



U.S. Department of Energy  
Idaho Operations Office

# **HWMA/RCRA Part B Permit Application for the Idaho National Laboratory**

## **Volume 3 General Information for INL Waste Management Units**

### **Book 1 of 1**

November 1985

Revision 1 – March 1986

Revision 2 – November 1986

Revision 3 – November 1987

Revision 4 – May 1991

Revision 5 – January 1993

Revision 6 – July 1993

Revision 7 – May 2001

Revision 8 – September 2001

Revision 9 – September 2002

Revision 10 – November 2002

Revision 11 – July 2004

Revision 12 – May 2005

Revision 13 – June 2006

Revision 14 – June 2008

Revision 15 – July 2010

Revision 16 – July 2013

Revision 17 – June 1, 2016

Revision 18 – July 2017

---

# **Idaho Cleanup Project**

# **HWMA/RCRA Part B Permit Application for the Idaho National Laboratory**

## **Volume 3**

## **General Information for INL Waste Management Units**

### **Book 1 of 1**

**November 1985**

**Revision 1 – March 1986**

**Revision 2 – November 1986**

**Revision 3 – November 1987**

**Revision 4 – May 1991**

**Revision 5 – January 1993**

**Revision 6 – July 1993**

**Revision 7 – May 2001**

**Revision 8 – September 2001**

**Revision 9 – September 2002**

**Revision 10 – November 2002**

**Revision 11 – July 2004**

**Revision 12 – May 2005**

**Revision 13 – June 2006**

**Revision 14 – June 2008**

**Revision 15 – July 2010**

**Revision 16 – July 2013**

**Revision 17 – June 1, 2016**

**Revision 18 – July 2017**



## CONTENTS

|  |       |
|--|-------|
| ACRONYMS.....  | vi    |
| INTRODUCTION .....   | 1     |
| Organization of Volume 3 of the HWMA/RCRA Permit Application.....  | 2     |
| PERMIT APPLICATION COMPLETENESS/TECHNICAL<br>EVALUATION CHECKLIST.....   | TEC-1 |
| A. PART A PERMIT APPLICATION.....  | A-1   |
| B. FACILITY DESCRIPTION.....   | B-1   |
| B-1 General Description [IDAPA 58.01.05.012; 40 CFR 270.14(b)(1)] .....  | B-2   |
| B-1(a) Facility Specific Information.....  | B-11  |
| B-2 Topographic Maps [IDAPA 58.01.05.012; 40 CFR 270.14(b)(19)] .....  | B-12  |
| B-2(a) Regional Topographic Maps .....   | B-12  |
| B-2(b) Wind Roses .....  | B-14  |
| B-2(c) Wells.....  | B-14  |
| B-2(d) Surrounding Land Use .....  | B-19  |
| B-2(e) Access Control.....   | B-21  |
| B-2(f) Other Structures .....  | B-21  |
| B-3 Location Information .....   | B-21  |
| B-3(a) Seismic Standard (IDAPA 58.01.05.008 and 58.01.05.012 [40 CFR<br>264.18(a) and 270.14(b)(11)(i-ii)]) .....  | B-21  |
| B-3(b) Floodplain Determination and Prevention of Washout (IDAPA<br>58.01.05.008 and 58.01.05.012 [40 CFR 264.18(b) and<br>270.14(b)(11)(iii-iv)]) ..... | B-22  |

|  |      |
|--|------|
| B-3(b)(1) Flood Potential from the Big Lost River.....   | B-24 |
| B-3(b)(2) Flood Diversion Systems at the INL.....  | B-25 |
| B-3(b)(3) INTEC 100-Year Storm Water Runoff and 25-Year<br>Runoff Analysis.....                      | B-25 |
| B-4 Traffic Information [IDAPA 58.01.05.012; 40 CFR 270.14(b)(10)] .....                             | B-25 |
| B-4(a) Off-Site Traffic.....   | B-25 |
| B-4(b) On-Site Traffic .....   | B-28 |
| B-4(b)(1) INTEC Traffic.....   | B-29 |
| B-4(b)(2) RWMC Traffic.....  | B-31 |
| B-4(b)(3) MFC Traffic .....  | B-31 |
| B-5 Literature Cited .....   | B-35 |
| C. WASTE CHARACTERISTICS.....  | C-1  |
| D. PROCESS INFORMATION .....   | D-1  |
| E. GROUNDWATER MONITORING.....   | E-1  |
| F. PROCEDURES TO PREVENT HAZARDS .....   | F-1  |
| F-1 Security IDAPA 58.01.05.008 and .012 [40 CFR 264.14(b) and(c),<br>and 270.14(b)(4)].....         | F-1  |
| G. CONTINGENCY PLAN .....  | G-1  |
| H. PERSONNEL TRAINING .....  | H-1  |
| I. CLOSURE AND POSTCLOSURE REQUIREMENTS .....  | I-1  |
| J. CORRECTIVE ACTION FOR SOLID WASTE MANAGEMENT UNITS<br>(IDAPA 58.01.05.008 [40 CFR 264.101]) ..... | J-1  |

K. OTHER FEDERAL LAWS (IDAPA 58.01.05.012 [40 CFR 270.14(b)(20) and 40 CFR 270.3])..... K-1

    K-1    The Wild and Scenic Rivers Act ..... K-1

    K-2    The National Historic Preservation Act of 1966 ..... K-1

    K-3    The Endangered Species Act..... K-1

    K-4    The Coastal Zone Management Act..... K-7

    K-5    The Fish and Wildlife Coordination Act..... K-7

    K-6    The Migratory Bird Treaty Act of 1918..... K-7

    K-7    Bald Eagle Protection Act..... K-7

    K-8    Management of Undesirable Plant on Federal Lands..... K-7

    K-9    Invasive Species Executive Order ..... K-7

    K-10   Public Land Orders 318, 545, 637, 1770 ..... K-8

    K-11   Clean Water Act..... K-8

L. HWMA/RCRA PERMIT APPLICATION CERTIFICATION [IDAPA 58.01.05.012 40 CFR 270.11(d) and 270.30(k)]

    DOE Idaho Operations Office Certification..... L-1

    Fluor Idaho Certification ..... L-2

APPENDICIES

Appendix I    Topographic Maps

Appendix II    Flood Insurance Rate Maps

Appendix III   Big Lost River Flood Hazard Study, Idaho National Laboratory,  
                  Idaho, U.S. Bureau of Reclamation, November 2005

                  INTEC 100-Year Flood Plain Map (RICOM Flow Model)

Appendix IV 100-Year Storm Water Runoff Floodplain and 25-Year Runoff Analyses for the Idaho Nuclear Technology and Engineering Center at the Idaho National Engineering and Environmental Laboratory (INEEL/EXT-03-001174, Revision 1, January 2004)

**EXHIBITS**

B-1. Map of the INL showing facility areas. .... B-3

B-2. Locations of INL seismic stations and normal faults and Quaternary Faults. .... B-5

B-3. Epicenters for historic earthquake events of a magnitude greater than 2.5 occurring from 1872 to 2014..... B-7

B-4. Generalized geology of the Eastern Snake River Plain showing locations of volcanic rift zones, young lava fields, and basin and range faults..... B-9

B-5. INTEC, ATR Complex, and TAN/SMC area wind roses..... B-15

B-6. CITRC, CFA, RWMC, MFC, and NRF area wind roses. .... B-16

B-7. INL sitewide locations of wells. .... B-17

B-8. Enlarged detail of the locations of wells at the ATR Complex, CFA, CITRC, INTEC, LSIT, MFC, NPR, NRF, PERC, RWMC, SMC, STF, TSF, VZPR and WRRTF. .... B-18

B-9. Grazing areas at the INL. .... B-20

B-10. USGS miscellaneous investigation map I-2330 . .... B-23

B-11. INL roads, highways, and railroads. .... B-26

B-12. Access and traffic control at INTEC..... B-30

B-13. Access and traffic control at RWMC..... B-33

B-14. Access and traffic control at MFC ..... B-34

F-1. Example of an INL boundary no trespassing sign..... F-2

F-2. Example of an INL boundary no grazing sign..... F-3

F-3. Locations of INL warning signs (INL Boundary), grazing boundaries, and current security stations..... F-5

**TABLES**

B-1. Description of the highway system in the INL vicinity..... B-27

B-2. Baseline traffic for selected highway segments in the vicinity of INL..... B-28

B-3. Baseline annual vehicle miles traveled for traffic related to the INL..... B-28

K-1. Listed and proposed endangered species, and candidate species, which may occur at the INL ..... K-2

## ACRONYMS

|    |             |  |
|----|-------------|--|
| 1  | AMWTP       | Advanced Mixed Waste Treatment Project                                   |
| 2  | ANL-W       | Argonne National Laboratory-West   |
| 3  | ARA         | Auxillary Reactor Area   |
| 4  | ARVFS       | Army Reentry Vehicle Facility Site                                       |
| 5  | ATR         | Advanced Test Reactor  |
| 6  | ATR Complex | Advanced Test Reactor Complex (formerly known as RTC)                    |
| 7  | BLM         | Bureau of Land Management  |
| 8  | BOR         | Bureau of Reclamation  |
| 9  | BORAX       | Boiling Water Reactor Experiment   |
| 10 | CITRC       | Critical Infrastructure Test Range Center (formerly known as WROC)       |
| 11 | CFA         | Central Facilities Area  |
| 12 | CFR         | Code of Federal Regulations  |
| 13 | DEQ         | Idaho Department of Environmental Quality                                |
| 14 | DOE         | Department of Energy   |
| 15 | DOE-ID      | Department of Energy Idaho Operations Office                             |
| 16 | EBR-I       | Experimental Breeder Reactor - I   |
| 17 | EDF         | engineering design file  |
| 18 | EIS         | environmental impact statement   |
| 19 | EO          | Executive Order  |
| 20 | EPA         | Environmental Protection Agency  |
| 21 | ESA         | Endangered Species Act   |
| 22 | ESRP        | Eastern Snake River Plain  |
| 23 | FDPA        | Fuel Dissolution Process Area (located within Building CPP-666 at INTEC) |
| 24 | FEMA        | Federal Emergency Management Act   |
| 25 | FFA/CO      | Federal Facility Agreement and Consent Order                             |
| 26 | FIA         | Federal Insurance Administration   |
| 27 | FIRM        | flood insurance rate map   |
| 28 | FSA         | Fues Storage Area (located within Building CPP-666 at INTEC)             |
| 29 | FWS         | U.S. Fish and Wildlife Service   |
| 30 | HWMA        | Hazardous Waste Management Act   |
| 31 | ICPP        | Idaho Chemical Processing Plant  |
| 32 | IDAPA       | Idaho Administrative Procedures Act                                      |

|    |       |   |
|----|-------|---|
| 1  | IET   | Initial Engine Test   |
| 2  | INEEL | Idaho National Engineering and Environmental Laboratory                 |
| 3  | INL   | Idaho National Laboratory (formerly known as INEEL)                     |
| 4  | INTEC | Idaho Nuclear Technology and Engineering Center                         |
| 5  | ISA   | interim storage area  |
| 6  | LSIT  | Large Scale Infiltration Test   |
| 7  | MFC   | Materials and Fuel Complex (formerly known as ANL-W)                    |
| 8  | MTR   | Materials Test Reactor  |
| 9  | NOTF  | Naval Ordnance Test Facility  |
| 10 | NPR   | New Production Reactor  |
| 11 | NRC   | Nuclear Regulatory Commission   |
| 12 | NRF   | Naval Reactors Facility   |
| 13 | PBF   | Power Burst Facility  |
| 14 | PERC  | INTEC Percolation Ponds   |
| 15 | RCRA  | Resource Conservation and Recovery Act                                  |
| 16 | RTC   | Reactor Test Complex [now known as ATR Complex (formerly known as TRA)] |
| 17 | RTF   | Remote Treatment Facility   |
| 18 | RWMC  | Radioactive Waste Management Complex                                    |
| 19 | SMC   | Specific Manufacturing Capability                                       |
| 20 | SNF   | spent nuclear fuel  |
| 21 | SPERT | Special Power Excursion Reactor Tests                                   |
| 22 | STF   | Security Training Facility  |
| 23 | TAN   | Test Area North   |
| 24 | TRA   | Test Reactor Area   |
| 25 | TREAT | Transient Reactor Test  |
| 26 | TSA   | Transuranic Storage Area  |
| 27 | TSDf  | treatment, storage, and/or disposal facility                            |
| 28 | TSF   | Technical Support Facility  |
| 29 | USC   | United States Code  |
| 30 | USGS  | United States Geological Survey   |
| 31 | WAG   | Waste Area Group  |
| 32 | WERF  | Waste Experimental Reduction Facility                                   |
| 33 | WROC  | Waste Reduction Operations Complex                                      |
| 34 | WRRTF | Water Reactor Research Test Facility                                    |



## INTRODUCTION

This Hazardous Waste Management Act/Resource Conservation and Recovery Act (HWMA/RCRA) permit application is for waste management units at the U.S. Department of Energy (DOE) Idaho National Laboratory (INL). The DOE uses a variety of contractors to operate the INL's numerous facilities and operations. The Certification, as contained in Section L of this volume, reflects the current contractor with the lead for RCRA. The facility (unit-specific) volumes that follow will similarly reflect responsible operators. The specific waste management units to be permitted under this application are listed in the HWMA/RCRA Work Plan for the INL. This permit application is prepared in conformance with the "A. T. Kearney" format typically used by the Idaho Department of Environmental Quality (DEQ) and the U.S. Environmental Protection Agency (EPA). This format consists of the following sections:

- A. Part A Permit Application
- B. Facility Description
- C. Waste Characteristics
- D. Process Information
- E. Groundwater Monitoring
- F. Procedures to Prevent Hazards
- G. Contingency Plan
- H. Personnel Training
- I. Closure and Postclosure Requirements
- J. Corrective Action for Solid Waste Management Units
- K. Other Federal Laws
- L. Certification.

The INL HWMA/RCRA permit application is, as reflected in the INL HWMA/RCRA Work Plan, a multivolume document organized as follows:

- Volume 1: HWMA/RCRA Part A Permit Application for the Idaho National Laboratory
- Volume 1a: Advanced Mixed Waste Treatment Project – Hazardous Waste Management Act/Resource Conservation and Recovery Act (HWMA/RCRA) Transuranic Storage Area Interim Status Document.

1           Volume 3:     General Information

- 2                     •       Section B, Facility Description
- 3                     •       Section F, Procedures to Prevent Hazards
- 4                     •       Section H, Personnel Training
- 5                     •       Section J, Corrective Action for Solid Waste Management Units
- 6                     •       Section K, Other Federal Laws
- 7                     •       Section L, Certification.
- 8                     •       Appendix I – Topographic Maps
- 9                     •       Appendix II – Flood Insurance Rate Maps (FIRMs)
- 10                    •       Appendix III – Big Lost River Flood Hazard Study, Idaho National  
11                    Laboratory (U.S, Bureau Of Reclamation, November 2005)
- 12                    •       Appendix IV – 100-Year Storm Water Runoff Floodplain and 25-Year  
13                    Runoff Analysis for the INTEC at the INEEL (INEEL/EXT-03-00174,  
14                    Revision 3, January 2004)

15           Additional volumes are waste management unit-specific and are generally numbered sequentially.  
16 Each waste management unit-specific volume provides detailed information for Sections A (Part A  
17 Permit Application) through I listed above; includes a permit application certification statement in Section  
18 L; and contains supplemental information (pictures, design drawings, maps, etc.) to support Sections A  
19 through I.

20                    **Organization of Volume 3 of the HWMA/RCRA Permit Application**

21           This volume (Volume 3) of the HWMA/RCRA permit application for the INL presents general  
22 information pertinent to the INL. Volume 3 contains the text of the permit application for Sections B, J,  
23 K, L (Certification), and supporting Appendices I through IV. Also, as directed by the State of Idaho,  
24 information is provided in Sections F and H that supplements the subsequent waste management unit-  
25 specific volumes.

26           Following this introduction is a Permit Application Completeness Evaluation Checklist that lists  
27 the HWMA/RCRA information requirements for Sections A through L and the corresponding location in  
28 the multivolume permit application where the information requirement is addressed. This checklist is  
29 provided to assist in the review of this permit application for completeness and technical content.



**Permit Application Completeness/Technical Evaluation Checklist**

| Information Requirement                                     | Complete (Y/N) | Technically Adequate (Y/N) | See Attached Comment | Location of Information   |
|---|----------------|----------------------------|----------------------|---|
| A. PART A APPLICATION                                       |                |                            |                      | INL HWMA/RCRA Permit Application, Volume 1, Fluor Idaho, LLC.; Advanced Mixed Waste Treatment Project – Hazardous Waste Management Act/Resource Conservation and Recovery Act (HWMA/RCRA) Transuranic Storage Area Interim Status Document (AMWTP-TSA-05); and in the Unit Specific Volumes |
| B. FACILITY DESCRIPTION                                     |                |                            |                      | INL HWMA/RCRA Permit Application, Volume 3, Sections B-1 through B-4  |
| B-1 General description                                     |                |                            |                      | INL HWMA/RCRA Permit Application, Volume 3, Section §B-1  |
| B-2 Topographic map   |                |                            |                      | INL HWMA/RCRA Permit Application, Volume 3, §B-2  |
| B-2a General requirements                                   |                |                            |                      | INL HWMA/RCRA Permit Application, Volume 3, §B-2  |
| B-2b Additional requirements for land disposal facilities   |                |                            |                      | Not Applicable (NA)   |
| B-3a Seismic standard                                       |                |                            |                      | INL HWMA/RCRA Permit Application, Volume 3, §B-3  |
| B-3b Floodplain standard                                    |                |                            |                      | INL HWMA/RCRA Permit Application, Volume 3, §B-3 and HWMA/RCRA Facility/Unit Specific Volumes (Unit Specific Volumes)   |
| B-3b(1) Demonstration of compliance                         |                |                            |                      | INL HWMA/RCRA Permit Application, Volume 3, §B-3 And Unit Specific Volumes  |
| B-3b(1)(a) Flood proofing and flood protection measures; or |                |                            |                      | INL HWMA/RCRA Permit Application, Volume 3, §B-3 And Unit Specific Volumes  |
| B-3b(1)(b) Floodplain                                       |                |                            |                      | INL HWMA/RCRA Permit Application, Volume 3, §B-3 And Unit Specific Volumes  |
| B-3b(2) Plan for future compliance with floodplain standard |                |                            |                      | See Unit Specific Volumes   |
| B-3b(3) Waiver for land storage and disposal facilities     |                |                            |                      | NA  |
| B-4 Traffic information                                     |                |                            |                      | INL HWMA/RCRA Permit Application, Volume 3, §B-4 And Unit Specific Volumes  |

**Permit Application Completeness/Technical Evaluation Checklist**

| Information Requirement   | Complete (Y/N) | Technically Adequate (Y/N) | See Attached Comment | Location of Information                                       |
|---|----------------|----------------------------|----------------------|---|
| C. WASTE CHARACTERISTICS  | _____          | _____                      | _____                | See Unit Specific Volumes                                     |
| D. PROCESS INFORMATION  | _____          | _____                      | _____                | See Unit Specific Volumes                                     |
| E. GROUNDWATER MONITORING   | _____          | _____                      | _____                | See Unit Specific Volumes                                     |
| F. PROCEDURES TO PREVENT HAZARDS  | _____          | _____                      | _____                | Volume 3, §F addresses the INL Site-wide security information |
| F-1 Security  | _____          | _____                      | _____                | Volume 3, §F  |
| F-1a Security procedures and equipment                                  | _____          | _____                      | _____                | Volume 3, §F  |
| F-1a(1) 24-hour surveillance system                                     | _____          | _____                      | _____                | Volume 3, §F  |
| F-1a(2) Barrier and means to control entry                              | _____          | _____                      | _____                | Volume 3, §F  |
| F-1a(2)(a) Barrier  | _____          | _____                      | _____                | Volume 3, §F  |
| F-1a(2)(b) Means to control entry                                       | _____          | _____                      | _____                | Volume 3, §F  |
| F-1a(3) Warning signs   | _____          | _____                      | _____                | Volume 3, §F  |
| F-1b Waiver   | _____          | _____                      | _____                | NA  |
| F-2 Inspection schedule   | _____          | _____                      | _____                | See Unit Specific Volumes                                     |
| F-3 Waiver or documentation of preparedness and prevention requirements | _____          | _____                      | _____                | See Unit Specific Volumes                                     |
| F-4 Preventive procedures, structures, and equipment                    | _____          | _____                      | _____                | See Unit Specific Volumes                                     |

**Permit Application Completeness/Technical Evaluation Checklist**

| Information Requirement  | Complete (Y/N) | Technically Adequate (Y/N) | See Attached Comment | Location of Information  |
|--|----------------|----------------------------|----------------------|--|
| F-5 Prevention of reaction of ignitable, reactive, and incompatible wastes | _____          | _____                      | _____                | See Unit Specific Volumes  |
| G. CONTINGENCY PLAN  | _____          | _____                      | _____                | See HWMA/RCRA Facility/Unit Specific Volumes   |
| H. PERSONNEL TRAINING  | _____          | _____                      | _____                | Volume 3, §H contains the core training program outline  |
| H-1 Outline of the training program  | _____          | _____                      | _____                | Volume 3, §H   |
| H-1a Job title/job description   | _____          | _____                      | _____                | See Unit Specific Volumes  |
| H-1b Training content, frequency, and techniques                           | _____          | _____                      | _____                | See Unit Specific Volumes  |
| H-1c Training director   | _____          | _____                      | _____                | See Unit Specific Volumes  |
| H-1d Relevance of training to job position                                 | _____          | _____                      | _____                | See Unit Specific Volumes  |
| H-1e Training for emergency response                                       | _____          | _____                      | _____                | See Unit Specific Volumes  |
| H-2 Implementation of training program                                     | _____          | _____                      | _____                | See Unit Specific Volumes  |
| H-3 Training records   | _____          | _____                      | _____                | See Volume 3, §H and Unit Specific Volumes   |
| I. CLOSURE AND POST CLOSURE REQUIREMENTS                                   | _____          | _____                      | _____                | See Unit Specific Volumes  |
| J. CORRECTIVE ACTION FOR SOLID WASTE MANAGEMENT UNITS                      | _____          | _____                      | _____                | Volume 3, §J contains the references to the sections of the Unit Specific Volume of each HWMA Partial-Permit that addresses/satisfies the HWMA/RCRA Corrective Action Requirements |
| K. OTHER FEDERAL LAWS  | _____          | _____                      | _____                | Volume 3, §K   |

Facility/Unit INL General Information  
 ID No. ID4890008952  
 Review Date July 2017  
 Reviewer \_\_\_\_\_

**Permit Application Completeness/Technical Evaluation Checklist**

| Information Requirement | Complete (Y/N) | Technically Adequate (Y/N) | See Attached Comment | Location of Information                |
|-------------------------|----------------|----------------------------|----------------------|--|
| L. PART B CERTIFICATION |                |                            |                      | Volume 3, §L and Unit Specific Volumes |



1  
2  
3  
4  
5  
6

**A. PART A PERMIT APPLICATION**

The information for this section is contained in: Volume 1 HWMA/RCRA Part A Permit Application for the INL; in the Advanced Mixed Waste Treatment Project – Hazardous Waste Management Act/Resource Conservation and Recovery Act (HWMA/RCRA) Transuranic Storage Area Interim Status Document; and in the waste management unit specific volumes of this permit application/permit.

This space was intentionally left blank.



## B. FACILITY DESCRIPTION

This section provides a general description of the U.S. Department of Energy (DOE) Idaho National Laboratory (INL), as required by the Idaho Administrative Procedures Act (IDAPA), 58.01.05.012 [Title 40, Code of Federal Regulations (CFR) Part 270.14(b)]. This permit application addresses hazardous waste and mixed waste management activities at the INL. For the purposes of this permit application, “mixed waste” means a waste that contains both Resource Conservation and Recovery Act (RCRA) hazardous waste (40 CFR 261.3) and source, special nuclear, or byproduct material subject to the Atomic Energy Act (40 CFR 266.210).

The INL is a large site (2,305 km<sup>2</sup> [890 mi<sup>2</sup>]) with several major facilities and contractors responsible for programs administered by various DOE operations offices.

The HWMA/RCRA Work Plan for the INL identifies the specific waste management units to be permitted, the waste management units that have received a permit from the Idaho Department of Environmental Quality (DEQ), and those waste management units that have interim status (see Volume 1 – HWMA/RCRA Part A Permit Application for the INL and the AMWTP HWMA/RCRA Transuranic Storage Area Interim Status Document) that are to be closed under interim status. The HWMA/RCRA Work Plan for the INL is available on the Internet at

<https://fluor-idaho.com/Outreach/Stakeholders>

The corrective action requirements for INL facilities (as applicable) are addressed under the following HWMA/RCRA Final Partial Permits (as applicable): Materials and Fuel Complex (MFC) Storage and Treatment Units HWMA/RCRA Final Permit (PER-116) – Module VI; Volume 18 – HWMA/RCRA Storage and Treatment Permit for the Idaho Nuclear Technology and Engineering Center (INTEC) and the Radioactive Waste Management Complex (RWMC) (PER-109) - Module VIII; and the Advanced Mixed Waste Treatment Project (AMWTP) HWMA/RCRA Permit, Module VI.

Section B is organized as follows:

Subsection B-1 provides a general description of the INL and identifies the location of the waste management units on the INL. The text in Subsection B-1 is supplemented by maps and organized according to the major facility areas at the INL.

Subsection B-2 contains topographic maps and wind rose data for the INL, along with supporting discussion. Subsection B-3 contains location information addressing seismic and floodplain standards. Subsection B-4 contains information on traffic volume and controls at the INL, including both on-Site and off-Site traffic.

1           **B-1 General Description [IDAPA 58.01.05.012; 40 CFR 270.14(b)(1)]**

2           The INL is owned by the United States Government and is operated by DOE. Management and  
3 operation of the INL is the responsibility of DOE-designated private contractors working under the  
4 direction of DOE Idaho Operations Office (DOE-ID) and the Idaho branch of the Pittsburgh Naval  
5 Reactors Office. Exhibit B-1 is a map of the INL that identifies the locations of the facility areas.

6           The INL was established in 1949, by the Atomic Energy Commission, as an area where various  
7 types of nuclear reactors, support plants, and associated equipment could be built, tested, and operated  
8 with maximum safety. To date, 52 reactors have been built at the INL, including reactors for aircraft  
9 propulsion, naval propulsion, fast-breeder reactor development, light-water safety tests, organic  
10 moderator and coolant development, materials testing, development of portable power reactors for use in  
11 space, and miscellaneous research. Two of these reactors are still operable, the Advanced Test Reactor  
12 (ATR), and the Neutron Radiography Reactor. A decontamination and decommissioning program is  
13 underway to ensure the safe closure of retired facilities and equipment.

14           INL's original emphasis on nuclear physics has been broadened to encompass the entire  
15 spectrum of the basic sciences. Presently, the INL is a science-based, applied engineering national  
16 laboratory dedicated to supporting the U.S. Department of Energy's missions in nuclear and energy  
17 research, science, and national defense. Additionally, paralleling and contributing to this growth in  
18 scientific and technical capabilities is the increased emphasis on and dedication of resources to solving  
19 the problems of environmental restoration and waste management.

20           The primary facility areas located at the INL are: Materials and Fuel Complex (MFC) [formerly  
21 known as the Argonne National Laboratory-West (ANL-W)], Central Facilities Area (CFA), Idaho  
22 Nuclear Technology and Engineering Center [(INTEC) formerly known as the Idaho Chemical  
23 Processing Plant], Naval Reactors Facility (NRF), Critical Infrastructure Test Range Center (CITRC)  
24 [formerly known as the Waste Reduction Operations Complex (WROC)/Power Burst Facility (PBF)],  
25 Radioactive Waste Management Complex (RWMC), Test Area North (TAN), and Advanced Test  
26 Reactor (ATR) Complex [formerly known as the Reactor Technology Complex (RTC) or the Test  
27 Reactor Area (TRA)].

28           The INL is located near the northwest margin of the Eastern Snake River Plain (ESRP), a  
29 prominent low-elevation arcuate feature of southeastern Idaho. Geographically, this region of the ESRP  
30 extends over five counties. The INL lies predominately in Butte County, although it extends into  
31 Bingham, Bonneville, Jefferson, and Clark counties. All waste management units are located in Butte  
32 County with the exception of MFC units, which are located in Bingham County.

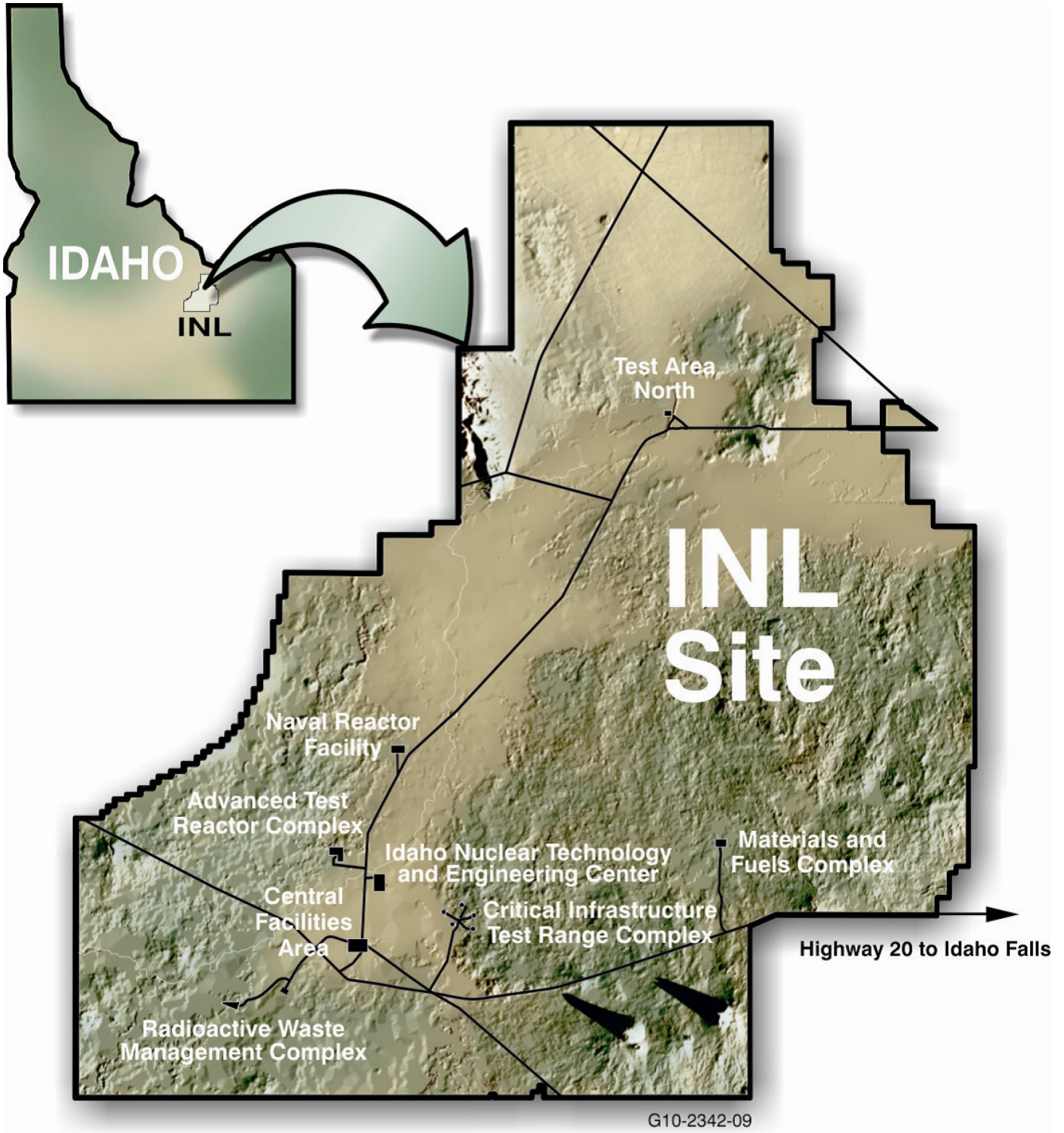


Exhibit B-1. Map of the INL showing facility areas.

1 The ESRP is relatively flat with an average elevation of 1,500 m (4,920 ft) above the mean sea level.  
2 Within the INL site, elevations generally range from 1,450 to 1,585 m (4,760 to 5,200 ft). A broad  
3 topographic ridge extends to the northeast along the central axis of the ESRP. This ridge effectively separates  
4 the drainage of the mountain ranges north and west of the INL site from the Snake River.

5 The ESRP is a northeast-trending zone of late Tertiary and Quaternary volcanism that transects the  
6 northwest-trending, normal-faulted mountain ranges of the surrounding Basin and Range Province. The  
7 mountain ranges bordering the ESRP, (e.g., Lost River, Lemhi, and Beaverhead) consist of Paleozoic- and  
8 Mesozoic-age rocks folded, intruded, and uplifted along normal faults during basin and range tectonism. The  
9 mountain ranges and their associated basin and range faults terminate along both sides of the low-lying  
10 basalt- and sediment-filled ESRP.

11 Volcanic rocks within the ESRP consist of late Tertiary rhyolitic rocks covered by the latest Tertiary  
12 to Holocene basaltic lava flows. At least 1 km (3,281 ft) of basaltic lava flows and intercalated sediments has  
13 accumulated over the past 4 million years in the ESRP following the rhyolitic volcanism related to passage of  
14 the Yellowstone mantle plume. Most basalt eruptions were effusive, similar to the style of basalt volcanism  
15 occurring at Kilauea, Hawaii, today. Throughout the ESRP, the basaltic vents typically formed linear arrays  
16 of fissure flows, small shields and pyroclastic cones, pit craters, and open fissures that collectively define  
17 northwest-trending volcanic rift zones. The most well known and recently active (2,000 years) is the Great  
18 Rift where eight eruptive episodes occurred at Craters of the Moon during the past 15,000 years. Basalt lava-  
19 flows within the boundaries of the INL range in age from 12,000 years to greater than 730,000 years old.

20 INL site surficial deposits are quite variable and include eolian (loess and sand dunes), alluvial  
21 (gravel, sand, and silt), and lacustrine (clay, silt, and sand) deposits. The surface soils vary widely in  
22 thickness and water-holding capacity. Sedimentary interbeds within the subsurface basalt stratigraphy exhibit  
23 the same characteristics as the surficial sediments.

24 The INL operates 33 seismic stations and 32 accelerometer sites to monitor earthquake activity  
25 occurring in the region. The seismic stations are located on the INL site, on the adjacent ESRP, and  
26 throughout the surrounding mountainous region (Exhibit B-2). Three component accelerometers are located  
27 in moderate and high-hazard facilities, at ground surface within facility areas, and at seismic stations. The  
28 INL monitors and records earthquake activity within a 161-km (100-mi) radius of the INL, to develop a  
29 historical database of times, dates, locations, and magnitudes of earthquakes. This information is used in  
30 ground motion analyses to estimate levels of ground shaking (ground motion) from future earthquakes. The  
31 seismic monitoring activity provides a way to validate current ground motion models and levels in the event  
32 of a large earthquake in the future. The INL seismic network also serves as an early warning detection system  
33 for future volcanism. Characteristic low-magnitude earthquake swarms accompany upward movement of  
34 magma through the crust of the earth and provide the means to monitor renewed volcanic activity.

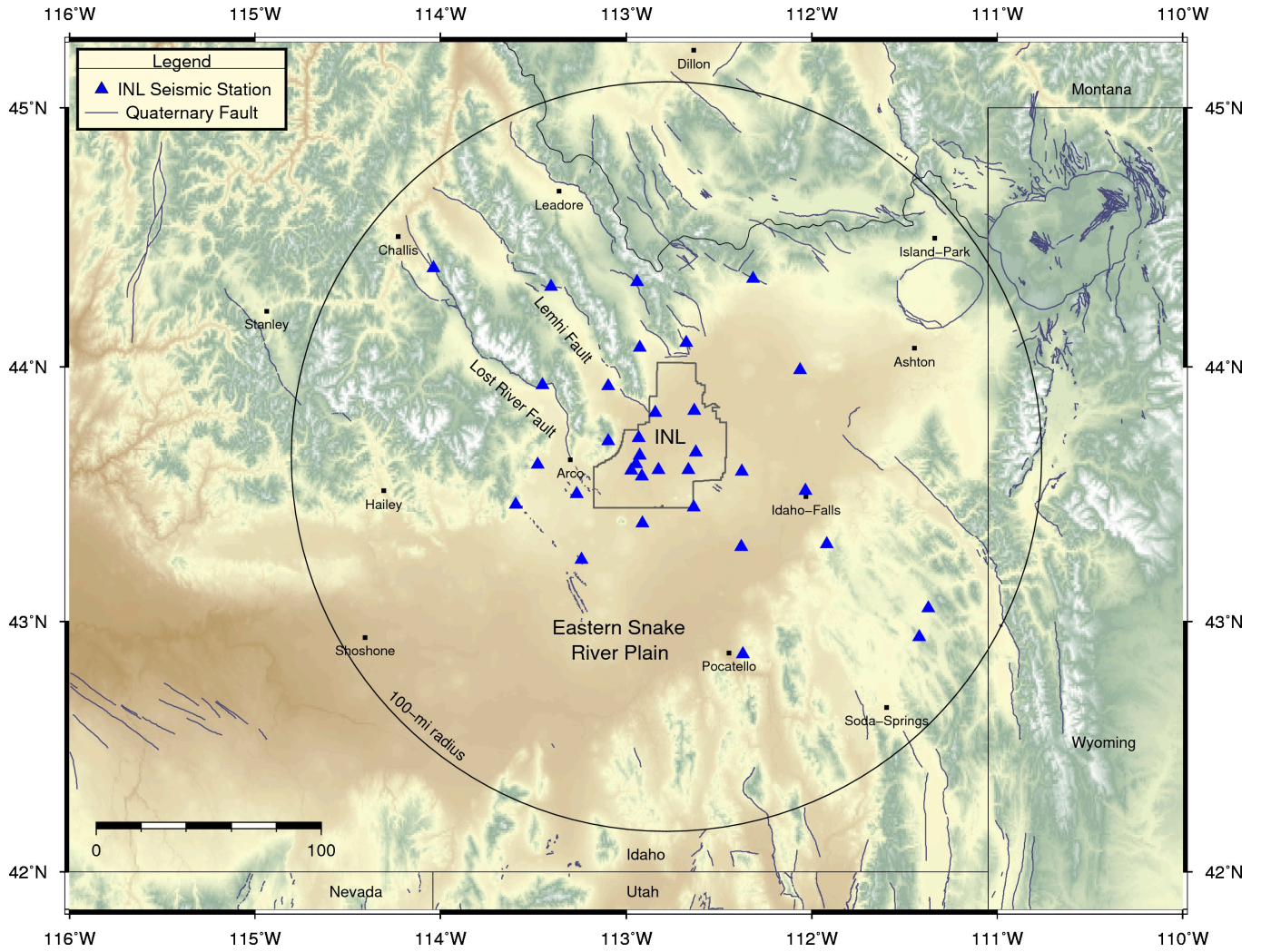


**Exhibit B-2.** Locations of INL seismic stations (blue triangles) and Quaternary faults (gray lines) from the U.S. Geological Survey and Idaho Geological Survey (2006).

1 INL earthquake data have been combined with earthquake data from nearby seismic networks to  
2 produce a historical earthquake record. The historical record from 1850 to 2014 for magnitude 2.5 and  
3 greater earthquakes shows that the ESRP is seismically quiet relative to the surrounding active Basin and  
4 Range Province. Detailed monitoring by the INL seismic network from 1972 to 2016 has located 95  
5 small magnitude microearthquakes ( $M < 2.5$ ), within the ESRP near the INL, 27 of which are located to  
6 the south of INL in the Great Rift (Exhibit B-4). Detailed analyses of focal depths and waveforms  
7 suggest that the microearthquakes in the ESRP are associated with tectonic or volcanic processes.  
8 Eighteen earthquakes with low frequency content ( $< 5$  Hz) at the northern end of the Great Rift are  
9 indicative of volcanic processes occurring at depths from 15 to 45 km. In contrast, thousands of tectonic  
10 earthquakes associated with faulting have occurred in the Basin and Range Province surrounding the  
11 ESRP.

12 During the past 20 years, the INL has spent a considerable amount of effort estimating the levels  
13 of ground shaking that can be expected at INL facilities from all earthquake sources in the region. The  
14 effort included investigating the faults closest to the INL (Exhibit B-2). The Lost River and Lemhi faults  
15 were studied in detail to estimate their maximum earthquake magnitudes, distances to INL facilities, ages  
16 of earthquakes, and recurrence intervals. The results of these investigations indicate that the closest fault  
17 segments are capable of generating magnitude 7 or greater earthquakes and that the most recent  
18 earthquakes occurred more than 15,000 years ago on these fault segments.

19 A probabilistic ground motion study was completed for all INL facilities in 1996 and recomputed  
20 in 2000. The method incorporated the range of possible seismologic and tectonic interpretations,  
21 including earthquake source characteristics (e.g., type of faulting, earthquake magnitude, and fault  
22 geometry), attenuation models (the manner in which seismic waves dissipate as they travel through the  
23 earth), and subsurface geologic conditions (the manner in which seismic waves are affected by the near-  
24 surface sediment and basalt layers). As part of this effort, modeling and earthquake monitoring were  
25 conducted to understand how seismic waves are affected by the alternating sequence of basalt lava flows  
26 and sedimentary interbeds that composes the ESRP subsurface. As seismic waves pass through layers of  
27 alternating competent (hard) basalt and loosely consolidated (soft) sediments scattering and dampening  
28 of seismic energy occurs which results in earthquake ground motion levels 15 to 25% less than would be  
29 exhibited in uniform rock. Sensitivity analyses were also performed to determine the important  
30 contributors to the seismic hazard and to assess the uncertainties in the hazard. The estimates are in the  
31 form of the levels of ground shaking that will not be exceeded in specified time periods (such as 500;  
32 1,000; 2,500; and 10,000 years).

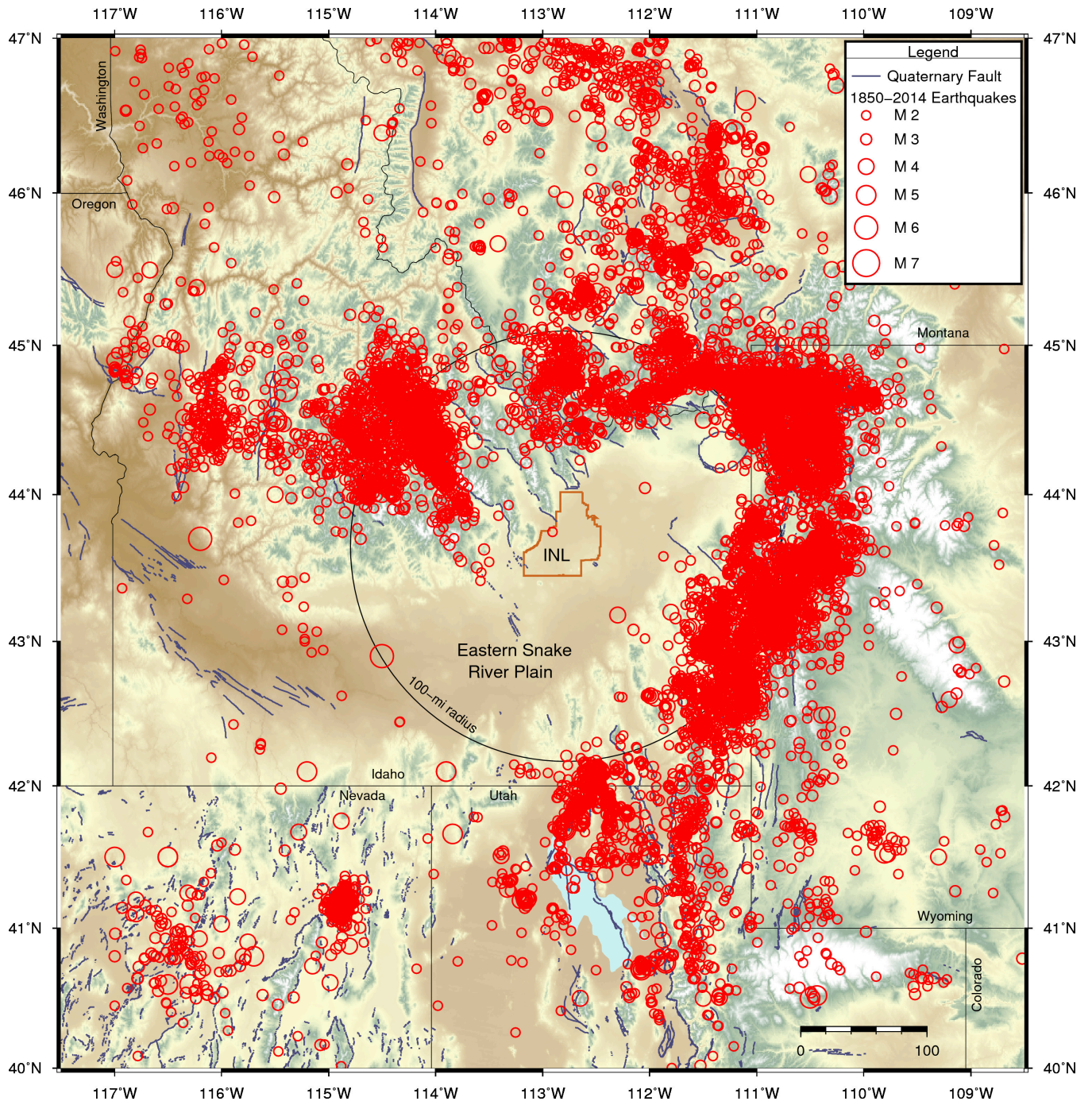


**Exhibit B-3.** Epicenters for historic earthquakes of magnitude greater than 2.5 occurring from 1872 to 2014.

1           These results were used to develop design basis earthquake parameters for rock conditions,  
2 which were documented in *Development of Probabilistic Design Earthquake Parameters for Moderate*  
3 *and High Hazard Facilities at INEEL* (Payne et al. 2002). The expected levels of earthquake ground  
4 motions (determined by the recent INL seismic hazards assessment) provide seismic design criteria for  
5 new facilities and indicate that past criteria are conservative. The revised seismic criteria are being used  
6 in assessments of existing facilities to ensure safety to the public, workers, and environment. INL  
7 seismic design criteria have been developed consistent with the requirements of DOE standards,  
8 American Society of Civil Engineering standards, Nuclear Regulatory Commission (NRC) requirements,  
9 American Nuclear Society (ANS) requirements, and nuclear quality assurance requirements.

10           Volcanic hazards assessments have been conducted for INL facilities since the ESRP is a  
11 volcanic province with recent eruptions of basalt lava flows, relative to geologic time, in association with  
12 volcanic rift zones (Exhibit B-4). Volcanism investigations (determination of ages of lava flows,  
13 mapping of volcano distribution and volcanic rift zone structures, and analysis of borehole data) have  
14 contributed greatly to improved understanding of the volcanic processes affecting the ESRP. This  
15 understanding has enabled completion of a rigorous probabilistic volcanic hazards assessment to support  
16 an NRC license that was recently granted for a new spent nuclear fuel (SNF) storage facility at the  
17 INTEC. Methodologies have been developed to assess the site-specific volcanic hazard for each facility.  
18 The shortest recurrence intervals (greatest annual probabilities of eruption) for INL volcanic rift zones  
19 are about 16,000 years (or  $6.2 \times 10^{-5}$  per year) for the axial volcanic zone and Arco volcanic rift zone.

20           Surface water at the INL consists of streams draining through intermountain valleys to the west  
21 and north, localized snowmelt, and rain. Streams entering the INL include the Big Lost River, Little Lost  
22 River, and Birch Creek. Flow from the Little Lost River and Birch Creek is generally diverted for  
23 irrigation purposes, before it reaches the INL. However, water from the Big Lost River and Birch Creek  
24 enters the INL during years without drought. During drought periods, flow does not reach the INL.  
25 These three drainage systems either terminate in one of four playas in the north-central part of the INL or  
26 terminate prior to reaching the playas. The INL is not crossed by any perennial streams. All surface  
27 outflows are a result of localized slope run-off.

28           Recharge waters from the Big Lost River to the Snake River Plain Aquifer have been significant  
29 during wet years. Except for evaporation losses, all water flowing in the Big Lost River through the  
30 ESRP is recharged to the ground.

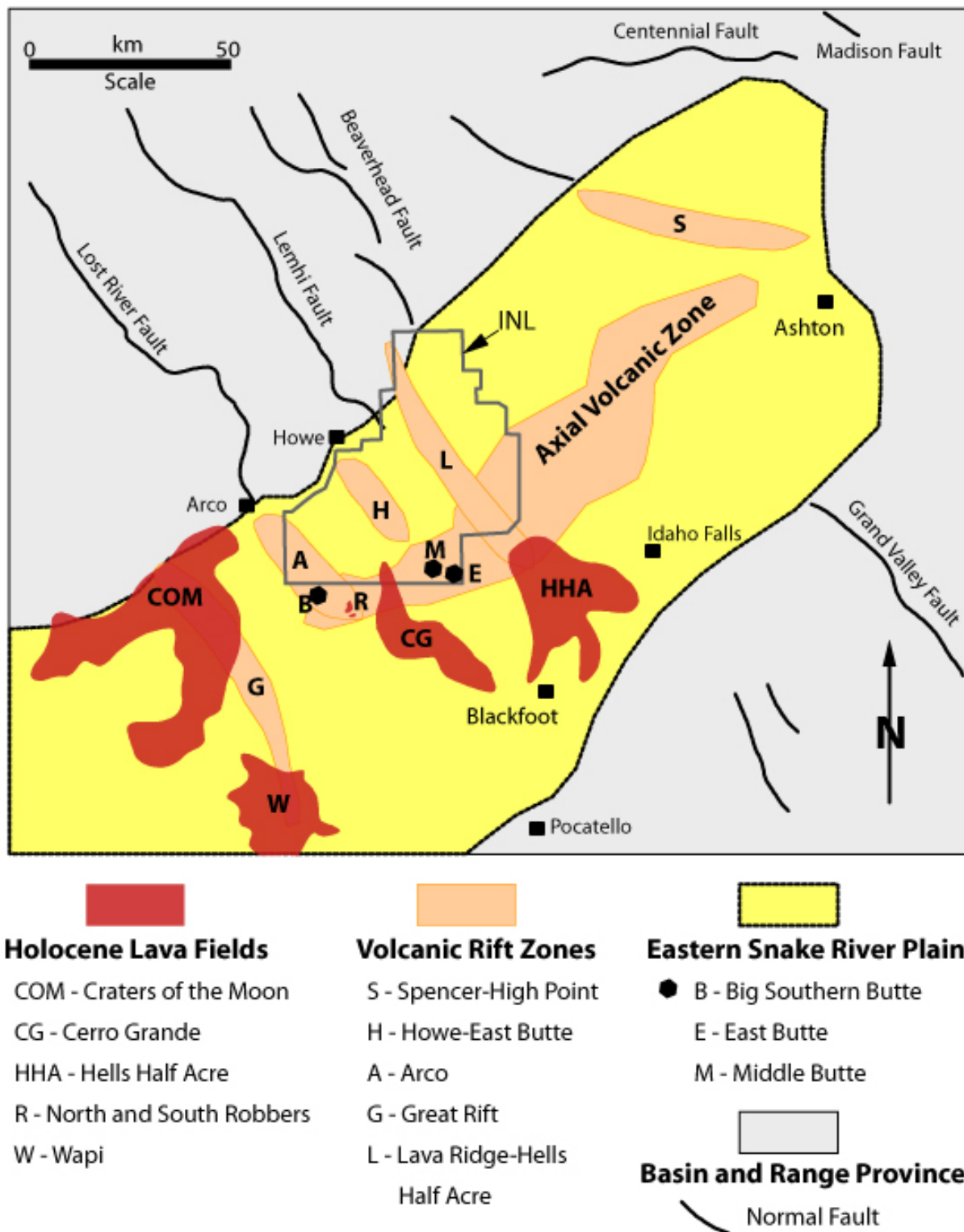


**Exhibit B-4.** Generalized geology of the Eastern Snake River Plain showing locations of volcanic rift zones, young lava fields, and basin and range faults.

1           The Snake River Plain Aquifer is a continuous body of groundwater that underlies nearly all of  
2 the ESRP. The section of the aquifer underlying the ESRP is approximately 320 km (198 mi) long and  
3 48 to 97 km (30 to 60 mi) wide. This section of thin basalt flows interbedded with layers of sediments  
4 comprises an area of approximately 24,900 km<sup>2</sup> (15,440 mi<sup>2</sup>). Most of the permeable zones in the aquifer  
5 occur along the upper and lower edges of the basaltic flows, which have large irregular fractures,  
6 cavities, and voids. This structure leads to a great degree of heterogeneity and anisotropy in the  
7 hydraulic properties of the aquifer. The thickness of the aquifer has not been established, but several  
8 holes at the INL indicate that the thickness of the most permeable part is between 100 and 400 m (328 to  
9 1,312 ft). The depth to the aquifer under the INL varies from 60 m (197 ft) in the northeast corner to 275  
10 m (902 ft) in the southwest corner.

11           Groundwater flows southwestward from the north and northeastern recharge areas. Tracer  
12 studies at the INL indicate groundwater velocities of 1.5 to 6.1 m (4.9 to 20 ft) per day. The aquifer  
13 contains 1,230 to 2,460 km<sup>3</sup> (300 to 600 mi<sup>3</sup>) of water, of which 616 km<sup>3</sup> (150 mi<sup>3</sup>) is recoverable. About  
14 8 km<sup>3</sup> (2 mi<sup>3</sup>) of groundwater is discharged annually through springs in the Hagerman, Idaho, area, and  
15 through irrigation-well withdrawals in the region west of Twin Falls, Idaho. The discharges from the  
16 springs make a significant contribution to the flow of the Snake River downstream from Hagerman.  
17 Besides providing water for INL operations, the aquifer supplies other industries. Water from springs  
18 emerging in the Twin Falls–Hagerman area is used commercially in the aquaculture industry. The spring  
19 water flow of 47 m<sup>3</sup>/sec (1,659 ft<sup>3</sup>/sec) constitutes 76% of the water used for the commercial production  
20 of fish in Idaho. Most of these fish farms discharge water directly into the Snake River.

21           The United States Geological Survey (USGS) maintains an office at the INL and conducts  
22 independent environmental monitoring. INL operations produce various types of radioactive effluents.  
23 The processes by which the radioactive wastes are produced and controlled at all of the INL facilities are  
24 generally similar. The major radioactive contaminants include short-lived nuclides (such as tritium,  
25 chromium-51, strontium-90, and cobalt-60) and long-lived nuclides (such as iodine-129, technetium-99,  
26 and carbon-14).

27           INL facilities routinely generate a variety of nonradioactive industrial and sanitary waste  
28 streams. These waste streams are primarily aqueous and may contain minor quantities of chemicals.  
29 Wastes include laboratory wastes, cooling water, effluent from boilers used in space and process steam  
30 heating, water treatment waste, and sanitary waste and sewage. Nonhazardous liquid wastes are  
31 generally routed to unlined impoundments. In the past, disposal wells have been used at the INL for such  
32 wastewater. Some of these wells have now been closed (filled with concrete and capped) or converted to  
33 monitoring wells. Several surface water run-off wells are also still in operation throughout the INL.  
34 Sanitary wastes and sewage are treated and then discharged to impoundments, evaporation lagoons, or  
35 shallow subsurface drainage fields. The ponds and wells described above are not addressed in this

1 permit application, as they are not currently receiving hazardous waste. These disposal areas are  
2 addressed under the Federal Facility Agreement and Consent Order (FFA/CO) involving DOE Idaho  
3 Operations Office, the State of Idaho, and EPA Region 10 (1991).

4 Hazardous wastes, mixed wastes, polychlorinated biphenyls (PCB), and PCB-contaminated  
5 materials are also generated at the INL. The hazardous wastes typically come from D & D activities,  
6 support operations, and laboratory activities conducted at the INL and include ignitable liquids, acids,  
7 bases, solvents, oxidizers, toxics, and reactives. Additional types of waste may include laboratory  
8 wastes, photographic wastes, spill residues, excess solutions, cleanup solutions, paint-stripping residues,  
9 and wastes generated by decontamination and demolition activities. The hazardous wastes may be  
10 accumulated on-Site in satellite accumulation areas (SAAs) and in “less than 90-day” storage areas  
11 (a.k.a. 90-day storage areas) in accordance with IDAPA 58.01.05.006 (40 CFR 262); stored and treated  
12 on-Site under a generator treatment plan or in a RCRA unit; or transported off-Site to a RCRA treatment,  
13 storage, and disposal facility (TSDF). PCB liquids, PCB-contaminated transformers, and other PCB-  
14 contaminated materials are sent off-Site for disposal, but may be stored on-Site pending shipment.

15 Mixed wastes that may be generated include, but are not limited to, contaminated metals,  
16 solvents, wastewater, laboratory wastes, and chemical-contaminated rags and other materials used in  
17 decontamination and waste generated during D & D activities. These wastes may be generated through a  
18 variety of processes and activities such as laboratory operations, equipment cleanup, paint stripping,  
19 decontamination operations, demolition activities, and other operations where contact with radioactive  
20 materials may occur. Some of these wastes are treated on-Site; others are stored, pending development  
21 of treatment or disposal capabilities on-Site or off-Site. Additionally, INL accepts mixed waste  
22 generated at other DOE facilities for treatment and certification for shipment to the Waste Isolation Pilot  
23 Plant (WIPP), in New Mexico. Furthermore, the INL also accepts mixed waste generated at other DOE  
24 Facilities for treatment and characterization for shipment to other off-Site treatment, storage, and  
25 disposal facilities (e.g., Energy Solutions, Nation Nuclear Security Administration, etc.), as well as to the  
26 WIPP.

### 27 **B-1(a) Facility Specific Information**

28 Facility specific information for INL facilities that have HWMA/RCRA units regulated under 40  
29 CFR 265 and 40 CFR 264 (IDAPA 58.01.05.009 and 58.01.05.008) may be found in the following Final  
30 Partial HWMA/RCRA Permits and HWMA/RCRA Permit Applications/Interim Status Documents:

- 31 • Volume 1 – HWMA/RCRA Part A Permit Application for the Idaho National Laboratory –  
32 Fluor Idaho, LLC (PER-101)

- 1           • AMWTP – HWMA/RCRA (HWMA/RCRA) Transuranic Storage Area Interim Status  
2           Document
  
- 3           • HWMA/RCRA Storage and Treatment Permit for the Materials and Fuels Complex  
4           (PER-116)
  
- 5           • Volume 14 – HWMA/RCRA Storage and Treatment Permit for the Liquid Waste  
6           Management System at the Idaho Nuclear Technology and Engineering Center on the Idaho  
7           National Laboratory (PER-111)
  
- 8           • Volume 18 – HWMA/RCRA Storage and Treatment Permit for the Idaho Nuclear  
9           Technology and Engineering Center and the Radioactive Waste Management Complex on  
10          the Idaho National Laboratory (PER-109)
  
- 11          • Volume 21 – HWMA/RCRA Post-Closure Permit for the INTEC Waste Calcine Facility and  
12          CPP-601/627/640 on the Idaho National Laboratory (PER-112)
  
- 13          • Volume 22 – HWMA/RCRA Storage Permit for the Calcine Solids Storage Facility at the  
14          Idaho Nuclear Technology and Engineering Center on the Idaho National Laboratory (PER-  
15          114)
  
- 16          • Advanced Mixed Waste Treatment Project (AMWTP) HWMA/RCRA Permit

17           **B-2 Topographic Maps [IDAPA 58.01.05.012; 40 CFR 270.14(b)(19)]**

18           This subsection presents topographic map information and supporting information on prevailing  
19           winds, wells, surrounding land use, access controls, and other structures present at the INL. This  
20           information satisfies the topographic map requirements.

21           **B-2(a) Regional Topographic Maps**

22           The topographic maps for the INL, provided in Appendix I, have been updated with the latest  
23           available USGS maps (as found to be available on the USGS website). Map #4 formerly identified by  
24           the USGS as Circular Butte 3 NW is currently identified by the USGS as East of Howe Peak. Map #5  
25           formerly identified by the USGS as Circular Butte 3 NE is currently identified by the USGS as North of  
26           Rye Grass Flat. Map #6 formerly identified by the USGS as Circular Butte 3 SW is currently identified  
27           by the USGS as North of Scoville. Map #7 formerly identified by the USGS as Circular Butte 2 SE is  
28           currently identified by the USGS as Rye Grass Flat. The information below cross-references the maps to

1 the waste management unit locations and other required information. Refer to the HWMA/RCRA Work  
2 Plan for specific units within the major facility areas.

3 Map No. 1 - Dubois 1:250,000 (1 in. = 20,833 ft) – Shows the INL legal boundary (northern-  
4 most portion of facility) and more than 305 m (1,000 ft) around the INL legal boundary. Map No. 1  
5 should be used in conjunction with Map #2. Map No. 1 has 200-ft contours; shows surface waters, land  
6 usage, highways, and property boundaries.

7 Map No. 2 - Idaho Falls 1:250,000 (1 in. = 20,833 ft) – Shows the INL legal boundary (southern  
8 portion of facility) and more than 305 m (1,000 ft) around the INL legal boundary. Map No. 2 should be  
9 used in conjunction with Map No. 1. Map. No. 2 has 200-ft contours; shows surface waters, land usage,  
10 highways, and property boundaries.

11 Map No. 3 - Circular Butte 1:24,000 (1 in. = 2,000 ft) – Shows TAN and SMC.

12 Map No. 4 - East of Howe Peak (Circular Butte 3 NW) 1:24,000 (1 in. = 2,000 ft) – Shows NRF.

13 Map No. 5 - North of Rye Grass Flat (Circular Butte 3 NE) 1:24,000 (1 in. = 2,000 ft) – There  
14 are no major facility areas on Map No. 5.

15 Map No. 6 - North of Scoville (Circular Butte 3 SW) 1:24,000 (1 in. = 2,000 ft) – Shows RTC,  
16 INTEC and CFA.

17 Map No. 7 - Rye Grass Flat (Circular Butte 3 SE) 1:24,000 (1 in. = 2,000 ft) – Shows CITRC and  
18 the Auxiliary Reactor Area (ARA).

19 Map No. 8 - Little Butte SW 1:24,000 (1 in. = 2,000 ft) – Shows MFC.

20 Map No. 9 - Arco Hills SE 1:24,000 (1 in. = 2,000 ft) – Shows the area north of RWMC. Map  
21 No. 9 should be used in conjunction with Map No. 10. Map No. 9 shows gauging stations on the Big  
22 Lost River and the diversion system.

23 Map No. 10 - Big Southern Butte 1:24,000 (1 in. = 2,000 ft) – Shows diversion areas for the Big  
24 Lost River diversion system. Map No. 10 should be used in conjunction with Map No. 9.

1 The INL encompasses 2,305 km<sup>2</sup> (890 mi<sup>2</sup>) of raised desert plain, with an average topographic  
2 elevation of approximately 1,500 m (4,920 ft) above mean sea level. The majority of the INL lies within  
3 Butte county, Idaho, although portions extend into Bingham, Bonneville, Jefferson, and Clark counties.  
4 All site activities and facilities are situated well within the INL boundaries, which extend for  
5 approximately 63 km (39 mi) north to south and 58 km (36 mi) east to west at their longest points.  
6 Exhibits B-1 and B-7 provide general facility location maps of the INL.

7 Appendix I provides regional topographic maps (Maps 1 and 2) of the INL complex, at a scale of  
8 1.0 in. = 20,833 ft. Additional topographic maps at a scale of 1 in. = 2,000 ft and contour intervals of 5,  
9 10, or 20 ft are also provided in Appendix I, as Maps 3 through 10, that are sufficient for this flat area as  
10 allowed under the regulation. Topographic maps with a smaller scale and smaller contour intervals are  
11 provided in the waste management unit-specific volumes of this permit application. The topographic  
12 maps in Appendix I show the topography, surface waters and intermittent streams, surrounding land  
13 usage, access roads, and well locations.

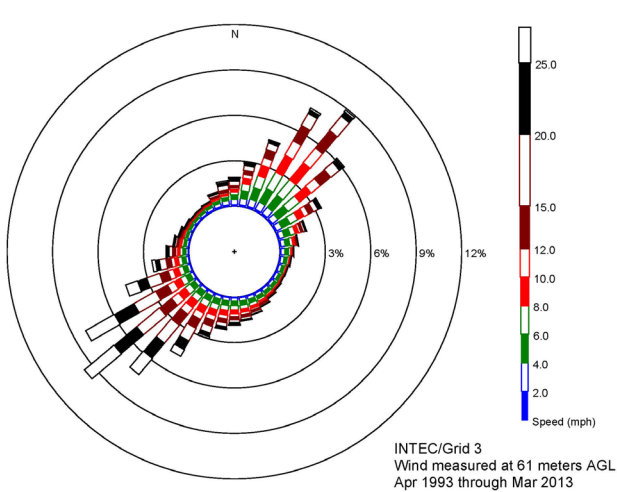
14 USGS topographic maps, which comply with the scale requirement of 1.0 in. = 200 ft under  
15 IDAPA 58.01.05.012 [40 CFR 270.14(b)(19)], are not available for the INL. From USGS maps  
16 provided, it is evident that the INL is located on an extremely flat desert plain.

### 17 **B-2(b) Wind Roses**

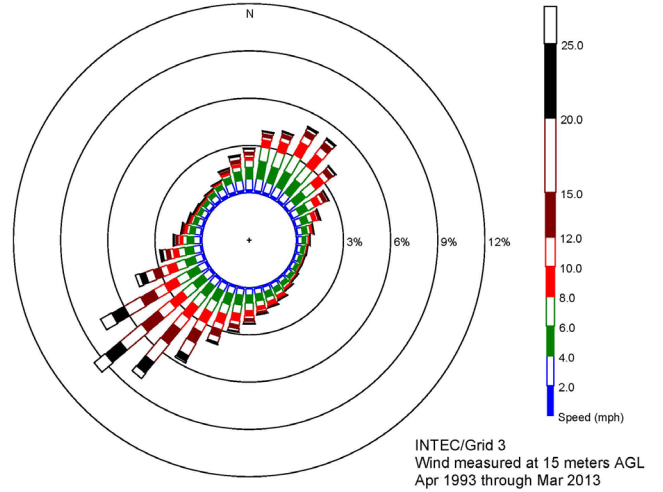
18 Wind rose data for INTEC and ATR, SMC, CITRC, CFA, NRF, RWMC, MFC, and NRF  
19 facilities and their surrounding areas are provided in Exhibits B-5 and B-6. These diagrams indicate a  
20 general northeast-southwest wind direction.

### 21 **B-2(c) Wells**

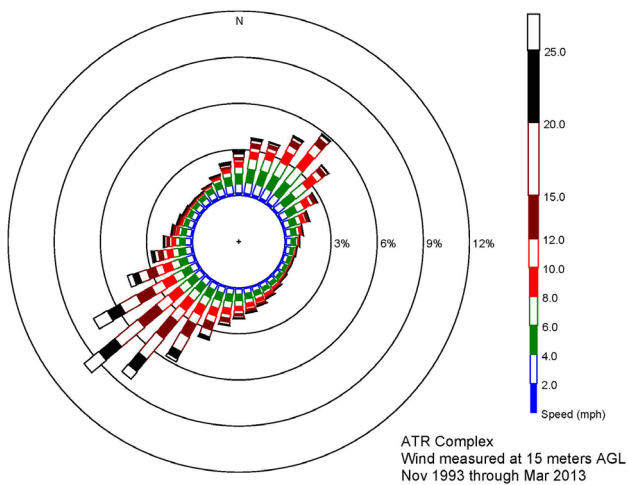
22 Updated maps showing the locations of all injection, withdrawal, and monitoring wells at and  
23 around the INL are included as Exhibits B-7 and B-8. Additionally, the State of Idaho has been provided  
24 with the Idaho National Engineering and Environmental Laboratory Environmental Monitoring Plan  
25 (DOE/ID-11088), which provides additional information on wells located at the INL.



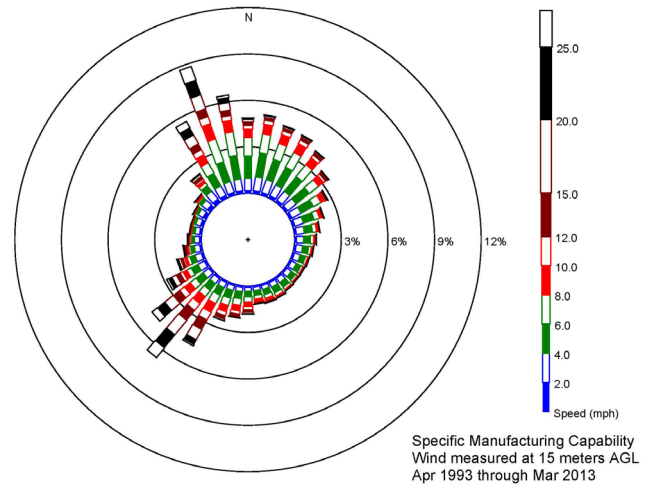
INTEC 61M



INTEC 15M

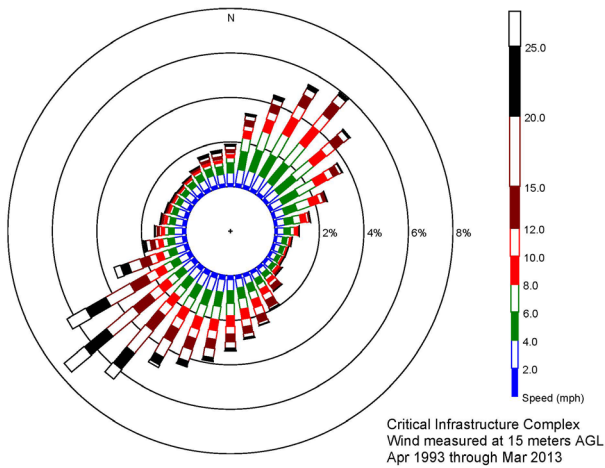


ATR 15M

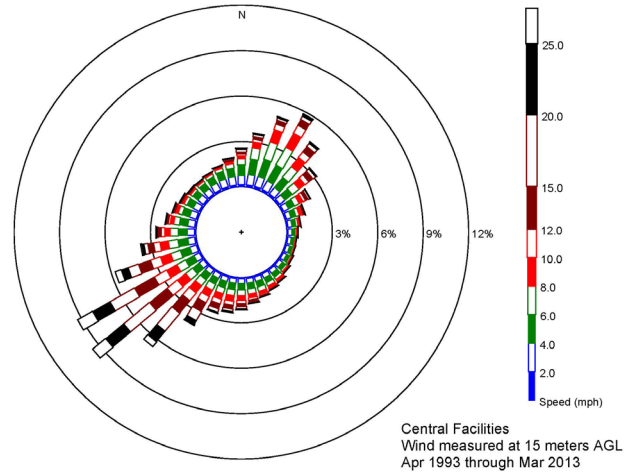


SMC 15M

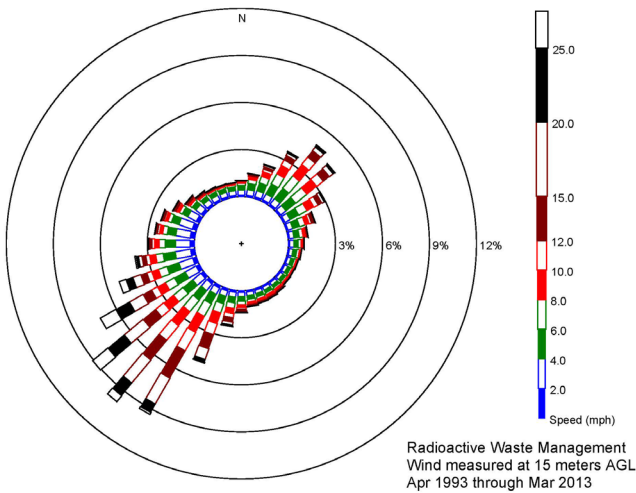
**EXHIBIT B-5.** INTEC, ATR Complex, and TAN/SMC area wind roses.



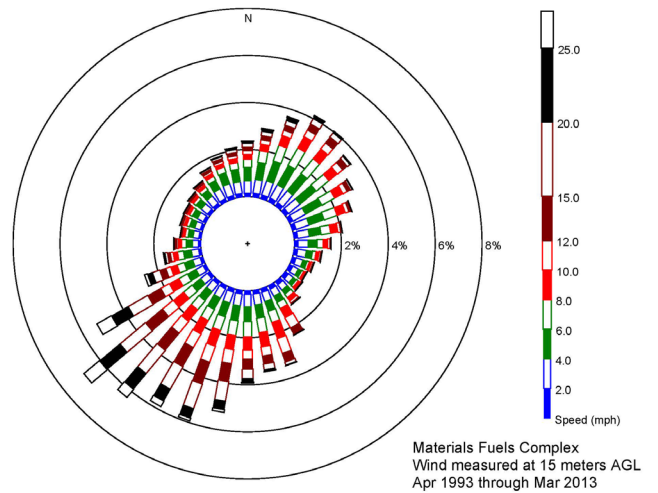
**CITRC 15M**



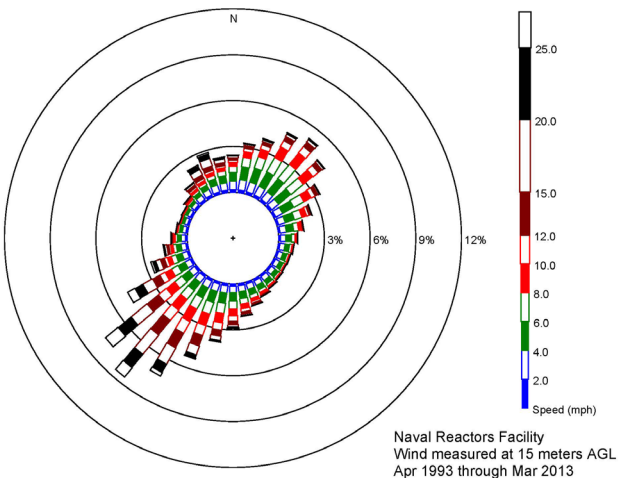
**CFA 15M**



**RWMC 15M**



**MFC 15M**



**NRF 15M**

**Exhibit B-6.** CITRC, CFA, RWMC, MFC and NRF area wind roses.

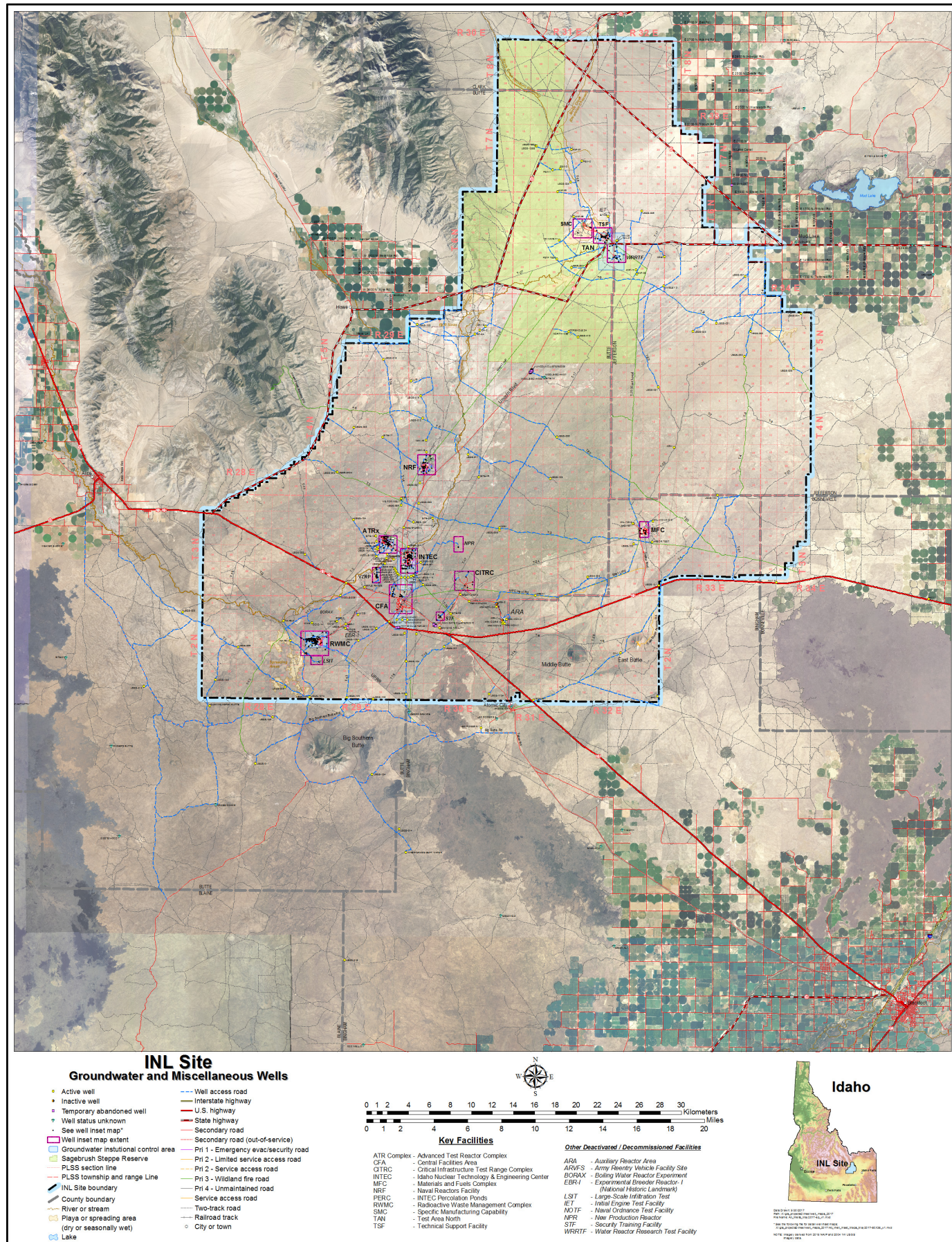
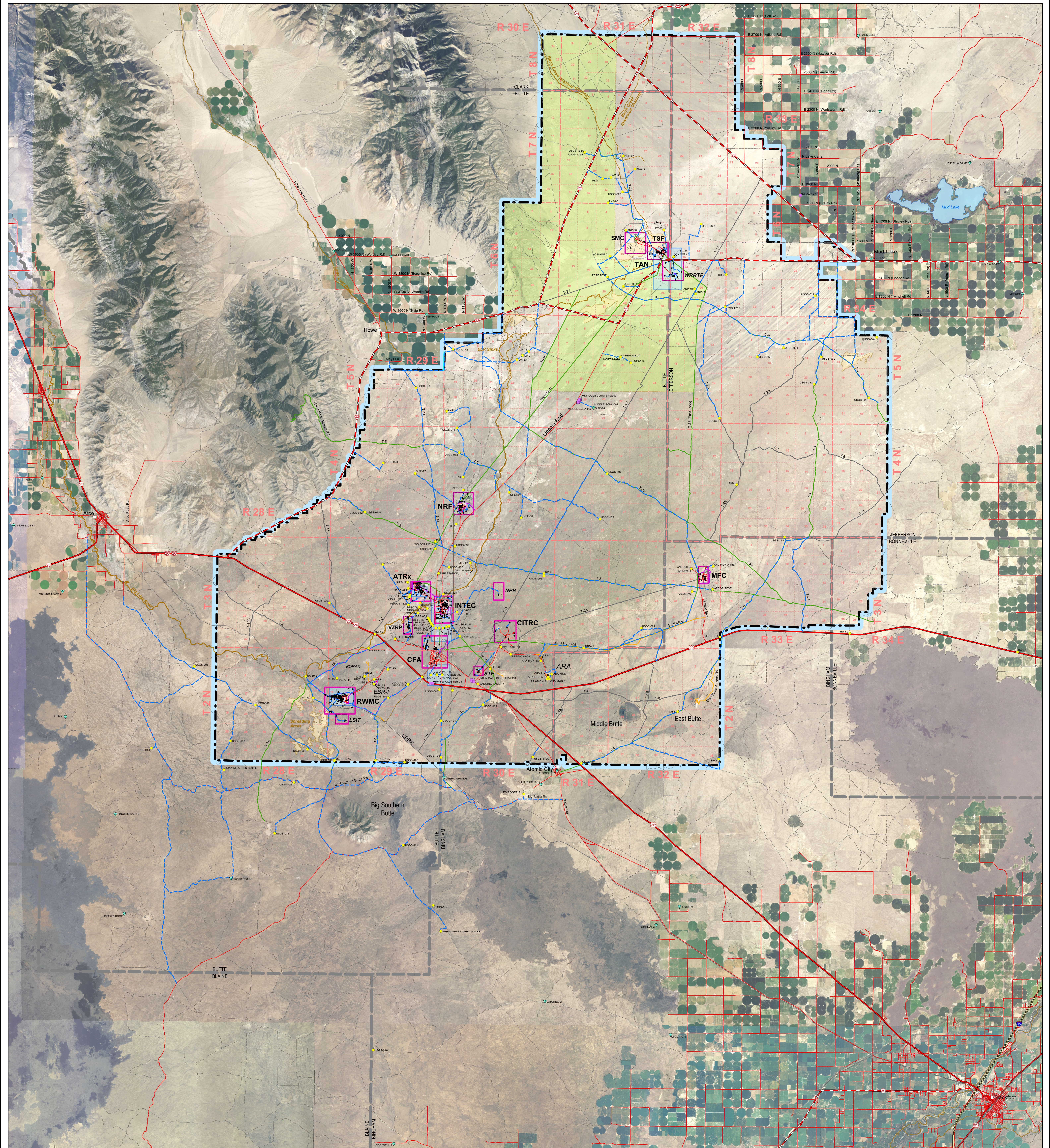
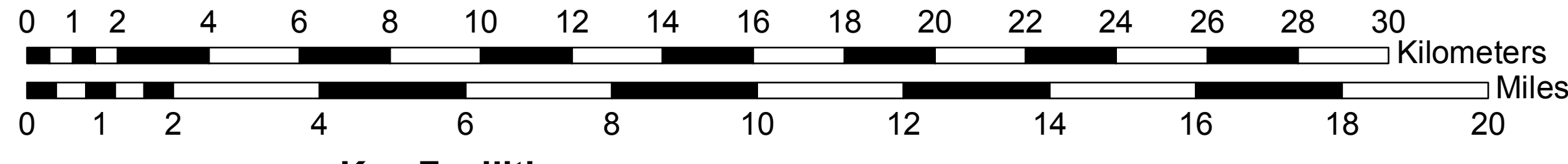


Exhibit B-7. INL sitewide locations of wells



## INL Site Groundwater and Miscellaneous Wells

- Active well
- Inactive well
- Temporary abandoned well
- Well status unknown
- See well inset map\*
- Well inset map extent
- Groundwater institional control area
- Sagebrush Steppe Reserve
- PLSS section line
- PLSS township and range Line
- ▬ INL Site boundary
- ▬ County boundary
- ▬ River or stream
- ▬ Playa or spreading area (dry or seasonally wet)
- ▬ Lake
- ▬ Well access road
- ▬ Interstate highway
- ▬ U.S. highway
- ▬ State highway
- ▬ Secondary road
- ▬ Secondary road (out-of-service)
- ▬ Pri 1 - Emergency evac/security road
- ▬ Pri 2 - Limited service access road
- ▬ Pri 2 - Service access road
- ▬ Pri 3 - Wildland fire road
- ▬ Pri 4 - Unmaintained road
- ▬ Service access road
- ▬ Two-track road
- ▬ Railroad track
- ▬ City or town



### Key Facilities

- ATR Complex - Advanced Test Reactor Complex
- CFA - Central Facilities Area
- CITRC - Critical Infrastructure Test Range Complex
- INTEC - Idaho Nuclear Technology & Engineering Center
- MFC - Materials and Fuels Complex
- NRF - Naval Reactors Facility
- PERC - INTEC Percolation Ponds
- RWMC - Radioactive Waste Management Complex
- SMC - Specific Manufacturing Capability
- TAN - Test Area North
- TSF - Technical Support Facility

### Other Deactivated / Decommissioned Facilities

- ARA - Auxiliary Reactor Area
- ARVFS - Army Reentry Vehicle Facility Site
- BORAX - Boiling Water Reactor Experiment
- EBR-I - Experimental Breeder Reactor-1 (National Historic Landmark)
- LSIT - Large-Scale Infiltration Test
- IET - Initial Engine Test Facility
- NOTF - Naval Ordnance Test Facility
- NPR - New Production Reactor
- STF - Security Training Facility
- WRRTF - Water Reactor Research Test Facility



Date Drawn: 5/20/2017  
 Path: X:\gis\_projects\inset\inset1\_maps\_2017  
 File Name: All\_Wells\_May2017\_ep\_v1.mxd  
 \*See the following file for detail well inset maps:  
 X:\gis\_projects\inset\inset\_2017\All\_Well\_Inset\_Maps\_May2017-60X36\_v1.mxd  
 NOTE: Imagery derived from 2015 NAD and 2004 1m USGS Imagery Data.

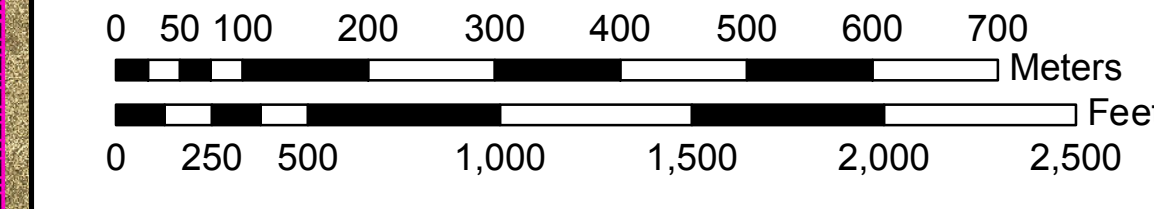


Exhibit B-8. Enlarged Detail of the Locations of Wells at the ATR Complex, CFA, CITRC, INTEC, LSIT, MFC, NPR, NRF, PERC, RWMC, SMC, STF, TSF, VZRP, and WRRTF

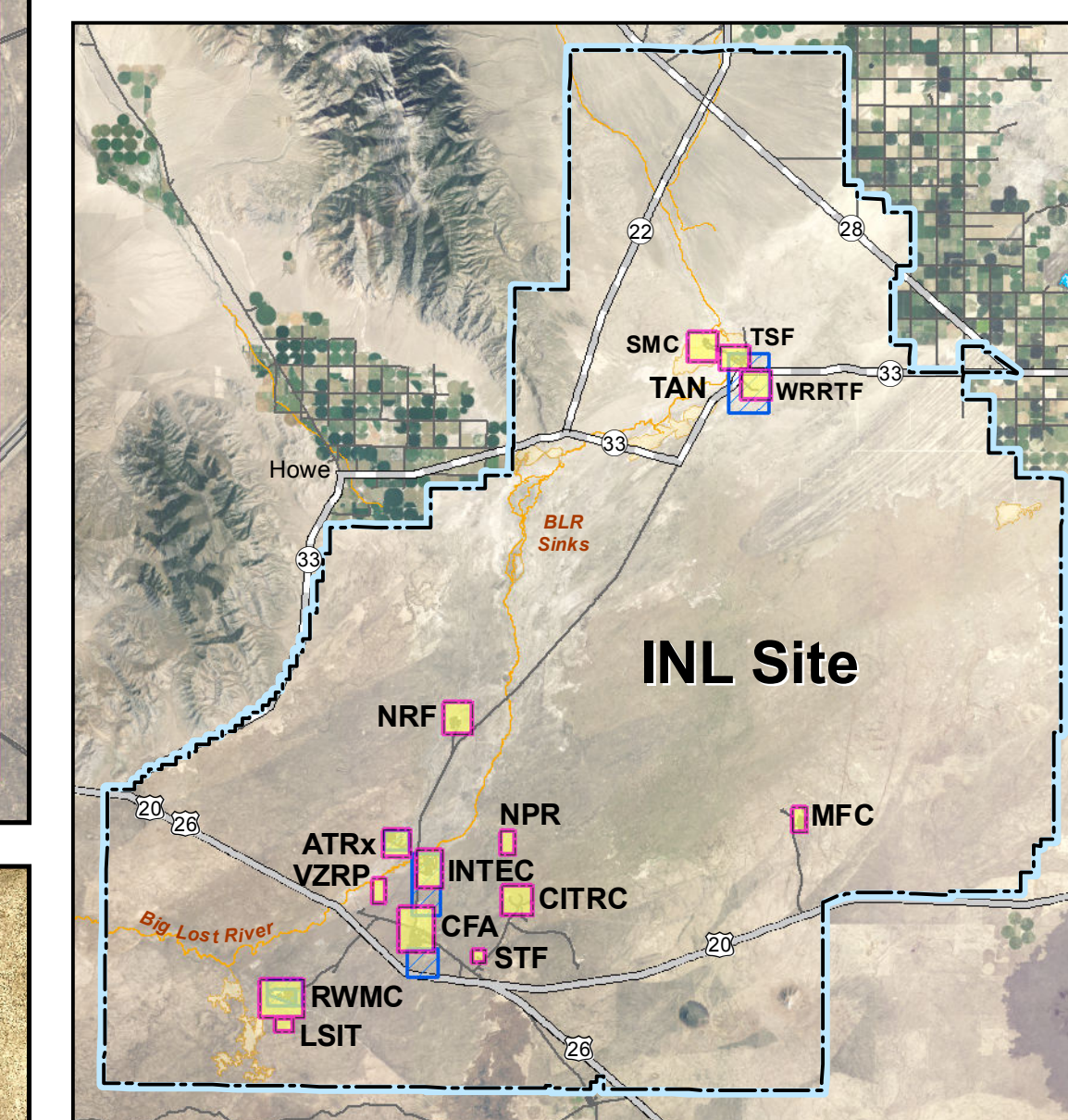
# INL Site Groundwater and Miscellaneous Wells

## Legend

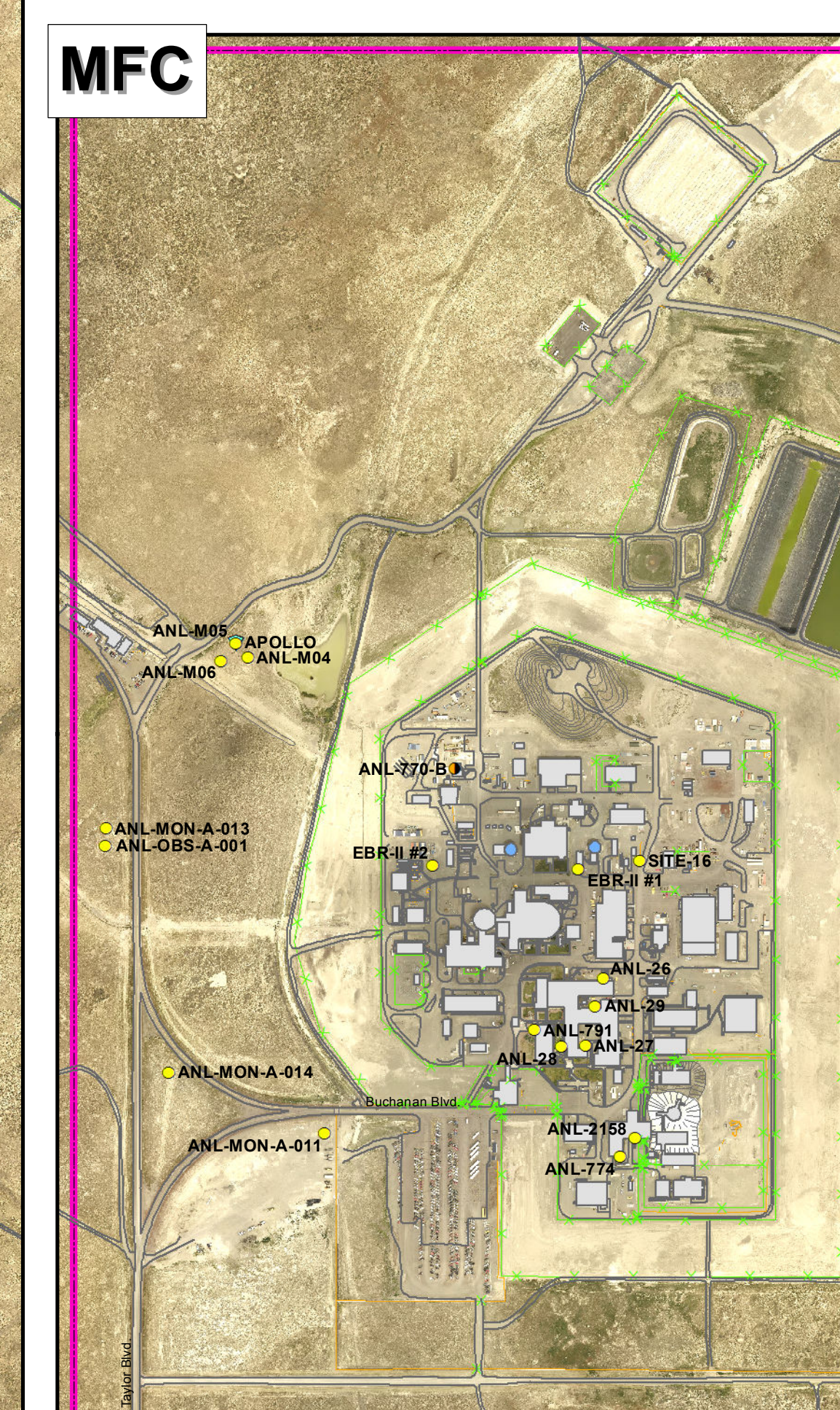
- Active well
- Inactive well
- Temporary abandoned well
- Well status unknown
- Groundwater institutional control area
- Well inset vicinity map extent
- Building or structure
- Tank
- Road
- Fence
- Barrier
- Railroad track
- Berm
- Center pivot
- Contaminated soil cap
- Waste water pond
- Storm water pond
- Playa or spreading area



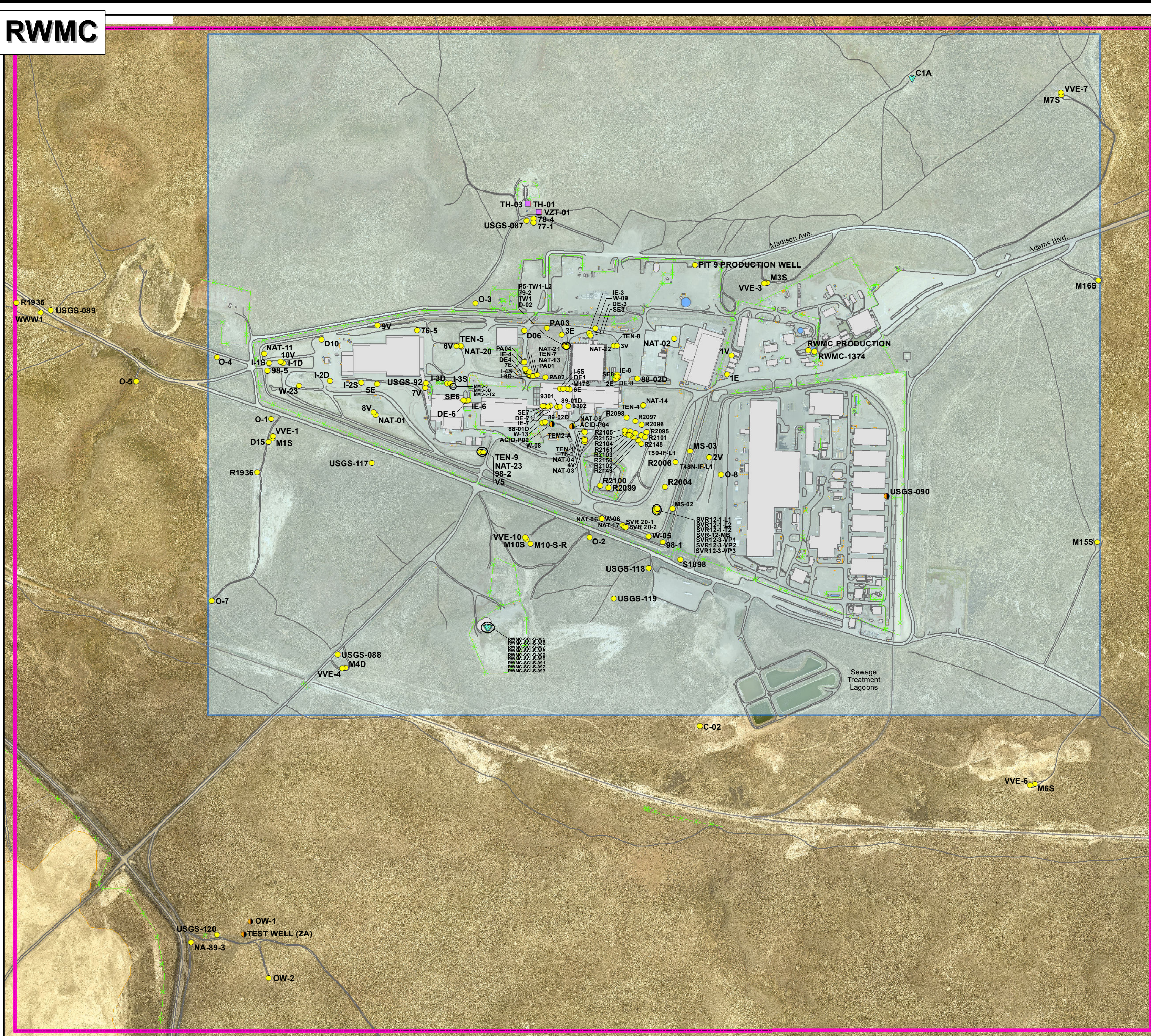
GIS Analyst: Don Madarski  
 Date: 02/02/2017  
 Path: \\g:\gsp\production\inl\map\_01\inl\_site\_groundwater\_mw\_010117.mxd  
 File Name: inl\_site\_groundwater\_mw\_010117.mxd



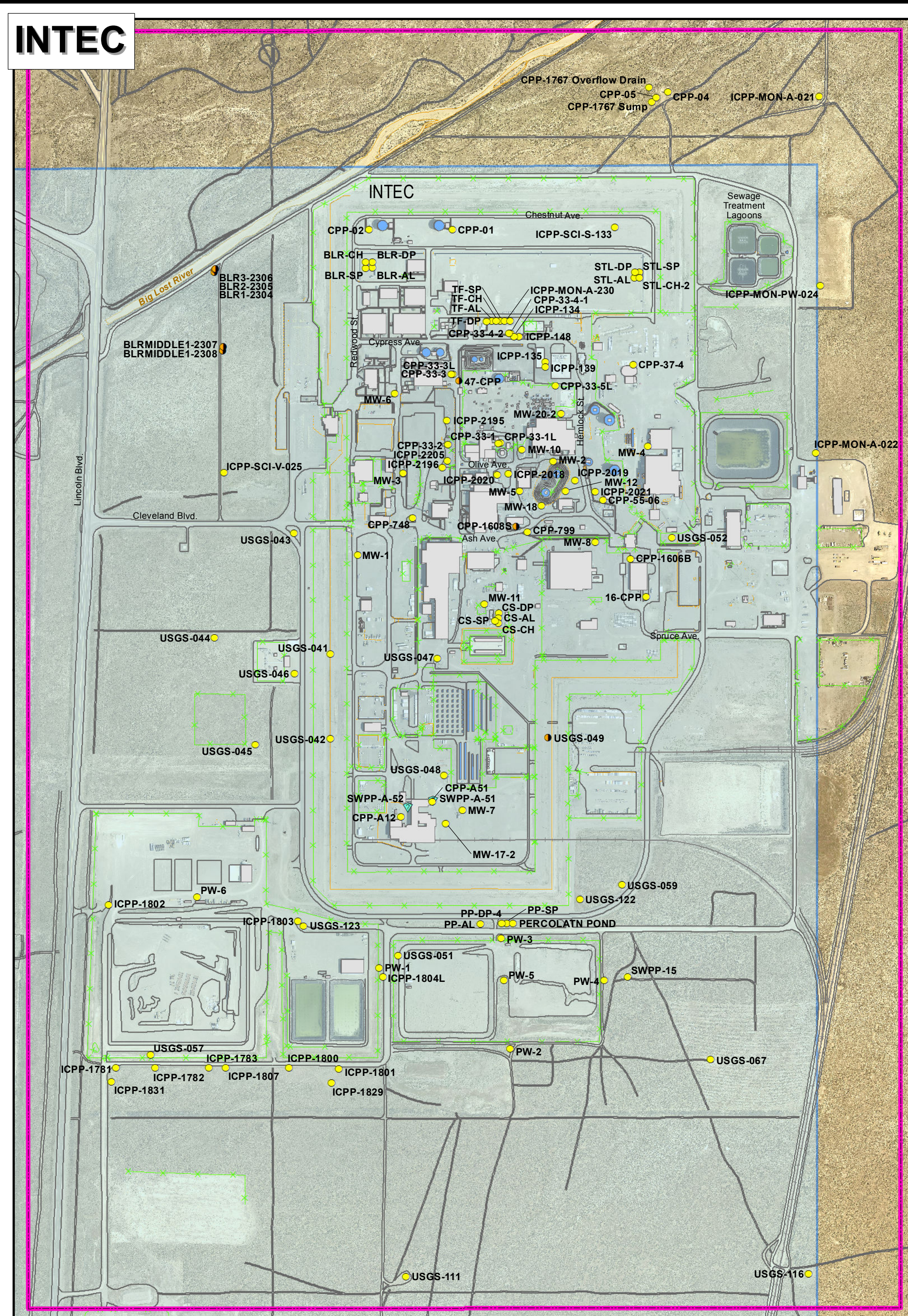
**Well Inset Vicinity Map**



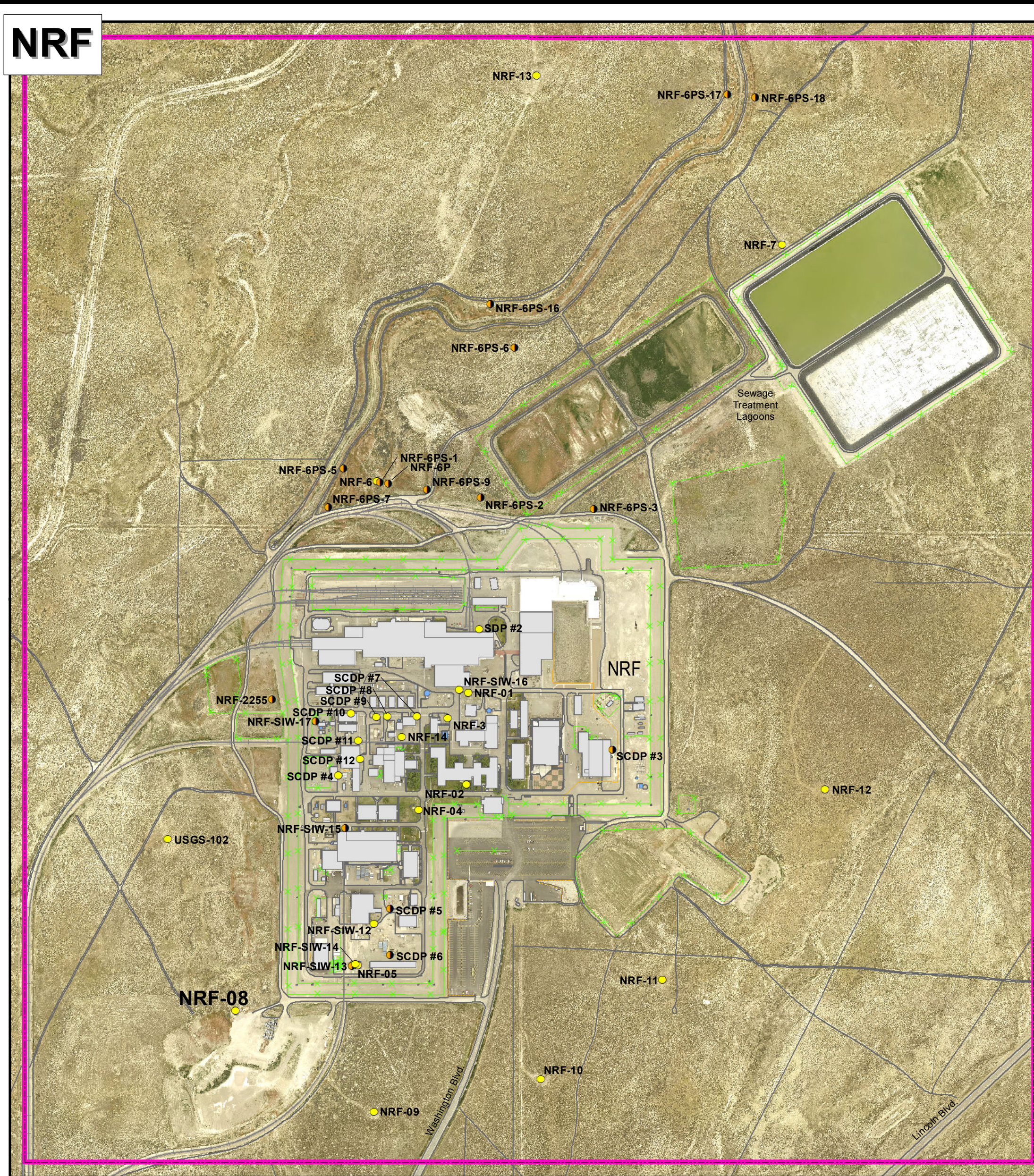
**MFC**



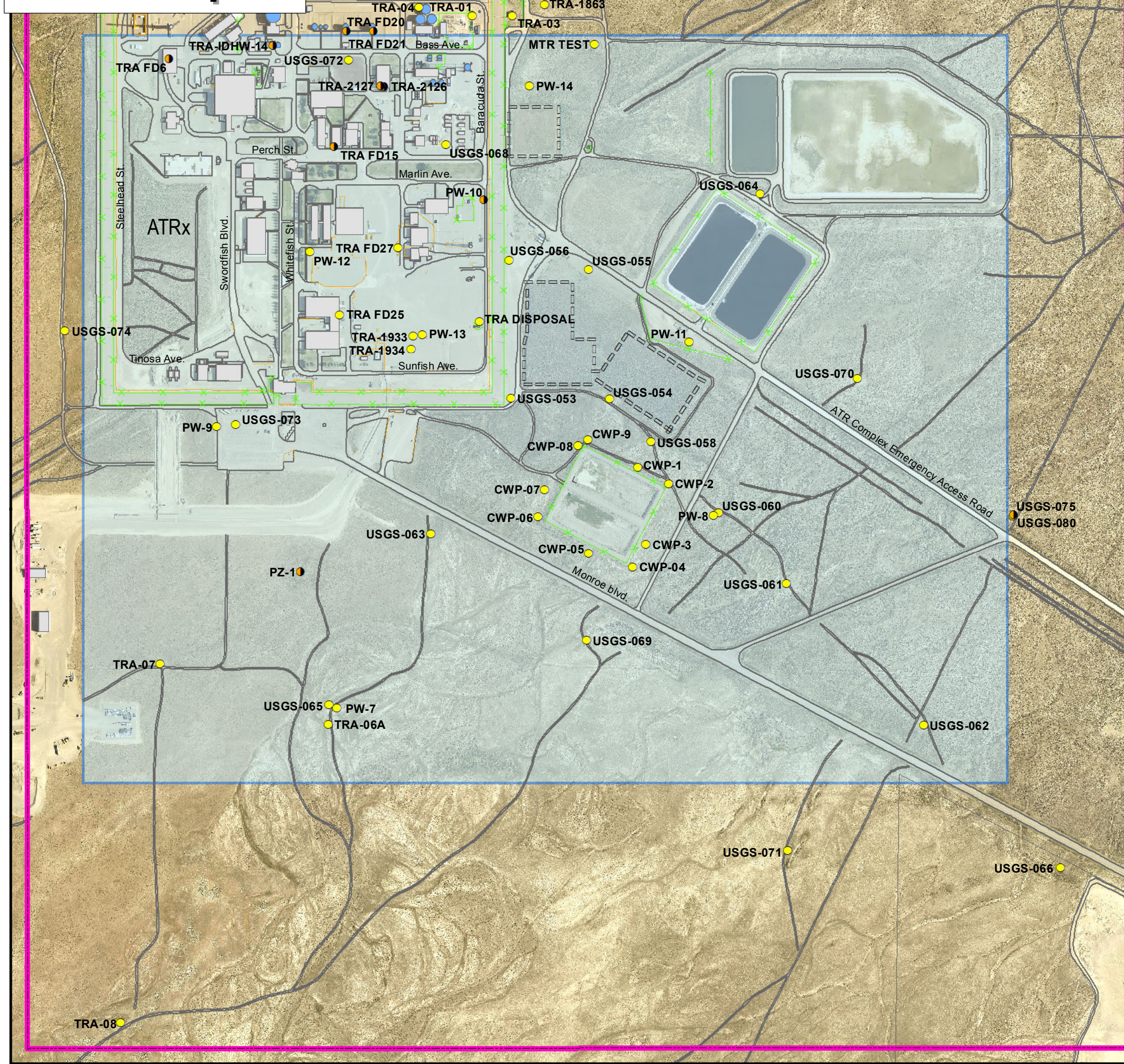
**RWMC**



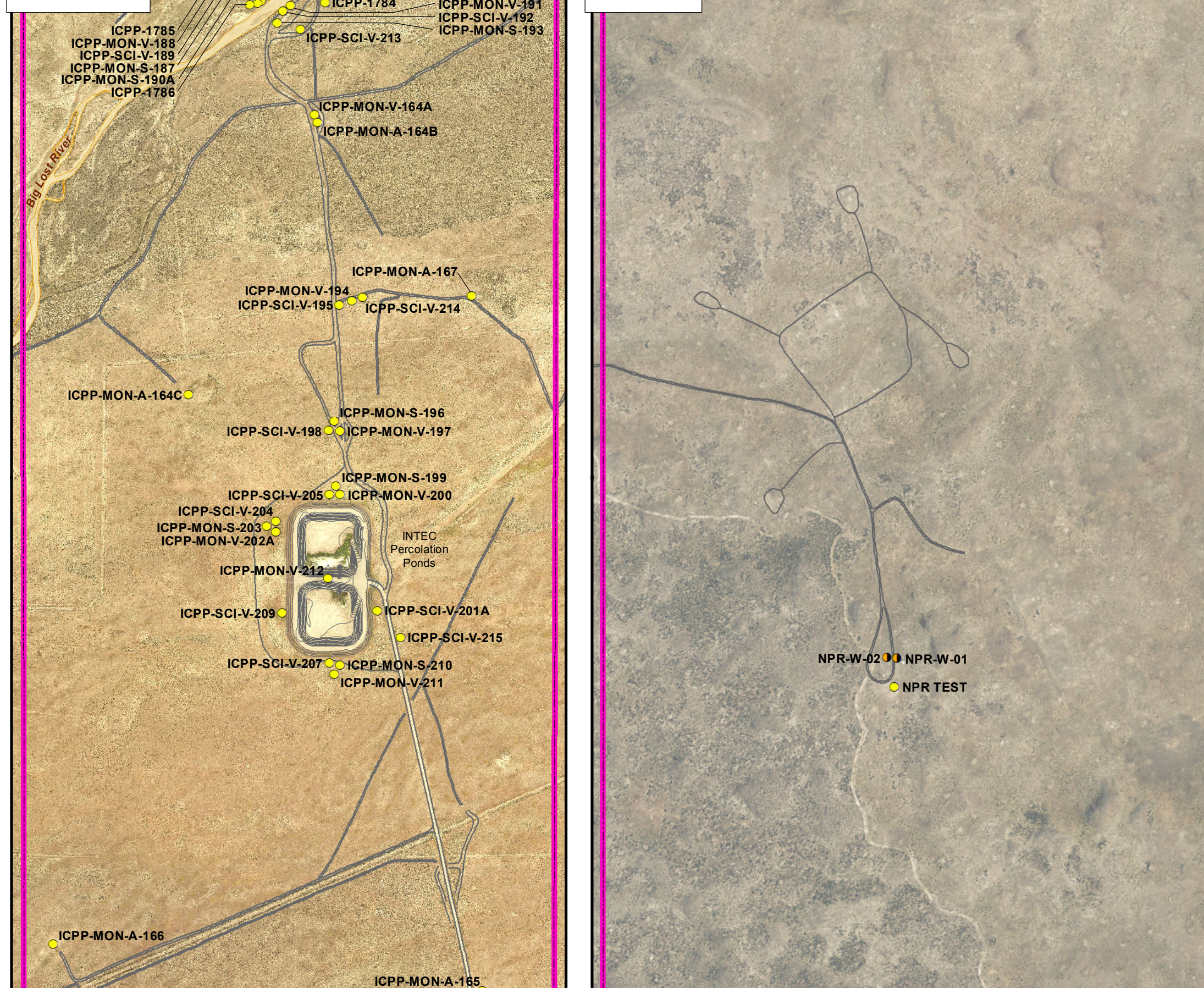
**INTEC**



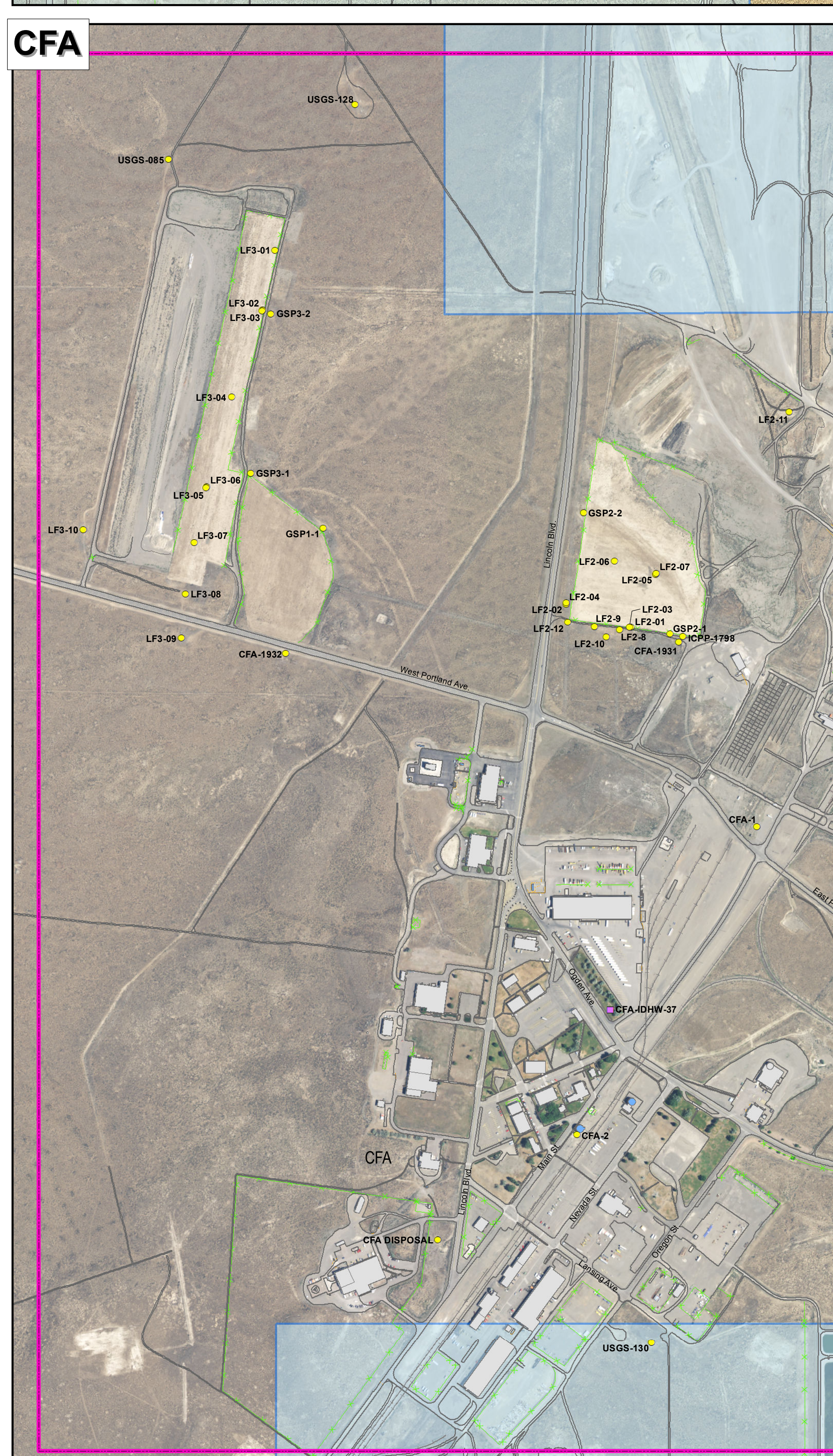
**NRF**



**ATR Complex**



**VZRP**



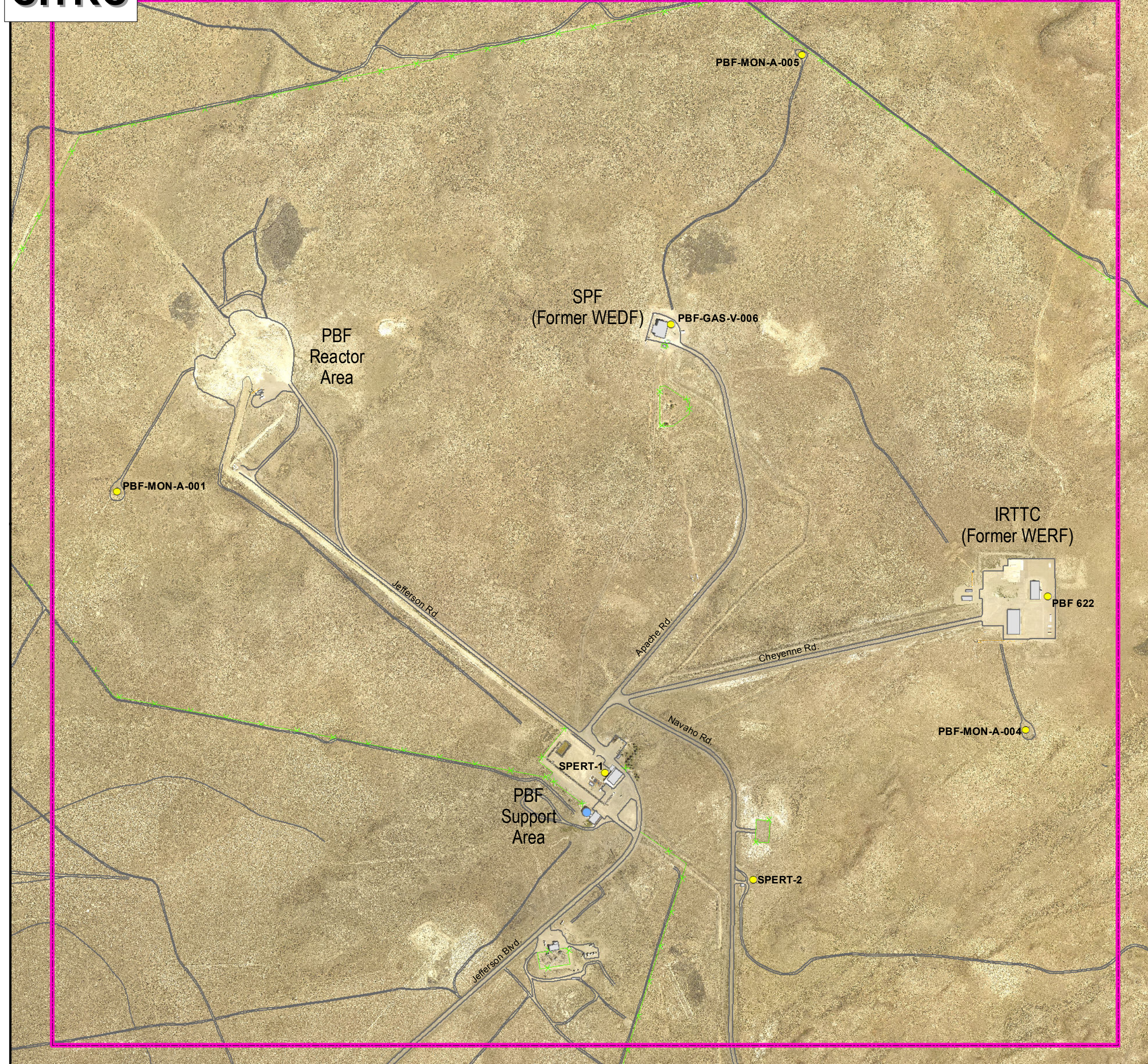
**CFA**



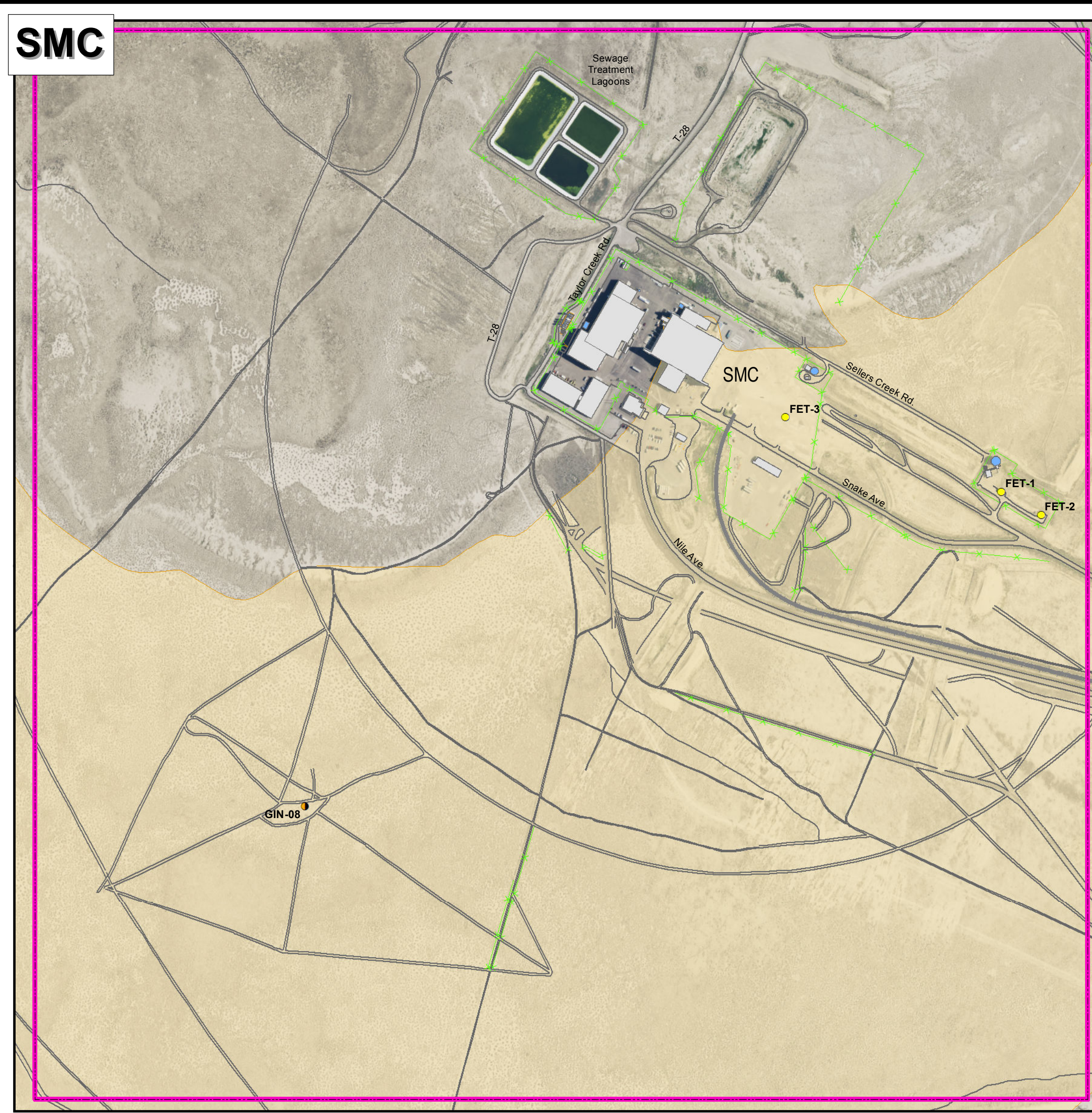
**LSIT**



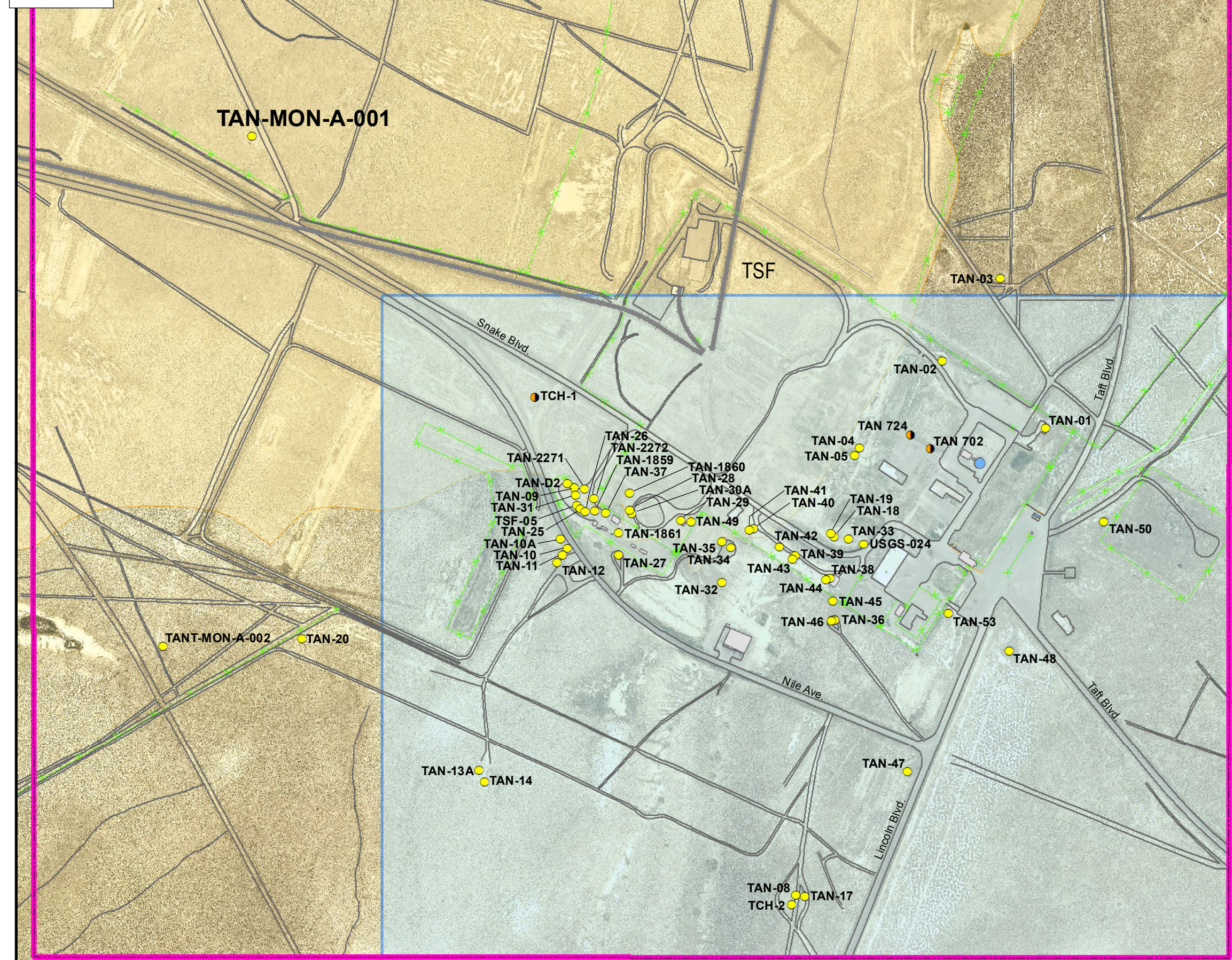
**STF**



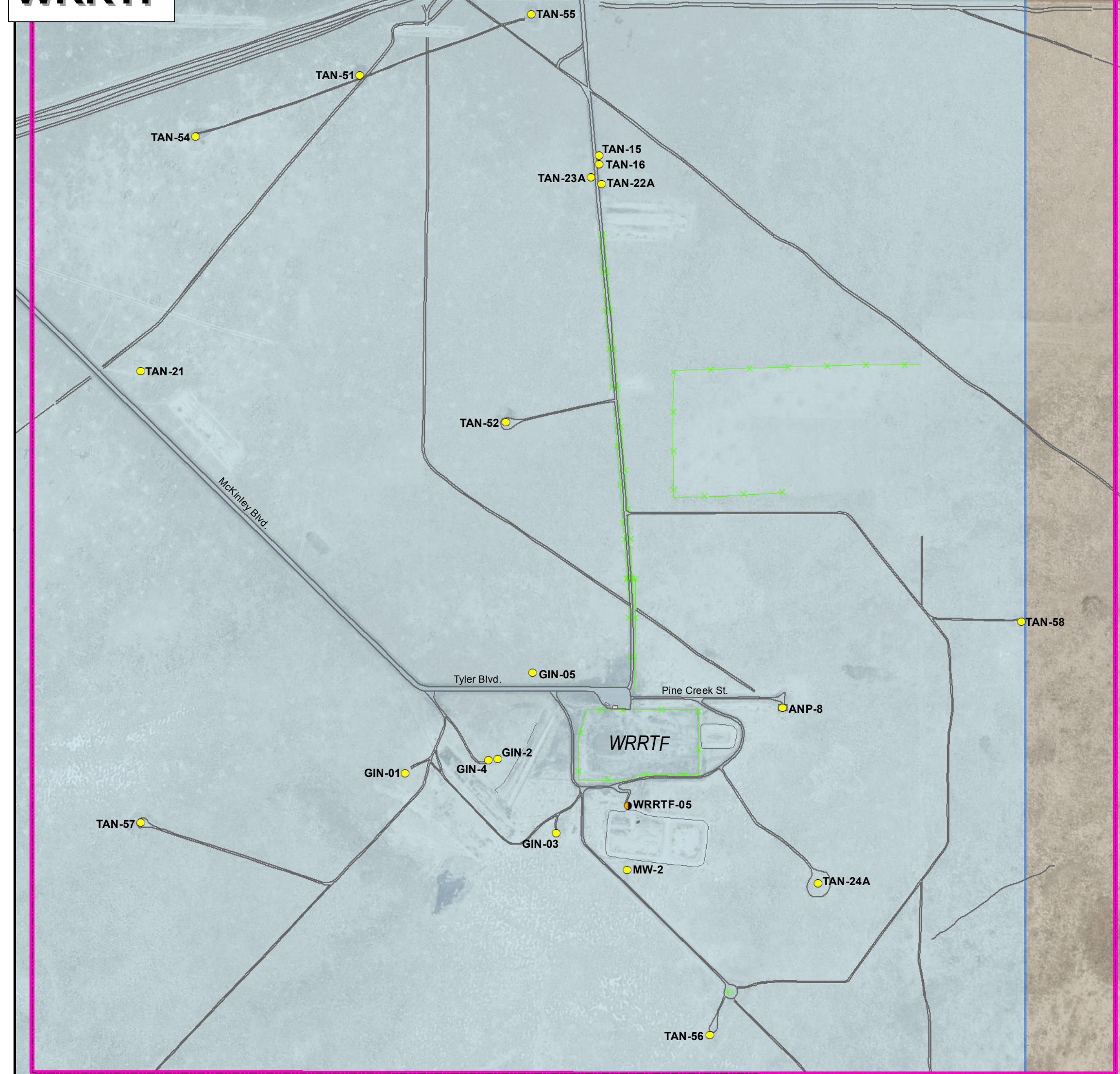
**CITRC**



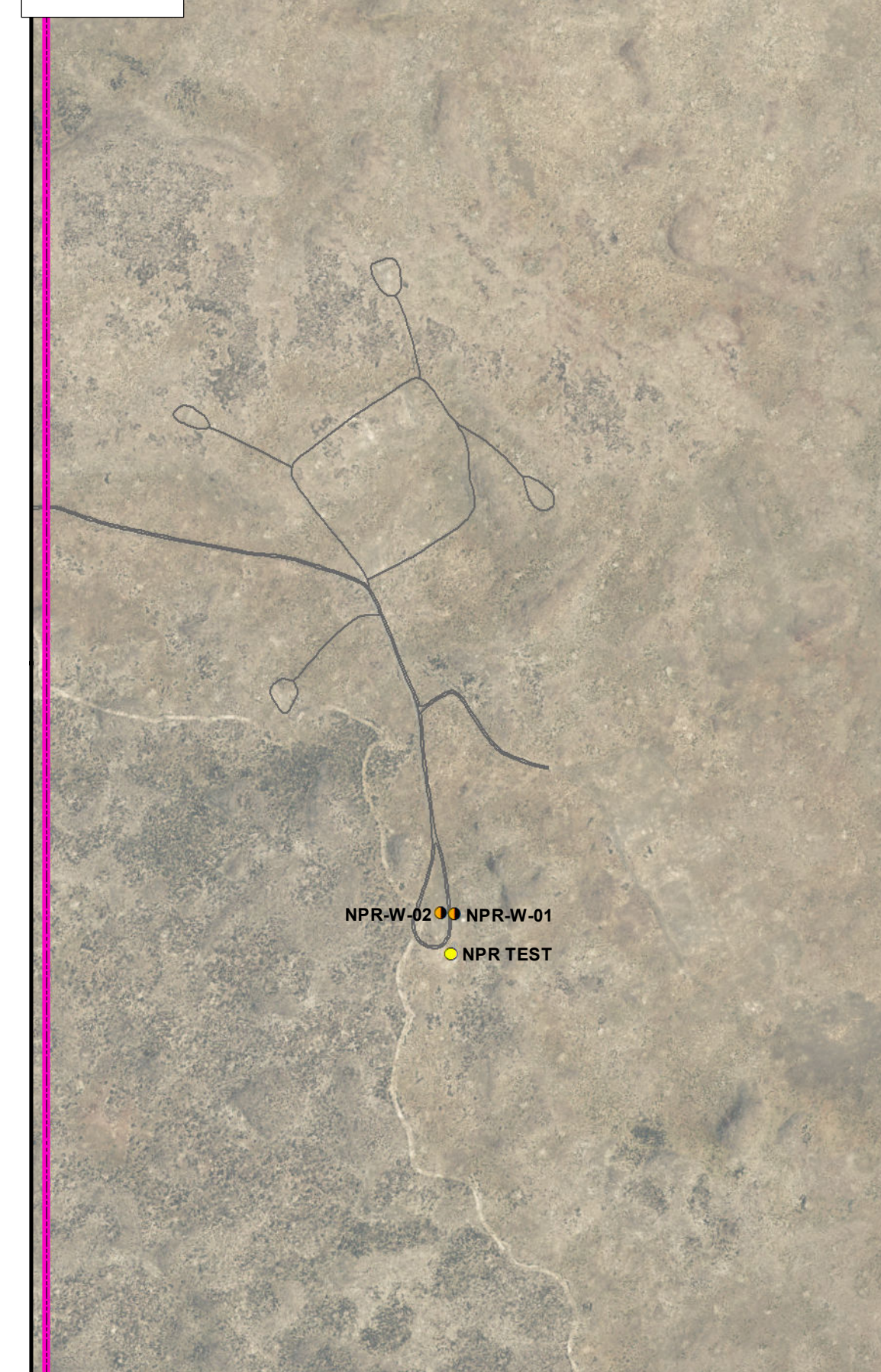
**SMC**



**TSF**



**WRRTF**



**NPR**

**MFC**

1           **B-2(d) Surrounding Land Use**

2           The federal government, the State of Idaho, and private parties own lands immediately  
3 surrounding the INL site. Land uses on federally owned land adjacent to the INL consist of grazing,  
4 wildlife management, mineral and energy production, and recreation. State-owned lands are used for  
5 grazing, wildlife management, and recreation. Private lands near the INL are used primarily for grazing  
6 and farming; irrigated farmlands make up approximately 25% of the land bordering the INL. Several  
7 small rural communities are scattered around the borders of the INL: Howe, Mud Lake, Terreton,  
8 Atomic City, Butte City, and Arco. The larger communities of Rexburg, Idaho Falls, Blackfoot, and  
9 Pocatello are located to the east and southeast of the INL site. The Fort Hall Indian Reservation is  
10 located southeast of the INL site.

11           Land immediately outside INL boundaries is used mainly for free-range livestock grazing.  
12 Within INL boundaries, approximately 60% of INL land area is open to cattle or sheep grazing by permit;  
13 Exhibit B-9 identifies these areas. Some irrigation farming occurs in areas near INL boundaries. Large  
14 areas of land are irrigated near the Snake River, approximately 32 km (20 mi) southeast of INL, and in  
15 the vicinity of Mud Lake.

16           The INL site and adjacent areas are not likely to experience large-scale residential and  
17 commercial development because the INL is remotely located from most developed areas. However,  
18 recreation and agricultural uses are expected to increase in the surrounding area in response to greater  
19 demand for these types of land uses.

20           Other uses of the land are severely limited because of the climate, lava flows, and general desert  
21 soil characteristics. The only INL land suitable for farming is near the terminations of the Big Lost River  
22 and Little Lost River, near the town of Howe, and to a distance of 13 km (8 mi) southeast from Howe.

23           Arable land with a moderate irrigation limitation (gravity irrigation) is present on both sides of  
24 the Big Lost River and in the remains of the lake bed of prehistoric Lake Terreton (between Mud Lake  
25 and Howe). The remainder of the INL, approximately 65% of the surface area, has a low subsurface  
26 water-holding capacity, is rocky or covered with basalt, or is classified as having moderate-to-severe  
27 limitations for agricultural irrigation.

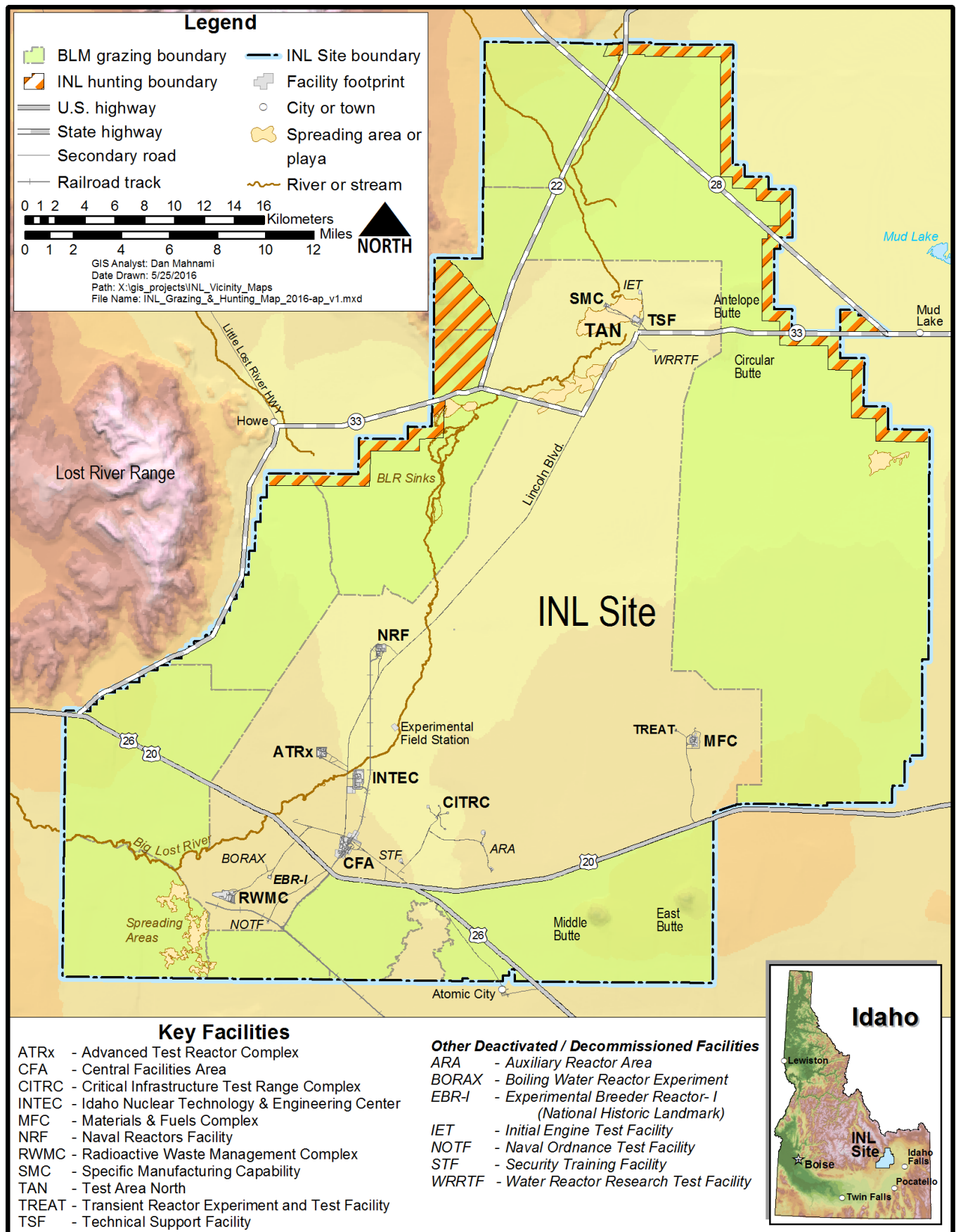


Exhibit B-9. Grazing areas at the INL.

1           **B-2(e) Access Control**

2           The INL is a restricted area patrolled by armed security personnel. No unauthorized access is  
3 permitted. Access control to the INL is maintained by security personnel stationed in gatehouses on East  
4 Portland Avenue, just off U.S. Route 20; on Van Buren Boulevard, just off U.S. Route 20/26; on Lincoln  
5 Boulevard near TAN; in route to MFC, and the RWMC. Access badges are required to proceed beyond  
6 these points. Additional access controls exist via gatehouses within the INL at ATR, INTEC, MFC, and  
7 NRF. Access controls in the vicinity of waste management units are described further in Subsection B-4  
8 of this permit application. Details on access controls and specific security features, such as fencing, are  
9 discussed in subsequent volumes of this permit application as pertinent to specific waste management  
10 units.

11           **B-2(f) Other Structures**

12           The term "other structures" refers to storm, sanitary, and process sewerage systems; loading and  
13 unloading areas; fire control facilities; and intake/discharge structures. These systems and facilities are  
14 described in subsequent volumes of this permit application as pertinent to specific waste management  
15 units. The INL has no intakes or discharges.

16           **B-3 Location Information**

17           The INL is located along the western edge of the ESRP in southeastern Idaho, approximately  
18 between latitudes N 43°28' to N 44°02' and longitudes E 112°26' to E 113°15'. The following subsections  
19 describe how the INL complies with the seismic and floodplain standards under IDAPA 58.01.05.008  
20 and .012 [40 CFR 264.18 and 40 CFR 270.14(b)(11)].

21           **B-3(a) Seismic Standard (IDAPA 58.01.05.008 and 58.01.05.012 [40 CFR 264.18(a)**  
22           **and 270.14(b)(11)(i-ii)])**

23           INL hazardous and mixed waste management units are located in either Butte or Bingham  
24 County. Only Bingham County is listed in IDAPA 58.01.05.008 (Appendix VI to 40 CFR 264) as  
25 requiring demonstration of compliance with the seismic standard. The MFC facility operates hazardous  
26 waste management units that are located in Bingham County, and thus, subject to the seismic standard  
27 compliance requirement which is addressed, as applicable, in the MFC HWMA/RCRA Final Partial Part  
28 B Permits.

29           USGS data, as detailed in USGS Miscellaneous Investigation Map I-2330, *Geologic Map of the Idaho*  
30 *National Engineering Laboratory and Adjoining Areas, Eastern Idaho, 1994*, indicates there are not any

1 faults or other known evidence of Holocene horizon motion within 914 m (3,000 ft) of the RTF. A copy  
2 of this map is included as Exhibit B-10.

3 **B-3(b) Floodplain Determination and Prevention of Washout (IDAPA 58.01.05.008**  
4 **and 58.01.05.012 [40 CFR 264.18(b) and 270.14(b)(11)(iii-iv)])**

5 As noted above, the INL hazardous and mixed waste management units are located in Butte and  
6 Bingham Counties. The Federal Emergency Management Agency (FEMA) Flood Insurance Rate Maps  
7 (FIRM) for Butte and Bingham Counties are provided in Appendix II.

8 Four flood zones are identified on the FIRMs: Zone A indicates areas subject to 100-yr floods;  
9 Zone B indicates areas between the limits of 100- and 500-yr floods; Zone C indicates areas of minimal  
10 flooding; and Zone D indicates areas of undetermined, but possible flood hazards.

11 Federal Insurance Administration (FIA) floodplain maps are normally used to delineate 100-yr  
12 floodplains and to determine if a given facility is located within or outside of a 100-yr riverine  
13 floodplain.

14 FIRMs exist for the portions of the INL that are within Bingham County. However, for the  
15 portions of the INL that are within Butte County, only a FIRM index map is available. The Butte County  
16 FIRM Index Map indicates that the map panels that would cover the areas of INL facilities were not  
17 published, which means FEMA did not perform hydrologic analyses in these areas. On the index map,  
18 these areas are classified as being in “Zone D,” which is defined as “undetermined but possible flood  
19 hazards.” For Butte County, all of the panels addressing the area covering the INL are within Zone D, as  
20 indicated in the footnote to the map. As shown on the county index map for the INL area, the following  
21 individual panels in map series 160033 have not been published: 0400 A, 0425 A, 0550 A, 0575 A, 0600  
22 A, 0775 A, 0800 A, 0825 A, 0850 A, 1000 A, 1025 A, 1050 A, 1075 A, 1100 A, 1225 A, 1250 A, 1275  
23 A, and 1300A.

24 For Bingham County, MFC facilities are located in the area addressed in Panel  
25 160018 0050 B; the footnote to the map indicates that this panel is not published, but the area is  
26 designated Zone C. Also, for Bingham County, Map Panel No. 25 of 750, Section 11, includes a small  
27 part of the west side of the MFC area designated as Zone C. Facilities located in that area are TREAT  
28 area Buildings 720 and 721. None of the hazardous or mixed-waste management units to be permitted  
29 are located in those buildings. Map panel no. 25 of 750 is also included in Appendix II.



1           Aside from indicating that there may be areas of undetermined but possible flood hazards, the  
2 existing FEMA maps do not clearly substantiate whether or not a facility is in the floodplain. As these  
3 maps indicate possible but undetermined flood hazards in areas within the INL, FIA equivalent mapping  
4 techniques have been employed to determine the elevations of the Big Lost River flood with respect to  
5 INL facilities.

6           The elevation of the 100-yr flood from the Big Lost River with respect to INL facilities is  
7 described in Subsection B-3(b)(1) below. The existing flood control systems at the INL are described in  
8 Subsection B-3(b)(2) below. Flood potential from localized events (such as the 25-yr, 24-hr storms, 100-  
9 yr precipitation events and rapid snowmelt) for INTEC are described in Section B-3(b)(3) below. The  
10 controls for protection against those events are presented in subsequent waste management unit-specific  
11 volumes of this permit application.

### 12           **B-3(b)(1) Flood Potential from the Big Lost River**

13           Floodplain determinations, engineering and structural analyses, in accordance with IDAPA  
14 58.01.05.012 [40 CFR § 270.14(b)(11)(iv and v)] are performed for RCRA facilities that are within the  
15 100-yr floodplain. The results of engineering analyses are reported in engineering design files (EDFs)  
16 generated by INL personnel and presented in the respective waste management unit-specific permits or  
17 applications. An EDF will typically provide a description of the RCRA facility's construction  
18 parameters, engineering analysis to indicate the various hydrodynamic and hydrostatic forces expected to  
19 result at the site as a consequence of a hypothetical 100-yr flood, structural or other engineering studies  
20 showing the design of operational units and flood protection devices at the facility and how these will  
21 prevent washout. If applicable, and in lieu of the above engineering analyses, a detailed description of  
22 procedures to be followed to remove hazardous waste to safety before the facility is flooded may be  
23 provided. Such procedures will be presented, if applicable, in subsequent waste management unit-  
24 specific volumes of this permit application.

25           In January 2006, the DOE-ID provided the contractors with the “Big Lost River Flood Hazard Study,  
26 Idaho National Laboratory, Idaho, U.S. Bureau of Reclamation, 2005” by D. A. Ostenna and D. H.  
27 O’Connell, to be used for all Big Lost River flood hazard characterization and delineation efforts on the  
28 INL. A copy of this study is provided electronically in Appendix III. This map will be used for  
29 determination of whether or not INTEC units are located within the 100-year floodplain of the Big Lost  
30 River. Since a previous study provided a more conservative and higher elevation floodplain, buildings  
31 previously determined to be within the floodplain have already been evaluated to the more conservative  
32 standard. As determinations of floodplain change or new facilities are added, additional EDFs will be  
33 prepared as necessary and modification to the unit specific permits will be submitted to the DEQ for  
34 approval and incorporation into the permits.

## **B-3(b)(2) Flood Diversion Systems at the INL**

The Big Lost River intermittently flows through the INL and is the nearest surface body of water with a potential influence to southwestern and central INL facilities. The Big Lost River is controlled by the Mackay Dam, an irrigation storage reservoir, 48 km (30 mi) northwest of Arco. In 1958, a flood diversion system was built along the Big Lost River near the western boundary of the INL, to divert flows on the river that might create flood hazards for INL facilities. This system consists of a small earthen diversion dam and a headgate that diverts water from the main channel, through a connecting channel, and into four spreading areas (A, B, C, and D). Spreading area A is bounded on the southeast by a dike; spreading area B is bounded on the northeast by a dike; and spreading area D is bounded on the southern edge by a dike. Spreading area C has no dike. The present capacity of the diversion system is 58,000 acre-ft at an elevation of 5,050 ft (1,540 m) (McKinney 1985). Flow upstream (near Arco) and downstream of the diversion dam, as well as into the diversion channel, is monitored by several USGS gauging stations (Stone et al. 1993).

## **B-3(b)(3) INTEC 100-Year Storm Water Runoff and 25-Year Runoff Analysis**

To ensure that all potential sources of flooding were evaluated for INTEC units, the report “100-Year Storm Water Runoff Floodplain and 25-Year Runoff Analyses for the Idaho Nuclear Technology and Engineering Center at the Idaho National Engineering and Environmental Laboratory” (INEEL/EXT-03-01174, Revision 1, January 2004) was prepared. A copy of this report is provided electronically in Appendix IV. This study evaluated the largest 25-year and 100-year storm water flood flows through and in the vicinity of INTEC and determined no flooding impacts to RCRA buildings at INTEC.

## **B-4 Traffic Information [IDAPA 58.01.05.012; 40 CFR 270.14(b)(10)]**

The following subsections describe the traffic pattern, volume of traffic (number, types of vehicles), and INL traffic controls used for off-Site and on-Site traffic.

### **B-4(a) Off-Site Traffic**

The INL is accessible from several highways, shown in Exhibit B-11 and described in Table B-1. Approximately 145 km (90 mi) of highways pass through the southern and northern sections of the INL and are used by the general public. U.S. Highways 20 and 26 are the main access routes through the southern portion of the INL, and Idaho State Routes 22, 28, and 33 pass through the northern portion of INL. Table B-2 shows the baseline (1995) traffic for several of these routes.

Four major modes of INL-related transit use the regional highways, community streets, and INL roads to transport people and property: DOE buses and shuttle vans, DOE motor pool vehicles, commercial vehicles, and personal vehicles. Table B-3 summarizes the baseline miles and actual 2004 miles for INL-related traffic. Bus traffic is heaviest on nearby highways between 5:00 and 8:00 a.m. and 4:00 and 7:00 p.m., Monday through Thursday.

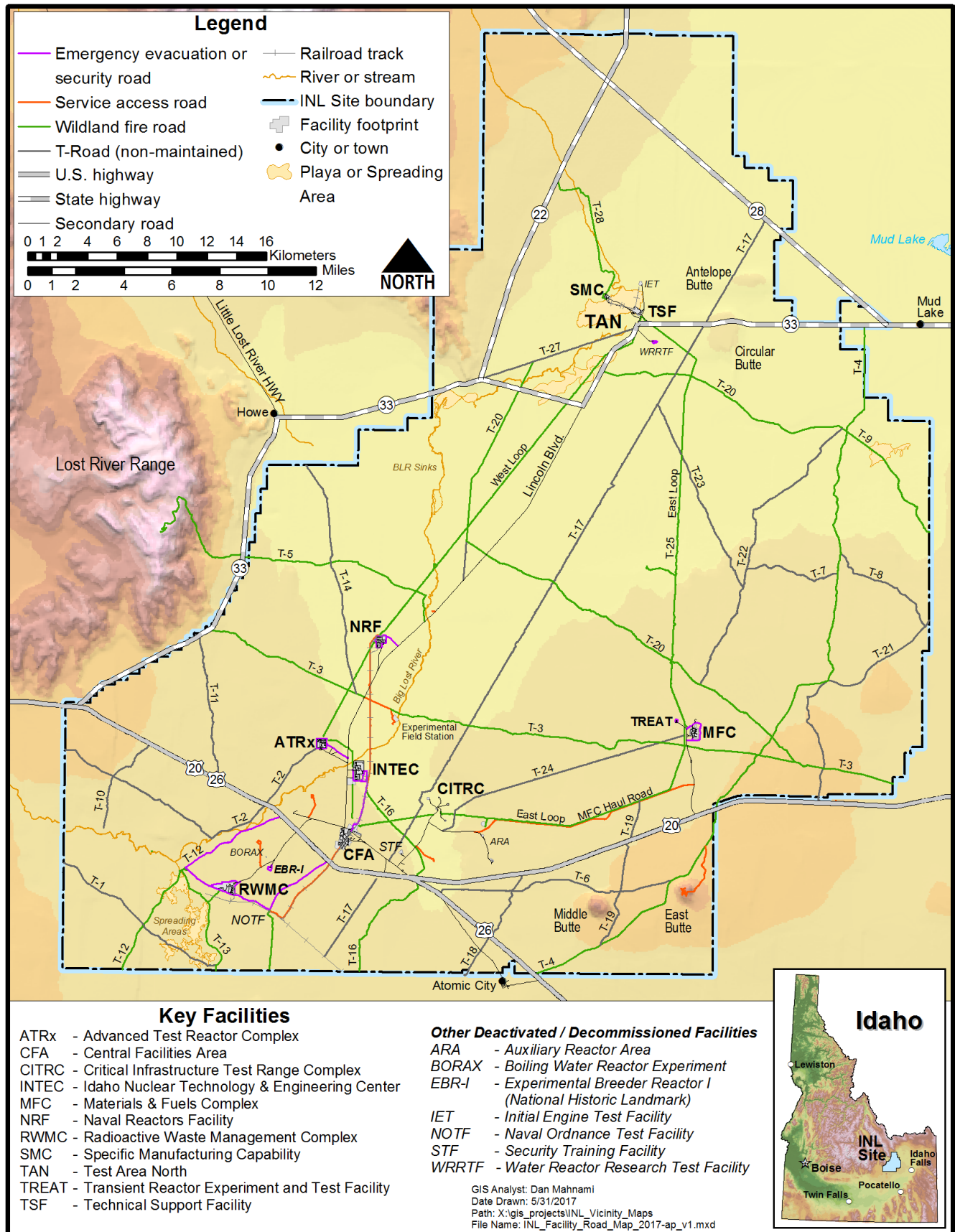


Exhibit B-11. INL roads, highways, and railroads.

**Table B-1.** Description of the highway system in the INL vicinity.

| <b>Route</b>     | <b>Description</b>  |
|------------------|---|
| I-15             | From the Utah/Idaho state line south of Malad northerly through Pocatello, Blackfoot, Idaho Falls, and Dubois to the Idaho/Montana state line at Monida Pass.   |
| I-84             | From the Oregon/Idaho state line south of Payette southeasterly through Boise, Mountain Home, Twin Falls and the Burley/Rupert area south to the Idaho/Utah state line.   |
| I-86             | From a junction with I-84 east of the Burley/Rupert area, northeasterly to a junction with I-15 in Pocatello.   |
| U.S. 20          | From the Idaho/Oregon state line near Nyssa, Oregon, easterly through Boise, Carey, Arco, Idaho Falls, Rigby, and Rexburg to the Idaho/Montana state line near West Yellowstone, Montana.                             |
| State Highway 22 | From a junction with U.S. 20/26 east of Arco northeasterly through Howe to Dubois; combines with State Highway 33 from its beginning at its junction with U.S. 20/26 to it's junction with State Hwy 33 east of Howe. |
| U.S. 26          | From the Idaho/Oregon state line near Nyssa, Oregon, easterly through Boise, Carey, Arco, Blackfoot, and Idaho Falls to the Idaho/Wyoming state line near Alpine.   |
| State Highway 28 | From a junction with I-15 north of Roberts, northwesterly to Terreton, Mud Lake, Leadore, and Lemhi to a junction with U.S. 93 in Salmon.   |
| State Highway 33 | From a junction with U.S. 20/26 east of Arco, easterly and northerly to Howe, Mud Lake, Terreton, and Rexburg, and then to the Idaho/Wyoming state line.  |

**Table B-2.** Baseline traffic for selected highway segments in the vicinity of INL.

| Route  | Average daily traffic<br>(number of vehicles) | Peak hourly traffic<br>(number of vehicles) |
|--|---|---|
| U.S. Highway 20-Idaho Falls to the Idaho National Engineering and Environmental Laboratory (INL) | 2,389   | 615   |
| U.S. Highway 20/26-INL to Arco   | 2,173   | 309   |
| U.S. Highway 26-Blackfoot to INL   | 1,200   | 184   |
| State Route 33-west from Mud Lake  | 585   | 88  |
| Interstate 15-Blackfoot to Idaho Falls   | 22,802  | 2,350                                       |

Source: DOE 1995 and Idaho Transportation Department roadway data web site @ <http://apps.itd.idaho.gov/road-data>

**Table B-3.** Baseline annual vehicle miles traveled for traffic related to the INL.

| Transit mode   | Vehicle miles traveled<br>Baseline 1995 | Actual mileage<br>traveled in 2016 |
|--|---|------------------------------------|
| Department of Energy (DOE) buses                               | 6,068,200                               | 2,618,125                          |
| Other DOE vehicles   | 9,183,100                               | 3,858,596                          |
| Personal vehicles on highways to the Idaho National Laboratory | 7,500,000                               | 23,195,787                         |
| Commercial vehicles  | 905,900                                 | 188,069                            |
| TOTAL  | 23,657,200                              |                                    |

Source: DOE 1995 and INL/BEA Transportation Services Division

**B-4(b) On-Site Traffic**

The INL has an additional 140 km (87 mi) of paved roads within its boundaries, not open to the public; approximately 30 km (18 mi) of the roads are considered service roads. Over 160 km (100 mi) of unpaved roads and trails at the INL are used for emergency, service, and security vehicle access.

The haul road is a single lane gravel road with turnouts beginning approximately 1.5 miles north of the intersection of Highway 20 and Taylor Blvd and extending approximately 12 miles, roughly parallel with T-25 to the intersection of Wilson and Jefferson Blvds at CITRC. The goal of the haul road in support of the Spent Nuclear Material program was to reduce the need to close Highway 20 for shipments defined as “out of commerce” from MFC to INTEC. The haul road is not a common use road at this time and will be barricaded at the MFC and CITRC ends to control use for safety, shipment, security, and maintenance concerns.

1 Union Pacific Railroad lines provide railroad freight service to Idaho Falls from Butte, Montana, to  
2 the north, and from Pocatello, Idaho, and Salt Lake City, Utah, to the south. The Union Pacific Railroad's  
3 Arco branch runs from Pocatello through Blackfoot to the INL. This branch crosses the southern portion of  
4 the Site, providing rail service to the INL. This branch connects at the Scoville siding with a DOE spur line,  
5 which links with developed areas within the INL. The Arco branch also passes approximately 0.8 km (0.5 mi)  
6 south of the RWMC. In 1974, a railroad spur to TSA was completed to permit direct shipment of waste to  
7 RWMC. Rail shipments to and from the INL usually are limited to bulk commodities, SNF, and radioactive  
8 waste.

9 The following subsections present on-Site traffic information for the INTEC, the RWMC, and the  
10 MFC, where permitted, interim status, and to be permitted waste management units are located. Traffic  
11 information for the AMWTP Facility (which is located within the boundary of the RWMC and has a separate  
12 security controlled entrance) may be found in the AMWTP HWMA/RCRA Storage Permit or the AMWTP  
13 HWMA/RCRA Treatment Permit.

#### 14 **B-4(b)(1) INTEC Traffic**

15 Access to INTEC is via Lincoln Boulevard to Cleveland Boulevard, which leads to the west side of  
16 the facility, the general parking area and primary access portal to the facility. The heaviest traffic on INL  
17 roads leading to INTEC occurs between 5:00 and 8:30 a.m. and again from 4:00 to 7:30 p.m., Monday through  
18 Thursday. Traffic consists primarily of site transit busses, employee private vehicles, and government  
19 contractor vehicles that come from various communities near/surrounding the INL.

20 The INTEC complex is surrounded by perimeter fence. Personnel access to and from the INTEC is  
21 through entry portals at locations on the east and west sides of the complex. Vehicles may only enter through  
22 the west guard gate at the Vehicle Monitoring Facility (CPP-661). Vehicles entering/exiting through the west  
23 guard gate must pass through a gate arrangement that allows security personnel to conduct thorough  
24 inspections. Personnel must pass through the security station to obtain proper dosimetry and verify they have  
25 the proper identification and access credentials to gain access to the complex. Personnel who do not have  
26 normal access to the INTEC complex are escorted by a person who does. Exhibit B-12 provides INTEC  
27 access and traffic control information.



1           **B-4(b)(2) RWMC Traffic**

2           U.S. Route 20/26 is the general access route for the RWMC. Van Buren Boulevard intersects  
3 U.S. 20/26 northeast of the RWMC and is the direct access road leading to EBR-I. Adams Boulevard  
4 intersects Van Buren Boulevard just north of EBR-I and is the direct access road leading to the RWMC  
5 personnel security and control area. Trucks transporting waste shipments to and from RWMC travel  
6 these roads. The heaviest traffic on the roads leading to RWMC occurs between 5:00 and 8:30 a.m. and,  
7 again, from 4:00 to 7:30 p.m., Monday through Thursday. Traffic consists primarily of site transit buses,  
8 employee-driven private vehicles, and government contractor vehicles that come from various  
9 communities near/surrounding the INL. From Memorial Day until Labor Day, private vehicle traffic  
10 increases slightly on Van Buren Boulevard, as tourists visit the EBR-I landmark.

11           The RWMC is contained within a security fence. There are two access security stations: one for  
12 the RWMC and one for the AMWTP. The following information does not pertain to the AMWTP.  
13 Vehicles entering the facility must pass through a one-gate arrangement that allows security personnel to  
14 conduct thorough inspections. Exhibit B-13 provides RWMC access and traffic control information.  
15 Personnel must pass through the security station to verify they have proper identification and access  
16 credentials. Personnel or visitors without proper credentials are escorted while on the RWMC site.  
17 While employees can get to the RWMC through the AMWTP, they are directed to go through the  
18 security station located at the RWMC entrance for access to the RWMC.

19           The roads accessing the RWMC are made of asphalt and all have load-bearing capacities of 68  
20 metric tons (75 tons). The daily volume of vehicles traveling to the RWMC and the AMWTP currently  
21 averages 350 to 400 vehicles, mainly cars or trucks. The average number of vehicles will vary depending  
22 upon activities taking place at the RWMC and the AMWTP locations. Typically, for the AMWTP, the  
23 daily volume of vehicles on the TSA access roads is approximately 125-130 vehicles (mainly cars, vans,  
24 and trucks) and site transit passenger busses that run twice per day. Additional AMWTP traffic  
25 information/exhibit may be found in the AMWTP HWMA/RCRA Permit.

26           **B-4(b)(3) MFC Traffic**

27           U.S. Route 20 is the general access route for MFC. Taylor Boulevard intersects U.S. 20 south of  
28 MFC and is the direct access road leading to the personnel security and control area. Taylor Boulevard is  
29 a 5.6 km paved roadway. A right turn off Taylor Boulevard leads to the MFC entrance. The heaviest  
30 traffic on the MFC site roads occurs between 6:00 and 8:30 a.m. and, again, from 4:00 to 6:30 p.m.,  
31 Monday through Thursday. Traffic consists primarily of site transit buses, employee-driven private  
32 vehicles, and government contractor vehicles from various communities near/surrounding the INL.

1           The MFC is located within a security fence. All access is attained through a security station  
2 located at the MFC entrance. Vehicles must pass through a two-gate arrangement that allows security  
3 personnel to conduct thorough inspections. Exhibit B-14 provides access and traffic control information  
4 for the MFC. Personnel must pass through the security station to obtain proper dosimetry and verify they  
5 have proper identification and access credentials. Personnel or visitors without proper credentials are  
6 escorted while on the MFC site.

7           Access to HWMA units and facilities within MFC is provided by a network of paved and gravel  
8 roadways. Any one of these roadways may be used to transport hazardous or mixed waste among MFC  
9 facilities. Transport from MCF facilities to other facilities on the INL site is done via U.S. 20. The roads  
10 accessing the MFC are constructed of asphalt, with load-bearing capacities of 68 metric tons (75 tons).  
11 Roads within the MFC area, used to transport hazardous/mixed waste, have been tested to 45,000 kg  
12 (100,000 lb) single-axle loading. Traffic is limited inside the MFC fenced area to security-approved  
13 vehicles, such as government and construction, and a speed limit of 10 mph.

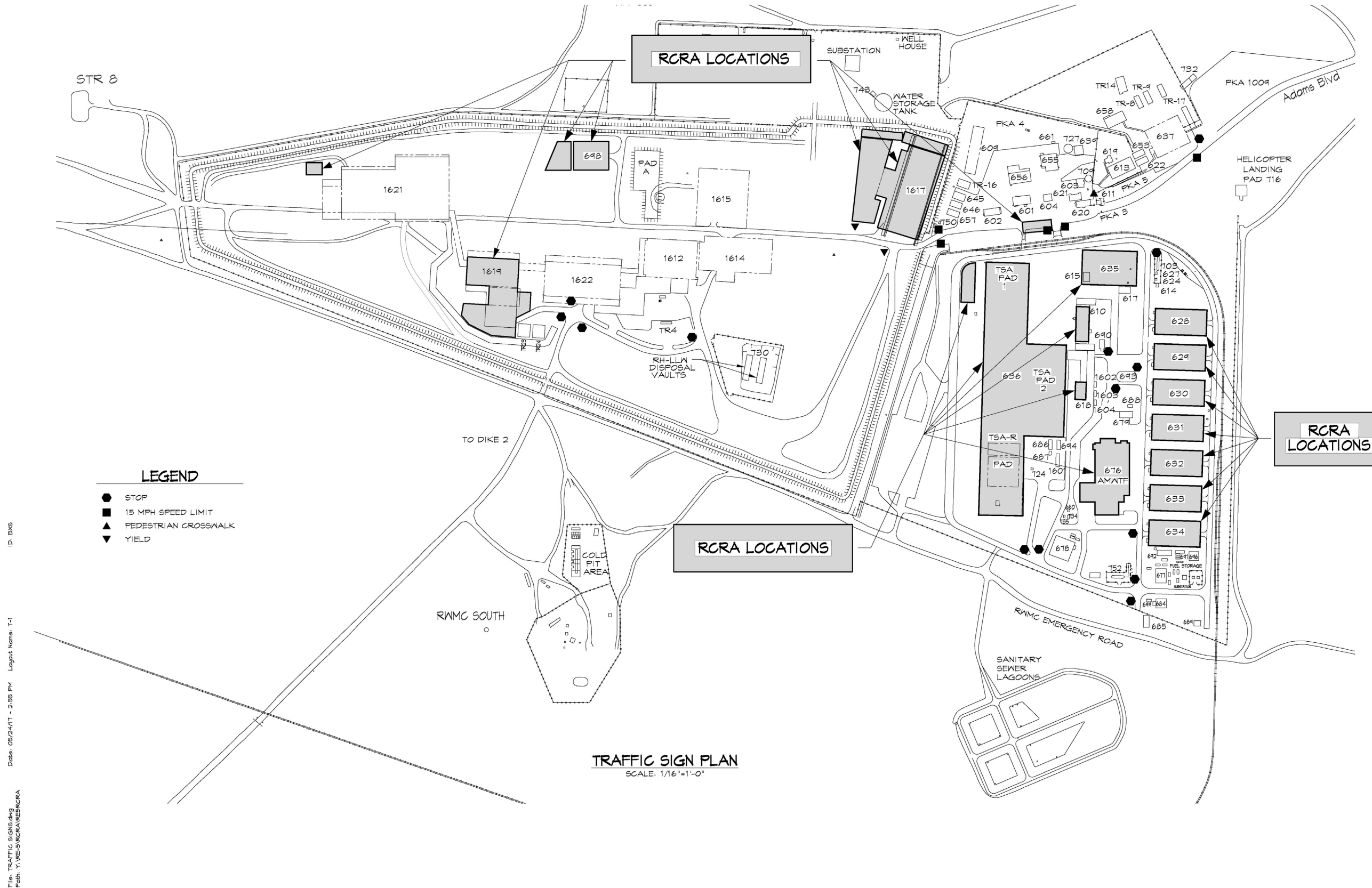


Exhibit B-13. Access and traffic control at RWMC

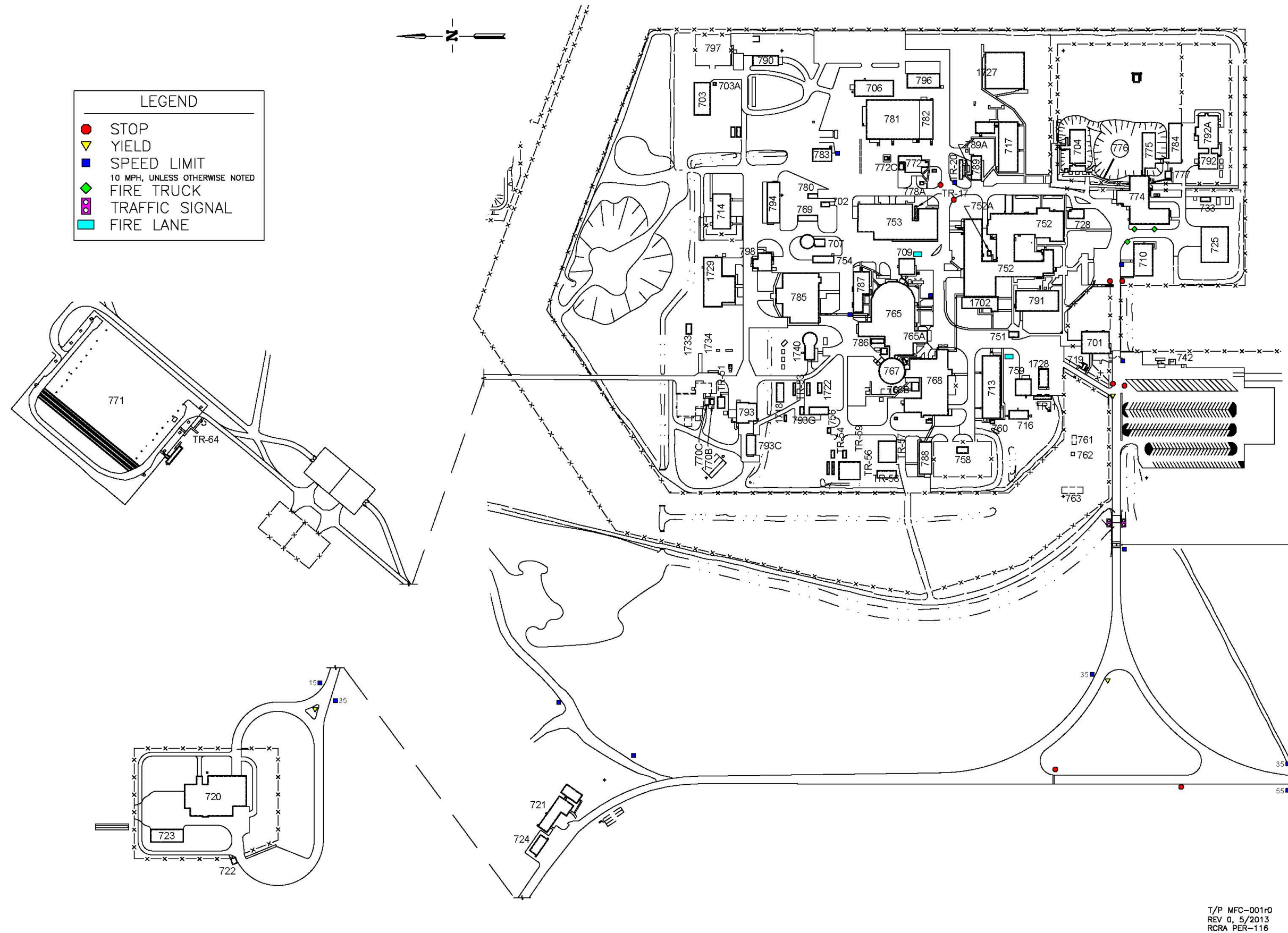


Exhibit B-14. Access and traffic control at MFC

1           **B-5 Literature Cited**

2           EPA/DOE/State of Idaho, 1991, *Federal Facility Agreement and Consent Order and Action Plan*, U.S.  
3           Department of Energy, Idaho Operations Office: Idaho Department of Health and Welfare,  
4           Division of Environmental Quality: U.S. EPA, Region 10, August 18.

5           DOE, Department of the Navy, State of Idaho, 1995, Settlement Agreement to Public Service Co. of  
6           Colorado v. Batt, No. CV 91-0035-S-EJL (D. Id.) and United States v. Batt,  
7           No. CV-91-0065-S-EJL (D. Id.). October 16.

8           DOE, 1995, *Department of Energy Programmatic Spent Nuclear Fuel Management and Idaho National*  
9           *Engineering Laboratory Environmental Restoration and Waste Management Programs Final*  
10           *Environmental Impact Statement*, Volumes 1, 2, & 3, EIS-0203F; U.S. Department of Energy,  
11           Office of Environmental Management, Idaho Operations, April.

12           DOE, 2005, *2005 Supplemental Analysis of the INL Site Portion of the April 1995 Programmatic Spent*  
13           *Nuclear Fuel Management and Idaho National Engineering Laboratory Environmental*  
14           *Restoration and Waste Management Programs Final Environmental Impact Statement*,  
15           DOE/EIS-0203-F-SA-02, United States Department of Energy, Idaho Operations Office, June.

16           DOE-ID, 2004, Idaho National Engineering and Environmental Laboratory Environmental Monitoring  
17           Plan, DOE/ID-11088, Department of Energy Idaho Operations Office, Idaho Falls, Idaho, April.

18           INL, 2013, *Hazardous Waste Management Act/Resource Conservation and Recovery Act*  
19           *(HWMA/RCRA) Work Plan for the Idaho National Laboratory (INL)*, EPA No. ID4890008952,  
20           Idaho National Laboratory, Idaho Falls, Idaho, April (or most current revision).

21           INEEL/EXT-03-01174 100-Year Storm Water Runoff Floodplain and 25-Year Runoff Analyses for the  
22           Idaho Nuclear Technology and Engineering Center at the Idaho National Engineering and  
23           Environmental Laboratory, Revision 1, January 2004.

24           McKinney, J. D., 1985, *Big Lost River 1983-1984 Flood Threat*, PPD-FPB-002, EG&G Idaho Inc., Idaho  
25           Falls, ID.

26           Ostenaar, D. A. and D. R.H. O'Connell, 2005, *Big Lost River Flood Study Idaho National Laboratory,*  
27           *Idaho, Summary Document*, Report 2005-2. Seismotectonics and Geophysics Group, Technical  
28           Service Center, Bureau of Reclamation, Denver, CO.

- 1 Payne S.J., Gorman V.W., Jensen S. A., Nitzel M.E., Russell M.J., and Smith R.P., 2002, Development  
2 of probabilistic design basis earthquake (DBE) parameters for moderate and high hazard  
3 facilities at INEEL, Bechtel BW XT Idaho, LLC, External Report INEEL/EXT-99-000775, Final  
4 Report, Rev 2, June, 101 pp.
- 5 Stone, M. A. J., L. J. Mann, and L. C. Kjelstrom, 1993, “Statistical Summaries of Streamflow Data for  
6 Selected Gaging Stations on and near the Idaho National Engineering Laboratory, Idaho,  
7 Through September 1990,” U. S. Geological Survey Water-Resources Investigations Report  
8 92-4196.
- 9 U.S. Geological Survey and Idaho Geological Survey, 2006, Quaternary fault and fold database for the  
10 United States, accessed 2011, from USGS web site: <http://earthquakes.usgs.gov/hazards/qfaults/>.

**SECTION C - WASTE  
CHARACTERISTICS**

1

### **C. WASTE CHARACTERISTICS**

2

The information for this section is contained in the waste management unit-specific volumes of

3

the INL HWMA/RCRA Part B permits, or permit applications.

**SECTION D -  
PROCESS  
INFORMATION**

1

**D. PROCESS INFORMATION**

2

The information for this section is contained in the waste management unit-specific

3

volumes of the INL HWMA/RCRA Part B permits, or permit applications.

**SECTION E -  
GROUNDWATER  
MONITORING**

1

**E. GROUNDWATER MONITORING**

2

The information for this section is contained in the waste management unit-specific volumes of

3

the INL HWMA/RCRA Part B permits, or permit applications.

**SECTION F -  
PROCEDURES TO  
PREVENT HAZARDS**

1 **F. PROCEDURES TO PREVENT HAZARDS**

2 **F-1 Security IDAPA 58.01.05.008 and .012 [40 CFR 264.14(b) and(c), and 270.14(b)(4)]**

3 Security at the INL is maintained by trained security personnel who monitor site access and  
4 provide security presence at the various complexes throughout the INL site. The size of INL (890 mi<sup>2</sup>),  
5 and its location with respect to highways (Idaho State Highways 22, 28, and 33, and U.S. Routes 20 and  
6 26), have made construction of a Site boundary security fence impractical. Rather, security at the INL  
7 and at the waste management units located therein is maintained by a security system, consisting of  
8 property warning signs and surveillance patrolling, security access control points placed at the entrances  
9 to the various complexes within the INL, and specific security measures taken at the individual areas,  
10 such as fencing, warning signs, and building security.

11 Property warning signs read "No Trespassing - By Order of the United States Department of  
12 Energy." Signs with this inscription are located along the INL property boundary and along the five  
13 public highways that pass through INL property. Exhibit F-1 is an example of this sign. The waste  
14 management unit-specific volumes of the INL HWMA/RCRA Part B permits and permit applications  
15 address access processes on a unit specific basis.

16 Areas along the boundary of the INL are open to grazing by livestock, as described in Subsection  
17 B-2, Surrounding Land Use. Limits of these grazing areas that lie inside the property boundary are  
18 denoted by the second type of sign; this sign has the same message as the first, with the addition of "No  
19 Grazing Beyond this Point." Exhibit F-2 is an example of this sign.

20 Both types of signs are legible from a distance of 7.6 m (25 ft) and are spaced at regular intervals.  
21 Signs are located closer together in areas where the line of sight is obstructed; in such cases, the warning  
22 signs are placed where they can be seen. Exhibit F-3 is a schematic diagram of the INL, identifying  
23 locations of warning signs, grazing boundaries, and current security stations.

24 Access control points are located at the entry and egress points to and from the various INL  
25 complexes. Only authorized personnel and escorted, authorized visitors holding the appropriate  
26 identification passes are cleared for entry and egress. Exhibit F-3 identifies the INL boundary and the  
27 current access control points. Visitors or authorized personnel without identification passes must check in  
28 at these stations.

DOE PROPERTY BOUNDARY SIGN

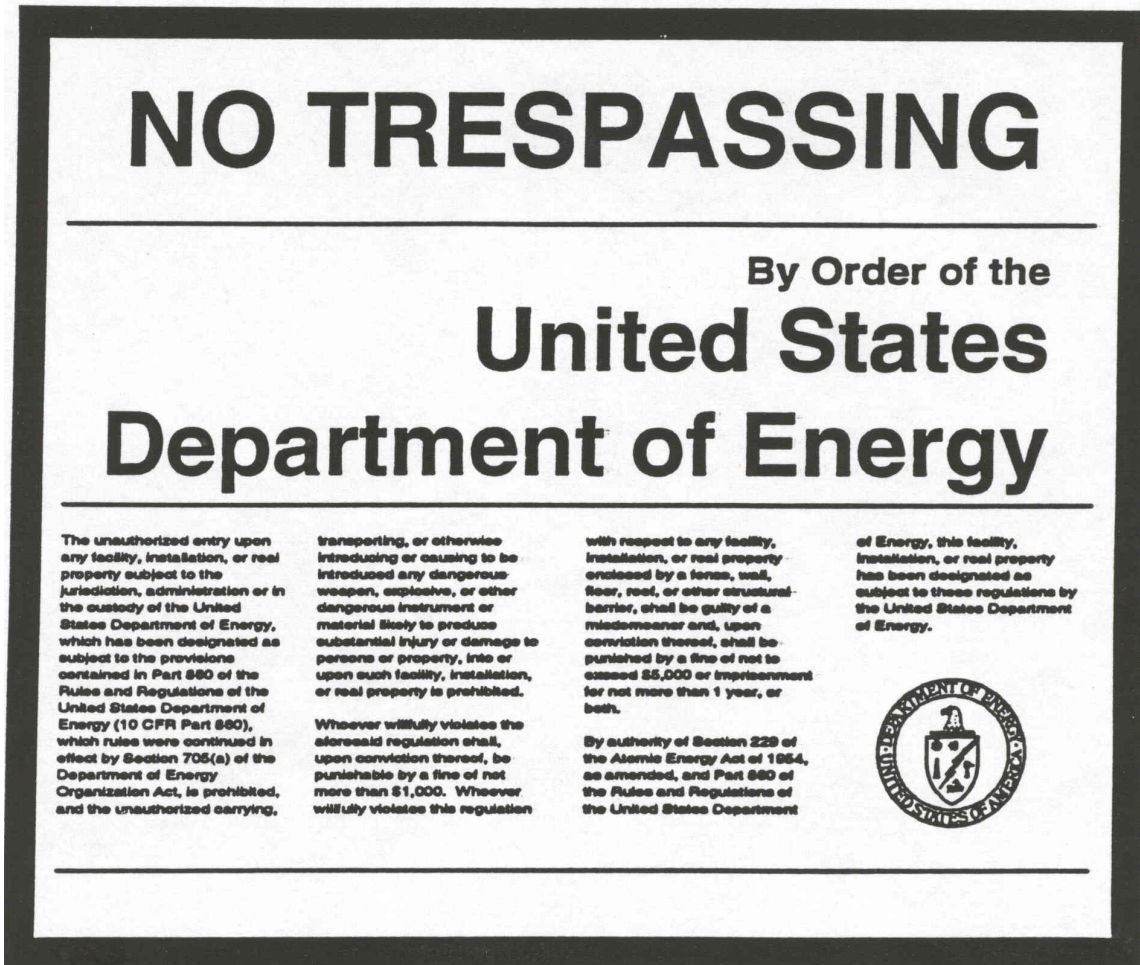
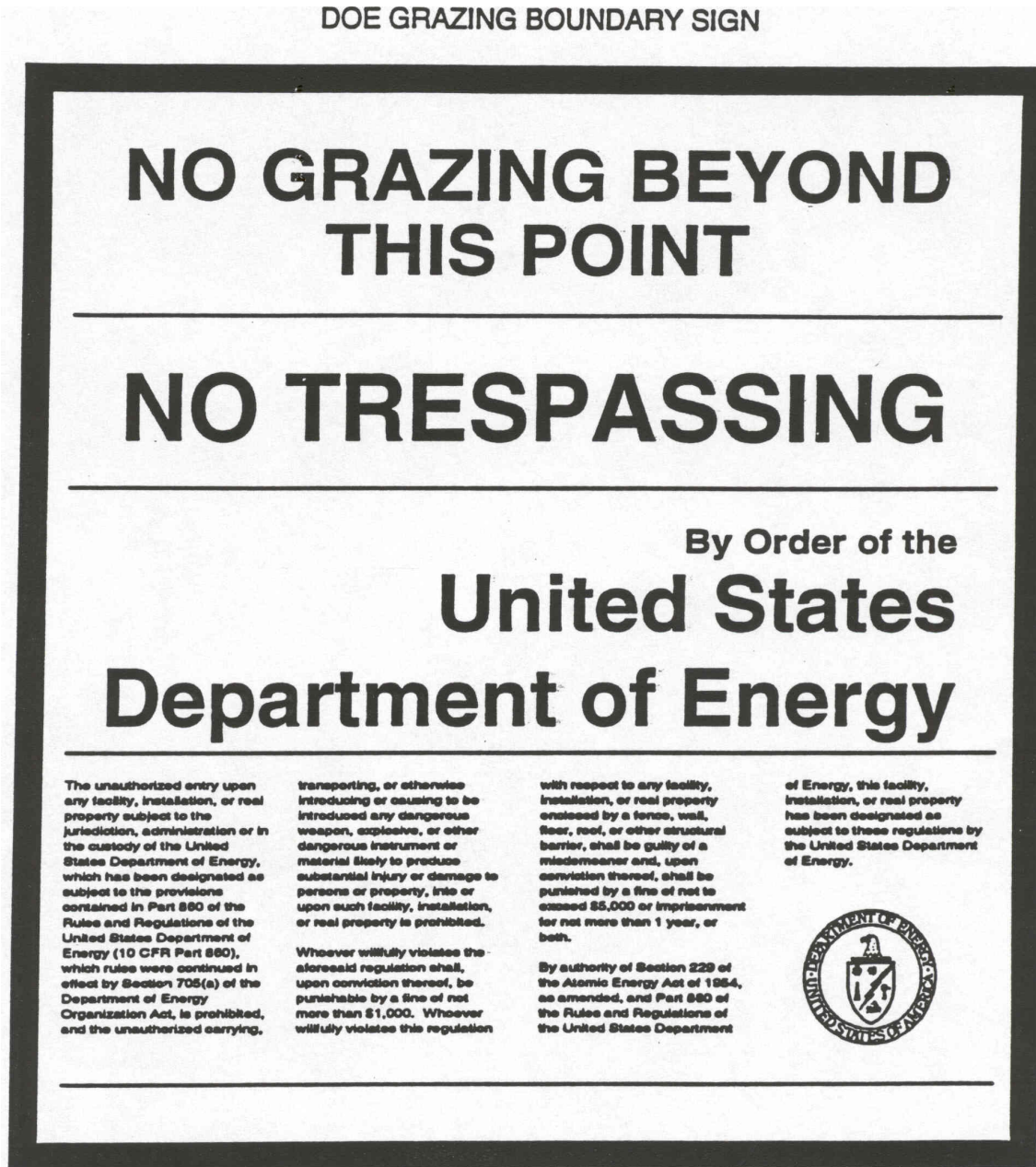


Exhibit F-1. Example of an INL boundary no trespassing sign.



**Exhibit F-2.** Example of an INL boundary no grazing sign.

1           In addition to the security presence at the manned stations, security personnel randomly patrol  
2 INL boundaries, roadways, and facilities in ground patrol vehicles and on foot. All patrol routes are  
3 nonrepetitive and random. When a domestic animal or a group of animals has entered an active portion  
4 of the INL beyond the designated grazing boundaries, security-surveillance personnel contact security  
5 personnel in the area in which the animals have wandered, and if the problem persists, they contact the  
6 Bureau of Land Management, who has jurisdiction over wildlife on the INL.

7           Security is specific to each INL area and its component buildings, and involves the use of security  
8 fencing, locks on gates, and warning signs placed on the exterior of buildings and within general building  
9 areas.

10           Additionally, several other features contribute to the safety and security of the INL, such as,  
11 ample lighting throughout the facility areas, security and operations personnel are equipped with two-way  
12 communication devices to report upset or trespass conditions, and an internal telephone system that  
13 encompasses most of the INL that is used for communication outside INL premises. The waste  
14 management unit-specific volumes of the INL HWMA/RCRA Part B permits and permit applications  
15 address the requirements associated with security, in more detail, on a unit-specific basis.

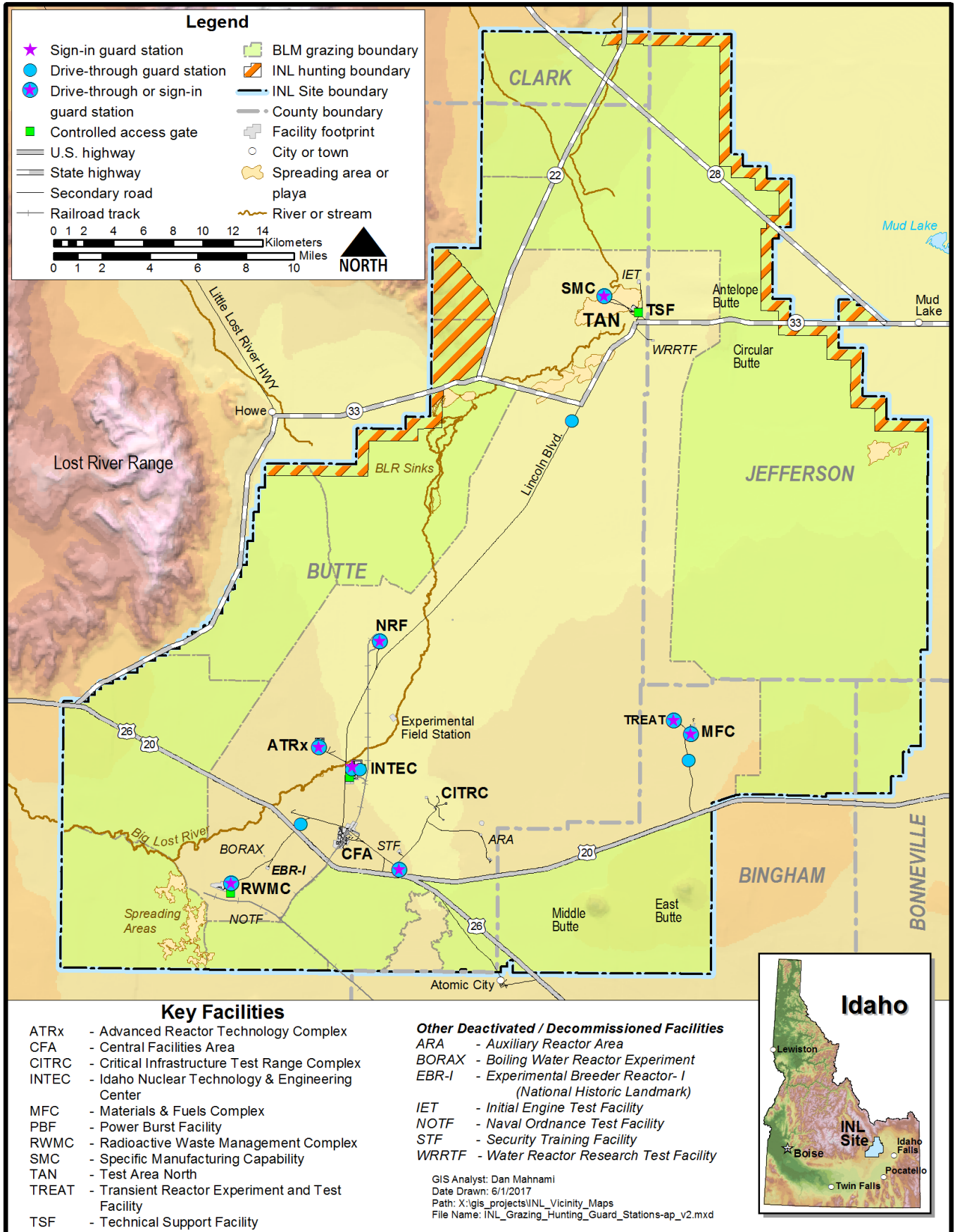


**Exhibit F-3.** Locations of INL warning signs (INL Boundary), grazing boundaries, and current security stations.



1

**G. CONTINGENCY PLAN**

2

The information for this section is contained in the waste management unit-specific volumes of

3

the INL HWMA/RCRA Part B permits, or permit applications.



1  
2  
3  
4  
5  
6  
7  
8  
9  
10  
11  
12  
13  
14  
15  
16  
17  
18  
19  
20  
21

## H. PERSONNEL TRAINING

DOE policy requires that all personnel involved with hazardous and mixed-waste handling, management, and unit operations be trained in the proper and safe receipt, handling, storage, and shipment of hazardous/mixed waste. Personnel receive training in the following HWMA areas, as appropriate to their individual job assignments:

- Occupational Safety and Health Administration (OSHA) 1910.120 Hazardous Waste Operations and Emergency Response Training (40- or 24-hour training as appropriate to job position). These courses are designed for all employees engaged in hazardous waste operations and have the potential of being exposed to a variety of hazards associated with such operations.
- Hazardous Materials Transportation Safety Training. This course provides a basic understanding of packaging, marking, labeling, and shipping requirements.
- Respirator Training. Provides information and guidance needed for the proper use, selection, and care of respirators.
- Hazard Communication. Provides awareness of the OSHA Hazard Communication Standard.
- General Employee Radiological Training. Provides basic information related to the “as low as reasonably achievable” (ALARA) principle.

The waste management unit-specific volumes of the INL HWMA/RCRA Part B permits and permit applications will address the requirements of IDAPA 58.01.05.008 and IDAPA 58.01.05.012 [40 CFR 264.16 and 40 CFR 270.14(b)(12)].

**SECTION I - CLOSURE  
AND POST CLOSURE**

1

## **I. CLOSURE AND POSTCLOSURE REQUIREMENTS**

2

The information for this section is contained in the waste management unit-specific volumes of

3

the INL HWMA/RCRA Part B permits, or permit applications.

**SECTION J -  
CORRECTIVE ACTION**

1                   **J. CORRECTIVE ACTION FOR SOLID WASTE MANAGEMENT UNITS**  
2   **(IDAPA 58.01.05.008 [40 CFR 264.101])**

3                   The corrective action requirements for INL facilities (as applicable) are addressed under the  
4 following HWMA/RCRA Final Partial Permits (as applicable): PER-116 – HWMA/RCRA Storage and  
5 Treatment Permit for the Materials and Fuel Complex – Module VI; PER-109 – HWMA/RCRA Storage  
6 and Treatment Permit for the Idaho Nuclear Technology and Engineering Center (Volume 18) – Module  
7 VIII; and Advanced Mixed Waste Treatment Project HWMA/RCRA Permit – Module VI.



1 **K. OTHER FEDERAL LAWS**  
2 **(IDAPA 58.01.05.012 [40 CFR 270.14(B)(20) AND 40 CFR 270.3])**

3 **K-1 The Wild and Scenic Rivers Act**

4 The activities under this permit application do not involve the construction of any water resource  
5 projects or other actions that will have any effect, adverse or otherwise, on the values for which a national  
6 wild and scenic river were established.

7 **K-2 The National Historic Preservation Act of 1966**

8 EBR-I, the first reactor built at the INL, was decommissioned in 1964. In 1966, EBR-I was  
9 officially designated a national historic landmark. The activities to be considered under this permit  
10 application will have no effect on EBR-I or any other properties currently on the national register or  
11 eligible for listing on the National Register of Historic Places.

12 **K-3 The Endangered Species Act (ESA)**

13 There are no known endangered or threatened plants or animal species on the INL Site.  
14 Table K-1 contains information on listed species, candidate species, and non-listed species of concern.  
15 There are several animal species that are known to, or having the potential to occur on or near the Site  
16 that are species of special concern. Among these species is the ferruginous hawk, which nests near the  
17 juniper woodlands and elsewhere on INL land. In addition, Townsend's big-eared bats roost in caves on  
18 the Site. Burrowing owls use the Site's grassland and sagebrush-steppe habitat, and loggerhead shrikes  
19 are found in the sagebrush areas and near facilities over much of the INL site. The relatively undisturbed  
20 areas of the INL site provide habitat for threatened, endangered, candidate, and other species.

**Table K-1.** ESA Listed Species, ESA Candidate Species, and species of concern, which may occur at the INL.

| Plants or Animals | ESA Listed Species  | Conservation Status Rank* and Comments   |
|-------------------|---|--|
|                   | None  | None   |
| Plants or Animals | ESA Candidate Species                                       | Conservation Status Rank and Comments  |
| Birds             | Greater sage-grouse<br>( <i>Centrocercus urophasianus</i> ) | G3, G4, and S2. On October 12, 2015 the U.S. Fish and Wildlife Service (FWS), announced a 12-month finding on petitions to list the greater sage grouse ( <i>Centrocercus urophasianus</i> ), both range wide and the Columbia Basin population, as an endangered or threatened species under the Endangered Species Act of 1973, as amended (Act). After review of the best available scientific and commercial information, the FWS found that the Columbia Basin population does not qualify as a distinct population segment. In addition, we find that listing the greater sage-grouse is not warranted at this time. |
|                   | Yellow-billed cuckoo<br>( <i>Coccyzus americanus</i> )      | G4 and S1B. October 3, 2013, the FWS published in the Federal Register a proposed rule (78 FR 61621) to list the western yellow-billed cuckoo. This rule finalizes our determination for listing the western yellow-billed cuckoo. The FWS has determined that the western yellow-billed cuckoo meets the definition of a threatened species and is likely to become endangered throughout its range within the foreseeable future, based on the immediacy, severity, and scope of the threats to its continued existence.   |
| Plants or Animals | Petitioned for ESA Listing                                  | Conservation Status Rank and Comments  |
| Mammals           | Wolverine ( <i>Gulo gulo luscus</i> )                       | G4 and S1. On August 12, 2014, the FWS announced today that it is withdrawing a proposal to list the North American wolverine in the contiguous United States as a threatened species under the Endangered Species Act (ESA). The wolverine does not meet the statutory definition of either a “threatened species” or an “endangered species” and does not warrant protection under the ESA. The wolverine has not been documented but may pass through the INL Site.   |
|                   | Little brown myotis<br>( <i>Myotis lucifugus</i> )          | G3 and S3. A 2010 status review of the little brown myotis concluded emergency listing under the ESA was warranted for this species; and the FWS is collecting information on this species to determine if, in addition to existing threats, white-nose syndrome may be increasing the extinction risk of this bat.  |

**Table K-1. (Continued)**

| Plants or Animals | Idaho Species of Greatest Conservation Need                    | Conservation Status Rank and Comments  |
|-------------------|--|--|
| Mammals           | Townsend’s big-eared bat<br>( <i>Corynorhinus townsendii</i> ) | G3, G4, and S3   |
|                   | Big brown bat ( <i>Eptesicus fuscus</i> )                      | G5 and S3. The FWS is proactively collecting information on this species, which is believed to be susceptible to white-nose syndrome to determine if, in addition to existing threats, the disease may be increasing the extinction risk of this bat.  |
|                   | Silver-haired bat<br>( <i>Lasionycteris noctivagans</i> )      | G4 and S3  |
|                   | Hoary bat ( <i>Lasiurus cinereus</i> )                         | G4 and S3  |
|                   | Western small-footed myotis ( <i>Myotis ciliolabrum</i> )      | G4G5 and S3  |
|                   | Pygmy rabbit<br>( <i>Brachylagus idahoensis</i> )              | G4 and S3. On September 29, 2010 the FWS announced that it has completed a status review, or 12-month finding, of the pygmy rabbit and concluded it does not warrant protection under the Endangered Species Act (ESA) in California, Nevada, Oregon, Idaho, Utah, Wyoming, and Montana. The status review was undertaken after the Service determined that a petition to list the pygmy rabbit under the ESA presented substantial information in January 2008, and that listing of the species may be warranted. |
|                   | Merriam’s shrew ( <i>Sorex merriami</i> )                      | G5 and S4  |
|                   | Gray Wolf ( <i>Canis lupus</i> )                               | G4, G5, and S4   |
| Birds             | Trumpeter Swan ( <i>Cygnus buccinators</i> )                   | G4, S1B, and S4N   |
|                   | Northern Pintail ( <i>Anas acuta</i> )                         | G5, S4B, and S4N   |
|                   | Lesser Scaup ( <i>Aythya affinis</i> )                         | G5, S3B, and S3N   |
|                   | Greater Sage-Grouse<br>( <i>Centrocercus urophasianus</i> )    | G3, G4, and S3   |
|                   | Western Grebe<br>( <i>Aechmophorus occidentalis</i> )          | G5 and S2B   |
|                   | Clark’s Grebe<br>( <i>Aechmophorus clarkia</i> )               | G5 and S2B   |
|                   | Great Egret ( <i>Ardea alba</i> )                              | G5 and S2B   |

**Table K-1. (Continued)**

| <b>Plants or Animals</b> | <b>Idaho Species of Greatest Conservation Need</b>            | <b>Conservation Status Rank and Comments</b> |
|--------------------------|---|--|
| Birds (continued)        | Snowy Egret ( <i>Egretta thula</i> )                          | G5 and S1B                                   |
|                          | Cattle Egret ( <i>Bubulcus ibis</i> )                         | G5 and S1B                                   |
|                          | Black-crowned Night-Heron<br>( <i>Nycticorax nycticorax</i> ) | G5, S2B, and S2N                             |
|                          | White-faced Ibis ( <i>Plegadis chihi</i> )                    | G5 and S2B                                   |
|                          | Bald Eagle ( <i>Haliaeetus leucocephalus</i> )                | G5 and S5                                    |
|                          | Swainson’s Hawk ( <i>Buteo swainsoni</i> )                    | G5 and S5B                                   |
|                          | Ferruginous Hawk ( <i>Buteo regalis</i> )                     | G4 and S3B                                   |
|                          | Golden Eagle ( <i>Aquila chrysaetos</i> )                     | G5 and S3                                    |
|                          | Merlin ( <i>Falco columbarius</i> )                           | G5 and S4                                    |
|                          | Peregrine Falcon ( <i>Falco peregrines</i> )                  | G4 and S3B                                   |
|                          | Sandhill Crane ( <i>Grus canadensis</i> )                     | G5 and S3B                                   |
|                          | Black-necked Stilt<br>( <i>Himantopus mexicanus</i> )         | G5 and S4B                                   |
|                          | American Avocet<br>( <i>Recurvirostra americana</i> )         | G5, S3B, and S3M                             |
|                          | Long-billed Curlew<br>( <i>Numenius americanus</i> )          | G5 and S2B                                   |
|                          | Wilson’s Phalarope<br>( <i>Phalaropus tricolor</i> )          | G5 and S4B                                   |
|                          | Franklin’s Gull ( <i>Larus pipixcan</i> )                     | G4, G5, and S3B                              |
|                          | California Gull ( <i>Larus californicus</i> )                 | G5, S3B, and S2N                             |
|                          | Caspian Tern ( <i>Sterna caspia</i> )                         | G5 and S1B                                   |
|                          | Forster’s Tern ( <i>Sterna forsteri</i> )                     | G5 and S2B                                   |
|                          | Black Tern ( <i>Chlidonias niger</i> )                        | G4 and S2B                                   |

**Table K-1. (Continued)**

| <b>Plants or Animals</b>                        | <b>Idaho Species of Greatest Conservation Need</b>  | <b>Conservation Status Rank and Comments</b>  |
|---|---|---|
| Birds (continued)                               | Burrowing Owl ( <i>Athene cunicularia</i> )   | G4 and S2B  |
|   | Short-eared Owl ( <i>Asio flammeus</i> )  | G5 and S3   |
|   | Brewer’s Sparrow ( <i>Spizella breweri</i> )  | G5 and S4B  |
|   | Sagebrush Sparrow ( <i>Artemisiospiza nevadensis</i> )  | G5 and S3B  |
| Plants  | Idaho Rare Plant List – Species with documented occurrences on the INL Site   |   |
|   | Lemhi milkvetch ( <i>Astragalus aquilonius</i> )  | G3 and S3. This species has been documented on the INL Site boundary in the Lemhi foothills but is unlikely to occur anywhere else onsite due to narrow habitat requirements. |
|   | Wing-seeded evening primrose ( <i>Camissonia pterosperma</i> )  | G4 and S2. This species has been documented within the INL Site boundaries, mostly in the limestone shale on the foothills in the northern extent of the Site.                |
|   | Spreading gilia ( <i>Ipomopsis polycladon</i> )   | G4 and S2. This species has been documented in and around juniper woodlands in the northern and western foothills within the INL Site boundary.                               |
|   | Hoary phacelia ( <i>Phacelia incana</i> )   | G3 and G4. This species has been documented within the INL Site boundary in the northern and western foothills.   |
|   | Middle Butte bladderpod ( <i>Lesquerella obdeltata</i> )  | G1, G3, and SNR. This species has been documented around the base of Middle Butte.  |
|   | <b>Idaho Rare Plant List – Species with appropriate habitat onsite and occurrences in close proximity to the INL Site</b> |   |
|   | Cusick’s giant hyssop ( <i>Agastache cusickii</i> )   | G3,G4, and SNR. Occurs on dry slopes, and rocky substrate.  |
|   | Custer milkvetch ( <i>Astragalus amnis-amissi</i> )   | G3 and S3. Habitat includes limestone cliffs and associated talus.  |
|   | Plains milkvetch ( <i>Astragalus gilviflorus</i> )  | G5 and S2. Occurs in sagebrush communities on barren knolls and stony hilltops.   |
|   | Desert dodder ( <i>Cuscuta denticulata</i> )  | G4, G5, and S1. Grows on shrubs in dry sandy, gravelly, and rocky soils.  |
|   | Crosby’s buckwheat ( <i>Eriogonum crosbyae</i> )  | GNR and SNR. This species is found on dry, windswept sites associated with the Lost River watersheds.   |
| Hooker’s buckwheat ( <i>Eriogonum hookeri</i> ) | G5 and S1. Habitat includes sandy soils in sagebrush and juniper communities.   |   |

**Table K-1. (Continued)**

| Plants or Animals   | Idaho Species of Greatest Conservation Need                            | Conservation Status Rank and Comments |
|---|--|---------------------------------------|
| <b>Idaho Rare Plant List (continued)</b>                            |  |                                       |
| St. Anthony Dunes evening primrose ( <i>Oenothera psammophila</i> ) | G3 and S3. Occurs in the interface between lava reefs and sand dunes.  |                                       |
| Mountain ball cactus ( <i>Pediocactus simpsonii</i> )               | G5 and SNR. Habitat includes juniper and/or sagebrush communities.     |                                       |
| Hidden phacelia ( <i>Phacelia inconspicua</i> )                     | G2 and S1. Grows on north-facing slopes with sagebrush in sandy soils. |                                       |

\*NatureServe Conservation Status Ranking system.

G is the global or range wide rank and S is the statewide range.

G1 or S1 – Critically imperiled.

G2 or S2 – Imperiled.

G3 or S3 – Vulnerable.

G4 or S4 – Apparently Secure.

G5 or S5 – Secure.

GNR – Global rank not yet assessed.

SNR – Not ranked. State conservation and status not yet assessed

B – Breeding Population.

N – Non-breeding population.

Q – Indicates questionable taxonomy

T1-T5 – Indicates an intraspecific taxon or the status of a subspecies or variety of the species being discussed

1           The activities under this permit application are relatively small in scale, confined, and consistent with  
2 ongoing operations at the INL Site. These activities are not likely to jeopardize the continued existence of any  
3 of the species presented in Table K-1.

4           **K-4 The Coastal Zone Management Act**

5           The activities under this permit application will not affect land or water use in any  
6 coastal zone.

7           **K-5 The Fish and Wildlife Coordination Act**

8           The activities under this permit application do not involve impoundment, diversion, or other control or  
9 modification of any body of water that might impact wildlife.

10          **K-6 The Migratory Bird Treaty Act of 1918**

11          The Migratory Bird Treaty Act governs the taking, killing, possession, transportation, and importation  
12 of migratory birds, their eggs, parts, and nests. The activities under this permit application are not likely to  
13 jeopardize the species protected under this act.

14          **K-7 Bald and Golden Eagle Protection Act (16 U.S.C. 668)**

15          This law provides for the protection of the bald eagle (the national emblem) and the golden eagle by  
16 prohibiting, except under certain specified conditions, the taking, possession and commerce of such birds. The  
17 activities under this permit application are not likely to jeopardize the species protected under this act.

18          **K-8 Management of Undesirable Plants on Federal Lands (7 U.S.C. 2814)**

19          This act provides that Federal agencies shall develop and coordinate an undesirable plants  
20 management program for control of undesirable plants on Federal lands under the agency's jurisdiction. The  
21 activities under this permit application are not likely to interfere with this program.

22          **K-9 Invasive Species Executive Order (EO 13112)**

23          This order established a council whose charter is to prevent the introduction of invasive species and  
24 provide for their control and to minimize the economic, ecological, and human health impacts that invasive  
25 species cause. The activities under this permit application will not interfere with this program.

1           **K-10 Public Land Orders 318, 545, 637, and 1770**

2           Public Land Orders 318, 545, 637, and 1770 are decrees for the public land withdrawals that provided  
3 the land for the INL. The activities under this permit application will not interfere with these orders.

4           **K-11 Clean Water Act (33 U.S.C. 1251 et. seq.)**

5           This act regulates the discharges of pollutants into the waters of the United States. The act also sets  
6 requirements for all contaminants in surface waters and makes it unlawful for any person to discharge any  
7 pollutant from a point source into navigable waters, unless a permit is its provisions. The activities under this  
8 permit application are not likely to interfere with this program.



**REGULATORY CERTIFICATION [IDAPA 58.01.05.012; 40 CFR 270.11(d) and 270.30(k)]**

**FOR THE HAZARDOUS WASTE MANAGEMENT ACT/RESOURCE CONSERVATION  
AND RECOVERY ACT PART B PERMIT APPLICATION FOR  
THE IDAHO NATIONAL LABORATORY  
VOLUME 3 – GENERAL INFORMATION FOR INL WASTE MANAGEMENT UNITS**

**REVISION 18 – JULY 2017**

**EPA I.D. Number ID4890008952**

The undersigned certifies as required per 40 CFR 270.11(d) and 270.30(k) as follows:

I certify under penalty of law that this document and all attachments were prepared under my direction or supervision according to a system designed to assure that qualified personnel properly gather and evaluate the information submitted. Based on my inquiry of the person or persons who manage the system, or those persons directly responsible for gathering the information, the information submitted is, to the best of my knowledge and belief, true, accurate, and complete. I am aware that there are significant penalties for submitting false information, including the possibility of fine and imprisonment for knowing violations.

Owner Signature



Richard B. Provencher, Manager  
Department of Energy, Idaho Operations Office

7/6/17  
Date

**REGULATORY CERTIFICATION [IDAPA 58.01.05.012; 40 CFR 270.11(d) and  
270.30(k)]**

**FOR THE HAZARDOUS WASTE MANAGEMENT ACT/RESOURCE  
CONSERVATION AND RECOVERY PART B PERMIT APPLICATION FOR  
THE IDAHO NATIONAL LABORATORY  
VOLUME 3 – GENERAL INFORMATION FOR INL WASTE MANAGEMENT  
UNITS**

**REVISION 18 – JULY 2017**

**EPA I.D. Number ID4890008952**

The undersigned certifies as required per 40 CFR 270.11(d) and 270.30(k) as follows:

I certify under penalty of law that this document and all attachments were prepared under my direction or supervision according to a system designed to assure that qualified personnel properly gather and evaluate the information submitted. Based on my inquiry of the person or persons who manage the system, or those persons directly responsible for gathering the information, the information submitted is, to the best of my knowledge and belief, true, accurate, and complete. I am aware that there are significant penalties for submitting false information, including the possibility of fine and imprisonment for knowing violations.

Operator Signature



Frederick P. Hughes, Program Manager, Fluor Idaho, LLC.



Date

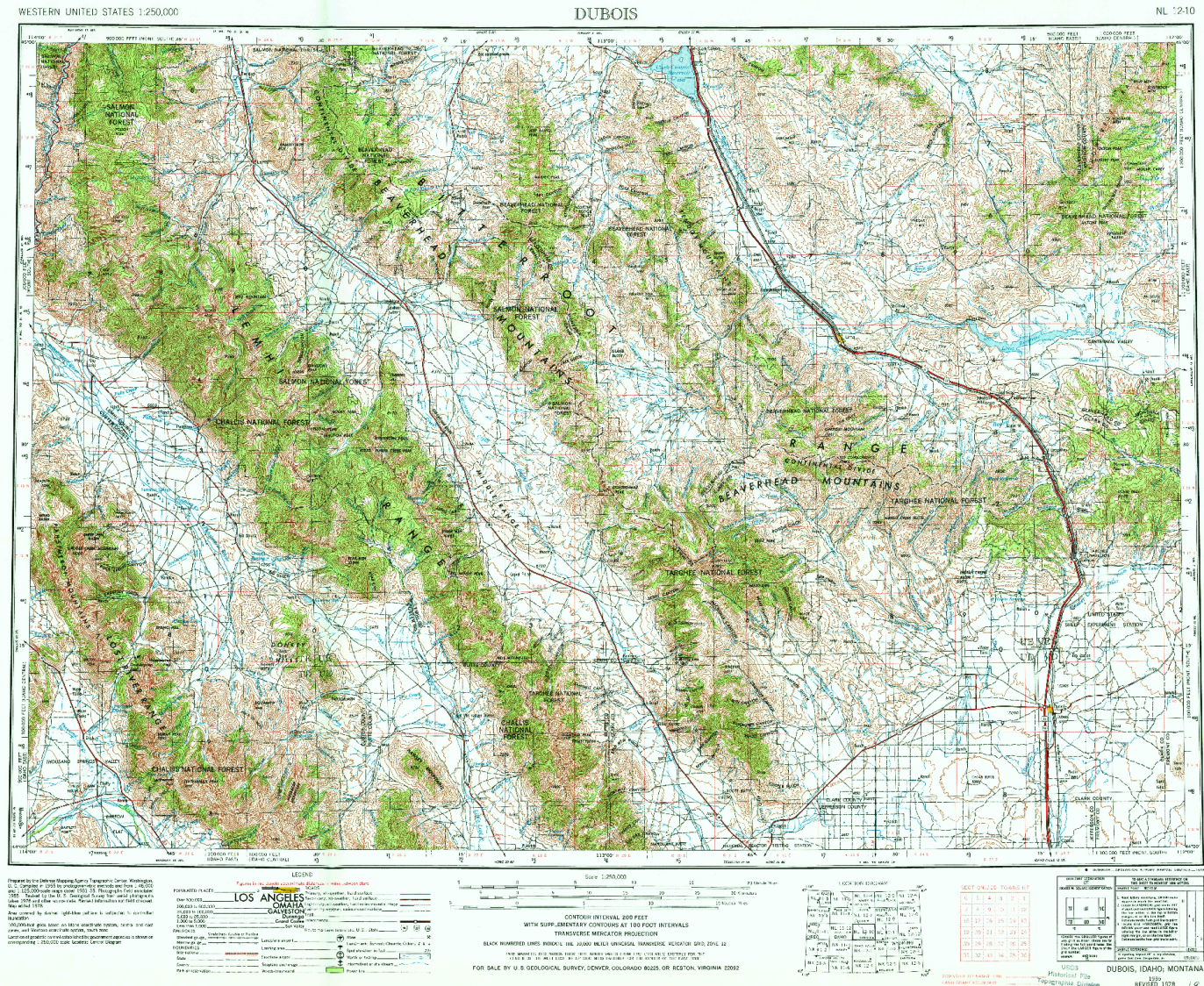


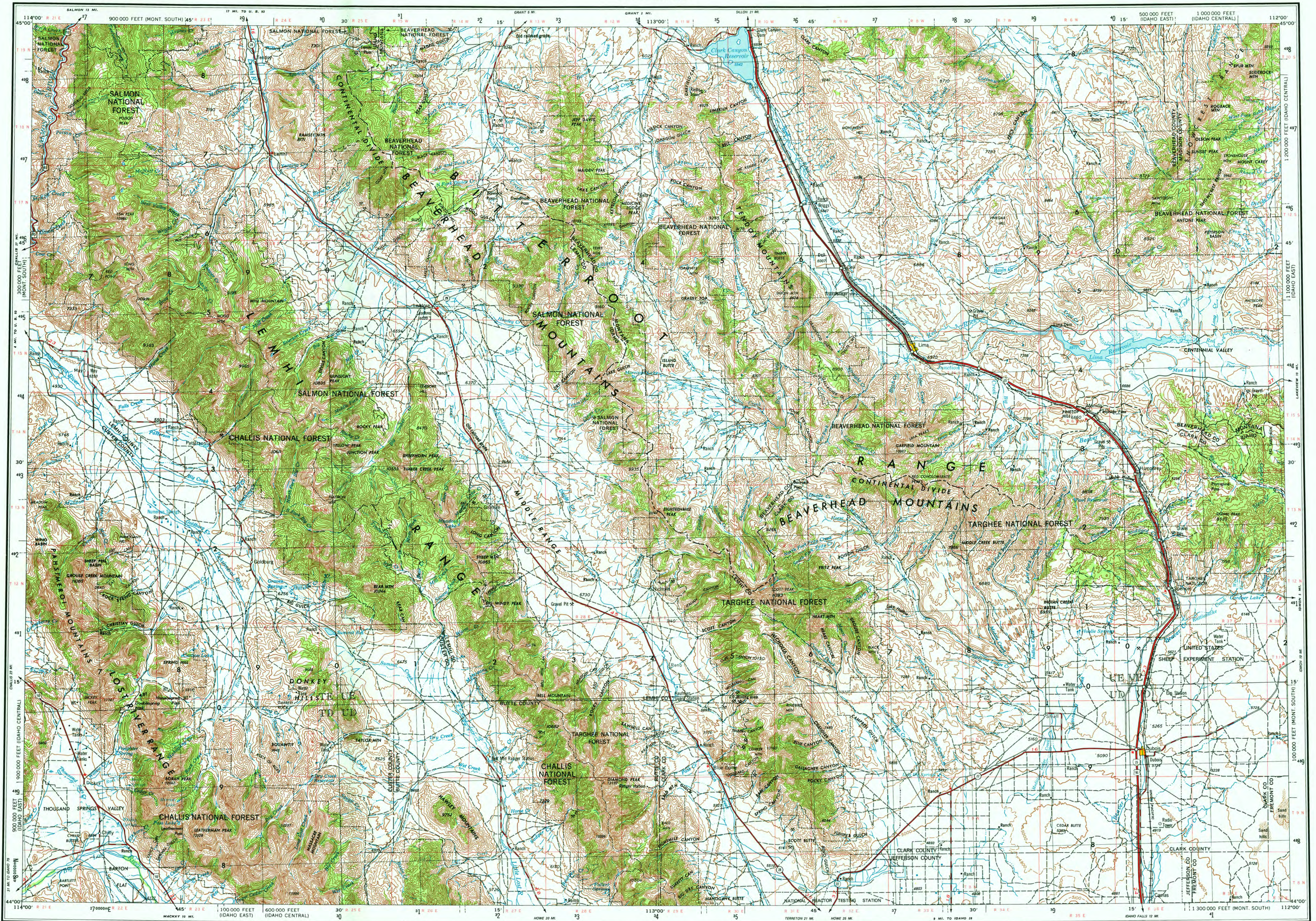
**APPENDIX I**  
**TOPOGRAPHIC MAPS**

## CONTENTS

- Map #1. Dubois (1:250,000) / INL Boundary (northern most portion of INL Site – Use in conjunction with Map #2) - Revision Date: 1978.
- Map #2. Idaho Falls (1:250,000) / INL Boundary (southern portion of INL Site – Use in conjunction with Map #1) - Revision Date: 1981
- Map #3. Circular Butte (1:24,000) / TAN, WRRTF, SMC - Revision Date: 2017
- Map #4. East of Howe Peak, ID (1:24,000) / NRF - Revision Date: 2017
- Map #5. North of Ryegrass Flat, ID (1:24,000) / ARVFS - Revision Date: 2017
- Map #6. North of Scoville, ID (1:24,000) / ATR, INTEC, CFA, NODA - Revision Date: 2017
- Map #7. Ryegrass Flat, ID (1:24,000) / SPERT II – IV, CITRC, ARA - Revision Date: 2017
- Map #8. Little Butte SW, ID (1:24,000) / MFC - Revision Date: 2017
- Map #9. Arco Hills SE, ID (1:24,000) / North of RWMC, EBR-I, Diversion System (use with Map #10) - Revision Date: 2017
- Map #10. Big Southern Butte, ID (1:24,000) / RWMC, Diversion System (use with Map #9) - Revision Date: 2017

# MAP #1 – DUBOIS (1:250,000) / INL BOUNDARY (northern most portion of INL Site – use in conjunction with Map #2).





Prepared by the Defense Mapping Agency Topographic Center, Washington, D. C. Compiled in 1955 by photogrammetric methods and from 1:48,000 and 1:125,000-scale maps dated 1951-55. Photographs field annotated 1955. Revised by the U. S. Geological Survey from aerial photographs taken 1976 and other source data. Revised information not field checked. Map edited 1978.

Area covered by dashed light-blue pattern is subjected to controlled inundation.

100,000-foot grids based on Idaho coordinate system, central and east zones, and Montana coordinate system, south zone.

Location of geodetic control established by government agencies is shown on corresponding 1:250,000-scale Geodetic Control Diagram.

**LEGEND**

Figures in red denote approximate distances in miles between stars.

**POPULATED PLACES**

- Over 500,000
- 100,000 to 500,000
- 25,000 to 100,000
- 5,000 to 25,000
- 1,000 to 5,000
- Less than 1,000

**RAILROADS**

- Standard gauge
- Narrow gauge
- International
- State
- County
- Park or reservation

**ROADS**

- Primary, all-weather, hard surface
- Secondary, all-weather, hard surface
- Light-duty, all-weather, hard or improved surface
- Fair or dry weather, unimproved surface
- Rail
- Interchange
- Route markers: Interstate, U.S., State
- Sun Valley

**LAND AND WATER FEATURES**

- Landplane airport
- Landing area
- Seaplane airport
- Seaplane anchorage
- Woods/brushwood
- Mine
- Landmark: School, Church, Other
- Spot elevation in feet
- Marsh or swamp
- Intermittent or dry stream
- Power line

Scale 1:250,000

0 5 10 15 20 25 30 Statute Miles

0 5 10 15 20 25 30 Kilometers

0 5 10 15 20 25 30 Nautical Miles

**CONTOUR INTERVAL 200 FEET**  
WITH SUPPLEMENTARY CONTOURS AT 100 FOOT INTERVALS

**TRANSVERSE MERCATOR PROJECTION**

BLACK NUMBERED LINES INDICATE THE 10,000 METER UNIVERSAL TRANSVERSE MERCATOR GRID, ZONE 12

1978 MAGNETIC DECLINATION FROM TRUE NORTH VARIES FROM 17°14' (310 MILS) EASTERLY FOR THE CENTER OF THE WEST EDGE TO 17° (300 MILS) EASTERLY FOR THE CENTER OF THE EAST EDGE

FOR SALE BY U. S. GEOLOGICAL SURVEY, DENVER, COLORADO 80225, OR RESTON, VIRGINIA 22092

**LOCATION DIAGRAM**

|              |              |              |              |
|--------------|--------------|--------------|--------------|
| WASH         | NL 12-4      | NL 12-5      | NL 12-6      |
| ILLINOIS     | ILLINOIS     | ILLINOIS     | ILLINOIS     |
| INDIANA      | INDIANA      | INDIANA      | INDIANA      |
| KENTUCKY     | KENTUCKY     | KENTUCKY     | KENTUCKY     |
| MICHIGAN     | MICHIGAN     | MICHIGAN     | MICHIGAN     |
| MONTANA      | MONTANA      | MONTANA      | MONTANA      |
| NEBRASKA     | NEBRASKA     | NEBRASKA     | NEBRASKA     |
| NEVADA       | NEVADA       | NEVADA       | NEVADA       |
| NEW YORK     | NEW YORK     | NEW YORK     | NEW YORK     |
| OHIO         | OHIO         | OHIO         | OHIO         |
| OREGON       | OREGON       | OREGON       | OREGON       |
| PENNSYLVANIA | PENNSYLVANIA | PENNSYLVANIA | PENNSYLVANIA |
| RHODE ISLAND | RHODE ISLAND | RHODE ISLAND | RHODE ISLAND |
| TENNESSEE    | TENNESSEE    | TENNESSEE    | TENNESSEE    |
| TEXAS        | TEXAS        | TEXAS        | TEXAS        |
| UTAH         | UTAH         | UTAH         | UTAH         |
| VIRGINIA     | VIRGINIA     | VIRGINIA     | VIRGINIA     |
| WISCONSIN    | WISCONSIN    | WISCONSIN    | WISCONSIN    |
| WYOMING      | WYOMING      | WYOMING      | WYOMING      |

**SECTIONIZED TOWNSHIP**

|    |    |    |    |    |    |
|----|----|----|----|----|----|
| 6  | 5  | 4  | 3  | 2  | 1  |
| 7  | 8  | 9  | 10 | 11 | 12 |
| 18 | 17 | 16 | 15 | 14 | 13 |
| 19 | 20 | 21 | 22 | 23 | 24 |
| 30 | 29 | 28 | 27 | 26 | 25 |
| 31 | 32 | 33 | 34 | 35 | 36 |

**GRID ZONE DESIGNATION**

12T

**TO GIVE A STANDARD REFERENCE ON THIS SHEET TO NEAREST 100 METERS**

**SECTION REFERENCE**

48Q9000

**USGS**

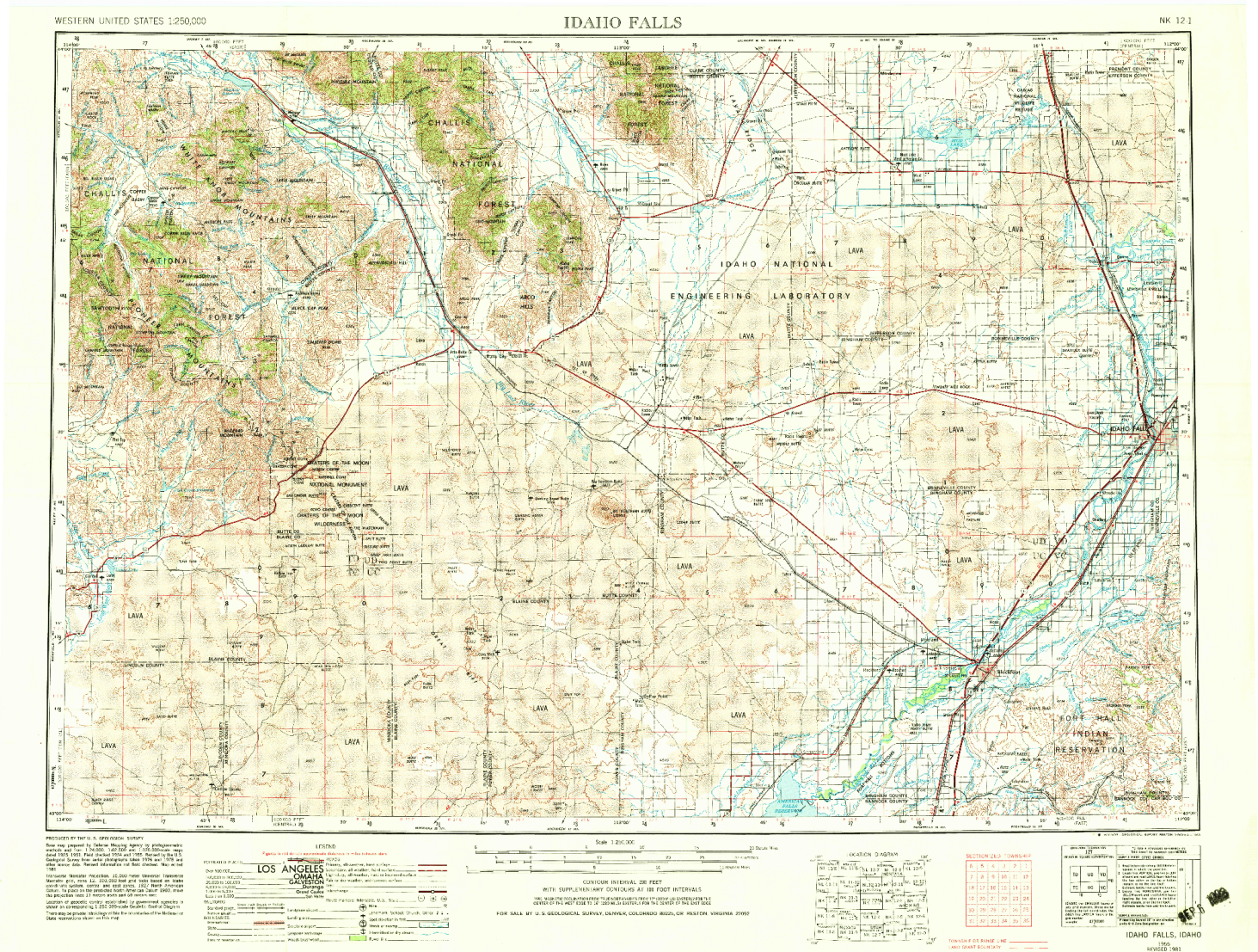
**DUBOIS, IDAHO; MONTANA**

1955  
REVISED 1978

NOV 27 1978

19,800

### MAP #2 – IDAHO FALLS (1:250,000) / INL BOUNDARY (southern portion of INL Site – use in conjunction with Map #1).





PRODUCED BY THE U. S. GEOLOGICAL SURVEY  
 Base map prepared by Defense Mapping Agency by photogrammetric methods and from 1:24,000, 1:62,500 and 1:125,000-scale maps dated 1925-1951. Field checked 1954 and 1955. Revised by the U.S. Geological Survey from aerial photographs taken 1976 and 1978 and other source data. Revised information not field checked. Map edited 1981.  
 Transverse Mercator Projection. 10,000-meter Universal Transverse Mercator grid, zone 12. 100,000-foot grid ticks based on Idaho coordinate system, central and east zones. 1927 North American Datum. To place on the predicted North American Datum 1983, move the projection lines 13 meters north and 68 meters east.  
 Location of geodetic control established by government agencies is shown on corresponding 1:250,000-scale Geodetic Control Diagram.  
 There may be private inholdings within the boundaries of the National or State reservations shown on this map.

**LEGEND**

Figures in red denote approximate distances in miles between stars

**POPULATED PLACES**

Over 500,000  
 100,000 to 500,000  
 25,000 to 100,000  
 5,000 to 25,000  
 1,000 to 5,000  
 Less than 1,000

**ROADS**

Primary, all-weather, hard surface  
 Secondary, all-weather, hard surface  
 Light-duty, all-weather, hard or improved surface  
 Fair or dry weather, unimproved surface  
 Trail  
 Interchange

**RAILROADS**

Single track  
 Double or Multiple track  
 Standard gauge  
 Narrow gauge

**LANDMARKS**

Landmark: School, Church, Other, etc.  
 Spot elevation in feet  
 Marsh or swamp  
 Intermittent or dry stream

**BOUNDARIES**

International  
 State  
 County  
 Park or reservation

**Other Symbols:**

Mine  
 Seaplane airport  
 Seaplane anchorage  
 Woods-brushwood  
 Power line

Scale 1:250,000

0 5 10 15 20 25 30 Statute Miles

0 5 10 15 20 25 30 Kilometers

0 5 10 15 Nautical Miles

CONTOUR INTERVAL 200 FEET  
 WITH SUPPLEMENTARY CONTOURS AT 100 FOOT INTERVALS

1981 MAGNETIC DECLINATION FROM TRUE NORTH VARIES FROM 17° (300 MILS) EASTERLY FOR THE CENTER OF THE WEST EDGE TO 10° (200 MILS) EASTERLY FOR THE CENTER OF THE EAST EDGE

FOR SALE BY U.S. GEOLOGICAL SURVEY, DENVER, COLORADO 80225, OR RESTON, VIRGINIA 22092

**LOCATION DIAGRAM**

|      |      |      |      |      |
|------|------|------|------|------|
| 118° | 119° | 120° | 121° | 122° |
| 41°  | 42°  | 43°  | 44°  | 45°  |

Grid showing townships and ranges with grid numbers.

**SECTIONIZED TOWNSHIP**

|    |    |    |    |    |    |
|----|----|----|----|----|----|
| 6  | 5  | 4  | 3  | 2  | 1  |
| 7  | 8  | 9  | 10 | 11 | 12 |
| 18 | 17 | 16 | 15 | 14 | 13 |
| 19 | 20 | 21 | 22 | 23 | 24 |
| 30 | 29 | 28 | 27 | 26 | 25 |
| 31 | 32 | 33 | 34 | 35 | 36 |

**GRID ZONE DESIGNATION**

12T

**TO GIVE A STANDARD REFERENCE ON THIS SHEET NEAREST 1000 METERS**

1. Read letters identifying 100,000-meter square in which the point lies.  
 2. Locate first VERTICAL grid line to LEFT of point and read LARGE figure labeling the line either in the top or bottom margin, or on the line itself.  
 3. Estimate meters from grid line to point.  
 4. Locate first HORIZONTAL grid line below point and read LARGE figure labeling the line either in the left or right margin, or on the line itself.  
 5. Estimate tenths from grid line to point.

**SAMPLE REFERENCE**

If reporting beyond 10" in any direction, prefix Grid Zone Designation, etc.  
 example: 4770000

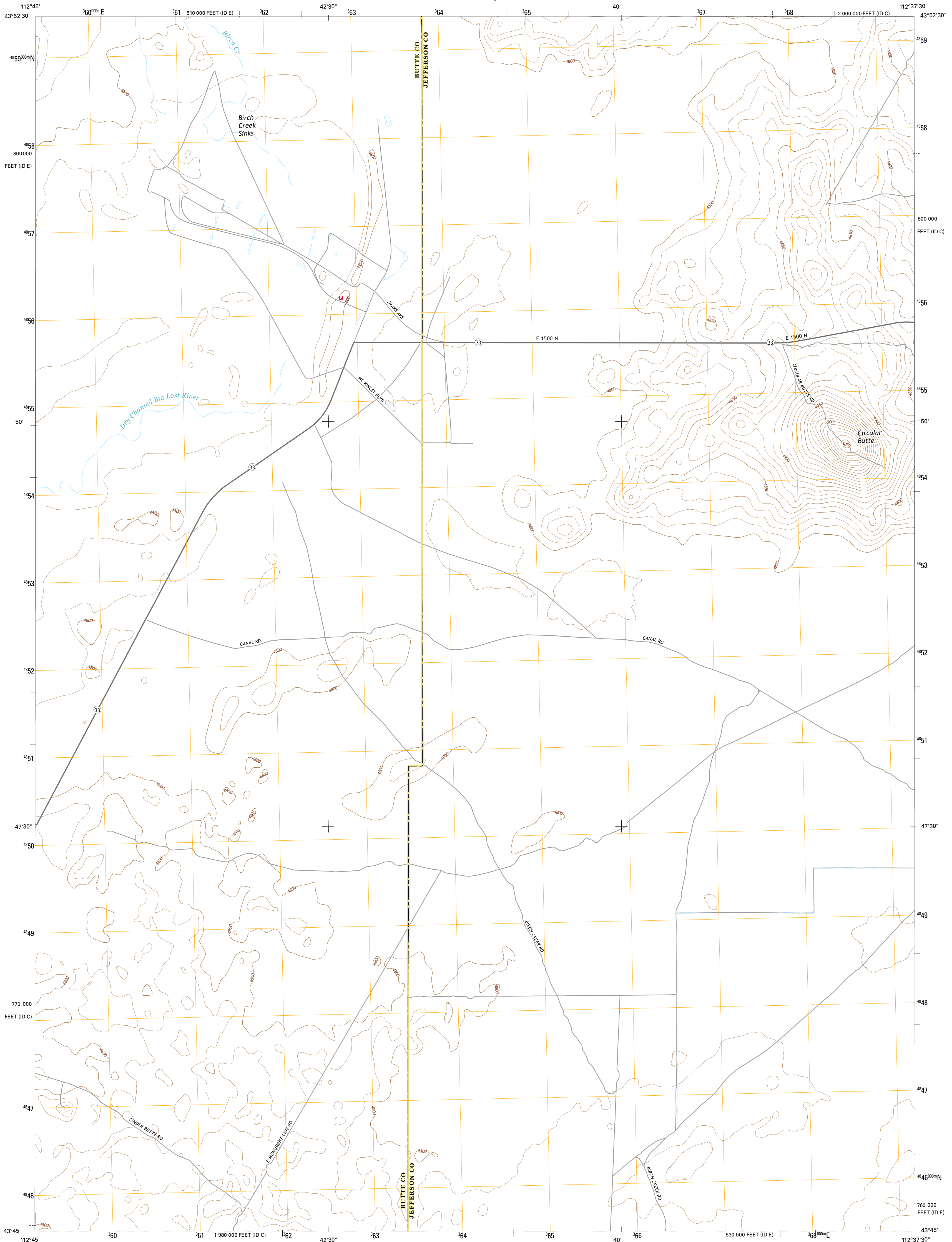




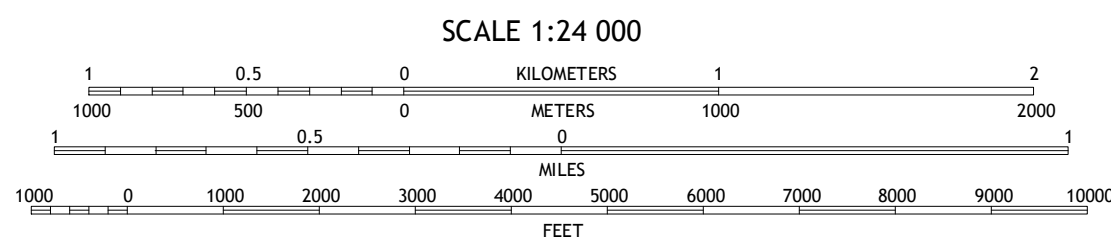
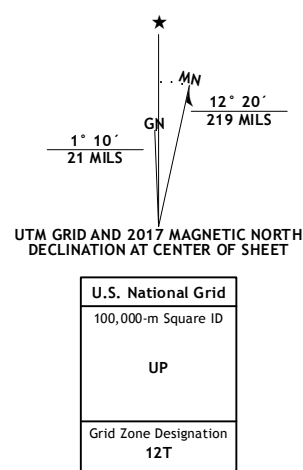
U.S. DEPARTMENT OF THE INTERIOR  
U.S. GEOLOGICAL SURVEY



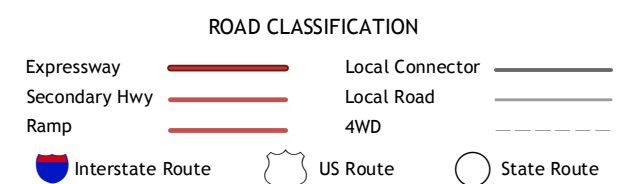
CIRCULAR BUTTE QUADRANGLE  
IDAHO  
7.5-MINUTE SERIES



Produced by the United States Geological Survey  
North American Datum of 1983 (NAD83)  
World Geodetic System of 1984 (WGS84), Projection and  
1 000-meter grid: Universal Transverse Mercator, Zone 12T  
10 000-foot ticks: Idaho Coordinate System of 1983 (east and  
central zones)  
This map is not a legal document. Boundaries may be  
generalized for this map scale. Private lands within government  
reservations may not be shown. Obtain permission before  
entering private lands.  
Imagery.....NAIP, January 2016  
Roads.....U.S. Census Bureau, 2015 - 2016  
Names.....GNIS, 2016  
Hydrography.....National Hydrography Dataset, 2016  
Contours.....National Elevation Dataset, 2002  
Boundaries.....Multiple sources; see metadata file 1972 - 2016  
Public Land Survey System.....BLM, 2015  
Wetlands.....FWS National Wetlands Inventory 1977 - 2014



QUADRANGLE LOCATION



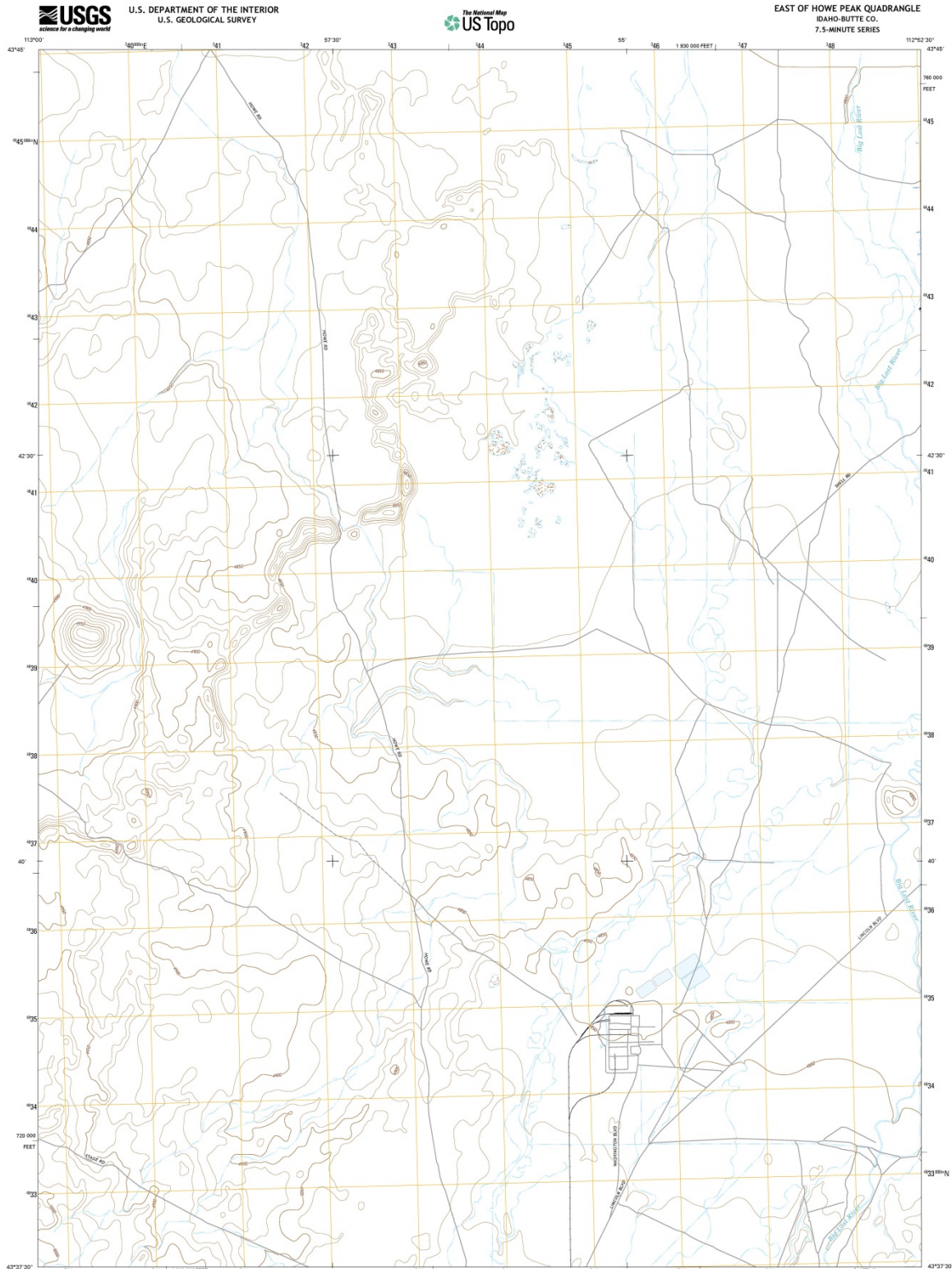
|   |   |   |
|---|---|---|
| 1 | 2 | 3 |
| 4 | 5 | 6 |
| 7 | 8 |   |

ADJOINING QUADRANGLES

CIRCULAR BUTTE, ID  
2017



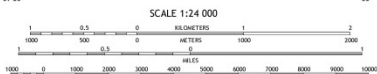
MAP #4 – EAST OF HOWE PEAK (1:24,000) / NRF



Produced by the United States Geological Survey  
 North American Datum of 1983 (NAD83)  
 World Geodetic System of 1984 (WGS84). Projected and  
 1 000 meter grid. Universal Transverse Mercator, Zone 12T  
 10 000 foot Grid. Idaho Coordinate System of 1983 (central  
 zone)

This map is not a legal document. Boundaries may be  
 generalized for this map scale. From land within government  
 boundaries may not be shown. Obtain permission before  
 entering private lands.

Source: ..... 2015  
 Rank: ..... U.S. Census Bureau, 2013 - 2014  
 Name: ..... 2015  
 Hydrography: ..... National Hydrography Dataset, 2015  
 Contour: ..... National Elevation Dataset, 2002  
 Boundaries: ..... Multiple sources; see metadata file 1972 - 2016  
 Public Land Survey System: ..... BLM, 2015  
 Wetlands: ..... FWS National Wetlands Inventory 1977 - 2014



ROAD CLASSIFICATION

|   |   |   |   |   |   |   |   |
|---|---|---|---|---|---|---|---|
| 1 | 2 | 3 | 4 | 5 | 6 | 7 | 8 |
| 1 | 2 | 3 | 4 | 5 | 6 | 7 | 8 |

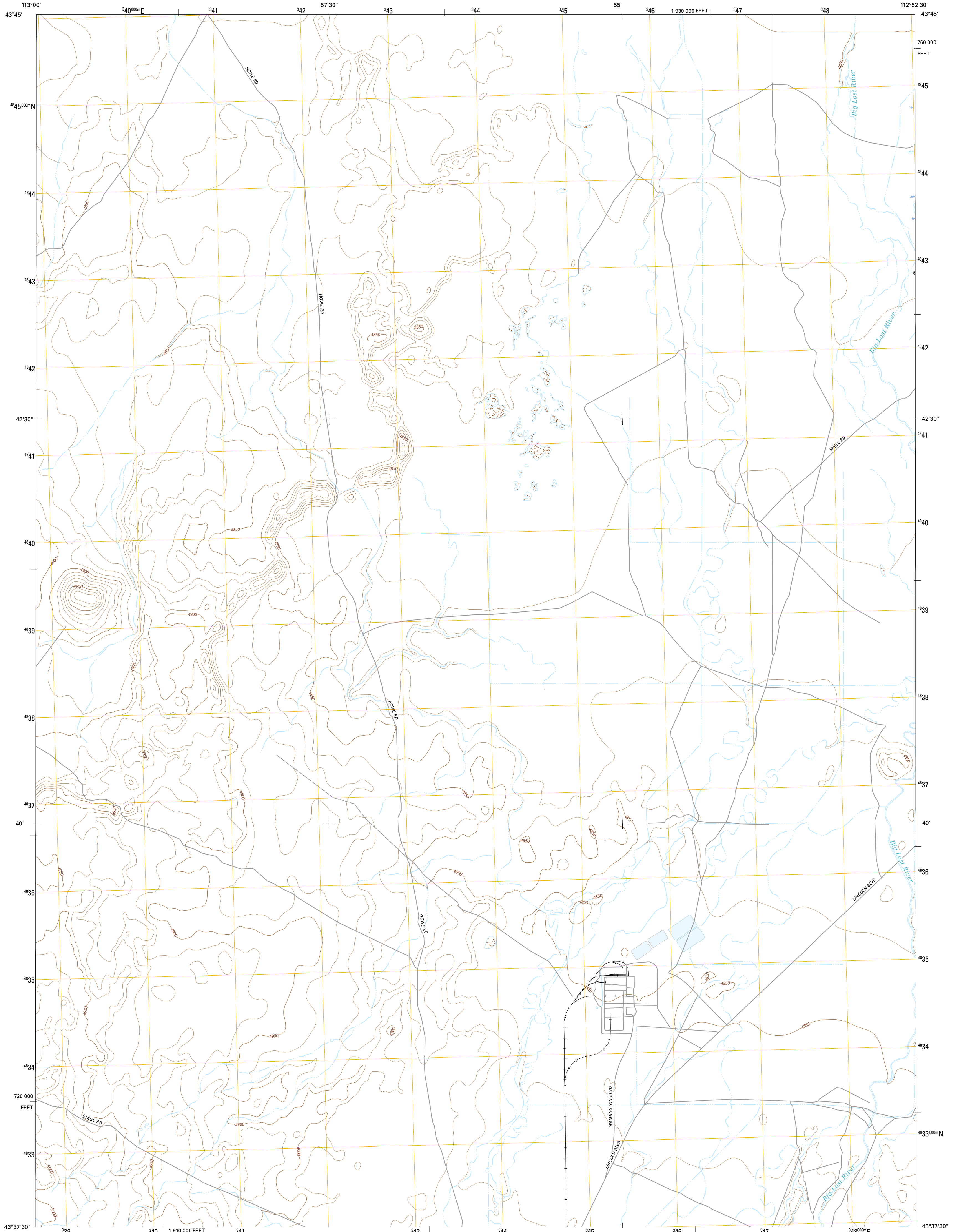
1 Howe  
 2 Little Lost River Sinks  
 3 Big Lost River Sinks  
 4 Howe Peak  
 5 North of Pegasus Flat  
 6 Area With U.C.  
 7 North of Scaville  
 8 Pegasus Flat

ROAD CLASSIFICATION

- Expressway
- Secondary Hwy
- Road
- Interstate Route
- US Route
- State Route
- Local Connector
- Local Road
- 4RD

EAST OF HOWE PEAK, ID  
 2017

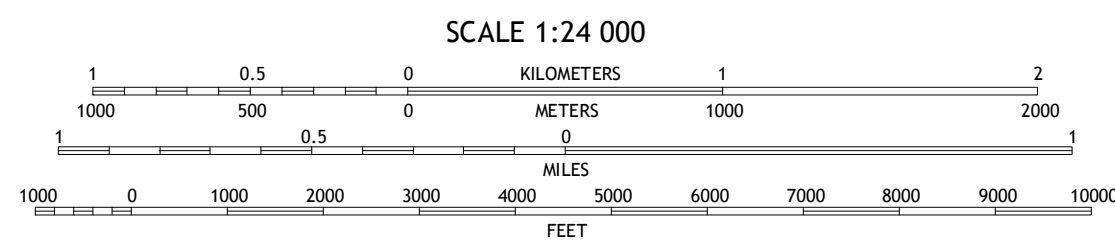
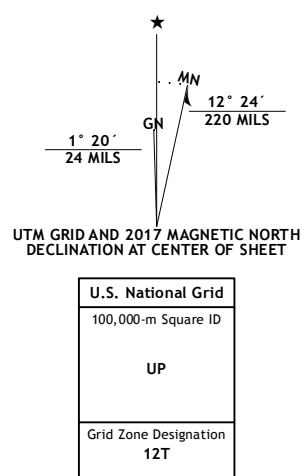




**Produced by the United States Geological Survey**  
North American Datum of 1983 (NAD83)  
World Geodetic System of 1984 (WGS84), Projection and  
1 000-meter grid: Universal Transverse Mercator, Zone 12T  
10 000-foot ticks: Idaho Coordinate System of 1983 (central  
zone)

This map is not a legal document. Boundaries may be  
generalized for this map scale. Private lands within government  
reservations may not be shown. Obtain permission before  
entering private lands.

Imagery.....N.A.P., December 2015  
Roads.....U.S. Census Bureau, 2015 - 2016  
Names.....National Hydrography Dataset, 2015  
Hydrography.....National Hydrography Dataset, 2015  
Contours.....National Elevation Dataset, 2002  
Boundaries.....Multiple sources; see metadata file 1922 - 2016  
Public Land Survey System.....BLM, 2015  
Wetlands.....FWS National Wetlands Inventory 1977 - 2014



CONTOUR INTERVAL 10 FEET  
NORTH AMERICAN VERTICAL DATUM OF 1988

This map was produced to conform with the  
National Geospatial Program US Topo Product Standard, 2011.  
A metadata file associated with this product is draft version 0.6.19



|   |   |   |
|---|---|---|
| 1 | 2 | 3 |
| 4 | 5 | 6 |
| 7 | 8 |   |

ADJOINING QUADRANGLES

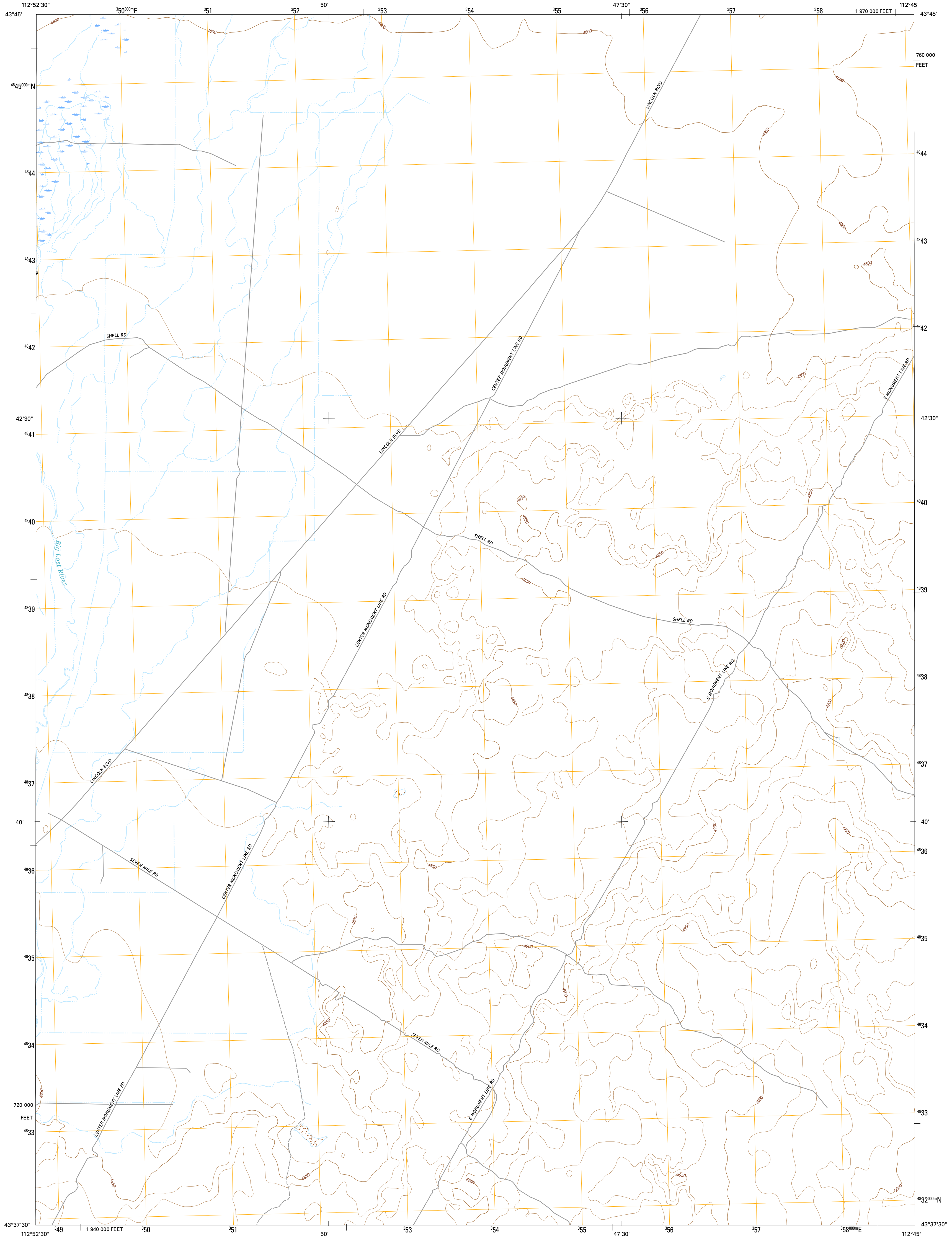
1 Howe  
2 Little Lost River Sinks  
3 Big Lost River Sinks  
4 Howe Peak  
5 North of Ryegrass Flat  
6 Arco Hills SE  
7 North of Scoville  
8 Ryegrass Flat

**EAST OF HOWE PEAK, ID**  
2017



# MAP #5 – NORTH OF RYE GRASS FLAT (1:24,000) / ARVFS

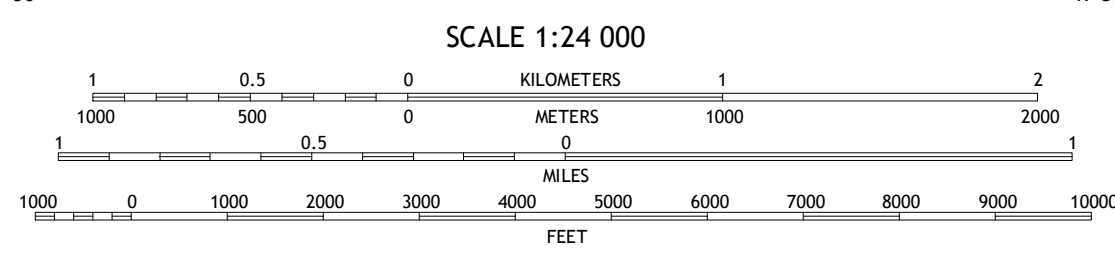
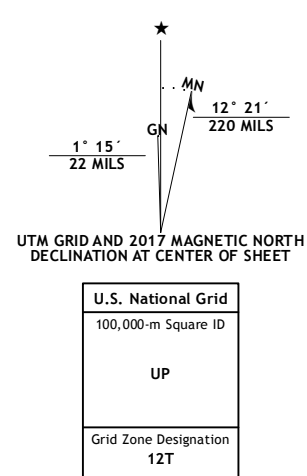




Produced by the United States Geological Survey  
North American Datum of 1983 (NAD83)  
World Geodetic System of 1984 (WGS84), Projection and  
1 000-meter grid: Universal Transverse Mercator, Zone 12T  
10 000-foot ticks: Idaho Coordinate System of 1983 (central zone)

This map is not a legal document. Boundaries may be generalized for this map scale. Private lands within government reservations may not be shown. Obtain permission before entering private lands.

Imagery.....N.A.I.P., December 2015  
Roads.....U.S. Census Bureau, 2015 - 2016  
Names.....G.N.S., 2016  
Hydrography.....National Hydrography Dataset, 2015  
Contours.....National Elevation Dataset, 2002  
Boundaries.....Multiple sources; see metadata file 1972 - 2016  
Public Land Survey System.....BLM, 2015  
Wetlands.....FWS National Wetlands Inventory 1977 - 2014



|   |   |   |
|---|---|---|
| 1 | 2 | 3 |
| 4 | 5 | 6 |
| 7 | 8 |   |

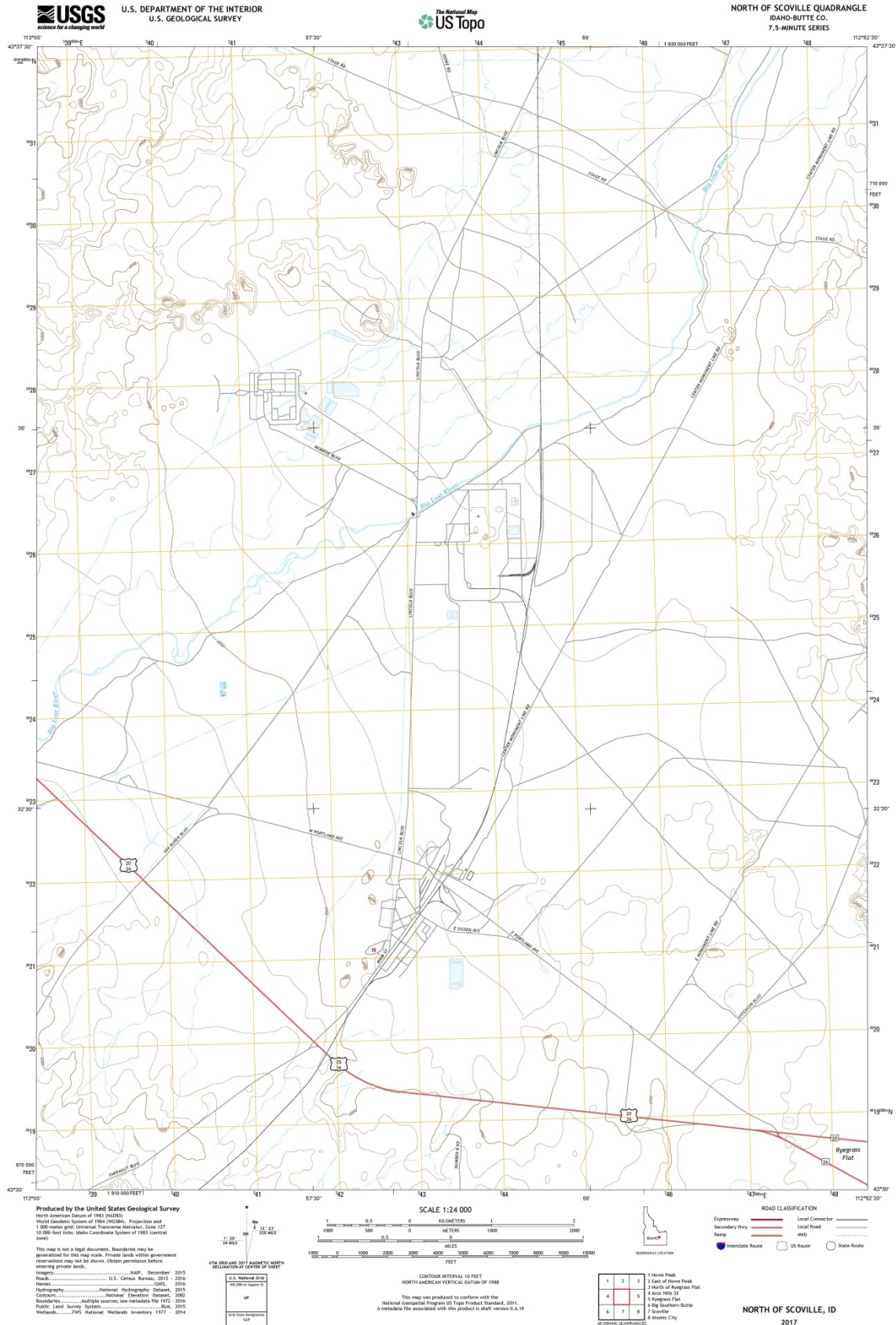
ADJOINING QUADRANGLES

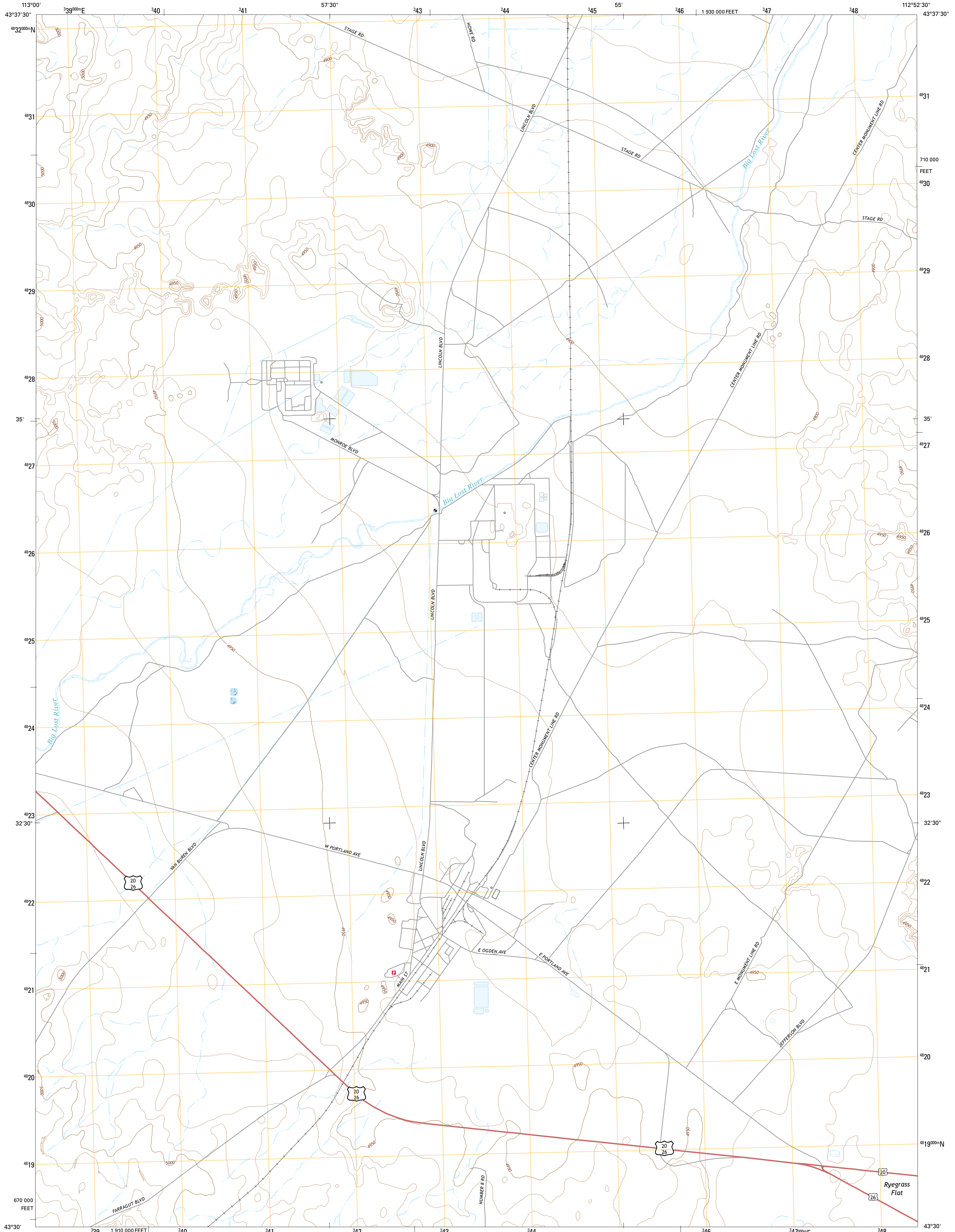
1 Little Lost River Sinks  
2 Big Lost River Sinks  
3 Circular Butte  
4 East of Howe Peak  
5 Little Butte NW  
6 North of Scoville  
7 Ryegrass Flat  
8 Little Butte SW

**NORTH OF RYEGRASS FLAT, ID**  
2017



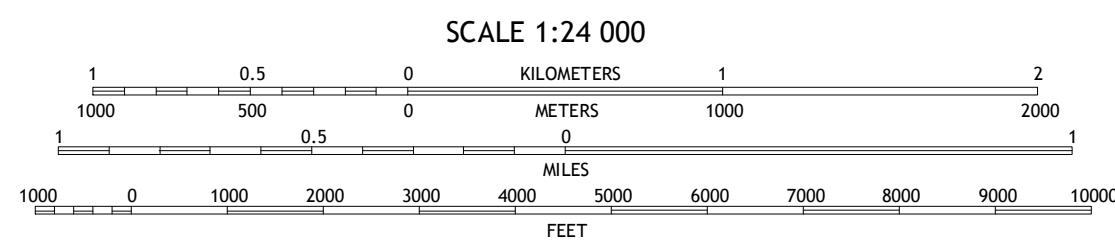
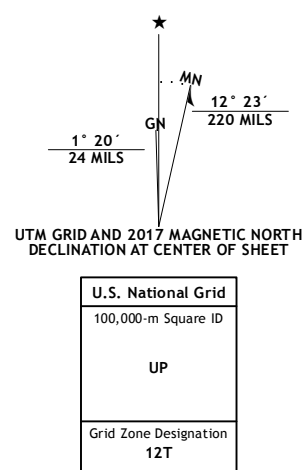
# MAP #6 – NORTH OF SCOVILLE (1:24,000) / ATR, INTEC, CFA, NODA





Produced by the United States Geological Survey North American Datum of 1983 (NAD83) World Geodetic System of 1984 (WGS84). Projection and 1 000-meter grid: Universal Transverse Mercator, Zone 12T 10 000-foot ticks: Idaho Coordinate System of 1983 (central zone)

This map is not a legal document. Boundaries may be generalized for this map scale. Private lands within government reservations may not be shown. Obtain permission before entering private lands. Imagery: NAIIP, December 2015 Roads: U.S. Census Bureau, 2015 Names: GNIS, 2016 Hydrography: National Hydrography Dataset, 2015 Contours: National Elevation Dataset, 2002 Boundaries: Multiple sources; see metadata file 1972 - 2016 Public Land Survey System: BLM, 2015 Wetlands: FWS National Wetlands Inventory 1977 - 2014

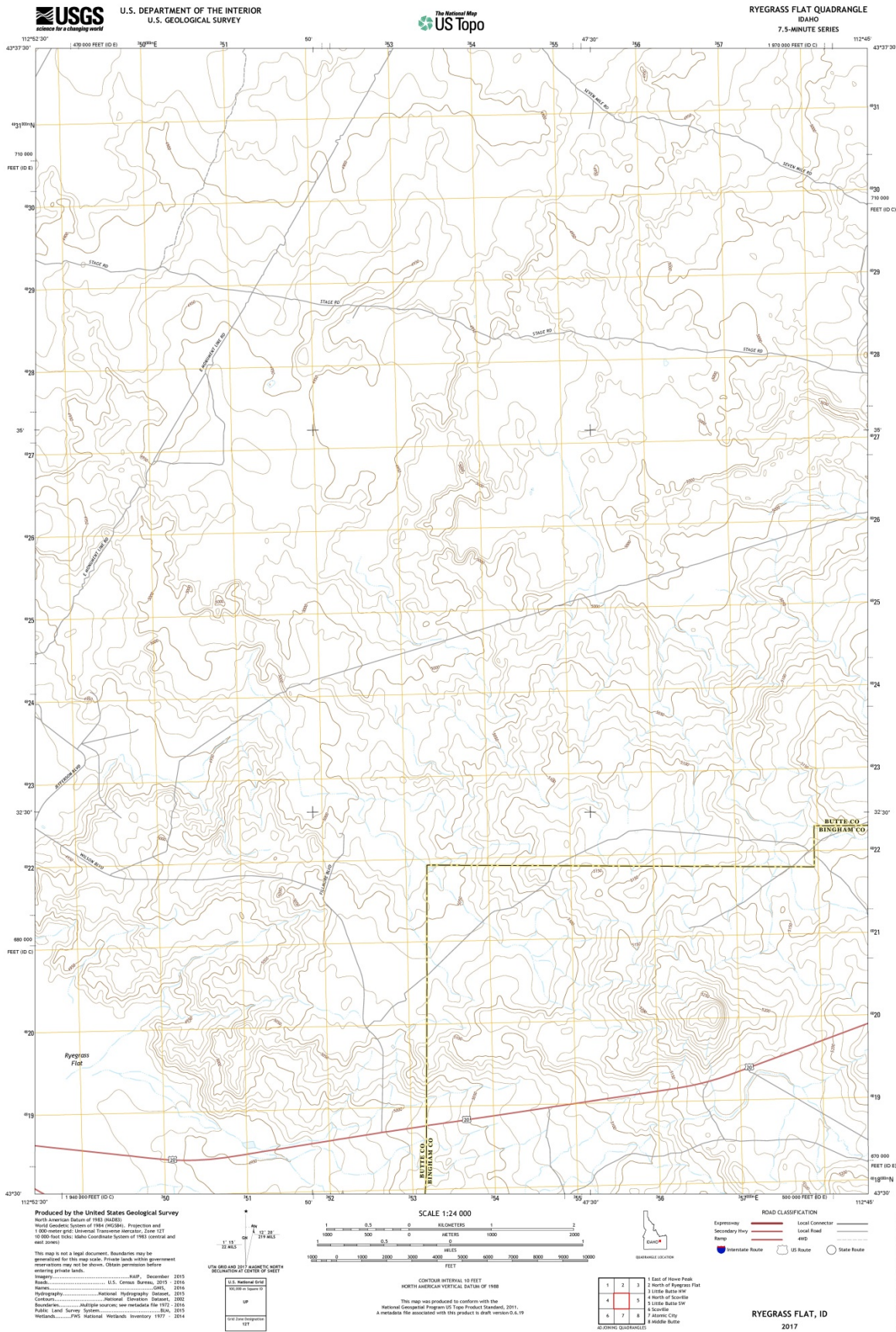


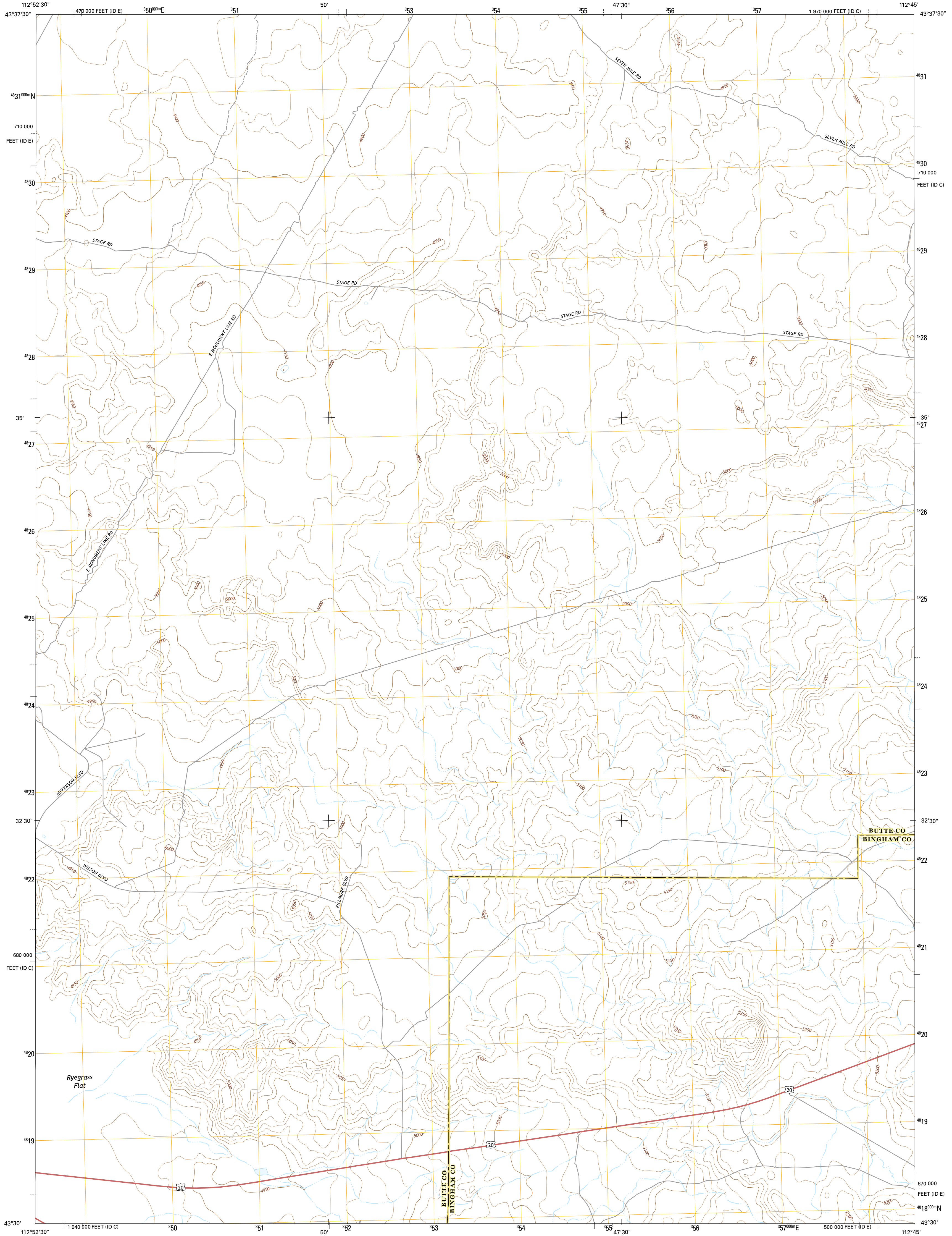
CONTOUR INTERVAL 10 FEET NORTH AMERICAN VERTICAL DATUM OF 1988 This map was produced to conform with the National Geospatial Program US Topo Product Standards, 2011. A metadata file associated with this product is draft version 0.6.19

ROAD CLASSIFICATION legend including symbols for Expressway, Secondary Hwy, Ramp, Interstate Route, US Route, State Route, Local Connector, Local Road, and 4WD. Includes a table for ADJOINING QUADRANGLES and a list of 8 landmarks: 1 Howe Peak, 2 East of Howe Peak, 3 North of Ryegrass Flat, 4 Arco Hills SE, 5 Ryegrass Flat, 6 Big Southern Butte, 7 Scoville, 8 Atomic City.



# MAP #7 – RYE GRASS FLAT (1:24,000) / SPERT II-IV, CITRC, ARA





Produced by the United States Geological Survey
North American Datum of 1983 (NAD83)
World Geodetic System of 1984 (WGS84). Projection and 1 000-meter grid: Universal Transverse Mercator, Zone 12T
10 000-foot ticks: Idaho Coordinate System of 1983 (central and east zones)
This map is not a legal document. Boundaries may be generalized for this map scale. Private lands within government reservations may not be shown. Obtain permission before entering private lands.
Imagery.....NAIP, December 2015
Roads.....U.S. Census Bureau, 2015 - 2016
Names.....GNIS, 2016
Hydrography.....National Hydrography Dataset, 2015
Contours.....National Elevation Dataset, 2002
Boundaries.....Multiple sources; see metadata file 1972 - 2016
Public Land Survey System.....BLM, 2015
Wetlands.....FWS National Wetlands Inventory 1977 - 2014

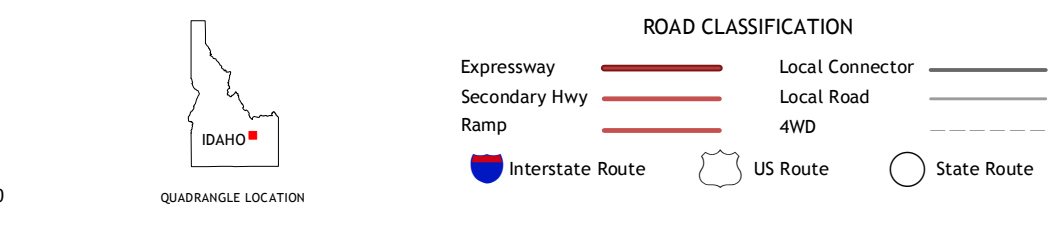
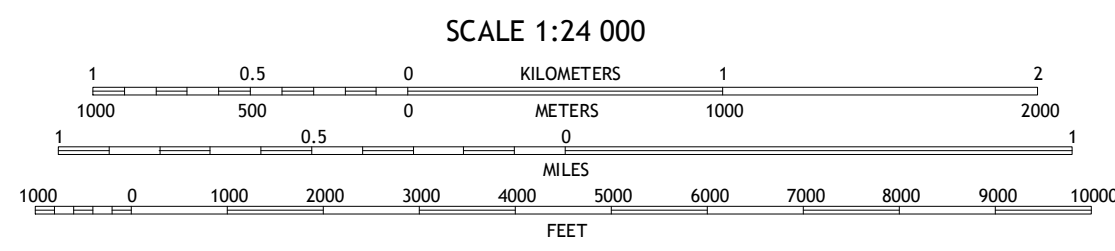
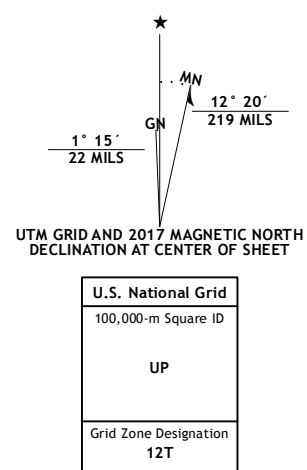
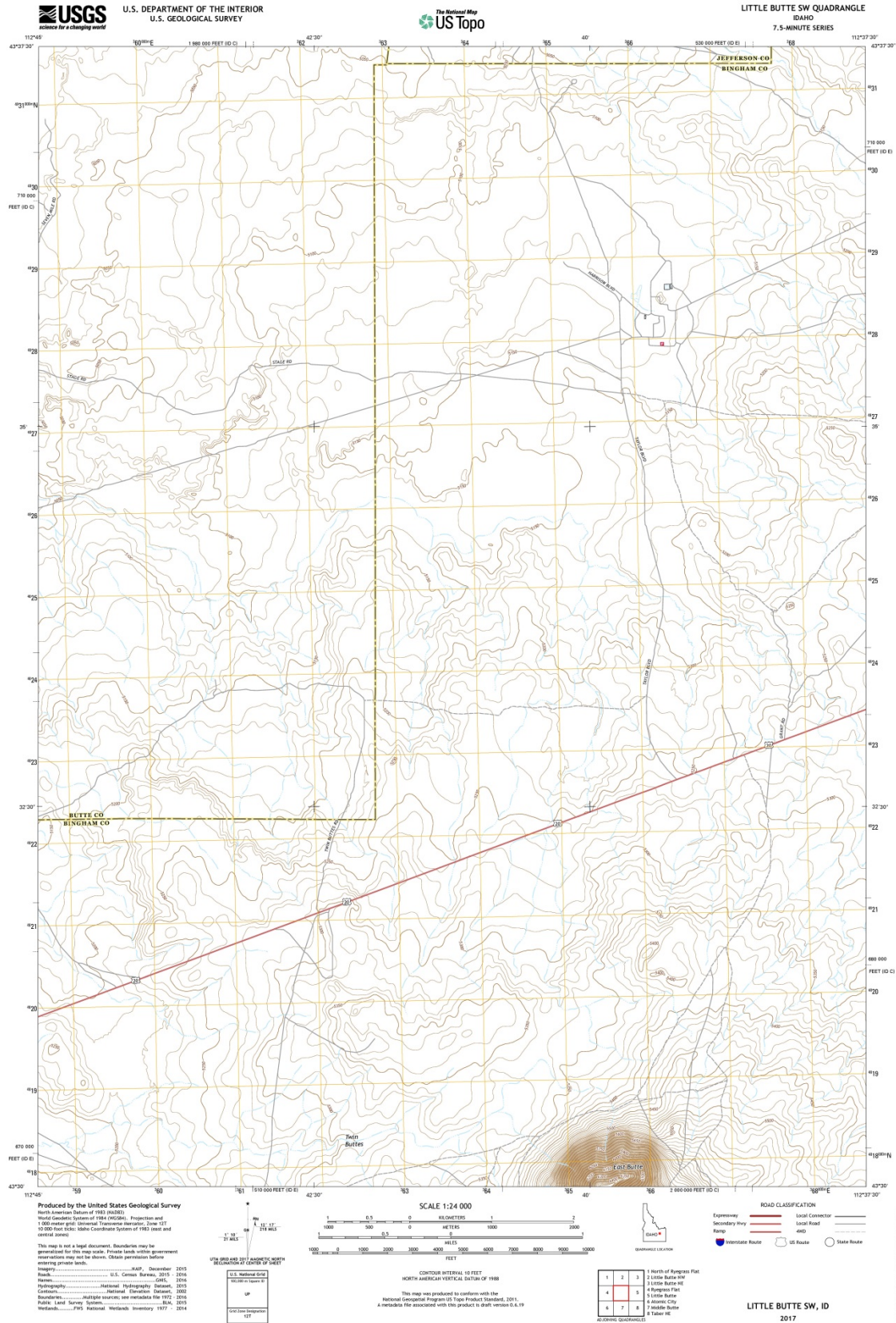
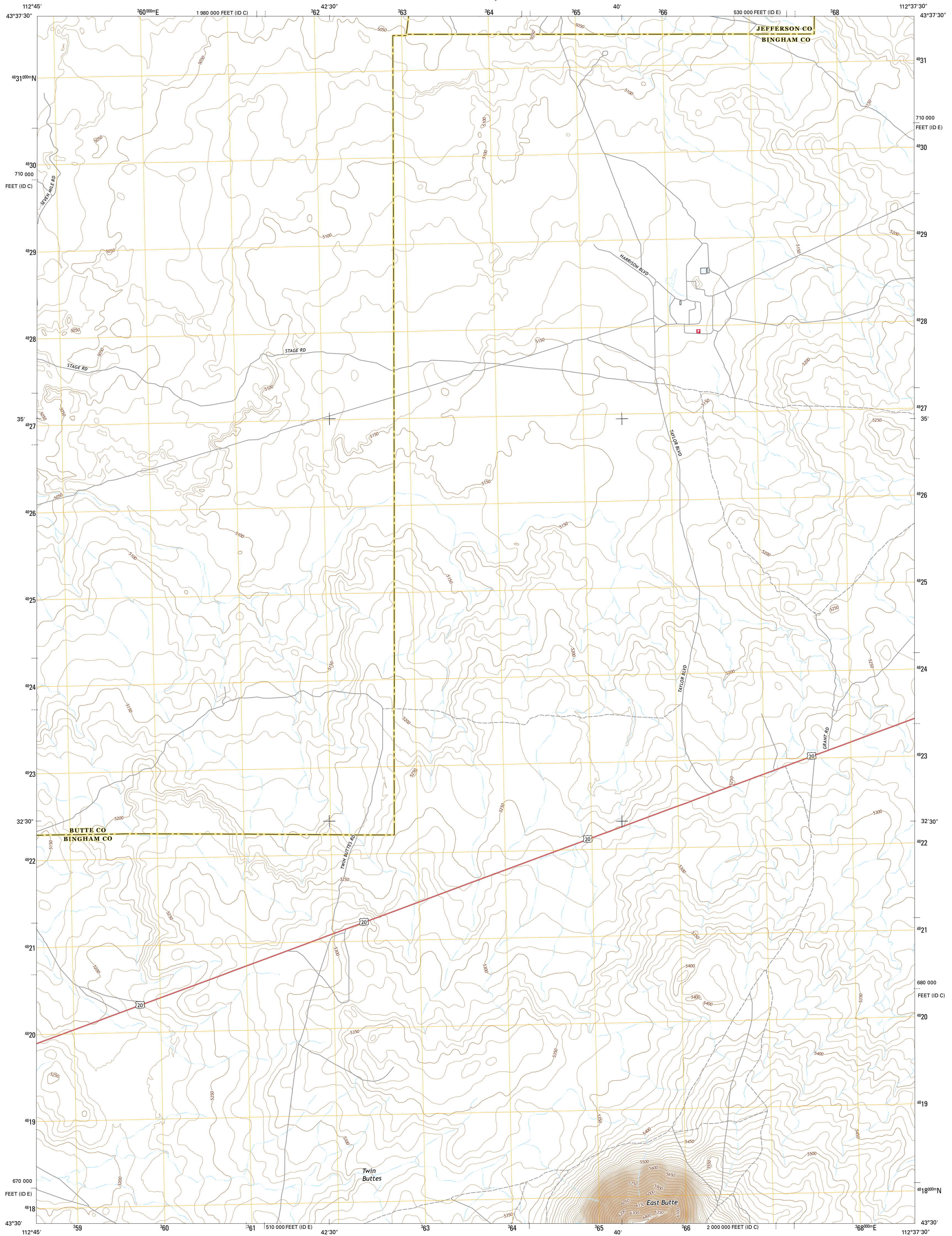


Table with 8 columns and 2 rows showing adjacent quadrangles: 1 East of Howe Peak, 2 North of Ryegrass Flat, 3 Little Butte NW, 4 North of Scoville, 5 Little Butte SW, 6 Scoville, 7 Alcanic City, 8 Middle Butte.



MAP #8 – LITTLE BUTTE SW (1:24,000) / MFC

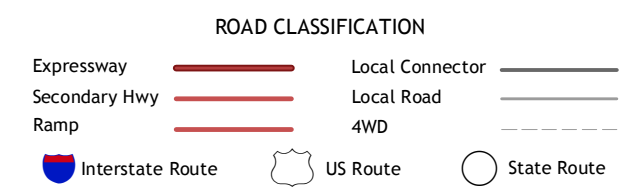
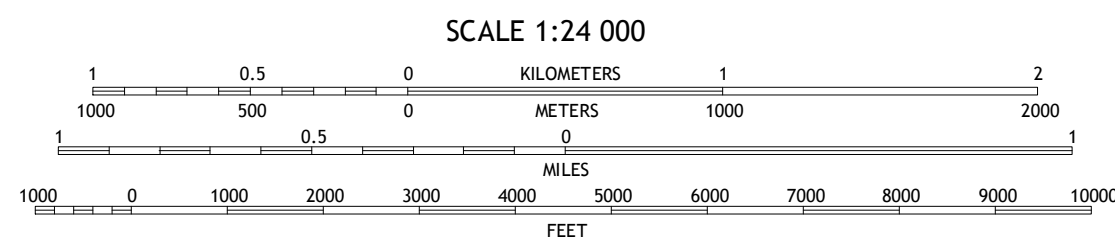
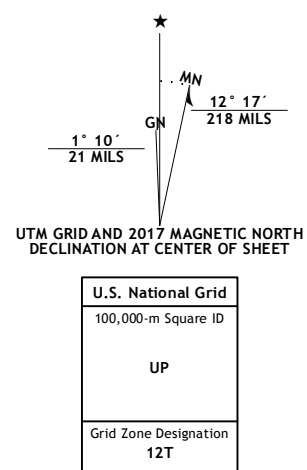




Produced by the United States Geological Survey  
North American Datum of 1983 (NAD83)  
World Geodetic System of 1984 (WGS84). Projection and  
1 000-meter grid: Universal Transverse Mercator, Zone 12T  
10 000-foot ticks: Idaho Coordinate System of 1983 (east and  
central zones)

This map is not a legal document. Boundaries may be  
generalized for this map scale. Private lands within government  
reservations may not be shown. Obtain permission before  
entering private lands.

Imagery.....NAIP, December 2015  
Roads.....U.S. Census Bureau, 2015 - 2016  
Names.....GNIS, 2016  
Hydrography.....National Hydrography Dataset, 2015  
Contours.....National Elevation Dataset, 2002  
Boundaries.....Multiple sources; see metadata file 1972 - 2016  
Public Land Survey System.....BLM, 2015  
Wetlands.....FWS National Wetlands Inventory 1977 - 2014



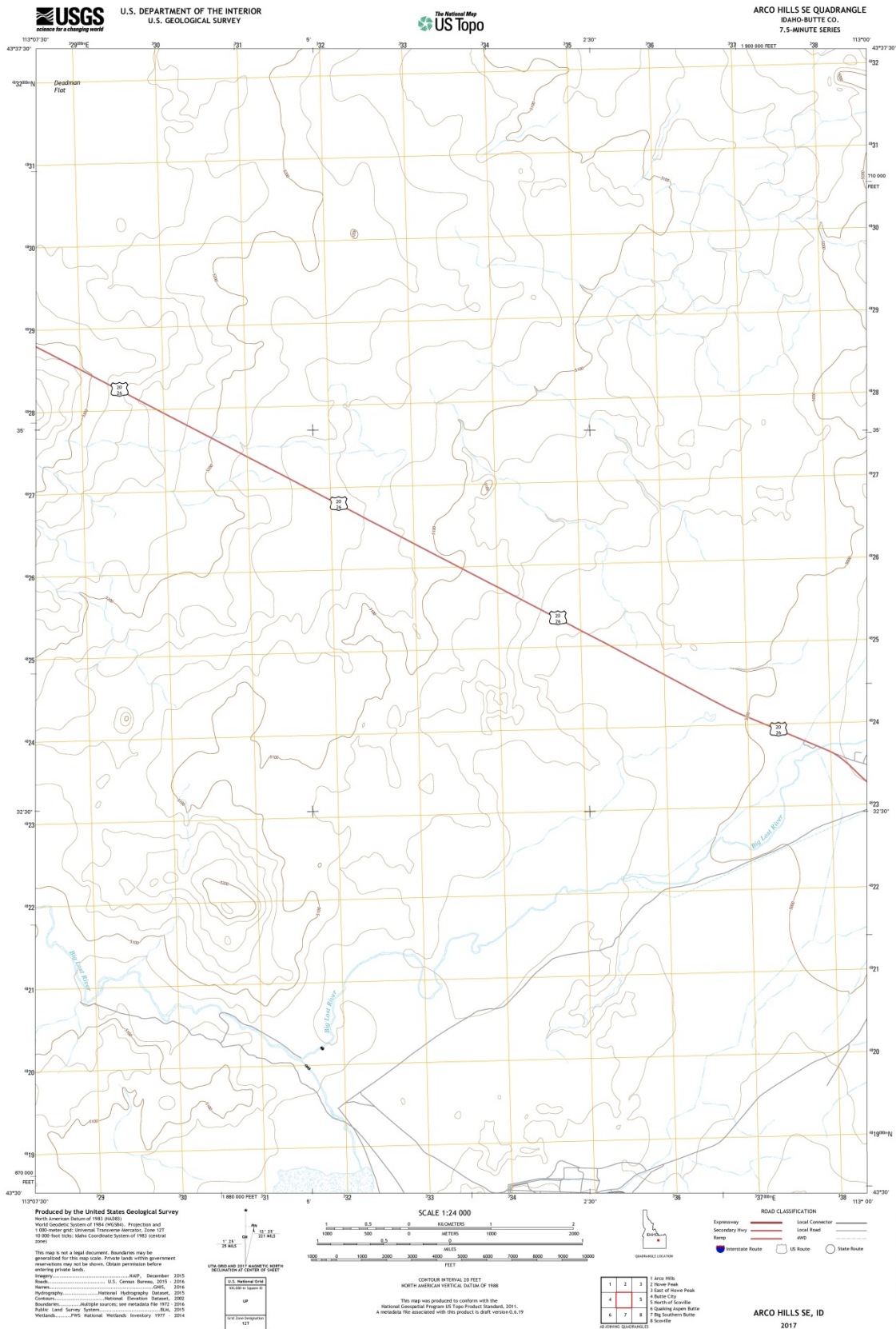
|   |   |   |
|---|---|---|
| 1 | 2 | 3 |
| 4 | 5 | 6 |
| 7 | 8 |   |

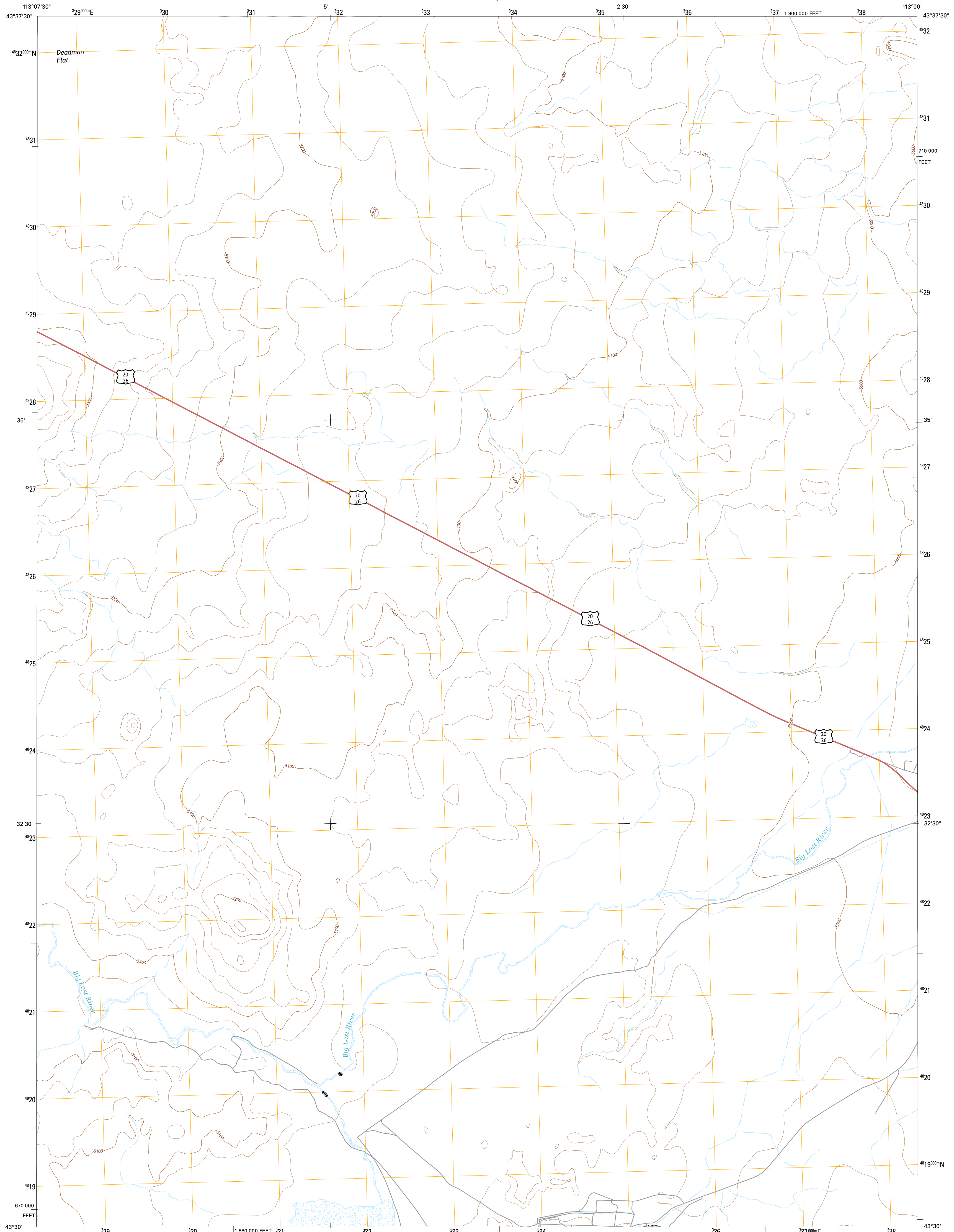
ADJOINING QUADRANGLES

**LITTLE BUTTE SW, ID**  
2017



# MAP #9 – ARCO HILLS SE (1:24,000) / NORTH OF RWMC (also see map #10), EBR-I, DIVERSION SYSTEM

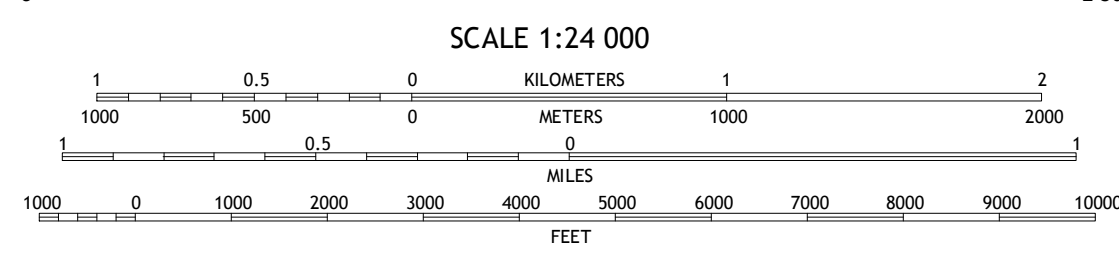
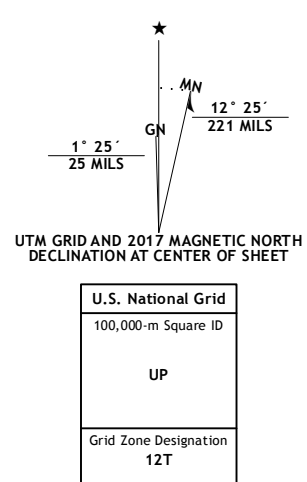




**Produced by the United States Geological Survey**  
North American Datum of 1983 (NAD83)  
World Geodetic System of 1984 (WGS84). Projection and  
1 000-meter grid: Universal Transverse Mercator, Zone 12T  
10 000-foot ticks: Idaho Coordinate System of 1983 (central  
zone)

This map is not a legal document. Boundaries may be  
generalized for this map scale. Private lands within government  
reservations may not be shown. Obtain permission before  
entering private lands.

Imagery.....N.A.I.P., December 2015  
Roads.....U.S. Census Bureau, 2015 - 2016  
Names.....GNIS, 2016  
Hydrography.....National Hydrography Dataset, 2015  
Contours.....National Elevation Dataset, 2002  
Boundaries.....Multiple sources; see metadata file 1922 - 2016  
Public Land Survey System.....BLM, 2015  
Wetlands.....FWS National Wetlands Inventory 1977 - 2014



**ROAD CLASSIFICATION**

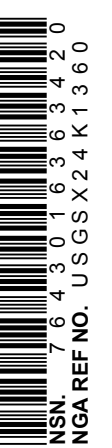
|                  |                 |
|------------------|-----------------|
| Expressway       | Local Connector |
| Secondary Hwy    | Local Road      |
| Ramp             | 4WD             |
| Interstate Route | US Route        |
|                  | State Route     |

**ADJOINING QUADRANGLES**

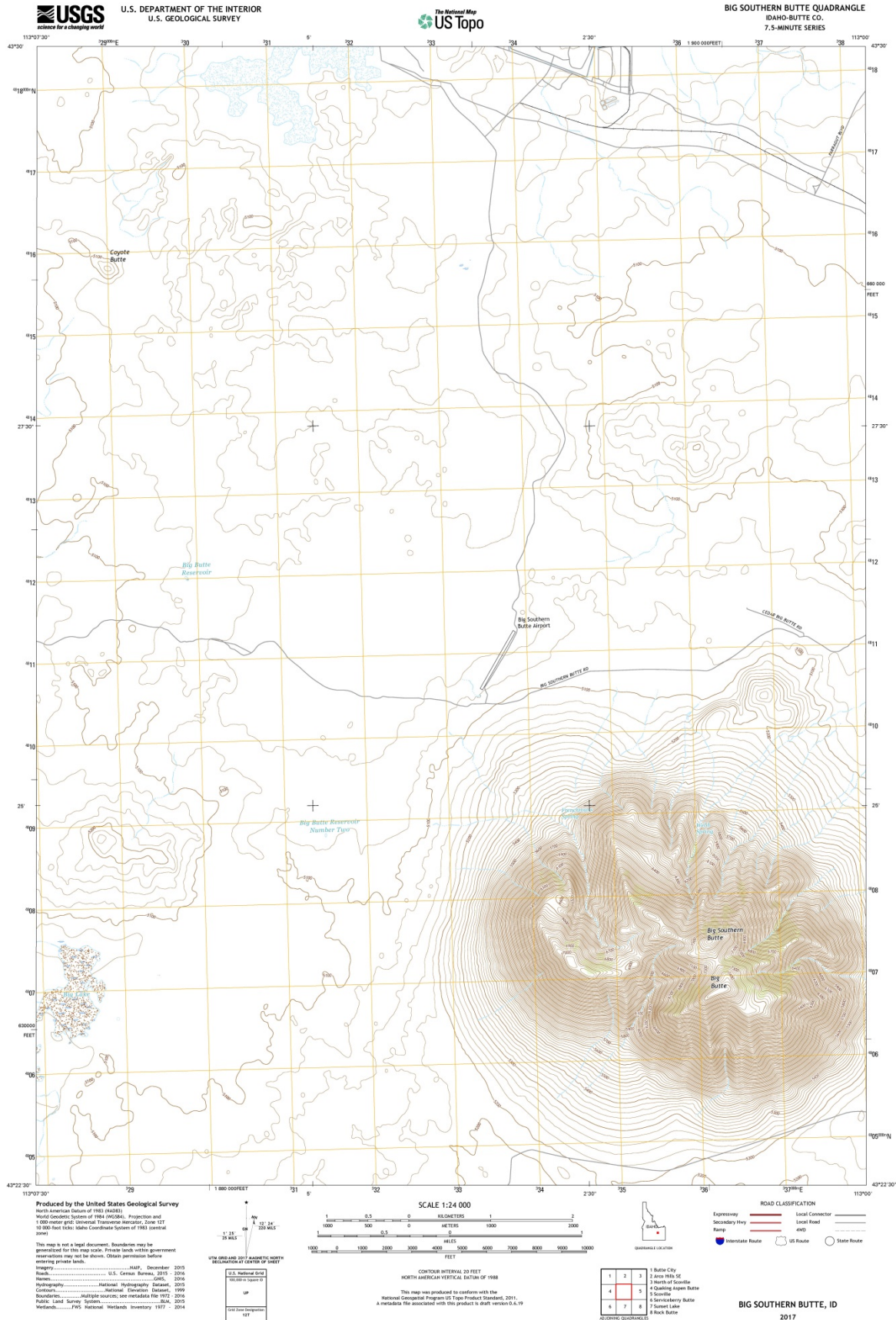
|   |   |   |
|---|---|---|
| 1 | 2 | 3 |
| 4 | 5 | 6 |
| 7 | 8 | 9 |

1 Arco Hills  
2 Howe Peak  
3 East of Howe Peak  
4 Butte City  
5 North of Scoville  
6 Quaking Aspen Butte  
7 Big Southern Butte  
8 Scoville

**ARCO HILLS SE, ID**  
2017



# MAP #10 – BIG SOUTHERN BUTTE (1:24,000) / RWMC (also see map #9), DIVERSION SYSTEM







**APPENDIX II**  
**FLOOD INSURANCE RATE MAPS**

## CONTENTS

- Map #1. Flood Insurance Rate Map of Bingham County, Idaho (unincorporated areas) – Community Panel Number 160018 0025 B – Effective Date: November 15, 1979.
- Map #2. Flood Insurance Rate Map of Butte County, Idaho (unincorporated areas) - Community Panel Numbers 160033 0001-475 – Effective Date: June 3, 1986.
- Map #3. Flood Insurance Rate Map of Bingham County, Idaho (unincorporated areas) – Community Panel Numbers 160018 0001-0750 – Effective Date: October 20, 1998





**KEY TO MAP**

500-Year Flood Boundary ————

100-Year Flood Boundary ————

Zone Designations\* With Date of Identification e.g., 10/2/74

100-Year Flood Boundary ————

500-Year Flood Boundary ————

Base Flood Elevation Line With Elevation In Feet\*\*

Base Flood Elevation In Feet Where Uniform Within Zone\*\*

Elevation Reference Mark

River Mile

**ZONE B**

**ZONE A1 DATE**

**ZONE A2 DATE**

**ZONE B**

—513—

(EL 987)

RM7x

•M1.5

\*\*Referenced to the National Geodetic Vertical Datum of 1929

- \*EXPLANATION OF ZONE DESIGNATIONS**
- | ZONE   | EXPLANATION  |
|--------|--|
| A      | Areas of 100-year flood; base flood elevations and flood hazard factors not determined.  |
| A0     | Areas of 100-year shallow flooding where depths are between one (1) and three (3) feet; average depths of inundation are shown, but no flood hazard factors are determined.  |
| AH     | Areas of 100-year shallow flooding where depths are between one (1) and three (3) feet; base flood elevations are shown, but no flood hazard factors are determined.   |
| A1-A30 | Areas of 100-year flood; base flood elevations and flood hazard factors determined.  |
| A99    | Areas of 100-year flood to be protected by flood protection system under construction; base flood elevations and flood hazard factors not determined.  |
| B      | Areas between limits of the 100-year flood and 500-year flood; or certain areas subject to 100-year flooding with average depths less than one (1) foot or where the contributing drainage area is less than one square mile; or areas protected by levees from the base flood. (Medium shading) |
| C      | Areas of minimal flooding. (No shading)  |
| D      | Areas of undetermined, but possible, flood hazards.  |
| V      | Areas of 100-year coastal flood with velocity (wave action); base flood elevations and flood hazard factors not determined.  |
| V1-V30 | Areas of 100-year coastal flood with velocity (wave action); base flood elevations and flood hazard factors determined.  |

**NOTES TO USER**

Certain areas not in the special flood hazard areas (zones A and V) may be protected by flood control structures.

This map is for flood insurance purposes only; it does not necessarily show all areas subject to flooding in the community or all planimetric features outside special flood hazard areas.

For adjoining map panels, see separately printed Index To Map Panels.

**INITIAL IDENTIFICATION:**  
JUNE 20, 1978

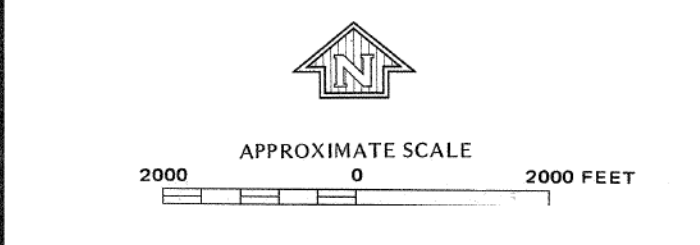
**FLOOD HAZARD BOUNDARY MAP REVISIONS:**

**FLOOD INSURANCE RATE MAP EFFECTIVE:**  
NOVEMBER 15, 1979

**FLOOD INSURANCE RATE MAP REVISIONS:**

Refer to the FLOOD INSURANCE RATE MAP EFFECTIVE date shown on this map to determine when actual rates apply to structures in the zones where elevations or depths have been established.

To determine if flood insurance is available in this community, contact your insurance agent, or call the National Flood Insurance Program, at (800) 638-6620, or (800) 424-8872.



**NATIONAL FLOOD INSURANCE PROGRAM**

**FIRM**  
FLOOD INSURANCE RATE MAP

**BINGHAM COUNTY, IDAHO**  
(UNINCORPORATED AREAS)

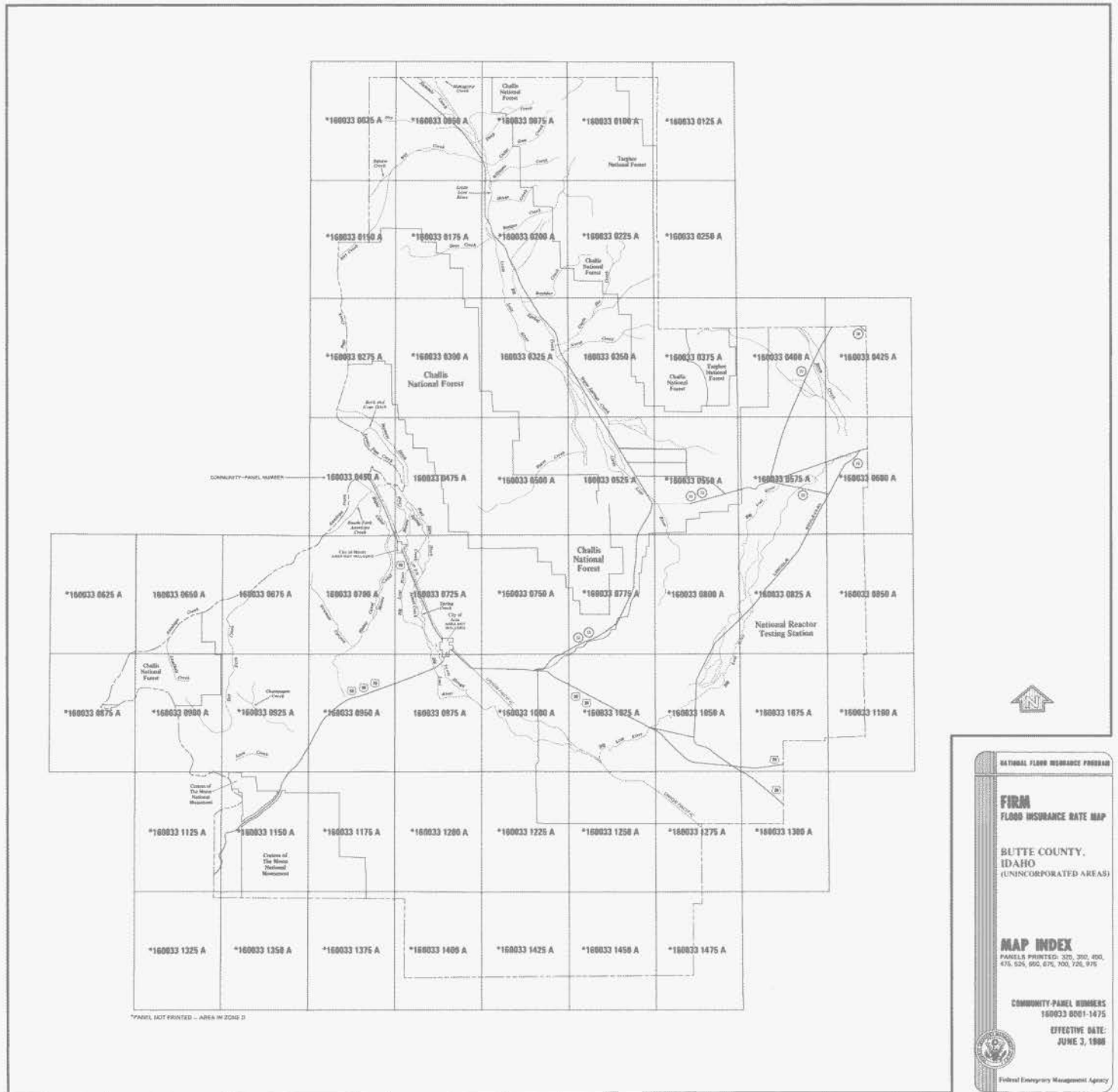
**PANEL 25 OF 750**  
(SEE MAP INDEX FOR PANELS NOT PRINTED)

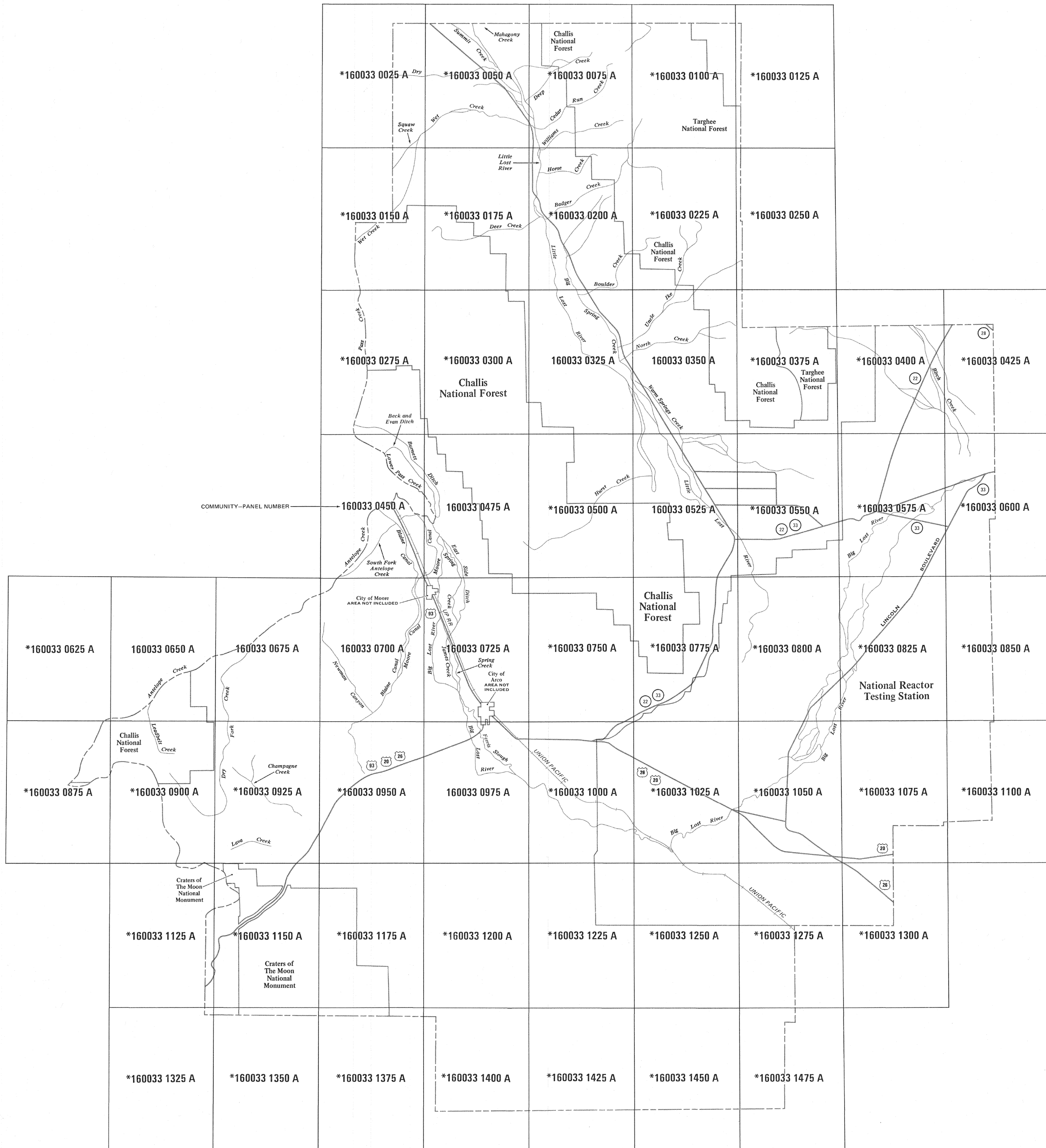
**COMMUNITY-PANEL NUMBER**  
160018 0025 B

**EFFECTIVE DATE:**  
NOVEMBER 15, 1979

**U.S. DEPARTMENT OF HOUSING AND URBAN DEVELOPMENT**  
FEDERAL INSURANCE ADMINISTRATION

### MAP #2 - Flood Insurance Rate Map of Butte County, Idaho (unincorporated areas) - Community Panel Numbers 160033 0001-475





\*PANEL NOT PRINTED - AREA IN ZONE D



NATIONAL FLOOD INSURANCE PROGRAM

**FIRM**  
FLOOD INSURANCE RATE MAP

BUTTE COUNTY,  
IDAHO  
(UNINCORPORATED AREAS)

**MAP INDEX**

PANELS PRINTED: 325, 350, 450,  
475, 525, 650, 675, 700, 725, 975

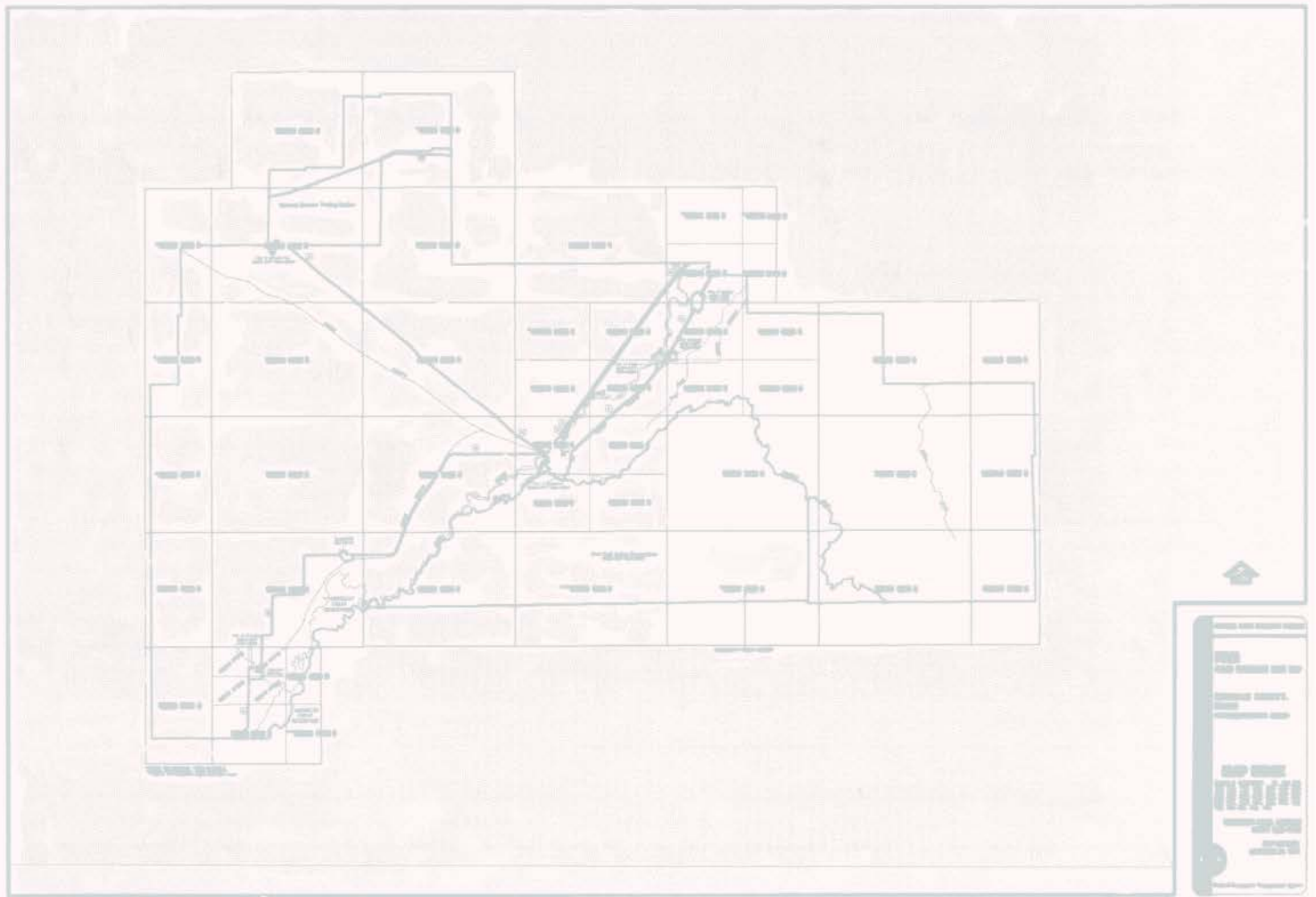
COMMUNITY-PANEL NUMBERS  
160033 0001-1475

EFFECTIVE DATE:  
JUNE 3, 1986



Federal Emergency Management Agency

**MAP #3 – Flood Insurance Rate Map of Bingham County, Idaho (unincorporated areas) – Community Panel Numbers 160018 0001-0750**







APPENDIX III

BIG LOST RIVER FLOOD HAZARD STUDY,  
IDAHO NATIONAL LABORATORY, U.S. BUREAUS OF RELCAMATION, 2005

**APPENDIX III. Big Lost River Flood Hazard Study, Idaho National Laboratory,  
Idaho, U.S. Bureau of Reclamation**

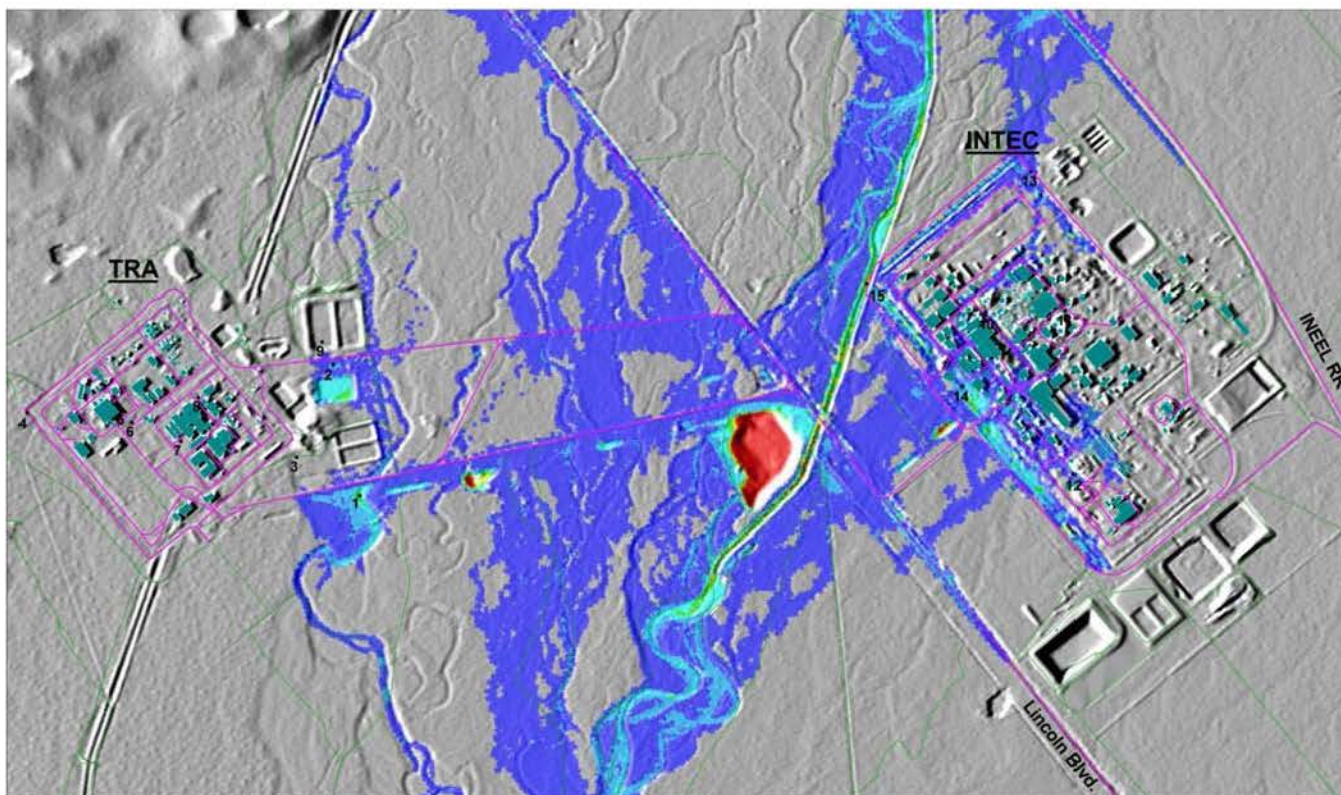
# RECLAMATION

*Managing Water in the West*

## Big Lost River Flood Hazard Study

Idaho National Laboratory, Idaho

Summary Document



U.S. Department of the Interior  
Bureau of Reclamation  
Technical Service Center  
Seismotectonics and Geophysics Group  
Denver, Colorado

November 2005

## **Mission Statements**

The mission of the Department of the Interior is to protect and provide access to our Nation's natural and cultural heritage and honor our trust responsibilities to Indian Tribes and our commitments to island communities.

The mission of the Bureau of Reclamation is to manage, develop, and protect water and related resources in an environmentally and economically sound manner in the interest of the American public.

# **Big Lost River Flood Hazard Study Idaho National**

**Idaho National Laboratory, Idaho**

**Summary Document**

**Report 2005-2**

*Prepared by*

**Dean A. Ostenaar  
Daniel R.H. O'Connell**



**U.S. Department of the Interior  
Bureau of Reclamation  
Technical Service Center  
Seismotectonics and Geophysics Group  
Denver, Colorado**

**November 2005**

Prepared by:

\_\_\_\_\_  
Dean A. Ostenaar

November 14, 2005  
Date

\_\_\_\_\_  
Daniel R.H. O'Connell

November 14, 2005  
Date

TSC Peer Review by:

\_\_\_\_\_  
Jon P. Ake

November 14, 2005  
Date

## OVERVIEW

### Introduction and Objectives

Paleoflood studies of the Big Lost River (Ostenaar et al., 1999; 2002) indicated that potential flood hazards for the Big Lost River at the Idaho National Laboratory (INL) (previously Idaho National Environmental and Engineering Laboratory (INEEL)) might be significantly different than portrayed by previous studies (e.g., Kjelstrom and Berenbrock, 1996). Because of the significant discrepancy between the previous studies (**Table SO-1**), additional studies aimed at reducing the uncertainty in flood hazard estimates at INL have been undertaken by both U.S. Geological Survey (USGS) (e.g., Hortness and Rousseau, 2003; Berenbrock and Doyle, 2004; Berenbrock et al., in prep.) and Bureau of Reclamation (BOR). The present document and the associated appendices describe the results from BOR studies of the Big Lost River flood hazard at INL. Differences in the estimate of the 100-year peak flow shown by previous studies (**Table SO-1**) are primarily due to the use of differing data in each of the analyses. Kjelstrom and Berenbrock (1996) and Hortness and Rousseau (2003) used stream-gage data from Big Lost River and surrounding region. Ostenaar et al. (1999, 2002) used stream-gage and paleoflood data from the Big Lost River at INL. Estimates of 100-year peak flow require extrapolation beyond the length of the available stream gage data record, whereas inclusion of geologic paleoflood data lengthens the record of peak flow to many times beyond a hundred-year time period.

The major objectives of the BOR studies are focused on two broad technical arenas; 1) geologic, geomorphic, and hydraulic modeling studies to reduce the uncertainty associated with paleohydrologic estimates used in flood frequency analyses, and 2) developing probabilistic flood stage estimates for specific facility locations at INTEC and TRA.

The paleohydrologic studies have focused on detailed studies of a 5-km (3-mi) reach of the Big Lost River that extends between the INEEL Diversion Dam and the historic Pioneer Diversion. In this reach, 1:4000-scale aerial photography flown in September 2000 was used to develop a 3-ft topographic grid that could be rendered as the base map for detailed geomorphic mapping of the study reach and as topographic input for updated two-dimensional hydraulic modeling. To improve the geologic data for paleoflood and paleohydrologic bound estimates, seven trenches at three detailed study sites were excavated within the study reach. From the geomorphic mapping,

trenching data and updated hydraulic modeling, revised estimates of paleofloods and paleohydrologic bounds for the Big Lost River were developed. These data were used to revise and update the unregulated flood frequency analyses for the Big Lost River.

**Table SO-1 Comparison of Revised Flood Frequency for the Big Lost River at the Diversion Dam with Previous Study Results.**

| AEP<br>(1/yr)        | Return<br>period<br>(yr) | Present Study             |  |                            | Previous Studies                               |  |  |
|----------------------|--------------------------|---------------------------|--|----------------------------|--|--|--|
|                      |                          | 5%<br>(m <sup>3</sup> /s) | mean<br>m <sup>3</sup> /s (ft <sup>3</sup> /s) | 95%<br>(m <sup>3</sup> /s) | Ostenaar et<br>al. (1999)                      | Kjelstrom<br>and<br>Berenbrock<br>(1996)       | Hortness<br>and<br>Rousseau<br>(2003)          |
|                      |                          |                           |  |                            | mean<br>m <sup>3</sup> /s (ft <sup>3</sup> /s) | mean<br>m <sup>3</sup> /s (ft <sup>3</sup> /s) | mean<br>m <sup>3</sup> /s (ft <sup>3</sup> /s) |
| 5 x 10 <sup>-2</sup> | 20                       | 63                        | 75 (2649)                                      | 83                         | 57 (2023)                                      |  |  |
| 2 x 10 <sup>-2</sup> | 50                       | 75                        | 83 (2931)                                      | 91                         | 72 (2545)                                      |  |  |
| 1 x 10 <sup>-2</sup> | 100                      | 78                        | 87 (3072)                                      | 97                         | 82 (2910)                                      | 206 (7260)                                     | 106 (3750)                                     |
| 5 x 10 <sup>-3</sup> | 200                      | 82                        | 96 (3390)                                      | 114                        | 92 (3252)                                      |  |  |
| 2 x 10 <sup>-3</sup> | 500                      | 89                        | 110 (3885)                                     | 137                        | 104 (3669)                                     |  |  |
| 1 x 10 <sup>-3</sup> | 1000                     | 101                       | 131 (4626)                                     | 163                        | 112 (3960)                                     |  |  |
| 5 x 10 <sup>-4</sup> | 2000                     | 127                       | 159 (5615)                                     | 194                        | 120 (4232)                                     |  |  |
| 2 x 10 <sup>-4</sup> | 5000                     | 148                       | 188 (6639)                                     | 236                        | 129 (4564)                                     |  |  |
| 1 x 10 <sup>-4</sup> | 10,000                   | 185                       | 279 (9853)                                     | 412                        | 136 (4796)                                     |  |  |
| 5 x 10 <sup>-5</sup> | 20,000*                  | 245                       | 416*(14691)                                    | 628*                       | 142 (5012)                                     |  |  |

\* Values with diminished or little statistical significance.  
AEP - Annual Exceedence Probability

Developing probabilistic stage estimates for INTEC and TRA facility sites included three major work activities: 1) reprocessing of the 1993 1:10,000-scale aerial photography along the Big Lost River to generate a 5-ft topographic grid for use in two-dimensional hydraulic modeling, 2) two-dimensional hydraulic modeling of multiple flow scenarios between the INEEL Diversion Dam to downstream of INTEC and TRA, and 3) estimating stage probability curves for facility sites that could include alternate views and uncertainties in flood frequency, infiltration, and culvert flows on the INL site.

Initial hydraulic modeling for the paleohydrologic studies based on the 3-ft grid topographic data for the Diversion Dam reach showed results that differed significantly from the previous studies

of Ostenaar et al. (1999, 2002) which used topographic data derived from the 1993 INEEL 2-ft contour map. Because the same two-dimensional hydraulic model was being used in both studies, the cause of this difference was clearly related to the input topography used in the models. To resolve these discrepancies, extensive GPS field surveys along the Big Lost River were conducted to assess the accuracy of the topographic mapping used in all phases of these studies. The GPS field surveys found that the 1993 INEEL 2-ft contour map did not appear to meet standards for 4-ft contour interval mapping and that in the area of the paleoflood study reach the surface defined by this mapping was apparently warped (**Appendix A**). The lack of resolution and accuracy associated with the 1993 2-ft contour map resulted in systematic overestimation of stages associated with discharge in the Big Lost River in the previous studies. Because similar issues to topographic accuracy would affect model estimates of flood stage probability at INTEC and TRA, data from the 1993 aerial photography was reprocessed to provide an updated topographic dataset for the hydraulic modeling. GPS field surveys of selected areas along the Big Lost River corridor demonstrate that the topographic data from the 2000 photography in the paleoflood study reach and reprocessed data from the 1993 photography both meet accuracy standards needed for the high-resolution flood modeling (**Appendix A**).

### **Outline of the Final Report**

The overall scope of the present study is large and has included extensive data acquisition, field investigations, and computational efforts. Documentation of the study is contained in three elements: 1) this Overview, 2) Summary Document, and 3) Appendices. This Overview provides the major results of these efforts and key conclusions for flood hazard studies of the Big Lost River at INL. Within the Summary Document, **Section 1** provides introduction and background. **Section 2** and **Section 3** describe the geologic, geomorphic and hydraulic modeling investigations to further evaluate the paleohydrologic data used for flood frequency estimates of the Big Lost River. **Section 4** provides an updated flood frequency analyses based on these data. **Section 5** describes the hydraulic modeling and conceptual framework for evaluating stage-probability estimates for selected sites at INTEC and TRA. Topographic and geomorphic maps for the Diversion Dam study reach are shown on **Plate 1** and **Plate 2**. Additional supporting documentation is contained in several appendices that accompany this report as follows:

**Appendix A - Quality Assurance of Topographic Data****Appendix B - Geologic Data**

Soil Profile Descriptions

Soil Particle Size Analysis Results from Colorado State University

Examination of Bulk Soil for Radiocarbon Datable Material from Along the Big Lost River on the Idaho National Engineering and Environmental Laboratory (INEEL) site by K. Puseman, Paleo Research Institute.

Radiocarbon Dating Results and Calibration Data from Beta Analytic

Summary Report on Detrital Zircon Ages of Samples from Big Lost River Trenches by P.K. Link, Idaho State Univ., and C.M. Fanning, Australian National University

Explanation, Plots, and Procedures for Point and Pebble Counts and Sieve Data by V. Sheedy, Idaho State Univ.

Gamma Ray Spectrometry Results from J. Budahn, U.S. Geological Survey

Trench Sample Listings

**Appendix B - Electronic Supplement - Trench Logs****Appendix C - Hydraulic Modeling Methodology and Quality Assurance**

Part A - Methodology, mesh generation, and models

Part B - Quality Assurance

**Appendix D - Hydraulic Modeling Results for Paleoflood Analyses**

Evaluating Paleohydrologic Data with Stream Power and Shear Stress Results from Hydraulic Models

**Appendix D - Electronic Supplement - Plots of Modeled Depth, Stream Power and Shear Stress for the Big Lost River, INEEL Diversion Dam Reach****Appendix E - Hydraulic Modeling to Estimate Big Lost River Flood Inundation at INEEL Facility Sites**

Estimating Channel Infiltration Parameters from Historical Flow Data at INEEL

Infiltration Rates to Support High-Resolution Hydraulic Modeling at Idaho National Engineering and Environmental Laboratory by F.R. Fiedler, University of Idaho

Culvert Survey Summary by C.O. Kingsford, Bechtel BWXT

Stage-Discharge Relations for Selected Culverts and Bridges in the Big Lost River Flood Plain at the Idaho National Engineering and Environmental Laboratory, Idaho by C. Berenbrock and J.D. Doyle, U.S. Geological Survey

**Appendix E - Electronic Supplement - Plots of Modeled Flood Inundation for the Big Lost River Downstream of the INEEL Diversion Dam****Appendix F - Stage Probability Plots for Selected Locations at INEEL Facility Sites**

## Geomorphic and Paleoflood Investigations

The paleohydrologic studies of the Diversion Dam study reach are a continuation and expansion of the studies described in previous reports (Ostenaar et al., 1999, 2002). The objective of further studies is to further identify and reduce the uncertainty associated with previous estimates. Field-scale investigations included four major tasks: 1) acquisition and processing of new detailed aerial photography to serve as a base map for geomorphic mapping and hydraulic modeling, 2) compilation of a detailed geomorphic map of the study reach, 3) trenching and detailed geologic descriptions and analyses in three areas of the study reach to confirm geologic/geomorphic relationships, and 4) additional two-dimensional hydraulic modeling using the new topographic data. The results of these investigations were expected to provide refined estimates, with improved understanding of the uncertainties, of the paleohydrologic parameters used in the prior flood frequency analyses. The present study results largely confirm and add additional details to the geologic components of the paleohydrologic parameters derived from the previous studies. However, because of the deficiencies associated with the topographic data (**Appendix A**) used in the earlier studies, hydraulic modeling for the present study results in substantially different estimates of discharge for the paleohydrologic parameters.

In evaluating discharge estimates for paleohydrologic bounds, the focus is on developing an estimate of the flood discharge required to modify or erode a geomorphic surface for which stability can be demonstrated for some prior length of time (e.g. Levish, 2002). Many geomorphologists have used stream power as a measure of the potential for channel and landscape modification with a focus on channel power or average cross section power (e.g., Baker and Costa, 1987; Magiligan, 1992). For engineering applications of erosion, channel stability, and sediment transport studies, many empirical and semi-theoretical relationships have been developed for hydraulic parameters such as depth, velocity, shear stress and stream power (e.g., see Carson and Griffiths, 1987 for a summary). However, in neither body of literature are there many examples of sites which might be considered long existing paleohydrologic bounds which have been overtopped by historical floods, and associated model estimates of the flow parameters associated with this overtopping developed. As noted by Jarrett and England (2002), documentation for the relationships between HWM (high water marks) and the estimated stage

required to modify a geomorphic surface and thus define a paleohydrologic bound is lacking in the general literature.

In the present study, we develop a more formal framework for the application of shear stress and stream power to the problem of specification of discharge estimates for paleohydrologic bounds. The difficulties associated with developing conclusions within this framework are similar to those faced in seismic hazard assessment (e.g., SSHAC, 1995), in that uncertainty of the estimates is derived from several sources including limited data, imperfect knowledge and models of salient physical processes, and legitimate differences of scientific opinion.

Three major types of information are used to estimate the discharge range associated with a paleohydrologic bound: 1) geomorphic/geologic map and unit descriptions, 2) hydraulic modeling results of depth, unit stream power, and bed shear stress for differing input parameters, and 3) a criterion for erosion/modification of geomorphic surfaces based on empirical data compilations of unit stream power and shear stress.

Geomorphic map units define the spatial extent of areas with similar geologic/geomorphic processes and history. Individual map units are characterized by similarity in relative and absolute age, geomorphic processes and history over broad areas. Differences in age, process, and history between different areas define different geomorphic units. Thus, based on detailed mapping along the Diversion Dam study reach of the Big Lost River (**Section 2, Plate 2, and Appendix B**), four major geomorphic map groups, H1-2, H3-4, P2, and P3, are of primary importance to the issues of specifying paleohydrologic bounds. The similarities and differences within these broad map units are highlighted and defined through "point" investigations with trenches or soil description sites where stratigraphic details are described in detail. These detailed site descriptions provide the basis for areal extrapolation represented by the areal extent of the geomorphic map units. Individual geomorphic map unit areas naturally define the spatial limits of areas within which the variability of hydraulic parameters such as unit stream power and bed shear stress can be evaluated when that geomorphic unit is inundated by a modeled flow.

Two-dimensional hydraulic modeling (**Section 2 and Appendix C**) based on small grid cells relative to channel width is used to develop detailed information on the extent and spatial

variability of flow for each modeled discharge. From the model results, shear stress and stream power are calculated for each grid cell providing a detailed depiction of the magnitude and spatial variability of these parameters over the inundated areas. This information can then be compared to the spatial extent and characteristics of differing geologic/geomorphic units. Results from the two-dimensional modeling of each discharge that are used to evaluate paleohydrologic information are 1) depth and spatial extent of inundation over a particular stratigraphic site or geomorphic surface, 2) magnitude and spatial extent of bed shear stress and/or unit stream power over a site or geomorphic surface, and 3) magnitude and spatial extent of bed shear stress and unit stream power in channel reaches. Evaluation based on depth and extent of inundation primarily considers whether or not a particular site or surface area is inundated by a given flow. For many sites, as a greater percentage of a given site or geomorphic surface is inundated, to progressively greater depths, the probability of surface modification and development of a preservable geologic record increases. Likewise, as the extent and depth of inundation increase, the magnitude and distribution of unit stream power and bed shear stress change across the geomorphic surface as well. The hydraulic conditions associated with flow across a geomorphic surface are varied and non-uniform due to topography, small- and large-scale roughness, turbulence, and mixing. Thus, actual and calculated values of stream power and shear stress vary spatially in magnitude across a given cross section and throughout the area of flow. The results or conclusions drawn from application of any criteria for surface modification is therefore dependent on the location chosen for evaluation. One advantage of the use of high-resolution, two-dimensional hydraulic models is that these models provide outputs that show the spatial variability of flow characteristics. Ideally, the spatial variability shown by hydraulic modeling can be evaluated separately for each geomorphic surface of interest.

The third major type of information used to estimate discharge associated with a paleohydrologic bound are empirical criteria and observational data on the magnitudes of stream power and shear stress that are likely associated with modification or erosion of differing geomorphic surfaces (**Appendix D**). From these data, limiting values for the estimated erosion or modification of differing surfaces can be subjectively estimated for the specific surface conditions and physical properties (e.g., vegetation, soil, and grain size) of each site or geomorphic surface. Because estimates of paleohydrologic bounds will ultimately have a probabilistic description for use in the

flood frequency analyses, these criteria are formulated as probability density functions (PDF) that relate the relative probability of surface modification to particular values of shear stress or stream power. In general, the PDF's that describe the probability of surface modification are triangular distributions based on three estimated values. A lower value of shear stress or stream power represents a limit for which there is judged to be a reasonable possibility based on the existing empirical data that significant erosion or surface modification will occur. A central or preferred value represents a large body of data with high confidence. For some PDF's, the central values include a range of equal relative likelihood. An upper value limit defines a boundary beyond which there is virtual certainty of significant erosion or modification based on the available data. For application to the Diversion Dam reach of the Big Lost River, three separate criteria have been developed for unit stream power and bed shear stress, respectively (**Appendix D**). Two of the criteria are for application to the differing site, soil, and geologic conditions associated the geomorphic surfaces along the Big Lost River. The third criteria describes the more general conditions under which significant geomorphic modification of portions of the Big Lost River channel might result from various discharge levels.

Soils and geologic data from the Big Lost River lead to two general categories for erosion and surface modification, termed soil erosion and terrace erosion, based on the contrasting physical and vegetative characteristics of the soils and terrace deposits. Most of alluvial soils have an upper horizon(s), usually less than 30 cm thick, composed of silt and sand which is generally loose and unconsolidated. These horizons, usually designated as A, AB, and sometimes Bw in soil descriptions (**Section 2** and **Appendix B**), lack carbonate cementation, are often bioturbated, and may include in their upper portions some component of recently active eolian sand. Some small grasses and plants have shallow roots in these horizons. In contrast, at most stream terrace sites, below a depth of more than 20-30 cm in most profiles, there is either carbonate cementation or gravel. In deposits that are mostly fine-grained, i.e., silty and sandy, soils with carbonate accumulation are stage I to II. In the gravel deposits maximum clast sizes are generally less than 200 mm, and carbonate stages range from Stage I to III. Larger plants, such as sage, have widely scattered roots that extend into the gravel horizons. Based on the carbonate cementation and generally larger clast size associated with the terrace deposits, larger values of stream power and shear stress are required to initiate erosion.

The criteria developed for channel stability is mainly derived from geomorphic study observations of major channel widening or change following floods (**Appendix D**). This criteria is only applicable to channels where banks are cut in alluvium. Most channel banks along the Big Lost River Diversion Dam study reach are composed of fine-grained alluvium with weakly to moderately developed carbonate soils similar to sections exposed in trenches T4, T5, T6, and description sites BLR2, BLR6, BLR7 and BLR8. Gravel, in Holocene fluvial deposits, is not present more than about 1 m above the present channel floor at these exposures. Based on geomorphic mapping (**Plate 2**), only very scattered sections of the channel banks are cut directly in the gravelly Pleistocene alluvium without an inset fine-grained fill terrace. More commonly, scattered basalt outcrops confine one or both channel banks. Within this varied channel setting, the hydraulic modeling results indicate large longitudinal variation in channel stream power and shear stress throughout the Diversion Dam study reach for a subset of modeled flows.

**Table S0-2** summarizes the conclusions and evidence for paleofloods and paleohydrologic bounds that resulted from the current study of the Diversion Dam reach, primarily based on the geologic observations gleaned from several trenches (**Section 2** and **Appendix B - Electronic Supplement**). As shown by previous studies (Ostenaar et al., 1999, 2002), there is clear evidence of late Holocene floods along the Big Lost River that are substantially larger than the largest historic floods. The present study confirms the approximate 400-yr age of one of these floods and suggests the possibility of infrequent, earlier floods of similar size as well as the existence of a more recent and slightly smaller paleoflood (**Section 2** and **Appendix B**). The geologic and geomorphic basis for paleohydrologic bounds based on these data are consistent with previous studies but discharge estimates for both paleofloods and paleohydrologic bounds are substantially revised based on the updated hydraulic modeling (**Section 2**, **Section 3** and **Appendix D**). Changes in these discharge estimates compared to previous studies are directly attributable to stage differences resulting from the use of new, more accurate topographic data in the current study (**Appendix A**). Results of the flow modeling are depicted on color-contoured plots of depth, unit stream power and bed shear stress overlain on shaded relief images of the high-resolution topography and the geomorphic map units from **Plate 2** in **Appendix D - Electronic Supplement**.

**Table S0-2 Big Lost River Paleofloods and Paleohydrologic Bounds**

| Event name   | Age or time span (Cal yrs or Cal yr B.P.) <sup>1</sup> | Discharge (m <sup>3</sup> /s) and type of distribution | Summary of Evidence  |
|--|--|--|--|
| Paleofloods  |  |  |  |
| "white flood"  | >100yr (pre-gaging) but less than 400-600yr            | 90 (80-100) uniform                                    | Based on thin deposit in T4. Not recognized in T5 or T6 (slightly higher sites). Possible correlative in T9(?). Age - most likely 100 to 150 years based on absence of soil development. Discharge - Upper limit based on rapid increase in power/shear stress at T4 and lack of deposit in T5/T6.   |
| "400-yr" flood   | 400 to 600 years                                       | 150 (130-175) triangular                               | Apparently correlative deposits in T4, T5, T6 (also BLR2, BLR7 & BLR8) with similar soils, stratigraphic setting, and radiocarbon ages. Soil has stage I- Bk horizon. Stripping of A- and AB/Bw horizons at T8c, partial stripping at T8b; lack of erosion at T8a. May represent more than one flood.  |
| "older flood"  | 1000 to 2000 years                                     | 150 (130-175) triangular                               | Deposits with Stage I to I+ Bk horizon that underlie "400-yr flood" deposits in T4, T5, T6 and T9. Appears to indicate long period of stability with little or no deposition at these sites before deposition of deposits associated with "400-yr" flood. Similar stratigraphy at BLR2 and BLR8. Likely represents multiple floods of similar or smaller maximum discharge. Minimum discharge must inundate FP1-FP4, FP6-8, most of FP7, FP11-13, FP17-18, and FP19-21, which are areas with H1-2 geomorphic surfaces that appear to indicate Holocene flooding. |
| Paleohydrologic Bounds   |  |  |  |
| 400-yr #1  | 400-600  | 130 (110-150) triangular                               | Preservation of recognizable stratigraphy at T4 and T6. No stripping of A-horizons from the youngest deposits at T4 and T6. Apparently correlative H1-2 geomorphic surfaces at FP1, FP3-4, FP7, FP11-13, FP17, and FP19-20.  |
| early Holocene (H1 surfaces)   | 6000 to 8000   | 225 (175-250) triangular                               | Preservation of stratigraphy in T6, T4, and T8a,b,c. Banks at BLR6 and continuity of H1-2 geomorphic surfaces along BLR.   |
| Pleistocene  | >10000   | 250 (225-400) triangular                               | Preservation of Pleistocene gravel surfaces throughout the study reach. Actual age of the underlying deposits is older than 12-15 ka (minimum age of deglaciation) and some may be older than 20-25 ka (Last glacial maximum). Length of time span for paleohydrologic bound is limited by post-glacial, warmer climate more similar to present.   |
| Notes: <sup>1</sup> All age distributions have uniform probability over the indicated time span uncertainty. |  |  |  |

## **Revised Big Lost River Flood Frequency Analyses**

The approach taken for this study is to incorporate paleoflood estimates and paleohydrologic bounds (Levish, 2002; Levish et al., 1994, 1996, 1997; Ostenaar and Levish, 1996) into nonparametric Bayesian flood frequency analysis that uses likelihood functions that incorporate both parameter and data (discharge and geologic age) measurement uncertainties (O’Connell et al., 1996, 1998; O’Connell, 2005).

A paleohydrologic bound is the time interval during which a given discharge has not been exceeded. Paleohydrologic bounds are not actual floods, but instead are limits on paleostage over a measured time interval. These bounds represent stages and discharges that have not been exceeded since a geomorphic surface stabilized. Through hydraulic modeling, discharge for a paleohydrologic bound can be derived from stage, just as a discharge is derived from the paleostage indicators of past floods. Used appropriately, paleohydrologic bounds are powerful constraints in flood frequency analyses, even if the number, timing, and magnitude of individual paleofloods are uncertain (Stedinger and Cohn, 1986).

It is necessary to revise flood frequency estimates from previous studies for two reasons. First, peak discharge values have been modified for several data points, including the paleohydrologic non-exceedence bounds. Second, the distribution of observed peak discharges and paleohydrologic information is sufficiently complex that parametric flood frequency functions are ill-suited to determine statistical quantities, such as credible or “confidence” limits for flood frequency estimates. Consequently, a newly-published nonparametric Bayesian flood frequency estimation approach (O’Connell, 2005) is used to obtain probabilistic minimum-bias estimates of flood frequency. This method accommodates complex flood behaviors such as event clustering (repeated instances of similar magnitude floods) and can use varied data, such as gage and historical peak discharges, and paleohydrologic upper and lower bounds on peak discharge, while rigorously accounting for a wide variety of measurement uncertainties. In contrast to nonparametric kernel estimation approaches, the stochastic assumption is used to generate flood frequency models that span the data and provide about twice the number of degrees of freedom of the data. Each generated flood frequency model is scored using likelihoods that account for data measurement uncertainties. A parametric estimation approach ensures high precision because

posterior sampling is known. However, parametric approaches can produce substantial biases because the classes of allowed flood frequency models are restricted. These biases are completely undetectable within a parametric paradigm. To minimize these types of biases, the nonparametric approach used here surrenders some precision, but produces greater overall accuracy and assurance; it reveals the annual probabilities where discharge becomes unconstrained by the data, thereby eliminating unsubstantiated extrapolation. Parametric flood frequency estimation introduces strong extrapolation priors that make it difficult, if not impossible, to determine when flood frequency is not longer constrained by the data. These problems are apparent in the parametric method of O'Connell et al. (2002) used in the previous INL flood-frequency analyses (Ostenaar et al., 1999, 2002).

Present results show limits of extrapolation on AEP to be inversely proportional to about twice the length of record, corresponding to a minimum AEP of  $\sim 1/20,000$  for which discharge estimation is credible. The data provide no constraints on how infrequent discharges larger than  $300 \text{ m}^3/\text{s}$  may be, but place strong constraints on the maximum AEPs that can be associated with any discharge.

The present analysis only assumes that for extreme floods, upstream regulatory structures and diversions do not increase flood magnitudes downstream compared to the unregulated natural flows, except for cases where upstream regulating structures might fail. Flood probabilities for such scenarios should be evaluated separately, and account for the overall failure probability of the structure under all conditions. The impacts of regulation and variations in smaller flows, such as those of historical experience, on frequency estimates of extreme floods were addressed through sensitivity analyses in previous analyses (Ostenaar et al., 1999).

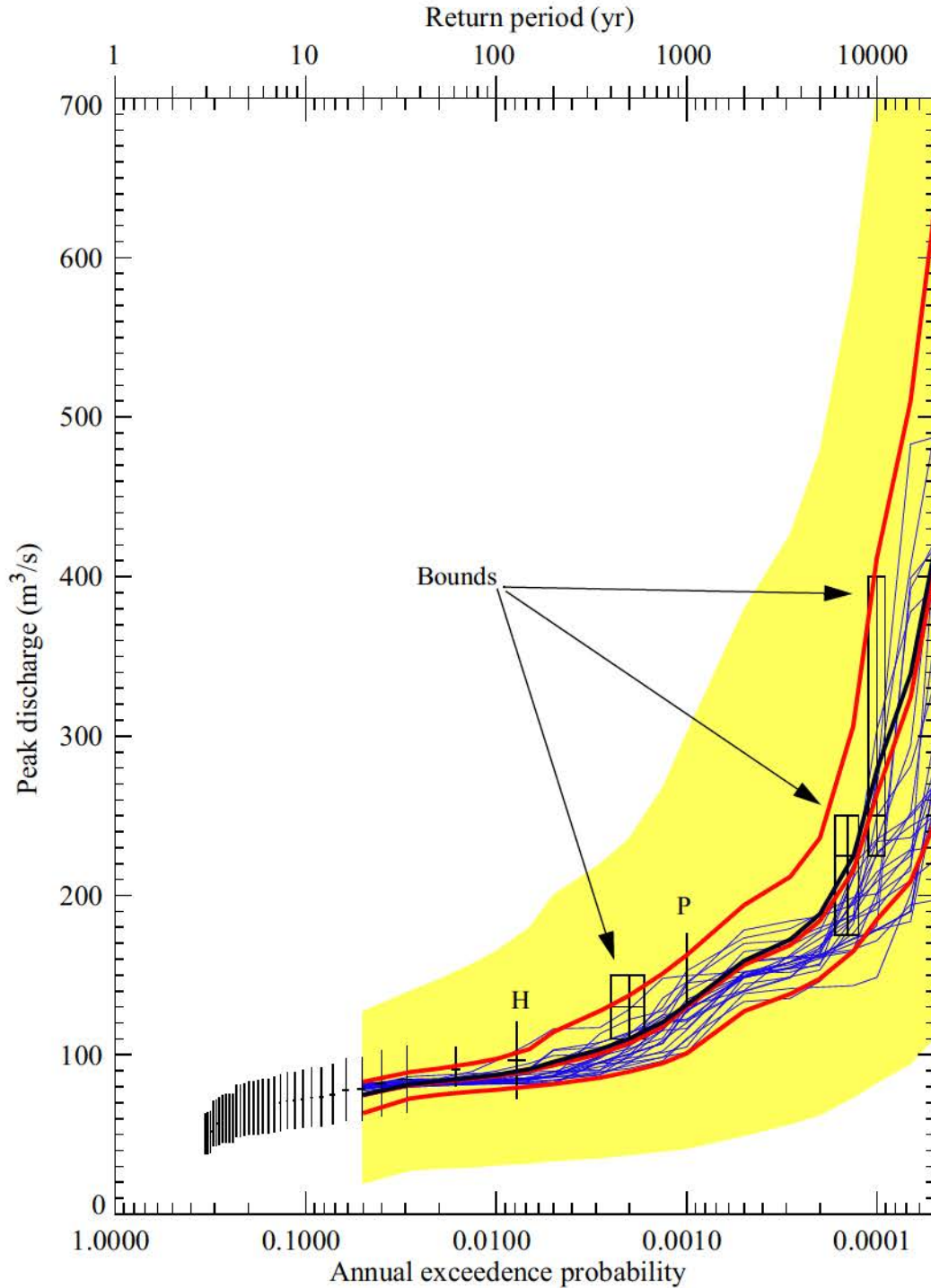


**Figure SO-1 Revised flood frequency for Big Lost River at the INEEL Diversion Dam.** Gaged flows (vertical black lines, with short horizontal lines indicating preferred discharge and plotting position uncertainty) are from Big Lost River at Howell Ranch (94 years) attenuated to the INEEL Diversion Dam based on methods of Hortness and Rousseau (2002). Geologic data includes two paleofloods (largest discharges labeled H and P) and three paleohydrologic bounds (black boxes - vertical lines indicate discharge range, horizontal lines indicate duration range). Lower and upper red curves are 5% and 95% credible limits (middle red is median, and middle black is mean). Blue curves are models with relative likelihoods > 0.25 of the maximum likelihood. Yellow region indicates the limits of sampling.

**Table SO-3 Nonparametric Flood Frequency for the Big Lost River at the Diversion Dam.**

| AEP<br>(1/yr)  | Return<br>period (yr) | 5%<br>(m <sup>3</sup> /s) | mean<br>(m <sup>3</sup> /s) | 95%<br>(m <sup>3</sup> /s) |
|--|-----------------------|---------------------------|-----------------------------|----------------------------|
| $5 \times 10^{-2}$   | 20                    | 63                        | 75                          | 83                         |
| $2.86 \times 10^{-2}$  | 35                    | 73                        | 81                          | 89                         |
| $2 \times 10^{-2}$   | 50                    | 75                        | 83                          | 91                         |
| $1.33 \times 10^{-2}$  | 75                    | 77                        | 86                          | 95                         |
| $10^{-2}$  | 100                   | 78                        | 87                          | 97                         |
| $6.67 \times 10^{-3}$  | 150                   | 80                        | 91                          | 104                        |
| $5 \times 10^{-3}$   | 200                   | 82                        | 96                          | 114                        |
| $2.86 \times 10^{-3}$  | 350                   | 86                        | 103                         | 127                        |
| $2 \times 10^{-3}$   | 500                   | 89                        | 110                         | 137                        |
| $1.33 \times 10^{-3}$  | 750                   | 95                        | 121                         | 151                        |
| $10^{-3}$  | 1000                  | 101                       | 131                         | 163                        |
| $5 \times 10^{-4}$   | 2000                  | 127                       | 159                         | 194                        |
| $2.86 \times 10^{-4}$  | 3500                  | 138                       | 172                         | 212                        |
| $2 \times 10^{-4}$   | 5000                  | 148                       | 188                         | 236                        |
| $1.33 \times 10^{-4}$  | 7500                  | 165                       | 224                         | 306                        |
| $10^{-4}$  | 10,000                | 185                       | 279                         | 412                        |
| $6.67 \times 10^{-5}$  | 15,000                | 209                       | 339*                        | 510*                       |
| $5 \times 10^{-5}$   | 20,000                | 245                       | 416*                        | 628*                       |
| * Values with diminished or little statistical significance. |                       |                           |                             |                            |

## **Probabilistic Flood Stage at INTEC and TRA**

The two-dimensional (depth-averaged) flow models TrimR2D and RiCOM (**Appendix C**) were used to calculate inundation and flow velocities for paleoflood and site inundation investigations at INL. TrimR2D uses a fixed-spacing staggered finite-difference approach that was used for hydraulic modeling of steady-state discharges in the paleoflood reach and with a larger grid spacing for the site inundation studies. RiCOM uses a staggered finite-element approach that provided an opportunity to employ high-resolution topography in a variable-sized element mesh constructed for the INL site inundation investigations. Both TrimR2D and RiCOM were used to investigate site inundation scenarios to assess the importance of parameters including topographic grid resolution, infiltration, and culvert performance, on estimated inundation corresponding to long-duration (~20 hour-steady-state) discharges. Results from both models were post-processed for estimates of unit stream power and bed shear stress.

Monte Carlo nonparametric flood frequency estimation was used to incorporate measurement uncertainties in gaged, historical, and paleoflood discharges and nonexceedence bounds and to produce fully probabilistic flood frequency estimates for annual exceedence probabilities of specific discharges of interest. These annual exceedence probabilities were combined with stage estimates from TrimR2D and RiCOM discharge, infiltration, culvert, and topographic resolution scenarios to produce scenario probabilistic stage hazard curves for 15 sites located in the TRA/INTEC facilities (**Appendix F**). Annual exceedence probabilities and associated credible limits are provided for map-scale inundation plots to provide scenario probabilistic inundation maps (**Appendix E**). These products provide a basis to develop weights for logic tree branches associated with infiltration and culvert performance scenarios to produce probabilistic inundation maps.

Two-dimensional hydraulic modeling using a broad range of discharges conducted for the reach of the Big Lost River downstream of the INEEL Diversion Dam to approximately the INEEL railroad grade downstream of INTEC and TRA provide one element needed for probabilistic flood stage estimates at these facilities. A conceptual framework for evaluating the model results and flood frequency information was developed in the early stages of this study to guide the evaluations. Uncertainties in probabilistic flood stage estimates are discussed in the context of

that framework. Based on this framework, results and uncertainties for stage - probability curves for fifteen specific sites within INTEC and TRA are discussed.

**Appendix E - Electronic Supplement** presents maps depicting the results of two-dimensional hydraulic modeling conducted to estimate probabilistic flood stage at INTEC and TRA. These maps show results for both the entire reach downstream of the INEEL Diversion Dam as well as enlarged views in the immediate vicinity of the facilities. For TrimR2D, the output flow quantities included water surface elevations and vector flow velocities interpolated to the water surface elevation positions at cell-centered positions in the staggered grid. Using the input topography, derived quantities such as depth, bed shear stress, and unit stream power were obtained. For RiCOM, the output flow quantities included water surface elevations and vector flow velocities interpolated to the element vertices using the finite-element basis functions. The inverse transformation operators were then applied to produce flow quantities in the INL state-plane coordinate system. For most modeled discharges, results are presented for modeled flow depth, unit stream power, and bed shear stress based on the TrimR2D results. RiCOM results are presented mostly as plots showing the difference in water-surface elevation from TrimR2D results for the same input discharge. A full set of RiCOM results (depth, unit stream power, bed shear stress) are presented only for four quantile results of the 100- and 500- yr discharges from the flood frequency analyses. Additional depth difference plots from TrimR2D models depict end member differences for infiltration and culvert scenarios.

Each of the inundation maps for a specific discharge could be associated with mean and credible limits on AEP associated with that discharge. However, such AEP's would not represent complete probabilistic inundation maps (PIM) for INL. There are additional probabilities (or weights) that must be assigned to aleatory (random-by-nature) parameters, such as infiltration and culvert conveyance. A conceptual framework for evaluating these uncertainties that was developed in the early stages of this study to guide the investigations. Epistemic uncertainties include factors such as flow model variability and appropriate scenario terrain models used in the simulations. Elicitation and assignments of weights to all aleatory and epistemic factors are required to produce comprehensive PIM's. Each of the major elements will be briefly described below.

Aleatory uncertainties include estimated flood frequency, hydrograph shape, infiltration, and culvert discharge characteristics. Several different infiltration and culvert performance scenarios were used to incorporate aleatory uncertainties associated with these parameters. A wide range of discharges were used to quantify the impacts of flood frequency aleatory uncertainty on probabilistic stage estimates. A long-duration steady-state flow assumption was used. Consequently, the impacts of varying hydrograph shape were not investigated. Generally, infiltration and culvert uncertainties had only small impacts relative to epistemic topography uncertainties, as discussed below.

Epistemic uncertainties include topography and computational flow models. Potential epistemic uncertainties associated with the two flow models are discussed in **Appendix C, Part B, Section 1**. These tests and output comparisons (difference plots in **Appendix E - Electronic Supplement**) show that negligible differences in water-surface elevation at most sites can be attributed to the choice of flow model. Much larger epistemic uncertainty is associated with the ability to accurately resolve subtle topographic features in the model inputs. Epistemic uncertainty associated with the input topography for the hydraulic models is not quantified in a statistical sense, but is shown by the differences in stage hazard plots for TrimR2D compared to RiCOM. These effects are often largest for flows less than about 200 m<sup>3</sup>/s where the differences in the ability of the input grids to resolve subtle features of the input topography leads to areas inundated to higher or lower levels between the flow models (See TrimR2D minus RiCOM difference plots in **Appendix E - Electronic Supplement**). A full appreciation of the impact of these factors on inundation characteristics is best provided by the large-scale inundation maps. The stage - AEP curves for the fifteen TRA/INTEC sites suggest these effects are mostly less than ~ 0.5 ft (**Appendix F**), but it is the maps (**Appendix E - Electronic Supplement**) that provide the best illustrations of the strong sensitivity of portions of the inundation to topographic resolution and relatively subtle topographic features such as roads and old diversion structures.

### **Inundation Discussion**

Stage hazard curves are provided in Appendix F for fifteen specific sites near TRA or INTEC as listed in **Table SO-4** and **Table SO-5**. For each site there are four plots of flow simulation results: 1) TrimR2D, 2) RiCOM, 3) TrimR2D - RiCOM comparisons, and 4) RiCOM Lincoln Ave

blockage scenarios. Comparisons within and between these four sets of plots isolate or compare specific factors that could influence estimated stages. The TrimR2D simulations are the primary suite of results for final estimate of stage hazard curves and isolate the effects of variations in infiltration and secondary culvert blockage. Generally, the secondary culverts have virtually no impact on inundation at most sites, with only minor impacts on inundation at sites outside TRA along Monroe Avenue. Infiltration has only a modest impact on inundation and generally does not change the hazard curves much. The RiCOM simulations and TrimR2D -RiCOM simulations illustrate the impacts of topographic resolution and persistent topographic features such as roads, old diversions, etc. These factors have the strongest impacts on inundation over the entire site. The RiCOM simulations with blockage of the Big Lost River channel at Lincoln Avenue has the strongest impact on inundation for portions of INTEC, particularly for the simulations of discharges less than about 250 m<sup>3</sup>/s.

The inundation maps in **Appendix E - Electronic Supplement** provide an essential tool to understand the stage hazard curves in **Appendix F**. It is clear that small-scale (possibly transient) changes to topography can significantly impact inundation at TRA and INTEC. This is a consequence of the relatively flat terrain in the vicinity of the Big Lost River and these INL facilities. However, the maps also provide a tool to determine small-scale changes to topography that could substantially reduce inundation hazards at TRA and INTEC. For instance, flow along the northern side of the old diversion channel west of TRA could be blocked by rather small-scale topographic modifications about 3.2 km west of TRA near the western end of the old diversion channel. The inundation impacts of topographic modification scenarios could be easily investigated by running new flows with modifications to the detailed topographic RiCOM mesh. Clearly, the performance of the Big Lost River culverts at Lincoln Avenue have a profound influence on stage hazards for several sites at INTEC, especially for the lower end of the discharges simulated. Similarly, although an explicit culvert blocking scenario was not constructed for the railroad embankment bridge downstream of INTEC, blockage of conveyance through the railroad embankment may also significantly influence stage hazards for portions of INTEC.

The stage hazard curves contained in Appendix F have the same limitations for extrapolation to small AEP ( $AEP < 0.0001$ ) as do the flood frequency results presented in **Section 4**. Because the flood frequency results are largely unconstrained for small AEP, no meaningful estimate of 95% limits is contained in the revised flood frequency analyses to promulgate into the stage probability estimate. Given the nearly unlimited upper bounds of extrapolation that might be possible for small AEP from the present flood frequency analyses, development of stage hazard curves for smaller AEP would also require additional hydraulic modeling for discharges much larger than  $700 \text{ m}^3/\text{s}$ , which is the largest discharge considered in the present study.

**Table SO-4 Probabilistic Stage Estimates for INTEC and TRA Sites (100- and 500-year floods).**

| Map Ref #   | Site Description         | AEP = 10 <sup>-2</sup><br>Return period = 100 yr |                 |                 | AEP = 2 x 10 <sup>-3</sup><br>Return period = 500 yr |                 |                 |
|-------------|--------------------------|--|-----------------|-----------------|--|-----------------|-----------------|
|             |                          | 5%   | mean            | 95%             | 5%   | mean            | 95%             |
| TRA Sites   |                          |  |                 |                 |  |                 |                 |
| 1           | TRA - Monroe Ave         | 4924.49-4924.56                                  | 4924.55-4924.60 | 4924.61-4924.65 | 4924.58-4924.63                                      | 4924.67-4924.70 | 4924.72-4924.75 |
| 2           | TRA-715 (evap. pond)     | 4918.36-4918.56                                  | 4918.50-4918.64 | 4918.63-4918.71 | 4918.57-4918.67                                      | 4918.73-4918.81 | 4918.81-4918.91 |
| 3           | TRA southeast corner     | dry  | dry             | dry             | dry  | dry             | dry             |
| 4           | TRA northwest corner     | dry  | dry             | dry             | dry  | dry             | dry             |
| 5           | TRA-670 (ATR)            | dry  | dry             | dry             | dry  | dry             | dry             |
| 6           | TRA-670 (ATR)            | dry  | dry             | dry             | dry  | dry             | dry             |
| 7           | TRA-632                  | dry  | dry             | dry             | dry  | dry             | dry             |
| 8           | TRA-621                  | dry  | dry             | dry             | dry  | dry             | dry             |
| 9           | TRA-715 (evap. pond)     | dry  | dry             | dry             | dry  | dry             | dry             |
| INTEC Sites |                          |  |                 |                 |  |                 |                 |
| 10          | INTEC Tank Farm          | 4912.57-4913.12                                  | 4912.92-4913.29 | 4913.26-4913.45 | 4913.09-4913.37                                      | 4913.50-4913.65 | 4913.72-4913.85 |
| 11          | NWCF (Bldg 659)          | dry  | dry             | dry             | dry  | dry             | dry             |
| 12          | CPP-749                  | 4916.30-4916.40                                  | 4916.42-4916.51 | 4916.54-4916.60 | 4916.48-4916.55                                      | 4916.63-4916.69 | 4916.71-4916.78 |
| 13          | INTEC - NE corner        | 4907.04-4907.17                                  | 4907.18-4907.27 | 4907.31-4907.35 | 4907.25-4907.31                                      | 4907.42-4907.47 | 4907.53-4907.59 |
| 14          | INTEC -nr west gate      | 4916.30-4916.40                                  | 4916.42-4916.51 | 4916.54-4916.60 | 4916.48-4916.55                                      | 4916.63-4916.69 | 4916.71-4916.78 |
| 15          | BLR - NW corner of INTEC | 4913.03-4913.10                                  | 4913.13-4913.18 | 4913.22-4913.26 | 4913.18-4913.22                                      | 4913.34-4913.38 | 4913.46-4913.50 |

**Table SO-5 Probabilistic Stage Estimates for INTEC and TRA Sites (2000- and 10,000-year floods).**

| Map Ref#    | Site Description         | AEP = $5 \times 10^{-4}$<br>Return period = 2000 yr |                 |                 | AEP = $1 \times 10^{-4}$<br>Return period = 10000 yr |                 |                 |
|-------------|--------------------------|---|-----------------|-----------------|--|-----------------|-----------------|
|             |                          | 5%  | mean            | 95%             | 5%   | mean            | 95%             |
| TRA Sites   |                          |   |                 |                 |  |                 |                 |
| 1           | TRA - Monroe Ave         | 4924.68-4924.71                                     | 4924.77-4924.80 | 4924.86-4924.90 | 4924.83-4924.86                                      | 4925.04-4925.09 | 4925.36-4925.43 |
| 2           | TRA-715 (evap. pond)     | 4918.74-4918.82                                     | 4918.91-4918.99 | 4919.06-4919.13 | 4919.01-4919.07                                      | 4919.36-4919.45 | 4919.89-4919.99 |
| 3           | TRA southeast corner     | dry   | dry-4922.21     | 4922.36-4922.45 | 4922.20-4922.37                                      | 4922.81-4922.96 | 4923.76-4924.02 |
| 4           | TRA northwest corner     | dry   | dry             | dry             | dry  | 4923.38-4923.52 | 4924.14-4924.20 |
| 5           | TRA-670 (ATR)            | dry   | dry             | dry             | dry  | dry             | dry             |
| 6           | TRA-670 (ATR)            | dry   | dry             | dry             | dry  | dry             | 4923.29-4923.32 |
| 7           | TRA-632                  | dry   | dry             | dry             | dry  | dry             | dry             |
| 8           | TRA-621                  | dry   | dry             | dry             | dry  | dry             | dry             |
| 9           | TRA-715 (evap. pond)     | dry   | dry             | dry             | dry  | dry             | dry             |
| INTEC Sites |                          |   |                 |                 |  |                 |                 |
| 10          | INTEC Tank Farm          | 4913.54-4913.68                                     | 4913.87-4913.98 | 4914.08-4914.18 | 4914.01-4914.11                                      | 4914.49-4914.57 | 4914.86-4914.89 |
| 11          | NWCF (Bldg 659)          | dry   | dry-4911.35     | 4911.77-4911.81 | 4911.22-4911.77                                      | 4911.93-4911.96 | 4912.03-4912.06 |
| 12          | CPP-749                  | 4916.64-4916.71                                     | 4916.79-4916.85 | 4916.93-4916.96 | 4916.88-4916.92                                      | 4917.15-4917.24 | 4917.45-4917.48 |
| 13          | INTEC - NE corner        | 4907.44-4907.49                                     | 4907.58-4907.64 | 4907.71-4907.77 | 4907.66-4907.72                                      | 4907.91-4907.95 | 4908.09-4908.13 |
| 14          | INTEC -nr west gate      | 4916.64-4916.71                                     | 4916.79-4916.85 | 4916.93-4916.96 | 4916.88-4916.92                                      | 4917.15-4917.22 | 4917.41-4917.45 |
| 15          | BLR - NW corner of INTEC | 4913.36-4913.40                                     | 4913.52-4913.62 | 4913.71-4913.75 | 4913.64-4913.71                                      | 4913.90-4913.93 | 4914.07-4914.13 |

## TABLE OF CONTENTS

| <u>Section</u> | <u>Title</u>  | <u>Page</u> |
|----------------|---|-------------|
|                | <b>OVERVIEW.....</b>  | <b>III</b>  |
| <b>1.0</b>     | <b>INTRODUCTION .....</b>   | <b>1</b>    |
| 1.1            | Present Study Objectives.....   | 1           |
| 1.2            | Acknowledgments .....   | 3           |
|                | Figures for <b>Section 1.0</b> .....  | 7           |
|                | Tables for <b>Section 1.0</b> .....   | 10          |
| <b>2.0</b>     | <b>GEOLOGIC AND GEOMORPHIC STUDIES OF THE DIVERSION DAM STUDY REACH .....</b>           | <b>12</b>   |
| 2.1            | Geologic and Geomorphic Setting of the Diversion Dam Study Reach .....                  | 12          |
| 2.1.1          | Big Lost River historical stream flow.....  | 13          |
| 2.1.2          | Big Lost River – Diversion Dam study reach.....   | 14          |
| 2.2            | Geomorphic Mapping of the Diversion Dam Study Reach.....                                | 17          |
| 2.2.1          | Quaternary Basalts - Rb, Rbe, Rd and Rde .....  | 17          |
| 2.2.2          | Pleistocene Units - P1 to P3 .....  | 19          |
| 2.2.2.1        | Age Constraints from Regional Glaciation.....   | 20          |
| 2.2.2.2        | Earth Mounds.....   | 21          |
| 2.2.2.3        | Geomorphic Evidence for Holocene Modification of the Pleistocene Units.....             | 23          |
| 2.2.3          | Holocene Units - H1 to H4 .....   | 24          |
| 2.2.4          | Channel Deposits.....   | 26          |
| 2.3            | Trenching Studies.....  | 27          |
| 2.3.1          | Trenches T1, T2, and T3 - Big Loop Study Area .....                                     | 28          |
| 2.3.1.1        | Trench T1.....  | 28          |
| 2.3.1.2        | Trench T2.....  | 29          |
| 2.3.1.3        | Trench T3.....  | 30          |
| 2.3.2          | Trenches T4, T5, T6, and T7 - Saddle Constriction Study Area .....                      | 31          |
| 2.3.2.1        | Trench T4.....  | 31          |
| 2.3.2.2        | Trench T5.....  | 33          |
| 2.3.2.3        | Trench T6.....  | 35          |
| 2.3.2.4        | Trench T7.....  | 37          |
| 2.3.3          | Trenches T8 and T9 - BLR8 Study Area.....   | 38          |
| 2.3.3.1        | Trench T8.....  | 39          |
| 2.3.3.2        | Trench T9.....  | 43          |
| 2.4            | Summary of Geomorphic and Geologic Data for Paleofloods and Paleohydrologic Bounds..... | 45          |
| 2.4.1          | Paleofloods .....   | 45          |
| 2.4.1.1        | "White Flood" .....   | 46          |
| 2.4.2          | "400-yr Flood" .....  | 46          |
| 2.4.3          | "Older Flood".....  | 47          |
| 2.4.4          | Paleohydrologic Bounds.....   | 48          |
| 2.4.4.1        | 400-yr Flood Bound.....   | 48          |
| 2.4.4.2        | Early Holocene (H1 surfaces) Bound .....  | 49          |
| 2.4.4.3        | Pleistocene Bound.....  | 49          |
| 2.5            | Hydraulic Modeling of the Diversion Dam Study Reach .....                               | 50          |

## TABLE OF CONTENTS

| <u>Section</u> | <u>Title</u>  | <u>Page</u> |
|----------------|---|-------------|
| 2.5.1          | Results .....   | 52          |
| 2.5.1.1        | Effects of Varied Manning's n.....  | 53          |
| 2.5.1.2        | Effects of Input Topography .....   | 53          |
| 2.5.1.3        | Comparisons to Previous Studies .....   | 54          |
| 2.5.1.4        | Results from Specific Study Areas .....   | 55          |
|                | Figures for <b>Section 2.0</b> .....  | 60          |
|                | Tables for <b>Section 2.0</b> .....   | 117         |
| <b>3.0</b>     | <b>PALEOFLOODS AND PALEOHYDROLOGIC BOUNDS FOR THE BIG LOST RIVER.....</b>   | <b>121</b>  |
| 3.1            | Background to the Use of Paleohydrologic Bounds.....  | 121         |
| 3.1.1          | Geologic and geomorphic evidence of flooding.....   | 121         |
| 3.2            | Criteria and Approach for Evaluating Paleohydrologic Information .....  | 122         |
| 3.2.1          | Evaluating Spatial Extent and Variability .....   | 127         |
| 3.2.1.1        | Uncertainty in Discharge Estimates of Modification for each Subarea.....  | 129         |
| 3.2.1.2        | Combining Estimates from Multiple Subareas .....  | 130         |
| 3.3            | Age and Discharge Estimates for Paleofloods .....   | 131         |
| 3.3.1          | "White Flood" .....   | 132         |
| 3.3.2          | "400-yr Flood" .....  | 133         |
| 3.3.3          | "Older Flood".....  | 134         |
| 3.4            | Age and Discharge Estimates for Paleohydrologic Bounds.....   | 135         |
| 3.4.1          | 400-yr Flood Bound.....   | 135         |
| 3.4.2          | Early Holocene (H1 surfaces) Bound.....   | 137         |
| 3.4.3          | Pleistocene Bound .....   | 138         |
| 3.4.3.1        | Catastrophic Channel Change.....  | 139         |
|                | Figures for <b>Section 3.0</b> .....  | 141         |
|                | Tables for <b>Section 3.0</b> .....   | 151         |
| <b>4.0</b>     | <b>REVISED FLOOD FREQUENCY FOR THE BIG LOST RIVER AT THE INEEL DIVERSION DAM.....</b>   | <b>161</b>  |
| 4.1            | Nonparametric Flood Frequency for the Big Lost River at INL.....  | 161         |
|                | Figures for <b>Section 4.0</b> .....  | 166         |
|                | Tables for <b>Section 4.0</b> .....   | 180         |
| <b>5.0</b>     | <b>PROBABILISTIC FLOOD STAGE AT INTEC AND TRA .....</b>   | <b>183</b>  |
| 5.1            | Topographic Input to Two-Dimensional Models.....  | 183         |
| 5.2            | Two Dimensional Hydraulic Modeling.....   | 183         |
| 5.2.1          | Infiltration Implementation and Scenarios .....   | 184         |
| 5.2.2          | Culvert Implementation and Scenarios.....   | 184         |
| 5.2.3          | Flow Initialization.....  | 184         |
| 5.2.4          | Flow Parameters .....   | 185         |
| 5.2.5          | Flow Completion .....   | 185         |
| 5.2.6          | Flow Output.....  | 186         |
| 5.3            | Conceptual Framework for Development of Probabilistic Inundation Maps and Flood Stage Estimates for Facility Sites at INL ..... | 186         |
| 5.3.1          | Aleatory Uncertainties .....  | 187         |

## TABLE OF CONTENTS

| <b><u>Section</u></b> | <b><u>Title</u></b>                        | <b><u>Page</u></b> |
|-----------------------|--|--------------------|
| 5.3.1.1               | Flood Frequency Analyses.....              | 187                |
| 5.3.1.2               | Hydrograph Shape .....                     | 188                |
| 5.3.1.3               | Infiltration .....                         | 188                |
| 5.3.1.4               | Culverts.....                              | 188                |
| 5.3.2                 | Epistemic Uncertainties .....              | 189                |
| 5.3.2.1               | Topography and Flow Model Uncertainty..... | 189                |
| 5.3.3                 | Scope of Results .....                     | 189                |
| 5.4                   | Evaluation of Results.....                 | 190                |
| 5.4.1                 | Flood Stage - Probability at TRA .....     | 191                |
| 5.4.2                 | Flood Stage - Probability at INTEC .....   | 191                |
| 5.5                   | Inundation Discussion .....                | 192                |
|                       | Figures for <b>Section 5.0</b> .....       | 194                |
|                       | Tables for <b>Section 5.0</b> .....        | 201                |
| <b>6.0</b>            | <b>REFERENCES</b> .....                    | <b>207</b>         |

## LIST OF FIGURES

| <b><u>Figure No.</u></b> | <b><u>Title</u></b>   | <b><u>Page</u></b> |
|--------------------------|---|--------------------|
| Figure SO-1              | Revised flood frequency for Big Lost River at the INEEL Diversion Dam.....  | xv                 |
| Figure 1-1               | Location map of INL (INEEL) and study area.....   | 8                  |
| Figure 1-2               | INL study area, Big Lost River and significant facility locations.....  | 9                  |
| Figure 2-1               | Annual peak discharge estimates for upstream (light shaded bars) and downstream gaging stations (dark shaded bars) on the Big Lost River..... | 61                 |
| Figure 2-2               | Area around Trenches T1, T2, and T3.....  | 62                 |
| Figure 2-3               | Area around "Saddle" and Trenches T4 and T5 downstream of saddle constriction .....   | 63                 |
| Figure 2-4               | Detail of area around Trenches T4, T5 and T6 downstream of saddle constriction .....  | 64                 |
| Figure 2-5               | Area around BLR8 and Trenches T8 and T9.....  | 65                 |
| Figure 2-6               | Modeled water surface elevation near trenches T4 and T5.....  | 66                 |
| Figure 2-7               | Modeled water surface elevation near trench T9.....   | 67                 |
| Figure 2-8               | Summary plot of age constraints for late Holocene paleofloods.....  | 68                 |
| Figure 2-9               | Channel power for the Diversion Dam study reach subareas.....   | 69                 |
| Figure 2-10              | Model results for 100 and 150 m <sup>3</sup> /s from Ostenaar et al. (1999, 2002) near the Saddle.....  | 70                 |
| Figure 2-11              | Figure 5 from Ostenaar et al. (2002) with revised stage estimates at BLR study sites .....  | 71                 |
| Figure 2-12              | 6-ft flow model results for 130 m <sup>3</sup> /s in the Big Loop study area.....   | 72                 |
| Figure 2-13              | 6-ft flow model results for 150 m <sup>3</sup> /s in the Big Loop study area.....   | 73                 |
| Figure 2-14              | 6-ft flow model results for 175 m <sup>3</sup> /s in the Big Loop study area.....   | 74                 |
| Figure 2-15              | 6-ft flow model results for 200 m <sup>3</sup> /s in the Big Loop study area.....   | 75                 |
| Figure 2-16              | 6-ft flow model results for 225 m <sup>3</sup> /s in the Big Loop study area.....   | 76                 |
| Figure 2-17              | 6-ft flow model results for 250 m <sup>3</sup> /s in the Big Loop study area.....   | 77                 |
| Figure 2-18              | 5-ft flow model results for 200 m <sup>3</sup> /s in the Big Loop study area.....   | 78                 |
| Figure 2-19              | 5-ft flow model results for 250 m <sup>3</sup> /s in the Big Loop study area.....   | 79                 |
| Figure 2-20              | 5-ft flow model results for 300 m <sup>3</sup> /s in the Big Loop study area.....   | 80                 |
| Figure 2-21              | 5-ft flow model results for 350 m <sup>3</sup> /s in the Big Loop study area.....   | 81                 |
| Figure 2-22              | 5-ft flow model results for 400 m <sup>3</sup> /s in the Big Loop study area.....   | 82                 |
| Figure 2-23              | 6-ft flow model results for 150 m <sup>3</sup> /s in the Saddle constriction study area.....  | 83                 |
| Figure 2-24              | 6-ft flow model results for 200 m <sup>3</sup> /s in the Saddle constriction study area.....  | 84                 |
| Figure 2-25              | 6-ft flow model results for 250 m <sup>3</sup> /s in the Saddle constriction study area.....  | 85                 |
| Figure 2-26              | 5-ft flow model results for 200 m <sup>3</sup> /s in the Saddle constriction study area.....  | 86                 |
| Figure 2-27              | 5-ft flow model results for 250 m <sup>3</sup> /s in the Saddle constriction study area.....  | 87                 |
| Figure 2-28              | 5-ft flow model results for 300 m <sup>3</sup> /s in the Saddle constriction study area.....  | 88                 |
| Figure 2-29              | 5-ft flow model results for 350 m <sup>3</sup> /s in the Saddle constriction study area.....  | 89                 |
| Figure 2-30              | 5-ft flow model results for 400 m <sup>3</sup> /s in the Saddle constriction study area.....  | 90                 |
| Figure 2-31              | 6-ft flow model results for 70 m <sup>3</sup> /s in the T4/T5/T6 study area.....  | 91                 |
| Figure 2-32              | 6-ft flow model results for 100 m <sup>3</sup> /s in the T4/T5/T6 study area.....   | 92                 |
| Figure 2-33              | 6-ft flow model results for 130 m <sup>3</sup> /s in the T4/T5/T6 study area.....   | 93                 |
| Figure 2-34              | 6-ft flow model results for 150 m <sup>3</sup> /s in the T4/T5/T6 study area.....   | 94                 |
| Figure 2-35              | 6-ft flow model results for 175 m <sup>3</sup> /s in the T4/T5/T6 study area.....   | 95                 |

## LIST OF FIGURES

| <b><u>Figure No.</u></b> | <b><u>Title</u></b>  | <b><u>Page</u></b> |
|--------------------------|--|--------------------|
| Figure 2-36              | 6-ft flow model results for 200 m <sup>3</sup> /s in the T4/T5/T6 study area.....  | 96                 |
| Figure 2-37              | 6-ft flow model results for 225 m <sup>3</sup> /s in the T4/T5/T6 study area.....  | 97                 |
| Figure 2-38              | 6-ft flow model results for 250 m <sup>3</sup> /s in the T4/T5/T6 study area.....  | 98                 |
| Figure 2-39              | 5-ft flow model results for 200 m <sup>3</sup> /s in the T4/T5/T6 constriction study area... ..                                      | 99                 |
| Figure 2-40              | 5-ft flow model results for 250 m <sup>3</sup> /s in the T4/T5/T6 constriction study area.....                                       | 100                |
| Figure 2-41              | 5-ft flow model results for 300 m <sup>3</sup> /s in the T4/T5/T6 constriction study area.....                                       | 101                |
| Figure 2-42              | 5-ft flow model results for 350 m <sup>3</sup> /s in the T4/T5/T6 constriction study area.....                                       | 102                |
| Figure 2-43              | 5-ft flow model results for 400 m <sup>3</sup> /s in the T4/T5/T6 constriction study area.....                                       | 103                |
| Figure 2-44              | 6-ft flow model results for 70 m <sup>3</sup> /s in the BLR8 study area.....   | 104                |
| Figure 2-45              | 6-ft flow model results for 100 m <sup>3</sup> /s in the BLR8 study area.....  | 105                |
| Figure 2-46              | 6-ft flow model results for 130 m <sup>3</sup> /s in the BLR8 study area.....  | 106                |
| Figure 2-47              | 6-ft flow model results for 150 m <sup>3</sup> /s in the BLR8 study area.....  | 107                |
| Figure 2-48              | 6-ft flow model results for 175 m <sup>3</sup> /s in the BLR8 study area.....  | 108                |
| Figure 2-49              | 6-ft flow model results for 200 m <sup>3</sup> /s in the BLR8 study area.....  | 109                |
| Figure 2-50              | 6-ft flow model results for 225 m <sup>3</sup> /s in the BLR8 study area.....  | 110                |
| Figure 2-51              | 6-ft flow model results for 250 m <sup>3</sup> /s in the BLR8 study area.....  | 111                |
| Figure 2-52              | 5-ft flow model results for 200 m <sup>3</sup> /s in the BLR8 constriction study area.....   | 112                |
| Figure 2-53              | 5-ft flow model results for 250 m <sup>3</sup> /s in the BLR8 constriction study area.....   | 113                |
| Figure 2-54              | 5-ft flow model results for 300 m <sup>3</sup> /s in the BLR8 constriction study area.....   | 114                |
| Figure 2-55              | 5-ft flow model results for 350 m <sup>3</sup> /s in the BLR8 constriction study area.....   | 115                |
| Figure 2-56              | 5-ft flow model results for 400 m <sup>3</sup> /s in the BLR8 constriction study area.....   | 116                |
| Figure 3-1               | Schematic representation of different types of geomorphic and stratigraphic evidence for paleofloods and paleohydrologic bounds..... | 142                |
| Figure 3-2               | Probability density functions for erosion based on shear stress and stream power for Big Lost River applications.....                | 143                |
| Figure 3-3               | Probability distributions for major channel modifications based on channel averaged stream power and shear stress values.....        | 144                |
| Figure 3-4               | Stream power and shear stress sample areas along Big Lost River Diversion Dam study reach.....                                       | 145                |
| Figure 3-5               | Example of stream power and shear stress results for subarea FP11.....   | 146                |
| Figure 3-6               | Combined discharge limits for late Holocene paleofloods and paleohydrologic bounds.....  | 147                |
| Figure 3-7               | Combined discharge limits for early Holocene paleohydrologic bound.....  | 148                |
| Figure 3-8               | Combined discharge limits for Pleistocene paleohydrologic bound.....   | 149                |
| Figure 3-9               | Combined discharge limits for catastrophic channel change.....   | 150                |
| Figure 4-1               | Measurement uncertainties for gage, bound, and paleoflood discharges on the Big Lost River at the INEEL Diversion Dam.....           | 167                |
| Figure 4-2               | Revised flood frequency for Big Lost River at the INEEL Diversion Dam.....   | 168                |
| Figure 4-3               | Peak discharges distributions for AEP's 0.01 and 0.00667 on the Big Lost River at the INEEL Diversion Dam.....                       | 169                |
| Figure 4-4               | Peak discharges distributions for AEP's 0.005 and 0.00286 on the Big Lost River at the INEEL Diversion Dam.....                      | 170                |
| Figure 4-5               | Peak discharges distributions for AEP's 0.002 and 0.00133 on the Big Lost River  |                    |

## LIST OF FIGURES

| <b><u>Figure No.</u></b> | <b><u>Title</u></b>  | <b><u>Page</u></b> |
|--------------------------|--|--------------------|
|                          | at the INEEL Diversion Dam.....  | 171                |
| Figure 4-6               | Peak discharges distributions for AEP's 0.001 and 0.0005 on the Big Lost River at the INEEL Diversion Dam. ....              | 172                |
| Figure 4-7               | Peak discharges distributions for AEP's 0.000286 and 0.00002 on the Big Lost River at the INEEL Diversion Dam.....           | 173                |
| Figure 4-8               | Peak discharges distributions for AEP's 0.000133 and 0.00001 on the Big Lost River at the INEEL Diversion Dam.....           | 174                |
| Figure 4-9               | Peak discharges distributions for AEP's 0.0000667 and 0.000005 on the Big Lost River at the INEEL Diversion Dam.....         | 175                |
| Figure 4-10              | AEP distributions for 250 m <sup>3</sup> /s and 300 m <sup>3</sup> /s on the Big Lost River at the INEEL Diversion Dam. .... | 176                |
| Figure 4-11              | AEP distributions for 400 m <sup>3</sup> /s and 700 m <sup>3</sup> /s on the Big Lost River at the INEEL Diversion Dam. .... | 177                |
| Figure 4-12              | AEP distributions for 106 m <sup>3</sup> /s and 150 m <sup>3</sup> /s on the Big Lost River at the INEEL Diversion Dam.....  | 178                |
| Figure 4-13              | AEP distributions for 176 m <sup>3</sup> /s and 200 m <sup>3</sup> /s on the Big Lost River at the INEEL Diversion Dam. .... | 179                |
| Figure 5-1               | Map of monitoring site locations (numbered black squares within blue boxes) for inundation at TRA and INTEC.....             | 195                |
| Figure 5-2               | Conceptual logic tree for probabilistic INL inundation modeling.....   | 196                |
| Figure 5-3               | Stage hazard curves for site TRA map ref #1. ....  | 197                |
| Figure 5-4               | Stage hazard curves for TRA-632 map ref #7. ....   | 198                |
| Figure 5-5               | Stage hazard curves for INTEC map ref #13.....   | 199                |
| Figure 5-6               | Stage hazard curves for the INTEC tank farm map ref #10. ....  | 200                |

## LIST OF TABLES

| <b><u>Table No.</u></b> | <b><u>Title</u></b>   | <b><u>Page</u></b> |
|-------------------------|---|--------------------|
| Table SO-1              | Comparison of Revised Flood Frequency for the Big Lost River at the Diversion Dam with Previous Study Results. .... | iv                 |
| Table S0-2              | Big Lost River Paleofloods and Paleohydrologic Bounds.....  | xii                |
| Table SO-3              | Nonparametric Flood Frequency for the Big Lost River at the Diversion Dam.xvi                                       |                    |
| Table SO-4              | Probabilistic Stage Estimates for INTEC and TRA Sites (100- and 500-year floods) .....                              | xxii               |
| Table SO-5              | Probabilistic Stage Estimates for INTEC and TRA Sites (2000- and 10,000-year floods) .....                          | xxiii              |
| Table 1-1               | Summary of some results from previous flood hazard studies at INL .....   | 11                 |
| Table 1-2               | Comparison of Measured and Required Accuracy Values for Areas Downstream of INEEL Diversion Dam (Appendix A) .....  | 11                 |
| Table 2-3               | Geologic and Geomorphic Summary for Big Lost River Paleofloods and Paleohydrologic Bounds .....                     | 117                |
| Table 2-1               | Discharge and modeling scenarios for the INEEL Diversion Dam study reach1 18  |                    |
| Table 2-2               | Soils and Radiocarbon Summary .....   | 119                |
| Table 2-3               | Geologic and Geomorphic Summary for Big Lost River Paleofloods and Paleohydrologic Bounds .....                     | 120                |
| Table 3-1               | Hydraulic modeling sample area characteristics - floodplain subareas .....  | 152                |
| Table 3-2               | Hydraulic modeling sample area characteristics - channel subareas .....   | 155                |
| Table 3-3               | Summary of limiting discharge values from hydraulic modeling sample areas157  |                    |
| Table 3-4               | Applicability of hydraulic modeling sample areas to paleofloods and paleohydrologic bounds estimates .....          | 158                |
| Table 3-5               | Big Lost River Paleofloods and Paleohydrologic Bounds.....  | 159                |
| Table 4-1               | Least frequent peak discharge generation nodes. ....  | 181                |
| Table 4-2               | Nonparametric Flood Frequency for the Big Lost River at the Diversion Dam.182                                       |                    |
| Table 5-1               | Discharge and modeling scenarios used to construct the stage - probability estimates.....                           | 202                |
| Table 5-2               | Discharge-AEP Results from the FFA.....   | 203                |
| Table 5-3               | Stage - Probability Sites.....  | 204                |
| Table 5-4               | Probabilistic Stage Estimates for INTEC and TRA Sites (100 and 500 floods).205                                      |                    |
| Table 5-5               | Probabilistic Stage Estimates for INTEC and TRA Sites (2000 and 10000 year floods) .....                            | 206                |

## List of Plates

(Folded sheets in pocket and PDF files on CD)

| <u>Plate</u> | <u>Title</u>   |
|--------------|--|
| 1            | Shaded Relief, Contour, and Orthophoto Maps of the INEEL Diversion Dam Study Reach - Big Lost River, Idaho |
| 2            | Geomorphic Maps of the INEEL Diversion Dam Study Reach - Big Lost River, Idaho                             |

## Appendices

(Separate documents or on CD's)

| <u>Appendix</u> | <u>Title</u> |
|-----------------|--------------|
|-----------------|--------------|

|          |   |
|----------|---|
| <b>A</b> | <b><i>Topographic Data for Flood Hazard Modeling at INEEL</i></b> |
|----------|---|

Quality Assurance of Topographic Data for the Big Lost River Flood Hazard Study, Idaho  
National Engineering and Environmental Laboratory, Idaho

Shaded Relief, Contour, and Orthophoto Maps of the INEEL Diversion Dam Study  
Reach - Big Lost River, Idaho

Shaded Relief, Contour, and Orthophoto Maps of the INEEL Reach - Big Lost River,  
Idaho

Coordinate and Photogrammetric Data Appendices

|          |                             |
|----------|-----------------------------|
| <b>B</b> | <b><i>Geologic Data</i></b> |
|----------|-----------------------------|

Soil Profile Descriptions

Soil Particle Size Results from Colorado State University

Examination of Bulk Soil for Radiocarbon Datable Material from Along the Big Lost River  
on the Idaho National Engineering and Environmental (INEEL) Site, Southern Idaho, by  
Kathryn Puseman, Paleo Research Institute.

Radiocarbon Dating Results and Calibration Data from Beta Analytic

Summary Report on Detrital Zircon Ages of Samples from Big Lost River Trenches, P.K  
Link, Idaho State University and C.M Fanning, Australian National University

Explanation, Plots, and Procedures for Point Count and Pebble Counts and Sieve Data, by V.  
Sheedy, Idaho State University

Gamma-Ray Spectrometry Results from J. Budahn, U.S. Geological Survey

Trench Sample Listings

**Appendix B - Electronic Supplement - Trench Logs**

|          |  |
|----------|--|
| <b>C</b> | <b><i>Hydraulic Modeling Methodology and Quality Assurance</i></b> |
|----------|--|

**Part A** - Methodology, Mesh Generation, and Models

**Part B** - Numerical Model Validation and Verification/Peer Review Comments

**D *Hydraulic Modeling Results for Paleoflood Analyses***

Evaluating Paleohydrologic Data with Stream Power and Shear Stress Results from Hydraulic Models

**Appendix D - Electronic Supplement** - Plots of modeled depth, stream power and shear stress for the Big Lost River, INEEL Diversion Dam Study Reach

**E *Hydraulic Modeling to Estimate Big Lost River Flood Inundation at INEEL Facility Sites***

Estimating Channel Infiltration Parameters from Historical Flow Data at INEEL

Infiltration Rates to Support High-Resolution Hydraulic Modeling at Idaho National Engineering and Environmental Laboratory by F.R. Fiedler, University of Idaho

Culvert Survey Summary by C.O. Kingsford, Bechtel BWXT

Stage-Discharge Relations for Selected Culverts and Bridges in the Big Lost River Flood Plain at the Idaho National Engineering and Environmental Laboratory, Idaho by C. Berenbrock and J.D. Doyle, 2003, DOE/ID-22184, WRIR 03-4066, U.S. Geological Survey

**Appendix E - Electronic Supplement** - Plots of modeled flood inundation for the Big Lost River downstream of the INEEL Diversion Dam

**F *Stage Probability Plots for Selected Locations at INEEL Facility Sites***



## 1.0 INTRODUCTION

Paleoflood studies of the Big Lost River (Ostenaar and others, 1999; 2002) indicated that potential flood hazards for the Big Lost River at the Idaho National Laboratory (INL) (**Figure 1-1**) might be significantly different than portrayed by previous studies (e.g., Kjelstrom and Berenbrock, 1996). Because of the significant discrepancy between the previous studies (**Table 1-1**), several further studies aimed at reducing the uncertainty in flood hazard estimates at INL have been undertaken by both USGS and BOR. The present document and the associated appendices describe the results from BOR studies of the Big Lost River flood hazard at INL.

In previous studies of flood hazard for the Big Lost River, Kjelstrom and Berenbrock (1996) and Hortness and Rousseau (2003) used stream-gage data from Big Lost River and surrounding region. Ostenaar et al. (1999, 2002) used stream-gage and geologic paleoflood data from the Big Lost River at INL. The differences in the resulting estimate of the 100-year peak flow shown by previous studies (**Table 1-1**) are primarily due to the use of differing data in each of the analyses. The lower peak flow estimate by Hortness and Rousseau (2003) can be attributed to their evaluation of flow attenuation within the Big Lost River system downstream of stream gages used to estimate flood frequency. The paleoflood study sites of Ostenaar et al. (1999, 2002) are downstream of the gages and should therefore include this attenuation. All estimates of 100-year peak flow require extrapolation beyond the length of the available stream gage data record. The geologic paleoflood data lengthens the available record of peak flow and constrain estimates of the 100-year peak flow to be within the data record of geologic observation.

### 1.1 Present Study Objectives

The major objectives of the BOR studies are focused on two broad technical arenas; 1) geologic, geomorphic, and hydraulic modeling studies to reduce the uncertainty associated with paleohydrologic estimates used in flood frequency analyses, and 2) developing probabilistic flood stage estimates for specified facility locations at INTEC and TRA.

The paleohydrologic studies have focused on detailed studies of a 5-km (3-mi) reach of the Big Lost River that extends between the INEEL Diversion Dam and the historic Pioneer Diversion (**Figure 1-2**) In this reach, 1:4000-scale aerial photography flown in September 2000 was used to

develop a 3-ft topographic grid that could be rendered as the base map for detailed geomorphic mapping of the study reach and as topographic input for updated two-dimensional hydraulic modeling (**Plate 1**). To improve the geologic data for paleoflood and paleohydrologic bound estimates, seven trenches at three detailed study sites were excavated within the study reach. From the geomorphic mapping, trenching data and updated hydraulic modeling, revised estimates of paleofloods and paleohydrologic bounds for the Big Lost River were developed. These data were used to revise and update the flood frequency analyses.

Developing probabilistic stage estimates for INTEC and TRA facility sites included three major work activities: 1) reprocessing of the 1993 1:10,000-scale aerial photography along the Big Lost River to generate a 5-ft topographic grid, 2) two-dimensional hydraulic modeling of multiple flow scenarios between the INEEL Diversion Dam to downstream of INTEC and TRA, and 3) estimating stage probability curves for facility sites that could include alternate views and uncertainties in flood frequency, infiltration, and culvert flows on the INL site.

Initial hydraulic modeling based on the 3-ft grid topographic data for the Diversion Dam reach showed results that differed significantly from the previous studies of Ostenaar and others (1999) which used topographic data derived from the 1993 INEEL 2-ft contour map. Because the same two-dimensional hydraulic model was being used in both studies, the cause of this difference was clearly related to the input topography used in the models. To resolve these discrepancies, extensive GPS field surveys along the Big Lost River were conducted to assess the accuracy of the topographic mapping used in all phases of these studies. The GPS field surveys found that the 1993 INEEL 2-ft contour map did not appear to meet standards for 4-ft contour interval mapping (**Table 1-2**) and that in the area of the paleoflood study reach the surface defined by this mapping was apparently warped (**Appendix A**). The lack of resolution and accuracy associated with the 1993 2-ft contour map resulted in systematic overestimation of stages associated with discharge in the Big Lost River in the previous studies. GPS field surveys of selected areas along the Big Lost River corridor demonstrate that the topographic data from the 2000 photography in the paleoflood study reach and reprocessed data from the 1993 photography both meet accuracy standards needed for the high-resolution flood modeling (**Table 1-2**) (**Appendix A**).

The two-dimensional (depth-averaged) flow models TrimR2D and RiCOM (**Appendix C**) were used to calculate inundation and flow velocities for paleoflood and site inundation investigations at INL. TrimR2D uses a fixed-spacing staggered finite-difference approach that was used for hydraulic modeling of steady-state discharges in the paleoflood reach and with a larger grid spacing for the site inundation studies. RiCOM uses a staggered finite-element approach that provided an opportunity to employ high-resolution topography in a variable-sized element mesh constructed for the INL site inundation investigations. Both TrimR2D and RiCOM were used to investigate site inundation scenarios to assess the importance of parameters including topographic grid resolution, infiltration, and culvert performance, on estimated inundation corresponding to long-duration (~20 hour-steady-state) discharges. Results from both models were post-processed for estimates of stream power and shear stress.

Monte Carlo nonparametric flood frequency estimation was used to incorporate measurement uncertainties in gaged, historical, and paleoflood discharges and nonexceedence bounds and to produce fully probabilistic flood frequency estimates for annual exceedence probabilities of specific discharges of interest. These annual exceedence probabilities were combined with stage estimates from TrimR2D and RiCOM discharge, infiltration, culvert, and topographic resolution scenarios to produce scenario probabilistic stage hazard curves for 15 sites located in the TRA/INTEC facilities (**Appendix F**). Annual exceedence probabilities and associated credible limits are provided for map-scale inundation plots to provide scenario probabilistic inundation maps (**Appendix E**). These products provide a basis to develop weights for logic tree branches associated with infiltration and culvert performance scenarios to produce probabilistic inundation maps.

## 1.2 Acknowledgments

This project has been funded through an Interagency Agreement (DE-AI07-00ID13972) between the Department of Energy (DOE) Idaho Operations Office and the Bureau of Reclamation (BOR) Technical Service Center in Denver. Robert Creed is the DOE Program Manager, who has enabled the extensive assistance and coordination required for the assembly of data and field activities on the INL site. Chris Martin (S.M. Stoller Corp.) developed initial QA documents and provided assistance with review activities.

The overall framework of this study as developed by R. Creed was intended to be a collaborative and inclusive effort that included contributions, inputs, and viewpoints from other individuals and institutions. While BOR was the primary lead on the paleohydrologic and hydraulic modeling components, assistance from a participatory review group following development of the initial scope of work consisting of N. Katapodes (University of Michigan), P.K. House (Nevada Bureau Mines and Geology), and K. Coppersmith (Coppersmith Consulting, Inc.) was highly beneficial. Other collaborators in the study including many INL staff, and study collaborators from USGS, University of Idaho, Idaho State University (ISU) also provided significant input.

J. Ake (BOR) worked with us and the participatory review group to develop the original and revised scope of work for this project. He also provided final review comments on the summary document.

Matt Jones (BOR) is a co-principal investigator responsible for production of many products that are integral to this project. Matt conducted the GPS surveys for the photogrammetry and topographic analyses, generated all of the photogrammetric products and topographic grid data used as input for the hydraulic modeling, and generated all of the visualizations used to display the results of the geomorphic mapping and hydraulic modeling.

Roger Denlinger of the USGS provided the 2D explicit finite-volume flow code and performed flow calculations on the Verde and Stanislaus rivers that provide a unique opportunity to provide an independent check of the TrimR2D and RiCOM flow codes (**Appendix C**). Roy Walters developed the TrimR2D and RiCOM flow codes and performed many tests of these codes to replicate and supplement testing performed by the authors of the report (**Appendix C**).

Collection and analyses of topographic data from the INL site could not have been completed without the extensive help of K. Beard (INL). Ken assisted with GPS surveys upstream of the INEEL Diversion Dam and graciously provided extensive assistance and consultations regarding the topographic and survey issues at the INL site. We also thank R. Smith (INL) for extensive help locating data needed for reanalyses of the 1993 aerial photography data. The INL GIS Laboratory provided several pieces of GIS data used to construct base maps for the inundation modeling.

Matt Norake (VECTORS, Inc.) assisted with reduction of much of GPS data used for control on the 2000 photography and with field surveys to evaluate the 1993 topographic results.

The insight and assistance of R. Smith (INL) with basalt stratigraphy and overall geologic processes at the INL was indispensable to this project. The initial phase of geomorphic mapping, conducted prior to the trenching, also benefited greatly from the insights and review comments of R. Klinger (BOR).

Logging and description of the trenches required extended field efforts and assistance from several individuals. Val Sheedy (ISU) provided extended assistance with logging and descriptions of the trenches and with sedimentological analyses. David Simpson (URS Consultants) assisted with soil descriptions for trenches T1 to T7. Lucy Piety (BOR) provided additional expertise in interpretations of the soils, and with extending the soil descriptions and mapping throughout the trenches. Piety and L. Anderson (BOR) also assisted in logging of trenches T8/T9. K. Duran and W. Gonzales (BOR) provided field assistance in the initial phases of trench gridding and surveying and extensive support in assembling the photomosaics used as base maps for trench logging (**Appendix B-electronic supplement**).

Many helpful and insightful comments were received along the way from G. Thackery and P. Link of ISU through several field visits and discussions during the mapping and trench logging. In addition, they provided oversight to V. Sheedy and the sedimentological analyses. P. Link conducted detrital zircon analyses of several samples.

Kathy Puseman at PaleoResearch Laboratories provided macrofloral identifications of samples from the trenches. Radiocarbon dating was conducted through Beta Analytic. Mel Kuntz (USGS) provided assistance with attempts to identify potential tephras in samples from the trenches. Jim Budahn (USGS) conducted gamma-ray spectrometry on a set of test samples to evaluate isotopic activity.

In February 2005, after most maps and supporting documentation for this report had been finalized, the Idaho National Laboratory (INL) became the new official name of the former Idaho National Environmental and Engineering Laboratory (INEEL). The new name has been adopted

in the text of this summary report for most references to the site and staff. Exceptions include figures where the boundaries and features are labeled with the INEEL name on underlying images and references to stream-gaging stations and data, all references to the INEEL Diversion Dam. The previous name was retained for consistency in this report because all of the supporting maps and images were completed with the old name. Most site references within appendices to this report were completed prior to the name change and thus retain the old name.

**Figures for Section 1.0**

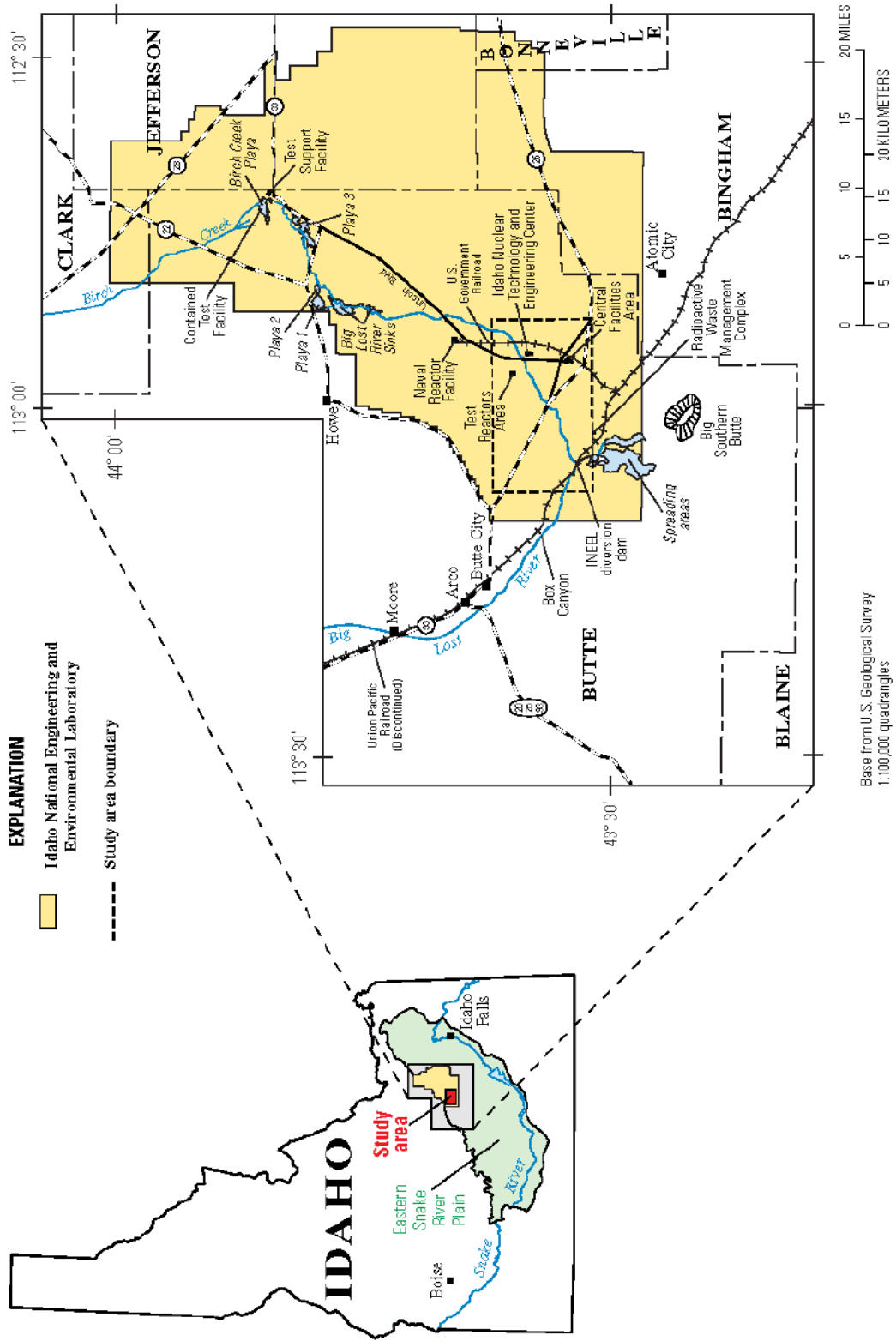


**Figure 1-1 Location map of INL (INEL) and study area. Diversion Dam study reach is located along the Big Lost River between the Union Pacific Railroad and Highway 26. Figure from Berenbrock and Doyle (2002).**

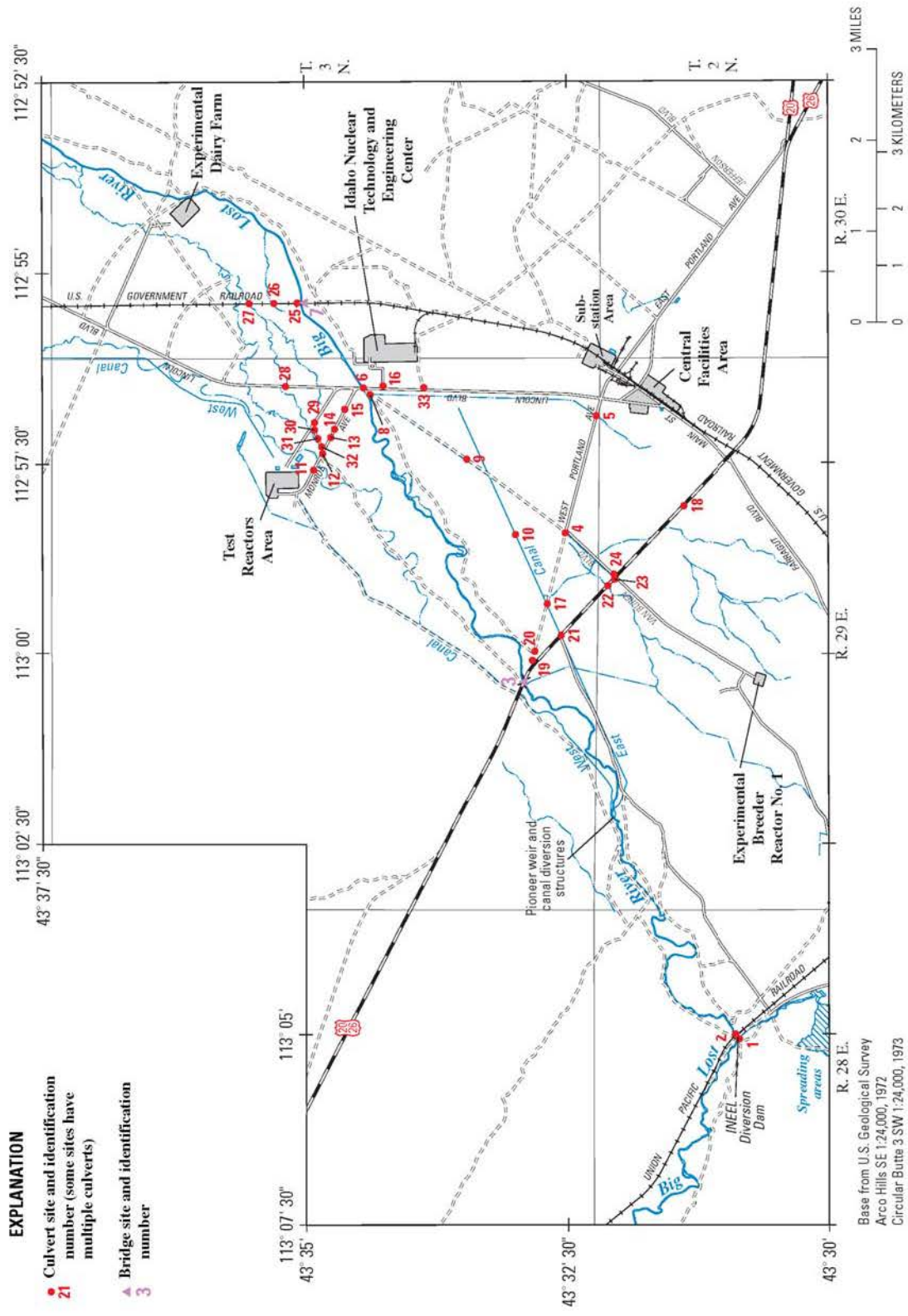


**Figure 1-2 INL study area, Big Lost River and significant facility locations.** Paleohydrologic studies were conducted for the reach between the INEEL Diversion Dam and the Pioneer diversion structures. Stage probability estimates are required for sites at the Test Reactor Area (TRA) and Idaho Nuclear Technology and Engineering Center (INTEC). Figure from Berenbrock and Doyle (Appendix E).

**Tables for Section 1.0**

**Table 1-1 Summary of some results from previous flood hazard studies at INL**

| Estimates of 100-year peak flow for the Big Lost River near INEEL Diversion Dam<br>m <sup>3</sup> /s (ft <sup>3</sup> /s) |                              |                              |
|---|------------------------------|------------------------------|
| Kjelstrom and Berenbrock (1996)   | Ostenaar et al. (1999, 2002) | Hortness and Rousseau (2003) |
| 206 (7260)  | 82 (2910)                    | 106 (3750)                   |

**Table 1-2 Comparison of Measured and Required Accuracy Values for Areas Downstream of INEEL Diversion Dam (Appendix A)**

| Map/Data Source  | Measured Values |          |                   | Required Values |         |                                    |         |
|--|-----------------|----------|-------------------|-----------------|---------|------------------------------------|---------|
|  | NSSDA           |          |                   | NMAS (Accuracy) |         | ASPRS class 1 (RMSE <sub>z</sub> ) |         |
|  | n=              | Accuracy | RMSE <sub>z</sub> | 2-ft CI         | 4-ft CI | 2-ft CI                            | 4-ft CI |
| <b>1993 AG 2-ft Contours (Paleoflood Study Reach)</b>  |                 |          |                   | 1.192           | 2.383   | 0.677                              | 1.333   |
| Aug. 2000 panel points   | 61              | 2.246    | 1.146             |                 |         |                                    |         |
| July 2002 check survey   | 827             | 3.038    | 1.550             |                 |         |                                    |         |
| (Downstream Hwy 20/26)   |                 |          |                   |                 |         |                                    |         |
| Oct. 2002 check survey   | 519             | 2.446    | 1.248             |                 |         |                                    |         |
| <b>2003 BOR 5-ft Grid (Paleoflood Study Reach)</b>   |                 |          |                   |                 |         |                                    |         |
| Aug. 2000 panel points   | 61              | 1.752    | 0.894             |                 |         |                                    |         |
| July 2002 check survey   | 827             | 1.746    | 0.891             |                 |         |                                    |         |
| (Downstream Hwy 20/26)   |                 |          |                   |                 |         |                                    |         |
| Oct. 2002 check survey   | 519             | 1.586    | 0.809             |                 |         |                                    |         |
| Shaded values do not meet NMAS standards or ASPRS class 1 standards for 4-ft contour mapping |                 |          |                   |                 |         |                                    |         |

## **2.0 GEOLOGIC AND GEOMORPHIC STUDIES OF THE DIVERSION DAM STUDY REACH**

The paleohydrologic studies of the Diversion Dam study reach are a continuation and expansion of the studies described in previous reports (Ostenaar et al., 1999, 2002). The objective of further studies is to identify and reduce the uncertainty of the previous estimates. Field-scale investigations included four major tasks: 1) acquisition and processing of new detailed aerial photography to serve as a base map for geomorphic mapping and hydraulic modeling, 2) compilation of a detailed geomorphic map of the study reach, 3) trenching and detailed geologic descriptions and analyses in three areas of the study reach to confirm geologic/geomorphic relationships, and 4) additional two-dimensional hydraulic modeling using the new topographic data. In the following sections, the setting of study reach is reviewed (**Section 2.1**), followed by discussions of the geomorphic mapping (**Section 2.2**), and trenching investigations (**Section 2.3**). **Section 2.4** summarizes the combined results of the geomorphic and trenching investigations. The scope and updated results from new two-dimensional modeling of the Diversion Dam study reach are in **Section 2.5**. **Section 3.0** describes the framework for evaluating the geomorphic and hydraulic modeling data to support conclusions regarding paleofloods and paleohydrologic bounds for the Big Lost River. These conclusions are outlined in **Section 3.3** and **Section 3.4** and used in the updated flood frequency analyses presented in **Section 4.0**.

### **2.1 Geologic and Geomorphic Setting of the Diversion Dam Study Reach**

Ostenaar et al. (1999, 2002) summarize the setting and extent of the Diversion Dam study reach, and the application of paleohydrologic bounds to the issues of estimating flood frequency for the Big Lost River.

The INL site is located on the eastern Snake River Plain of Idaho (**Figure 1-1**), a large area of Quaternary basaltic lava flows that are mantled with extensive, thin, wind-blown deposits and lesser areas of alluvium and lacustrine deposits (Kuntz et al., 1994). Mid- to late Cenozoic extension in the Basin and Range Province mountains that lie to the north and south is overprinted by the volcanic activity on the eastern Snake River Plain, presumably in response to passage of the Yellowstone Hot Spot (e.g., Pierce and Morgan, 1992).

The headwaters of the Big Lost River are in the glaciated mountains of the Idaho Basin and Range Province north of the Snake River Plain. The upper basin includes peaks that exceed elevation 3500 m in the northeast-facing basins of the Pioneer Mountains and the southeastern portion of the steep southwest-facing front of the Lost River Range. The river flows southeast for a distance of about 80-km through the Big Lost River Valley, a late Cenozoic structural basin filled with alluvium. Mackay Reservoir, about 30-km upstream of Arco, stores irrigation water for users in the downstream Big Lost River Valley. At the northern edge of the Snake River Plain near Arco, the drainage basin includes an area of about 3650 km<sup>2</sup> that lies above an elevation of 1550 m. About 10-km downstream of Arco, the river flows onto the INL site where it turns northeast and flows another 35 km to its natural terminus in the Big Lost River Sinks and several playas at the northern edge of the INL site. The last portion of the river course parallels the axis of the Big Lost Trough, a late Cenozoic depositional center on the north side of the eastern Snake River Plain (Geslin et al., 2002). Subsidence along the Big Lost Trough has been more or less matched by the rate of volcanic and sedimentary infill (Geslin et al., 2002). Thus, on the Snake River Plain and the INL site, a sequence of late Pleistocene terraces along the Big Lost River records only a few meters of net incision in the last 95 ka (Ostenaar et al., 1999; Simpson et al., 1999).

**2.1.1 Big Lost River historical stream flow.** Average annual precipitation in the Big Lost River basin ranges from about 1250 mm/yr in the mountainous upper basin areas to about 200 mm/yr across much of the INL site on the Snake River Plain. This precipitation occurs mostly in the winter months and is largely derived from moisture from the northern Pacific Ocean (Kjelstrom, 1991). During the late spring and summer snowmelt period, the air flow from the Pacific generally consists of relatively dry, subtropical air that produces only sporadic thunderstorms across Idaho. Southeastern Idaho can be affected as well by summer monsoon flow from the south and southwest, which can cause increased precipitation (Kjelstrom, 1991). Meteorological conditions favorable for long-duration winter rainfall are uncommon (Kjelstrom, 1991), especially for large drainage basins.

Annual stream flow, and the largest annual peak discharge, in the Big Lost River are dominated by the spring and early summer snowmelt and runoff from the mountains in the upper drainage basin. Stream flow records are available from the upper basin since 1904 and from the Arco area

since 1947 (Ostenaar et al., 1999, 2002) (**Figure 2-1**). The timing of the snowmelt is regular, usually beginning in late May or early June of each year, with significant flows extending into July. The magnitude of the annual peak discharge typically decreases in a downstream direction with increasing drainage area. Significant downstream decreases in peak discharge, even in the wettest years, indicate that the decrease is at least in part due to large amounts of natural channel infiltration and storage in the Big Lost River Valley (Stearns et al., 1938). Additional decreases in peak discharge result from storage in Mackay Reservoir, about 65 km upstream of the INL site, and irrigation diversions upstream of Arco and the INL site. Hortness and Rousseau (2003) evaluated the changes in peak discharge at gaging stations along the Big Lost River and documented a systematic attenuation in peak discharge from the upstream gaging stations to the INL area. This attenuation appears to exist even for the largest historical streamflows and is not solely due to regulation effects.

**2.1.2 Big Lost River – Diversion Dam study reach.** South of Arco, the Big Lost River leaves the alluvium-filled Big Lost River valley (**Figure 1-1**) and flows across middle to late Quaternary basalt on the Snake River Plain that is locally mantled with alluvium of varied thickness (Kuntz et al., 1994). Near Box Canyon (**Figure 1-1**), the river is incised from 5- to 30-m into the basalt, and only small areas of alluvium are preserved in the canyon. Downstream of Box Canyon, on the southwestern portion of the INL site, Kuntz et al. (1994) mapped extensive areas of alluvium along the Big Lost River. However, even in this reach, basalt exposures are common in the bed and banks of the river and as isolated outcrops on the alluvial surfaces near the channel, indicating that the alluvium overlying the basalt is relatively thin in this area (**Plate 2**).

The geologic and geomorphic descriptions, and hydraulic modeling analyses, focus on a 6-km-long study reach just downstream of the INEEL Diversion Dam (**Plates 1 and 2**). Throughout the Diversion Dam reach, the Big Lost River is incised about 2- to 4-m into the relatively flat alluvial surfaces on either side. Areas of relief are associated with Pleistocene basalt outcrops that stick out above the alluvium. Previous mapping depicts most of this alluvium as Pleistocene in age based on the degree of soil development and alluvial surface morphology (e.g., Rathburn, 1991; Kuntz et al., 1994). The Pleistocene alluvium is gravelly with a 0.5- to 1-m-thick cover of loess, mostly deposited before about 10 ka (Forman et al., 1993). Exposures in nearby gravel pits,

stream banks, and trenches excavated for this study show a moderate- to well-developed soil with stage II or greater calcium carbonate accumulation in the gravel and loess.

Soils at sites BLR3 and BOR25 contain stage II or greater calcium carbonate accumulation (Ostenaar et al., 1999, 2002) as do soils exposed in the trench intervals excavated into the Pleistocene alluvium (e.g., T1, T2, T3, T6, T7, T8 and T9; see **Plate 2** for locations). Soils in the gravelly alluvium and overlying loess have well developed calcic horizons, (stage II to III), generally considered indicative of a late Pleistocene age (e.g., Scott, 1982; Birkeland, 1999).

Topographic maps and images of the Pleistocene surfaces show a distinct pattern of relic channels with a subdued morphology (**Plate 2**). The pattern of these channels is consistent with the development of these surfaces as Pleistocene glacial outwash plains, as is the sedimentology of the gravels exposed in the trenches. The youngest fluvial-related features on these gravel surfaces are 1- to 1.5-m deep braid channels infilled with fine sand and silt in which a Stage II carbonate soil is developed, consistent with a Pleistocene age. The surfaces also have a well-developed pattern of earth mounds, which often follow and overprint the channels (Tullis, 1995).

The overall channel configuration of the Big Lost River in this study reach (**Plate 2**) is controlled by several locations where the river crosses outcrops of basalt. The sharp bend at the INEEL Diversion Dam results from the impingement of the Big Lost River on a flow tongue of Quaking Aspen Basalt. Downstream of this bend, through the study reach extent shown on **Plates 1 and 2**, the overall sinuosity is about 1.5. However, upstream of BLR2 (see **Plate 1** for locations), sinuosity is about 1.2. The central section from BLR2 to the Saddle Constriction area has sinuosity of 2.4, while downstream sections have an overall sinuosity of about 1.2. The most sinuous sections of the channel are formed in reaches with mostly alluvial banks upstream of where the Big Lost River impinges on partially buried basalt outcrops, such as at the Saddle Constriction study area (**Plate 2** and **Figure 2-3**). Reaches with relatively lower sinuosity tend to have more areas of outcropping basalt in the channel bed and banks, suggesting that the stream course and form is primarily controlled by interactions with rock outcrops. The basalt outcrops in the study reach form constrictions that locally create hydraulic controls on flow and indicate that the overall configuration of the channel has been stable since the river incised below the level of the Pleistocene surfaces. Well-developed soils on some of the inset fine-grained terraces, such as

at BLR6 and in Trench T6 and T8, and radiocarbon ages from these deposits (**Table 2-2**), indicate that this incision has an age of at least 10 ka and more likely 13 ka.

In the central portion of the Diversion Dam study reach, the Big Lost River flows through a narrow basalt constriction (**Saddle Constriction study area - Plate 2**). This constriction is formed by a ridge of basalt that extends across the Big Lost River and protrudes above the level of the Pleistocene alluvial surface south of the river. Upstream of this constriction lies a meandering reach of the river that is flanked by an extensive area of Holocene alluvium inset below the level of the Pleistocene alluvial surfaces on either side (**Plate 2**). On the north side of the river, a low ridge apparently underlain by basalt forms the contact between the Holocene and Pleistocene alluvium (**Figure 2-3**). The surface of the ridge is capped with gravel and eolian deposits. The low point along this ridge, informally known as the Saddle, is a location where high flows could spill over onto the Pleistocene surface downstream of the ridge due to elevated stage caused by hydraulic ponding at the basalt constriction.

Throughout the Diversion Dam study reach are Holocene surfaces with distinctly different morphology that are inset within, and below the level of the Pleistocene surfaces. An extensive area of Holocene alluvium lies just upstream of the Saddle (**Plate 2**), but elsewhere in the reach these deposits are of limited extent. Downstream of the Saddle, Holocene surfaces are limited to narrow terraces that mostly parallel the main channel, but which are somewhat wider at locations where high flows have cut across bends, such as near site BLR8 (**Figure 2-5**). On the higher Holocene surfaces, approximately 2- to 3-m above the low-flow channel, the surface morphology is generally smooth, with only small, subdued channels evident. In contrast to the Pleistocene surfaces, earth mounds are absent. A 0.5- to 1-m-high terrace riser is often present at the back edge of these surfaces defining the contact with the Pleistocene surfaces. On the geomorphic maps these surfaces are mapped as the H1-2 units (**Appendix B** and **Plate 2**). Surfaces that are less than 2-m above the low-flow channel are distinctly channeled (H3-4 units on **Plate 2**). Floated historical debris indicates that these lower surfaces and deposits have been flooded by recent flows.

Descriptions in trenches T4, T5, T6, T8 and T9, (**Section 2.3**) and at sites BLR2, BLR7, and BLR8, (Ostenaar et al., 1999, 2002) in the Diversion Dam reach show that the Holocene terrace

deposits of the Big Lost River are generally fine-grained, consisting of sand and silt. Gravel is generally present only as small bars in the channel, or underlying the fine-grained deposits in these terraces. Rathburn (1991) also noted that the Holocene deposits of the Big Lost River on the INL site are more fine-grained than the Pleistocene alluvium.

## **2.2 Geomorphic Mapping of the Diversion Dam Study Reach**

Mapping of the Diversion Dam study reach was done using stereo photography and digital terrain models using Intergraph ZI Imagestation Software. Imagery and terrain models were obtained from the 2000 aerial photography flown for this study (**Appendix A**). Most final contacts were not field checked in detail, but the mapping was heavily supplemented with field notes compiled on 1993 and 2000 aerial photography and their associated topographic map products, as well as data from previous mapping. One major mapping objective was to characterize the spatial extent of the significant geomorphic units within the study reach for comparison and analyses with the results of the two-dimensional flow modeling. A second objective was identify and characterize sites for subsurface investigations of stratigraphy and soils. Characteristics of the major units depicted on **Plate 2** are discussed in the following subsections, followed by summaries of the setting of the sites identified for further investigations.

**2.2.1 Quaternary Basalts - Rb, Rbe, Rd and Rde.** Previous geologic mapping of the INL site area (Kuntz et al., 1994) depicts two Quaternary basalt units in the area of the Diversion Dam study reach. An older unit, previously mapped as Qbd, includes basalt flows with estimated ages of 400 to 730 ka, mostly derived from sources north of the present Big Lost River. For the present study (**Plate 2**), flows of this group are mapped as Rd, and Rde for outcrop areas discontinuously and thinly covered by eolian sand and loess. A younger unit, previously mapped as Qbb, includes flows dated between 15 to 200 ka. Qbb flows in the Diversion Dam study reach have sources near Quaking Aspen Butte, several km to the southwest. Dating studies near the RWMC, just south of the Diversion Dam study reach, indicate that the flow at that site is about 95 ka (Forman et al., 1993; Kuntz et al., 1994). For the present study, the Quaking Aspen flows are mapped as Rb, and Rbe for outcrop areas discontinuously and thinly covered by eolian sand and loess.

Both of the basalt map units are locally covered by a variable thickness of loess and eolian cover. Locally, many areas have a well-developed stone pavement consisting of angular basalt pebbles and carbonate detritus. Earth mounds are present in some areas where loess accumulation is apparently thicker. The flow tops are highly irregular, with local surface relief that exceeds 5 m.

At least two flows from the Quaking Aspen Butte lava field (Rb) intercepted the course of the Big Lost River in the map area (**Plate 2**). One flow tongue extends northeast from the INEEL Diversion Dam for about 2 km and appears to have deflected the late Pleistocene course of the Big Lost River to the northeast. A second flow extends across the course of the Big Lost River from the Saddle area to the Old Pioneer Diversion Dam area. This flow tongue extends southeast to the RWMC area where it has an estimated age of 95 ka (Forman et al., 1993; Kuntz et al., 1994). Pleistocene gravel sheets, mapped here as P1-2, bury the margins of the flow tongues, and have breached the low areas of both flow tongues as shown by radial, fan-shaped surfaces downstream of the Rb flows. In addition, the Pleistocene gravel surface extends around the northwest side of the Rb flow about 2 km north of the Old Pioneer Diversion Dam. Rb outcrops are present in bed and banks of the Big Lost River channel at the INEEL Diversion Dam, and from the Saddle area to the Old Pioneer Diversion Dam area. Outcrops that protrude above the Pleistocene surfaces by more than about 1 m generally retain primary cooling features including vesicular plates on flow tops. Limited areas of loess accumulation are present on larger outcrops, which often have well-developed pavements of basalt fragments. Fissures along the crests of pressure ridges are only partially infilled with eolian deposits. In hand specimens, the Rb flows are distinguished by very fine-grained groundmass with common olivine phenocrysts.

The Rd units are part of a large area of basalt, mapped as Qbd by Kuntz et al. (1994) that lies north and northwest of Big Lost River downstream of the INEEL Diversion Dam. The margins of these flows are buried by Pleistocene alluvium. Extensive outcrops are present in the river channel bed and banks downstream of the INEEL Diversion Dam near BOR20, and scattered outcrops are present along the river downstream from BLR7 to BLR2 and the meander bend upstream of BLR3. The Rd units generally have a thicker cover of eolian deposits and more subdued morphology than Quaking Aspen (Rb) flows. In hand specimen, these basalts are

distinguished by fine-grained groundmass, common plagioclase phenocrysts, and rare olivine phenocrysts.

**2.2.2 Pleistocene Units - P1 to P3.** Initial mapping of the study reach defined three relative-age subdivisions, termed P1-2, P2, and P3, of the Pleistocene surfaces within the Diversion Dam study reach. The oldest surfaces, P1-2, are composed of broad, low-relief, fan-shaped surfaces that radiate from low saddles in the basalt ridges. Relic channels are subdued or not apparent, and large earth mounds up to 0.5-m-high are common and appear evenly spaced or random across the surface (**Plate 2**). The P1-2 surfaces are generally most distant from the present Big Lost River channel and are about 4.0 to 4.5 m above the channel.

The P2 surfaces are the most extensive Pleistocene surface within the Diversion Dam study reach and are generally 3.5 to 4.0 m above the channel. These surfaces have prominent relic cutoff and braid channels that are clear on aerial photography, and typically have 0.5-m relief as shown by contour maps. Because these surfaces are slightly inset relative to the P1-2 surface, the radial pattern from saddles in the basalt ridges is slightly subdued, but is still present. Large earth mounds up to 0.5-m-high are also common on the P2 surfaces. In some areas, the mounds often appear to follow relic channels, but are also present on interfluves. Over some large areas of P2 surfaces the mound pattern is subdued, but other morphology is unchanged. The mapped extent of P2 includes some slightly higher areas that are gradational to P1-2 and not mapped separately.

The gravel deposits that underlie the P1-2 and P2 surfaces are distal, glacial outwash from late Pleistocene glaciation in the upper Big Lost River drainage (Kuntz et al., 1994). The surface morphology on these units indicates deposition as an extensive gravel braid-plain, that predates the incision and establishment of the present Big Lost River channel. Thus, surface slopes and patterns on the P1-2 and P2 surfaces are generally unrelated to the present Big Lost River channel system. Rathburn (1991) also noted this, but viewed the gravels as having been deposited by the waning stages of a late Pleistocene glacial outburst flood, about 20 ka (Cerling et al., 1994). Subsequent work has suggested that any exceptionally large glacial outburst flood on the Big Lost River is likely older than about 50 ka (Ostenaar et al., 1999; Knudsen et al., 2002).

The gravel deposits that underlie the P1-2 and P2 surfaces are typically overlain by 25-150 cm of loess, with stage II-III carbonate developed in the loess and underlying gravel (Ostenaar et al., 1999, 2002; and **Section 2.3** following).

The P3 surfaces, 3.0 to 3.5 m above the Big Lost River channel are of limited extent compared to older P1-2 and P2 surfaces (**Plate 2**). In contrast to the older Pleistocene surfaces, the average surface gradient of the P3 surfaces is generally consistent with the Holocene channel and the inset H1-2 surfaces, although some P3 surfaces have a gentle slope towards the channel. A pattern of earth mounds are apparent on aerial photography and digital imagery (**Plates 1 and 2**), but larger mounds with topographic relief are present only on the rear, higher portions of these surfaces. Mounds with topographic relief are absent along lower portions. A distinct plant mound pattern is apparent on all surfaces; more developed than on H1 surfaces. The P3 surfaces are underlain by gravels, capped by a layer of loess which is generally thinner than on the P1-2 or P2 surfaces. Soils generally have Stage II carbonate in the gravels (**Section 2.3** following).

#### **2.2.2.1 Age Constraints from Regional Glaciation.**

Regional approaches have linked loess deposition to glaciation because the landscapes associated with regional glaciation such as aggraded river valleys, active alluvial fans, and fluctuating pluvial lake margins, provide the most viable sources for the loess (Forman et al., 1993). Based on luminescence ages from loess samples at INL, Forman et al. (1993) concluded that the latest period of loess deposition commenced about 35,000 to 40,000 years ago and ceased approximately 10,000 years ago. The youngest luminescence ages for loess on the eastern Snake River Plain near INL are 20-30 ka, and the age for cessation of loess deposition was based on age estimates for deglaciation in the Eastern Snake River Plain region.

Limiting ages for glaciation in the region surrounding the Snake River Plain are available from three areas, 1) Yellowstone, Wyoming to the east, 2) Wallowa Mountains Oregon to the northwest, and 3) Sawtooth Mountains, Idaho, to the north.

Radiocarbon ages on materials recovered from drill holes at Jackson Lake, Wyoming indicate that the southern outlet glaciers of the Yellowstone Plateau ice cap had retreated from maximum

positions in the Jackson Lake area by about 15,000  $^{14}\text{C}$  yr B.P., an age roughly equivalent to 17,000 to 18,000 calendar years (Pierce and Good, 1992; Good and Pierce, 1997; Connor, 1998). Northern outlet glaciers may have reached maximum positions somewhat later, about  $16,200 \pm 300$   $^{10}\text{Be}$  yr B.P. ( $16,500 \pm 400$   $^3\text{He}$  yr B.P.) possibly reflecting differences in ice accumulation source area characteristics (Licciardi et al., 2001). Earlier work in the area had suggested somewhat older ages for glacial maximums in northern Yellowstone (e.g., Sturchio et al., 1994), but all agree that deglaciation of the area was well underway, or even nearly complete, no later than about 14,000 cal. yr B.P. (e.g., Licciardi et al., 2001; Whitlock, 1993; Richmond, 1986; Pierce, 1979). In the Wallowa Mountains, Oregon, Licciardi et al., 2004 infer significant glacial advances at about  $17,000 \pm 300$   $^{10}\text{Be}$  yr B.P. based on ages from moraines located only a short distance upvalley of the LGM moraines dated to  $21,100 \pm 400$   $^{10}\text{Be}$  yr B.P. In the Sawtooth Mountains of Idaho, just to the west of the headwaters of the Big Lost River, Thackery et al. (2004) showed that the maximum glacial advances occurred shortly before about  $\sim 14,000$   $^{14}\text{C}$  yr B.P. ( $16,900$  cal. yr B.P.), roughly 4000 years later than the regional LGM. These ice positions were either maintained until or reoccupied as late as about 11,900  $^{14}\text{C}$  yr B.P. ( $13,950$  cal. yr B.P.), followed shortly by major deglaciation.

**2.2.2.2 Earth Mounds.** A ubiquitous feature of the Pleistocene surfaces, particularly the P1 and P2 surfaces, are large circular features termed earth mounds by Tullis (1995) in a previous study of these features on the INL. Tullis reviewed the extensive literature on the similar features which exist throughout the world, with several potential origins, including biological (primarily burrowing animals) and cryogenic (related to past glacial climates). Although unable to fully characterize all aspects of the origin of the earth mounds, Tullis (1995) concluded that a cryogenic origin was most likely for the INL mounds, although biological activity was a clear factor in the present mound characteristics. Soil development within and between the mounds indicated that the mounds developed during the late Pleistocene (Tullis, 1995) and many areas between the mounds have a weak to moderate gravel pavement (e.g., McFadden et al., 1998). Recent literature provides additional mechanisms for the initial origin of the mounds that would be consistent with a cryogenic origin (e.g., Kessler and Werner, 2003), as well as concepts for the biological exploitation of such sites (Johnson and Johnson, 2003).

Trench exposures (**Appendix B - Electronic Supplement** and **Section 2.3** following) through eleven mounds for this study confirm the relative antiquity and longevity of the mounds. The mounds formed in a variety of stratigraphic settings, clearly post-date gravel deposition, but also include strongly developed soils that indicate long-term spatial persistence. The trench exposures did not reveal evidence for eroded or abandoned mound sites. Only limited evidence of mound-related cryogenic features were observed in the trenches for this study. As noted by Tullis (1995), the mounds are preferred locations for Holocene biological activity based on abundant active and inactive burrows and disrupted soils of various development and ages.

Soil development within the mounds that indicates long-term spatial persistence, probably since the late Pleistocene, together with the occasional observations of associated cryogenic features noted in the trenches and by Tullis (1995), seems to support the hypothesis that the initiating condition for the mounds at INL was likely cryogenic. Mechanisms such as those discussed by Kessler and Werner (2003) would have led to formation of shallow depressions that would initially provide thicker sites of finer sediments on the gravel braid plain. Most likely these would then become colonizing sites for biological activity (e.g., Johnson and Johnson, 2003) and the process of building the topographic relief that distinguishes the present mounds. This framework of origin and mound growth implies a cryogenic process for initial subsurface relief and expression of the mounds, which are then strongly modified by the biological activity that is primarily responsible for building the surface relief and expression of the mounds. It further implies a strong likelihood that the topographic expression of the mounds on the Pleistocene surfaces has been gradually increasing, primarily due to biological processes, since they were initiated.

The surficial expression of the mounds consist largely of loess (Tullis, 1995) and would be highly erodible, as would the loess cover on the Pleistocene alluvium, if there was significant surface flow around or over the mounds. As shown on **Plate 2**, there are significant variations in the expressions of the earth mounds throughout the study reach. On the older Pleistocene surfaces, P1-2 and P2, these variations are not clearly related to obvious any patterns of flow that develop based on modeling of extreme flood discharges through the study reach. A likely cause of some of the observed variations is mound deflation due to wind following the August 2000 wildfire which

burned over most of Diversion Dam study reach a few weeks prior to the flight for aerial photography used for the base map images of **Plates 1 and 2**. In other areas, mounds have been modified by cultural activities at INL, especially early agriculture and grazing.

In contrast to the older Pleistocene surfaces, the geomorphic expression of the mounds on the P3 surfaces does appear to be modified by flow related to the present Big Lost River system. Earth mounds are only prominent on the higher, more distal portions of the P3 surfaces. The absence of mounds on the inset Holocene surfaces is more complex. Similar mounds may not have formed due to differences in the materials underlying the Holocene surfaces, or if the initial origin of the mounds required a much colder climate, the Holocene surfaces may post-date periods of climate favorable for mound initiation. Alternately, the expression of mounds on the Holocene surfaces may have been modified by younger floods.

#### **2.2.2.3 Geomorphic Evidence for Holocene Modification of the Pleistocene**

**Units.** The pattern of relic braid channels on the P1-2 and P2 surfaces shows no evident relation to potential patterns of large flows associated with the present Big Lost River channel. Rather, these channels are directly related to the overall radial fan shape of the P1-2 and P2 surfaces that is controlled by breaches through low saddles in the basalt ridges that flank and cross the Big Lost River (**Plate 2**). The braid channels have overall similar morphology, and do not display geomorphic evidence of having conveyed any significant, recent flow. One site that could appear as a possible exception to this is located about 250 m northeast of trench T1 (**Figure 2-2 and Plate 1**) where a sharp cut is present in the terrace riser onto the P2 surface. Field inspection of this feature suggests that it was excavated for vehicle access and was not an erosional feature and there are numerous other old wheel tracks and ruts in this area. About 150 m north of that site, the upstream continuation of the same terrace riser intersects a channel at the back edge of the highest P3 surface in this area, and at this location there appears to be a small fan built from the mouth of this channel onto the H1-2 surface. Trench T3 crosses this channel about 80 m to the west (upchannel) from this site. Exposures in trench T3 are permissive of small flows and limited amounts of sediment transport (**Section 2.3.1.3** following).

The morphology of several areas of the P3 surface contrasts sharply with the P1-2 and P2 surfaces. The large area mapped as P3 on the northwest edge of the Big Loop study area (**Plate 2**)

lacks earth mound morphology and there is subtle evidence of small fans built off the downstream edge of this surface. Just downstream, on the north side of the Big Lost River between the large meanders, another large area of P3 has smoother morphology, and small erosional features on its downstream edge. On the higher portions of the surface, more distant from flow, earth mounds are present. This area also appears to have been plowed or farmed, as evidenced by the surface morphology and by diversion canals built across it and on the upstream edge. It is not clear how much of the morphology results from anthropomorphic activities versus geomorphic modifications due to floods. On the next meander bend, on the south side of the river, the P3 surface also shows two distinct morphologies. To the northwest, on the lower portions of the surface closest to the river bend, the surface is smooth, and downstream edges of terrace risers appear to be channelled and eroded. To the southeast, the surface is slightly higher, and the surface is rougher, with obvious earth mounds. These morphology differences on the P3 surfaces appear to bracket the limits of significant flow modification by floods that are much younger than the surfaces. Two other areas of P3 surfaces, one upstream across from BLR7, and a section downstream of the Saddle Constriction study area near trenches T6 and T7, are both slightly higher and do not display geomorphic evidence of recent flooding.

**2.2.3 Holocene Units - H1 to H4.** Previous mapping has recognized the presence of a generally fine-grained fill inset within the Pleistocene gravels along the Big Lost River (Rathburn, 1991; Kuntz et al., 1994). The oldest portions of this fill likely relate to the latest Pleistocene deglaciation and changes in flow regime at the end of the Pleistocene (Rathburn, 1991). Subsequently, the fill has been partially reworked and a series of surfaces, cut onto the original fill and younger deposits.

In the present mapping, four groups of surfaces, H1 to H4 were defined according to their geomorphic characteristics. The oldest surface, H1, is preserved only as small, often narrow, remnants along the outer, higher, margins of the Holocene fill deposits. These surfaces appear to be underlain by an intact early Holocene soil characterized by >0.5-m-thick Bk-horizons with Stage II carbonate accumulation. The slope of these surfaces generally follows the present channel slope and these surfaces are typically ~ 2.5 to 3.0 m above the channel.

Inset H2 surfaces record erosion and deposition by at least one late Holocene flood (s), most recently about 400-600 years ago (Ostenaar et al., 1999, 2002). Locally, the boundary of H1-2 surfaces is expressed by a subtle break in slope with < 0.5-m relief, but in other areas, there is only a gradual slope or rise towards the back edge of the Holocene surfaces. The H2 surfaces are typically ~1.8 to 2.2 m above the present channel. Areas of the H2 surfaces that are more than a few meters from the bank of the Big Lost River appear to be mostly underlain by early Holocene fine-grained fill deposits with variably stripped remnants of a soil similar to that developed on the H1 surfaces as shown by exposures in trenches T6 and T8 (**Section 2.3.2.3** and **Section 2.3.3.1** following). The outer margins of the H2 surfaces, and streambank exposures along the edge of the H2 surfaces typically expose a ~1-m-thick section of fine-grained fill in which the upper-most deposits have weakly developed soils and a Bk horizon with Stage I- carbonate accumulation. Radiocarbon ages from the upper-most deposits indicate an age of 400-600 years, for the units with Stage I- carbonate in the Bk horizon (Ostenaar et al., 1999, 2002). Some of these soils may be partly cumulic, and the subsequent addition of thin deposits (1-5 cm) of fine sand and silt to the uppermost soil horizons probably cannot be ruled out.

In some of the lowest exposures along the edges of the H2 surfaces, for example trench T4 (**Section 2.3.2.1** following), these younger additions to the soil profile are readily recognizable and appear to indicate a subsequent, and smaller discharge paleoflood. In most other exposures, it appears that the deposits of the 400-600 year flood extend to the present ground surface with only a few cm of eolian sand mixed into the upper most A-horizon. Deposits of the 400-600 year flood are typically 20-50 cm thick in the streambank exposures, e.g., BLR2, 7, and 8 (Ostenaar et al., 1999, 2002). In trench exposures T4, T5, and T6, deposits of 400-600 year old late Holocene flood thicken toward the streambanks, to a maximum of 0.5 m, but all of the trench exposures begin about 1-2 m from present bank margin. In most bank exposures, and in channel-ward ends of the trench exposures, ~1 m of stratified silt and sand underlie the deposits of the 400-600 flood. Locally, these deposits retain a variably developed, and sometimes eroded carbonate horizon, indicating that a wide range in ages for the underlying deposits. Where there is sufficient depth of exposure, gravels often underlie the fine-grained section, but generally only to elevations about 1 m above the current streambed. Exposures at T8b and T8c (**Section 2.3.3.1** following) are an

exception to this, where channel-facies, fine gravels are higher in the section of the early Holocene deposits just upstream of a bedrock constriction.

Deposits that underlie the H3 and H4 surfaces are not exposed in any of the trenches, and were not described as soil description sites in this or previous studies (e.g., Ostenaar et al, 1999, 2002). Field reconnaissance of many bank exposures along the margins of the H3 and H4 surfaces shows that deposits that underlie these surfaces are well stratified, with very weakly developed soils. Recognizable soil horizons are limited to thin A- and AB- horizons, consistent with the inferred historical ages of these surfaces. With the exception of the meandering reach of the Big Lost River that lies upstream of the Saddle constriction and downstream of BLR7, H3 surfaces are generally limited to very narrow, <1 m wide, terrace treads that are inset below the edges of the more extensive H2 surfaces. Within the meandering reach upstream of the Saddle constriction, H3 surfaces are more extensive and the underlying deposits are more heterogeneous. In that subreach, deposits underlying H3 surfaces likely include stripped and eroded remnants of the early Holocene fine-grained fill deposits that underlie H1 surfaces, abandoned channel and associated overbank deposits of early- to late-Holocene ages, and late Holocene to historic fine-grained deposits capping older units. The upper limit of the H3 surfaces is typically about 1.8 m above the present channel and is often expressed as a subtle scallop on gently sloping surfaces. At a few locations, near BLR2 and the Saddle Constriction area, this limit appeared to coincide the floated, milled timber, suggesting that this may have been associated with an earlier, historic flood. However, much this evidence was burned in the August 2000 wildfire.

Throughout the Diversion Dam study reach, the H4 surfaces are characterized by narrow, paired, terrace treads, typically <1- to 5- m wide, that are about 1 m above the low-flow channel. These surfaces are often capped by thin sand deposits from the 1997 flows, which resulted in shallow overtopping of the H3 surfaces, and these surfaces support a thicker cover of grass and vegetation than any other surfaces. The underlying deposits consist of well stratified silt, sand, and gravel. Soil profiles consist of very thin A-horizons, although silty and fine sand units are significantly bioturbated and there are extensive roots which penetrate throughout exposures in these deposits.

**2.2.4 Channel Deposits.** Sand and gravel within the low-flow channel are the most recent deposits of the Big Lost River. These deposits occur in small bedforms, generally less than

0.5 to 1 m in height. Over much of the study reach the bed is armored with small cobbles. Near constrictions, the armor is absent and bedforms composed of finer gravel are present. Many of these bedforms appear fresh and likely were reactivated during flows in 1995-1999, when there was peak flow in the range of 10-13 m<sup>3</sup>/s on multiple occasions downstream of the INEEL Diversion Dam (**Appendix E**). Downstream of bedrock constrictions, there are often small pendant and lateral bars composed of larger, more angular blocks of basalt that appear to be locally derived from the outcrop constriction immediately upstream. Maximum clasts in these bars are typically less than about 0.5 m, and bar heights are similar.

Berenbrock et al. (2003) characterized the bed armor and channel deposits in the central part of the study area from near BLR8 to upstream of the Saddle Constriction study area (**Plate 1**). They found that  $d_{50}$  of the armor layer ranged from 6-49 mm and was typically 15-35 mm at sites away from constrictions. The underlying channel deposits were slightly finer, with  $d_{50}$  ranging from 0.17-35 mm. Trench exposures showed that these deposits ranged from massive to stratified. Maximum clast sizes in the underlying gravels were typically less than about 50 mm.

### 2.3 Trenching Studies

Within the Diversion Dam study reach, three areas were selected based on the initial geomorphic mapping as sites for subsurface investigations and more detailed study: 1) Big Loop, 2) Saddle Constriction, and 3) BLR8 (**Plate 2**). The overall objectives of additional detailed investigations were to improve the characterization of the Big Lost River paleofloods and paleohydrologic bounds portrayed in Ostenaar et al. (1999, 2002). Each of the areas identified had the potential to provide differing types of data towards those goals based on their individual geomorphic and hydraulic setting. Improved characterization of the paleoflood record required excavation at sites where deposits of paleofloods might be preserved and at sites where erosion from these floods might be evident. It was also hoped that these sites would yield additional datable samples that could improve the knowledge of the age(s) of Big Lost River paleoflood(s). Improved characterization of the paleohydrologic bounds required extension of the trenching to additional sites where no geomorphic evidence of recent floods was apparent. At these sites, exposures of soils and stratigraphy would permit better assessment of the time spans over which the geomorphic conclusions could be extended.

In 2002, nine shallow trenches with a total length of 635 m were excavated at the three study sites. Trench configurations and procedures were generally similar at all three study areas and are described in **Appendix B - Electronic Supplement**. The trench logs were mapped in the field on a photographic base and are presented in that format here. The final logs (**Appendix B - Electronic Supplement**) are compiled at a scale of ~1:45 when printed on 11x17-inch paper. This permits assembly of pairs of 15-m long sections of the trenches on a single sheet and facilitates visualization of the lateral continuity of the deposits. In the digital version, high resolution is maintained and the logs can be printed on larger sheets or in sections at a larger scale. Two sets of logs are presented in **Appendix B - Electronic Supplement**, one set with interpretations, and a second set of unmarked photographs. On the interpretive logs, stratigraphic contacts and units are labeled with lithofacies codes adapted from Miall (1996); soil horizons use nomenclature adapted from Birkeland (1999). Soil profile descriptions are contained in **Appendix B**. Sample locations are labeled and numbered on the logs. Data from sample analyses and disposition of samples are compiled in **Appendix B**.

**2.3.1 Trenches T1, T2, and T3 - Big Loop Study Area.** The Big Loop study area encompasses three trenches, T1, T2, and T3, sited on the large expanse of Pleistocene surfaces south of the Big Lost River about 0.5- to 1.5-km downstream of the INEEL Diversion Dam (**Plate 1**). Much of this area is mapped as P2, but the study area includes the transition area between P2 and P3 (**Section 2.2.2**). Braid channels and large earth mounds are prominent throughout the area and the three trenches were sited to intersect both types of features (**Figure 2-2**). The objectives of trenching in this area include: 1) to evaluate whether differences in the morphology of the P3 units compared to P2 might have resulted from Holocene paleoflood inundation of those surfaces; 2) to evaluate further the characteristics of the earth mounds, particularly in areas where they appeared somewhat subdued or muted; and 3) to confirm, with soils and stratigraphic observations, the geomorphic conclusion that the braid channels on the P2 surfaces were relic features, and were not features produced by post-Pleistocene modification of the P2 surface.

**2.3.1.1 Trench T1.** Trench T1, about 73-m long, was sited across an area that is transitional between P2 surfaces and P3 surfaces (**Figure 2-2**). The southern end of the trench begins with a short section on the P2 surface, then drops down a small terrace riser into a channel

bounding an slightly lower area mapped as P3. The trench alignment exposed two earth mounds, centered at stations 25 and 53.

Trench logs for trench T1 are contained on three sheets (**Appendix B- Electronic Supplement**). No age dates were obtained from samples in this trench. No sedimentological analyses were conducted on samples from this trench. Soil profiles were described at Stations 3, 15, 20, and 61; particle size data is available for all four profiles. (**Appendix B**).

The basal units in trench T1 are a sequence of lateral accretion gravels composed of beds ~20 - 100-cm thick. The uppermost bed in this sequence is coincident with the surface channel at approximately stations 15 to 35. The channel fill, massive-to-poorly-stratified, pebbly-to-silty sand, is best expressed near stations 8 - 14. Loess, 30-50 cm thick, extends the entire length of the trench although it is difficult to distinguish from the channel fill in many areas. The sequence of loess over gravel and soil development in these deposits illustrated in soil descriptions at stations 3, 15, 20, and 61 appears typical of that repeated on the Pleistocene deposits throughout the study reach.

Soil horizons mapped in the gravels, vary laterally, but continue through the channel sequence suggesting the channel is similar in age to the gravels. Within the channel, there is no deposit or erosional feature that disrupts stratigraphy or soil horizons implying significant Holocene flow through this channel. Conversely, carbonate morphology through the channel section of trench T1 is somewhat weaker compared to channels in trenches T2, T3, T6, and T7. Thus, if Holocene flow has been present in the channel at T1, it was limited to amounts that did not result in any significant soil erosion at the site.

**2.3.1.2 Trench T2.** Trench T2, about 44-m long, crosses a prominent braid channel on the interior of the P2 surface (**Figure 2-2**). The braid channel follows a terrace riser that separates slightly lower areas of the P2 surface to the north from slightly higher areas to the south. In addition to crossing the channel and flanking surfaces, the trench alignment crossed and exposed two earth mounds, centered on stations 19 and 36.

Trench logs for trench T2 are contained on three sheets (**Appendix B- Electronic Supplement**). No age dates were obtained from samples in this trench. No sedimentological analyses were conducted on samples from this trench. Soil profiles were described at Stations 1, 20, and 28. Particle size data is available for profiles at stations 1 and 28. (**Appendix B**).

The basal units in trench T2 are a sequence of lateral accretion gravels composed of beds ~20 - 100 cm thick. These gravels are overlain throughout the trench by 30-50 cm of sandy to pebbly silt, of which loess is a major component. Frequency of pebbles decreases upward from the gravel contact and where the finer deposits thicken; Bk horizons are formed in the finer units.

Earth mounds in trench T2 are large and well-developed. Carbonate accumulation beneath the mounds is enhanced, suggesting long-term spatial stability. Deposits and soils within the mounds are highly variable and disrupted, indicating continued bioturbation within the mounds.

**2.3.1.3 Trench T3.** Trench T3, about 57-m long, crosses a prominent braid channel on the back side of the P2 surface (**Figure 2-2**). The braid channel follows a terrace riser that separates the slightly higher P1-2 areas to the south from the main extent of P2 surfaces to the north. At the T3 site, the riser is very subdued, and the trench did not extend far enough south to expose a soil that might be fully representative of soils associated with the P1-2 surfaces. The south end of trench T3 begins on this subdued riser, drops into the channel and extends onto the main P2 surface to the north. Two earth mounds are crossed by the alignment, centered at stations 15 and 53.

The log of trench T3 is contained on three sheets (**Appendix B- Electronic Supplement**). No age dates were obtained from samples in this trench. Pebble and point counts were done on a sample from station 5 and sieve analyses of a sample from station 20 (**Appendix B**). Soil profiles were described at stations 2, 15, and 28. Particle size data is available for profiles at stations 2 and 28 (**Appendix B**).

The basal units in trench T3 are a sequence of lateral accretion gravels composed of beds ~30 - 50 cm thick. The uppermost bed in this sequence is gently undulatory along the length of the trench and appears to have a low point that would be approximately coincident with the surface channel

at stations 13 to 17, where a large earth mound is located and no channel fill deposits are recognized. Stage III carbonate is extensive beneath this mound, as well as the mound at station 54, and there is high variability of soils within both mounds. Between the two mound crossed by trench T1, loess that overlies the gravel is ~25-cm thick. The base of the loess in this area is highly irregular, suggesting disruption by frost wedges and bioturbation.

**2.3.2 Trenches T4, T5, T6, and T7 - Saddle Constriction Study Area.** The Saddle Constriction study area encompasses four trenches, T4, T5, T6, and T7, that include two very distinct settings (**Plate 1** and **Figure 2-3**). Trenches T4, T5, and the southern portion of T6 are sited on narrow areas of H1-2 surfaces that flank the river downstream of a bedrock constriction (**Figure 2-4**). These sites were chosen because they appeared likely to preserve a record of vertical accretion deposits from Holocene floods and/or a record of erosion resulting from floods that may have overtopped them. The lower portions of trenches T4, T5, and T6, were located on portions of the H1-2 surface that appeared to include deposits of the "400-yr" paleoflood identified in the previous study (Ostenaar et al., 1999, 2002). The northward extension of trenches T6 and T7 extend across higher P3 and P2 units, and lie downstream of the feature known as the Saddle, from previous studies (Ostenaar et al., 1999, 2002) (**Section 2.1.2**). The objectives of these trenches are to evaluate, through soils and geomorphic observations, whether or not there was evidence on these surfaces of flow having overtopped the saddle during the Holocene. Geomorphic evidence, shown by faint channels on the P3 surface at trench T6 and the southern end of T7 suggests that the youngest flow on these surfaces was associated with the inset of the P3 surface into the P2 surface and that flow was through the bedrock constriction at the present channel location (**Figure 2-3**). Flow through the saddle would be in a direction orthogonal to these channels. Similar to the objective for trenching in the Big Loop area, the northern continuation of trench T7 would allow evaluation of whether differences in the morphologies of P3 and P2 surfaces might be related to younger flooding, and to confirm geomorphic conclusions related to the origins and ages of the braid channels on the P2 surfaces and issues related to the earth mounds.

**2.3.2.1 Trench T4.** Trench T4, about 21-m-long, is located on a small H1-2 terrace about 100 m downstream of the Saddle bedrock constriction (**Figure 2-3**). The terrace is inset on the downstream side of a basalt outcrop that deflects the channel slightly to the north. The south

end of the trench was limited by a small road and lies on the edge of the slope off the P2 surface south of the river. That portion of the trench encountered a small area of gravels overlain by a pebbly silt that is probably related to a poorly expressed earth mound whose expression was muted by activity along the road and position coincident with the terrace riser on the north. Excavation depth of the trench was limited by outcrops of basalt through much of the central and sloping section of the trench which crosses the terrace riser. Loess, colluvium, and deposits related to the earth mound are intermixed in the central portion of the trench, then grade laterally and downslope to stratified sequence of fine-grained flood deposits that underlie the flattest portion of the H1-2 surface.

Trench logs for T4 are contained on a single sheet (**Appendix B- Electronic Supplement**). Five radiocarbon ages were obtained from samples in this trench (**Table 2-2**). Gamma-ray spectrograph data is available for three samples from station 20 and one sample from the H4 terrace deposit immediately below the trench (**Appendix B**). No sedimentological analyses were conducted on samples from this trench. One soil profile was described at station 20 (**Appendix B**).

The sequence of flood units exposed in the lower portion of trench T4, stations 17-21, provides evidence of at least three late Holocene paleofloods. The basal unit in this section of trench T4 is a ~1-m-thick silty fine sand with a stage II carbonate morphology in the upper portion. A radiocarbon age of 7320-7200 cal yr B.P. from this soil horizon provides a minimum age for this deposit (**Table 2-2** and **Appendix B**). Similar ages, sedimentology, and soil development are observed in other sections that underlie the higher portions of H1-2 surfaces along the Big Lost River (**Section 2.2.3**). The top of this unit is eroded, and three separate overlying silty-fine sand units are recognized primarily through soil properties. The lower and thickest unit is wedge-shaped and increases in thickness from about 40 cm at station 18 to nearly 1 m at station 21. In the upper portion of the unit, an ~20-cm thick Ab1 horizon with no visible carbonate morphology overlies a thicker Bk1b horizon with stage I- carbonate morphology. Radiocarbon ages from this unit at stations 19 and 20 range between 1000 to 2000 cal yr B.P. (**Table 2-2** and **Appendix B**). This age range may represent a minimum time range for deposition and subsequent soil formation. Alternatively, it could indicate that the deposit includes multiple stratigraphic units

whose boundaries have been overprinted by soil development. This deposit is considered part of the evidence for the "older paleoflood" discussed in later sections.

The second sand unit is less than 20-30 cm thick, and extends from about stations 18.5-21. The soil in the underlying unit does not suggest significant erosion associated with this deposit, but the basal contact is inset into the underlying soil upslope. This unit is mostly at the surface and includes the A1/A2 horizons of the soil on the present H1-2 surface at this site. A single radiocarbon age in the lower part of this unit from station 20 indicates an age of 630-510 cal yr B.P. (**Table 2-2** and **Appendix B**). This is the age range associated with other similar flood deposits on the lower portions of the H1-2 surfaces. These sites collectively are evidence for the "400-yr" paleoflood.

The third, and youngest flood deposit in trench T4 consists of a thin, 5-10 cm layer of highly calcareous silty fine sand, slightly lighter in color than is present only about station 20-21 and is referred to as the "white flood". This unit is at the surface and has minimal soil development. It must be considerably younger than the underlying soil because the underlying A-horizon is relatively depleted in carbonate and much less effervescent. No datable material was recovered from samples of this unit. Cesium and lead activity from a sample at station 20 was similar to that in the underlying deposits, but substantially lower than a sample from an H4 terrace in the bank just below the trench (**Appendix B**). The H4 terrace is overtopped by post-INEEL Diversion Dam flows and is therefore likely younger than the mid-1950's. The lower activity in the samples from this unit appears to indicate that it pre-dates that time period.

**2.3.2.2 Trench T5.** Trench T5, about 10-m long, is located on a H1-2 surface about 100-m downstream of the Saddle bedrock constriction and directly across from trench T4 (**Figure 2-3**). The T5 site is at the very upstream end of a long, narrow H1-2 terrace that extends several hundred meters downstream on the north side of the river. The H1-2 surface at T5 is slightly higher than at trench T4 (**Figure 2-6**).

The south or lower end of T5, beneath the flattest portion of the H1-2 surface, exposed a sequence of fine-grained flood deposits that are generally similar to those in trench T4. These flood deposits are cut into well-bedded gravels that dip moderately to the north and which underlie the back

portion of the H1-2 surface and lower portion of the terrace riser at the back edge of the surface. Trench excavation was rapidly limited by basalt outcrops which were overlain by loess and colluvium.

The log for Trench T5 is contained on a single sheet (**Appendix B- Electronic Supplement**). Two radiocarbon ages were obtained from samples in this trench (**Table 2-2**). No sedimentological analyses were conducted on samples from this trench. One soil profile was described at station 2 (**Appendix B**).

The gravels that underlie the terrace slope between stations 4-10 dip moderately to the north and other than orientation they appear similar to P2/P3 gravels in all other trenches. Stratification and bedding in the gravels is disrupted in a steeply dipping zone between stations 6-7 and suggests that these gravels are possibly involved in a small bank failure that rotated and displaced them slightly. The fill of colluvium and loess near the upper end of the trench straddles the contact between basalt outcrops and the gravels. Significant carbonate accumulation in this fill suggests that the block has been stable for at least a few thousand years.

A sequence of flood deposits are cut into the gravels between stations 0-5. A basal colluvium is overlain by a stratified sequence of sand to sandy silt that probably represents one or more paleofloods. This sequence is capped by a Bk1b soil horizon at a depth of about 20-25 between stations 0-2. Overlying this contact and soil horizon boundary between stations is a thin deposit of silty fine sand that appears to be inset into an A1/A2 horizon in silty eolian deposits south of station 2. A radiocarbon age of 760-660 cal yr B.P. at station 0, from the top of the Bk1b indicates the minimum age of burial of this unit by the upper silty fine sand. The underlying deposit has an interval of stronger carbonate development at a depth of 56-74 cm, is also more silty than units above and below. This interval may represent an older, eroded soil buried by two flood deposits, or has more carbonate because of the finer texture. The contact and horizon boundary is not obviously erosional, based on sharpness and irregularity. Deposits below this interval are distinctly more pebbly and incorporate clasts derived from the underlying colluvium. A radiocarbon age near the base of the lower unit gave an age of 1900-1720 cal yr B.P. (**Table 2-2** and **Appendix B**).

Based on the radiocarbon ages and soils from this site, the upper silty fine sand south of station 2 is correlated to the "400-yr flood" and the underlying deposits are considered correlative with the "older flood".

**2.3.2.3 Trench T6.** Trench T6, about 121 m long, is located about 100 m downstream of trench T5 (**Figure 2-3**). The south end of T6 begins on the same H1-2 surface as trench T5, extends north across that surface, then up the terrace riser onto the adjacent P3 surface. The southernmost section of the trench, stations 1-5, exposes late Holocene flood deposits similar to those in trenches T4 and T5. Stations 5 to 25 expose mid- to early-Holocene soils and fine-grained channel fill. The sequence of deposits beneath the terrace riser, stations 25-45, includes a sequence of gravels that records the lateral migration and incision of the Big Lost River below the level of the P3 surface. Overlying slope colluvium and soils on the riser grade into equivalent units that underlie the H1-2 surface to the south. The remainder of the trench, stations 45-121, exposes mostly plane-stratified gravels, similar to those in trenches T1, T2, and T3. The gravels are overlain in most areas by ~20 cm of finer gravels which grade laterally into a pair of channels between stations 66 to 96. The finer gravels and channels appear to represent the last phase of fluvial erosion and deposition on the P3 surface. Loess, typically ~20 cm thick, overlies the entire sequence from stations 45-121 and forms the upper horizons of the carbonate soil developed through all the deposits. The low point in the same ridge to the west, termed the Saddle, lies about 50-70 west of the section of trench T6 near stations 75-100. Near station 95, an earth mound deposit overprints the edge of the channel sequence.

Trench logs for Trench T6 are compiled on four sheets (**Appendix B- Electronic Supplement**). Six radiocarbon ages were obtained from samples in this trench (**Table 2-2**). Detrital zircons were analyzed from samples at stations 12 and 66 (**Appendix B**). Pebble and point counts were done on samples from stations 23 and 99 (**Appendix B**). Gamma-ray spectrograph data is available for two samples each from stations 0 and 4 (**Appendix B**). Seven soil profiles were described at stations 1, 7, 17, 43, 57, 72, and 118. Particle size data are available for profiles at stations 43 and 57 (**Appendix B**).

The physical stratigraphy and soils at the southern end of T6, stations 1-5, appear very similar to the sequences in trenches T4 and T5. A stratified wedge of silty-fine sand, with relatively weakly

developed soils, truncates sand silt and sand units with much stronger carbonate soils. At station 1-2, this wedge appears to consist of a single unit of silty fine sand which contains an increasing percentage to the north of carbonate-cemented cicada clasts that appear to be derived from Bk soil units similar to those between stations 4-20. The basal part of the wedge is contains about 10 per cent pieces of older soil. At station 4, two radiocarbon ages from a bulk sample of this unit barely overlap in the range of 790-540 cal yr B.P. Based on these ages and the associated soil development, it appears most likely that this deposit is correlative to the "400-yr" flood. Deposits correlative to an "older flood" may be represented by the lower-most units at the very end of the trench.

Trench T6 extends across the entire H1-2 terrace at this location and the trench exposure demonstrates the lateral continuity of stratigraphy and soils beneath the surface. From the south end of the trench to near station 23, a thick basal sand unit, locally stratified, is overlain by a similarly thick silty fine sand in which a strong Bk horizon is developed with abundant cicada burrows. From the south to north in this interval, the surface horizons that overlie this Bk horizon become thicker and more complex. Beyond about station 14, to station 25, the horizons are consistent and thick. This change, near station 14, appears to mark the northern limit of erosion associated with the younger flood deposit that contains clasts of Bk material near stations 1-4.

Three radiocarbon ages potentially limit the age of Bk soil and associated deposits in the southern end of trench T6. At station 4, a radiocarbon age on a mixture of very small charcoal fragments recovered from a large bulk soil sample has an age of 3480-3360 cal yr B.P. (**Table 2-2** and **Appendix B**). The sample site is surrounded by prominent burrows, and has an anomalously young age compared to samples from other sites with similar soil development. A similarly anomalous age was obtained at station 20, again on a mixture of very small charcoal fragments recovered from a bulk sample of the basal sand unit. This sample had an age of 2870-2760 cal yr B.P. (**Table 2-2** and **Appendix B**). An apparently more reliable age is from a snail shell recovered from a bulk sample of the basal sand at station 6. This sample had an age of 12,800 - 11,940 cal yr B.P. (**Table 2-2** and **Appendix B**). This age implies a very late Pleistocene age for incision of the Big Lost River that is consistent with the regional glacial chronology (**Section 2.2.2.1**) and with

ages from similar soils at trench T4 (**Section 2.3.2.1**) and BLR6 (Ostenaar et al., 1999, 2002) located just downstream of trench T6 (**Plate 1**).

The ages, soil development, and continuity of the stratigraphy and soils beneath the H1-2 terrace indicate that this surface has been largely unmodified by floods through much of the Holocene. Stabilization of the surface, and formation of the Bk soil horizon in the silty fine sand unit, likely post-dates deposition of the basal sand at 12 ka, but is still most likely early Holocene, based on comparisons to ages at other sites. Since that time, there has been only limited modification of the surface, as recorded by the sequence of deposits at stations 1-4 which are cut into the Bk horizon, and which stripped the upper horizons to approximately station 14.

The objectives of extending trench T6 north across the P3 surface downstream of the Saddle were to determine if there was evidence of erosion due to flows through the Saddle during the Holocene. From station 45-121, the trench exposes stratified gravels, which in many areas are capped with a finer, sandy gravel that appears to laterally grade into fine-grained channel fills. A thin loess, in turn capped by a very thin layer of eolian sand, overlies both the gravels and the channel fills. Basal units in the channels are typically sandy to pebbly and fine upwards to silty fine sands that are texturally similar to loess. A carbonate soil with highly variable, but common stage II morphology, appears to be continuous across the entire sequence. Variability in the soil is apparently related to small variations in texture of the uppermost gravels. A single radiocarbon age was obtained from near the top of the Bk in the channel fill at station 68. The age of 660-540 cal yr B.P. (**Table 2-2** and **Appendix B**) is a very minimum age that reflects the continuing input of young material into the soil profile.

There is no apparent stratigraphic evidence of erosion removing significant thicknesses of loess, or of erosion affecting the top of the gravels. The channel fills coincide with faint geomorphic suggestions of flow parallel to the ridge that forms the Saddle, suggesting that they are related to flow from south to north on the P3 surface, not west to east indicated by flow through the Saddle (**Figure 2-3**).

**2.3.2.4 Trench T7.** Trench T7, about 256 m long, overlaps and continues north from the north end of trench T6 (**Figure 2-3**). The southern portion of T7, stations 1-25, exposes gravels

with channel fill, loess thickness, and soils that are similar to those in the central and northern portions of trench T6. This section of trench T7 coincide with the mapped extent of the P3 surface (**Plate 1**) and a ~0.4-m-step in the ground surface between stations 25-30. From about station 25 to 50, excavation depth was limited by basalt beneath the gravels. Thin exposures of gravels are overlain by another group of channel deposits and loess that underlie a slightly higher surface than the area near stations 1-25. Beyond station 50, the surface steps up another 0.3-0.4 m to the level of the main P2 surface downstream of the northern continuation of the ridge near the saddle. North from station 50, channel fill deposits that overlie the main gravel units thin, and laterally grade to thin sandy gravel and gravelly sand units. These are in turn typically overlain by 20-30 cm of loess, and a variable thickness of eolian sand, including locally mappable accumulations of post-2000 sand. These are identified where they overlie the 2000 burn horizon. Beyond station 130, to the north end of the trench at station 256, the upper sandy units are not present, and variably stratified gravels are overlain by 20-40 cm of loess. Earth mound deposits interrupt the stratigraphic continuity along the trench near stations 60, 116, 166, and 258.

Trench logs for T7 are compiled on nine sheets (**Appendix B- Electronic Supplement**). No radiocarbon ages were obtained from samples in this trench. Detrital zircons were analyzed from samples at stations 107 and 109 (**Appendix B**). Pebble and point counts were done on a sample from station 231 and sieve analyses of a sample from station 136 (**Appendix B**). Seven soil profiles were described at stations 36, 44, 95, 108, 158, 167, and 237 (**Appendix B**).

Similar to trench T6, there is no apparent stratigraphic evidence of erosion removing significant thicknesses of loess or of erosion affecting the top of the gravels throughout the length of trench T7. The channel fills coincide with faint geomorphic suggestions of flow parallel to the ridge that forms the Saddle, suggesting that they are related to flow from south to north on the P3 surface, not west to east, as indicated by flow through the Saddle (**Figure 2-3**).

**2.3.3 Trenches T8 and T9 - BLR8 Study Area.** The BLR8 study area includes two trenches, T8 and T9, on the south side of a sharp bend located upstream of a bedrock constriction (**Figure 2-5**). The BLR8 site of Ostenaar (1999, 2002) is on the opposite bank. Trench T8 is located mostly on an H1-2 surface, the lower part of which appears correlative to the position of BLR8. The site is downwind and adjacent to extensive areas of basalt outcrops and associated eolian

sand deposits (**Plate 1**). Thus, all units in this area have relatively thicker eolian surface units than most other sites. Trench T8 was originally proposed as a continuous excavation that extended from the H3-4 units through the H1-2 and into units mapped as P3. However, pre-trenching archaeological investigations showed this to be a potentially significant cultural site. A scaled-back trench layout was adopted consisting of three short trenches, each about 6 to 7 m long, designated T8a, T8b, and T8c. Prior to excavation of these smaller trenches, an extensive archaeological mitigation investigation was carried out which included excavating several test units along the trench alignments (Peterson and Harding, 2002). The final trenches partly incorporated and retained the archaeology units so that stratigraphy in those units could be related to the trenches. Trench T9 was excavated on the upstream side of the bedrock constriction where the channel impinged on the edge of the P3 surface. Because the sites were located upstream of a bedrock constriction, and based on the exposures at BLR8, there appeared to be potential for both trenches to expose a datable record of paleofloods. This would be most likely in the northern end of the trenches. The southern end of both trenches extended onto higher and older surfaces, thus providing the potential to define the limits of erosion associated with past floods.

**2.3.3.1 Trench T8.** The final excavation for Trench T8 consisted of three trench segments (**Figure 2-5**), labeled from south to north, T8a, T8b, and T8c. The locations of two archaeology units not incorporated in the final trenches, designated Locality A, 101N/100E and 105N/100E (Peterson and Harding, 2002) lie between T8b and T8c. Correlation of units described by Peterson and Harding with those mapped in the trenches follows discussion of the three trenches.

Trench logs for T8 are compiled on one sheet (**Appendix B - Electronic Supplement**). No radiocarbon ages were obtained from samples in this trench. Artifacts recovered by the archaeology investigations provide some evidence for the age of these sites. Pebble and point counts were done on a sample from T8a, station 3 (**Appendix B**). No soil profiles were described separately; horizons are mapped on the logs.

**Trench T8a.** Trench T8a, the southernmost of the three trenches was about 7 m long and sited on the edge of a small P3 surface surrounded by basalt (**Plate 1**). Gravels, with overlying loess and eolian sand at the southern end of this trench are similar to and have similar soils to the

Pleistocene gravels in trenches at the Big Loop (**Section 2.3.1**) and Saddle Constriction study areas (**Section 2.3.2**). These gravels interfinger with a channel fill, also with stage II carbonate morphology, and again are very similar to the channel fills and soils exposed in T6 and T7 at the Saddle Constriction study area. The stratigraphic relationships of the gravels and channel fill in T8a, and the soil developed across these boundaries demonstrate the late Pleistocene age of these channel fills on the P3 and P2 surfaces. Pebble stringers, found near the middle of the channel fill at stations 4-5, show that much of the fill is fluvial. The upper portion of the fill grades upwards and laterally with loess that overlies the gravels. The complete soil profile, and upper eolian units are truncated or removed from the northern portion of the trench and reflected in the surface topography by a 20-30 cm high, gentle scarp. Removal of these upper units is old enough that the top of the Bk in the channel fill section and parallels the ground surface and maintains a constant depth.

**Trench T8b.** Trench 8b is the middle trench at site and is about 6 m long. Locality A, 96N/100E and 95N/100E units of Peterson and Harding (2002) are partially retained in the north end of the trench. The basal units exposed in T8b are fluvial as shown by beds of sand and fine sandy silt. The section fines upward, becoming more silty and similar in texture to loess. Extensive cicada burrows and soil carbonate have overprinted any bedding or stratification. The section in T8b is slightly coarser than the channel fill in T8a and is likely the lateral extension of the same channel fill unit. Stratification of the upper part of the fill in T8b is based primarily on the relatively abrupt increase in soil carbonate (2Bk1/2Bk2 horizon boundary). The same horizon boundary in T8a is gradational. This difference may be due to subtle texture differences in the original stratified fill, or to erosion and redeposition of the upper unit in T8b. Carbonate morphology of the Bk1 horizons in both trenches is similar. Surficial soils in T8b and the north end of T8a are similar, suggestive of removal or stripping of surface horizons in the past few hundreds of years.

**Trench T8c.** Trench T8c is the northernmost trench at the site, about 6 m long, and closest to the Big Lost River channel (**Figure 2-5**). The basal units exposed in T8c are fine pebbly sands and sandy gravels which may or may not be a lateral facies of the channel fill sands exposed in T8b and T8a. The lower units in T8c are capped by the eroded remnants of a well-developed

carbonate soil, similar to that present in the other trenches. The uppermost unit in T8c is mostly a massive sand that contains abundant carbonate-cemented cicada burrow clasts. These appear to be derived from a Bk horizon of channel fill or a fine-grained fluvial deposit similar to those exposed in the southern portion of T6 (**Section 2.3.2.3**). Soil development in this upper unit is very weak, limited to scattered occurrences of stage I carbonate morphology on occasional pebbles and filaments on the edges of the cicada clasts.

**Correlation to Archaeological Stratum.** Peterson and Harding (2002) designated the area around trench T8 as Locality A, and defined twelve stratigraphic units (stratum) based on bedding, grain size, and soil development. The oldest, basal stratum is designated I, and the youngest stratum at the surface is XII. They divided the recovered cultural remains into two components based on the diagnostic projectile points and natural stratigraphy. Diagnostic materials for the younger component were recovered on the surface, but were associated with stratums X, XI, and XII based on soil development. Diagnostic points from the older component were identified in stratum IX and at the top of stratum VIII at depths of 30-40 cm in Locality A, 95N/100E and 105N/101E.

The location of 95N/100E at Locality A corresponds to stations 4-6 in trench T8b. In trench T8b, stratum XII and XI of Peterson and Harding (2002) appear to correspond to eolian sand and the AB soil horizon, about 10-15 cm thick across the trench. A 2Bk1 soil horizon formed in the upper fluvial sand corresponds to stratum IX and X of Peterson and Harding. A 2Bk2 soil horizon formed in a lower fluvial sand corresponds to stratum VIII. The depth range of 30-40 is coincident with the contact between two the fluvial units.

105N/101E at Locality A is located 10 m north of T8b, and 5 south of T8c (**Figure 2-5**). We did not remap this exposure, but from field inspection, it appears that the eolian sand is thinner and that more likely, stratum XI corresponds to an A-horizon formed in fluvial silty sand. Stratum IX includes a Bk horizon forming in silty sand that appears to include re-worked cicada burrow clasts similar to the uppermost fluvial unit and Bk horizon in trench T8c. Correlation of this unit to the upper fluvial unit in T8b is less clear, because reworked and broken cicada clasts are not so obvious in T8b, and the upper fluvial unit in T8b is slightly finer. The irregular contact at the base of stratum IX in 105N/101E suggests it is erosional, as does the significant increase in carbonate

morphology observed in stratum VIII beneath this contact. Because of the irregularity of the basal contact, the recovered artifacts may have been originally part of either unit. Stratum VIII to I in 105N/101E resemble lateral equivalents of the lower fluvial units in trench T8c. The lower fluvial units in T8c are finer, and the lower units in 105N/101E and T8c may either be equivalent lateral facies to T8b or a younger inset.

Peterson and Harding (2002) Locality A site 111N/1000E and 112N/100E correspond to stations 0-2 of trench T8c. In T8c, units mapped as eolian sand correspond to stratum XI and XII. The upper most fluvial unit in T8c includes all of Peterson and Harding stratum IX and X, as well as portions of stratum VIII. This fluvial unit contains extensive broken and reoriented cicada burrow clasts and has an irregular, erosional basal contact. Below this contact are eroded remnants of a Bk horizon with stage II+ carbonate formed in a bedded sequence of silt, sand, and gravel beds and lenses. Peterson and Harding designated individual beds within this fluvial sequence as stratum II through VIII. From the larger exposure of trench T8c, it appears that most of their stratum VIII corresponded to the eroded remnant of a well-developed Bk horizon formed in a silty sand capping a well-bedded fluvial sequence. Variability in carbonate accumulation within the sequence is the result of variations of carbonate accumulation in the lower portions of soil profile in beds of differing initial texture.

Peterson and Harding (2002) and Harding (2002) identified two Northern Side-notched projectile points from their Component I, which are considered to range in age from 7500 to 4400 years ago. Recovery of these points at depths of 30-40 cm suggests that they were most likely entrained in the upper fluvial unit exposed in T8c, and possibly T8b as well. These units appear to contain reworked clasts of cicada burrows derived from the underlying soils. It seems less likely that these points had been worked into the underlying Bk horizon of the lower fluvial unit in the trenches, because artifact recovery decreased dramatically below 30-40 cm depths. Artifacts recovered at the surface have a potential age range of ~100 to 1700 years. This age range brackets the possible age range of late Holocene paleofloods along the Big Lost River and is thus not diagnostic here.

**T8 Combined Interpretations.** The lack of continuous exposure across the T8 site somewhat limits interpretations, but the physical stratigraphy and soils have enough similarities that some conclusions can be reached. Soils and stratigraphy in the southern portion of T8a,

stations 1-3, are very similar to those found on the Pleistocene surface elsewhere in trenches T1, T2, T3, T6, and T7. This appears to be typical of the soil profile and stratigraphy developed on unmodified Pleistocene surfaces throughout the site, with the addition of eolian sand on top of the loess. Long-term stability of the site is shown by the development of stage II Bk-horizons across the boundary of gravel, fine-grained channel fill, and loess units. Soil horizons and stratigraphy are truncated at the northern end of T8a, indicating a lateral limit to erosion in this trench at about stations 3-4. Erosion of the profile in the underlying loess/channel fill sequence is minimal in the northern section of the trench. Depth-to-top of Bk horizon is ~20 cm, suggesting this erosion is at least a few hundred years in age. The upper portion of trench T8b is somewhat more stratified than T8a, but is generally similar to the channel fill/loess sequence in T8a. The presence of two Bk horizons may result from burial of an older soil by the upper-most fluvial unit or increased carbonate accumulation due to subtle difference in texture of the original deposits. Horizons at the surface are similar in both trenches.

The stratigraphy of the upper unit in trench T8c is distinctly different. The uppermost fluvial unit in T8c is a fine sand that contains clasts of broken and reoriented carbonate-cemented cicada burrows. Coarser sand and pebbly lenses along the base are cut into a Bk horizon with stage II morphology developed in an underlying fluvial sequence. The Bk in the upper fluvial unit has stage I- morphology, suggesting an age of no more than a few hundred years. The cicada burrow clasts consist of carbonate-cemented silty, fine sand that could be derived older channel fill units or H1 age units. Incorporation of Middle Prehistoric artifacts (7500 - 4500 years old) would be consistent with the apparent age of soils incorporated as clasts in this much younger deposit. These ages may indirectly indicate a minimum age for the underlying deposits in T8c as well.

**2.3.3.2 Trench T9.** Trench T9 is approximately 35-m long and extends on the south from the relatively flat, sand covered P3 surface down a ~2-m-high terrace riser onto a small H3-4 terrace (**Figure 2-5**). The site is located just upstream of a bedrock constriction, which results in backwater effects even for moderate flows (see plots in **Appendix D - Electronic Supplement**). In this setting the H3-4 terrace was inferred as likely site of fine-grained deposition during floods, and the presence of several subtle steps and inflections in the terrace riser (see log profile at stations 30 and 32) suggested a possibility of an extended record of paleofloods at this site. The

trench was extended back onto the P3 surface to expose the continuity of stratigraphy through the riser and because preliminary hand-auger borings suggested a thick, fine-grained sequence was present. Pre-trenching archaeological investigations (Peterson and Harding, 2002) along this trench alignment found only a few artifacts. The final trench incorporates a portion of archaeological excavations between stations 11-14. No diagnostic artifacts were recovered at this site.

Trench logs for T9 are compiled on one sheet (**Appendix B - Electronic Supplement**). Three radiocarbon ages were obtained from samples in this trench (**Table 2-2**). Pebble and point counts were done on a sample from station 18 and on a sample from a mid-channel bar just below the end of the trench (**Appendix B**). No soil profiles were described separately; horizons are mapped on the logs.

At the south end of trench T9, the basal gravels exposed from stations 1-30, resemble the Pleistocene gravels that underlie P2 and P3 surfaces in other trenches. These gravels are interrupted between stations 23-28 by a channel fill with steeply inclined stratification along one side. In the southern portion of the trench, the gravels are overlain by about 1 m of fine sand. A well-developed Bk horizon in this sand has stage II and locally stage III carbonate morphology and to the north, as the sand thins, the strong Bk horizon extends from the sand into the gravel. A radiocarbon age of about 2750 cal yr B.P on a small piece of charcoal (**Table 2-2** and **Appendix B**) found in the lower part of the sand at station 2 is anomalously young based on soil development in the sand. Extensive burrowing in the sand is likely responsible for downward transport of young charcoal to this depth. The burrowing has also disrupted the soil to a significant extent. The upper horizons of the soil in the southern part of the trench show that there is significant input of younger sand across this surface at this site. Soil profile development in the sands, channel fill, into the gravels are similar to profiles developed in Trench 8a, as well as other trenches on the Pleistocene P2 and P3 surfaces at the Big Loop (**Section 2.3.1**) and Saddle Constriction study areas (**Section 2.3.2**). A similar age is inferred at trench T9 for the gravels, channel fill and overlying sand with strong Bk development. The uppermost sands above the Bk are possibly younger, reflecting new eolian input from sand dunes on the basalt to southwest (upwind) of this site. North of station 14, the slope steepens, and near the edge of the terrace riser

these upper loose, sandy horizons thin and terminate northward. Similar to soil evidence at T8a and T8b, some stripping of the uppermost portion of the Pleistocene profile between stations 14 to 28.

Colluvium on the terrace riser slope grades downslope to a sequence of fine-to-medium sand beds. Between stations 32-33, these are separated by A/Bw horizons, with abundant organic material. Radiocarbon ages from this section calibrate to ages less than 300 cal yr B.P. and include historic ages (**Table 2-2** and **Appendix B**). The high limit of these deposits on the terrace riser slope corresponds to a discharge of about 70 m<sup>3</sup>/s (**Figure 2-7** and **Section 2.5.1.4** following), roughly the upper limit of historic flood discharge in the Big Lost River (**Section 2.1.1**). Some of these deposits could potentially correlate to the youngest flood deposit in trench T4 (**Section 2.3.2.1**), but this correlation is only speculative. The radiocarbon ages, and discharge range that inundates this site, suggest that these deposits are most likely associated with floods that pre-date the INEEL Diversion Dam and had discharges near or only slightly larger than the largest historical floods.

The lowest deposits in trench T9 are a sequence of sand beds that underlie the flat portion of the H3-4 terrace at station 34-35. This inset sequence is inundated by discharges of less than 50 m<sup>3</sup>/s (**Figure 2-7**) and likely accumulated from historic floods. Minimally developed soils in these deposits are consistent with a young age.

## **2.4 Summary of Geomorphic and Geologic Data for Paleofloods and Paleohydrologic Bounds**

The geologic studies described in the preceding sections found evidence of at least three late Holocene paleofloods, and are the basis for describing three paleohydrologic bounds that can be used with these data in the flood frequency analyses (**Section 4.0**).

**2.4.1 Paleofloods.** From the geomorphic mapping and trenching investigations, evidence of three paleofloods have been identified within the Diversion Dam study reach of the Big Lost River (**Table 2-3**). This evidence is briefly reviewed below. Studies to date have not located any site along the study reach that dependably preserves a long or detailed full record of large floods. Rather, over time, there is a progressive self-censoring (House et al., 2002) such that

only successively smaller floods can be recognized for shorter periods of time. For the sites observed, any large flood essentially obliterates the record of smaller floods that preceded it. Likewise, only limited remnants of larger, but older floods might remain. The primary focus for selecting sites for this study has been of evaluating evidence for floods that potentially much larger than the largest historical floods. All but a small portion of 1 of the trenches used for this study are located outside the inundation limits of historic floods.

**2.4.1.1 "White Flood".** Stratigraphic evidence for this flood is recognized at a single site, Trench T4 (**Section 2.3.2.1**). A thin, ~ 7 cm, deposit of silty sand caps the sequence of flood deposits exposed beneath the lowest surface at the end of trench T4, stations 19-21, and appears to bury the soil formed on deposits of the "400-yr" flood. Soil descriptions (**Appendix B**) designate this unit as the A1-horizon of the present soil and soil development is weak in comparison to other sites. The deposit is not associated with historic floods because no historic floods would have been large enough to inundate the site (**Section 2.1.1** and **Figure 2-6**). No similar deposit is present or recognized in trenches T5 or T6, both of which are only slightly higher relative to the discharge at which they are inundated (e.g. **Figure 2-6**) and it does not appear that soils in deposits of the "400-yr" flood were eroded more recently at these sites (**Section 2.3.2.2** and **Section 2.3.2.3**). A radiocarbon age from the underlying A2 horizon at T4 has a calibrated age range between 630-510 cal yr B.P. (**Table 2-2** and **Appendix B**). Deposits in lowest portions of trench T9 have young radiocarbon ages (**Section 2.3.3.2** and **Table 2-2**), but are also inundated by discharges that might have occurred prior to construction of the INEEL Diversion Dam (**Figure 2-7**). Thus, the age of a paleoflood associated with this deposit is constrained to be prior to the beginning of stream-gaging records (A.D.1903) by the minimum discharge required to reach the site. The deposit is younger than the 630-510 cal yr B.P. age from the underlying soil, and is most likely about 100-150 years based on the relative soil development.

**2.4.2 "400-yr Flood".** Stratigraphic evidence for this paleoflood was recognized in the earlier paleoflood study by Ostenaar et al. (1999, 2002) at four sites in the Diversion Dam study reach (**Figure 2-11**). Deposits with similar soils and stratigraphy that are apparently correlative are present in trenches T4, T5 and T6 (**Table 2-3** and **Section 2.3.2**). These deposits appear to be associated with the prominent geomorphic expression of the H2 surface that can be mapped

throughout the study reach (**Plate 2** and **Section 2.2.3**). Soil development in these deposits, and radiocarbon ages from these deposits and from underlying deposits constrain the age to about 600 - 400 cal yr B.P. (**Figure 2-8**).

Because the flood deposits recognized by Ostenaar (1999, 2002) and in the trenches for this study appear to be associated with H2 geomorphic surface (**Plate 2**), one constraint for evaluating the discharge of this paleoflood is that the discharge be large enough to inundate the full extent of this surface throughout the study reach.

**2.4.3 "Older Flood"**. Trench and bank exposures along the H1-2 surface all demonstrate that the deposits of the "400-yr" paleoflood overlie eroded soils developed in slightly older, similar flood deposits (Ostenaar et al., 1999, 2002; and **Section 2.3**). The soils in these deposits are generally similar, or slightly more developed than soils developed in the past 400-600 years. This implies a similar length of time over which no flood either eroded or resulted in significant deposition over these deposits. Likewise, the limited extent of the deposits of the "400-yr" flood relative to the H1-2 surface indicate that overall the surface must be a composite of deposits with similar origins, but differing ages. The significant scatter in radiocarbon ages from site to site, and the variability in soils that underlie the "400-yr" flood deposits appear to support this concept. As shown on **Figure 2-8**, there is much less correlation of the potential time brackets for a single older flood than for the "400-yr" paleoflood and some possibility that multiple floods may have occurred in the time interval since about 3000 cal yr B.P. However, both the stratigraphic and the chronologic resolution to define multiple floods in this time period are lacking in the present exposures. The existing age constraints appear to indicate that a conservative age range for this flood would lie in the range of 2000 to 1000 Cal yr B.P.

The stratigraphy in trenches T4 and T5, where evidence of this flood is best expressed, could also be interpreted as evidence for more than one flood. Interpretations of multiple floods in these sections is most supported by breaking out beds in the lower portions of these stratigraphic sections. If that is done, the upper stage limit to associate with these floods is no longer associated with the H1-2 surface, but is down in the section at an elevation below the stage level that would be associated with the largest historic floods,  $\sim 70 \text{ m}^3/\text{s}$  (**Figure 2-6**). The addition of temporally sparse data in that discharge range does not improve the assessment of the flood frequency. This

type of information would be more useful if it could be independently reasoned that these floods must have been much larger than historical floods, either near or exceeding the discharge of the "400-yr" flood.

Because deposits that are associated with the "older flood" underlie the H1-2 surfaces, inundation of the full spatial extent of those surfaces provides a constraint for evaluating the discharge associated with this paleoflood.

**2.4.4 Paleohydrologic Bounds.** For use in the flood frequency analyses, geomorphic and stratigraphic data are used to define three paleohydrologic bounds that span differing time intervals over the past 10,000 years (**Table 2-3**). The geologic basis for each of these bounds is summarized below.

The geologic data show that over different time intervals and areas along the Big Lost River, there is evidence of relative geomorphic stability. Thus, the preservation of paleoflood deposits as the surface units on portions of the H1-2 geomorphic surfaces shows that no floods large enough to modify or remove these deposits have occurred since the time of those paleofloods. As summarized in, there is stratigraphic and geologic data along the Big Lost River that allows for defining three paleohydrologic bounds. Geomorphic mapping delineates the characteristics and extent of surfaces of similar age that are potentially useful as paleohydrologic bounds (**Section 2.1.2**). Stratigraphic data from trenches and exposures defines the characteristics of the surfaces and the evidence for relative surface stability over time.

**2.4.4.1 400-yr Flood Bound.** In trenches at the Saddle Constriction study area, deposits of a paleoflood with an age of 400- to 600- years are the parent materials of the surface soils (**Section 2.3.2**). Weakly developed soils developed in the flood deposits at these sites indicate that no significant erosion or deposition by other floods or other geomorphic processes have disrupted these surfaces in that time span. Similar relationships, preserved at multiple sites, demonstrate stability of these surfaces since the time of the "400-yr" flood, approximately 400- to 600-years ago (**Section 2.4.2**). Even at trench T4, where the "400-yr" deposits are buried by thin deposit of a younger paleoflood, the soil profile in the underlying deposits is intact, indicating that this site was not significantly eroded by that flood (**Section 2.4.1.1**), and hence has been stable

since deposition 400-600 years ago. Throughout the reach, the H1-2 surfaces which include these deposits are unmodified by younger erosion (**Section 2.2.3** and **Plate 2**).

The H1-2 surfaces and deposits of the "400-yr" flood are preserved in many differing hydraulic settings throughout the Diversion Dam study reach. Thus, for use as a paleohydrologic bound, some of these sites are much more strongly limiting than others (**Section 3.2.1.2** following). In particular, at Trench T4, unit stream power and bed shear stress increase very rapidly with increasing discharge and thus that site is very important to discharge limits for "400-yr" bound.

**2.4.4.2 Early Holocene (H1 surfaces) Bound.** The stratigraphic evidence to support this paleohydrologic bound is the preservation of extensive areas of generally fine-grained fluvial sediments with well-developed carbonate soils that underlie the H1-2 surfaces. The most extensive exposures of these sediments and soils are in trench T6, stations 1 to ~30, and in the disconnected sequence of trenches at BLR8 study area, T8a,b,c (**Section 2.3.2.3**, and **Section 2.3.3.1**). Smaller remnants are present at T4, stations 16 to 20 (**Section 2.3.2.1**), and at BLR6 (Ostenaar et al., 1999, 2002). These deposits and soils apparently are part of an aggradational fill of latest Pleistocene to early Holocene age (**Section 2.2.3**). Stage II carbonate soil horizons in these deposits are generally 50- to 100 cm thick, indicative of an early Holocene age for stabilization of the surface, and radiocarbon ages from these deposits ranging from about 12,800-7200 cal yr B.P support this age (**Section 2.2.3** and **Section Table 2-2**). Based on these data, a conservative time interval of 6000 to 8000 years has been chosen for use as a paleohydrologic bound. Most of radiocarbon ages from these sites are older than this range, but the shorter time interval reflects the possibility interpretation that aggradation of the sequence continued and the surfaces did not stabilize and begin forming soils until somewhat later.

**2.4.4.3 Pleistocene Bound.** The extensive areas of unmodified Pleistocene surfaces that flank the Big Lost River are the stratigraphic and geomorphic basis for this paleohydrologic bound (**Table 2-3**). The Pleistocene P2 surfaces have a braid-channel morphology that is inherited from Pleistocene gravel deposition and unrelated to present flows in the Big Lost River (**Section 2.2.2**). The more limited areas of Pleistocene P3 surfaces generally follow the present river channel and are also underlain by gravels, and likely represent the last episode of Pleistocene deglaciation (**Section 2.2.2**). Trench exposures in T6, T7, T8 and T9 indicate that the last phase of

deposition on these surfaces was aggradation of fines in small channels on the P3 surfaces (**Section 2.2.2**, **Section 2.3.2**, and **Section 2.3.3**). Subsequent deposition, shown by the inset deposits that underlie the Holocene surfaces has been dominated by fines. Soils on the Pleistocene surfaces are characterized by an upper loess cap, generally less than 0.5-m-thick in the Diversion Dam study reach and well-developed carbonate morphology (**Section 2.2.2**). The Pleistocene age of both the P2 and P3 surfaces is established regionally by depositional links to regional glaciation, and in a local context by radiocarbon ages of ~10,000 to 12,800 cal yr B.P. obtained from the inset fine-grained deposits (**Section 2.2.2** and **Table 2-2**).

## 2.5 Hydraulic Modeling of the Diversion Dam Study Reach

TrimR2D (**Appendix C, Part A**; Ostenaar et al., 1999) was used with the topographic data for the Diversion Dam reach (**Appendix A**) to calculate steady-state 2D inundation and flow velocities using a 6-ft cell flow grid for the discharges listed in **Table 2-1**. A 3 ft-spacing uniform grid was produced after a clockwise rotation of 31.4° of a subset of the high-resolution topographic grid (2000 photography, **Appendix A**) for the Diversion Dam study reach, which was subsampled by TrimR2D to produce a 6-ft staggered finite-difference grid. To accommodate the larger inundated areas associated with discharges larger than 200 cms, a larger region of topography containing the Diversion Dam study reach was extracted from the 5-ft spacing topographic mesh from the reprocessed 1993 aerial photography at INL (**Appendix A**) after a 36.9° clockwise rotation of the topographic mesh and interpolated to produce a 2.5-ft-spacing topographic input grid for TrimR2D. TrimR2D then subsampled the 2.5-ft-spacing topographic grid to produce a 5-ft-spacing staggered finite-difference grid. To ensure that flow was entrained within the grid to the downstream edges of the grids, high elevation walls were added to the western, northern, and southern edges of the grids. The impact of these walls in the 6-ft grid is most clearly apparent for the larger discharges (generally discharges of 200 cms or larger, see **Table 2-1** and plots in **Appendix D**) and motivated the development of the 5-ft grid that encompassed a larger area south of the channel to allow more realistic routing of discharges of 200 cms or larger.

In both grids the minimum elevation in the grid was removed from all points in the grid to maximize numerical precision in quantities involving elevations. Coordinate transformation

equations were constructed for both the 5-ft and 6-ft TrimR2D flow grids to convert the TrimR2D local grid coordinates to their original INL state-plane coordinates and elevations.

The grids were initially wetted using springs distributed along the channel and that were activated for several minutes of flow to partially fill the channels. To produce steady-state flows for specific discharges, springs were activated immediately downstream of the diversion dam in the active channel with a total flux equal to the specific discharge. For the smaller flows on the 6-ft grid, 22 springs were used to minimize stages in the vicinity of the springs and 28 springs were used with the larger discharges on the 5-ft grid. Flows for all discharges were calculated using a sequential approach, where the first flow calculation started with the smallest discharges. The results of the preceding smaller discharge were used as the initial wetting condition to start flow calculations for the next larger discharge. This minimized the impact of transient flow features like bores on the wetted area. Outlet flow water surface elevations were set to ensure subcritical outflow conditions.

Time steps were established at 5 s for the 6-ft grid and the smaller discharges to ensure Courant numbers of larger than 4 given main channel flow velocities of 1-2 m/s for discharges of 10 cms to ~200 cms. Main channel flow velocities for discharges of 200 cms and larger were generally > 2 m/s. Consequently, a time step of 3 s for the 5-ft grid to ensure Courant number larger than 4. As indicated in **Table 2-1**, two bed roughness scenarios using Manning's  $n$  of 0.030 and 0.038 were implemented in the 6-ft-grid flow calculations.

A total of 15 hydrograph monitoring positions were established throughout the channel sections of the study reaches. These hydrographs were monitored to determine when the flows had reached steady state. Typically, flow times of about four hours were required to achieve steady-state conditions throughout both study reaches. Steady-state conditions were defined as attaining an essentially static water surface elevation at all the hydrograph monitoring positions (natural high-frequency water surface elevation oscillations, typically of several centimeters, were ignored).

The flow quantities output included water surface elevations and vector flow velocities interpolated to the water surface elevation positions at cell-centered positions in the staggered grid. Using the known topography, derived quantities such as depth, shear stress, and power were

obtained. The inverse transformation operators were then applied to produce flow quantities in the INL state-plane coordinate system.

**2.5.1 Results.** Complete results of the flow modeling are depicted on maps contained in **Appendix D - Electronic Supplement**. Color-contoured plots of depth, stream power and shear stress are overlain on shaded relief images of the high-resolution topography and the geomorphic map units shown on **Plate 2**. Plots showing differences in flow depth for simulations with varied inputs of Manning's  $n$  or the input topographic grid are also included in **Appendix D - Electronic Supplement**. Plots in **Appendix F (Figures D3-6 through D3-37)** depict the effects of these same variations on unit stream power and bed shear stress in each of the sampling subareas. The plots in **Appendix F** can be used to directly assess the affects of the varied inputs on the estimated discharges associated with paleofloods and paleohydrologic bounds (see **Section 3.2**).

The model results show that depth, stream power, and shear stress vary significant throughout the study reach based on the local conditions of flow. For example, along the length of the channel, unit stream power increases and decreases significantly for areas with more or less constricted flow (**Figure 2-9**). Unit stream power increases with discharge in reaches which are less constricted; but locally decreases significantly upstream of some constrictions as flow stagnates with increasing discharge. The smallest flows simulated, 10, 12, and 15 m<sup>3</sup>/s, correspond to the range of the largest gaged flows downstream of the INEEL Diversion Dam, including a series of flows from 1995-1999 (**Appendix E**). In channel values of unit stream power and bed shear stress from this range of discharge that generally remain within the ranges of values associated with soil erosion (**Appendix D and Figure 3-2**) appear to be qualitatively consistent with field observations of a mostly intact, armored gravel bed through many areas of the central part of the study reach (**Section 2.2.4**). Areas at channel constrictions have somewhat higher values unit stream power and bed shear stress, and appear to be areas where sediment was mobilized by these flows.

For simulations up to about 70 m<sup>3</sup>/s, most flow remains confined to the main channel system with progressively greater inundation of flanking H3-4 and locally, limited areas of some H1-2 surfaces. Flows up to this level generally do not reach the geomorphic surfaces of interest for this study. The complex network of abandoned and cutoff channels in the Big Loop area and upstream

of the Saddle constriction gradual inundates with relatively low velocity and stagnated flow that is independent of the pattern of channel cutoffs, but instead controlled by changing patterns of flow constrictions through and downstream of the Big Loop area. Simulations for discharges of 100 and 130 m<sup>3</sup>/s show that essentially all areas of H1-2 surfaces along the Big Lost River become inundated by shallow flow, and simulations for 150 m<sup>3</sup>/s and larger discharges show progressive encroachment of this flow into the lowest areas of Pleistocene deposits and surfaces along the river. Discharges greater than 200 m<sup>3</sup>/s show progressive expansion of flows through the networks of braid channels on the Pleistocene surfaces.

**2.5.1.1 Effects of Varied Manning's  $n$ .** Difference plots of TrimR2D flow depth with varied Manning's  $n$  of 0.038 and 0.030, for discharges of 100, 200, and 250 m<sup>3</sup>/s, show that effects on the flow depth from variations in this parameter vary spatially throughout the study reach (**Appendix D - Electronic Supplement**). The largest differences are present in subreaches where flow accelerates, and flow depths for the lower  $n$ -value are reduced by 0.5 - 1-ft (0.1 - 0.3 m). In subreaches where flow stagnates, which includes large areas of the study reach, this parameter has little effect on flow depth. Thus, simulations based on a Manning's  $n$  of 0.030 indicate slightly reduced depths as flow is initiated through braid channels leading to trench T3, and in the straight reach between trenches T4/T5 and T6. However, initiation of flow over the Saddle and across the large area of Pleistocene (P2) surfaces north of the Big Lost River between the Saddle and the BLR8 site is unaffected by variations of Manning's  $n$  because flow depth in those areas is controlled by backwater effects at bedrock constrictions in the channel.

Effects on estimates of unit stream power and bed shear stress also vary spatially throughout the reach. On the plots in **Appendix F (Figures D3-6 through D3-37)**, dotted lines depicting the results for simulations using a Manning's  $n$  of 0.030 are close to, or shifted slightly to the right of lines for simulations using a Manning's  $n$  of 0.038. This implies a potential increase in the discharge associated with a threshold criteria of about 0 - 25 per cent, depending on the characteristics of flow through any specific subarea.

**2.5.1.2 Effects of Input Topography.** Most flow simulations for the study reach were used a 6-ft computational grid derived from the 2000 topographic data. However, as modeling commenced, it became clear that the extent model reach needed to expanded to simulate

the larger discharges. Thus, a 5-ft topographic grid of larger extent was derived from the reprocessed 1993 topographic data. As shown in **Appendix A**, the 1993 data has somewhat reduced accuracy compared to the 2000 data resulting in a lower resolution topographic input model, particularly in channelled or confined areas. These effects were shown on difference plots of flow depth for two discharges, 200 and 250 m<sup>3</sup>/s, common to both sets of simulations (**Appendix D - Electronic Supplement**). In general, simulations based on the 1993 topographic data resulted in flow depths that were 0.5 - 1 ft (0.1 - 0.3 m) larger throughout most of the study reach. Effects on estimates of unit stream power and bed shear stress are complex and controlled by local flow conditions (See plots in **Appendix D, Figures D3-6 through D3-37**). In some areas, unit stream power and bed shear stress increase due to the higher stage and flow velocity represented in the 5-ft grid model. In other areas, higher stage results in increased backwater and flow stagnation, leading to a reduction in unit stream power and bed shear stress.

**2.5.1.3 Comparisons to Previous Studies.** Initial inspections of model results derived from the 6-ft grid showed significant differences compared to the flow results developed for previous studies (Ostenaar et al., 1999, 2002) using the same flow model. These differences are illustrated by results from the Saddle area depicted in Ostenaar et al. (1999, 2002) (**Figure 2-10**). Increasing discharge from 100 m<sup>3</sup>/s to 150 m<sup>3</sup>/s resulted in a new path for flow named the Saddle, and development of high values of unit stream power on the geomorphic surfaces just downstream of the Saddle. In contrast, results from the 6-ft grid for this study showed that for a discharge of 150 m<sup>3</sup>/s (**Figure 2-23**), flow through the Saddle did not commence until modeled discharge reached of 250 m<sup>3</sup>/s (**Figure 2-24** and **Figure 2-25**). The smallest discharge modeled with the 5-ft grid was 200 m<sup>3</sup>/s (**Figure 2-26**) and these results showed significant flow through the Saddle as well as at a similar location slightly upstream. Because the initiation of through the Saddle is controlled by the backwater effects at the bedrock constriction (Ostenaar et al., 1999, 2002, and **Figure 2-10**) it appears that much of this difference is attributable to the lack of resolution in the original 2-ft contour data used in the earlier modeling. This resulted in higher stages upstream of the constriction for relatively lower discharges compared to the topographic models used as inputs for the present study.

Initial comparisons of modeling results for other areas of the study reach did not show a consistent difference (**Section Figure 2-11**). At BLR7, the most upstream site in the Diversion Dam study reach, modeled stage increased by about 0.5 m compared to the previous results. At BLR2, BLR6, and BLR8, modeled stage decreased by about 0.1-0.2 m compared to the previous results. When evaluation of the topographic data (**Appendix A**) revealed discrepancies in the accuracy of the 2-ft contour data used as input for the modeling by Ostenaar et al. (1999, 2002), the previous modeling results were eliminated from further consideration.

**2.5.1.4 Results from Specific Study Areas.** As a supplement to the reach-scale plots of the flow simulation results contained in **Appendix D - Electronic Supplement**, large-scale plots near the detailed geologic study areas were prepared that show unit stream power and bed shear stress. The plots in this section illustrate results for TrimR2D simulations using a Manning's  $n$  of 0.038, and results are shown for both 6-ft and 5-ft topographic grids. Only the larger flow simulations, those which are pertinent to the evaluations of paleofloods and paleohydrologic bounds for each of the study reaches are included. The full set of flow simulations is included in **Appendix D - Electronic Supplement** and used to define specific discharge limits as discussed in **Appendix D, Figures D3-6 through D3-37**, and following this section in **Section 3.2**.

**Big Loop Study Area, Trenches T1, T2 and T3.** Trenches T1, T2, and T3 were all located across braid channels on the extensive Pleistocene (P2) surface (**Plates 1, 2, and Section 2.3.1**). Trench T1 is lowest of these sites, and flow through the channel at T1 and on the P3 surface surrounding the trench is seen in simulations for discharges of 130 m<sup>3</sup>/s and larger (**Figure 2-12**). For modeled flows of 150 and 175 m<sup>3</sup>/s (**Figure 2-13** and **Figure 2-14**), inundation extent extends across most of the P3 surface and low values of unit stream power (<2 W/m<sup>2</sup>) and bed shear stress (1-5 N/m<sup>2</sup>) are present in limited areas of channels where flow is concentrated. For larger discharges, 200, 225, and 250 m<sup>3</sup>/s (**Figure 2-15** through **Figure 2-17**), the magnitude and extend of unit stream power exceeding 2 W/m<sup>2</sup> and bed shear stress exceeding 1-5 N/m<sup>2</sup> increases with discharge, particularly as flow concentrates in the braid channels and is diverted around small area of higher topography. For this discharge range, some flow is beginning in upstream braid channels on the P2 surface, but no flow has reached trenches T2 or T3.

Flow simulations using the 5-ft topographic grid for discharges of 200 and 250 m<sup>3</sup>/s (**Figure 2-18** and **Figure 2-19**) show increased flow depth and extent compared to the simulations using the 6-ft topographic grid (discussed above in **Section 2.5.1.2**). Thus, flow extent, and the magnitude and extent of values of unit stream power and bed shear stress for 200 m<sup>3</sup>/s on the 5-ft grid is only slightly less than values shown for 250 m<sup>3</sup>/s on the 6-ft grid (compare **Figure 2-18** and **Figure 2-17**). Flow simulations for 300, 350, and 400 m<sup>3</sup>/s (**Figure 2-20** through **Figure 2-22**) show increased flow across the P2 surface in the Big Loop study area, first concentrated in former braid channels, but gradually expanding across much of the surface. For this range of discharges, unit stream power and bed shear stress commonly reach values of 10-30 W/m<sup>2</sup> and 10-25 N/m<sup>2</sup>, respectively, in the braid channels on the P2 surface where flow first concentrates. In the braid channels crossed by trenches T2 and T3, unit stream power and bed shear stress reach values of 5-10 W/m<sup>2</sup> and 5-10 N/m<sup>2</sup>, respectively.

**Saddle Constriction and T4/T5/T6 Study Areas.** The initiation of flow through the Saddle area and onto the extensive Pleistocene (mostly P2) surfaces downstream of the Saddle was an important piece of evidence used by Ostenaar et al. (1999, 2002) to define the basis for a paleohydrologic bound over the past 10,000 years (**Section 2.3.2**). As noted above, (**Section 2.5.1.3**), flow simulations for this study, using the 6-ft grid derived from the 2000 topography, showed that flow was not initiated across the Saddle except for discharges of 250 m<sup>3</sup>/s and larger (**Figure 2-23** through **Figure 2-25**). Trenches T6 and T7 were sited to determine if there was geologic evidence downstream of the Saddle area of such flows. Flow simulations using the 5-ft topographic grid from the 1993 topography again show higher stages compared to simulations based on the 6-ft topographic grid (**Section 2.5.1.2**). For the smallest discharge simulated using the 5-ft grid, 200 m<sup>3</sup>/s, significant flow is present through the saddle, as well as at a second location about 200 m to the northwest (**Figure 2-26**). For the northernmost portion of trench T6 and a small area at the south end of trench T7, unit stream power and bed shear stress exceed 5-10 W/m<sup>2</sup> and 5-10 N/m<sup>2</sup>, respectively, due to flow through the Saddle. Simulations based on either the 6-ft or 5-ft topographic grid (**Figure 2-25** and **Figure 2-26**) indicate that the initial flow onto the P3 surface from the Saddle would cross the geomorphic patterns on the P3 surface downstream of the Saddle. Flows that would follow channel patterns on the P3 surface at trench T6 and the southern end of trench T7 must reach that surface due to high stages in the Big Lost River downstream of

the Saddle constriction. Flow simulations based on the 5-ft grid indicate that this does not happen except for discharges of  $250 \text{ m}^3/\text{s}$  and larger (**Figure 2-27** through **Figure 2-30**). These simulations show that as flow across the topographic barrier associated with the Saddle increases, unit stream power and bed shear stress commonly reach values of  $10\text{-}30 \text{ W/m}^2$  and  $10\text{-}25 \text{ N/m}^2$ , respectively, in the braid channels on the P2 surface downstream as flow re-concentrates in these channels.

The T4/T5/T6 study area is located along the main Big Lost River channel downstream of the Saddle constriction (**Plate 1**). For flow simulations as large as about  $70 \text{ m}^3/\text{s}$  (**Figure 2-31**), flow remains confined to the relatively straight channel flanked by H1-2 and P2 surfaces. Flow simulations of  $100 \text{ m}^3/\text{s}$  (**Figure 2-32**) show inundation of the lowest portions of H1-2 surfaces, such as near T4, and for a discharge of  $130 \text{ m}^3/\text{s}$  (**Figure 2-33**), the entire H1-2 surface near T4/T5/T6 is inundated. In some areas, such as the north end of trench T4, unit stream power and bed shear stress increase rapidly with increased discharge and begin to exceed  $30 \text{ W/m}^2$  and  $25 \text{ N/m}^2$ , at a discharge of  $100 \text{ m}^3/\text{s}$ . In other areas, such as along the main H1-2 surface on the north side of the river between T5 and T6, the increase is slower and patchy, with unit stream power and bed shear stress generally  $<5 \text{ W/m}^2$  and  $5 \text{ N/m}^2$  for a discharge of  $130 \text{ m}^3/\text{s}$ . Increasing discharge results in progressive increases in the extent of larger values of unit stream power and bed shear stress on the H1-2 surfaces. For a discharge of  $150 \text{ m}^3/\text{s}$  (**Figure 2-34**), large areas of unit stream power and bed shear stress in the range of  $10\text{-}30 \text{ W/m}^2$  and  $10\text{-}25 \text{ N/m}^2$ , respectively, are shown on the H1-2 surface, and these expand over most of that surface in simulations for  $175 \text{ m}^3/\text{s}$  (**Figure 2-35**). These values continue to increase in simulations for 200, 225, and  $250 \text{ m}^3/\text{s}$  (**Figure 2-36** through **Figure 2-38**). Simulations for  $225 \text{ m}^3/\text{s}$  show unit stream power and bed shear stress in the range of  $30\text{-}50 \text{ W/m}^2$  and  $25\text{-}50 \text{ N/m}^2$ , respectively, over most of H1-2 surface between T5 and T6, and unit stream power exceeding  $50 \text{ W/m}^2$  in many areas for a discharge of  $250 \text{ W/m}^2$ .

Simulation results for the T4/T5/T6 study area based on the 5-ft topographic grid again show greater flow depth than do equivalent discharge simulations based on the 6-ft topographic grid (**Section 2.5.1.2**). However, for discharges of  $200 \text{ m}^3/\text{s}$ , unit stream power and bed shear stress magnitude and extent on the H1-2 surfaces are generally similar, near  $30 \text{ W/m}^2$  and  $25 \text{ N/m}^2$ , respectively, for simulations using either the 5-ft or 6-ft topographic grid (compare **Figure 2-36**

and **Figure 2-39**). Because of the higher stage present in the 5-ft grid model, flow overtops edge of the P3 surface north of the river, resulting in slightly reduced unit stream power and bed shear on the flanking H1-2 surface. For larger discharges simulated using the 5-ft topographic grid (**Figure 2-40** through **Figure 2-43**), the high values unit stream power and unit stream power are present across the entire extent of the H1-2 surface near trenches T5 and T6.

In both sets of flow simulations, for discharges larger than  $150 \text{ m}^3/\text{s}$ , unit stream power exceeds  $100 \text{ W/m}^2$  bed shear stress approaches  $100 \text{ N/m}^2$  over most of the channel area through this subreach.

**BLR8 Study Area, Trenches T8 and T9.** For discharges up to  $70 \text{ m}^3/\text{s}$  (**Figure 2-44**), flow simulations indicate that the main path of flow follows the Big Lost River channel around the sharp bends that define this subreach. For the larger discharges in this range, there is a decrease in channel power and shear stress in the downstream portion of the reach, and an increase in area near the Rb outcrops flanking the downstream bedrock constriction. Near trench T8a,b,c, the inundation extent for a discharge of  $70 \text{ m}^3/\text{s}$  is roughly coincident with the transition between H1-2 and H3-4 surfaces (**Figure 2-44**). Deposits at the north end of trench T9 are inundated by discharges of less than  $50 \text{ m}^3/\text{s}$ , and unit stream power and bed shear stress remains low at this site through the full range of simulated discharges flow depth increases. Discharges of  $100$  and  $130 \text{ m}^3/\text{s}$  (**Figure 2-45** and **Figure 2-46**) both inundate the full extent of H1-2 surfaces to the vicinity of trench T8b. Unit stream power and bed shear values increase significantly near trench T8c with each increase in the modeled discharge, but remain low at the edge of the flow near trench T8b. Discharge of  $150 \text{ m}^3/\text{s}$  (**Figure 2-47**) results in inundation to the southern end of trench T8a and is roughly coincident with the lower edge of the P3 surface near trench T9. At this discharge and larger, unit stream power and bed shear stress near trench T8c, the northernmost trench, remain generally above values of  $50 \text{ W/m}^2$  and  $25 \text{ N/m}^2$ . For discharges of  $175$ ,  $200$ ,  $225$ , and  $250 \text{ m}^3/\text{s}$  (**Figure 2-48** through **Figure 2-51**) flow depth progressively increases in the areas of T8a and T8b, increasing the range unit stream power and bed shear stress to  $5\text{-}25 \text{ W/m}^2$  and  $5\text{-}30 \text{ N/m}^2$ , respectively. Near T8c, values of unit stream power and bed shear stress increase somewhat but remain above  $50 \text{ W/m}^2$  and  $25 \text{ N/m}^2$ . Near trench T9, increasing discharge above  $150 \text{ m}^3/\text{s}$ ,

results in gradual southward extension of the inundation extent with low unit stream power and bed shear stress values.

Simulations of the larger discharges using the 5-ft grid topography have higher stages and greater flow depths (**Section 2.5.1.2**), but the most significant difference from the 6-ft grid results is a small shift to the south in the band of highest intensity unit stream power and bed shear stress across the H1-2 surface near T8b and T8c. The results based on the 5-ft topographic grid for 200 and 250 m<sup>3</sup>/s (**Figure 2-52** and **Figure 2-53**) show a distinctly different pattern of high values of unit stream power and bed shear stress compared to results based on the 6-ft topographic grid (**Figure 2-49** and **Figure 2-51**). For the larger discharges modeled, 300, 350 and 400 m<sup>3</sup>/s (**Figure 2-54** through **Figure 2-56**) the full extent of the P3 surface near the trenches becomes inundated. In the largest flows, unit stream power and bed shear stress begin to decrease across the site due to backwater effects from the bedrock outcrops at the downstream edge of the study area.

**Figures for Section 2.0**

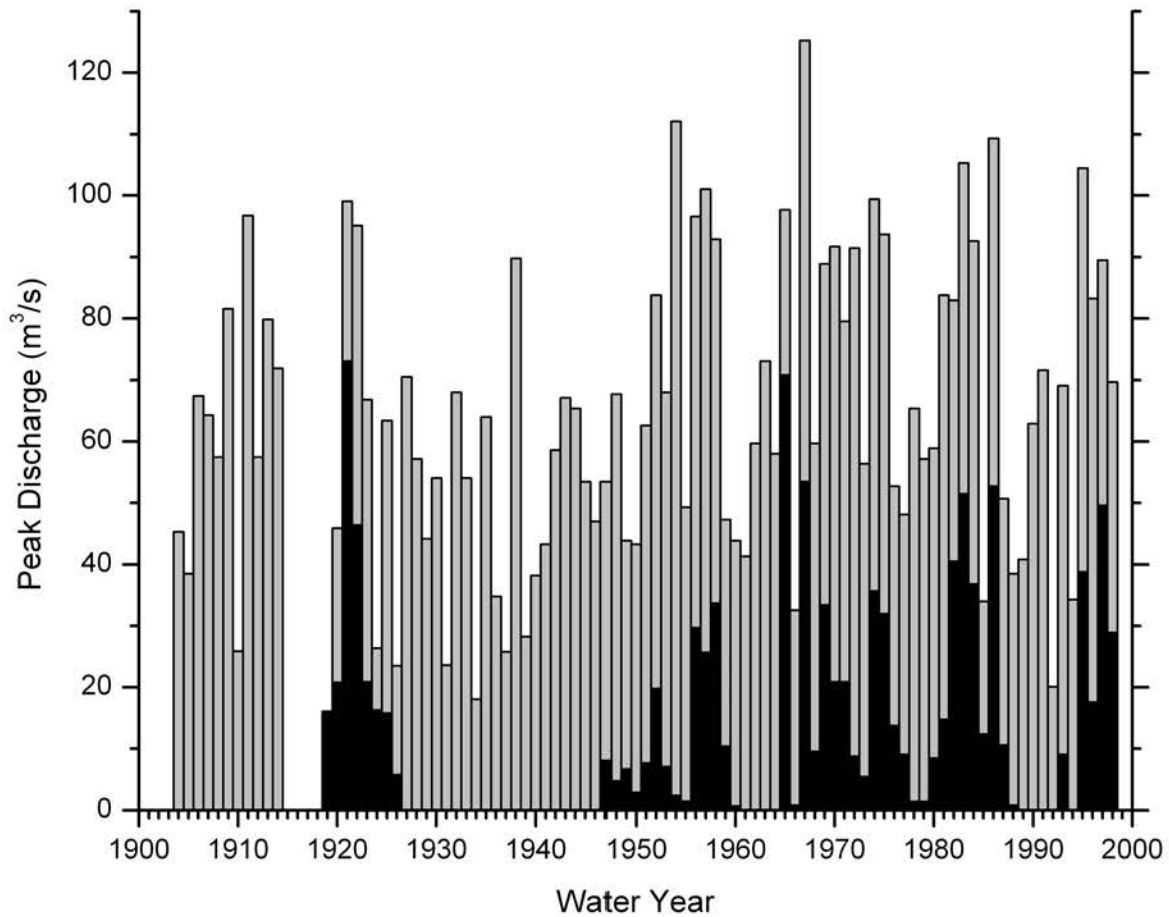


**Figure 2-1 Annual peak discharge estimates for upstream (light shaded bars) and downstream gaging stations (dark shaded bars) on the Big Lost River.** Upstream estimates are from Big Lost River at Howell Ranch from 1904 to 1998. Downstream estimates are from Big Lost River near Arco from 1947 to 1998 except for period 1919 to 1926 which are peak discharge estimates from stations at Leslie and near Moore, early gages located a short distance upstream of Arco. No peak discharge estimates are available from sites near Arco for the periods 1905 to 1918, 1927 to 1945, and 1962 to 1964. Figure from Ostenaar et al., 2002.

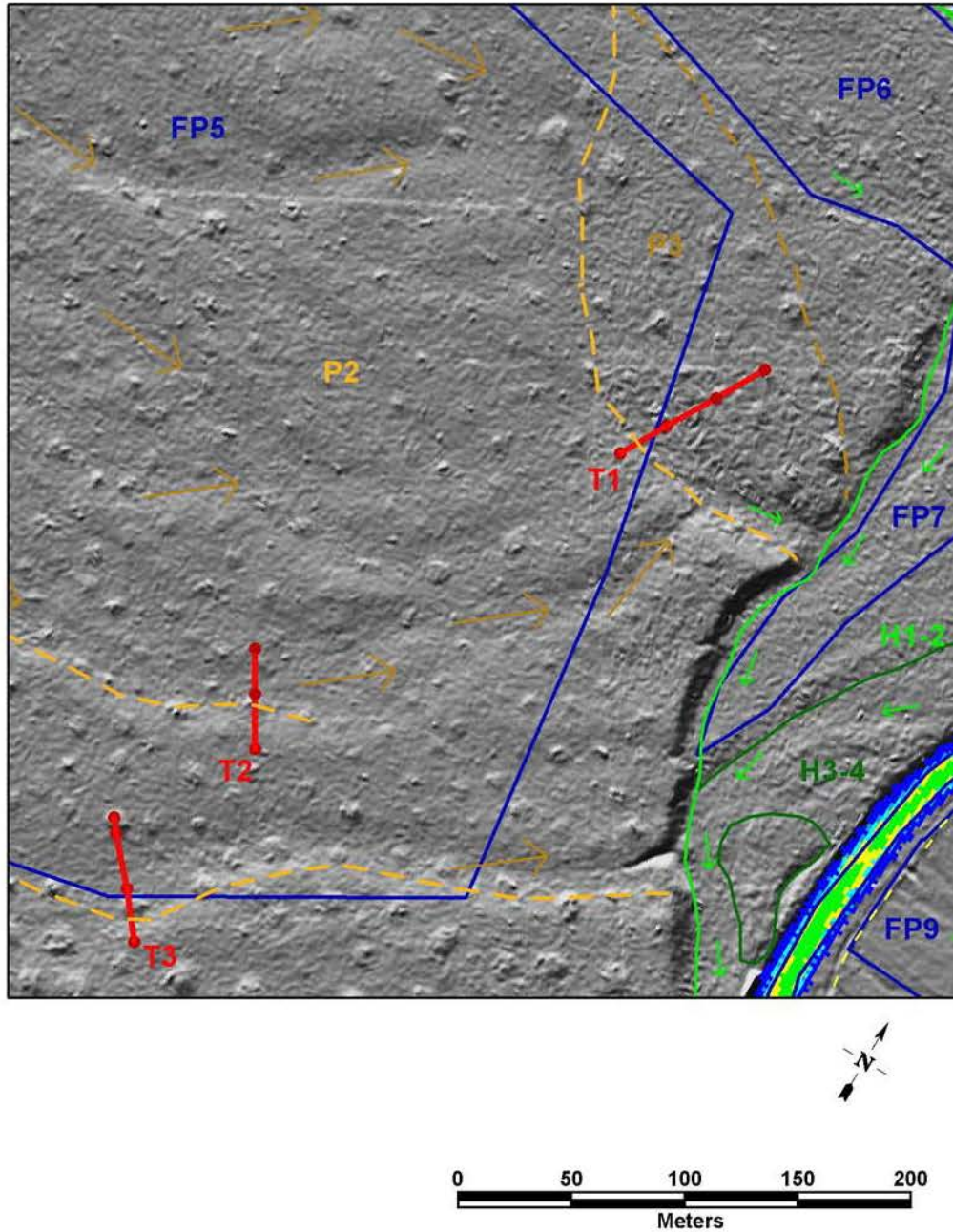


**Figure 2-2 Area around Trenches T1, T2, and T3.** Shaded relief image and geology from **Plate 2**. Blue boxes are stream power and shear stress sample areas (**Section 3.2**). Red lines are trench locations; red dots along the lines show end stations and 25-m stationing intervals beginning at south end. See **Plate 2** for explanation of geologic symbols and labels. Flow direction in Big Lost River is from upper left to lower right.

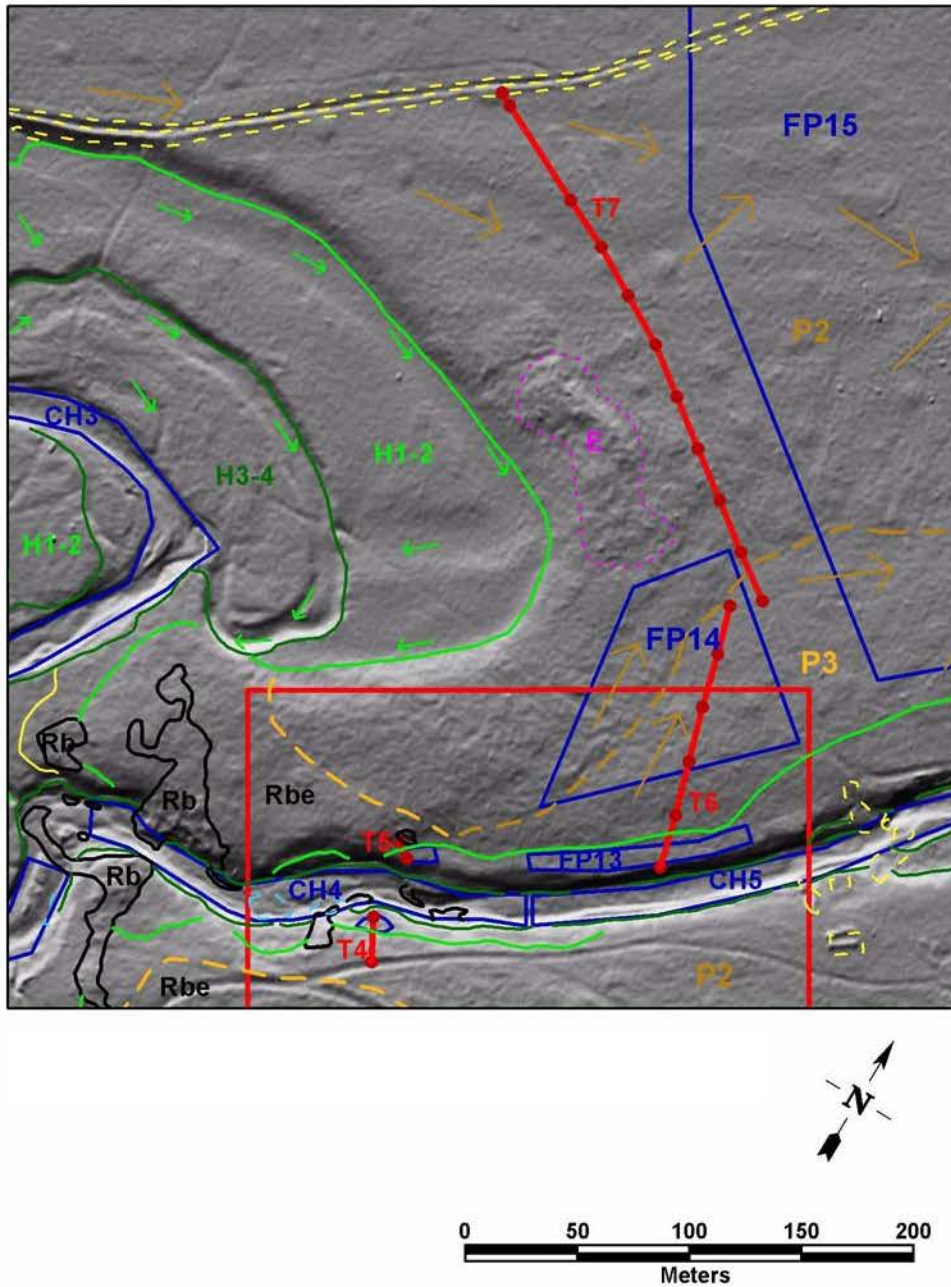


**Figure 2-3 Area around "Saddle" and Trenches T4 and T5 downstream of saddle constriction.**

Shaded relief image and geology from **Plate 2**. Blue boxes are stream power and shear stress sample areas (**Section 3.2**). Red lines with dots and labels show trench locations; red dots along the lines show end stations and 25-m stationing intervals beginning at south end. Red box in lower part of figure shows partial extent of inset area shown in **Figure 2-4**. See **Plate 2** for explanation of geologic symbols and labels. River flow direction is from left to right.

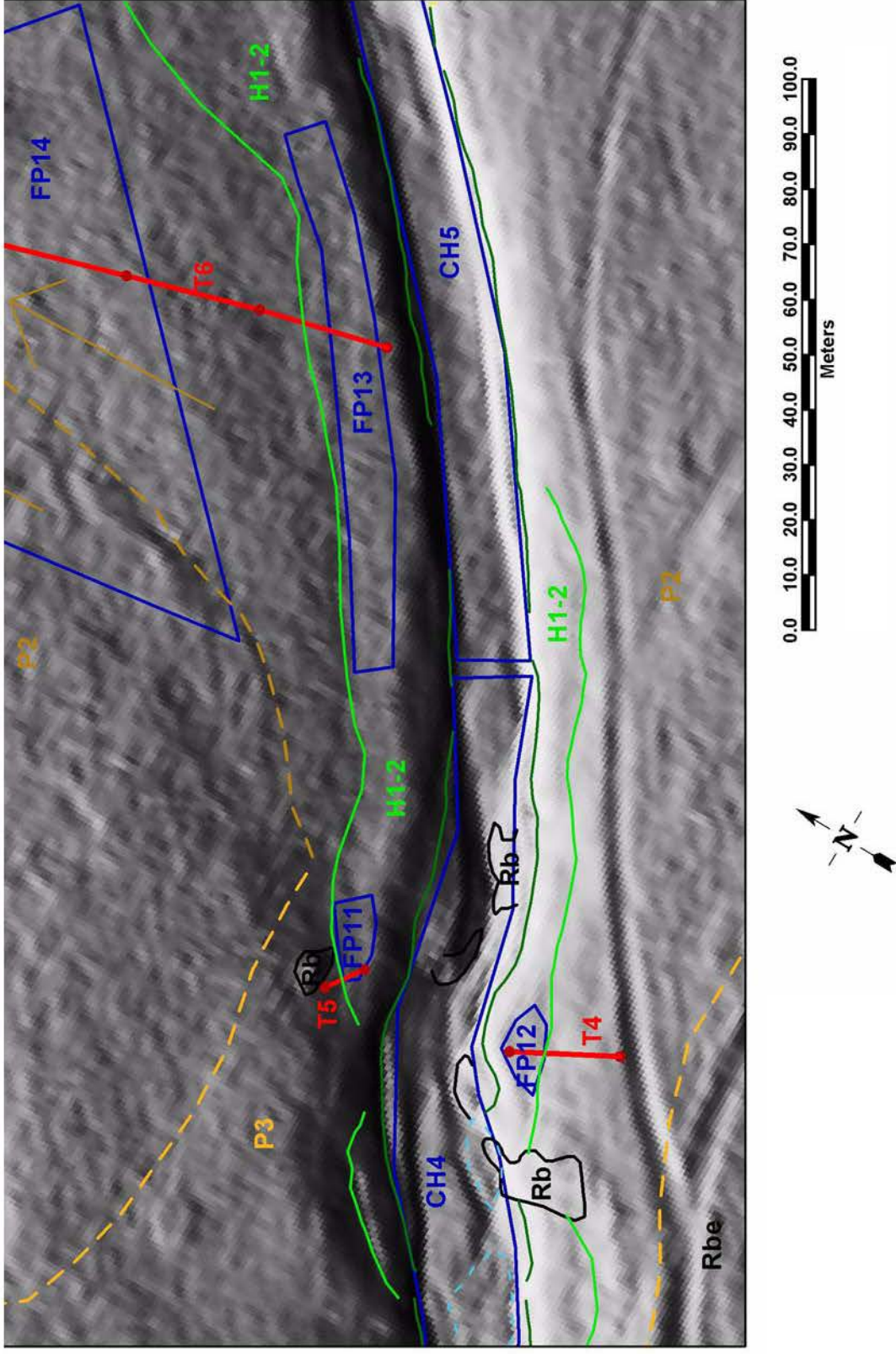


**Figure 2-4 Detail of area around Trenches T4, T5 and T6 downstream of saddle constriction.** Shaded relief image and geology from **Plate 2**. Blue boxes are stream power and shear stress sample areas (**Section 3.2**). Red lines with dots and labels show trench locations; red dots along the lines show end stations and 25-m stationing intervals beginning at south end. See **Plate 2** for explanation of geologic symbols and labels.

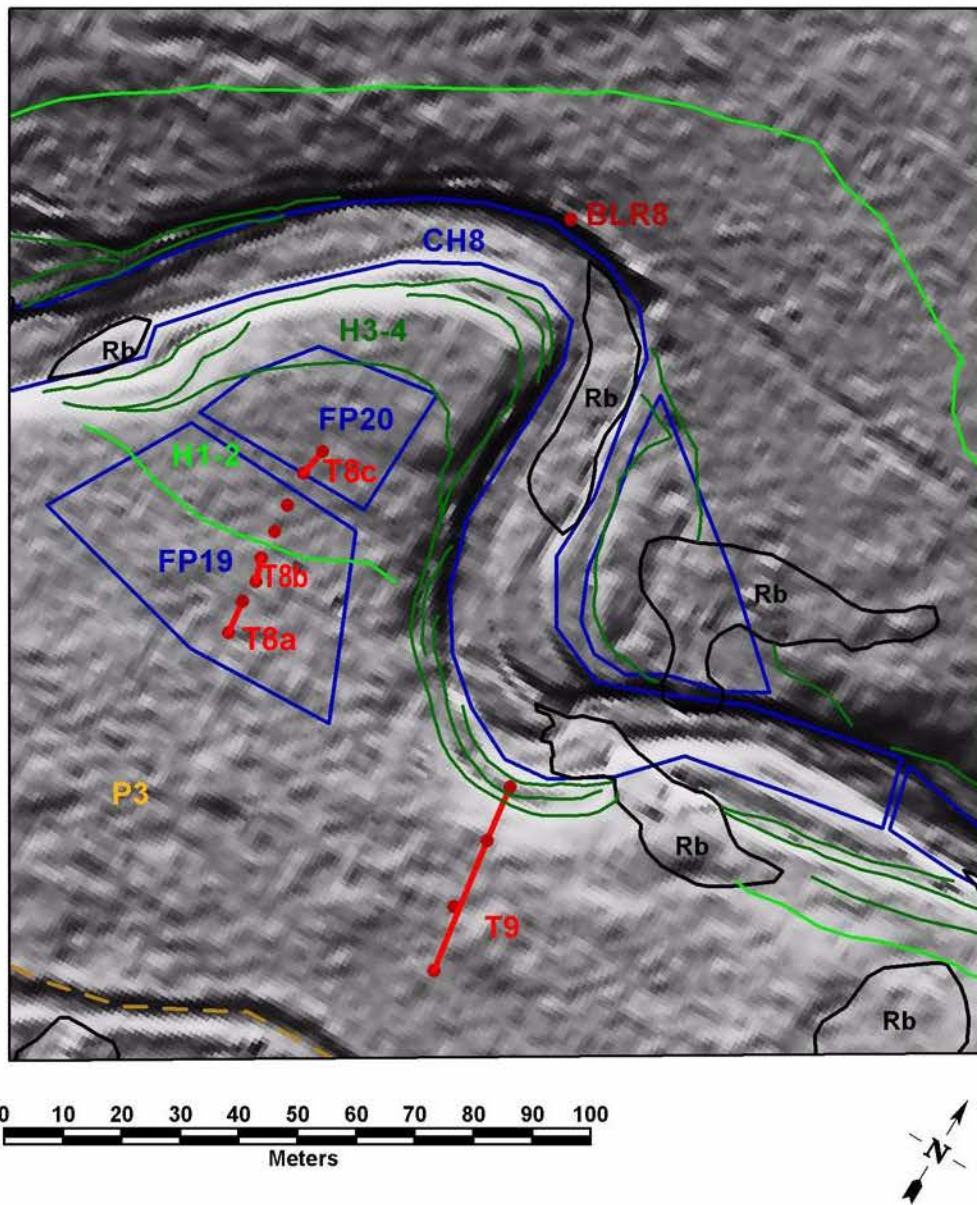


**Figure 2-5 Area around BLR8 and Trenches T8 and T9.** Shaded relief image and geology from **Plate 2**. Blue boxes are stream power and shear stress sample areas (**Section 3.2**). Red lines with dots and labels show trench locations; red dots along the lines show end stations and 25-m stationing intervals beginning at south end. See **Plate 2** for explanation of geologic symbols and labels. River flow is from left to right.

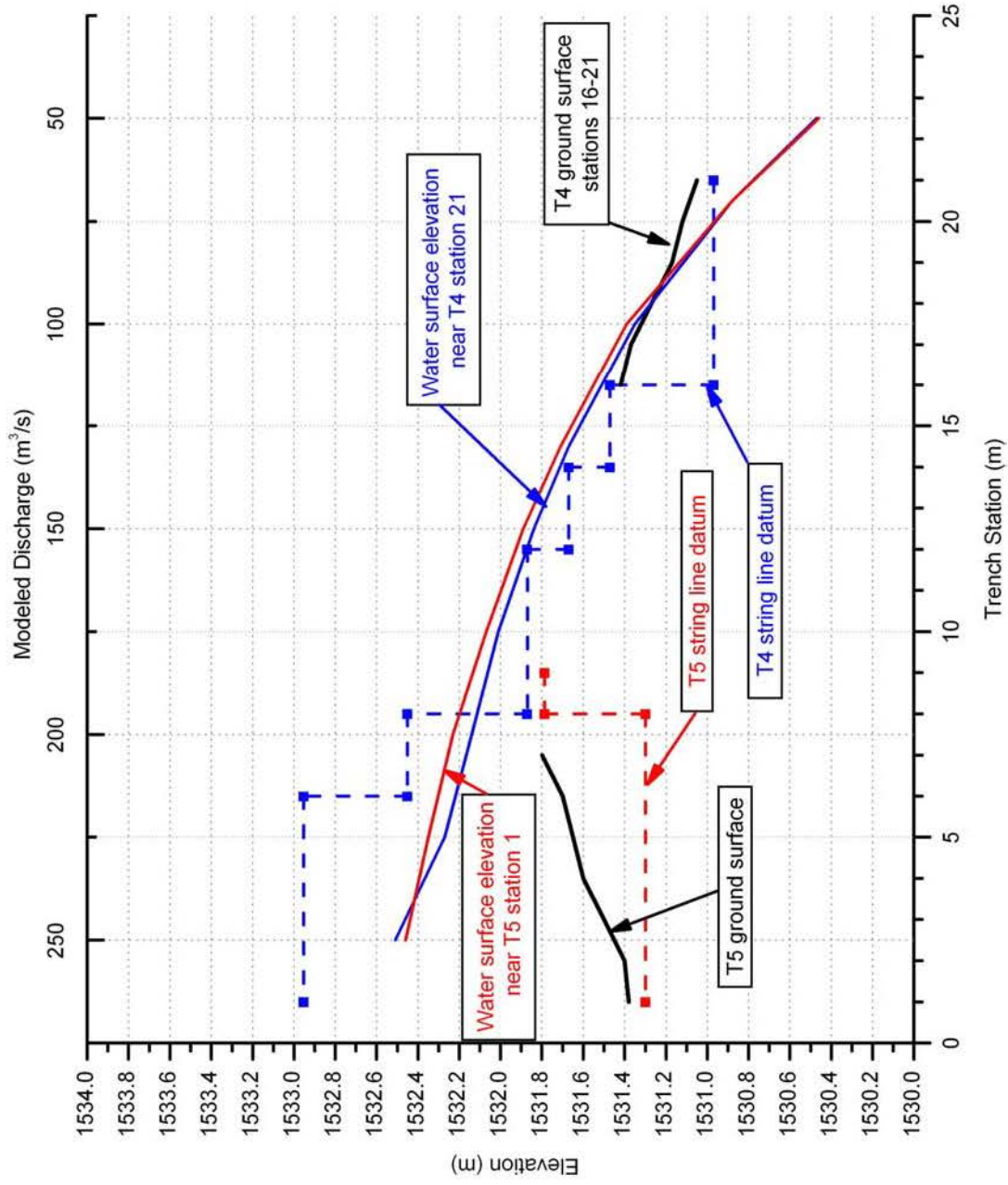


Figure 2-6 Modeled water surface elevation near trenches T4 and T5. Results for  $n=0.038$  from TrimR2D models on 6-ft topographic grid. S

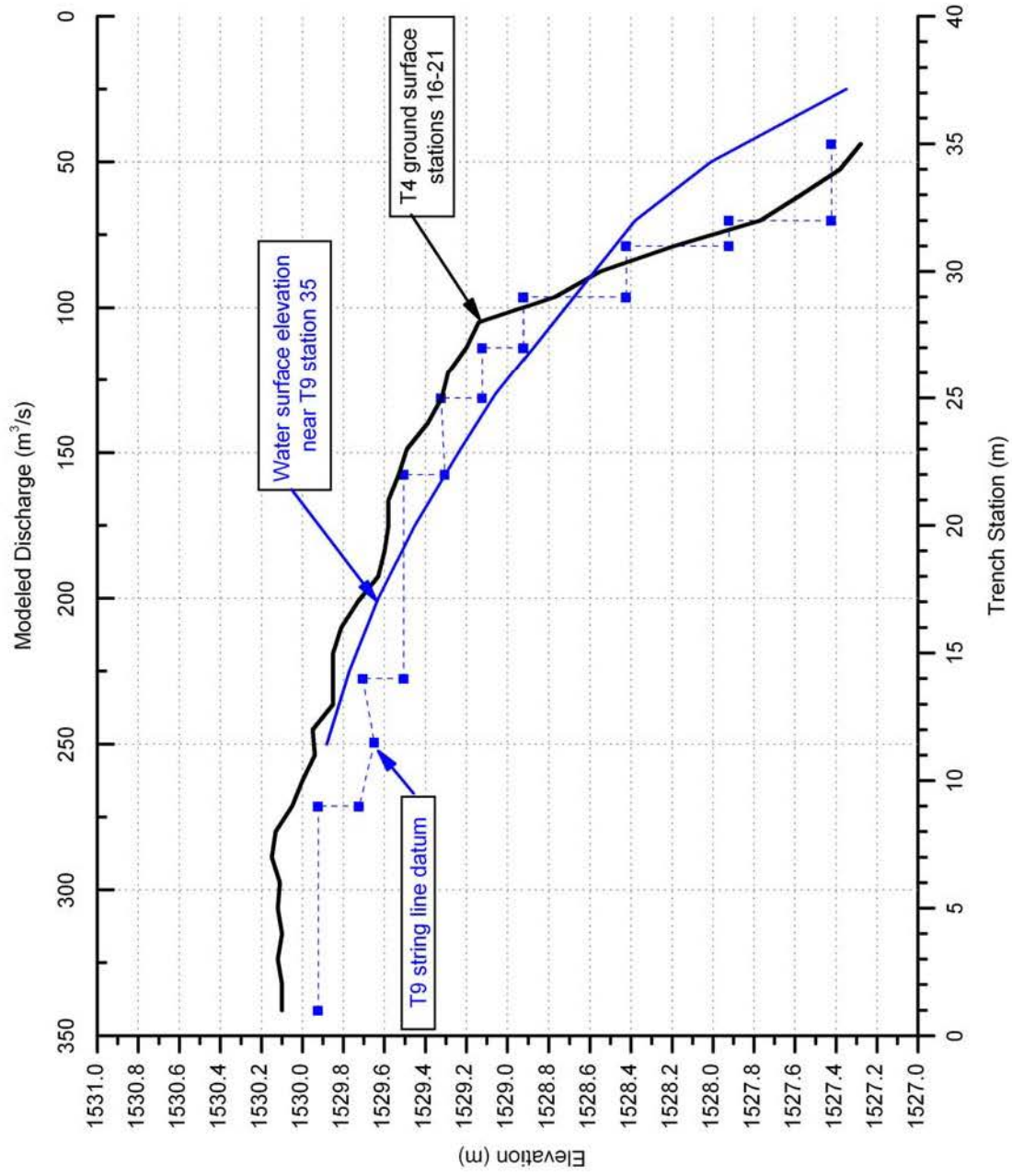
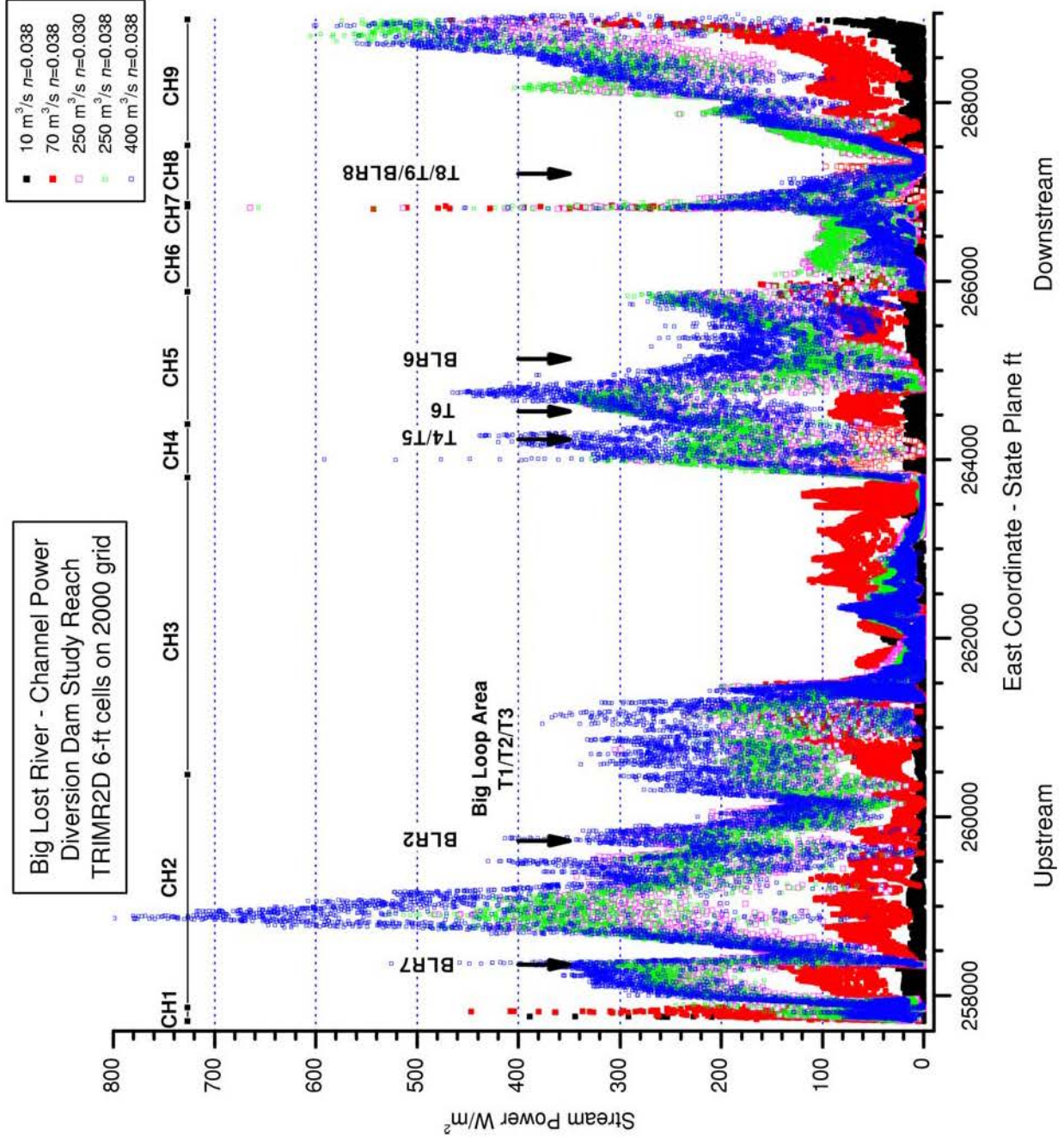


Figure 2-7 Modeled water surface elevation near trench T9. Results for n=0.038 from TrimR2D models on 6-ft topographic grid. S





**Figure 2-9 Channel power for the Diversion Dam study reach subareas.** Longitudinal extent of channel reach subareas is shown by bars along top of plot. Subarea extent and sampling is described in Appendix D.

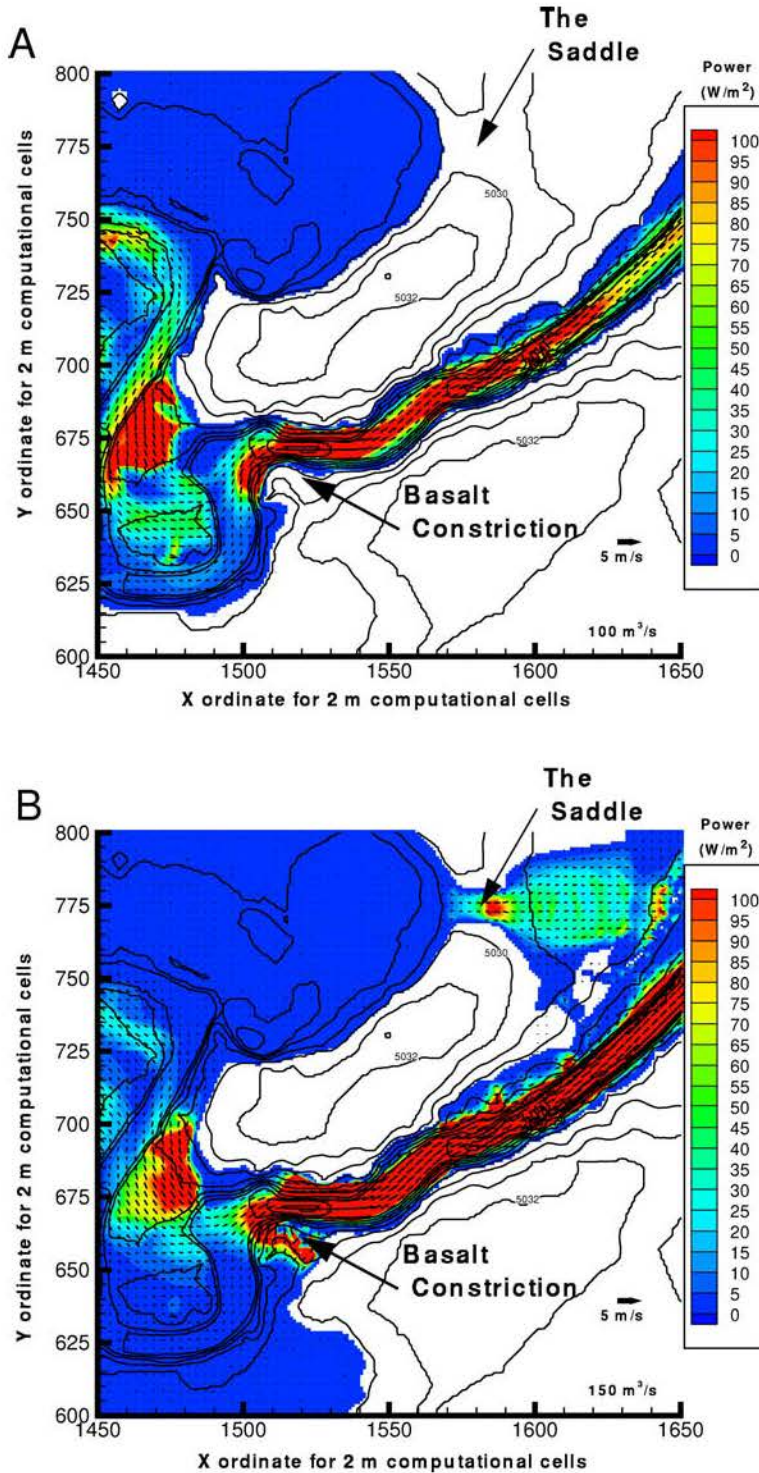


Figure 2-10 Model results for 100 and 150 m<sup>3</sup>/s from Ostenaar et al. (1999, 2002) near the Saddle. A) Inundation and unit stream power for 100 m<sup>3</sup>/s; B) Inundation and unit stream power for 150 m<sup>3</sup>/s. Flow is from left to right in both plots.

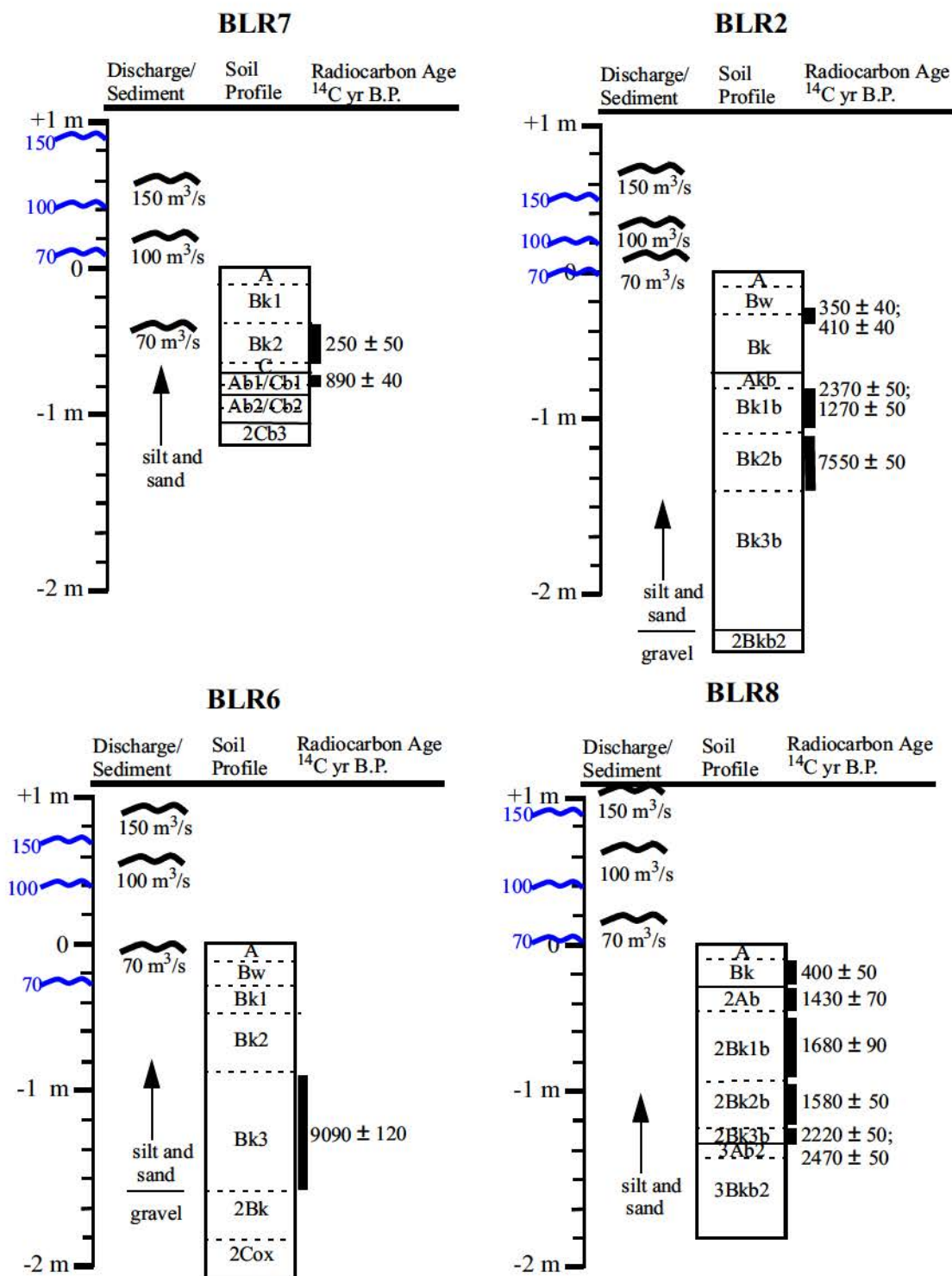


Figure 2-11 Figure 5 from Ostenaar et al. (2002) with revised stage estimates at BLR study sites. Wavy blue lines along axis show current study model results from 6-ft grid for  $n=0.038$ . All other data from Ostenaar et al. (2002). Study site locations are shown on Plates 1 and 2.

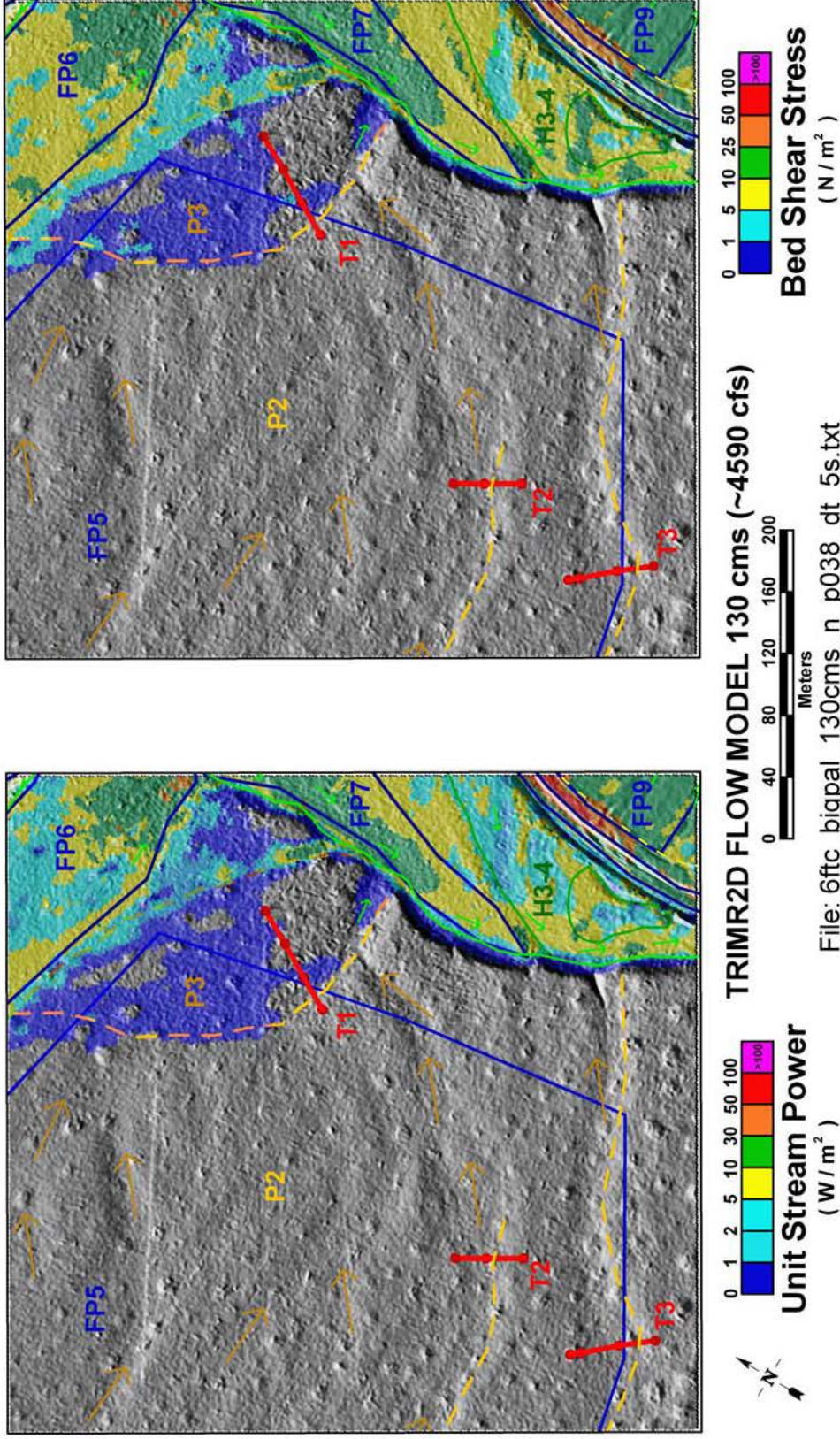


Figure 2-12 6-ft flow model results for  $130\text{ m}^3/\text{s}$  in the Big Loop study area. Base map symbology is from Figure 2-3 and Plate 2.

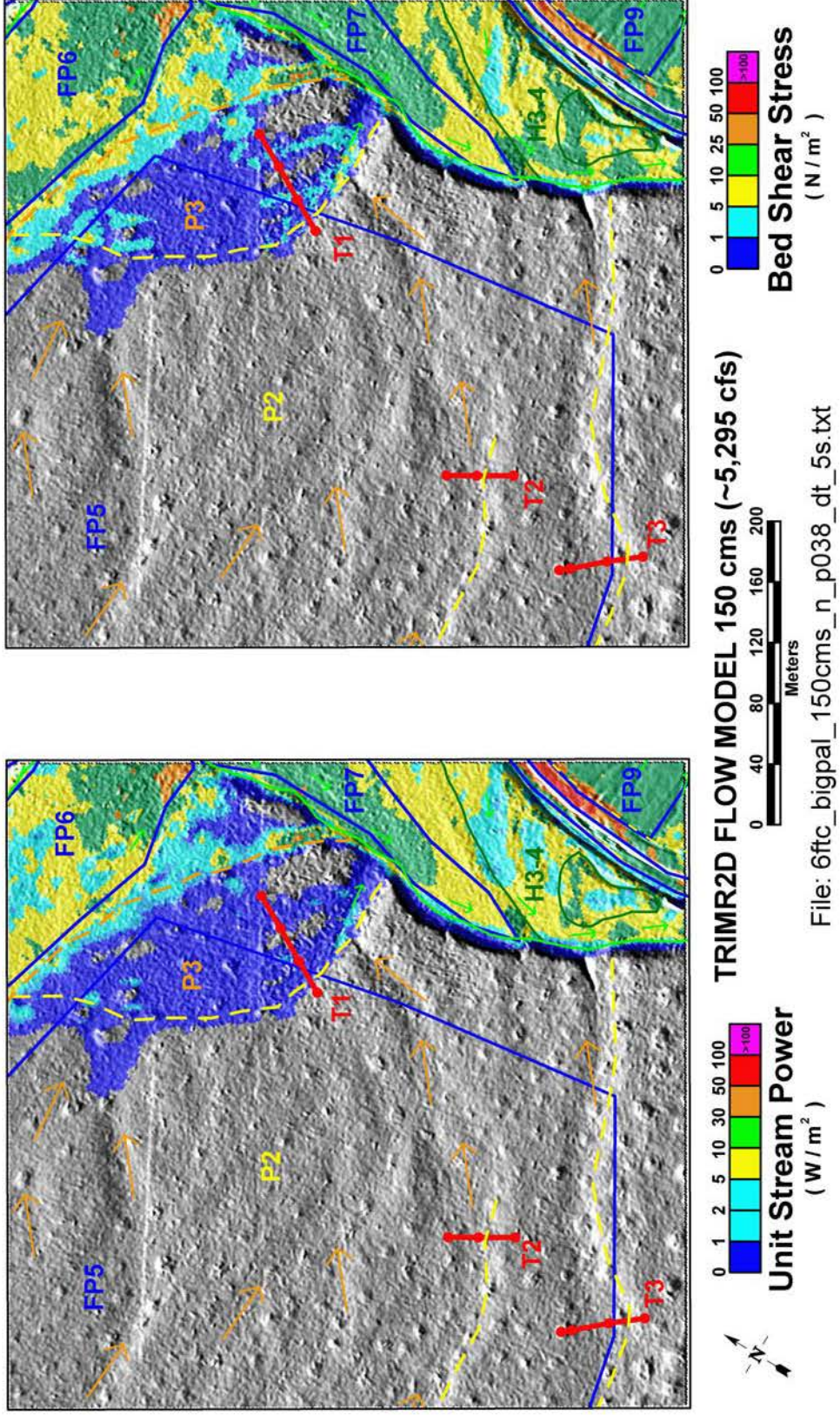


Figure 2-13 6-ft flow model results for 150 m<sup>3</sup>/s in the Big Loop study area. Base map symbology is from Figure 2-3 and Plate 2.

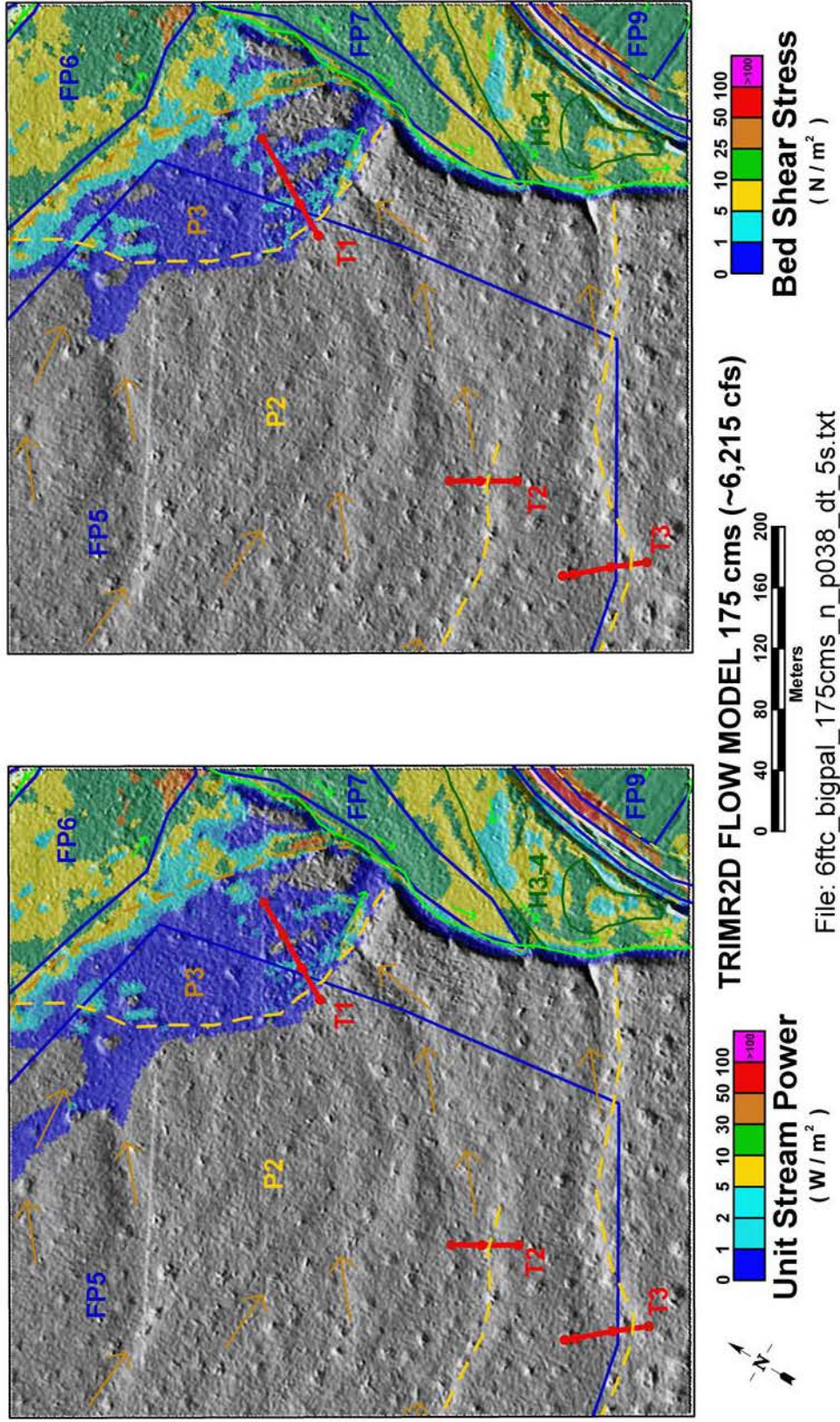


Figure 2-14 6-ft flow model results for 175 m<sup>3</sup>/s in the Big Loop study area. Base map symbology is from Figure 2-3 and Plate 2.

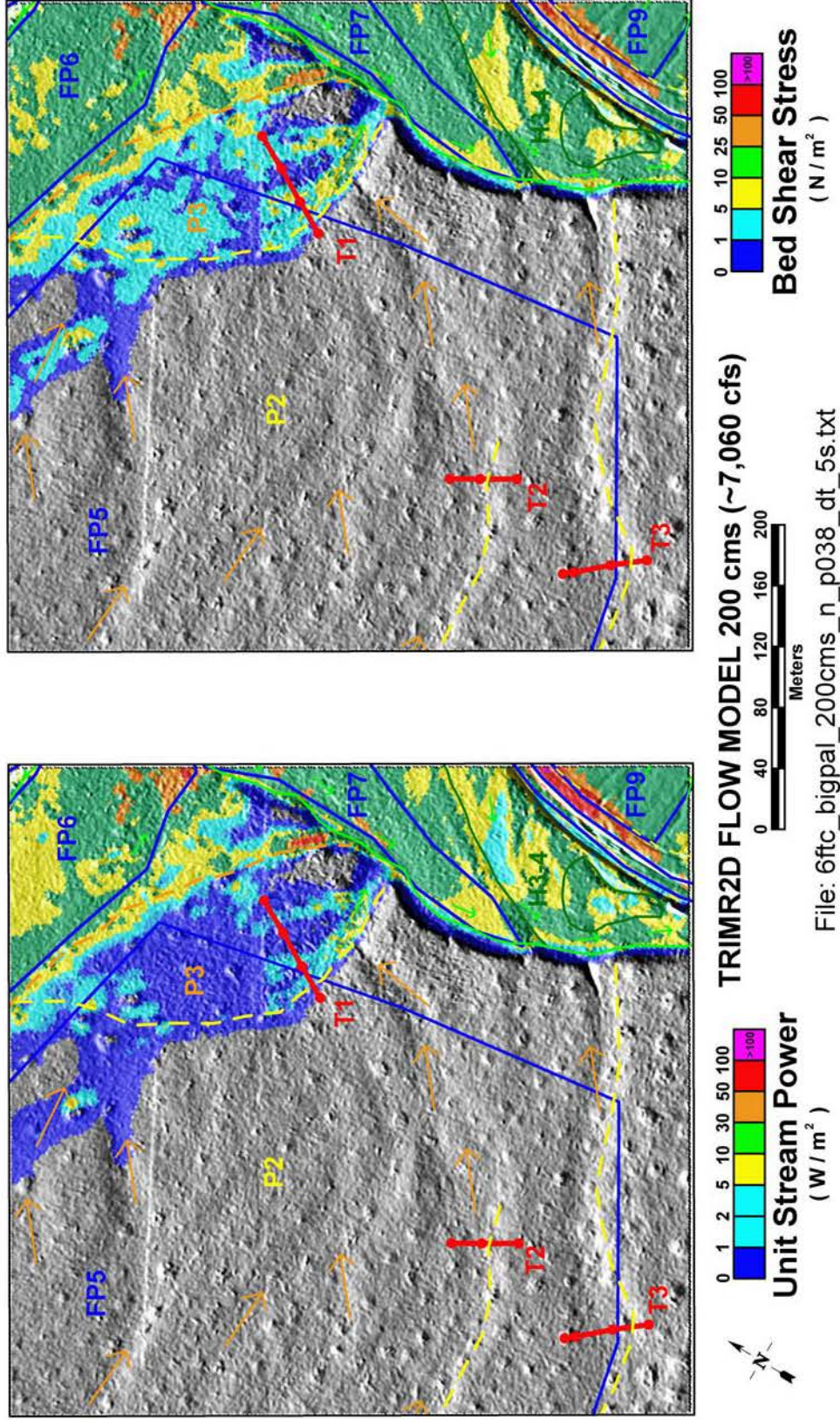


Figure 2-15 6-ft flow model results for  $200 \text{ m}^3/\text{s}$  in the Big Loop study area. Base map symbology is from Figure 2-3 and Plate 2.

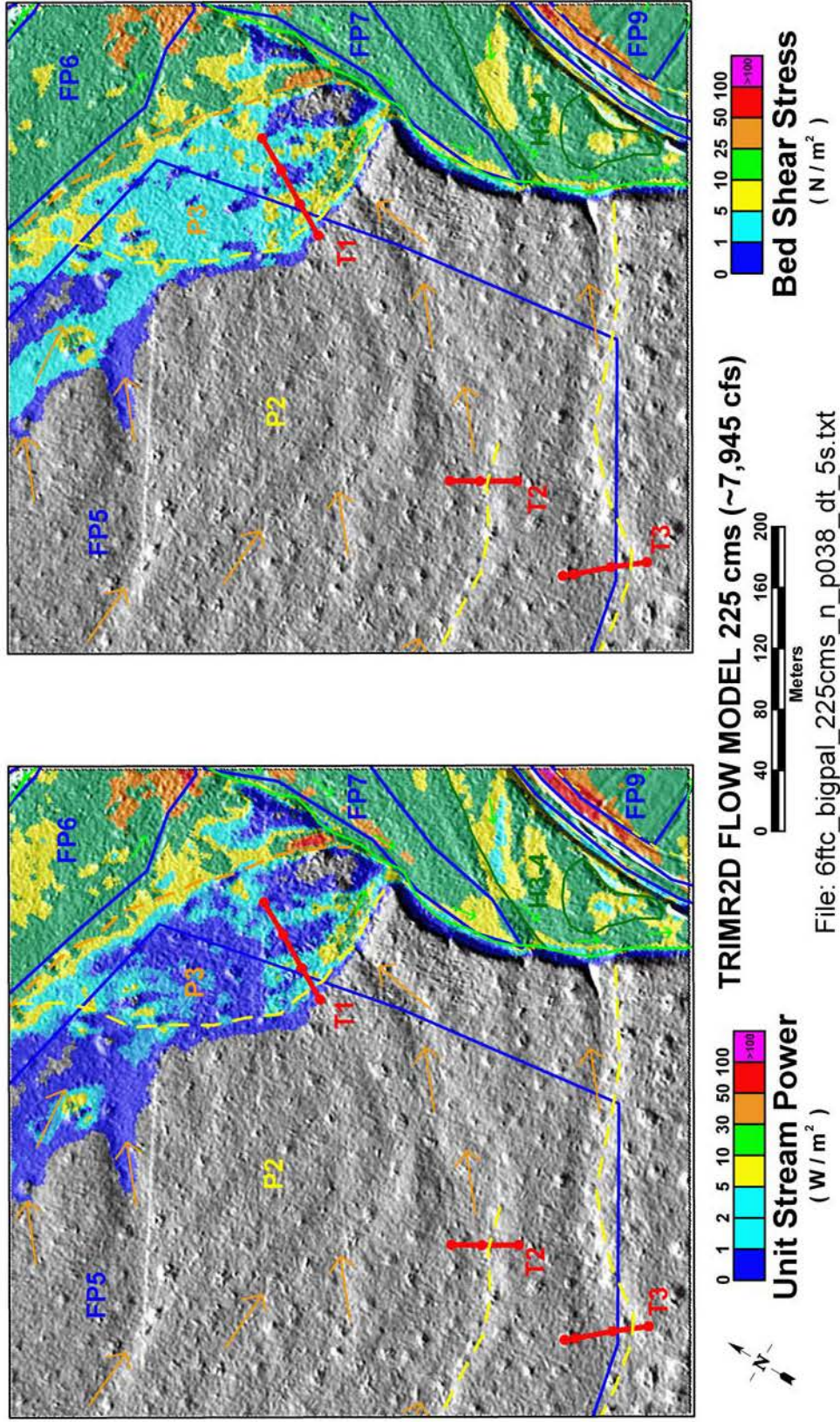


Figure 2-16 6-ft flow model results for  $225\text{ m}^3/\text{s}$  in the Big Loop study area. Base map symbology is from Figure 2-3 and Plate 2.

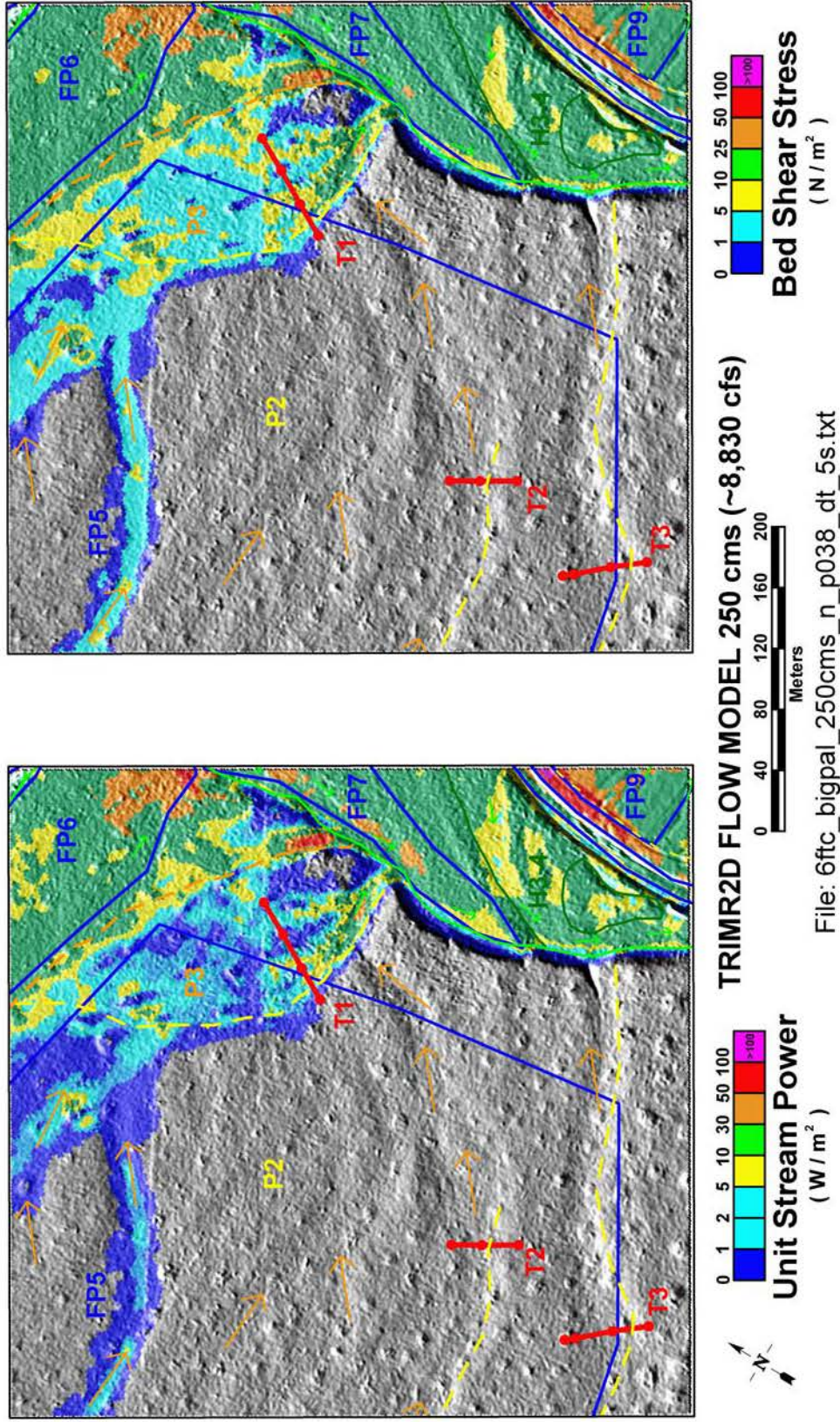


Figure 2-17 6-ft flow model results for  $250 \text{ m}^3/\text{s}$  in the Big Loop study area. Base map symbology is from Figure 2-3 and Plate 2.

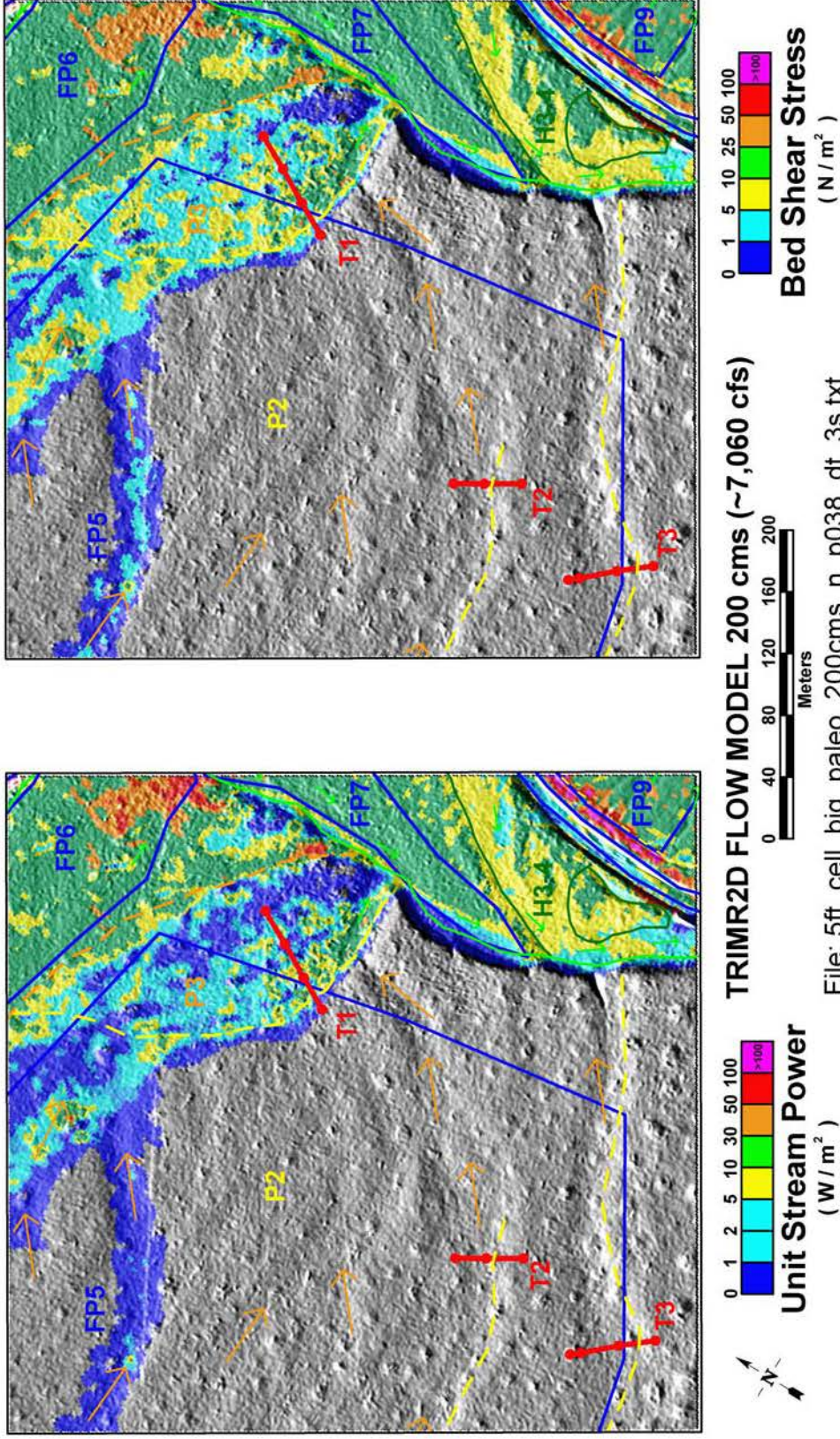


Figure 2-18 5-ft flow model results for 200 m<sup>3</sup>/s in the Big Loop study area. Base map symbology is from Figure 2-3 and Plate 2.

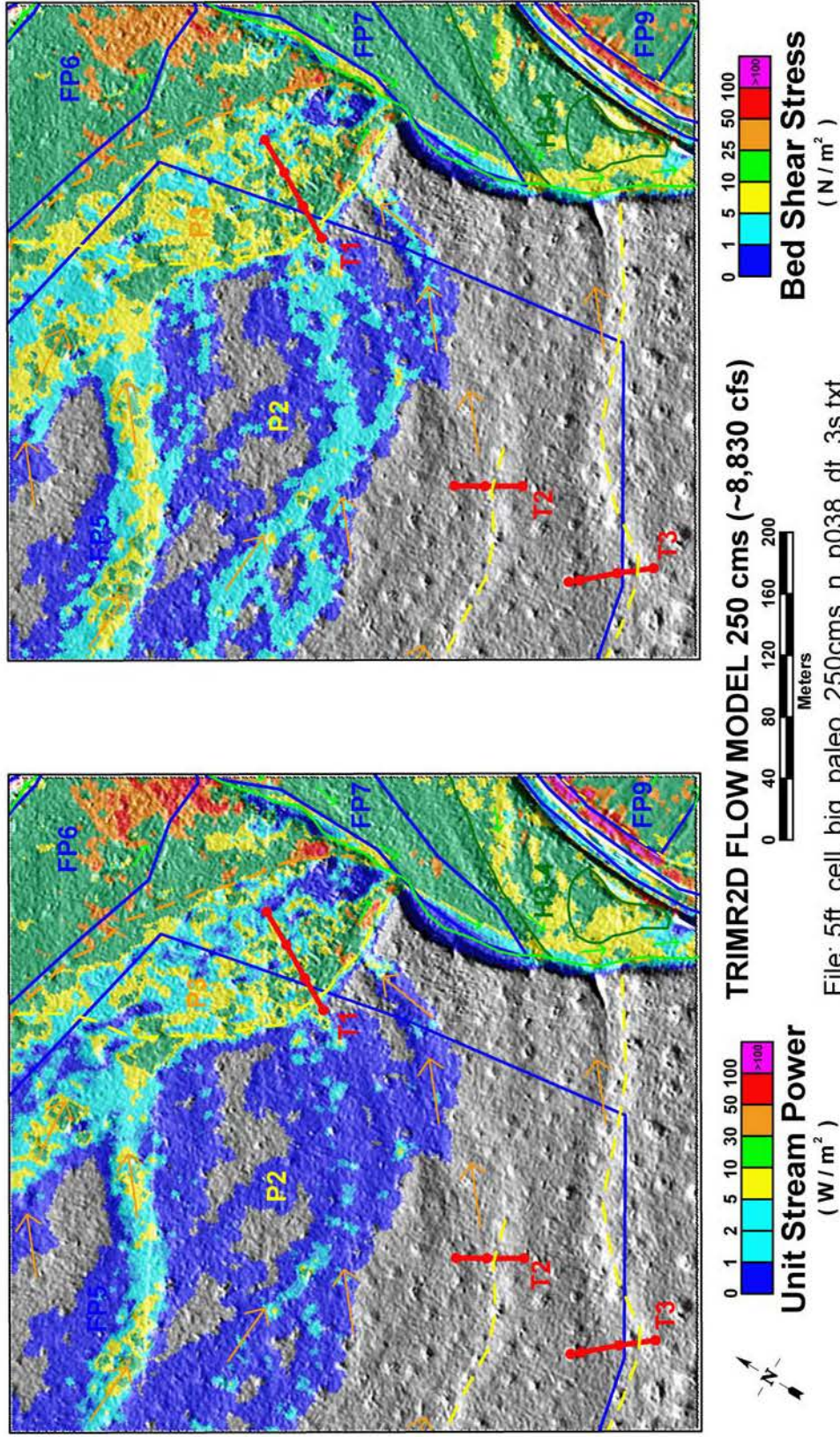


Figure 2-19 5-ft flow model results for  $250\text{ m}^3/\text{s}$  in the Big Loop study area. Base map symbology is from Figure 2-3 and Plate 2.

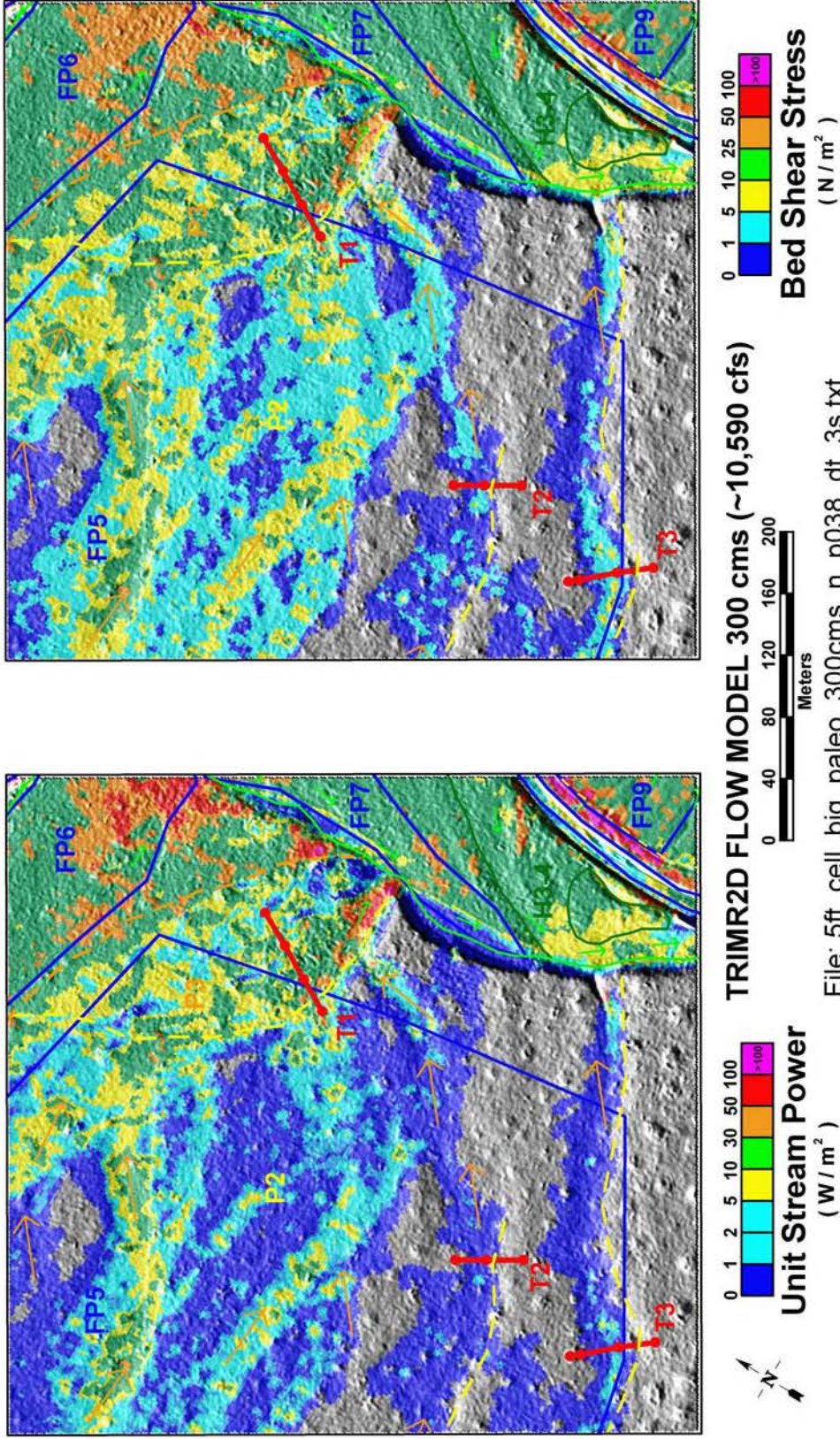


Figure 2-20 5-ft flow model results for  $300\text{ m}^3/\text{s}$  in the Big Loop study area. Base map symbology is from Figure 2-3 and Plate 2.

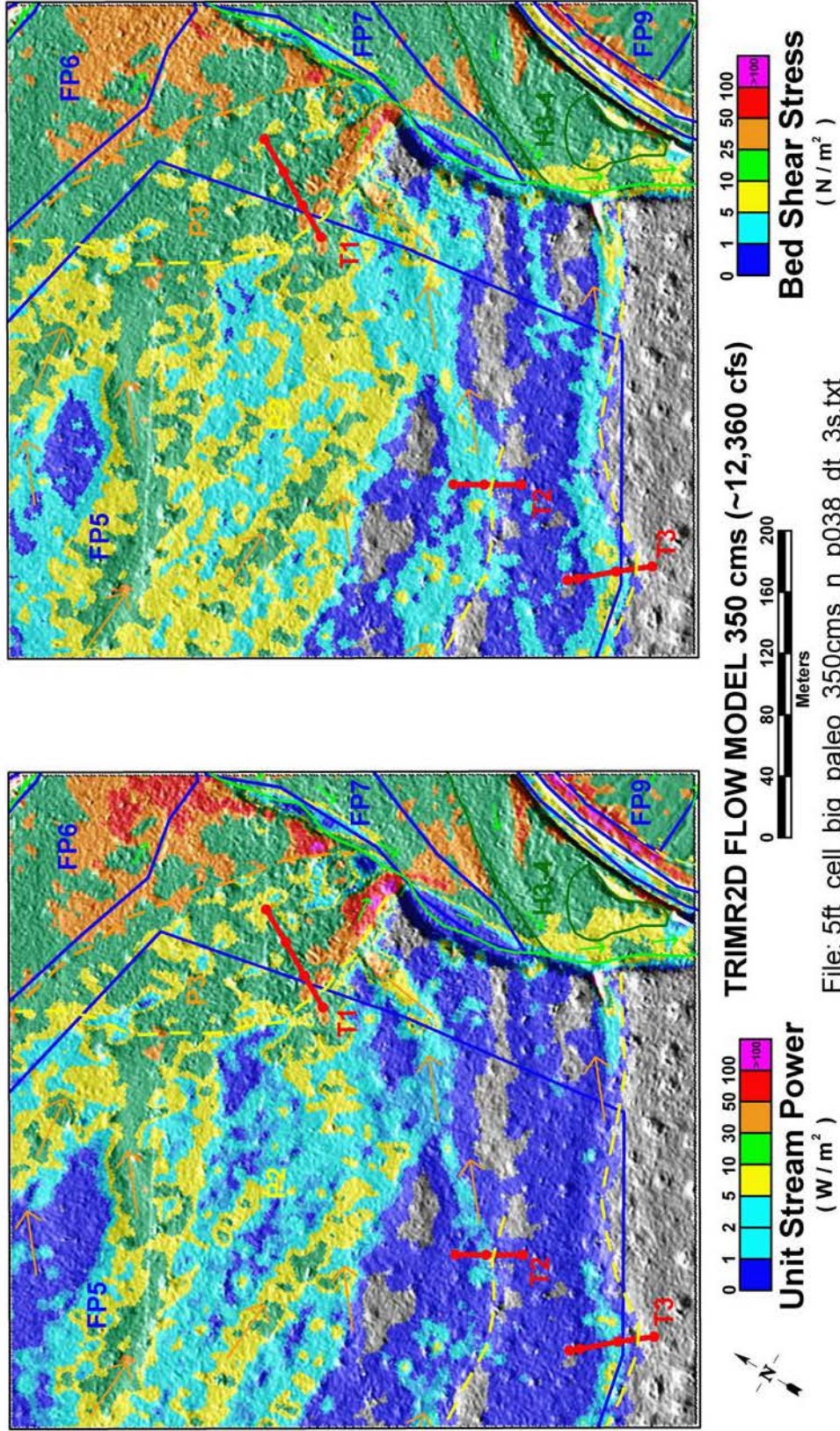


Figure 2-21 5-ft flow model results for 350 m<sup>3</sup>/s in the Big Loop study area. Base map symbology is from Figure 2-3 and Plate 2.

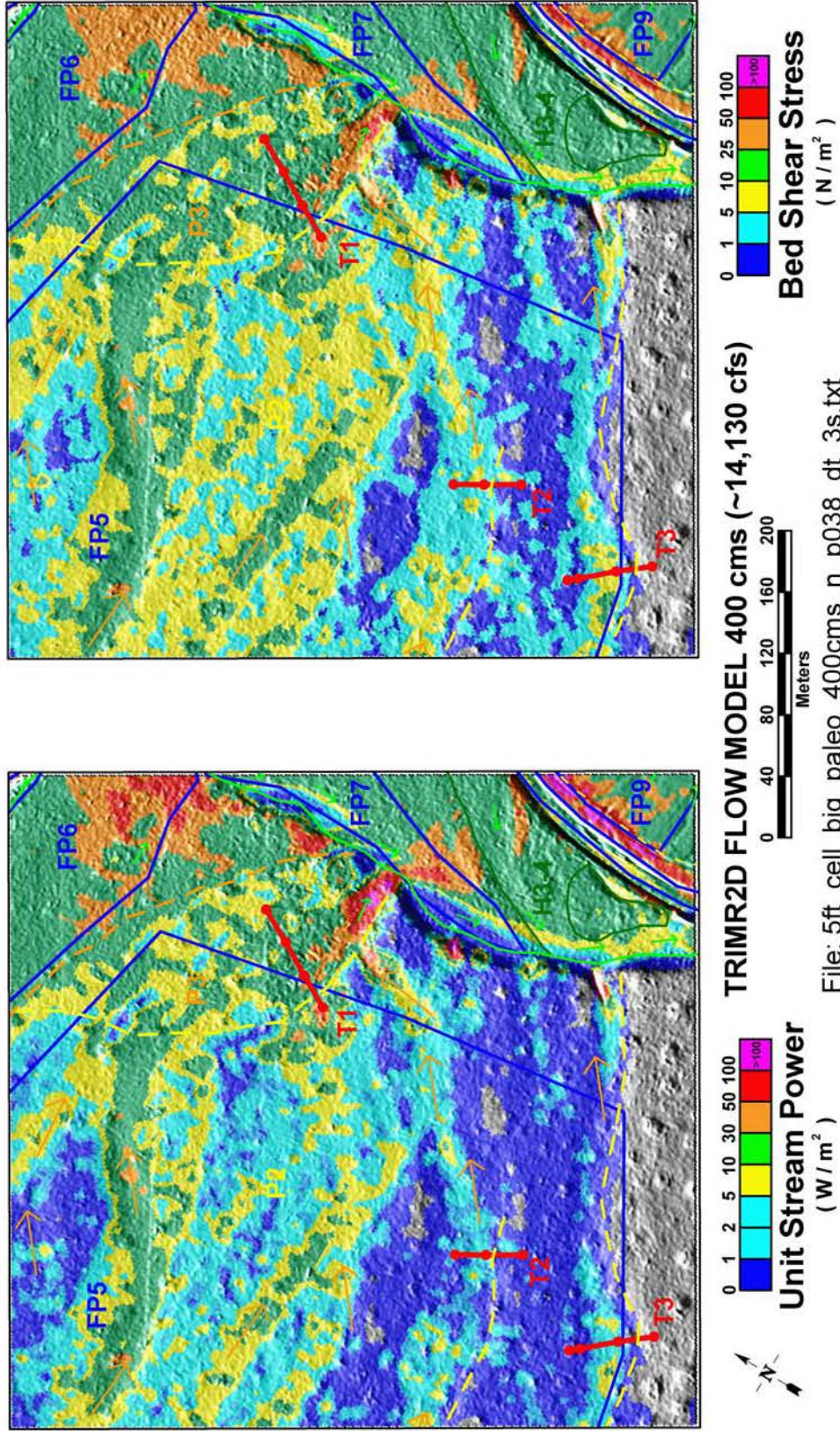


Figure 2-22 5-ft flow model results for 400 m<sup>3</sup>/s in the Big Loop study area. Base map symbology is from Figure 2-3 and Plate 2.

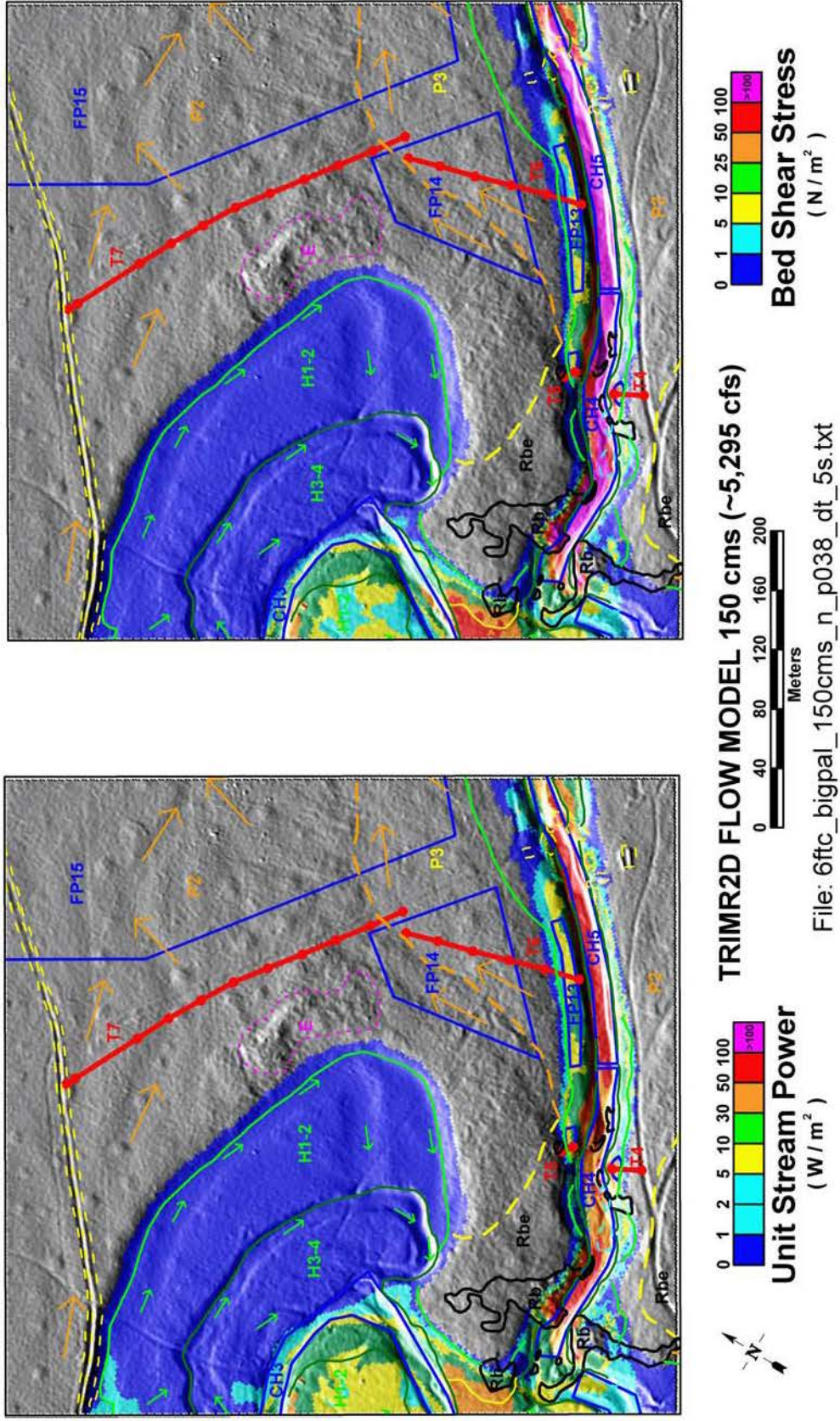


Figure 2-23 6-ft flow model results for  $150 m^3/s$  in the Saddle constriction study area. Base map symbology is from Figure 2-3 and Plate 2.



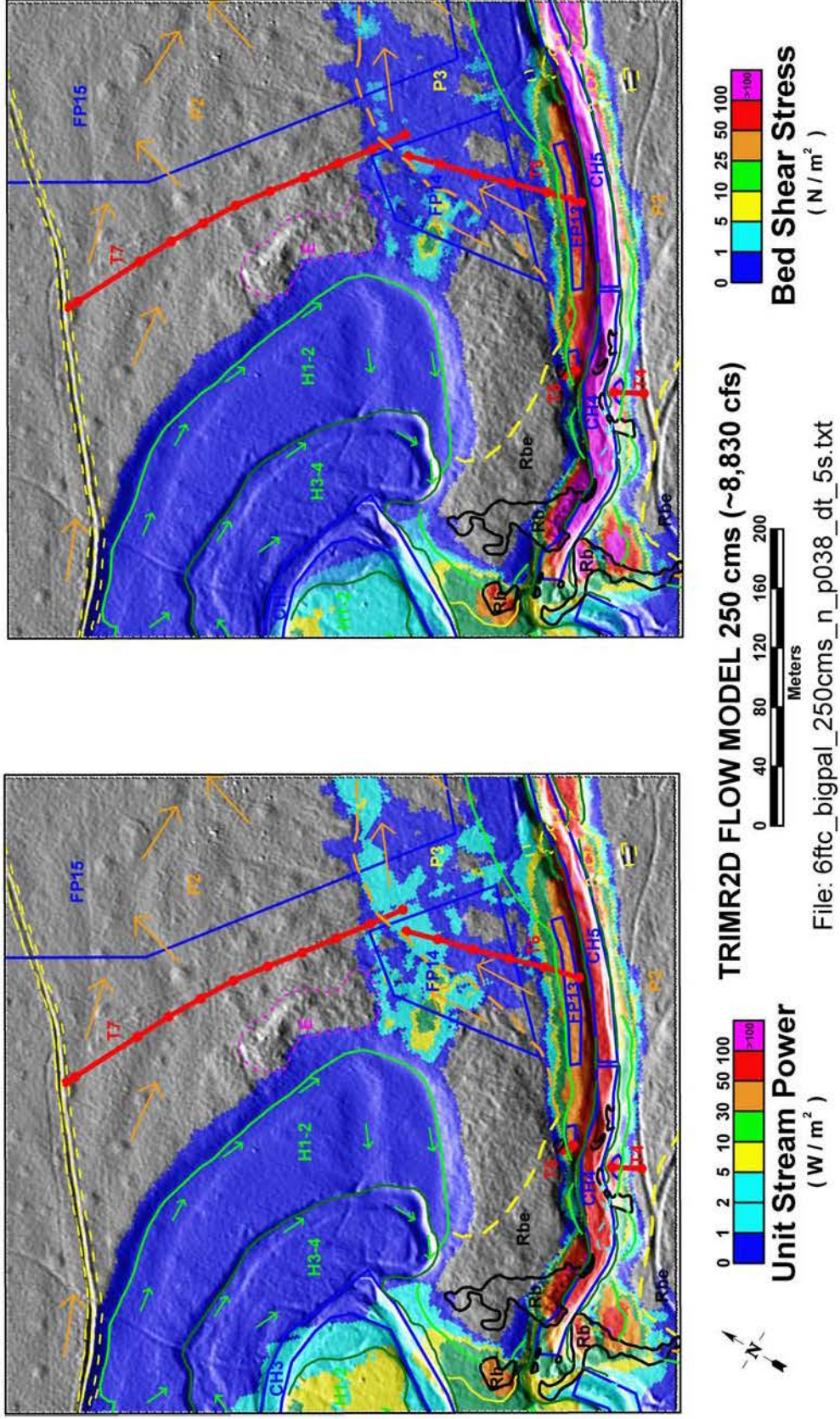


Figure 2-25 6-ft flow model results for 250 m<sup>3</sup>/s in the Saddle constriction study area. Base map symbology is from Figure 2-3 and Plate 2.

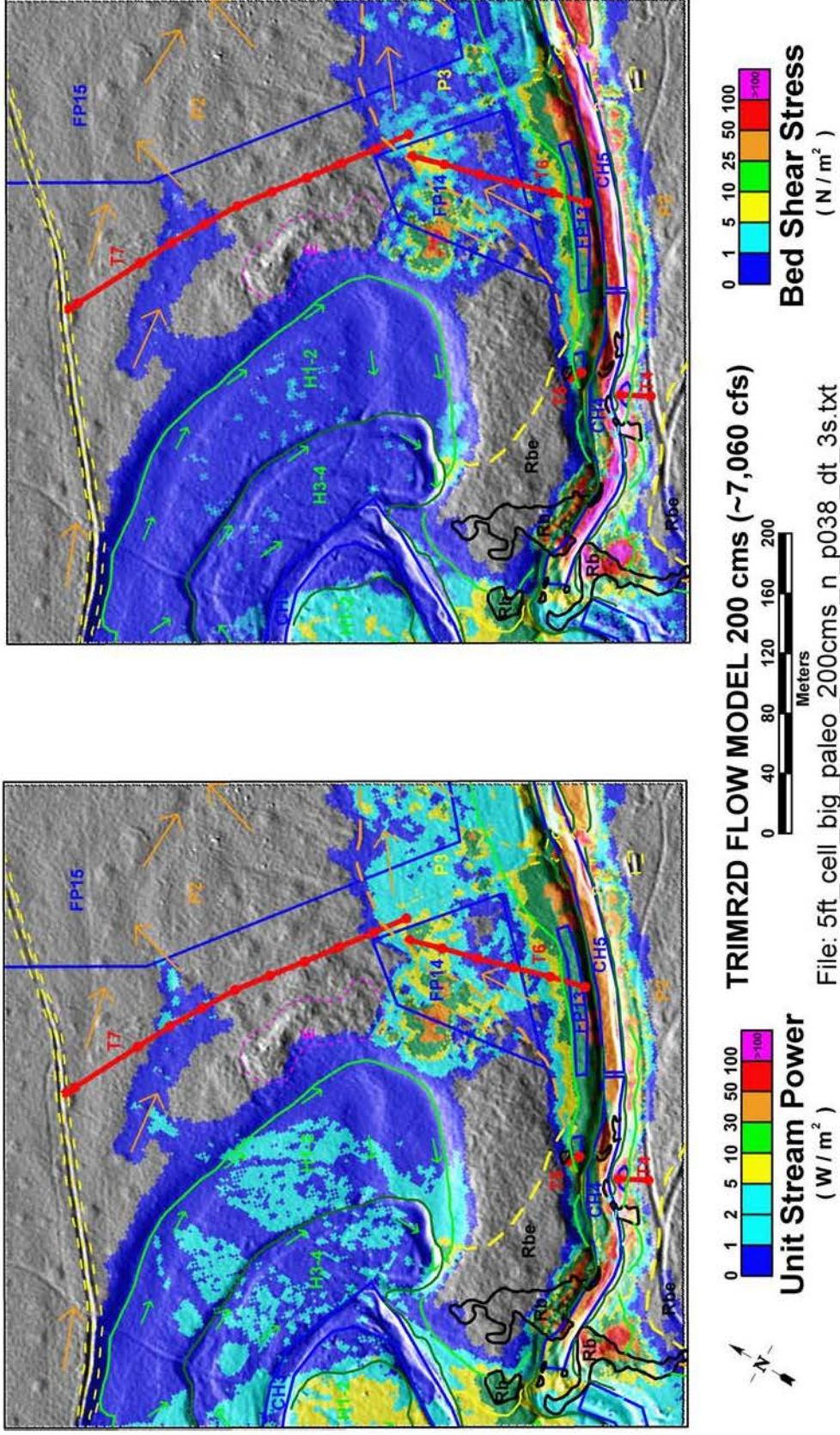


Figure 2-26 5-ft flow model results for 200 m<sup>3</sup>/s in the Saddle constriction study area. Base map symbology is from Figure 2-3 and Plate 2.

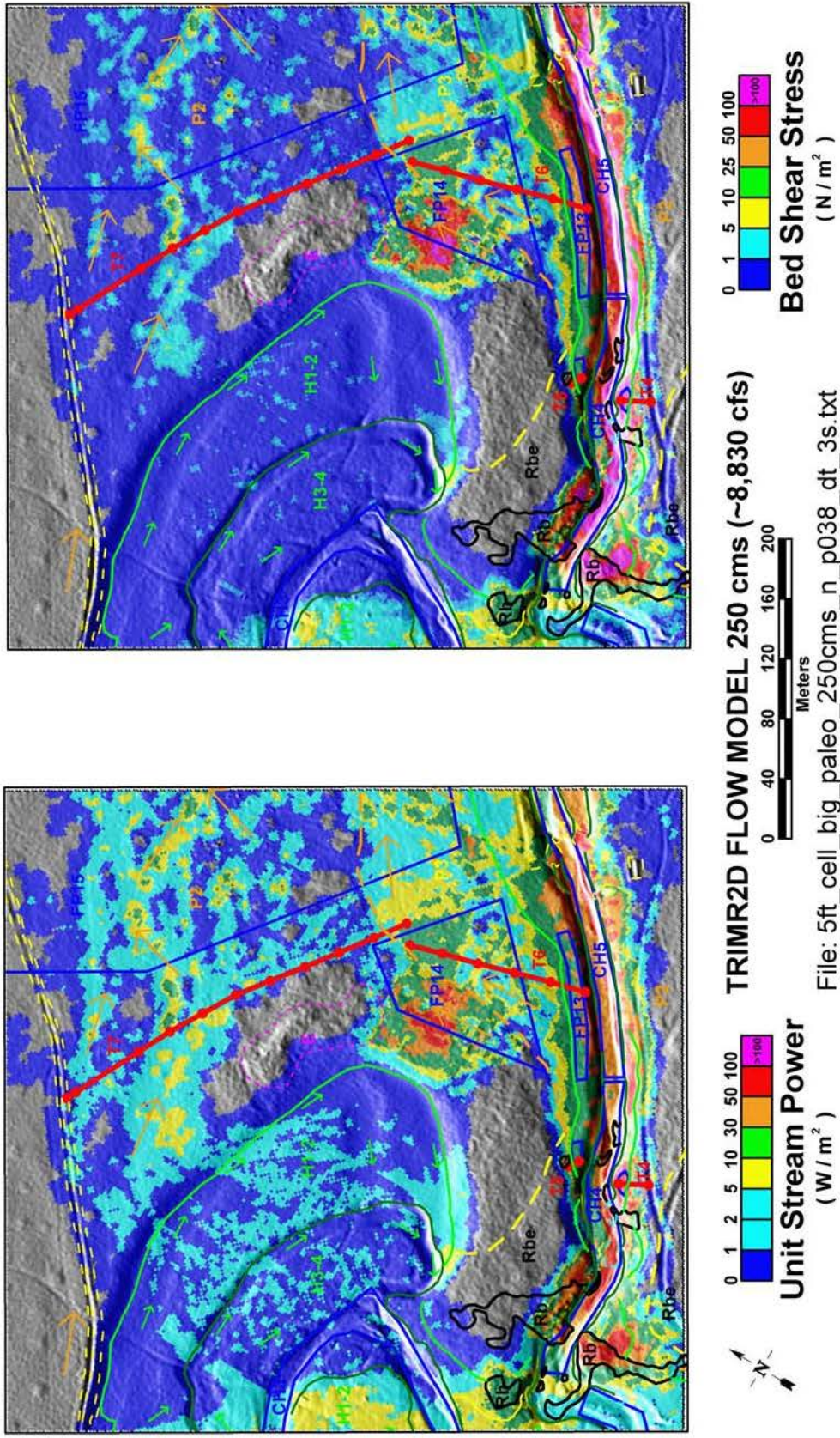


Figure 2-27 5-ft flow model results for 250 m<sup>3</sup>/s in the Saddle constriction study area. Base map symbology is from Figure 2-3 and Plate 2.

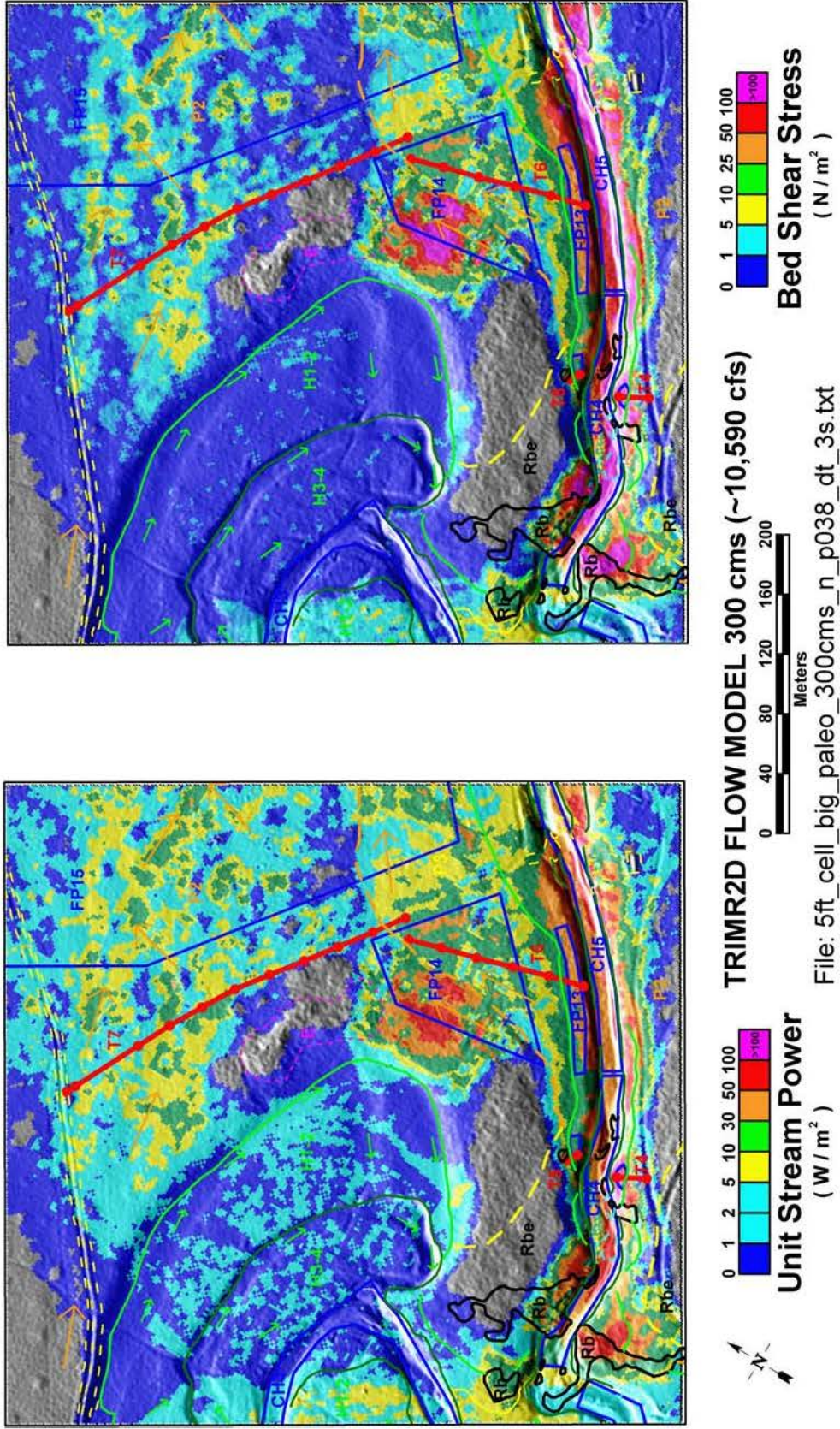


Figure 2-28 5-ft flow model results for 300 m<sup>3</sup>/s in the Saddle constriction study area. Base map symbology is from Figure 2-3 and Plate 2.

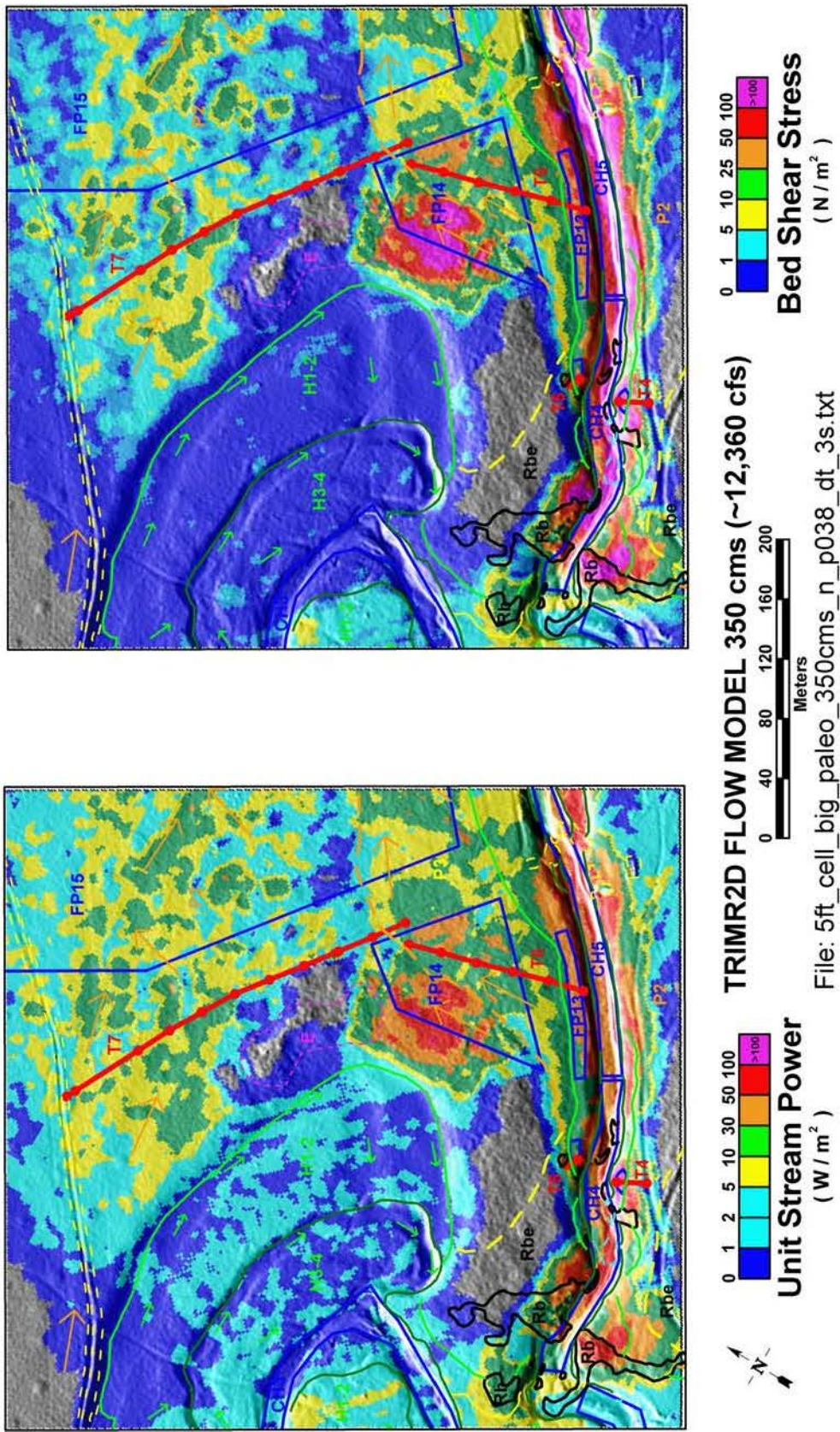


Figure 2-29 5-ft flow model results for  $350\text{ m}^3/\text{s}$  in the Saddle constriction study area. Base map symbology is from Figure 2-3 and Plate 2.

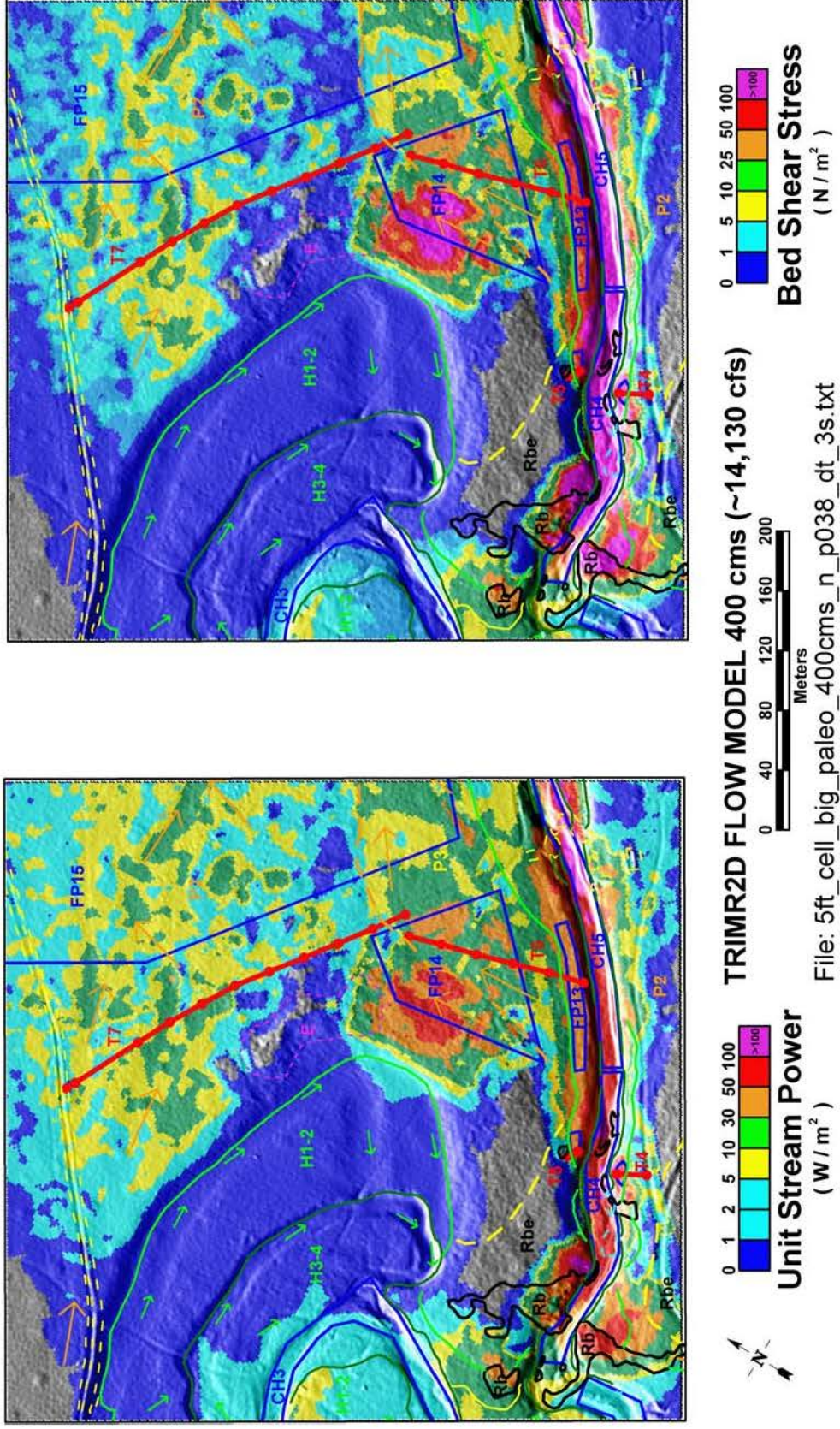


Figure 2-30 5-ft flow model results for 400 m<sup>3</sup>/s in the Saddle constriction study area. Base map symbology is from Figure 2-3 and Plate 2.

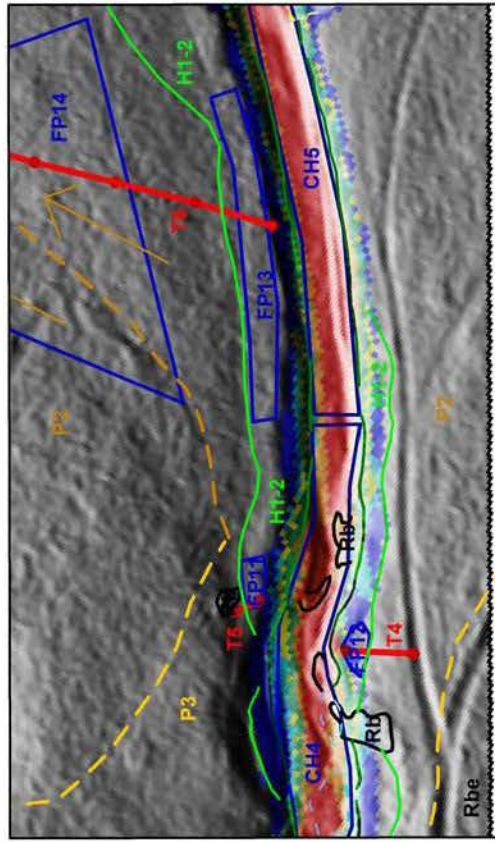
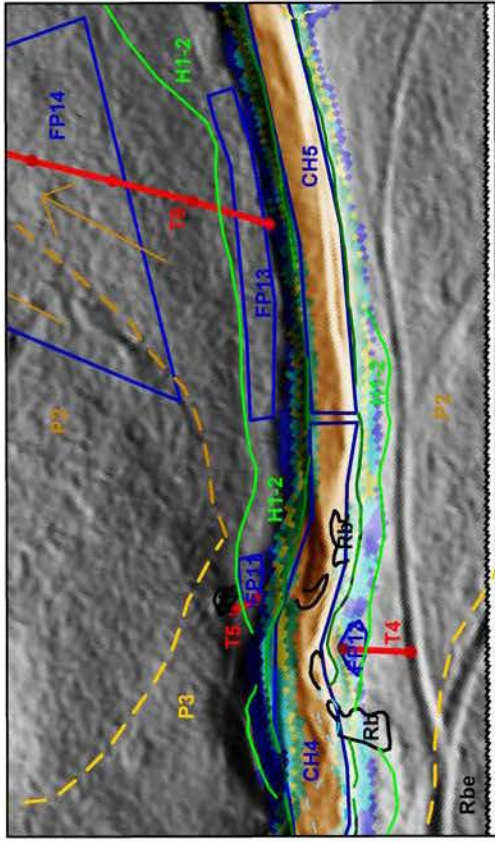


Figure 2-31 6-ft flow model results for 70 m<sup>3</sup>/s in the T4/T5/T6 study area. Base map symbology is from Figure 2-3 and Plate 2.

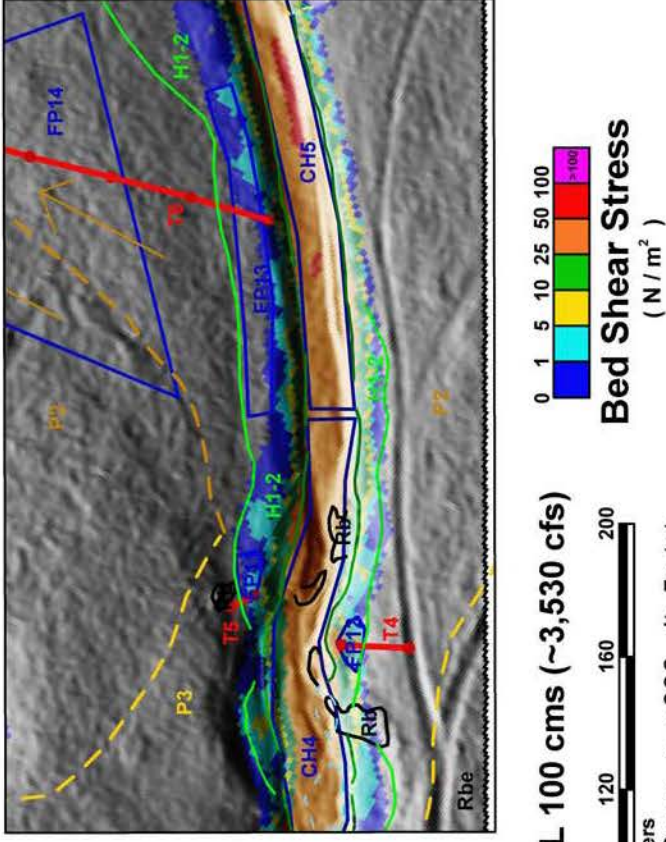
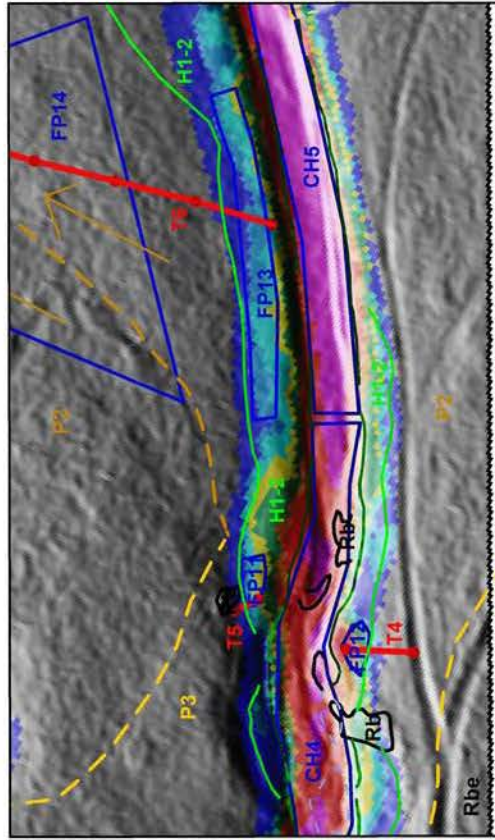
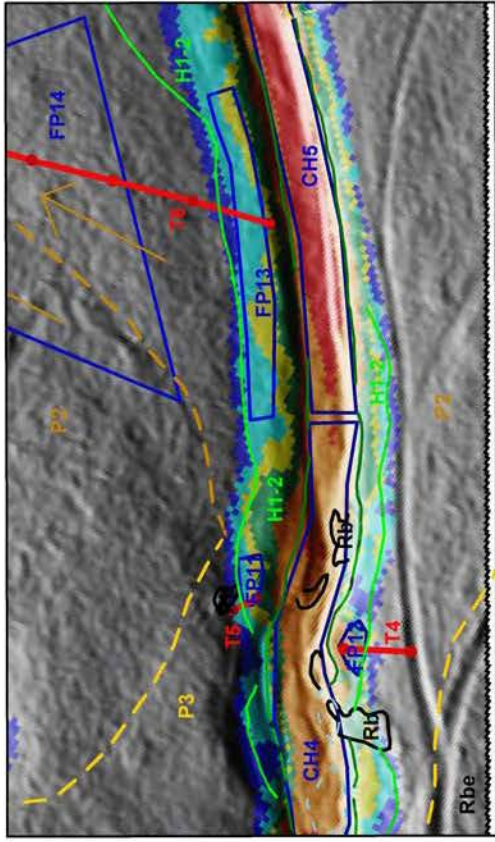


Figure 2-32 6-ft flow model results for 100 m<sup>3</sup>/s in the T4/T5/T6 study area. Base map symbology is from Figure 2-3 and Plate 2.



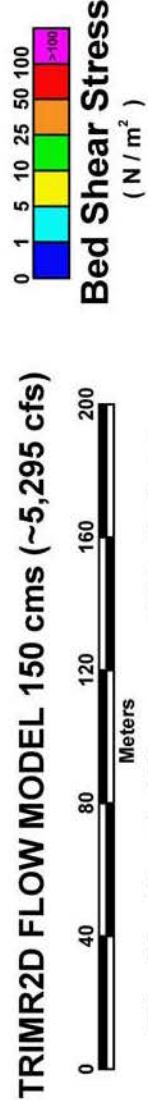
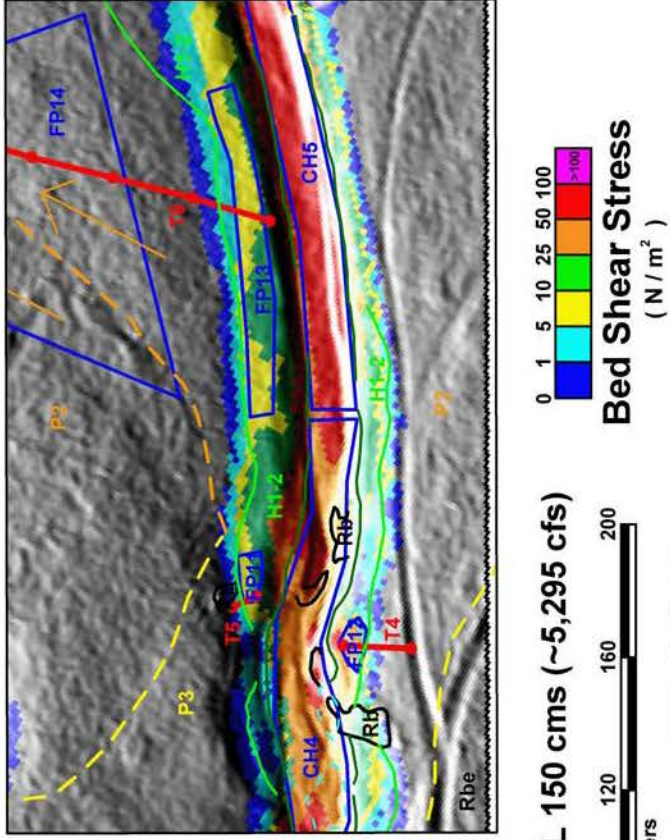
**TRIMR2D FLOW MODEL 130 cms (~4,590 cfs)**

Meters

0 40 80 120 160 200

File: 6ftc\_big\_pal\_130cms\_n\_p038\_dt\_5s.txt

Figure 2-33 6-ft flow model results for  $130\text{ m}^3/\text{s}$  in the T4/T5/T6 study area. Base map symbology is from Figure 2-3 and Plate 2.



File: 6ftc\_bigpal\_150cms\_n\_p038\_dt\_5s.txt

**TRIMR2D FLOW MODEL 150 cms (~5,295 cfs)**

Figure 2-34 6-ft flow model results for  $150 \text{ m}^3/\text{s}$  in the T4/T5/T6 study area. Base map symbology is from Figure 2-3 and Plate 2.

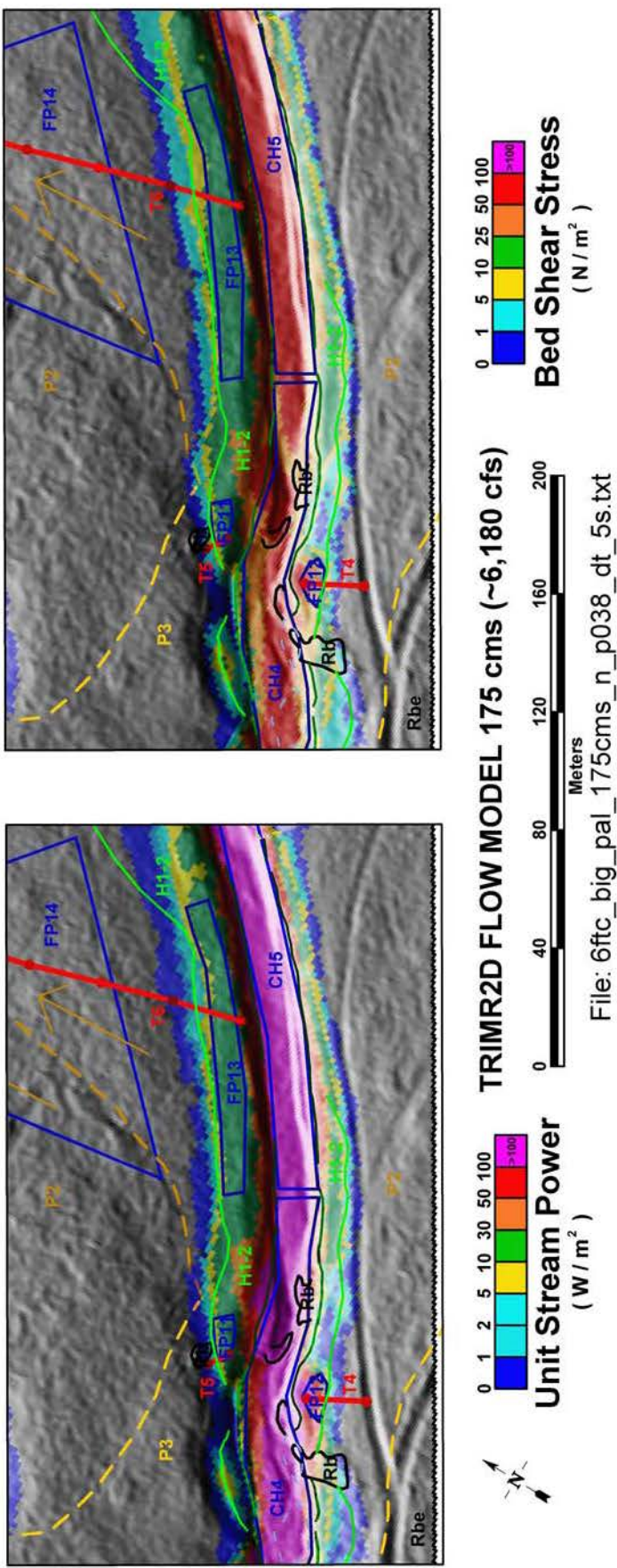
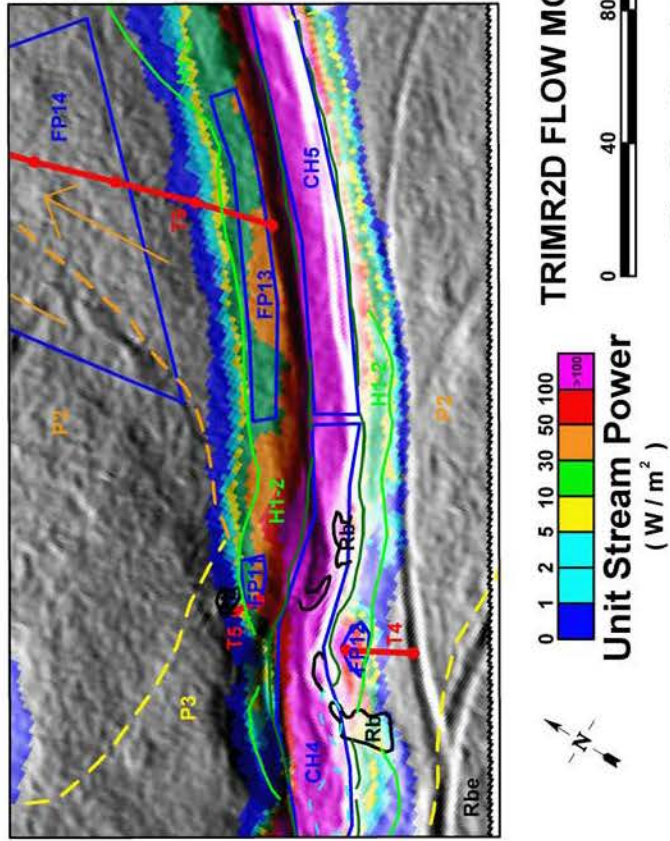
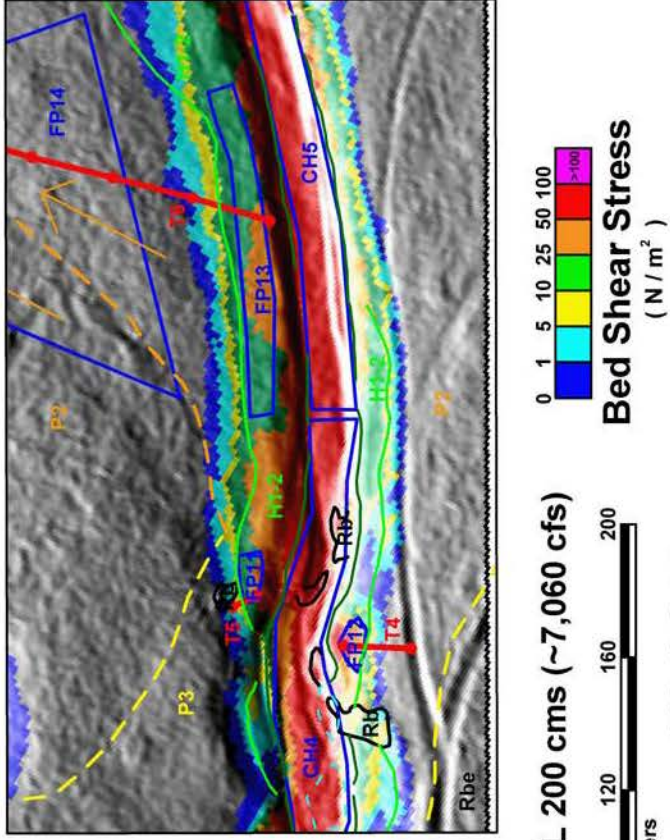
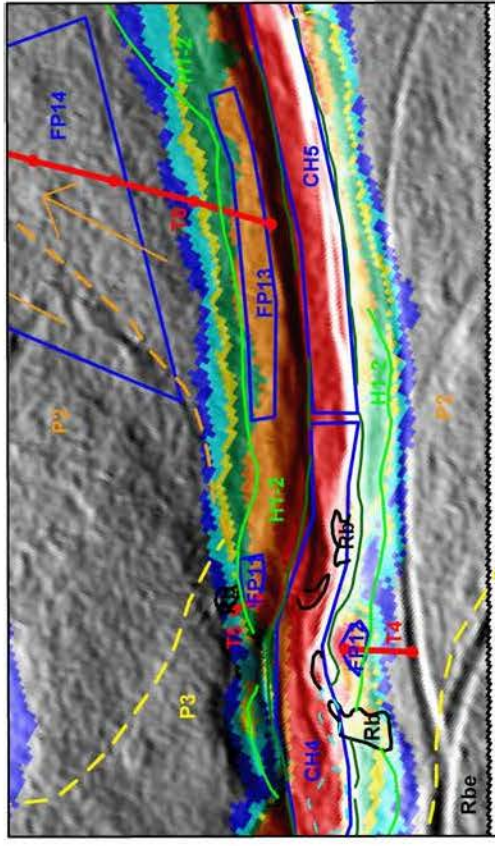


Figure 2-35 6-ft flow model results for  $175 \text{ m}^3/\text{s}$  in the T4/T5/T6 study area. Base map symbology is from Figure 2-3 and Plate 2.



**TRIMR2D FLOW MODEL 200 cms (~7,060 cfs)**

Figure 2-36 6-ft flow model results for  $200 \text{ m}^3/\text{s}$  in the T4/T5/T6 study area. Base map symbology is from Figure 2-3 and Plate 2.



**TRIMR2D FLOW MODEL 225 cms (~7,945 cfs)**



**Bed Shear Stress (N/m²)**



Figure 2-37 6-ft flow model results for 225 m<sup>3</sup>/s in the T4/T5/T6 study area. Base map symbology is from Figure 2-3 and Plate 2.

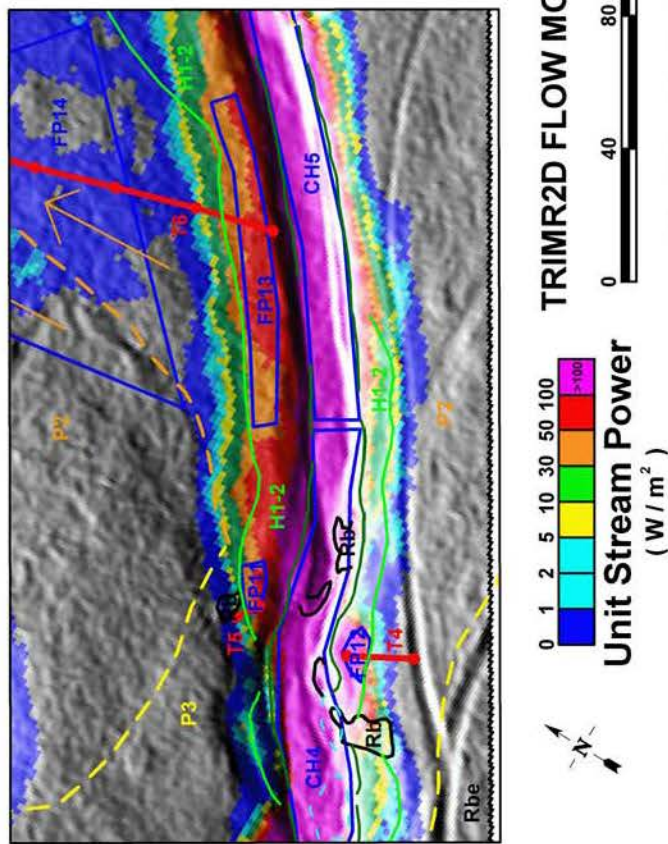
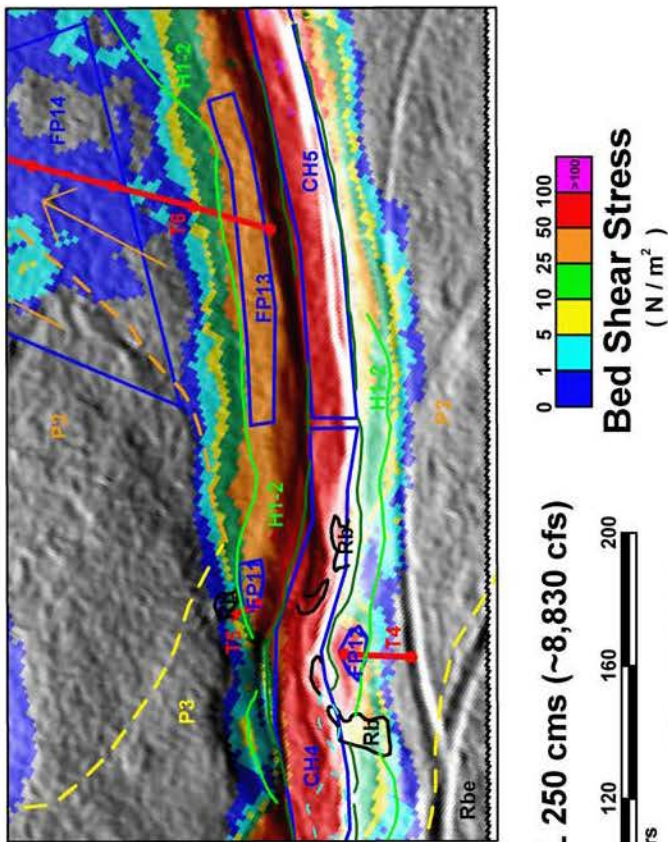


Figure 2-38 6-ft flow model results for  $250 \text{ m}^3/\text{s}$  in the T4/T5/T6 study area. Base map symbology is from Figure 2-3 and Plate 2.

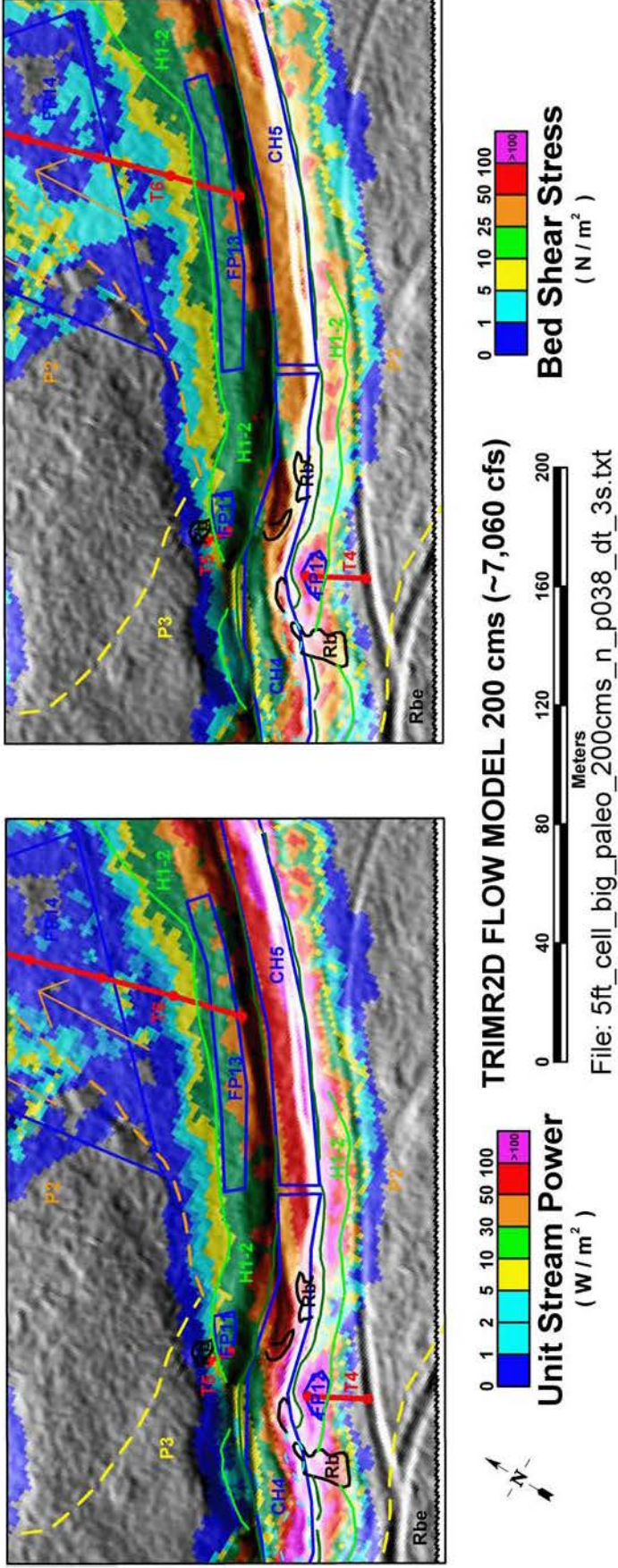


Figure 2-39 5-ft flow model results for  $200 \text{ m}^3/\text{s}$  in the T4/T5/T6 constriction study area. Base map symbology is from Figure 2-3 and Plate 2.

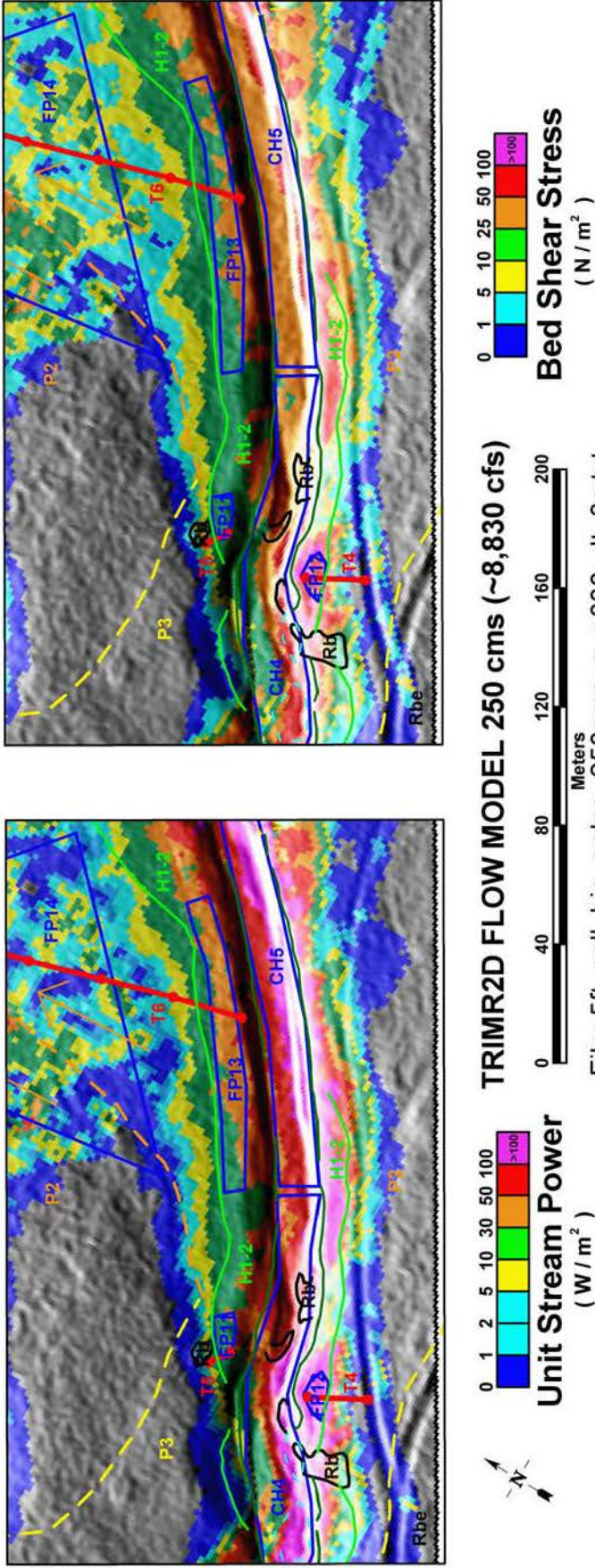


Figure 2-40 5-ft flow model results for  $250\text{ m}^3/\text{s}$  in the T4/T5/T6 constriction study area. Base map symbology is from Figure 2-3 and Plate 2.

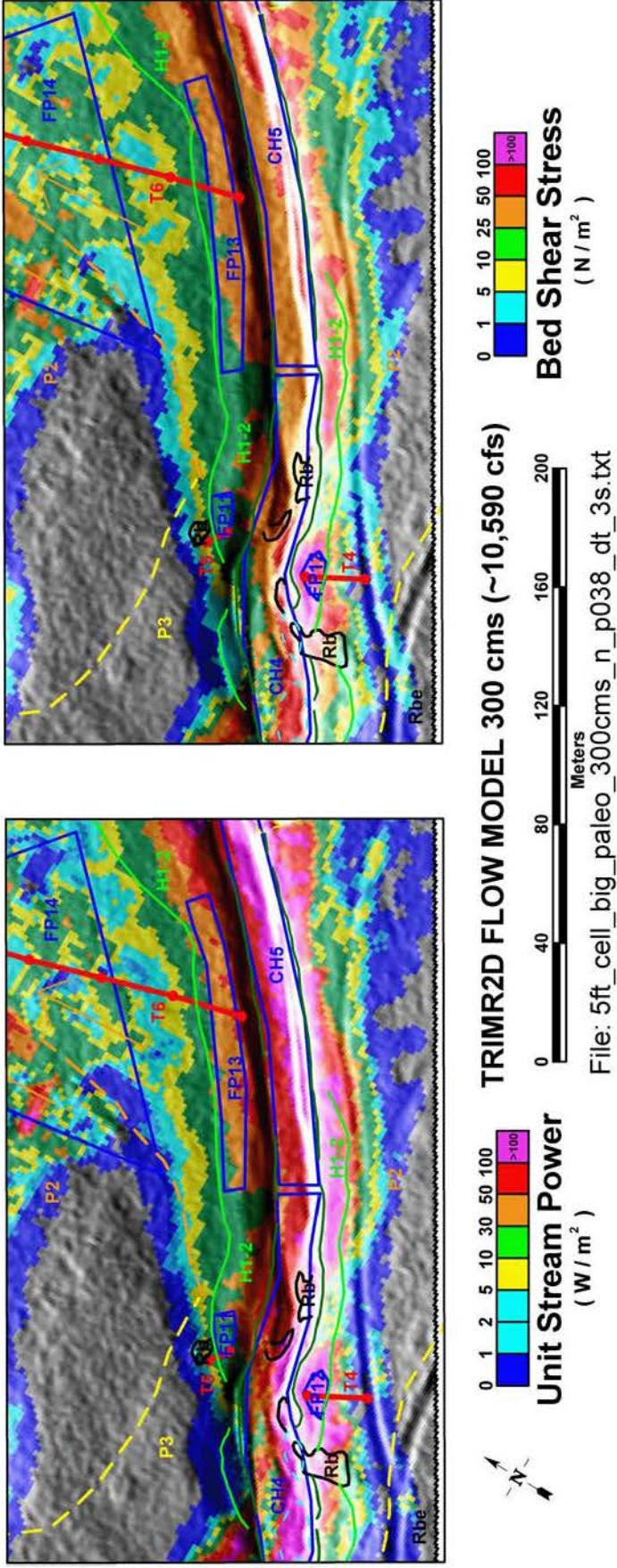


Figure 2-41 5-ft flow model results for  $300\text{ m}^3/\text{s}$  in the T4/T5/T6 constriction study area. Base map symbology is from Figure 2-3 and Plate 2.

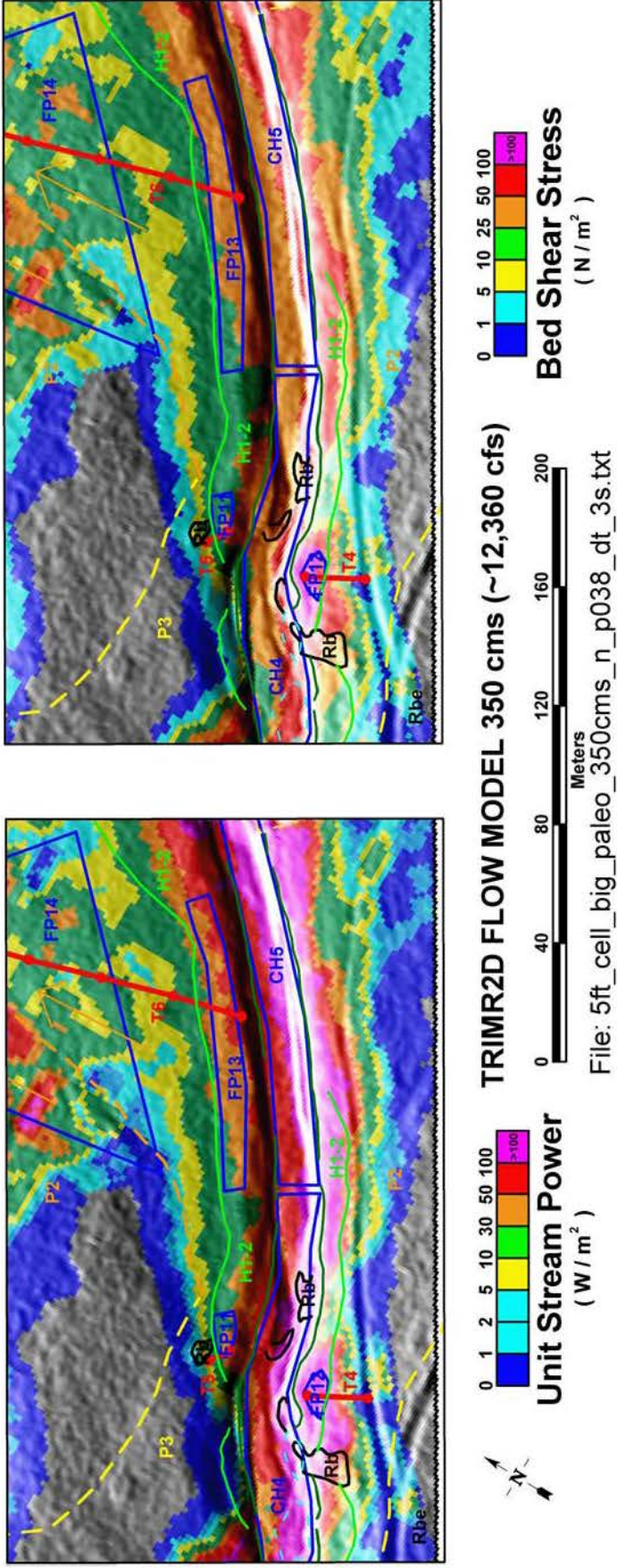


Figure 2-42 5-ft flow model results for  $350 m^3/s$  in the T4/T5/T6 constriction study area. Base map symbology is from Figure 2-3 and Plate 2.

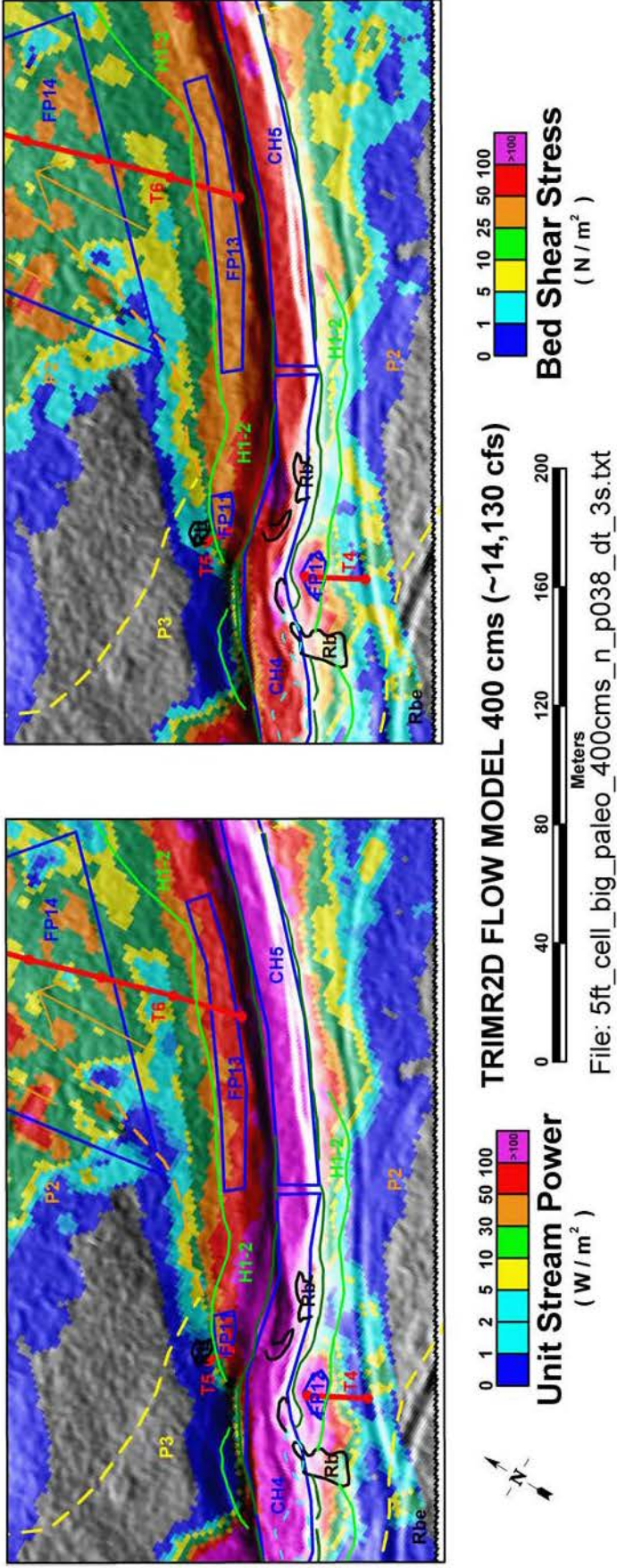
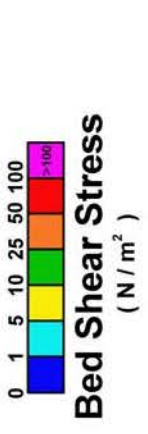
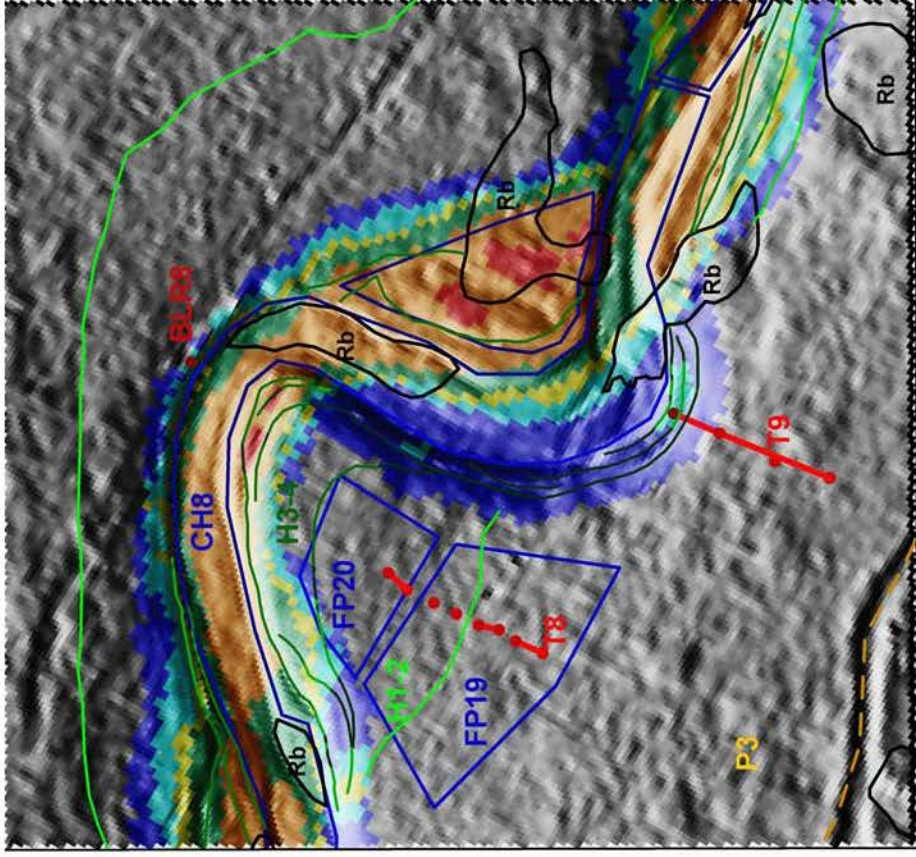


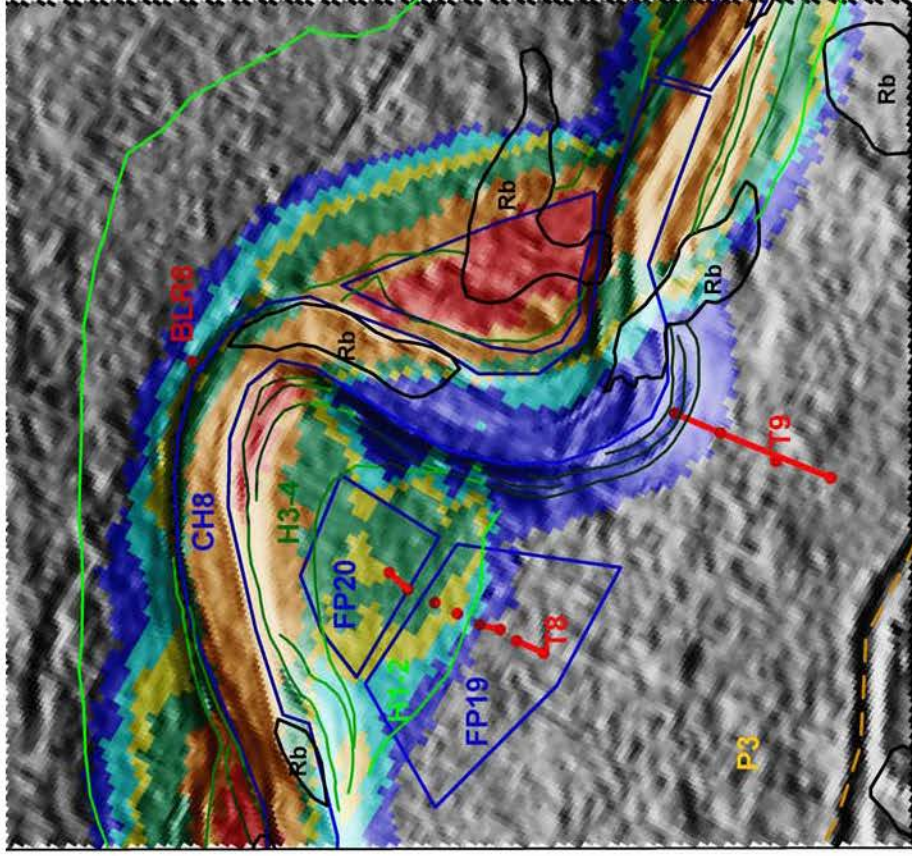
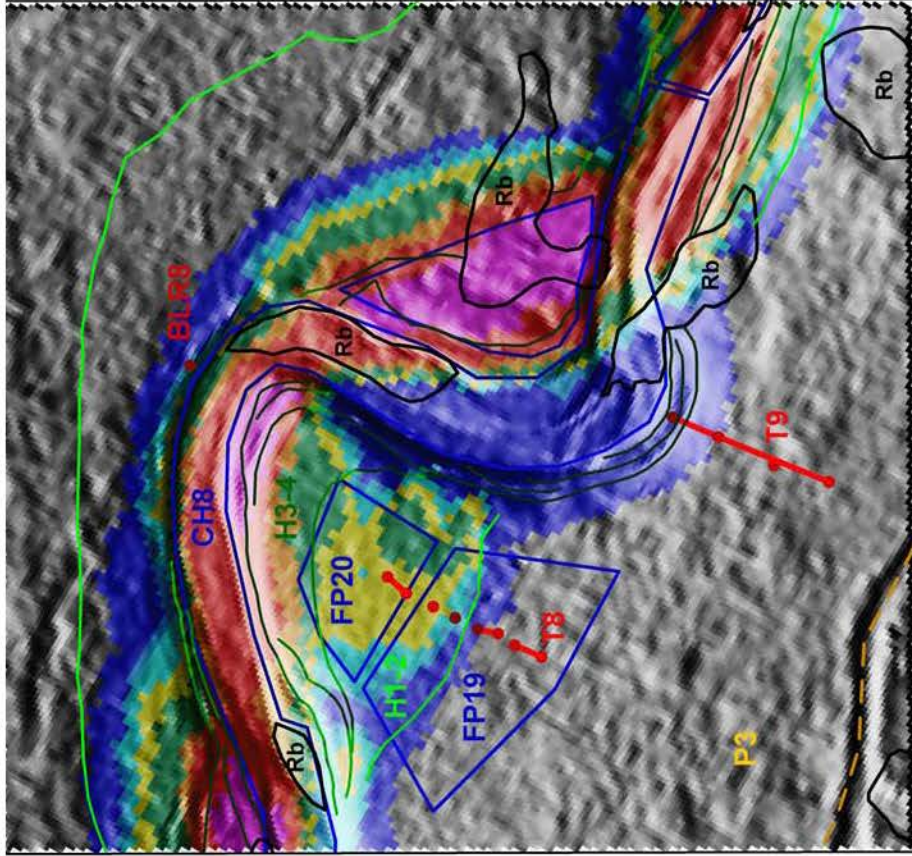
Figure 2-43 5-ft flow model results for  $400\text{ m}^3/\text{s}$  in the T4/T5/T6 constriction study area. Base map symbology is from Figure 2-3 and Plate 2.



TRIMR2D FLOW MODEL 70 cms (~2470 cfs)

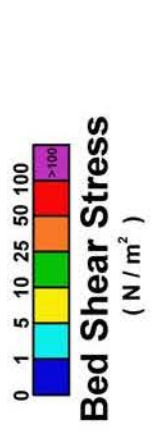
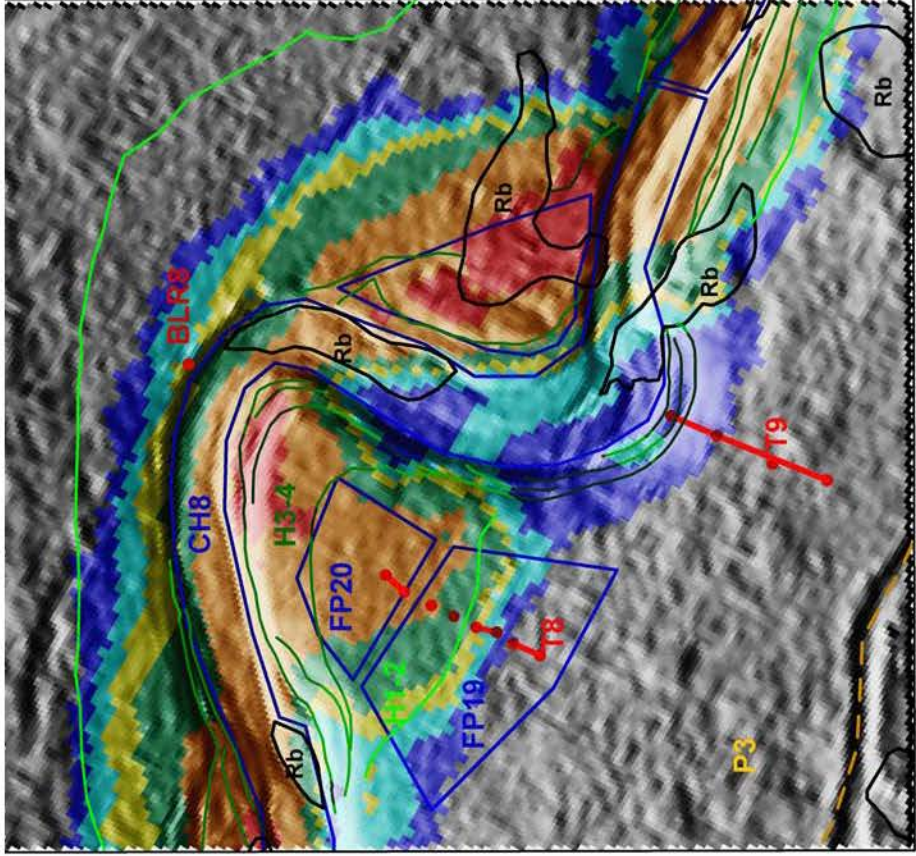
File: 6ftc\_cell\_big\_paleo\_70cms\_n\_p038\_dt\_5s.txt

Figure 2-44 6-ft flow model results for 70 m<sup>3</sup>/s in the BLR8 study area. Base map symbology is from Figure 2-3 and Plate 2.



**TRIMR2D FLOW MODEL 100 cms (~3530 cfs)**

Figure 2-45 6-ft flow model results for  $100\text{ m}^3/\text{s}$  in the BLR8 study area. Base map symbology is from Figure 2-3 and Plate 2.



TRIMR2D FLOW MODEL 130 cms (~4590 cfs)

File: 6ftc\_cell\_big\_paleo\_130cms\_n\_p038\_dt\_5s.txt

Figure 2-46 6-ft flow model results for 130 m<sup>3</sup>/s in the BLR8 study area. Base map symbology is from Figure 2-3 and Plate 2.

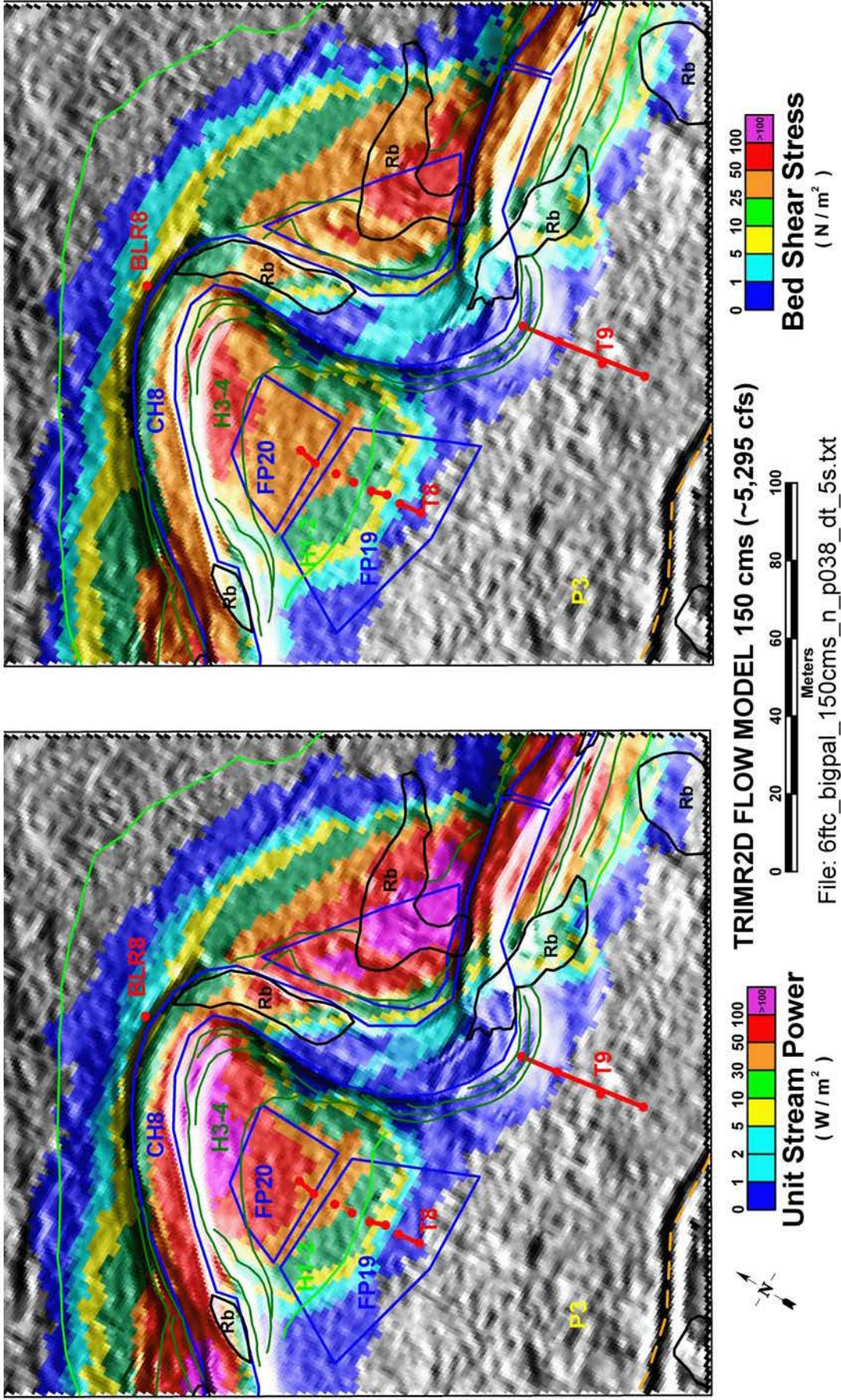


Figure 2-47 6-ft flow model results for 150 m<sup>3</sup>/s in the BLR8 study area. Base map symbology is from Figure 2-3 and Plate 2.

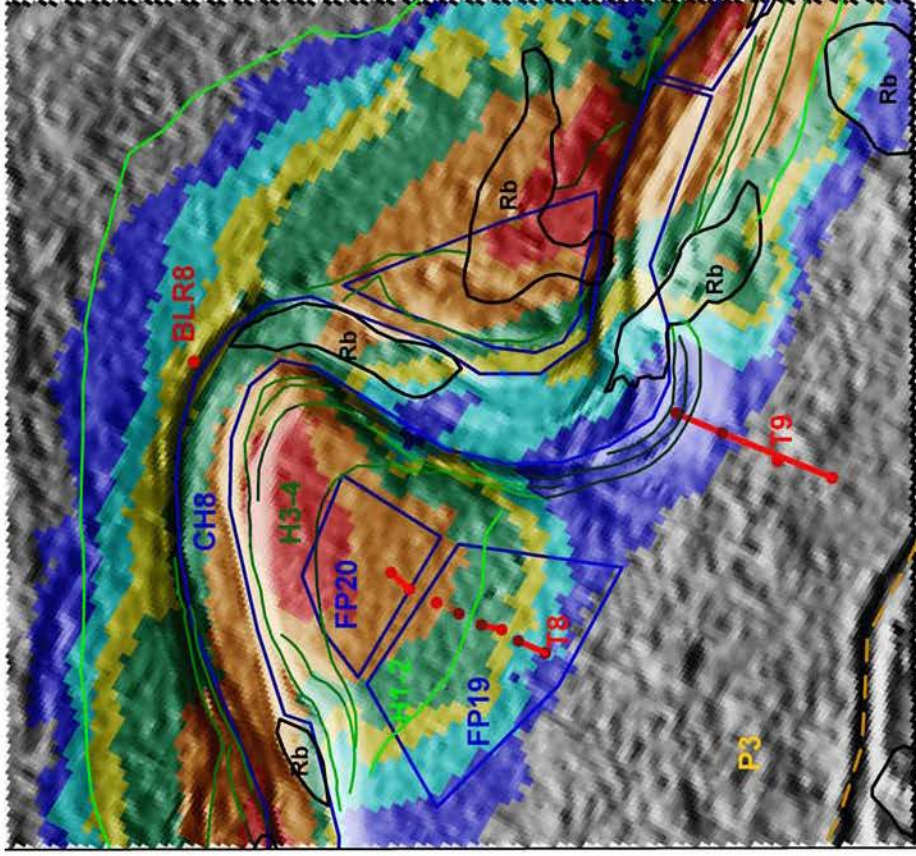
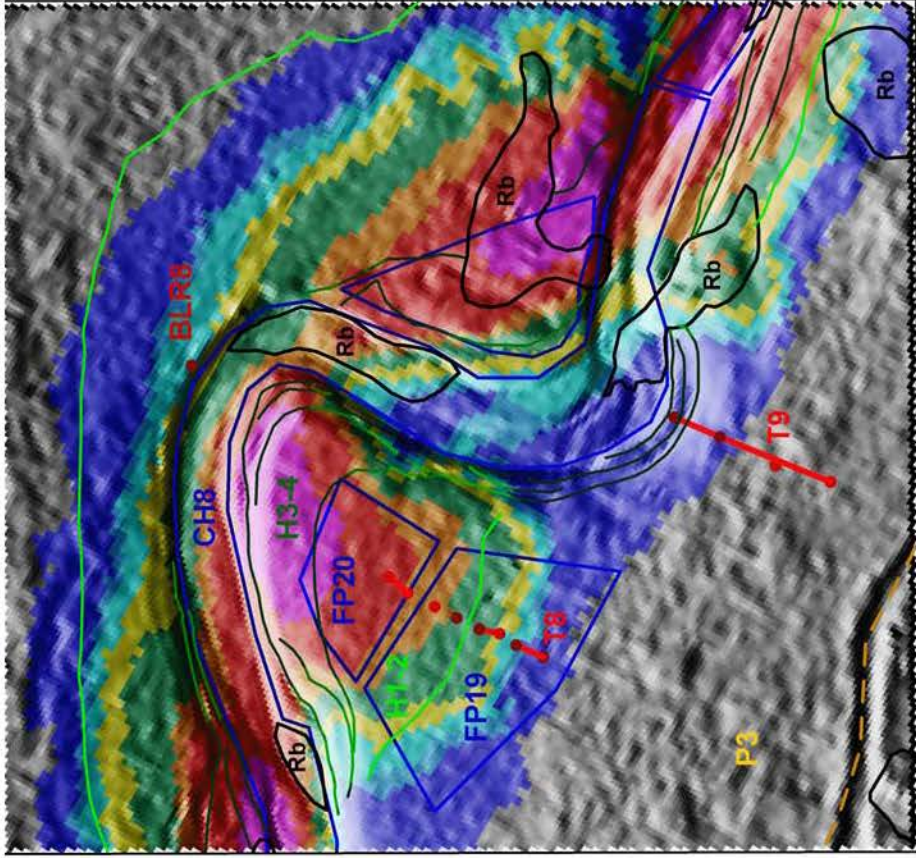


Figure 2-48 6-ft flow model results for 175 m<sup>3</sup>/s in the BLR8 study area. Base map symbology is from Figure 2-3 and Plate 2.

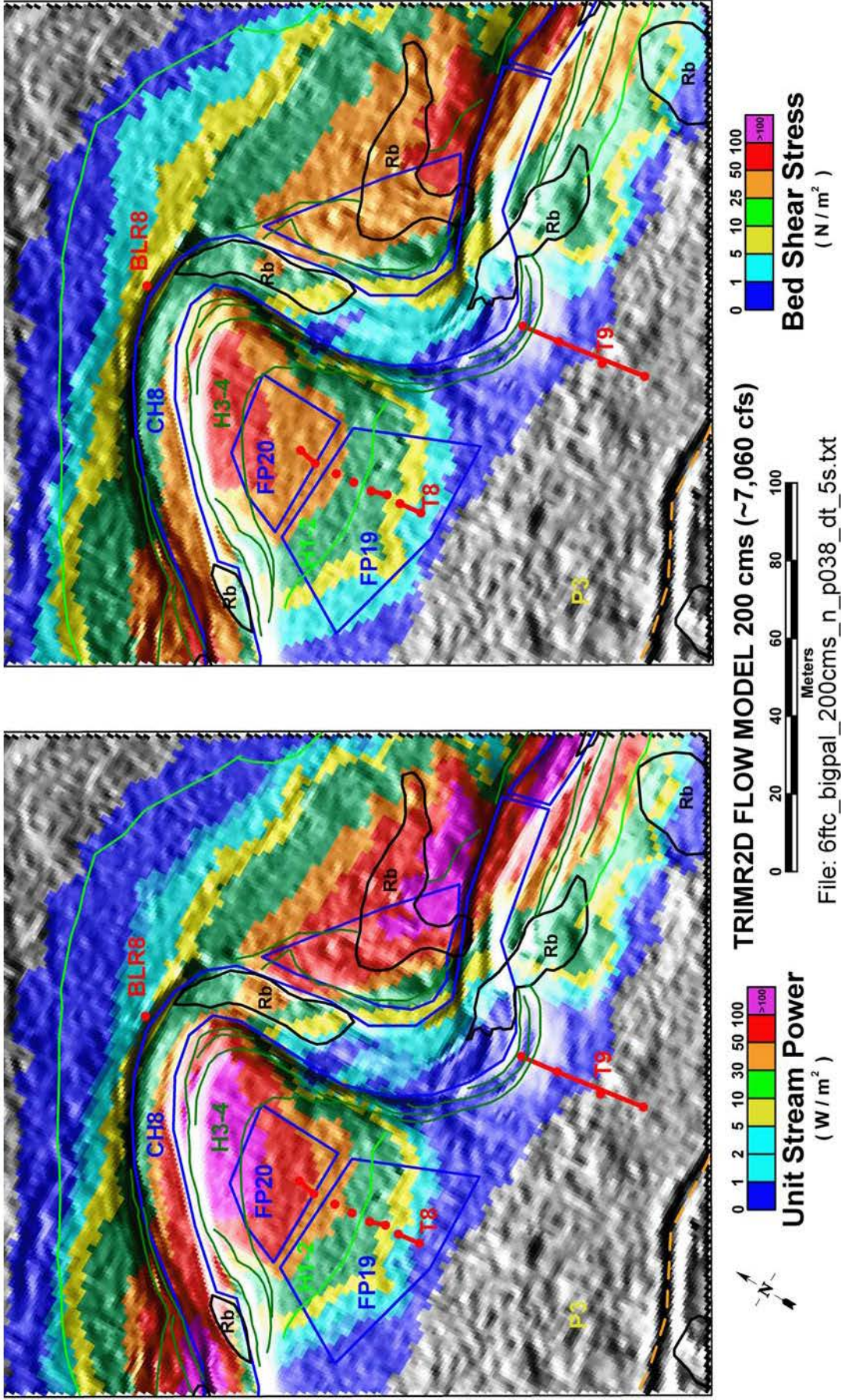


Figure 2-49 6-ft flow model results for 200 m<sup>3</sup>/s in the BLR8 study area. Base map symbology is from Figure 2-3 and Plate 2.

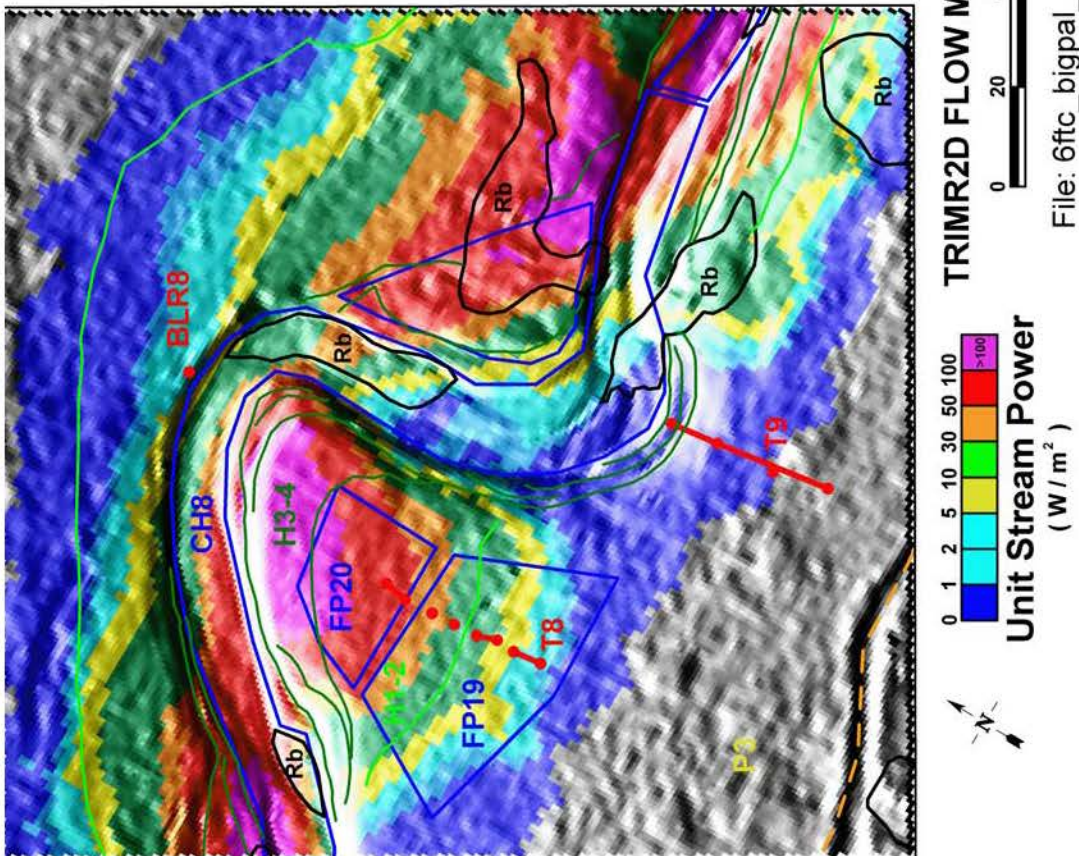
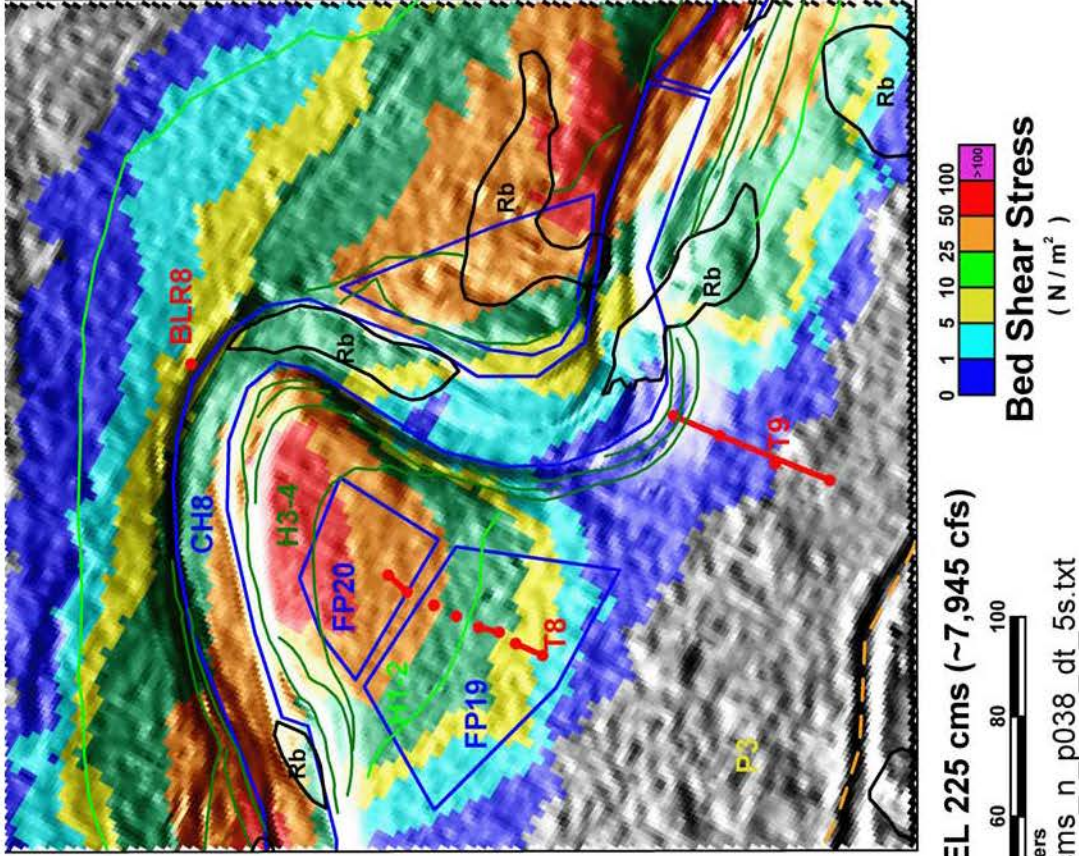


Figure 2-50 6-ft flow model results for 225 m<sup>3</sup>/s in the BLR8 study area. Base map symbology is from Figure 2-3 and Plate 2.

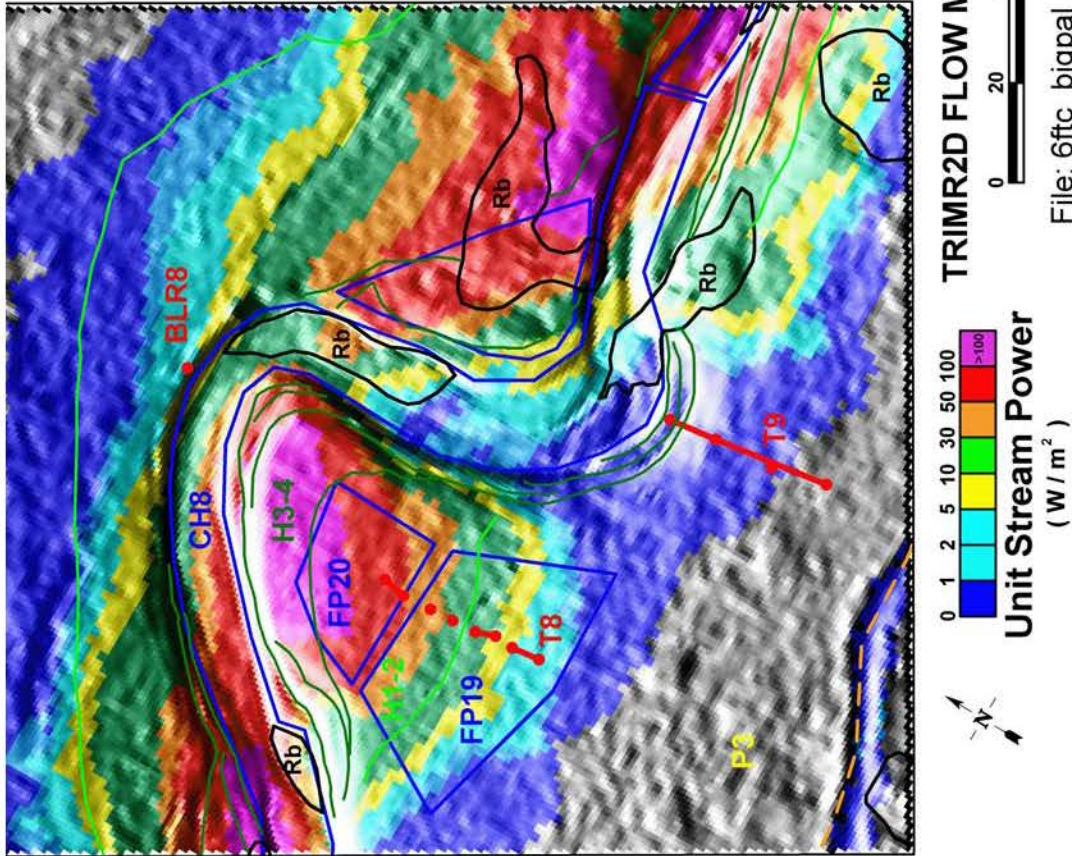
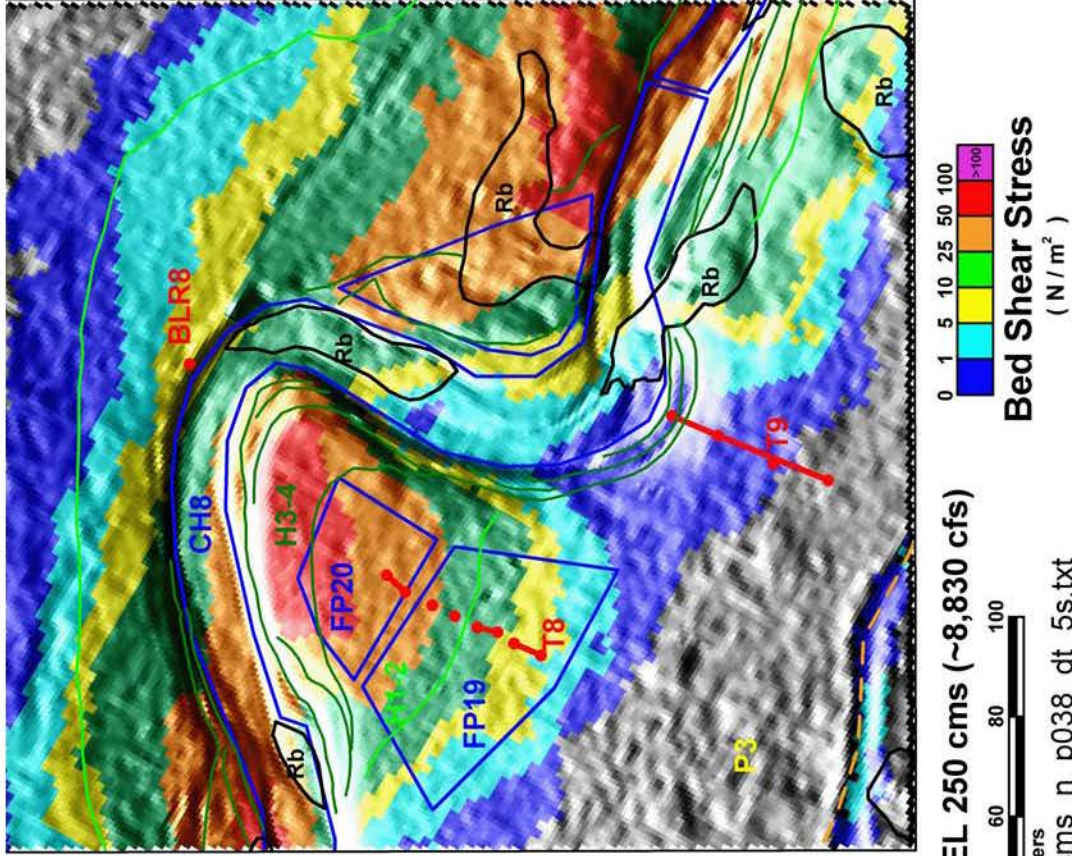
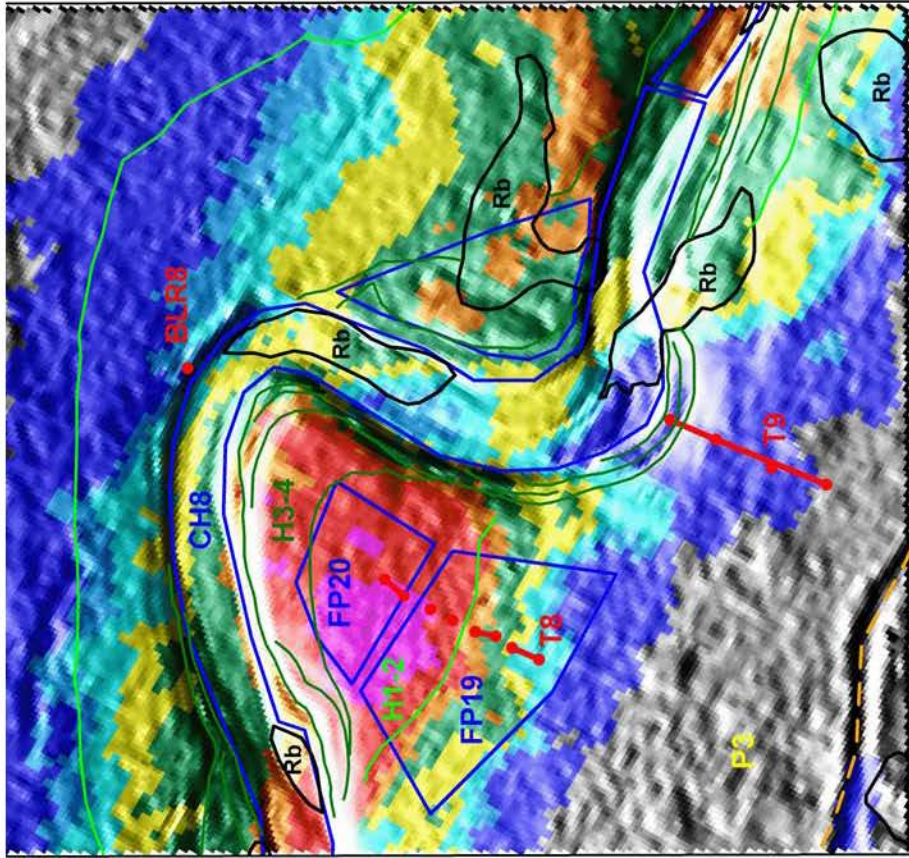
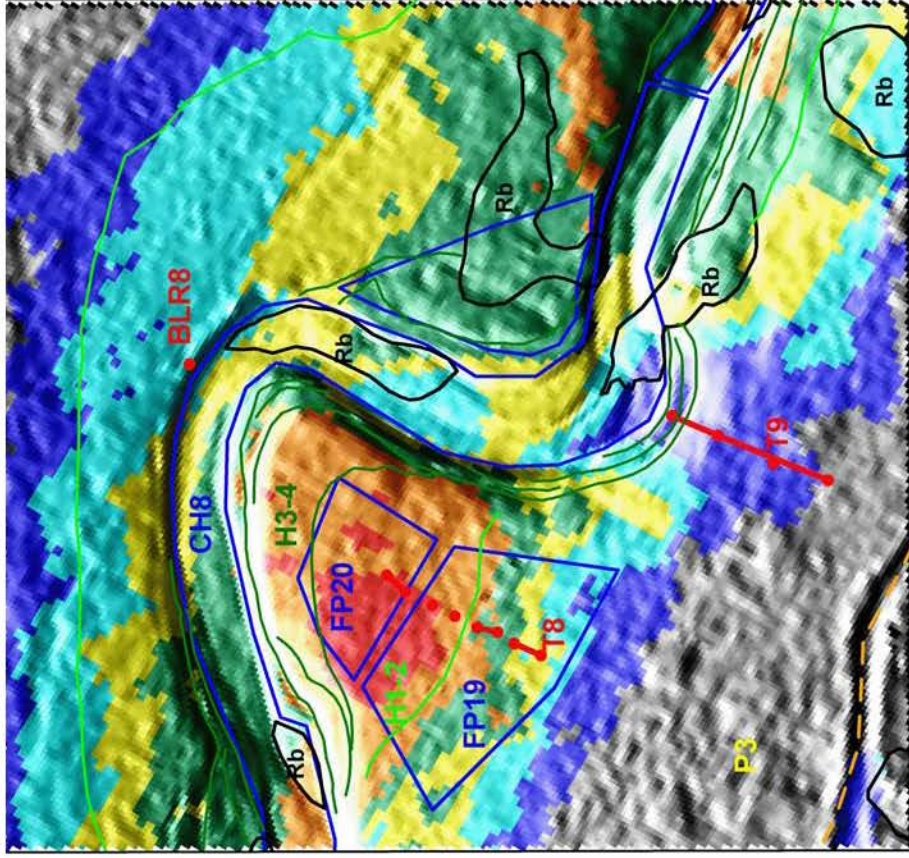


Figure 2-51 6-ft flow model results for 250 m<sup>3</sup>/s in the BLR8 study area. Base map symbology is from Figure 2-3 and Plate 2.



**Unit Stream Power**  
(  $W / m^2$  )



**Bed Shear Stress**  
(  $N / m^2$  )

**TRIMR2D FLOW MODEL 200 cms (~7,060 cfs)**  
 File: 5ft\_cell\_big\_paleo\_200cms\_n\_p038\_dt\_3s.txt

Figure 2-52 5-ft flow model results for  $200 \text{ m}^3/\text{s}$  in the BLR8 constriction study area. Base map symbology is from Figure 2-3 and Plate 2.

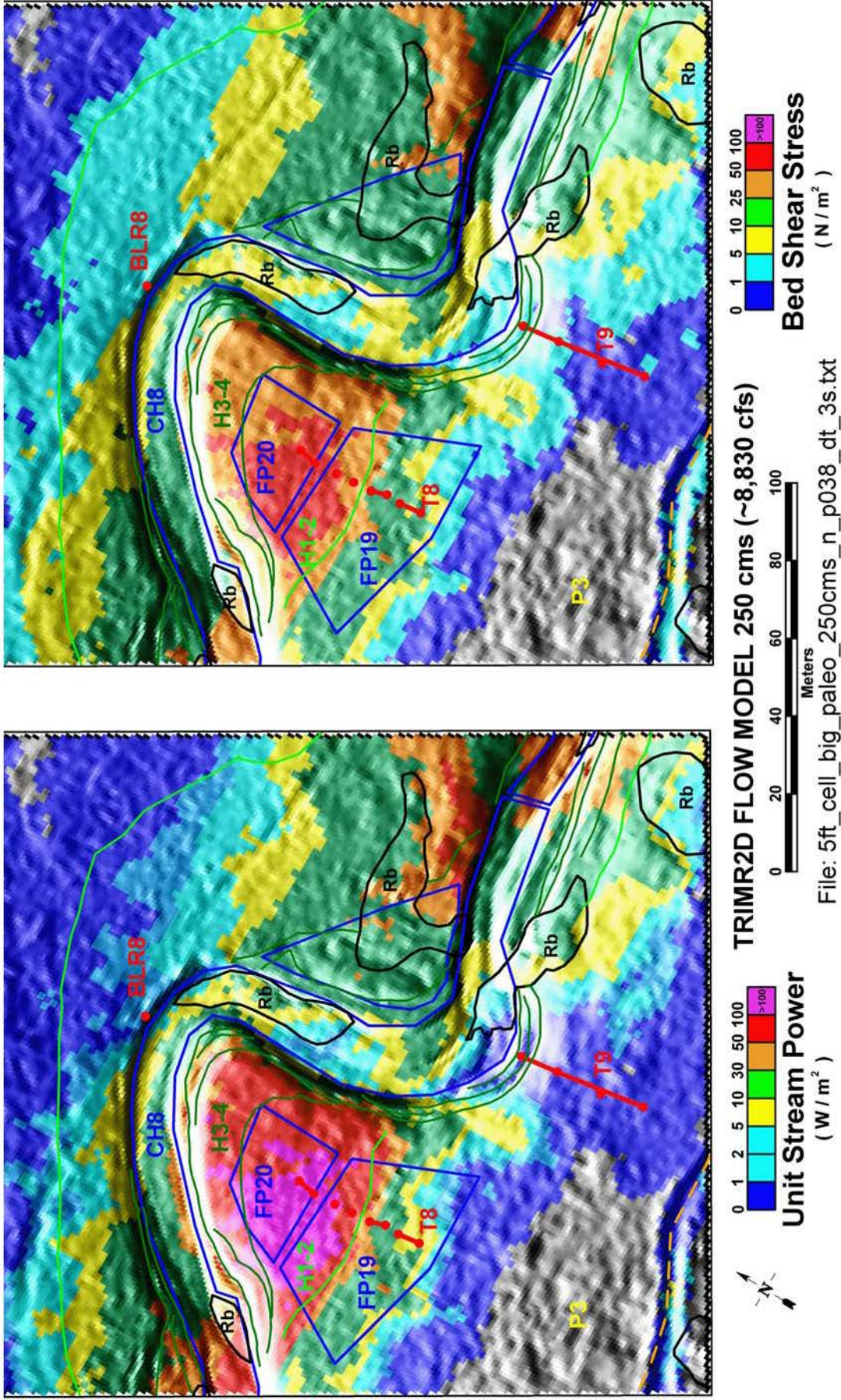
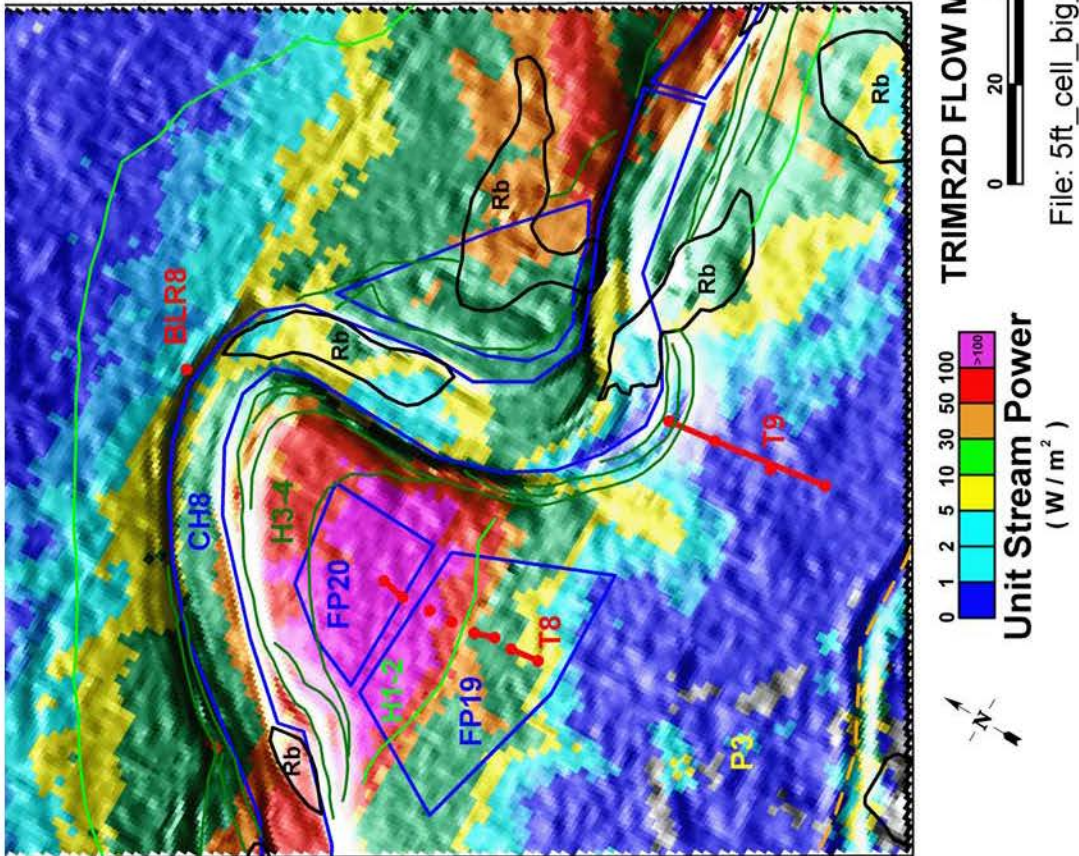
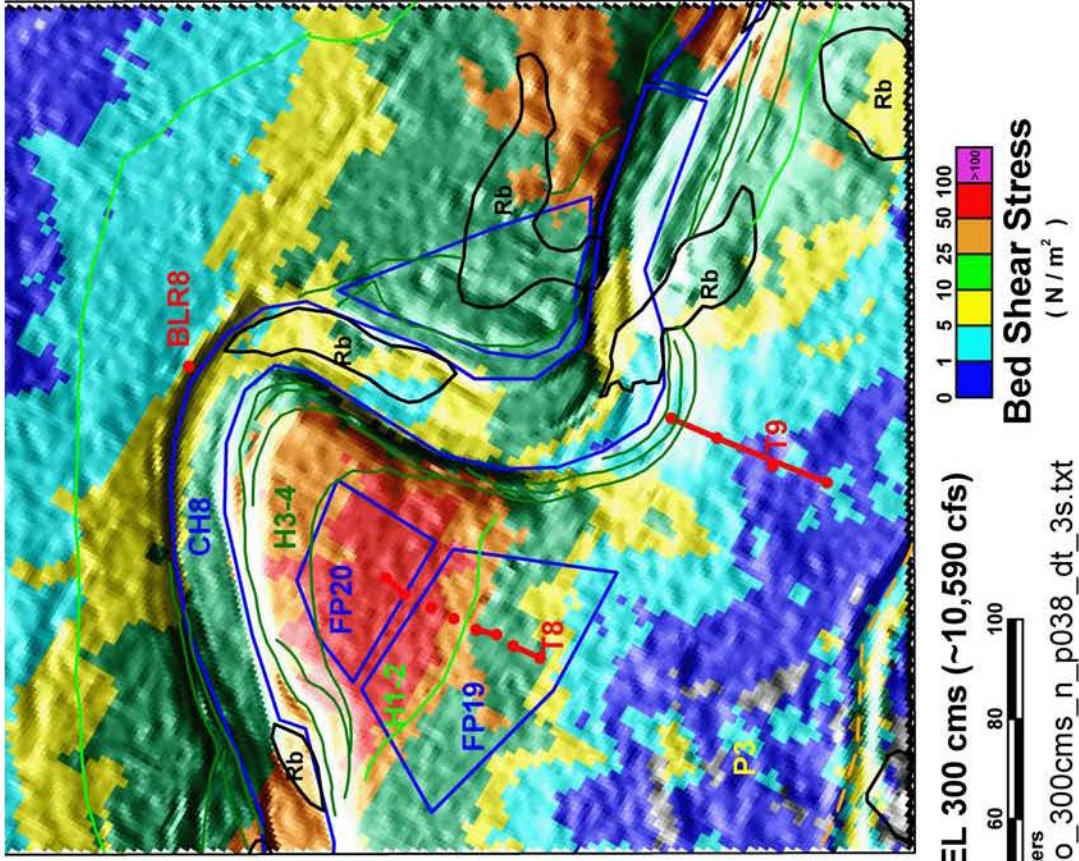


Figure 2-53 5-ft flow model results for 250 m<sup>3</sup>/s in the BLR8 constriction study area. Base map symbology is from Figure 2-3 and Plate 2.



**TRIMR2D FLOW MODEL 300 cms (~10,590 cfs)**

File: 5ft\_cell\_big\_paleo\_300cms\_n\_p038\_dt\_3s.txt

Figure 2-54 5-ft flow model results for  $300\text{ m}^3/\text{s}$  in the BLR8 constriction study area. Base map symbology is from Figure 2-3 and Plate 2.

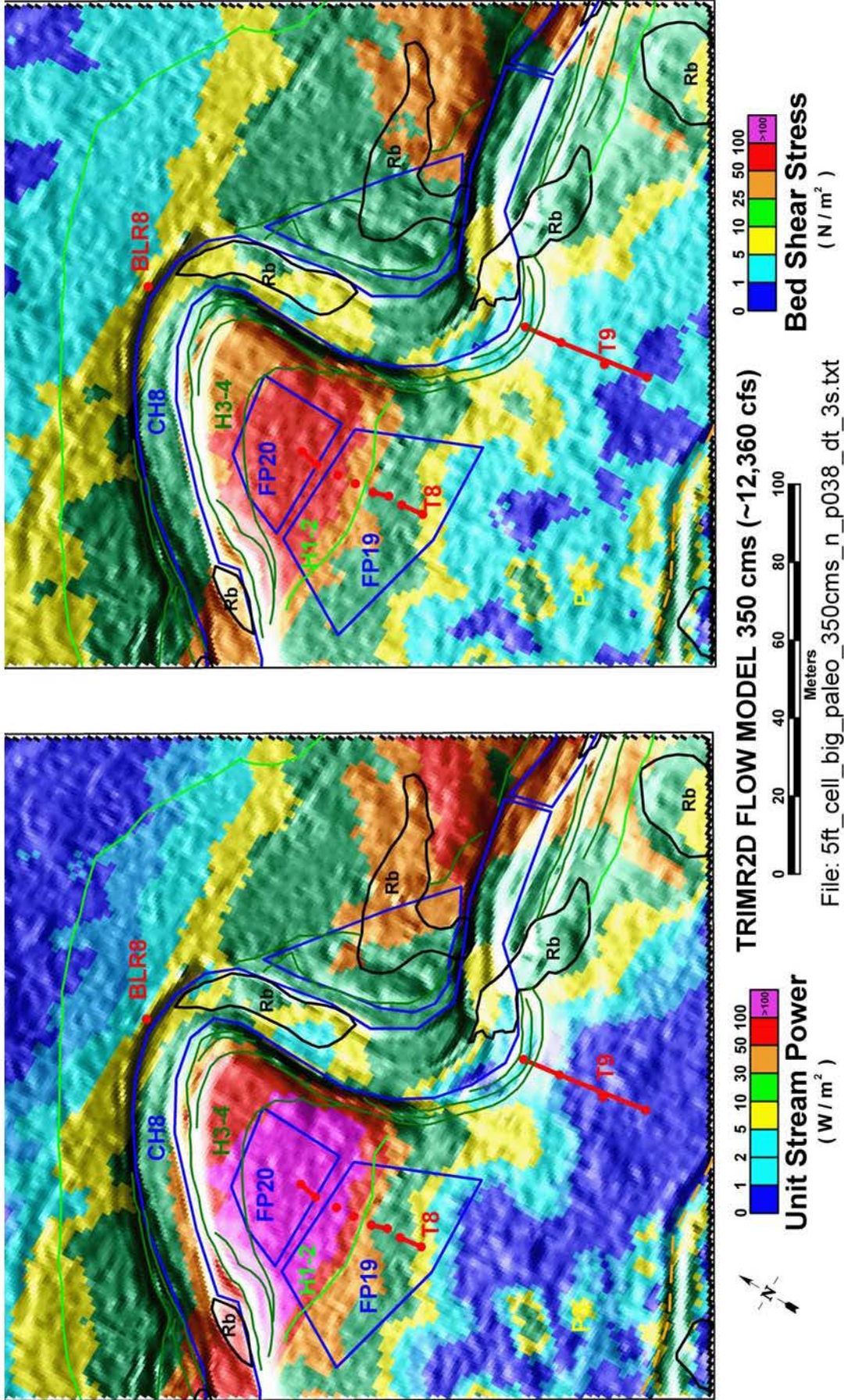


Figure 2-55 5-ft flow model results for 350 m<sup>3</sup>/s in the BLR8 constriction study area. Base map symbology is from Figure 2-3 and Plate 2.

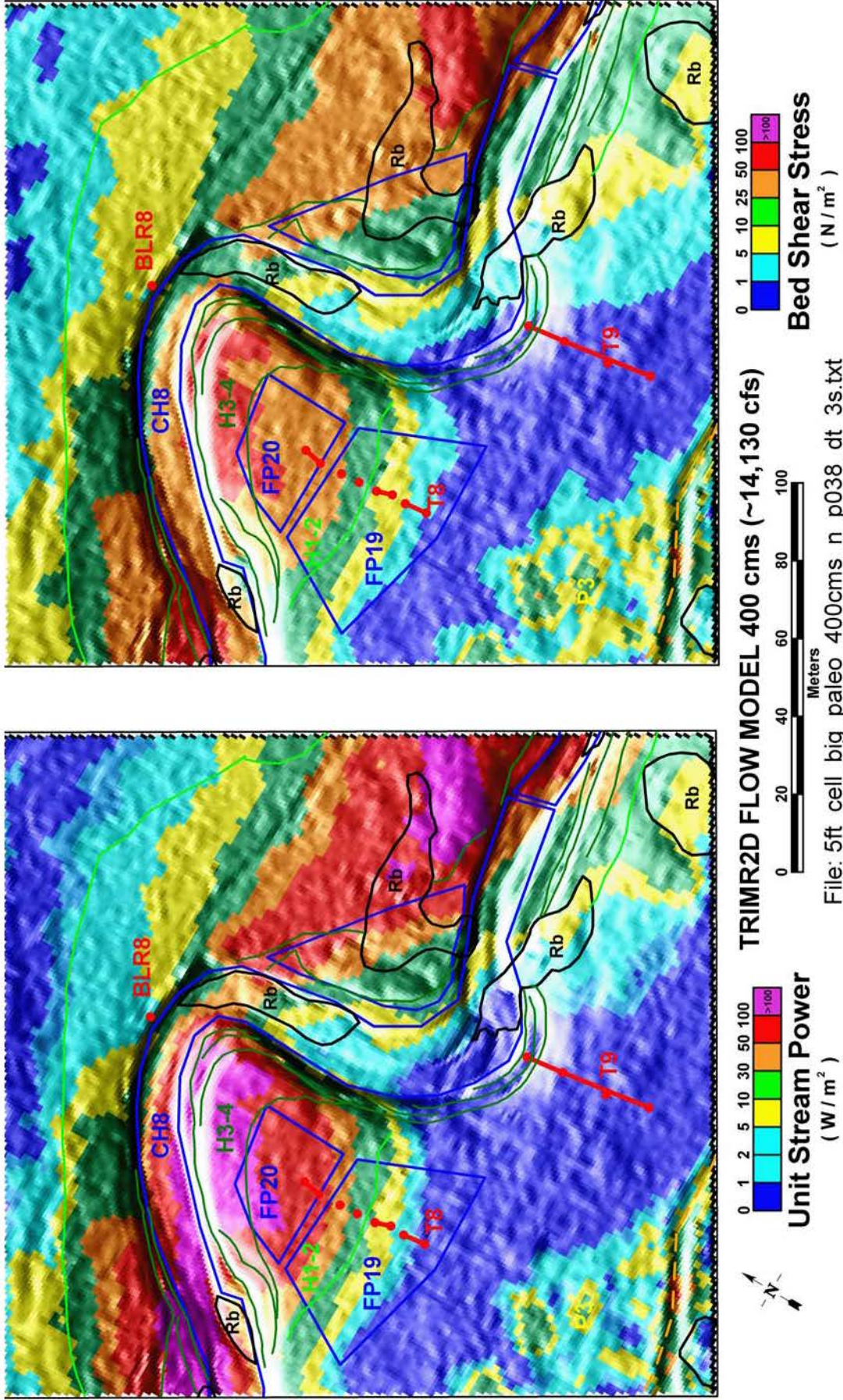


Figure 2-56 5-ft flow model results for  $400\text{ m}^3/\text{s}$  in the BLR8 constriction study area. Base map symbology is from Figure 2-3 and Plate 2.

**Tables for Section 2.0**

**Table 2-1 Discharge and modeling scenarios for the INEEL Diversion Dam study reach**

| Modeled Discharge <sup>1</sup><br>m <sup>3</sup> /s (ft <sup>3</sup> /s)   | Topography <sup>2</sup> |                 |                               | Potential Significance of Modeled Discharge   |
|--|-------------------------|-----------------|-------------------------------|---|
|  | 2000 6-ft grid          |                 | Reprocessed<br>1993 5-ft grid |   |
|  | <i>n</i> =0.030         | <i>n</i> =0.038 | <i>n</i> =0.038               |   |
| 10 (~355)  | X                       | X               |                               | Approximate maximum gaged flow downstream of INEEL Diversion (since 1984)                                   |
| 12 (~425)  | X                       | X               |                               |   |
| 15 (~530)  | X                       | X               |                               |   |
| 25 (~885)  | X                       | X               |                               | Approximate INEEL Diversion Dam release capacity  |
| 50 (~1765)   | X                       | X               |                               | Range for largest estimated historic floods near INEEL Diversion Dam  |
| 70 (~2470)   | X                       | X               |                               |   |
| 100 (~3530)  | X                       | X               |                               | Revised USGS 100-yr flood is 106 m <sup>3</sup> /s (~3740 ft <sup>3</sup> /s) (Hortness and Rousseau, 2002) |
| 130 (~4590)  | X                       | X               |                               |   |
| 150 (~5295)  | X                       | X               |                               | Median value for 10,000 yr paleohydrologic bound (Ostenaar and others, 1999)                                |
| 175 (~6180)  | X                       | X               |                               | Approximate USGS 100-yr flood downstream of INEEL Diversion Dam (Kjelstrom and Berenbrock, 1998)            |
| 200 (~7060)  | X                       | X               | X                             |   |
| 225 (~7945)  | X                       | X               |                               |   |
| 250 (~8830)  | X                       | X               | X                             |   |
| 300 (~10,590)  |                         |                 | X                             |   |
| 350 (~12,360)  |                         |                 | X                             |   |
| 400 (~14,130)  |                         |                 | X                             |   |
| Notes:   |                         |                 |                               |   |
| <sup>1</sup> Steady-state discharge input at upstream end of reach, downstream of the INEEL Diversion Dam        |                         |                 |                               |   |
| <sup>2</sup> All scenarios modeled with TRIMR2D with 5- or 6-ft rectangular grid with input topography as noted. |                         |                 |                               |   |

Table 2-2 Soils and Radiocarbon Summary

| Trench No. | Field Sample No. | Sample Depth (cm) | Material dated                | Laboratory number | Radiocarbon age ( $^{14}\text{C}$ yr B.P.) $\pm 1 \sigma$ | Calibrated age range (cal yr B.P.) $\pm 2 \sigma$ |
|------------|------------------|-------------------|-------------------------------|-------------------|---|---|
| T4         | T4-20-1AR        | 20-25             | <i>Artemisia</i> charcoal     | Beta - 174101     | 520 $\pm$ 40  | 630-600; 560-510                                  |
|            | T4-20-2AR        | 38-51             | <i>Artemisia</i> charcoal     | Beta - 174102     | 1070 $\pm$ 40   | 1060-930  |
|            | T4-19-1AR        | 50-60             | <i>Artemisia</i> charcoal     | Beta - 174099     | 1130 $\pm$ 40   | 1160-950  |
|            | T4-19-1CO        | 50-60             | Conifer charcoal              | Beta - 174100     | 1980 $\pm$ 40   | 2000-1860   |
|            | T4-19-3CH        | 140-155           | <i>Chrysothamnus</i> charcoal | Beta - 172812     | 6330 $\pm$ 40   | 7320-7200   |
| T5         | T5-0-1AR         | 22-32             | <i>Artemisia</i> charcoal     | Beta - 174103     | 780 $\pm$ 40  | 760-660   |
|            | T5-0-2CO         | 110-130           | Conifer charcoal              | Beta - 174104     | 1880 $\pm$ 40   | 1900-1720   |
| T6         | T6-4-1SA         | 12-25             | <i>Salicaceae</i> charcoal    | Beta - 174106     | 630 $\pm$ 40  | 660-540   |
|            | T6-4-1AR         | 12-25             | <i>Artemisia</i> charcoal     | Beta - 174105     | 830 $\pm$ 40  | 790-680   |
|            | T6-6-1YS         | 95-105            | snail shell                   | Beta - 183387     | 10390 $\pm$ 50  | 12800-11940                                       |
|            | T6-4-2MIX        | 103-121           | charcoal fragments            | Beta - 172813     | 3210 $\pm$ 40   | 3480-3360   |
|            | T6-20-2MIX       | 110-140           | charcoal fragments            | Beta - 183388     | 2710 $\pm$ 40   | 2870-2760   |
|            | T6-68-1AR        | 30-40             | <i>Artemisia</i> charcoal     | Beta - 174107     | 620 $\pm$ 40  | 660-540   |
| T9         | T9-32-1PO        | 35-45             | <i>Populus</i> charcoal       | Beta - 183391     | 170 $\pm$ 40  | 290-250; 230-130; 110-70; 30-0                    |
|            | T9-32-2CM        | 105-115           | <i>Chrysothamnus</i> charcoal | Beta - 183392     | 130 $\pm$ 40  | 290-0   |
|            | T9-2-2AR         | 105-115           | <i>Artemisia</i> charcoal     | Beta - 183389     | 2610 $\pm$ 40   | 2730-2780   |
|            |                  |                   |                               |                   |   |   |

**Table 2-3 Geologic and Geomorphic Summary for Big Lost River Paleofloods and Paleohydrologic Bounds**

| Event name   | Age or time span (Cal yrs or Cal yr B.P) <sup>1</sup> | Summary of Evidence  |
|--|---|--|
| <b>Paleofloods</b>   |   |  |
| "white flood"  | >100yr (pre-gaging) but less than 400-600yr           | Based on thin deposit in T4. Not recognized in T5 or T6 (slightly higher sites). Possible correlative in T9(?). Age - most likely 100 to 150 years based on absence of soil development  |
| "400-yr" flood   | 400 to 600 years                                      | Apparently correlative deposits in T4, T5, T6 (also BLR2, BLR7 & BLR8) with similar soils, stratigraphic setting, and radiocarbon ages. Soil has stage I- Bk horizon. Stripping of A and AB/Bw horizons at T8c, partial stripping at T8b; May represent more than one flood.   |
| "older flood"  | 1000 to 2000 years                                    | Deposits with Stage I to I+ Bk horizon that underlie "400-yr flood" deposits in T4, T5, T6 and T9. Appears to indicate long period of stability with little or no deposition at these sites before deposition of deposits associated with "400-yr" flood. Similar stratigraphy at BLR2 and BLR8. Likely represents multiple floods of similar or smaller maximum discharge. Minimum discharge must inundate FP1-FP4, FP6-8, most of FP7, FP11-13, FP17-18, and FP19-21, which are areas with H1-2 geomorphic surfaces that appear to indicate Holocene flooding. |
| <b>Paleohydrologic Bounds</b>  |   |  |
| 400-yr #1  | 400-600   | Preservation of recognizable stratigraphy at T4 and T6. No stripping of A-horizons from the youngest deposits at T4 and T6. Apparently correlative H1-2 geomorphic surfaces at FP1, FP3-4, FP7, FP11-13, FP17, and FP19-20.  |
| early Holocene (H1 surfaces)   | 6000 to 8000  | Preservation of stratigraphy in T6, T4, and T8a,b,c. Banks at BLR6 and continuity of H1-2 geomorphic surfaces along BLR.   |
| Pleistocene  | >10000  | Preservation of Pleistocene gravel surfaces throughout the study reach. Actual age of the underlying deposits is older than 12-15 ka (minimum age of deglaciation) and some may be older than 20-25 ka (Last glacial maximum). Length of time span for paleohydrologic bound is limited by post-glacial, warmer climate more similar to present.   |
| Notes: <sup>1</sup> All age distributions have uniform probability over the indicated time span uncertainty. |   |  |

### **3.0 PALEOFLOODS AND PALEOHYDROLOGIC BOUNDS FOR THE BIG LOST RIVER**

#### **3.1 Background to the Use of Paleohydrologic Bounds**

The approach taken for this paleohydrologic analysis is similar to that used for the previous paleohydrologic studies at INL (Ostenaar et al., 1999, 2002) as well as several Bureau of Reclamation flood hazard evaluations for dams throughout the western United States (e.g., Ostenaar et al., 1996, 1997; Ostenaar and Levish, 1997). Flood frequency analyses for these studies incorporate paleoflood estimates and paleohydrologic bounds (Levish, 2002; Levish et al., 1994, 1996, 1997; Ostenaar and Levish, 1996) into nonparametric Bayesian analyses that use likelihood functions that incorporate both parameter and data (discharge and geologic age) measurement uncertainties (O'Connell et al., 1996, 1998; O'Connell, 2005).

A paleohydrologic bound is the time interval during which a given discharge has not been exceeded. Paleohydrologic bounds are not actual floods, but instead are limits on paleostage over a measured time interval. These bounds represent stages and discharges that have not been exceeded since a geomorphic surface stabilized. Through hydraulic modeling, discharge for a paleohydrologic bound can be derived from stage, just as a discharge is derived from the paleostage indicators of past floods. Used appropriately, paleohydrologic bounds are powerful constraints in flood frequency analyses, even if the number, timing, and magnitude of individual paleofloods are uncertain (Stedinger and Cohn, 1986).

In this context, the present analysis only assumes that for extreme floods, upstream regulatory structures and diversions do not increase flood magnitudes downstream compared to the unregulated natural flows, except for cases where upstream regulating structures might fail. Flood probabilities for such scenarios should be evaluated separately, and account for the overall failure probability of the structure under all conditions. The impacts of regulation and variations in smaller flows, such as those of historical experience, on frequency estimates of extreme floods are addressed through sensitivity analyses.

**3.1.1 Geologic and geomorphic evidence of flooding.** There are many different types of geologic and geomorphic information in fluvial systems that provide a direct indication of the

magnitude and frequency of floods (e.g., Baker et al., 1988). Gravel bars and slackwater terraces indicate the minimum stage of past floods. Likewise, evidence for past erosion such as channels on terrace surfaces and truncated soil profiles also indicates the minimum stage of past floods. The age and frequency of the floods that produced these features can be determined by the degree of soil development, the morphology and extent of weathering on surface features, and radiocarbon analysis of organic material within the deposits. For historical or more recent paleofloods, floated debris and subtle erosional scars are a shorter-lived record of the maximum stage.

A complementary indication of the limits of past floods is the recognition of the amount of time during which floods have not modified geomorphic features or deposits. Soil development and the geomorphic evolution of deposits and surfaces are time-dependent processes (e.g., Birkeland, 1999). Thus, the age of stable, non-flood-modified geomorphic surfaces adjacent to streams is an indication of the minimum length of time since last flooding (Costa, 1978). Evidence of modification of these surfaces by floods includes the deposition of sediment resulting in burial of soils, erosion and truncation of soils, erosion of channels on the surfaces, or erosion of the deposits themselves. Estimates of the stage required to modify these surfaces can come from empirical comparisons to data from historical floods or by comparison to hydraulic model results of observed flows. The minimum depth of flow required for the initiation of large-scale erosion or deposition on geomorphic surfaces can also be evaluated formally in terms of shear stress or stream power (e.g., Parker, 1978; Andrews, 1984; Baker and Costa, 1987). This type of approach is expanded upon here based on the criteria discussed below and in **Appendix D**.

### **3.2 Criteria and Approach for Evaluating Paleohydrologic Information**

In evaluating discharge estimates for paleohydrologic bounds, the focus is on developing an estimate of the flood discharge required to modify or erode a geomorphic surface for which stability can be demonstrated for some prior length of time (e.g. Levish, 2002). Evidence of surface stability is primarily shown by the consistency of soil development and stratigraphy that underlie the surface. These geomorphic surfaces are most often terraces, adjacent to the main stream channel. Many geomorphologists have used stream power as a measure of the potential for channel and landscape modification with a focus on channel power or average cross section

power (e.g., Baker and Costa, 1987; Magiligan, 1992). For engineering applications of erosion, channel stability, and sediment transport studies, many empirical and semi-theoretical relationships have been developed for hydraulic parameters such as depth, velocity, shear stress and stream power (e.g., see Carson and Griffiths, 1987 for a summary). However, in neither body of literature are there many examples of sites which might be considered long existing paleohydrologic bounds which have been overtopped by historical floods, and associated model estimates of the flow parameters associated with this overtopping developed. As noted by Jarrett and England (2002), documentation for the relationships between HWM (high water marks) and the estimated stage required to modify a geomorphic surface and thus define a paleohydrologic bound is lacking in the general literature.

Previous paleohydrologic studies of the Big Lost River recognized the value of using stream power or shear stress as quantitative measures of the erosional potential of stream flow across geomorphic surfaces that might be considered as paleohydrologic bounds (Ostenaar et al., 1999, 2002). However, no quantitative criteria for application of these measures to evaluating discharge and associated uncertainty estimates for paleohydrologic bounds were proposed. Ostenaar et al. (1999) noted the presence of "high" stream power and inundation depths typically in the range of 25-90 cm (1-3 ft) as a justification for establishing bounds. Ostenaar et al. (2002) compared modeled channel stream power for a discharge that had significant gravel bedload transport to modeled power on Pleistocene surfaces downstream of a site termed the Saddle. Power in both cases was noted to be in the range of 50 to  $>100 \text{ W/m}^2$ . Ranges of inundation depths were noted along with observations that shear stress calculations would indicate potential mobility of 2 mm particles for flow depths as shallow as 5-18 cm.

In the present study, we develop a more formal framework for the application of shear stress and stream power to the problem of specification of discharge estimates for paleohydrologic bounds. The difficulties associated with developing conclusions within this framework are similar to those faced in seismic hazard assessment (e.g., SSHAC, 1995), in that uncertainty of the estimates is derived from several sources including limited data, imperfect knowledge and models of salient physical processes, and legitimate differences of scientific opinion.

Three major types of information are used to estimate the discharge range associated with a paleohydrologic bound: 1) stratigraphic and geomorphic data, 2) hydraulic modeling results of depth, stream power, and shear stress for differing input parameters, and 3) a criterion for erosion/modification of geomorphic surfaces based on empirical data compilations of unit stream power and bed shear stress. Results of the geologic/geomorphic investigations were described and compiled in **Section 2.4**, **Plate 2**, and **Appendix B**. The hydraulic modeling approach and results were discussed in **Section 2.5** and portrayed on plots in **Appendix D**. A criterion for erosion/modification of geomorphic surfaces based on stream power and shear stress is developed in **Appendix D** and implemented below.

Geomorphic map units define the spatial extent of areas with similar geologic/geomorphic processes and history. Individual map units are characterized by similarity in relative and absolute age, geomorphic processes and history over broad areas. Differences in age, process, and history between different areas define different geomorphic units. Thus, based on detailed mapping and trenching investigations along the Diversion Dam study reach of the Big Lost River (**Plate 2**, **Appendix B**, and **Section 2.4**), three major geomorphic map groups, H1-2, H3-4, and P2-3, are of primary importance to the issues of specifying paleohydrologic bounds. The similarities and differences within these broad map units are highlighted and defined through "point" investigations with trenches or soil description sites where stratigraphic details are described in detail. These detailed site descriptions provide the basis for areal extrapolation represented by the areal extent of the geomorphic map units. Individual geomorphic map unit areas naturally define the spatial limits of areas within which the variability of hydraulic parameters such as stream power and shear stress can be evaluated when that geomorphic unit is inundated by a modeled flow.

Two-dimensional hydraulic modeling based on relatively small grid cells is used to develop detailed information on the extent and spatial variability of flow for each modeled discharge. From the model results, shear stress and stream power are calculated for each grid cell providing a detailed depiction of the magnitude and spatial variability of these parameters over the inundated areas. This information can then be compared to the spatial extent and characteristics of differing geologic/geomorphic units. Results from the two-dimensional modeling of each discharge that are

used to evaluate paleohydrologic information are 1) depth and spatial extent of inundation over a particular stratigraphic site or geomorphic surface, 2) magnitude and spatial extent of shear stress and/or stream power over a site or geomorphic surface, and 3) magnitude and spatial extent of shear stress and stream power in channel reaches. Evaluation based on depth and extent of inundation primarily considers whether or not a particular site or surface area is inundated by a given flow. For many sites, as a greater percentage of a given site or geomorphic surface is inundated, to progressively greater depths, the probability of surface modification and development of a preservable geologic record increases. Likewise, as the extent and depth of inundation increase, the magnitude and distribution of stream power and shear stress change across the geomorphic surface as well.

The hydraulic conditions associated with flow across a geomorphic surface are varied and non-uniform due to topography, small- and large-scale roughness, turbulence, and mixing. Thus, actual and calculated values of stream power and shear stress vary spatially in magnitude across a given cross section and throughout the area of flow. The results or conclusions drawn from application of any criteria for surface modification is therefore dependent on the location chosen for evaluation. One advantage of the use of high-resolution, two-dimensional hydraulic models is that these models provide outputs that show the spatial variability of flow characteristics. Ideally, the spatial variability shown by hydraulic modeling can be evaluated separately for each geomorphic surface of interest.

The third major type of information used to estimate discharge associated with a paleohydrologic bound are empirical criteria and observational data on the magnitudes of stream power and shear stress that are likely associated with modification or erosion of differing geomorphic surfaces (**Appendix D**). From these data, limiting values for the estimated erosion or modification of differing surfaces can be subjectively estimated for the specific surface conditions and physical properties (e.g., vegetation, soil, and grain size) of each site or geomorphic surface. Because estimates of paleohydrologic bounds will ultimately have a probabilistic description for use in the flood frequency analyses (**Section 4.0**), these criteria are formulated as Probability Density Functions (PDF) that relate the relative probability of surface modification to particular values of shear stress or stream power. In general, the PDF's that describe the probability of surface

modification are triangular distributions based on 3 estimated values. A lower value of shear stress or stream power represents a limit for which there is judged to be a reasonable possibility based on the existing empirical data that significant erosion or surface modification will occur. A central or preferred value represents a large body of data with high confidence. For some PDF's, the central values include a range of equal relative likelihood. An upper value limit defines a boundary beyond which there is virtual certainty of significant erosion or modification based on the available data. For application to the Diversion Dam reach of the Big Lost River, three separate criteria have been developed for stream power and shear stress, respectively (**Figure 3-2** and **Figure 3-3**) and **Appendix D**). Two of the criteria are for application to differing site, soil, and geologic conditions associated the geomorphic surfaces along the Big Lost River (**Figure 3-2**). The third criteria describes the more general conditions under which significant geomorphic modification of portions of the Big Lost River channel might result from various discharge levels (**Figure 3-3**).

Soils and geologic data from the Big Lost River lead to two general categories for erosion and surface modification, termed soil erosion and terrace erosion, based on the contrasting physical and vegetative characteristics of the soils and terrace deposits. Most of the alluvial soils have an upper horizon(s), usually less than 30 cm thick, composed of silt and sand which is generally loose and unconsolidated. These horizons, usually designated as A, AB, and sometimes Bw in soil descriptions (**Section 2.1** and **Appendix B**), lack carbonate cementation, are often bioturbated, and may include in their upper portions some component of recently active eolian sand. Some small grasses and plants have shallow roots in these horizons. In contrast, at most stream terrace sites, below a depth of more than 20-30 cm in most profiles, there is either carbonate cementation or gravel. In deposits that are mostly fine-grained, i.e., silty and sandy, soils with carbonate accumulation are stage I to II. In the gravel deposits maximum clast sizes are generally less than 200 mm, and carbonate stages range from Stage I to III. Larger plants, such as sage, have widely scattered roots that extend into the gravel horizons. Based on the carbonate cementation and generally larger clast size associated with the terrace deposits, larger values of stream power and shear stress are required to initiate erosion relative to the alluvial soils.

The criteria developed for channel stability (**Figure 3-3**) is mainly derived from geomorphic study observations of major channel widening or change following floods (**Appendix D**). This criteria is only applicable to channels where banks are cut in alluvium. Most channel banks along the Big Lost River Diversion Dam study reach are composed of fine-grained alluvium with weakly to moderately developed carbonate soils similar to sections exposed in T4, T5, T6, BLR2, BLR6, BLR7 and BLR8. Gravel, in Holocene fluvial deposits, is not present more than about 1 m above the present channel floor at these exposures. Based on geomorphic mapping (**Plate 2**), only very scattered sections of the channel banks are cut directly in the gravelly Pleistocene alluvium without an inset fine-grained fill terrace. More commonly, scattered basalt outcrops confine one or both channel banks.

### **3.2.1 Evaluating Spatial Extent and Variability.**

The geomorphic maps and the hydraulic modeling results are both two-dimensional datasets that can be overlain and evaluated jointly. This approach allows the spatial extent of geomorphic surfaces and inundation to be evaluated along with the spatial variability of hydraulic modeling results for specific sets of geomorphic surfaces. This type of evaluation could be done in a strict GIS-style, where the full extent of each map unit is evaluated separately, but that approach has not been used here because the mapped geomorphic units include many transitional slopes and areas that are not ideally representative of sites that would be suitable for evaluating paleohydrologic bounds. Specifically, this includes areas such as broad slopes on risers between terraces where some slope erosion and deposition is ongoing, irrespective of the paleoflood and fluvial processes of the Big Lost River. Long-term geomorphic stability cannot generally be demonstrated for these types of transitional areas. For that reason, a more restricted subset of the key geomorphic surfaces were selected for evaluation. Within the Big Lost River Diversion Dam reach, 30 subareas were defined based on geomorphic characteristics (**Figure 3-4**). The boundaries of each subarea were drawn to generally lie within the extent of a single geomorphic map unit along the Big Lost River. Most of the subareas are of sufficient size to include hundreds of computational cells from the hydraulic modeling results and include thousands of square meters of individual geomorphic surfaces. One way of reducing uncertainty associated with paleohydrologic conclusions is to expand the spatial extent of that data throughout a study reach.

The detailed geomorphic and spatial characteristics of the subareas are summarized in **Table 3-1** and **Table 3-2**. Twenty-one subareas, FP1 to FP21, are located on the Holocene and Pleistocene geomorphic surfaces adjacent to the Big Lost River. These subareas range from small areas surrounding the individual trenches, (e.g., FP12 near T4) to subareas which encompass extensive areas of the Pleistocene surfaces flanking the Big Lost River (e.g., FP5 and FP15). Nine subareas, CH1 through CH9, were defined within the channel of the Big Lost River. These channel reaches differ in sinuosity, bed and bank materials, and hydraulic characteristics.

Within each subarea, values for inundation, stream power, and shear stress from each flow simulation are plotted relative to the threshold values for modification defined by empirical data (e.g., end points and peaks on **Figure 3-2** and **Figure 3-3**). From the resulting plots (e.g., **Figure 3-5** and remaining plots in **Appendix D**) a range of discharge values can be defined for each subarea that corresponds to the subjective probability thresholds for modification based on stream power or shear stress. A minimum discharge level for these values is first imposed by the requirement that 90-100 percent of the subarea is inundated by the simulated discharge. This is imposed to assure the uniformity of geomorphic processes within each subarea. Because the subarea boundaries are primarily defined by geomorphic boundaries, and because the age of geomorphic surfaces within each subarea are interpreted to be constrained by similar geologic factors, for flood modification of these surfaces nearly complete inundation is generally a minimum requirement. Inundation extent that is less than 100 percent is allowed for surfaces that include original depositional or erosional relief unrelated to flood modification. This would include transitional areas such as terrace risers that exist between surfaces of differing ages, or constructional relief associated with abandoned bars and channel features. Discharge values that correspond to the erosion/modification thresholds (i.e., PDF of **Figure 3-2** and **Figure 3-3**) are then estimated by choosing a percentage of the subarea that must exceed the threshold value for erosion/modification. The two-dimensional hydraulic modeling demonstrates the spatial variability of hydraulic conditions across individual surfaces. Because the subareas are very large (see **Table 3-1** for sizes), and the scale of geomorphic mapping and observation is also large, geomorphic change that is detectable within the scale of this investigation should result when threshold values are exceeded over much less than 100 per cent of most of the subareas. For the present scale of mapping along the Big Lost River, geomorphic features that are less than about

10 m<sup>2</sup> (108 ft<sup>2</sup>), such as outcrops, dunes, mounds, and small channels, are readily observable and detectable. Thus, even for the smallest of the subareas, use of a value of 50 percent area for exceedence of the threshold values of stream power or shear stress corresponds to minimum areas of 35 m<sup>2</sup> (377 ft<sup>2</sup>), and for most subareas, it is hundreds or thousands of square meters. The subarea percentages and the discharge ranges derived from analysis of each of the subareas are tabulated in **Table 3-3**.

#### **3.2.1.1 Uncertainty in Discharge Estimates of Modification for each Subarea.**

Overall, the uncertainty in the discharge ranges estimated from each subarea is mostly derived from three main sources. The first is the variability in calculated stream power and shear stress that results from changes in the input hydraulic model parameters such as discharge, roughness, or topographic model. This uncertainty is displayed for each subarea by comparison of the curves based on similar discharge, but varied roughness or topographic input, or comparing changes resulting from successive discharge values (e.g. **Figure 3-5** and plots in **Appendix D**). As such, the ranges compiled in **Table 3-3** directly incorporate this uncertainty for range of input parameters used in the simulations.

The second source of uncertainty lies in the PDF's (e.g., **Figure 3-2**) that describe the relative probability of erosion or modification associated with variation in stream power or shear stress. This source of uncertainty is directly linked to the choices and relevance of threshold values from empirical data to associate with surface modification (**Appendix D**). The tabulated empirical data on which these thresholds are based were collected according to a wide variety of scientific and engineering protocols. It is therefore difficult to directly link all of these results directly to the present framework of flow simulation and calculation used in the present study. Further research and data compilation, conducted specifically within the framework of modern two- and three-dimensional flow modeling, is needed to rigorously evaluate whether the present range of values chosen to characterize the erosion/modification thresholds are appropriate, or not. Determining the proper basis for describing and characterizing the spatial variability of flow parameters and erosion over extent varied geomorphic surfaces is a critical component of this uncertainty.

The third source of uncertainty lies in the delineation and choices for the areal extent of a subarea or geomorphic surface which must meet the threshold criteria. This latter factor is somewhat

minimized because stream power and shear stress values develop rapidly over most of the individual subareas with increases in discharge. Thus, the curves on **Figure 3-5** and the additional plots in **Appendix D** are generally very steep, meaning that for most subareas, changing the required percentage that must exceed the threshold does not substantially change the estimate of discharge. Additional small uncertainty is derived directly from the delineation of the subarea boundaries from the geomorphic and geologic data. The extent to which the subareas are reasonable subdivisions or groupings of the geomorphic units can be judged subjectively by comparison of the subareas and geomorphic mapping. As noted above, use of the presently mapped geomorphic boundaries in lieu of the subareas would result in inclusion of larger percentages of transitional topography with increased geologic complexity and variability.

**3.2.1.2 Combining Estimates from Multiple Subareas.** Sample subareas for stream power and shear stress are located throughout the Diversion Dam study reach (**Figure 3-4**). Hydraulic conditions vary throughout the study reach and although many subareas are located on geomorphic surfaces of similar age where there will be variability within a subarea (**Section 3.2.1**), estimates of unit stream power and bed shear stress are expected to vary between subareas as well. Thus, a consistent approach for combining results from multiple subarea sites is required. For paleofloods, the observed geologic or geomorphic evidence should relate to a pattern of modeling results that is consistent with a single discharge range throughout the study reach. Thus, the estimated discharge for the paleoflood must 1) inundate all sites where correlative flood deposits are observed; and 2) have stream power and shear stress distributions that are consistent with the observed distributions of fine- and coarse-grained deposits of the paleoflood as well as any evidence of erosion that can be associated with the flood. Estimates from multiple sites should be generally consistent if all the sites are associated with a common paleoflood discharge. In contrast, because a paleohydrologic bound represents an exceedence of prior events, and is possibly a hypothetical event that was not associated with deposition of the preserved deposits or geomorphic surfaces, modeled hydraulic conditions may vary greatly between sites of similar age within a reach. Some sites will inevitably be much more strongly limiting than other sites even though they may be of the same general age. This is perhaps most easily illustrated by considering the broad areas of the Pleistocene P2 surfaces that flank the Big Lost River. As the hydraulic modeling results show, these surfaces are slowly and variably inundated over a broad range of

discharge (**Section 2.5** and **Section 3.2.1**). Thus, the estimated discharge required to modify any subsection of the P2 surfaces will vary substantially and for some sites, the criteria for modification (e.g., **Figure 3-2**) may never be met, regardless of discharge. In contrast, some areas of the Pleistocene surfaces may be sites where modification is highly likely at very shallow inundation. These types of sites are more strongly limiting as a basis for evaluating a paleohydrologic bound.

Comparison of possible discharge estimates from several subareas for any group of similar-age surfaces might yield a broad range of discharge values for a paleohydrologic bound, but the final choice of values to describe the bound can be limited to a more narrow range that best describes the uncertainty associated with estimates for a subset of the most strongly limiting sites. Limiting the range based on fewer sites may still be conservative depending on the number and characteristics of the initial group of subareas evaluated. There is no assurance that the subareas chosen include the most strongly limiting site for any age group. On the other hand, initial delineation of the subareas (**Section 3.2.1**) is based on a requirement that the subareas be large enough to include a geologic/geomorphic record or deposit that could be preserved and recognized over geologic time scales.

### **3.3 Age and Discharge Estimates for Paleofloods**

The geologic investigations summarized in **Section 2.4** identified stratigraphic evidence for at least three paleofloods along the Big Lost River that exceeded the stage and discharge of floods in the historic record (**Table 3-5**). Stratigraphic data from trenches and exposures defines the number, relative sizes, and relative ages of these paleofloods. Geologic age-dating methods provide the absolute ages and uncertainty ranges (**Section 2.3** and **Figure 2-8**). Estimates of discharge ranges for the paleofloods are based on the hydraulic modeling results (**Section 2.5**) and the approaches discussed above in **Section 3.2**. The basis for reaching age and discharge conclusions for each of the paleofloods is discussed separately below. Summary data for discharge limits from each subarea are compiled in **Table 3-3**. **Table 3-4** summarizes the applicability of each subarea to evaluation of the individual paleofloods and paleohydrologic bounds.

**3.3.1 "White Flood"**. Stratigraphic evidence for this flood is recognized at a single site, Trench T4 (**Section 2.3.2.1**). A thin, ~ 7 cm, deposit of silty sand caps the sequence of flood deposits in lowest portion of trench T4, stations 19-21, and appears to bury the soil formed on deposits of the underlying "400-yr" flood. Soil descriptions (**Appendix B**) designate this unit as the A1-horizon of the present soil and soil development is weak in comparison to other sites. The deposit is not associated with historic floods because no historic floods would have been large enough to inundate the site (**Section 2.1.1** and **Figure 2-6**). No similar deposit is present or recognized in trenches T5 or T6, both of which are only slightly higher relative to discharge at which they are inundated (e.g. **Figure 2-6**) and it does not appear that soils in deposits of the "400-yr" flood are eroded more recently at these sites (**Section 2.3.2.2** and **Section 2.3.2.3**). A radiocarbon age from the underlying A2 horizon at T4 has a calibrated age range between 630-510 cal yr B.P. (**Table 2-2** and **Appendix B**). Deposits in lowest portions of trench T9 have young radiocarbon ages (**Section 2.3.3.2** and **Table 2-2**), but are also inundated by discharges that might have occurred prior to construction of the INEEL Diversion Dam (**Figure 2-7**). Thus, the age of a paleoflood associated with this deposit is constrained to be prior to the beginning of stream-gaging records (A.D.1903) by the minimum discharge required to reach the site. The deposit is younger than the 630-510 cal yr B.P. age from the underlying soil, and is most likely about 100-150 years based on the relative soil development.

The discharge range for this flood is narrowly constrained by modeling results at the site. A minimum discharge of 70-80 m<sup>3</sup>/s is required to inundate the deposit (**Figure 2-6**). As discharge increases, unit stream power and bed shear stress increase very rapidly at trench T4 (**Figure 2-31**, **Figure 2-32**, and subarea FP12 in **Table 3-3** and **Appendix D - Figure D3-17**). This constraint indicates that a discharge of more than 100 m<sup>3</sup>/s would have been very likely to have resulted in erosion of the underlying deposits between stations 20-21 of trench T4. Discharges larger than 100 m<sup>3</sup>/s (**Figure 2-32**) would also result in inundation of the "400-yr" deposits in the lower elevation portions of trenches T5 and T6. Discharge less than 100 m<sup>3</sup>/s is consistent with the lack of evidence for very young erosion at the Big Loop subarea FP9 (**Appendix D - Figure D3-14**) and at the BLR8 study area (subarea 20 - **Appendix D - Figure D3-25** and trench T8c - **Section 2.3.3.1**). These constraints lead to limiting the estimated discharge for this paleoflood to a range of 80-100 m<sup>3</sup>/s (**Table 3-5**).

**3.3.2 "400-yr Flood".** Stratigraphic evidence for this paleoflood was recognized in the earlier paleoflood study by Ostenaa et al. (1999, 2002) at four sites in the Diversion Dam study reach (**Figure 2-11**). Deposits with similar soils and stratigraphy that are apparently correlative are present in trenches T4, T5 and T6 (**Figure 2-8** and **Section 2.3.2**). These deposits appear to be associated with the prominent geomorphic expression of the H2 surface that can be mapped throughout the study reach (**Plate 2** and **Section 2.2.3**). Soil development in these deposits, and radiocarbon ages from these deposits and from underlying deposits constrain the age to about 600 - 400 cal yr B.P. (**Figure 2-8**).

Because the flood deposits recognized by Ostenaa et al. (1999, 2002) and in the trenches for this study appear to be associated with H2 geomorphic surface, one constraint for the discharge of this paleoflood is that the discharge be large enough to inundate the full extent of this surface throughout the study reach. As shown by the plots in **Appendix D - Electronic Supplement** that cover the entire study reach and the individual study area plots (**Figure 2-12** through **Figure 2-56**) this constraint is met for modeled discharges between 100 to 130 m<sup>3</sup>/s. The most strongly limiting sites for the lower discharge limit of this flood appear to be the H1-2 surface in the vicinity of trench T6 (**Figure 2-33**) and at the BLR8 study site near trench T8a (**Figure 2-46**). Modeled discharges of only slightly less than 130 m<sup>3</sup>/s are required at both of these sites to inundate the extent of flood deposits (T6 - **Section 2.3.2.3**) or young erosion (T8a,b - **Section 2.3.3.1**).

An upper limiting discharge for this paleoflood is derived from the observation that in trenches T4, T5, and T6 (**Section 2.3.2**) deposits of the "400-year" paleoflood overlie only slightly eroded soils formed in older flood deposits. At T8a,b (**Section 2.3.3.1**), preservation of Bk horizons in older flood deposits suggests that the primary record of the "400-yr" paleoflood at that site is only limited erosion of upper-most soil horizons. Comparison of unit stream power and bed shear stress values from the subareas that include these sites, and other H1-2 surfaces in the study reach indicates that once discharge exceeds about 175 m<sup>3</sup>/s, the criteria for terrace erosion is being exceeded at multiple sites throughout the reach (**Table 3-3** and **Figure 3-6**). Thus, if the paleoflood discharge exceeded 175 m<sup>3</sup>/s, much more extensive erosion should have been associated with these deposits in the trench exposures. Discharge in the range of 130 - 175 m<sup>3</sup>/s is consistent with the muted expression of earth mounds on the large area of P3 surface northwest of trench T1

(**Plate 2** and subarea FP 6, **Figure 3-4**). In this discharge range, unit stream power and bed shear stress criteria for soil erosion are exceeded over most of this surface (**Appendix D - Figure D3-11** and **Figure 3-6**). In the same discharge range, minor flow is initiated through the braid channel traversed by trench T1, consistent with soils and stratigraphy in the trench and nearby geomorphology (**Section 2.3.1.1**). However, for discharge greater than  $175 \text{ m}^3/\text{s}$ , unit stream power and bed shear stress increase in this channel (e.g., **Figure 2-15**) implying that significant erosion would be expected.

**3.3.3 "Older Flood"**. Trench and bank exposures along the H1-2 surface all demonstrate that the deposits of the "400-yr" paleoflood overlie eroded soils developed in slightly older, similar flood deposits (Ostenaar et al., 1999, 2002; and **Section 2.3**). The soils in these deposits are generally similar, or slightly more developed than soils developed in the past 400-600 years. This implies a similar length of time over which no flood either eroded or resulted in significant deposition over these deposits. Likewise, the limited extent of the deposits of the "400-yr" flood relative to the H1-2 surface indicate that overall, the surface must be a composite of deposits with similar origins, but differing ages. The significant scatter in radiocarbon ages from site to site, and the variability in soils that underlie the "400-yr" flood deposits appear to support this concept. As shown on **Figure 2-8**, there is much less correlation of the potential time brackets for a single older flood than for the "400-yr" paleoflood and some possibility that multiple floods may have occurred in the time interval since about 3000 cal yr B.P. However, both the stratigraphic and the chronologic resolution to define multiple floods in this time period are lacking in the present exposures. The existing age constraints appear to indicate that a conservative age range for this flood would lie in the range of 2000 to 1000 Cal yr B.P.

The discharge range estimate (**Table 3-5**) for older flood(s) represented within deposits that underlie the H1-2 surface is similar to that for the "400-yr" flood. A minimum discharge must inundate the full extent of the H1-2 surface; an upper limiting discharge must not impose unit stream power and bed shear stress loads that would result in erosion of underlying and adjacent deposits. For these reasons, the same range of discharge,  $130 - 175 \text{ m}^3/\text{s}$ , is judged to be appropriate for possible "older" paleofloods as for the "400-yr" paleoflood. The spatial extent, and depth of flow, associated with this range of discharge envelopes all of the stratigraphic and

geomorphic evidence of Holocene paleofloods that has been observed along the Diversion Dam study reach (**Section 2.4**).

### **3.4 Age and Discharge Estimates for Paleohydrologic Bounds**

The geologic data show that over different time intervals and areas along the Big Lost River, there is evidence of relative geomorphic stability. Thus, the preservation of paleoflood deposits as the surface units on portions of the H1-2 geomorphic surfaces shows that no floods large enough to modify or remove these deposits have occurred since the time of those paleofloods. As summarized in **Section 2.4**, there is stratigraphic and geologic data along the Big Lost River that allows for defining three paleohydrologic bounds that span differing time intervals over the past 10,000 years (**Table 3-5**). Geomorphic mapping delineates the characteristics and extent of surfaces of similar age that are potentially useful as paleohydrologic bounds (**Section 2.1.2**). Stratigraphic data from trenches and exposures defines the characteristics of the surfaces and the evidence for relative surface stability over time. Geologic age-dating methods provide the absolute ages and uncertainty ranges (**Section 2.3** and **Figure 2-8**). Estimates of discharge ranges for the paleohydrologic bounds are based on the hydraulic modeling results (**Section 2.5**) and the approaches discussed above in **Section 3.2**. The basis for reaching age and discharge conclusions for each of the paleohydrologic bounds is discussed separately below. Summary data for discharge limits from each subarea are compiled in **Table 3-3**. **Table 3-4** summarizes the applicability of each subarea to evaluation of the individual paleofloods and paleohydrologic bounds.

**3.4.1 400-yr Flood Bound.** In trenches at the Saddle Constriction study area, deposits of a paleoflood with an age of 400- to 600- years are the parent materials of the surface soils (**Section 2.3.2**). Weakly developed soils developed in the flood deposits at these sites indicate that no significant erosion or deposition by other floods or other geomorphic processes have disrupted these surfaces in that time span. Similar relationships, preserved at multiple sites, demonstrate stability of these surfaces since the time of the "400-yr" flood, approximately 400- to 600-years ago (**Section 3.3.2**). Even at trench T4, where the "400-yr" deposits are buried by thin deposit of a younger paleoflood, the soil profile in the underlying deposits is intact, indicating that this site was not significantly eroded by that flood (**Section 3.3.1**), and hence has been stable since

deposition 400-600 years ago. Throughout the reach, the H1-2 surfaces which include these deposits are unmodified by younger erosion (**Section 2.2.3** and **Plate 2**).

The H1-2 surfaces and deposits of the "400-yr" flood are preserved in many differing hydraulic settings throughout the Diversion Dam study reach. Thus, for use as a paleohydrologic bound, some of these sites are much more strongly limiting than others (**Section 3.2.1.2**). In particular, at Trench T4, unit stream power and bed shear stress increase very rapidly with increasing discharge (**Figure 2-31**, **Figure 2-32**, and subarea FP12 in **Table 3-3** and **Appendix D - Figure D3-17**). These data indicate that this site would be likely be subject to significant soil erosion at a discharge exceeding about 100 m<sup>3</sup>/s, and terrace erosion once discharge exceeded 110-120 m<sup>3</sup>/s. Modeled values of unit stream power and bed shear stress in this discharge range increase even more rapidly near trench T8c in subarea 20 at the BLR8 study area (**Figure 2-45** and **Figure 2-46**, **Table 3-3** and **Appendix D - Figure D3-25**), where no deposits clearly younger than 400- to 600-years are present (**Section 2.3.3.1**). Unit stream power and bed shear stress values from subarea 17, located on an unmodified H1-2 surface midway between the Saddle Constriction and BLR8 study areas (**Figure 3-4**), also increase rapidly (**Appendix D - Figure D3-22**). Compiled unit stream power and bed shear stress results from subareas throughout the reach show that large areas of the "400-yr" flood deposits would likely be subject to significant soil erosion at relatively low discharges (**Figure 3-6**). In contrast to estimating the discharge for the paleoflood, no requirement to inundate the entire H1-2 surface is imposed. Preservation and demonstration of stability at multiple sites which provide strongest limits on the discharge which might modify these sites is sufficient basis to establish the paleohydrologic bound (**Section 3.2.1.2**). Thus, the discharge limits for the paleohydrologic bound based on the deposits of the "400-year" paleoflood can be somewhat smaller than the discharge estimated for the paleoflood, because even a smaller flood would have a high likelihood of modifying extensive areas of the "400-year" deposits (**Table 3-5**). As discussed above, there are several sites where modification of the "400-year" flood deposits becomes increasingly certain for discharges above 110 m<sup>3</sup>/s. To characterize the discharge range of the paleohydrologic bound, a modified triangular distribution of relative likelihood is used, with a lower discharge limit of 110 m<sup>3</sup>/s. A peak is chosen at 130 m<sup>3</sup>/s, with uniform likelihood extended to 150 m<sup>3</sup>/s (see **Figure 4-1**).

**3.4.2 Early Holocene (H1 surfaces) Bound.** The stratigraphic evidence to support this paleohydrologic bound is the preservation of extensive areas of generally fine-grained fluvial sediments with well-developed carbonate soils that underlie the H1-2 surfaces. The most extensive exposures of these sediments and soils are in trench T6, stations 1 to ~30, and in the disconnected sequence of trenches at BLR8 study area, T8a,b,c (**Section 2.3.2.3, Section 2.3.3.1, and Appendix B - Electronic Supplement**). Smaller remnants are present at T4, stations 16 to 20 (**Section 2.3.2.1 and Appendix B - Electronic Supplement**), and at BLR6 (Ostenaar et al., 1999, 2002). These deposits and soils apparently are part of an aggradational fill of latest Pleistocene to early Holocene age (**Section 2.2.3**). Stage II carbonate soil horizons in these deposits are generally 50- to 100 cm thick, indicative of an early Holocene age for stabilization of the surface, and radiocarbon ages from these deposits ranging from about 7200 to 12,800 cal yr B.P support this age (**Section 2.2.3 and Section Table 2-2**). Based on these data, a conservative time interval of 6000 to 8000 years has been chosen for use as a paleohydrologic bound. Most of radiocarbon ages from these sites are older than this range, but the shorter time interval reflects the possible interpretation that aggradation of the sequence continued and the surfaces did not stabilize and begin forming soils until later.

There are fewer sites that constrain discharge estimates for this paleohydrologic bound than for the bound based on the "400-yr" flood (**Table 3-4, compare Figure 3-6 and Figure 3-7**). Discharge constraints based on the exposures at trenches T6 (subarea FP13) and T8a,b (subarea 20) (**Figure 3-7**) indicate that unit stream power and bed shear stress at these sites are high enough and extensive enough to indicate significant terrace erosion at these sites for discharges of 175 m<sup>3</sup>/s and larger. The H1-2 surface at FP17 (**Figure 3-4**) is similarly impacted. Many sites on Pleistocene P3 surfaces (**Section 2.2.2**) are significantly affected by modeled flows of 175 m<sup>3</sup>/s and larger as well. Terrace erosion is likely initiated in extensive areas of subareas FP6 and FP8 (**Figure 3-4 and Figure 3-7**), both sites that show geomorphic evidence of the "400-yr" flood (**Section 3.3.2 and Plate 1**). Results also indicate the initiation of soil erosion at sites on the older Pleistocene P2 surfaces (**Section 2.2.2**), such as in subareas FP5 and FP16 (**Figure 3-4 and Figure 3-7**). The geomorphology in these areas indicates that they are beyond the limits of any Holocene floods (**Section 2.4 and Plate 1**). For discharges larger than 250 m<sup>3</sup>/s, judged to be the upper confidence limit for this paleohydrologic bound, significant terrace erosion is indicated for all the

subareas (**Figure 3-7**). At larger discharges, flow also overtops the saddle area (**Section 2.5.1.4**) and impacts significant areas in, and adjacent to, subareas FP14 and FP15.

The paleohydrologic bound based on the early Holocene deposits (**Table 3-5**) potentially includes some conservatism in the time estimates for the bound, 6000 to 8000 years, in that most of the dating results indicate these deposits are likely somewhat older. The discharge range used for this bound, 175 to 250 m<sup>3</sup>/s, is a range of values beyond any observed evidence for Holocene floods in the Diversion Dam study reach of the Big Lost River.

**3.4.3 Pleistocene Bound.** The extensive areas of unmodified Pleistocene surfaces that flank the Big Lost River are the stratigraphic and geomorphic basis for this paleohydrologic bound (**Table 3-5**). The Pleistocene P2 surfaces have a braid-channel morphology that is inherited from Pleistocene gravel deposition and unrelated to present flows in the Big Lost River (**Section 2.2.2**). The more limited areas of Pleistocene P3 surfaces generally follow the present river channel and are also underlain by gravels, and likely represent the last episode of Pleistocene deglaciation (**Section 2.2.2**). Trench exposures in T6, T7, T8 and T9 indicate that the last phase of deposition on these surfaces was aggradation of fines in small channels on the P3 surfaces (**Section 2.2.2**, **Section 2.3.2**, and **Section 2.3.3**). Subsequent deposition, shown by the inset deposits that underlie the Holocene surfaces has been dominated by fines. Soils on the Pleistocene surfaces are characterized by an upper loess cap, generally less than 0.5-m-thick in the Diversion Dam study reach and well-developed carbonate morphology (**Section 2.2.2**). The Pleistocene age of both the P2 and P3 surfaces is established regionally by depositional links to regional glaciation, and in a local context by radiocarbon ages of ~10,000 to 12,800 cal yr B.P. obtained from the inset fine-grained deposits (**Section 2.2.2** and **Table 2-2**).

The lower discharge limits for the Pleistocene bound are based on discharges at which significant terrace erosion is indicated on the P3 surfaces, mostly in areas that are slightly modified by the "400-yr" paleoflood (**Figure 3-8**). Within subareas FP6, FP8, and FP19, discharges of 225 m<sup>3</sup>/s and larger result in unit stream power and bed shear stress values over extensive areas that exceed upper limits for soil erosion and indicate significant potential for terrace erosion. In addition, near this discharge, model results indicate that flow is initiated over multiple locations near the Saddle area (**Section 2.5.1.4**), which produces localized areas with large values of unit stream power and

bed shear stress on the Pleistocene surfaces just downstream. Over broad areas of the Pleistocene surfaces, increasing discharge leads to progressive increases in the extent of significant soil erosion and localized channeling. As discharge approaches 400 m<sup>3</sup>/s, considered the upper discharge limit for this bound, unit stream power and bed shear stress values reach or exceed the preferred values for terrace erosion over significant portions of all the subareas located on the Pleistocene surfaces. The majority of these exceedences are concentrated braid channels such as those traversed by trenches T1, T2, T3, and T7 where the Pleistocene deposits and soils demonstrate long-term stability of these surfaces and channels (**Section 2.4**).

**3.4.3.1 Catastrophic Channel Change.** An alternative approach to determine discharge estimates for bounds over long, but non-specific time frames is to estimate the discharge which might result in "catastrophic" channel change (**Appendix D** and **Figure 3-3**). Unlike other estimates, this approach is not specific to the conditions of the Big Lost River, with the caveat that only in reaches where the channel banks are mostly composed of alluvium does this approach apply.

For each of the channel subareas (**Figure 3-4**), a range of values for catastrophic channel change is evaluated based on the subarea results, (**Figure 3-9**; derived from **Appendix D - Figures D3-29 to D3-37**), and the channel profile plots (**Figure 2-9**). A minimum discharge range for bounds has been estimated from the plots based on approximately 10 percent of the channel subarea exceeding the minimum criteria for either unit stream power >200 W/m<sup>2</sup> or bed shear stress >100 N/m<sup>2</sup>, realizing that some subareas have sections with rock channels and minimum values should be higher in those subreaches (see **Table 3-2** for descriptions of individual channel subareas). A preferred value is taken when there is significant exceedence on the plots (**Appendix D - Figures D3-29 to D3-37**), of the 400 W/m<sup>2</sup> or 200 N/m<sup>2</sup>, and these exceedences are apparent as well on the channel profile plots (**Figure 2-9**). The existence of large areas of rock outcrops in the channel is a factor that will make this approach non-conservative, but is hard to quantify. Modeling does not extend to large enough discharges to estimate a true upper bound; and this approach is inherently subjective, but we do expect these values to have a degree of consistency with the estimates of paleohydrologic bounds that have durations of thousands of years.

Results from each subarea combined are shown on **Figure 3-9**. A bounding range of discharge that would be associated with catastrophic channel change on this reach of the Big Lost River is judged to be 250 - 450 m<sup>3</sup>/s based on the compiled results. Within this range five of the subreaches exceed the basis for reaching preferred values. Subarea CH1 is largely discounted because it may include some effects due to flow initiation in the upstream portion of the model, especially for larger flows and because long portions of this subreach include rock channels. Subareas CH4 and CH7 also include significant sections of rock outcrop, but are also representative of the types of sites where empirical data on which this approach is based might have been collected (**Appendix D**). The absence of higher values of unit stream power or bed shear stress in subareas CH3, CH6, and CH8 results from flow stagnation due to downstream channel constrictions (**Section 2.5.1.4**).

Evaluation based on catastrophic channel change is not linked directly to a time period associated with a specific paleohydrologic bound or used subsequently in the flood frequency analyses. For the Big Lost River, these results appear to qualitatively support the range of bounds independently evaluated for periods of 1000's to 10,000 years. Thus, the occurrence of floods with discharges that appear likely to significantly modify the Pleistocene surfaces (**Section 3.4.3**), would also be considered "catastrophic" in a geomorphic sense.

**Figures for Section 3.0**

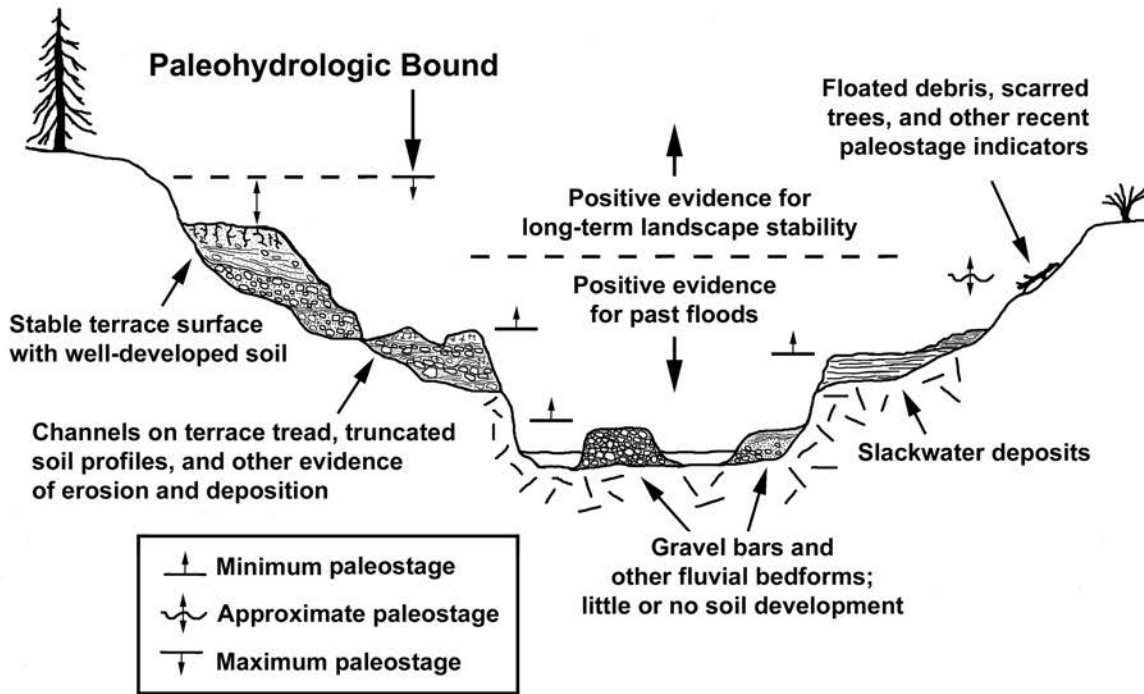


**Figure 3-1 Schematic representation of different types of geomorphic and stratigraphic evidence for paleofloods and paleohydrologic bounds.**

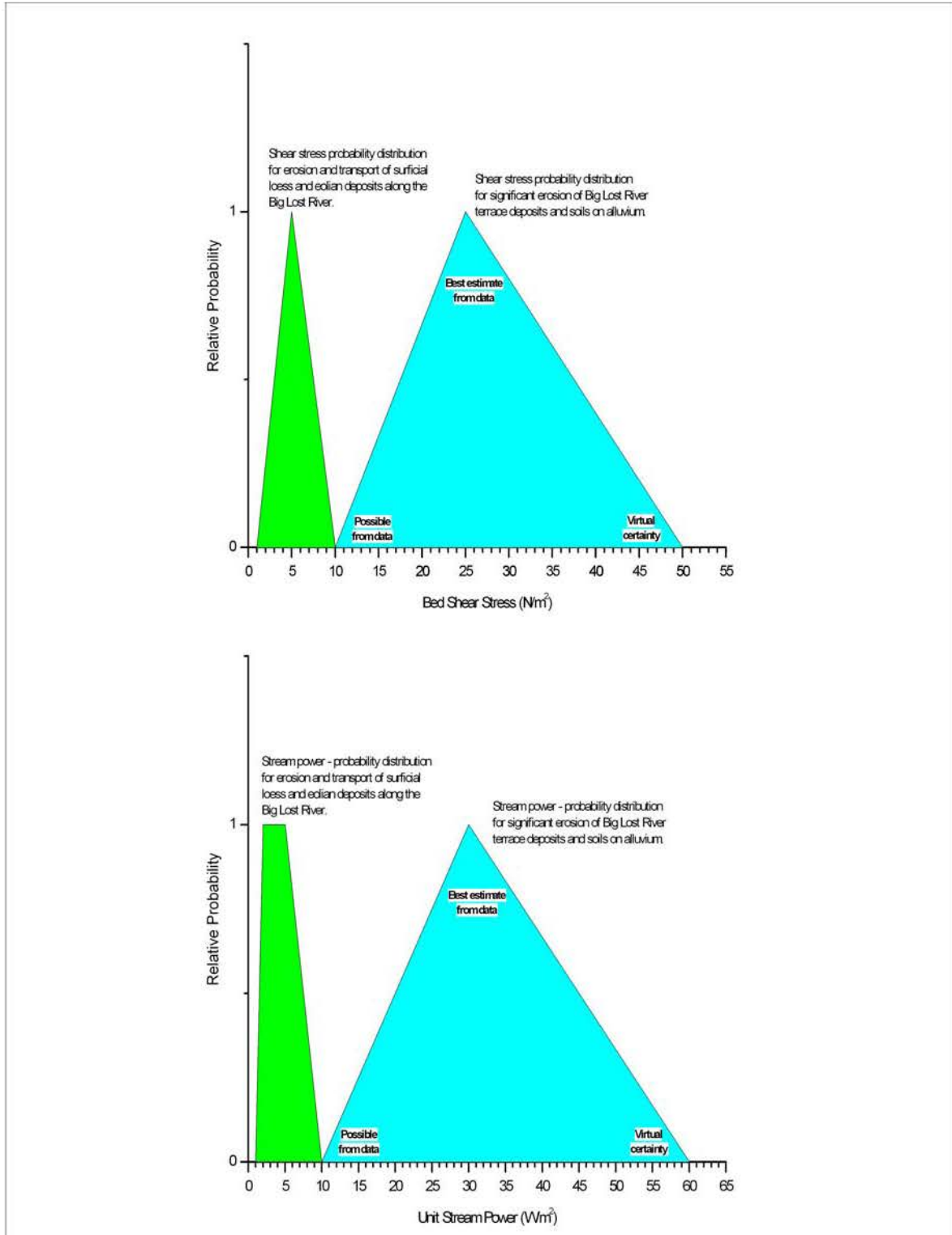


**Figure 3-2 Probability density functions for erosion based on shear stress and stream power for Big Lost River applications. See Appendix D for discussion of data used to define these distributions**

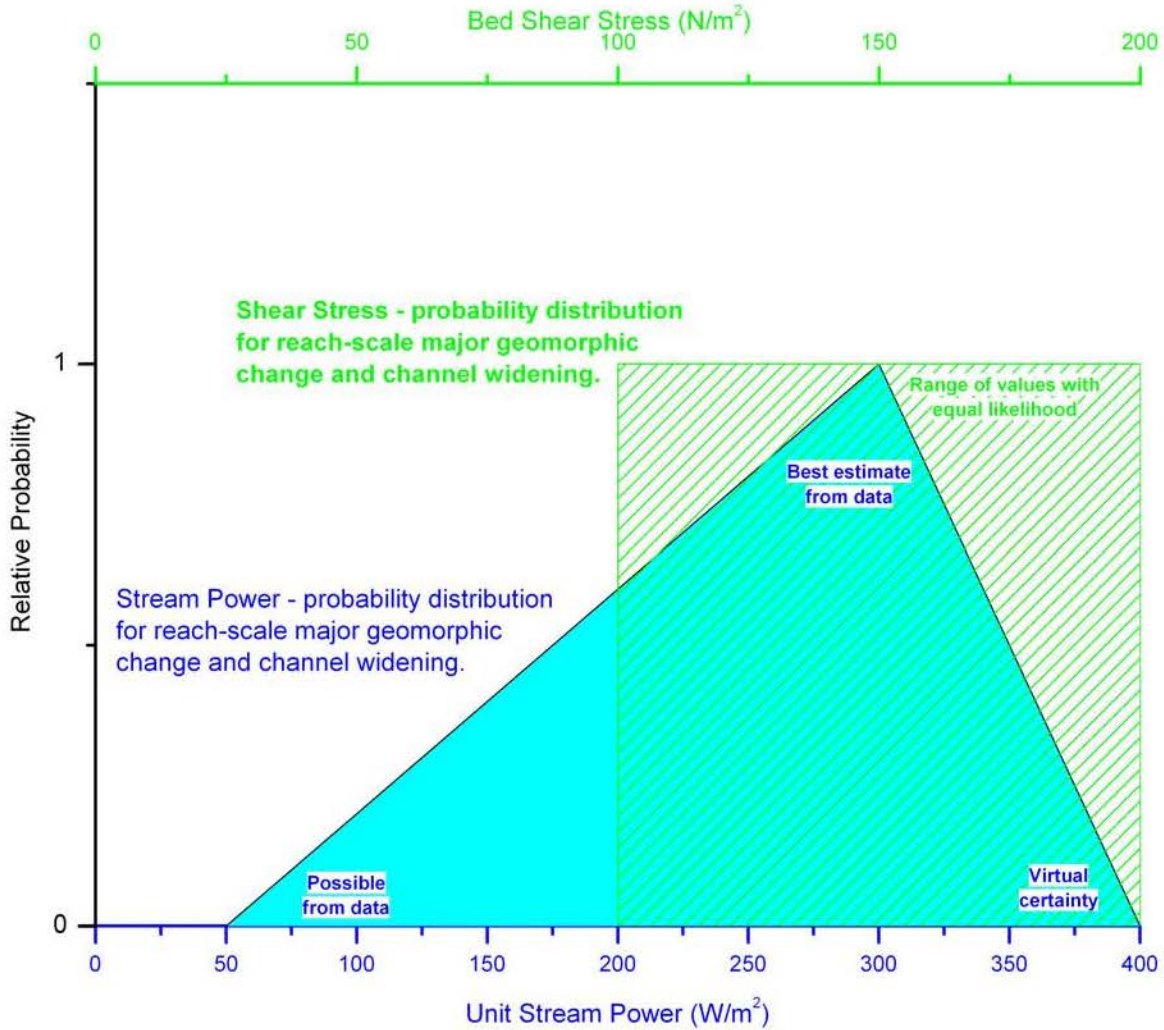


**Figure 3-3 Probability distributions for major channel modifications based on channel averaged stream power and shear stress values. See Appendix D for discussion of data used to define these distributions**

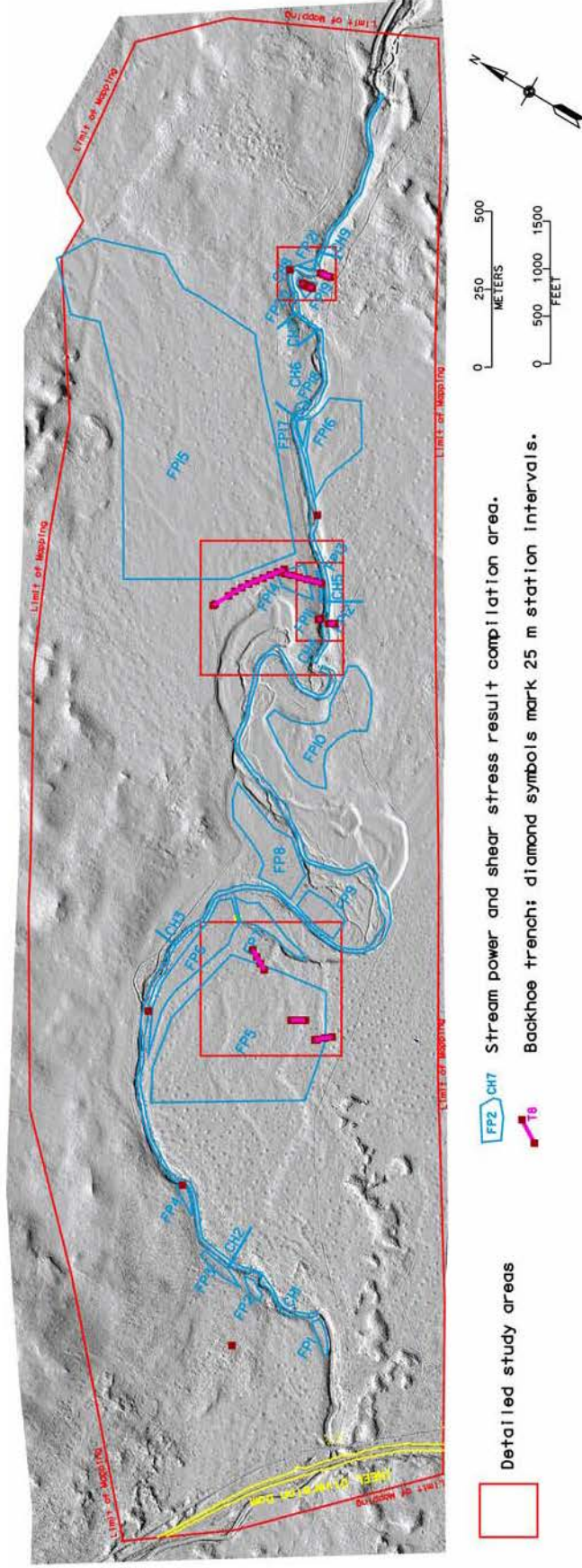


**Figure 3-4 Stream power and shear stress sample areas along Big Lost River Diversion Dam study reach. See Table 3-1 and Table 3-2 for summary of characteristics of each subarea.**

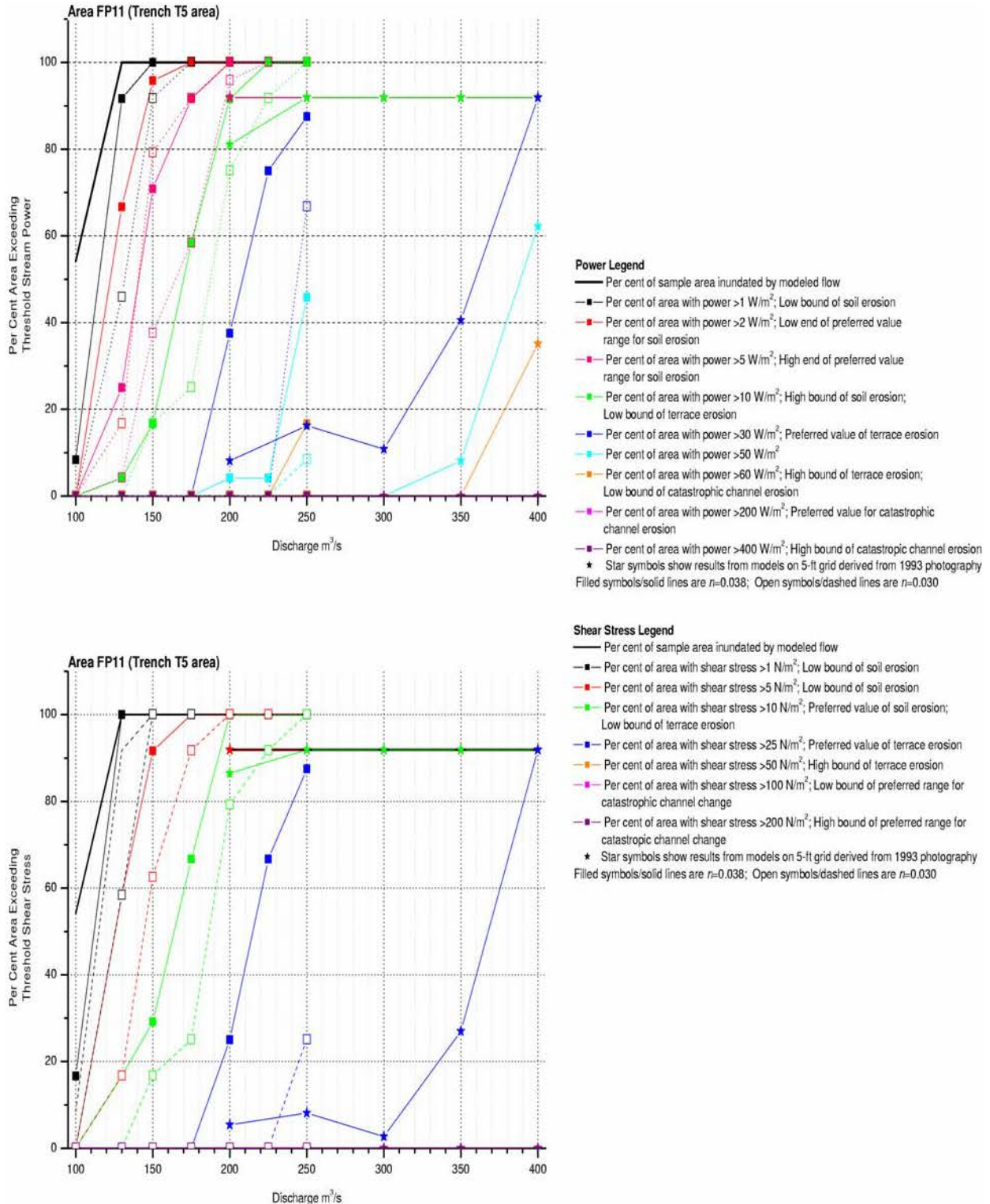


**Figure 3-5 Example of stream power and shear stress results for subarea FP11.** Colored lines and symbols correspond to key values (listed in legend above) on the PDF of **Figure 3-2**. Each symbol represents the percent area exceeding the threshold values for a single flow simulation. Colored lines between symbols represent change between simulations of different discharge. Lines with colored stars are data from models on 5-ft grid derived from 1993 photography.

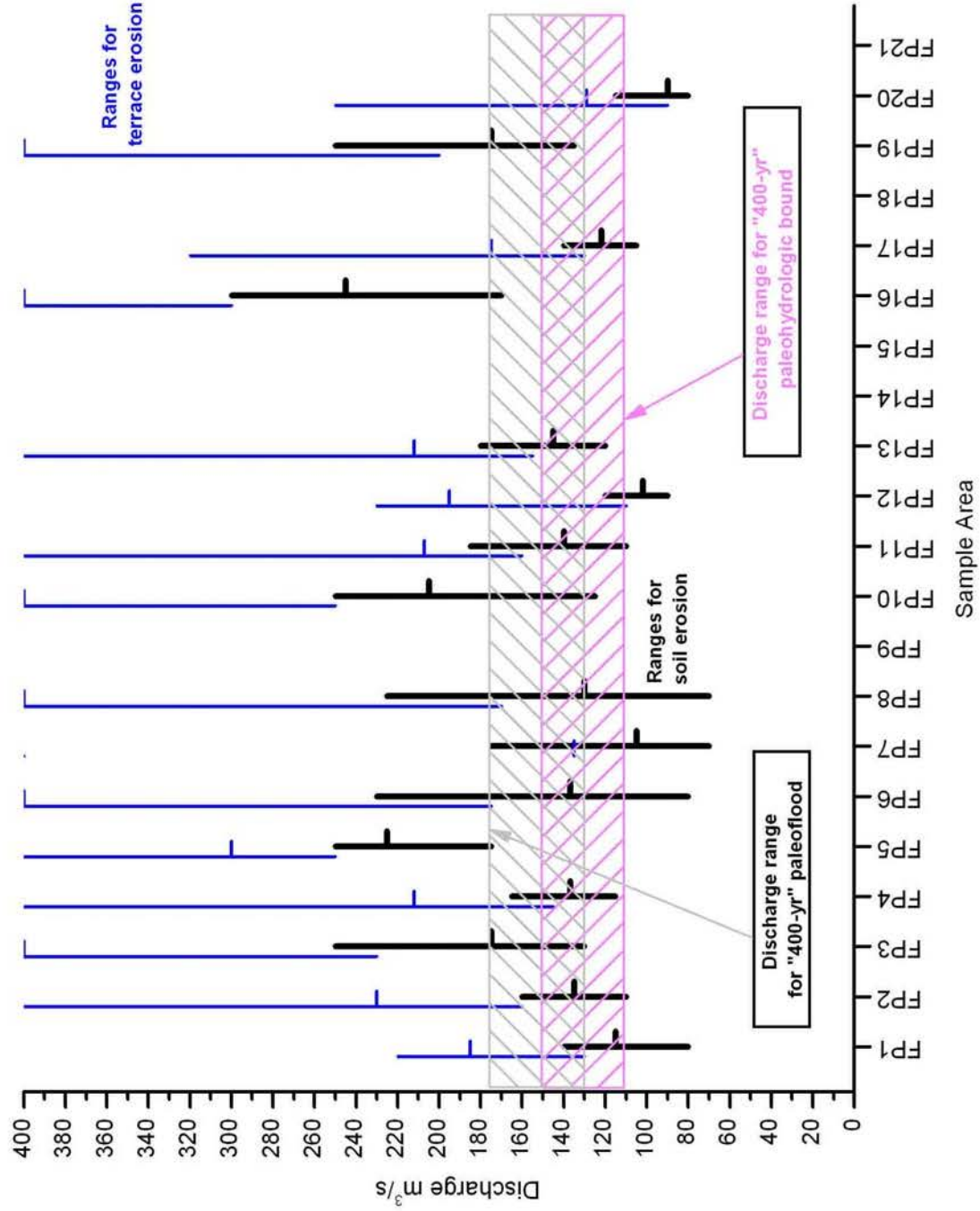


**Figure 3-6 Combined discharge limits for late Holocene paleofloods and paleohydrologic bounds.** Estimated discharge ranges for soil erosion, black bars and terrace erosion, blue bars are from (Table 3-3). Gray cross-hatching shows discharge range for paleofloods; magenta cross-hatch shows range for paleohydrologic bound (Table 3-5). See (Figure 3-4) for sample area locations, (Table 3-4) for applicability, and (Table 3-1) for sample area descriptions.

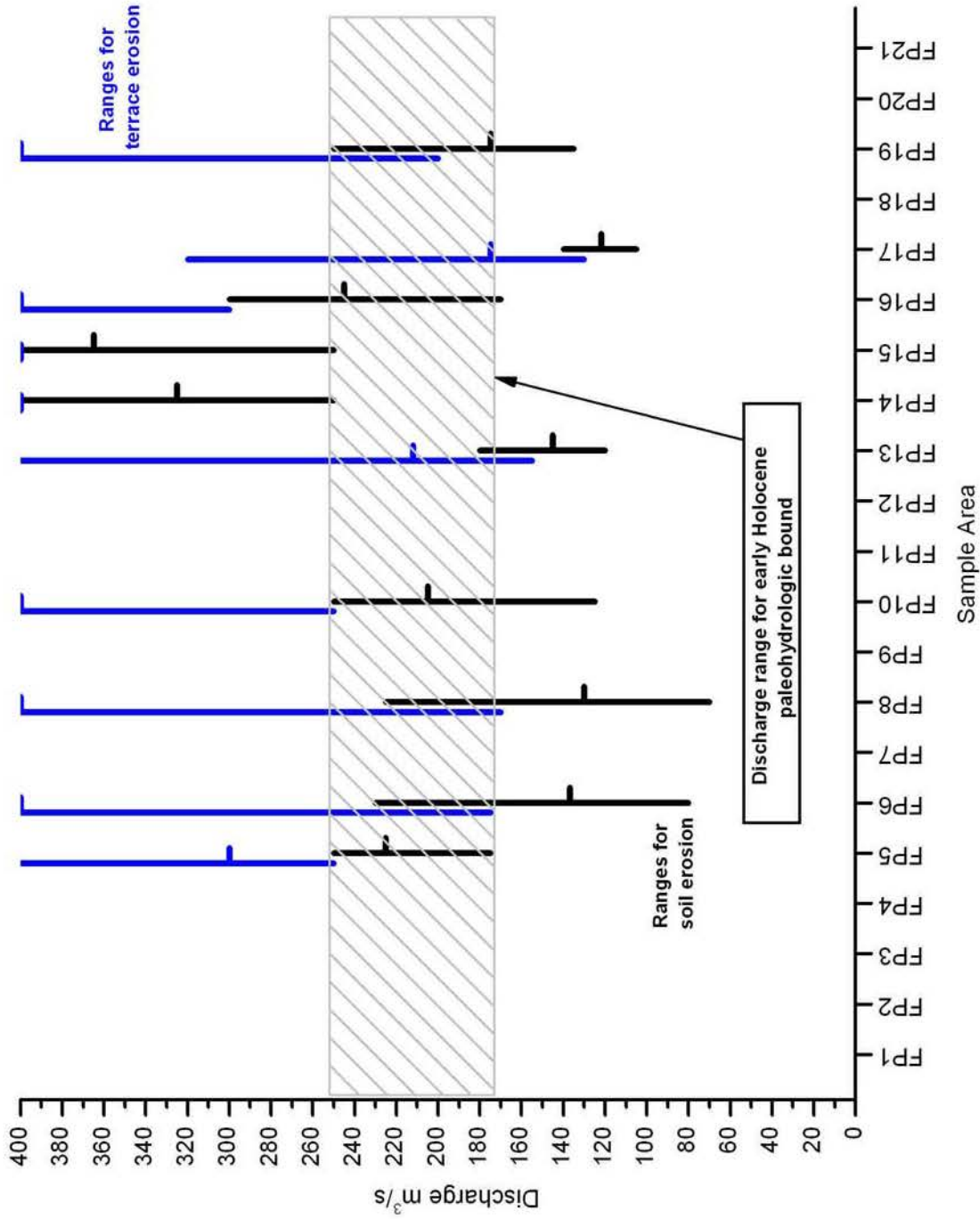


**Figure 3-7 Combined discharge limits for early Holocene paleohydrologic bound.** Cross hatching shows discharge range for early Holocene (T1) paleohydrologic bound (Table 3-5). See (Figure 3-6) for additional explanation of symbols.

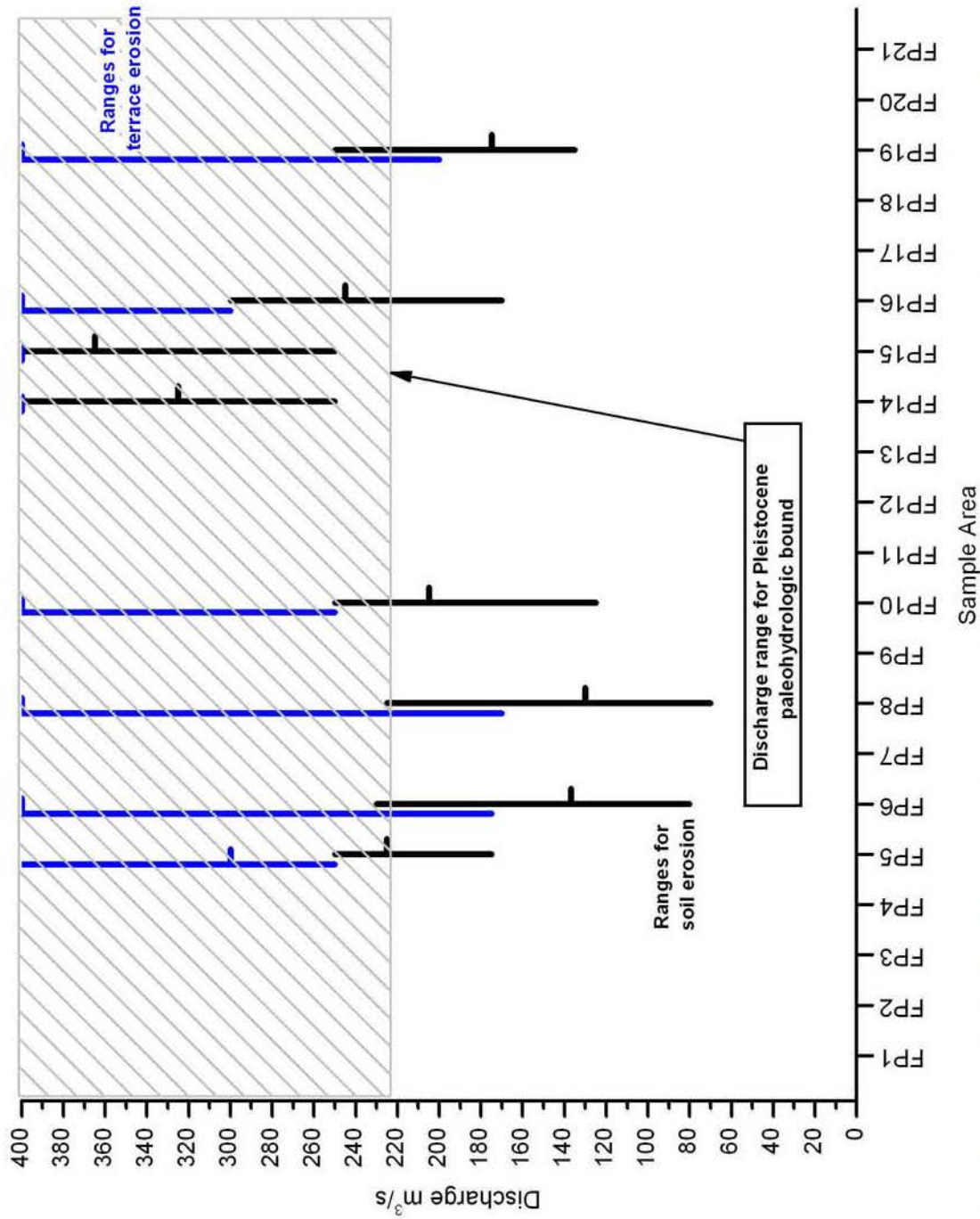


**Figure 3-8 Combined discharge limits for Pleistocene paleohydrologic bound.** Cross hatching shows discharge range for Pleistocene paleohydrologic bound (Table 3-5). See (Figure 3-6) for additional explanation of symbols.

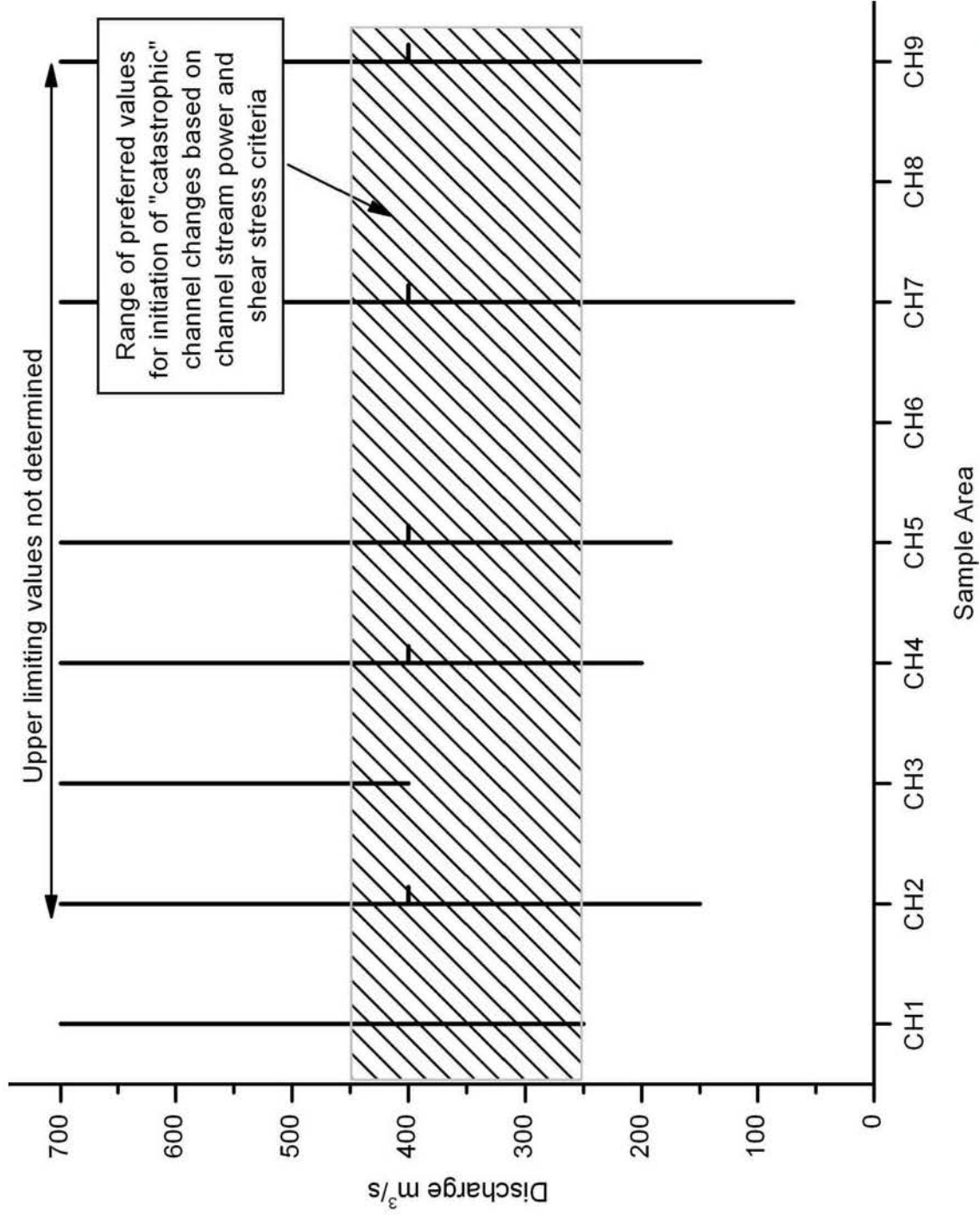


**Figure 3-9 Combined discharge limits for catastrophic channel change.** Upper limiting values are arbitrarily plotted at 700 m<sup>3</sup>/s. See **Figure 3-6** for additional explanation of symbols. Sample area descriptions are in **Table 3-2**. Subarea data from **Appendix D, Figure D3-27** through **D3-37**.

**Tables for Section 3.0**

**Table 3-1 Hydraulic modeling sample area characteristics - floodplain subareas**

| Sub-area | Area and Number of Cells          |                                   | Geomorphic and Geologic Characteristics |   |  |  |                          |   |
|----------|-----------------------------------|-----------------------------------|---|---|--|--|--------------------------|---|
|          | Number of 6-ft cells <sup>1</sup> | Area                              |   | Map unit and surface morphology                             | Surficial deposits /soil               | Underlying deposits                            | Trenches or sites        | Other   |
|          |                                   | ft <sup>2</sup> (m <sup>2</sup> ) | acres (hectare)                         |   |  |  |                          |   |
| FP1      | 902                               | 32472 (3017)                      | 0.74 (0.30)                             | H1-2; smooth terrace surface                                | silt and sand                          | not exposed                                    | n.a                      | Beginning of model reach  |
| FP2      | 595                               | 21420 (1990)                      | 0.49 (0.20)                             | H3 and Rd; overflow channel; and basalt outcrop             | silt and sand in channel; rock outcrop | basalt(?)                                      | n.a.; Juniper Bends site | Probable flow in channel from pre-INEEL Diversion floods                                  |
| FP3      | 1068                              | 38448 (3572)                      | 0.88 (0.36)                             | H1-2 onlap onto Qbd outcrops                                | silt and sand; minor areas of basalt   | Thin(?) veneer of fluvial sediment over basalt | n.a.; Juniper Bends site |   |
| FP4      | 538                               | 19368 (1799)                      | 0.44 (0.18)                             | H2; smooth terrace surface                                  | silt and sand                          | > 1m of fine sediment                          | BLR7 on d/s edge         |   |
| FP5      | 60286                             | 2170296 (201627)                  | 49.69 (20.11)                           | P2; subdued braided channels with large earth mounds        | silt and sand with local pavement      | ±0.5 m silt and sand overlying gravel          | T1, T2, T3               |   |
| FP6      | 9435                              | 339660 (31555)                    | 7.78 (3.15)                             | P3/H1-2; smooth terrace; few muted earth mounds             | silt and sand                          | gravel(?)                                      | n.a.                     | BLR2 is on inset terrace at upstream end of FP6 area                                      |
| FP7      | 3390                              | 122040 (11338)                    | 2.79 (1.13)                             | H1-2; mostly smooth surface; minor channels                 | silt and sand                          | (?)  | n.a.                     |   |
| FP8      | 10401                             | 374436 (34786)                    | 8.57 (3.47)                             | P3/H1; smooth terrace; few muted earth mounds               | silt and sand                          | thin silt and sand gravel(?)                   | n.a.                     | Historical irrigation ditch on u/s side is not eroded; historical use as field or pasture |
| FP9      | 3469                              | 124884 (11602)                    | 2.86 (1.16)                             | H2/H3; mostly smooth terrace with channels on lower portion | silt and sand                          | (?)  | n.a.                     | Historical irrigation ditch on u/s side is not eroded; historical use as field or pasture |

Notes: <sup>1</sup> For 5-ft grid models, average number of cells is ~145% of number of 6-ft grid cells.

**Table 3-1 Hydraulic modeling sample area characteristics - floodplain subareas**

| Sub-area | Area and Number of Cells          |                                   | Geomorphic and Geologic Characteristics |   |                          |  |                   | Other   |
|----------|-----------------------------------|-----------------------------------|---|---|--------------------------|--|-------------------|---|
|          | Number of 6-ft cells <sup>1</sup> | Area                              |   | Map unit and surface morphology   | Surficial deposits /soil | Underlying deposits                                | Trenches or sites |   |
|          |                                   | ft <sup>2</sup> (m <sup>2</sup> ) | acres (hectare)                         |   |                          |  |                   |   |
| FP10     | 15504                             | 558144 (51853)                    | 12.78 (5.17)                            | P3/H1; smooth terrace; few muted earth mounds; eroded d/s margin                          | silt and sand            | silt and sand overlying gravel(?)                  | n.a.              | Western portion eroded; earth mounds more prevalent in eastern half; Affected by backwater from saddle constriction |
| FP11     | 24                                | 864 (80)                          | 0.02 (0.01)                             | H1-2; smooth terrace and riser to P2 surface  | silt and sand            | basalt outcrops in stream bank                     | T5                |   |
| FP12     | 23                                | 828 (77)                          | 0.02 (0.01)                             | H1-2; small area between basalt outcrops  | silt and sand            | basalt outcrops in banks; gravel on higher surface | T4                |   |
| FP13     | 236                               | 8496 (789)                        | 0.19 (0.08)                             | H1-2; long, narrow, smooth terrace  | silt and sand            | >1 m fine sediments                                | T6                |   |
| FP14     | 2095                              | 75420 (7007)                      | 1.73 (0.70)                             | P3; minor eolian sand; smooth terrace surface   | silt and sand            | <0.5 m silt and sand overlying gravel              | T6                |   |
| FP15     | 152753                            | 5499108 (510884)                  | 125.90 (50.95)                          | P1-2; subdued braided channels with large earth mounds; minor areas of eolian sand sheets | silt and sand            | ±0.5 m silt and sand overlying gravel              | T7                | Several wheel tracks; includes circular area cleared as target for old bombing range                                |

Notes: <sup>1</sup> For 5-ft grid models, average number of cells is ~145% of number of 6-ft grid cells.

**Table 3-1 Hydraulic modeling sample area characteristics - floodplain subareas**

| Sub-area | Area and Number of Cells          |                                   | Geomorphic and Geologic Characteristics |   |                             |  |                   |   |
|----------|-----------------------------------|-----------------------------------|---|---|-----------------------------|--|-------------------|---|
|          | Number of 6-ft cells <sup>1</sup> | Area                              |   | Map unit and surface morphology                 | Surficial deposits /soil    | Underlying deposits                                | Trenches or sites | Other   |
|          |                                   | ft <sup>2</sup> (m <sup>2</sup> ) | acres (hectare)                         |   |                             |  |                   |   |
| FP16     | 10913                             | 392868 (36499)                    | 8.99 (3.64)                             | P2/P3; braided channels with large earth mounds | silt and sand               | ±0.5 m silt and sand overlying gravel(?)           | n.a.              | T6 is on inset terrace near upper end of area |
| FP17     | 477                               | 17172 (1595)                      | 0.39 (0.16)                             | H1-2; smooth terrace                            | silt and sand               | (?)  | n.a.              |   |
| FP18     | 199                               | 7164 (666)                        | 0.16 (0.07)                             | Rb; scoured basalt outcrop                      | basalt; minor sand and silt | basalt   | n.a.              |   |
| FP19     | 427                               | 15372 (1428)                      | 0.35 (0.14)                             | H1; smooth terrace surface                      | silt and sand               | silt and sand; minor fine gravel                   | T8b,c             |   |
| FP20     | 178                               | 6408 (595)                        | 0.15 (0.06)                             | H2; smooth terrace surface                      | silt and sand               | silt and sand; increasing gravel away from channel | T8a,b             | BLR8 on similar inset surface across channel  |
| FP21     | 266                               | 9576 (890)                        | 0.22 (0.09)                             | Rb; scoured basalt outcrop                      | basalt; minor silt and sand | basalt   | n.a.              |   |

Notes: <sup>1</sup> For 5-ft grid models, average number of cells is ~145% of number of 6-ft grid cells.

Table 3-2 Hydraulic modeling sample area characteristics - channel subareas

| Sub-area | Number of Cells <sup>1</sup> , Area <sup>2</sup> and Length |                                   |                 | Geomorphic and Geologic Characteristics |  |   |   |
|----------|---|-----------------------------------|-----------------|---|--|---|---|
|          | Number of 6-ft cells  | Area                              |                 | Channel form                            | Bed/bank materials   | Notes   |   |
|          |   | ft <sup>2</sup> (m <sup>2</sup> ) | acres (hectare) |   |  |   | Length<br>ft (m)                                |
| CH1      | 1305  | 46980 (4365)                      | 1.08 (0.44)     | 1154 (352)                              | Mostly straight with small amplitude bends. Single thread; rock controlled.  | Common rock outcrops in bed and banks with rock constrictions; long section of fluted and scoured rock bed. Some banks of P2 gravels and fine-grained lateral accretion deposits (H1/H2/H3).  | "Juniper Bends area"                            |
| CH2      | 4533  | 163188 (15161)                    | 3.74 (1.51)     | 3773 (1150)                             | Gently curving; one sharp bend at BLR2 (FP4). Single thread.   | Scattered rock outcrops in bed throughout length; some rock in banks near and upstream of BLR2 (FP4). Bed mostly sand and fine gravel. Right bank mostly fine-grained lateral accretion deposit (H1-2) against P2 gravel. Left bank mostly H2/H3 fine-grained deposits. | BLR2 and BLR7 bank exposures are in this reach. |
| CH3      | 9920  | 357120 (33178)                    | 8.18 (3.31)     | 7830 (2387)                             | Large amplitude s-bends; tighter radius at downstream end. Single thread at upstream end, multi thread in central portion of meanders. | Sand and gravel in bed and banks. Rock outcrops in bed and banks are limited to scattered occurrences at downstream end of sample area just upstream of Saddle constriction. Bank materials are heterogeneous mix of silty/sandy alluvium and gravel of all ages.       | "Big Loop"                                      |

Notes: <sup>1</sup> For 5-ft grid models, average number of cells is ~145% of number of 6-ft grid cells.

<sup>2</sup> Channels are oblique to orientation of rectangular grid in most areas. Sample areas are defined along base of bank for low-flow channel. At most sections, this typically includes 3-5 cells across channel floor, so typical width is about 5-9 m (~18-30 ft).

**Table 3-2 Hydraulic modeling sample area characteristics - channel subareas**

| Sub-area | Number of Cells <sup>1</sup> , Area <sup>2</sup> and Length |                                   | Geomorphic and Geologic Characteristics |              |  | Notes   |   |
|----------|---|-----------------------------------|---|--------------|--|---|---|
|          | Number of 6-ft cells  | Area                              |   | Channel form | Bed/bank materials   |   |   |
|          |   | ft <sup>2</sup> (m <sup>2</sup> ) | acres (hectare)                         |              |  |   | Length<br>ft (m)  |
| CH4      | 877   | 31572 (2933)                      | 0.72 (0.29)                             | 668 (204)    | Straight reach with very gentle s-bend and large rock constrictions. Single thread, rock controlled. | Bed is mostly sand and gravel with scattered rock outcrops. Rock section in bed just upstream. Banks are controlled by rock outcrops. Intervening bank areas are H1/H2 lateral accretion terraces.                  | "Saddle constriction". Trench sites T4 and T5 (FP11 and FP12) are adjacent to the downstream portion of this reach. |
| CH5      | 2444  | 87984 (8174)                      | 2.01 (0.82)                             | 1965 (599)   | Mostly straight reach. Single thread.  | Bed is gravel. Right bank mostly P2/P3 gravel with narrow H1/H2 lateral accretion terrace and few rock outcrops. Left bank is wider H1/H2 terrace.  | Trench T6 is on left bank in upstream section; BLR6 is on right bank, mid-reach.                                    |
| CH6      | 1322  | 47592 (4421)                      | 1.09 (0.44)                             | 1030 (314)   | 90° bend at upstream end; mostly straight with gentle left bends. Single thread with rock control.   | Rock in bed near upstream portion. Scattered outcrops in bed downstream, otherwise gravel. Scattered rock outcrops along banks; most banks H1/H2/H3 terraces.   |   |
| CH7      | 198   | 7128 (662)                        | 0.16 (0.07)                             | 260 (79)     | Rock constriction. Straight, single thread.  | Gravel bed. Banks are rock, with small areas of fine-grained H1/H2 deposits between outcrops.   | "Bridge constriction"   |
| CH8      | 1195  | 43020 (3997)                      | 0.98 (0.40)                             | 934 (285)    | Tight s-bend with rock controls. Single thread.  | Mostly gravel bed with many rock outcrops. Large areas of rock control in middle of reach. Rock banks and constriction on middle/downstream portion. Upstream banks are H2/H3 fine-grained deposits.                | BLR8 on right bank mid-reach. T8 and T9 trenches on right banks in middle portion of reach.                         |
| CH9      | 1444  | 51984 (4829)                      | 1.19 (0.48)                             | 1852 (564)   | Mostly straight with gentle bends. Single thread with rock control.                                  | Bed is gravel with several rock outcrops. Right bank has narrow H4 fine-grained terrace along most of length with scattered rock outcrops. Left bank is H2/H3/H4 fine-grained terrace with scattered rock outcrops. |   |

Notes: <sup>1</sup> For 5-ft grid models, average number of cells is ~145% of number of 6-ft grid cells.

<sup>2</sup> Channels are oblique to orientation of rectangular grid in most areas. Sample areas are defined along base of bank for low-flow channel. At most sections, this typically includes 3-5 cells across channel floor, so typical width is about 5-9 m (~18-30 ft).

**Table 3-3 Summary of limiting discharge values from hydraulic modeling sample areas**

| Sample Area | Per Cent Area Meeting Erosion Criteria | Discharge (m <sup>3</sup> /s) |                 |            |                 |                 |             |
|-------------|--|-------------------------------|-----------------|------------|-----------------|-----------------|-------------|
|             |  | Soil Erosion                  |                 |            | Terrace Erosion |                 |             |
|             |  | Low Bound                     | Preferred Value | High Bound | Low Bound       | Preferred Value | High Bound  |
| FP1         | 50                                     | 80-110                        | 115             | 130-140    | 130-140         | 170-200         | 220         |
| FP2         | 50                                     | 110                           | 120-150         | 160        | 160             | 220-240         | >400(?)     |
| FP3         | 50                                     | 130-140                       | 160-190         | 230-250    | 230-250         | >400(?)         | >400(?)     |
| FP4         | 50                                     | 115                           | 120-145         | 145-165    | 145-165         | 205-220         | 350-400(?)  |
| FP5         | n.a.*                                  | 175                           | 225             | 250        | 250             | 300             | 400         |
| FP6         | 50                                     | 80-100                        | 115-160         | 175-230    | 175-230         | >400(?)         | >400(?)     |
| FP7         | 50                                     | <70                           | <90-125         | 135-175    | 135-175         | >400(?)         | >400(?)     |
| FP8         | 50                                     | <70                           | 95-160          | 170-225    | 170-225         | >400(?)         | >400(?)     |
| FP9         | 50                                     | <70                           | <70             | 80-100     | 80-100          | 250             | >400(?)     |
| FP10        | n.a.*                                  | 125-160                       | 160-250         | 250        | 250             | >400(?)         | >400(?)     |
| FP11        | 50                                     | 110                           | 120-160         | 160-185    | 160-185         | 200-215         | >400(?)     |
| FP12        | 50                                     | 90                            | 95-110          | 110-120    | 110-120         | 130-160         | 160-230     |
| FP13        | 50                                     | 115-120                       | 130-160         | 155-180    | 155-180         | 205-220         | 270->400(?) |
| FP14        | n.a.*                                  | 250                           | 300-350         | 400-450    | 400-450         | >400(?)         | >400(?)     |
| FP15        | n.a.*                                  | 250                           | 330-400         | >400(?)    | >400(?)         | >400(?)         | >400(?)     |
| FP16        | n.a.*                                  | 170-220                       | 220-270         | 300        | 300             | >400(?)         | >400(?)     |
| FP17        | 50                                     | 105-110                       | 115-130         | 130-140    | 130-140         | 165-185         | 220-320     |
| FP18        | 50                                     | 60                            | 65-70           | 80         | 80              | 100-110         | 130-190     |
| FP19        | 50                                     | 135-140                       | 150-200         | 200-250    | 200-250         | >400(?)         | >400(?)     |
| FP20        | 50                                     | 80                            | 90              | 90-115     | 90-115          | 120-140         | 155-250     |
| FP21        | 50                                     | 30                            | 35              | 40         | 40              | 45-60           | 60-90       |

Notes:  
\* n.a. - Flow in these areas is concentrated in paleochannels where initial erosion would preferentially be concentrated in small portions of the sample area.

**Table 3-4 Applicability of hydraulic modeling sample areas to paleofloods and paleohydrologic bounds estimates**

| Sample Area | Event Name    |                |                  |                        |                              |             |
|-------------|---------------|----------------|------------------|------------------------|------------------------------|-------------|
|             | Paleofloods   |                |                  | Paleohydrologic Bounds |                              |             |
|             | "white flood" | "400-yr" flood | "older flood(s)" | 400-yr #1              | early Holocene (H1 surfaces) | Pleistocene |
| FP1         |               | G              |                  | G                      |                              |             |
| FP2         |               | G              |                  |                        |                              |             |
| FP3         |               |                | G                | G                      |                              |             |
| FP4         |               | S              | G                | G,S                    |                              |             |
| FP5         |               |                | G,S              |                        | G                            | G,S         |
| FP6         |               | G,S            | G,S              | G,S                    | G                            | G           |
| FP7         |               | G              |                  | G                      |                              |             |
| FP8         |               | G              | G                | G                      | G                            | G           |
| FP9         | G             |                |                  |                        |                              |             |
| FP10        |               | G              | G                | G                      | G                            | G           |
| FP11        | S             | G,S            | G,S              | G,S                    |                              |             |
| FP12        | S             | G,S            | G,S              | G,S                    |                              |             |
| FP13        | S             | G,S            | G,S              | G,S                    | G,S                          |             |
| FP14        |               |                |                  |                        |                              | G,S         |
| FP15        |               |                |                  |                        |                              | G,S         |
| FP16        |               | G              | G                | G                      | G,S                          | G           |
| FP17        |               | G              | G                | G                      | G                            |             |
| FP18        | G             |                |                  |                        |                              |             |
| FP19        |               | S              | S                | G,S                    | G,S                          | G,S         |
| FP20        |               | S              | S                | G,S                    |                              |             |
| FP21        | G             |                |                  |                        |                              |             |

Notes: S = Stratigraphic evidence; G = Geomorphic evidence

**Table 3-5 Big Lost River Paleofloods and Paleohydrologic Bounds**

| Event name   | Age or time span (Cal yrs or Cal yr B.P) <sup>1</sup> | Discharge (m <sup>3</sup> /s) and type of distribution | Summary of Evidence  |
|--|---|--|--|
| Paleofloods  |   |  |  |
| "white flood"  | >100yr (pre-gaging) but less than 400-600yr           | 90 (80-100) uniform                                    | Based on thin deposit in T4. Not recognized in T5 or T6 (slightly higher sites). Possible correlative in T9(?). Age - most likely 100 to 150 years based on absence of soil development. Discharge - Upper limit based on rapid increase in power/shear stress at T4 and lack of deposit in T5/T6.   |
| "400-yr" flood   | 400 to 600 years                                      | 150 (130-175) triangular                               | Apparently correlative deposits in T4, T5, T6 (also BLR2, BLR7 & BLR8) with similar soils, stratigraphic setting, and radiocarbon ages. Soil has stage I- Bk horizon. Stripping of A- and AB/Bw horizons at T8c, partial stripping at T8b; lack of erosion at T8a. May represent more than one flood.  |
| "older flood"  | 1000 to 2000 years                                    | 150 (130-175) triangular                               | Deposits with Stage I to I+ Bk horizon that underlie "400-yr flood" deposits in T4, T5, T6 and T9. Appears to indicate long period of stability with little or no deposition at these sites before deposition of deposits associated with "400-yr" flood. Similar stratigraphy at BLR2 and BLR8. Likely represents multiple floods of similar or smaller maximum discharge. Minimum discharge must inundate FP1-FP4, FP6-8, most of FP7, FP11-13, FP17-18, and FP19-21, which are areas with H1-2 geomorphic surfaces that appear to indicate Holocene flooding. |
| Paleohydrologic Bounds   |   |  |  |
| 400-yr #1  | 400-600   | 130 (110-150) triangular                               | Preservation of recognizable stratigraphy at T4 and T6. No stripping of A-horizons from the youngest deposits at T4 and T6. Apparently correlative H1-2 geomorphic surfaces at FP1, FP3-4, FP7, FP11-13, FP17, and FP19-20.  |
| early Holocene (H1 surfaces)   | 6000 to 8000  | 225 (175-250) triangular                               | Preservation of stratigraphy in T6, T4, and T8a,b,c. Banks at BLR6 and continuity of H1-2 geomorphic surfaces along BLR.   |
| Pleistocene  | >10000  | 250 (225-400) triangular                               | Preservation of Pleistocene gravel surfaces throughout the study reach. Actual age of the underlying deposits is older than 12-15 ka (minimum age of deglaciation) and some may be older than 20-25 ka (Last glacial maximum). Length of time span for paleohydrologic bound is limited by post-glacial, warmer climate more similar to present.   |
| Notes: <sup>1</sup> All age distributions have uniform probability over the indicated time span uncertainty. |   |  |  |



## **4.0 REVISED FLOOD FREQUENCY FOR THE BIG LOST RIVER AT THE INEEL DIVERSION DAM**

It is necessary to revise flood frequency estimates for two reasons. First, peak discharge values have been slightly modified for several data points, including the paleohydrologic non-exceedence bounds. Second, the distribution of observed peak discharges and paleohydrologic information is sufficiently complex that parametric flood frequency functions are ill-suited to determine statistical quantities, such as credible or “confidence” limits for flood frequency estimates. Consequently, a newly-published nonparametric Bayesian flood frequency estimation approach (O’Connell, 2005) is used to obtain probabilistic minimum-bias estimates of flood frequency.

### **4.1 Nonparametric Flood Frequency for the Big Lost River at INL**

The nonparametric Bayesian Monte Carlo method of O’Connell (2005) is used to estimate flood frequency. This method accommodates complex flood behaviors such as event clustering (repeated instances of similar magnitude floods) and can use varied data, such as gage and historical peak discharges, and paleohydrologic upper and lower bounds on peak discharge, while rigorously accounting for a wide variety of measurement uncertainties. In contrast to nonparametric kernel estimation approaches, the stochastic assumption is used to generate flood frequency models that span the data and provide about twice the number of degrees of freedom of the data. Each generated flood frequency model is scored using likelihoods that account for data measurement uncertainties. A parametric estimation approach ensures high precision because posterior sampling is known. However, parametric approaches can produce substantial biases because the classes of allowed flood frequency models are restricted. These biases are completely undetectable within a parametric paradigm. To minimize these types of biases, the nonparametric approach used here surrenders some precision, but produces greater overall accuracy and assurance; it reveals the annual probabilities where discharge becomes unconstrained by the data, thereby eliminating unsubstantiated extrapolation. Parametric flood frequency estimation introduces strong extrapolation priors that make it difficult, if not impossible, to determine when flood frequency is no longer constrained by the data. These

problems are apparent in the parametric method of O'Connell et al. (2002) used in the previous INL flood-frequency analyses (Ostenaar et al., 1999).

Measurement uncertainty is included using discrete pdf's. Gaussian measurement uncertainties of  $2\sigma=25\%$  are used for the gage data (see **Figure 4-1** for an example for the largest gage flood). The smaller (historical) paleoflood is assigned a uniform likelihood for discharges from 80 m<sup>3</sup>/s (cms) to 105 cms and its corresponding non-exceedence bound is assigned a uniform likelihood for discharges from 80 cms to 110 cms. The non-uniform measurement uncertainties for the rest of the nonexceedence bounds and paleofloods are shown in **Figure 4-1**.

Monte Carlo integration is used with a total of 320,000 randomly-created flood-frequency models to produce posterior estimates of probability density for peak discharge at target annual exceedence probabilities (AEP) and for cumulative probability (which is transformed to AEP for plotting) associated with target peak discharges. The 25 least frequent AEP positions used to randomly generate peak discharge values are shown in **Table 4-1** which reflect about twice the number of degrees of freedom represented by the data for AEP's < 0.1.

Peak discharges were randomly generated at all data points plotted in **Figure 4-2**, with the caveat that the peak discharges for  $T < 10$  years were rescaled to a maximum of half their values to avoid having the reordering of small flows influence the distribution of the large flows of interest. The cumulative frequency (*cf*) node positions at  $T=30,000$  years and  $T=40,000$  years were added to provide an extrapolation limit for the computation. As shown in **Figure 4-2** non-informative peak discharge priors were selected for AEP's < 0.1 by expanding the prior to include discharges much larger than the observed data. These priors adequately represent an ignorance function relative to the magnitude of floods and bounds in the input data. Construction of such a prior is essential for determining the AEP limit where observed data no longer provide any meaningful constraints on flood frequency. The range of peak discharges included in the Bayesian estimation of flood frequency as a function of AEP and return period are shown in **Figure 4-2** by the yellow region. The maximum number of peak discharge resorting operations allowed before rejecting a random flood frequency model was set to seven and represented less than a third of the total number of degrees of freedom.

Monte Carlo nonparametric flood frequency results using 320,000 random models are shown in **Figure 4-2**. Formal Monte Carlo relative errors are 2.7% based on the approach used in O'Connell (2005), but actual convergence appears to be much faster, because flood frequency estimates obtained using 8000, 40,000 and 320,000 random models are virtually the same. Sampling density functions are substantially broader than the nonzero regions of posterior density (**Figure 4-2**). The best-fitting models reproduce all the observed data well (**Figure 4-2**). This result is expected since arbitrary flood frequency shapes can be generated by the nonparametric process. It is instructive to inspect sampling functions, posterior pdf's and *cf*'s for individual return periods that show more detail than can be portrayed in **Figure 4-2**.

The cluster of floods in the 80-90 cms range (**Figure 4-2**) places strong constraints on the  $T=100$  year and  $T=150$  year discharges, although the  $T=150$ -year pdf begins to develop a longer tail at maximum discharges (**Figure 4-3**). The increased uncertainty in estimated discharges for AEP's  $< 0.01$  is apparent in the expanding upper tail in the discharge pdf's for  $T=200$  years and  $T=350$  years (**Figure 4-4**) which is also clearly apparent in **Figure 4-2**. Since the only definite information available about the occurrence of floods in this region are the historical and paleoflood, a wide range of peak discharge scenarios are consistent with the flood and nonexceedence bound data for  $T=150$  years to  $T=500$  years, as indicated by the wide region of blue curves in **Figure 4-2** and the expanding upper tails in **Figure 4-3**, **Figure 4-4**, and **Figure 4-5**.

While the discharge mode is dominated by the largest paleoflood for  $T=1000$  years and  $T=2000$  years (**Figure 4-6**) a relatively large range of discharges are allowed because there is little density information in the form of actual floods (only the historical and paleoflood). Consequently, the higher likelihood discharges vary over a wide range constrained mostly by the nonexceedence bounds and the single paleoflood for AEP's  $< 1/1000$  (**Figure 4-2**). This is particularly evident for  $T=3500$  years and  $T=5000$  years, where discharges from slightly the lower limit of the largest paleoflood discharge up to the upper limits of the early Holocene nonexceedence bound are allowed (**Figure 4-7**). For  $T=7500$  years and  $T=10,000$  years, the only constraints are that discharge be as large as the largest paleoflood, but smaller than the late Holocene nonexceedence bound (**Figure 4-8**). As  $T$  extends beyond 10,000 years, the available data provide diminishing constraints with increasing  $T$  (**Figure 4-9**). Once  $T$  is about twice the length of record ( $T=20,000$

years), constraints on the upper bound for discharge become weak, while the constraint that discharge must be as large as the largest paleoflood remain (**Figure 4-9**). This is evident in the large discharge ranges of high likelihood models for AEP's  $< 0.0001$  (shown as blue lines in **Figure 4-2**).

For discharges  $> 100$  cms credible intervals for AEP can be quite large because there is only positive evidence for the actual occurrence of one such discharge (P in **Figure 4-2**). Consequently, AEP's for discharges  $> 100$  cms are only weakly bounded to the right in **Figure 4-2** and in fact become virtually unbounded to the right (are not required to ever occur) for discharges significantly exceeding the largest observed discharge. This means that the right credible limit for discharges  $> \sim 300$  cms becomes a cumulative frequency of one or AEP of zero (**Figure 4-2**, **Figure 4-10**, and **Figure 4-11**). Thus for discharges  $> \sim 300$  cms the most meaningful statistics are bounds to the left in **Figure 4-2** which limit the maximum frequencies of occurrence. Central tendency measures like the mean or median lose statistical significance in these situations. However, for all discharges, the nonexceedence discharge bounds place strong limits on the maximum AEP's that can be associated with particular discharges (**Figure 4-2**).

The densities in **Figure 4-10**, **Figure 4-11**, **Figure 4-12**, and **Figure 4-13** look peculiar relative to the cumulative frequencies because all density/cumulative frequencies calculations are performed in cumulative frequency space and then transformed to AEP/T for plotting. This is why it appears that there is more density to the right (small AEP's) than indicated by the cumulative frequency curves or credible limits in **Figure 4-10**, **Figure 4-11**, **Figure 4-12**, and **Figure 4-13**. For example, the AEP density distribution for a discharge of 106 cms appears unbounded to the right, but the cumulative frequency density is well behaved and provides a useful right credible limit (**Figure 4-12**). When the right credible limits are significant (discharges  $< \sim 300$  cms), they indicate a 90% probability that the AEP is greater than the right credible limit AEP. The wide ranges of AEP's represented between the 10% and 90% credible limits for discharges  $< 300$  cms (**Figure 4-11**, **Figure 4-12**, and **Figure 4-13**) indicate the large range of recurrence uncertainties that result from the lack of strong density information, i.e., multiple observed discharges or discharge exceedences  $> 100$  cms.

As discussed above for this particular dataset there is more statistical significance to the left credible limits, than the mean or right credible limits for discharges  $> \sim 300$  cms. For discharges  $> \sim 300$  cms right credible limits may just as easily extend to AEP=0 as the values reported in the nonparametric flood frequency calculations, and the shape of the densities are generally not compatible with a measure of central tendency, such as a mean. Consequently, mean flood frequency estimates for AEP's  $< 0.0001$  are flagged with stars in **Table 4-2**.

**Figures for Section 4.0**

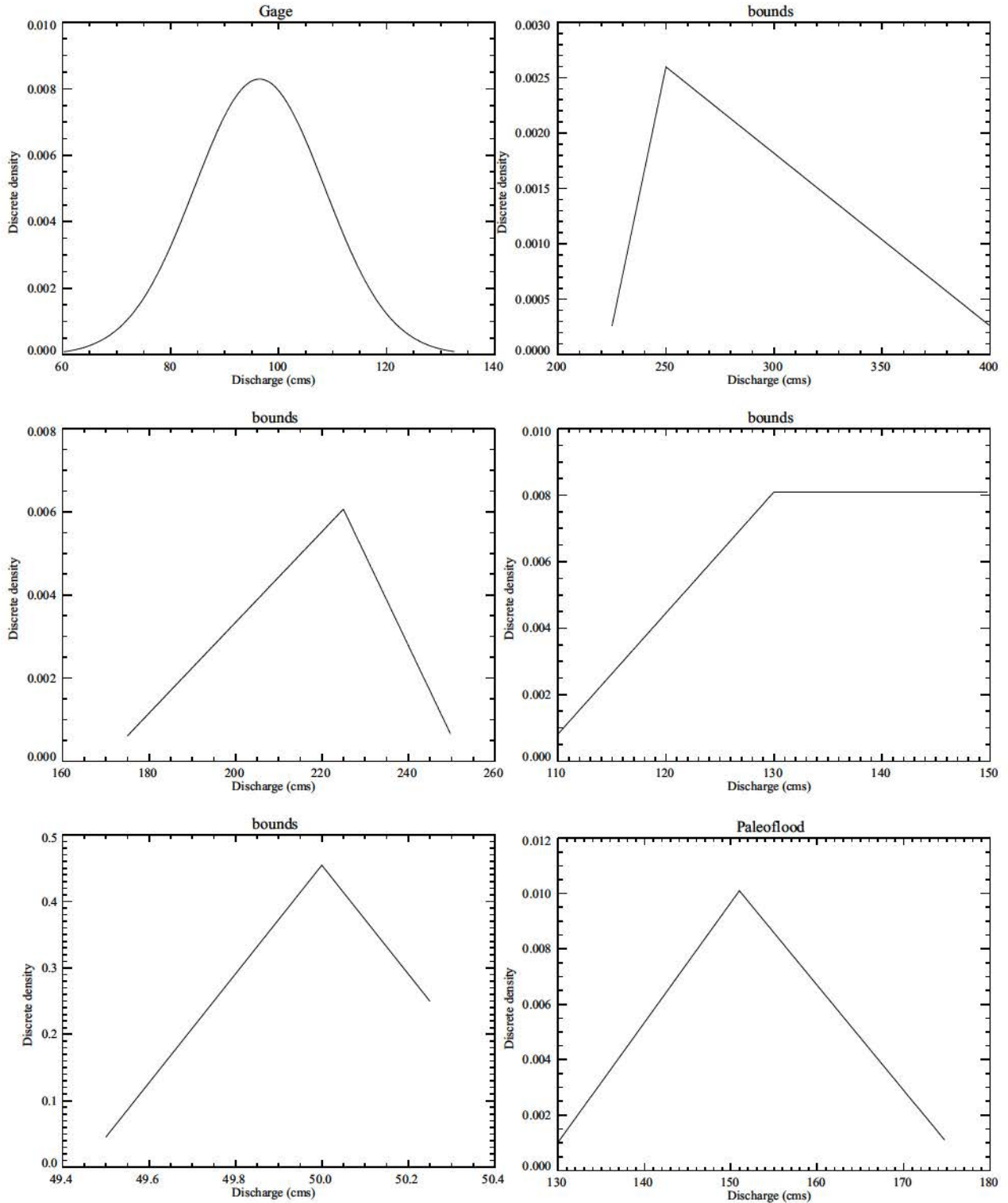


**Figure 4-1 Measurement uncertainties for gage, bound, and paleoflood discharges on the Big Lost River at the INEEL Diversion Dam..**

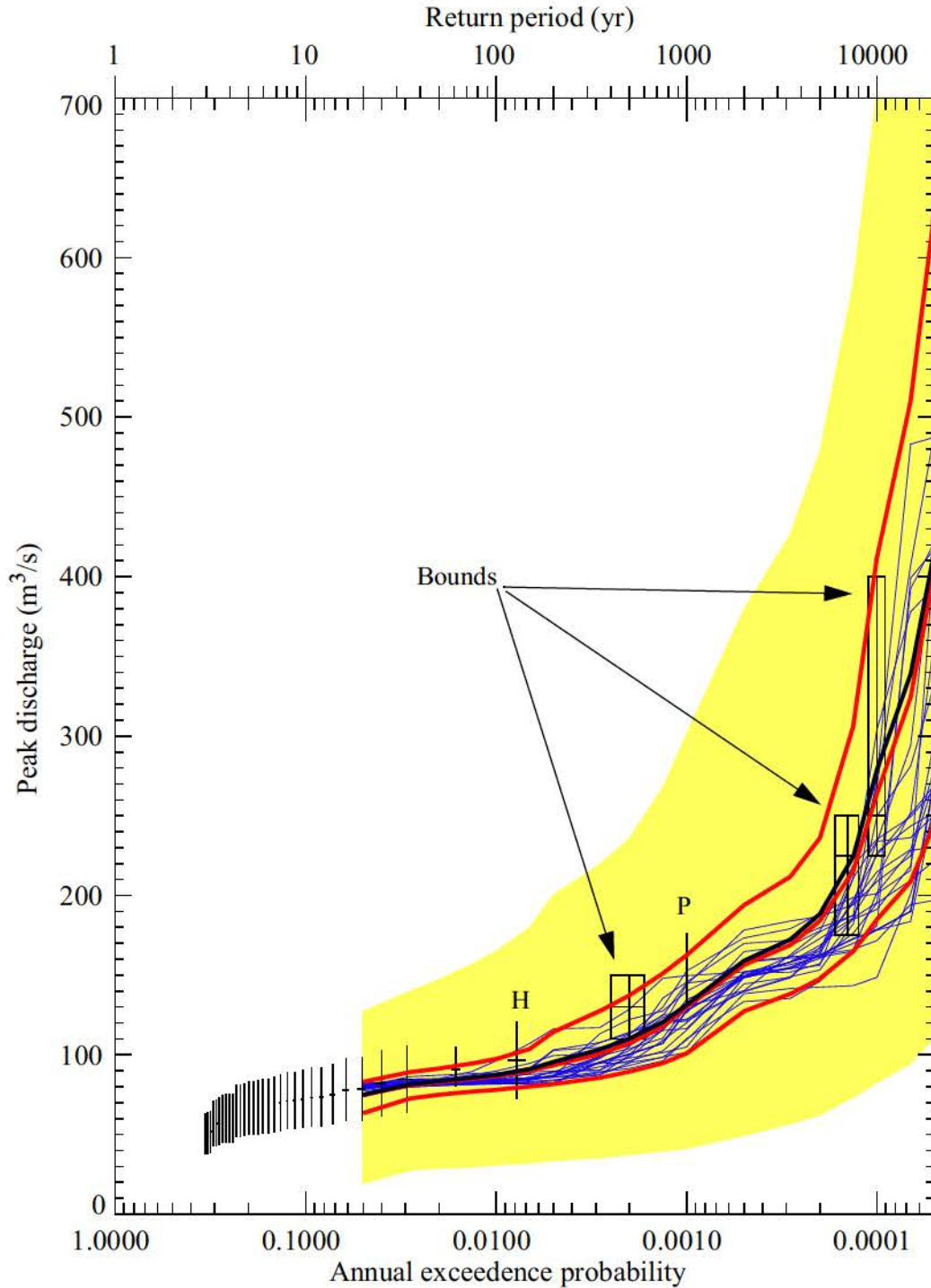


**Figure 4-2 Revised flood frequency for Big Lost River at the INEEL Diversion Dam.** Gaged flows (vertical black lines, with short horizontal lines indicating preferred discharge and plotting position uncertainty) are from Big Lost River at Howell Ranch (94 years) attenuated to the INEEL Diversion Dam based on methods of Hortness and Rousseau (2002). Geologic data includes two paleofloods (largest discharges labeled H and P) and three paleohydrologic bounds (black boxes - vertical lines indicate discharge range, horizontal lines indicate duration range). Lower and upper red curves are 5% and 95% credible limits (middle red is median, and middle black is mean). Blue curves are models with relative likelihoods > 0.25 of the maximum likelihood. Yellow region indicates the limits of sampling.

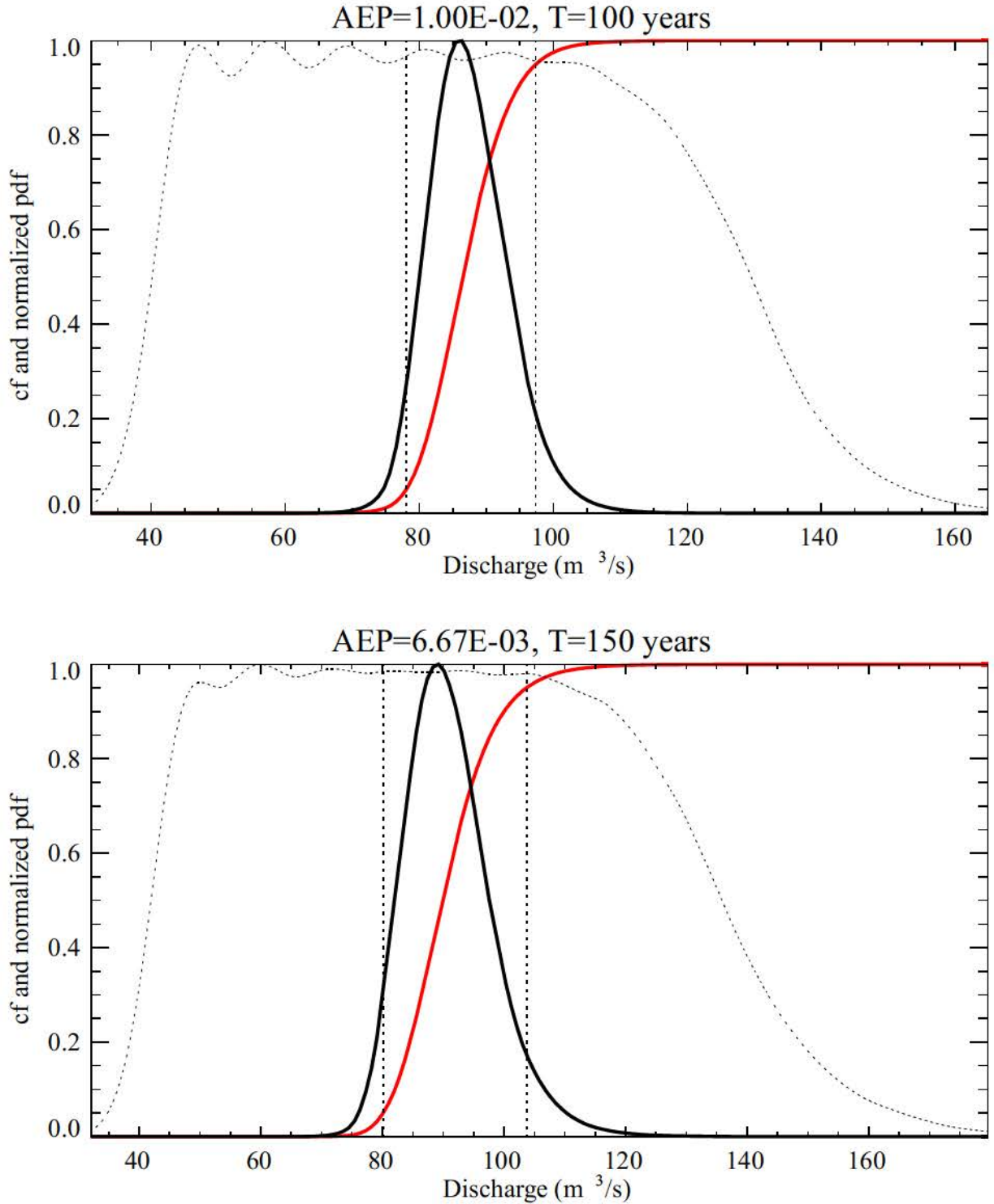


**Figure 4-3 Peak discharges distributions for AEP's 0.01 and 0.00667 on the Big Lost River at the INEEL Diversion Dam. Red curves are cumulative probability, dotted curves are sampling density, and black curves are probability density. Vertical dotted lines represent 5% and 95% credible limits.**

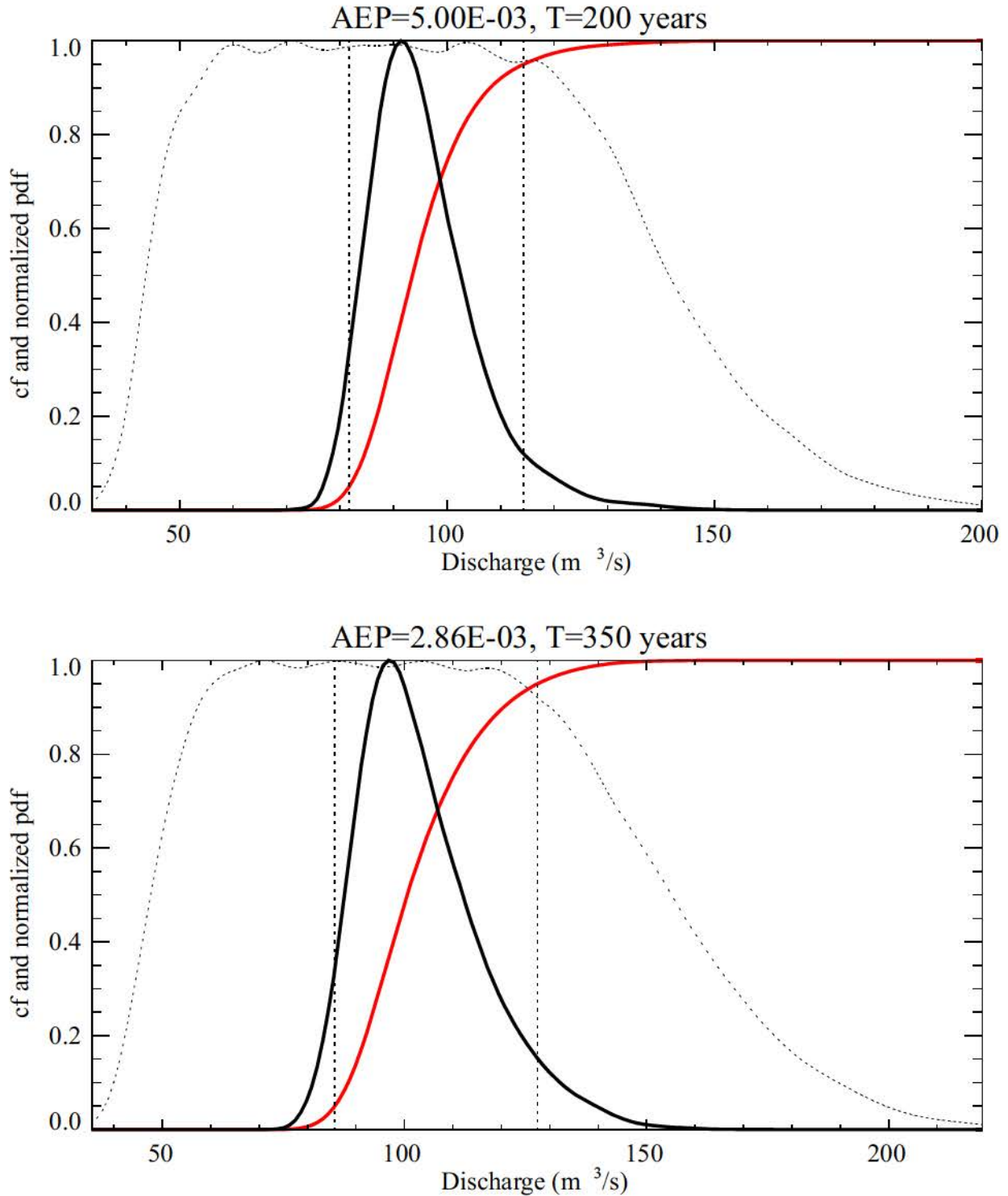


**Figure 4-4 Peak discharges distributions for AEP's 0.005 and 0.00286 on the Big Lost River at the INEEL Diversion Dam. Red curves are cumulative probability, dotted curves are sampling density, and black curves are probability density. Vertical dotted lines represent 5% and 95% credible limits.**

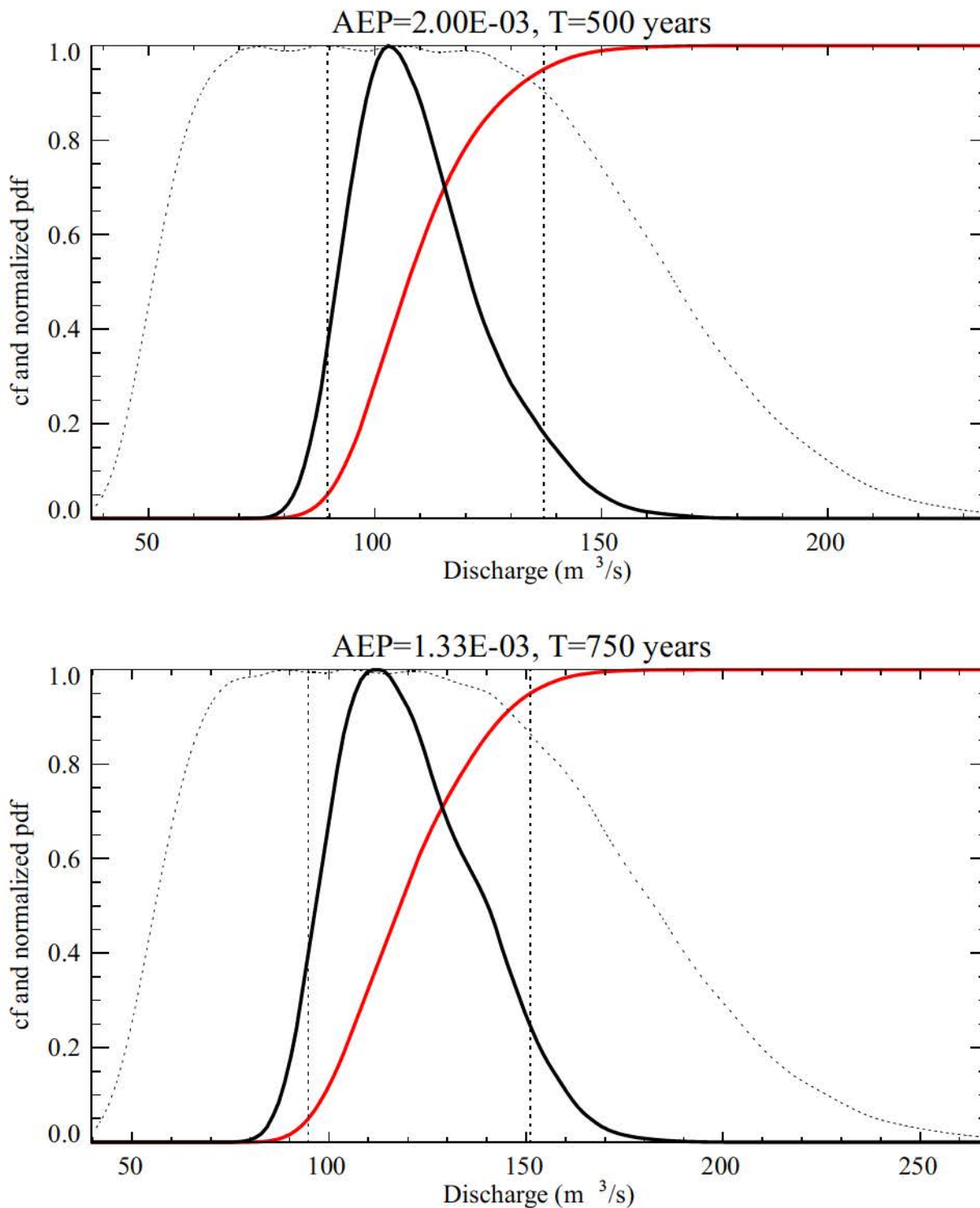


**Figure 4-5 Peak discharges distributions for AEP's 0.002 and 0.00133 on the Big Lost River at the INEEL Diversion Dam. Red curves are cumulative probability, dotted curves are sampling density, and black curves are probability density. Vertical dotted lines represent 5% and 95% credible limits.**

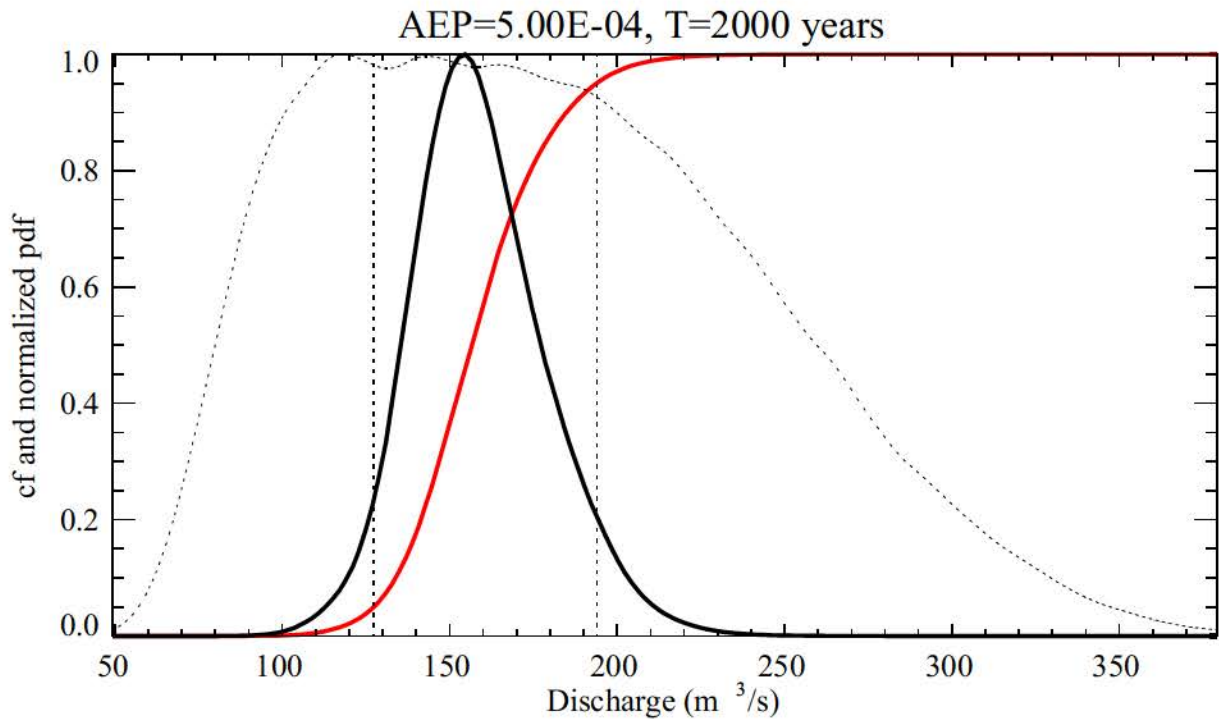
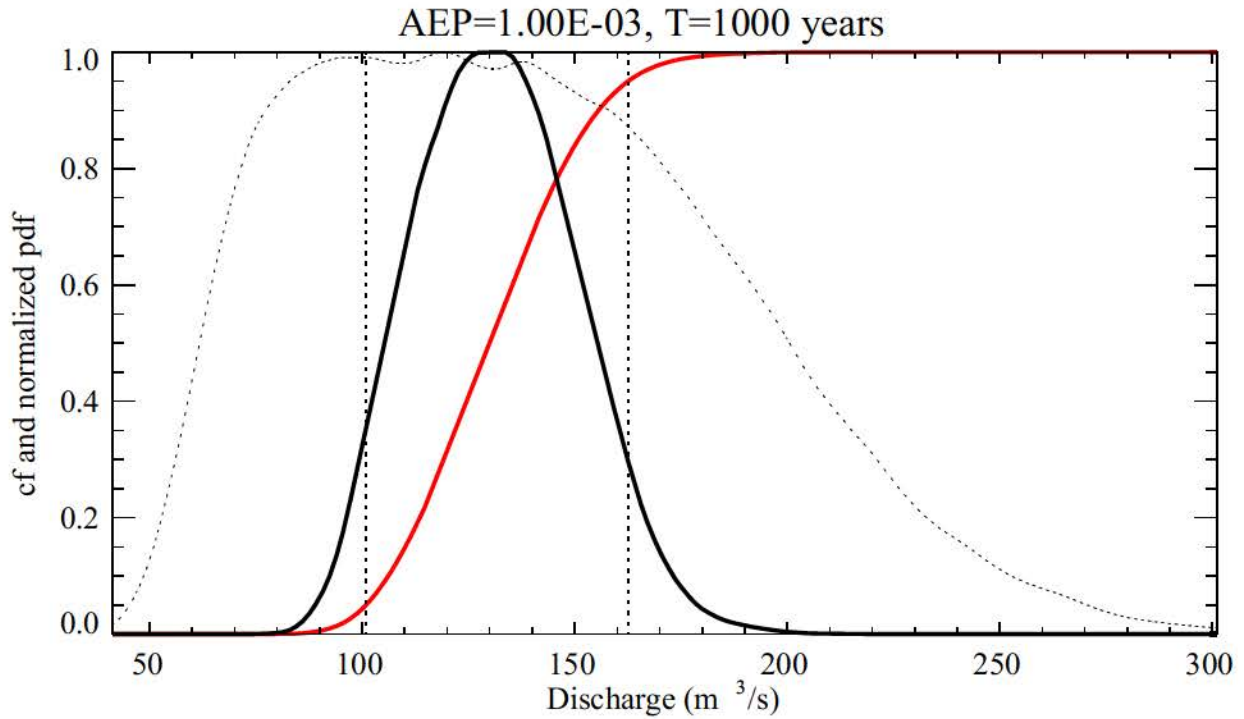


**Figure 4-6 Peak discharges distributions for AEP's 0.001 and 0.0005 on the Big Lost River at the INEEL Diversion Dam. Red curves are cumulative probability, dotted curves are sampling density, and black curves are probability density. Vertical dotted lines represent 5% and 95% credible limits.**

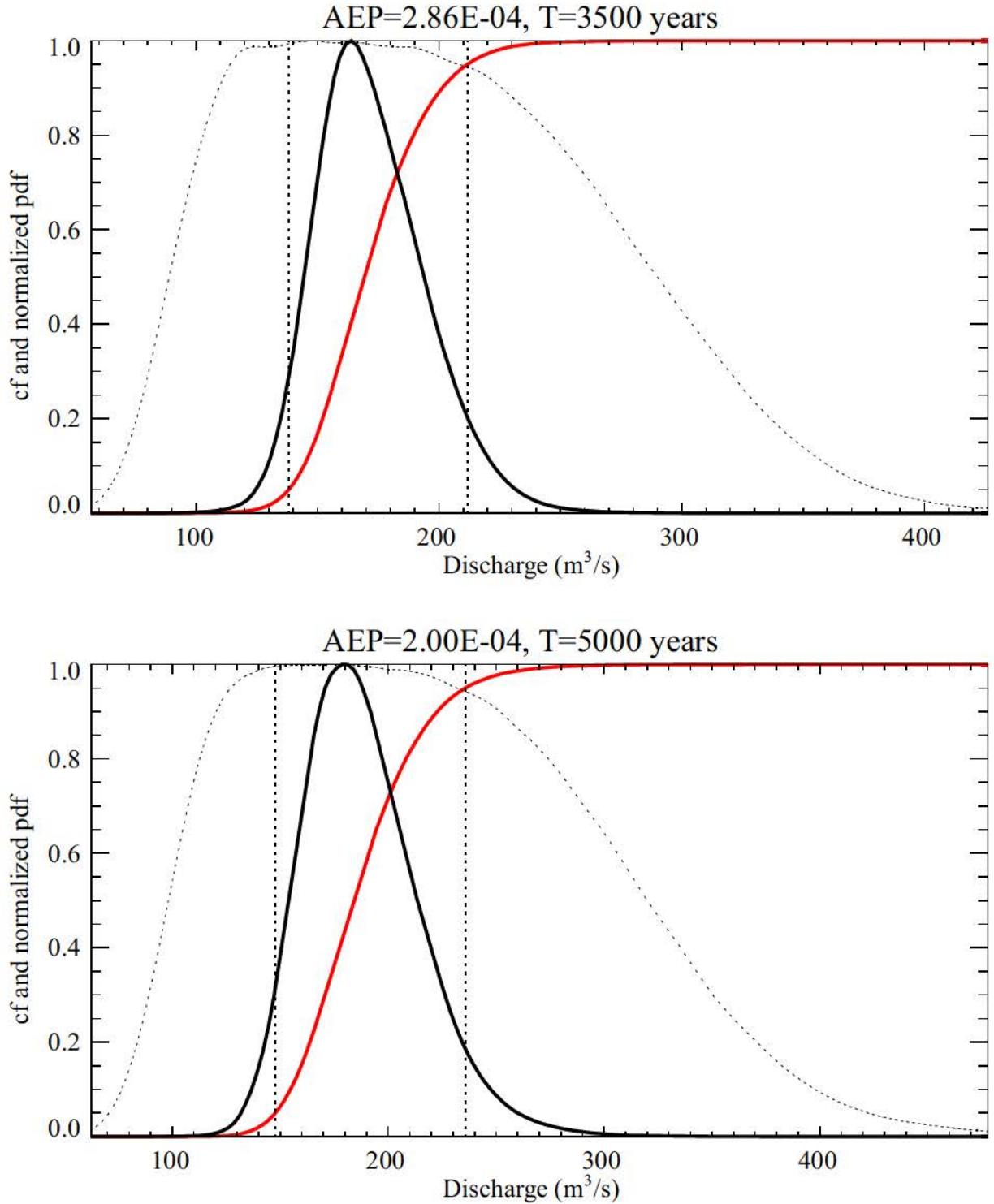


**Figure 4-7 Peak discharges distributions for AEP's 0.000286 and 0.00002 on the Big Lost River at the INEEL Diversion Dam. Red curves are cumulative probability, dotted curves are sampling density, and black curves are probability density. Vertical dotted lines represent 5% and 95% credible limits.**

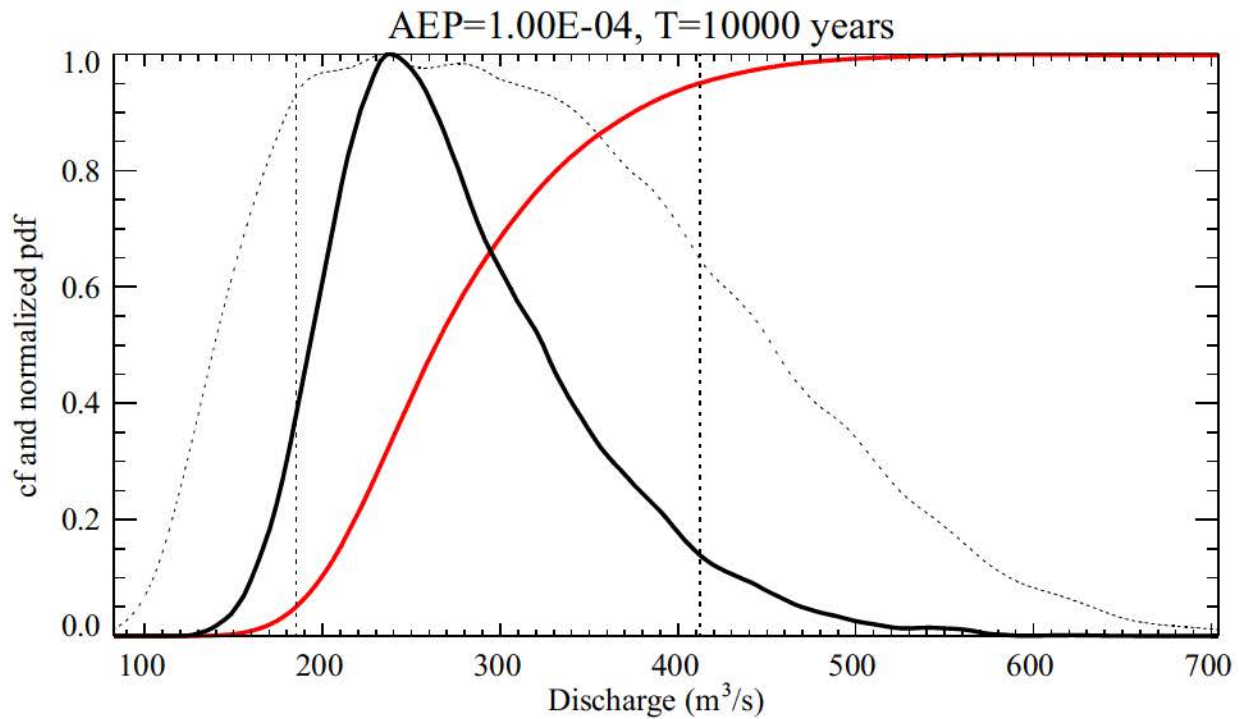
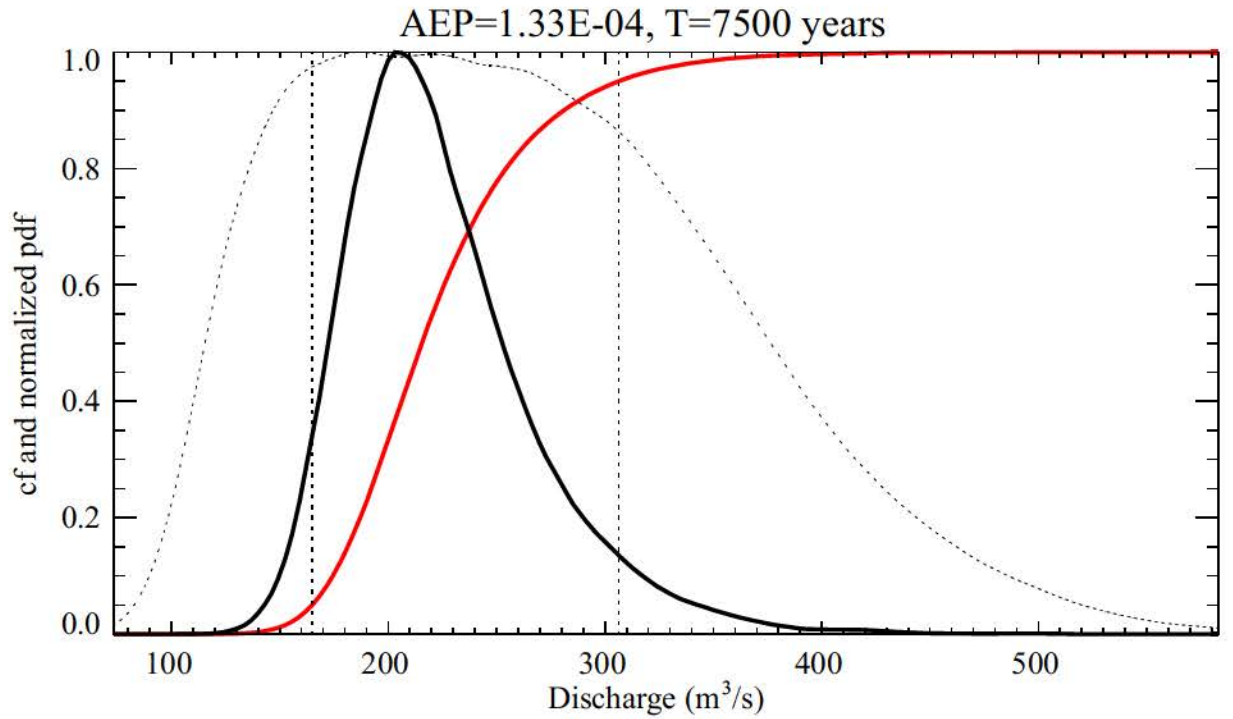


**Figure 4-8 Peak discharges distributions for AEP's 0.000133 and 0.00001 on the Big Lost River at the INEEL Diversion Dam. Red curves are cumulative probability, dotted curves are sampling density, and black curves are probability density. Vertical dotted lines represent 5% and 95% credible limits.**

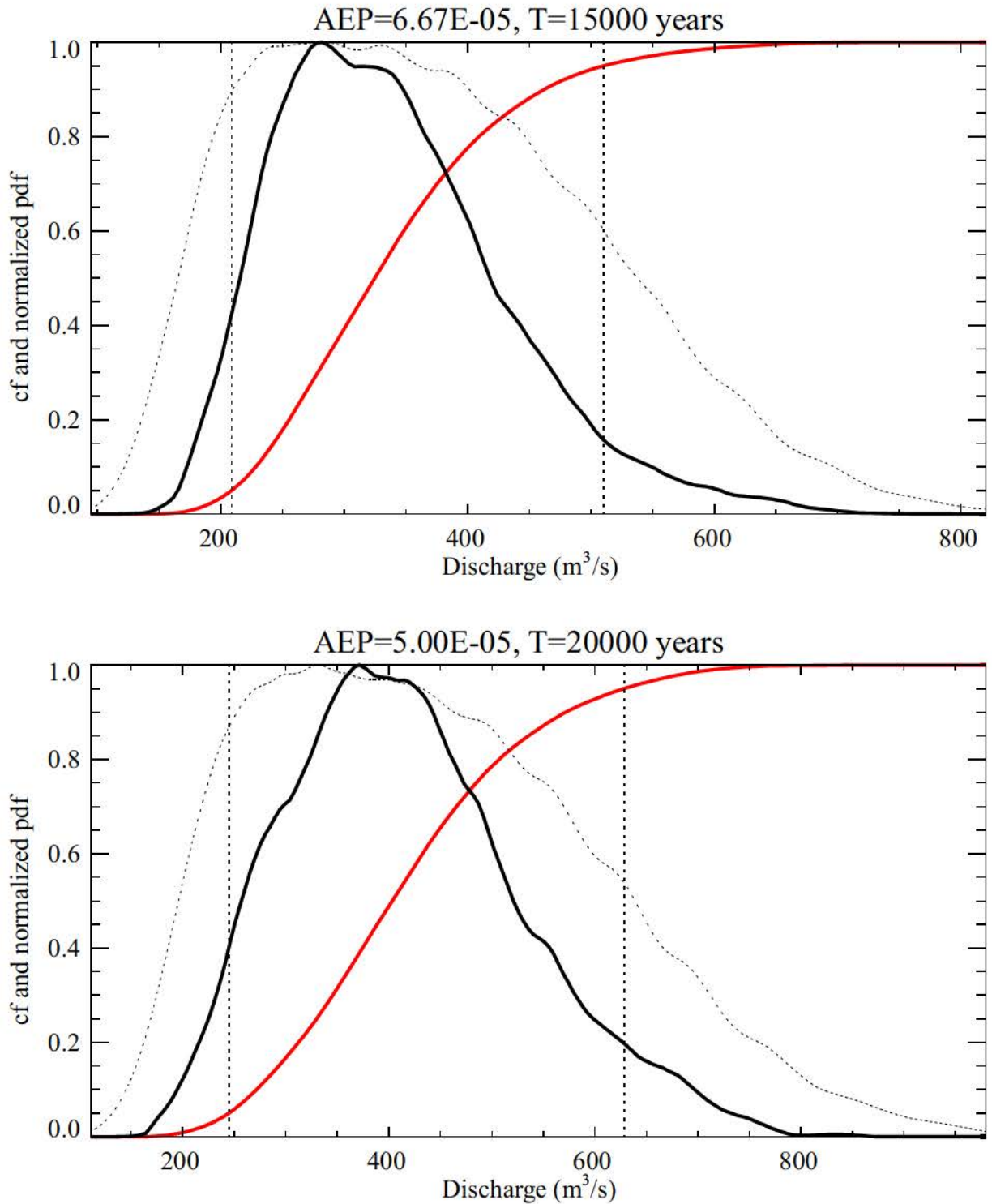


**Figure 4-9 Peak discharges distributions for AEP's 0.0000667 and 0.000005 on the Big Lost River at the INEEL Diversion Dam.** Red curves are cumulative probability, dotted curves are sampling density, and black curves are probability density. Vertical dotted lines represent 5% and 95% credible limits.

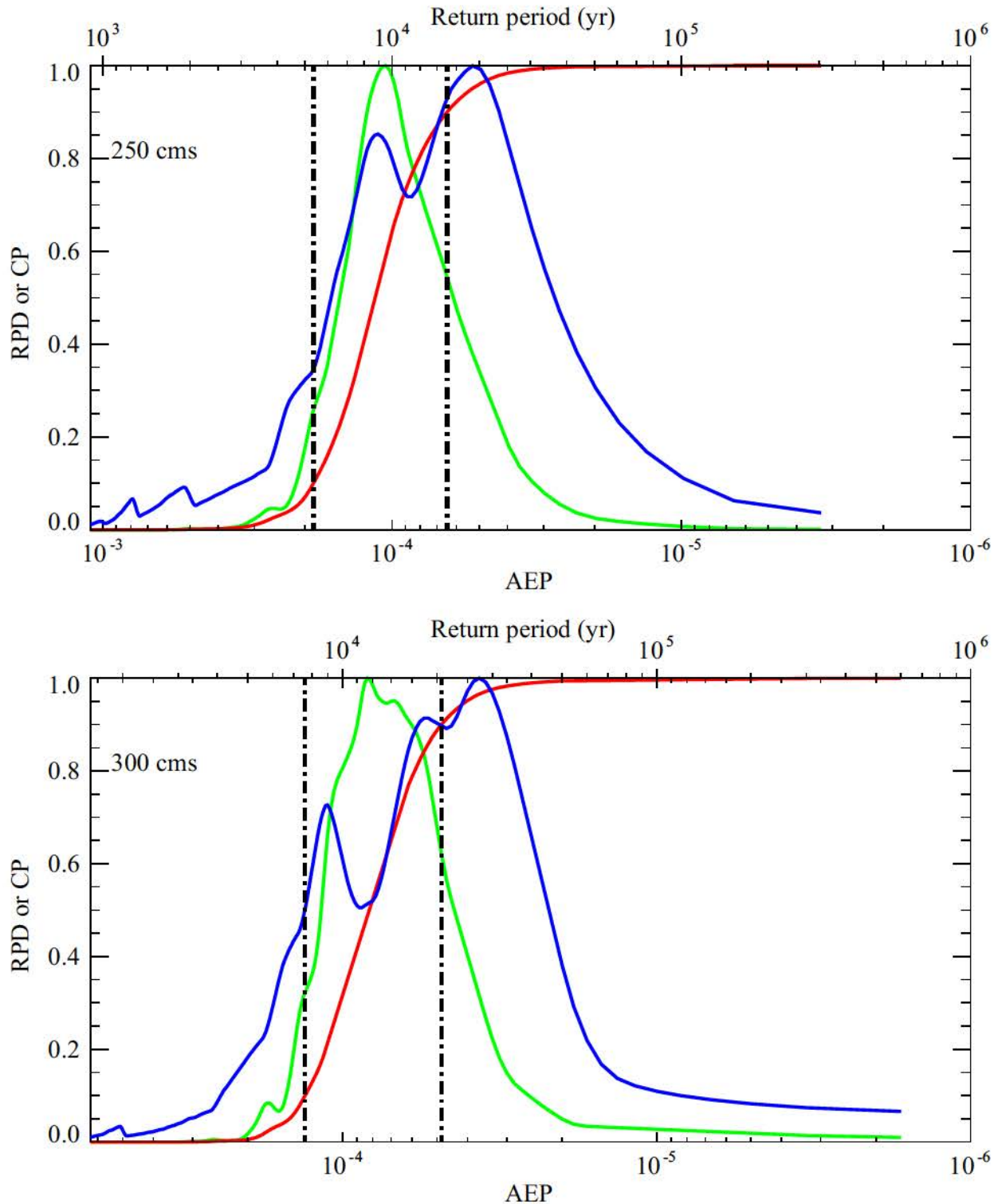


**Figure 4-10 AEP distributions for 250 m<sup>3</sup>/s and 300 m<sup>3</sup>/s on the Big Lost River at the INEEL Diversion Dam.** Red curves are cumulative probability, blue curves are sampling density, and green curves are probability density (from cumulative probability and transformed to AEP). Vertical lines represent 10% and 90% credible limits on AEP, but are not really defined for 300m<sup>3</sup>/s because nonzero density extends to AEP=0.

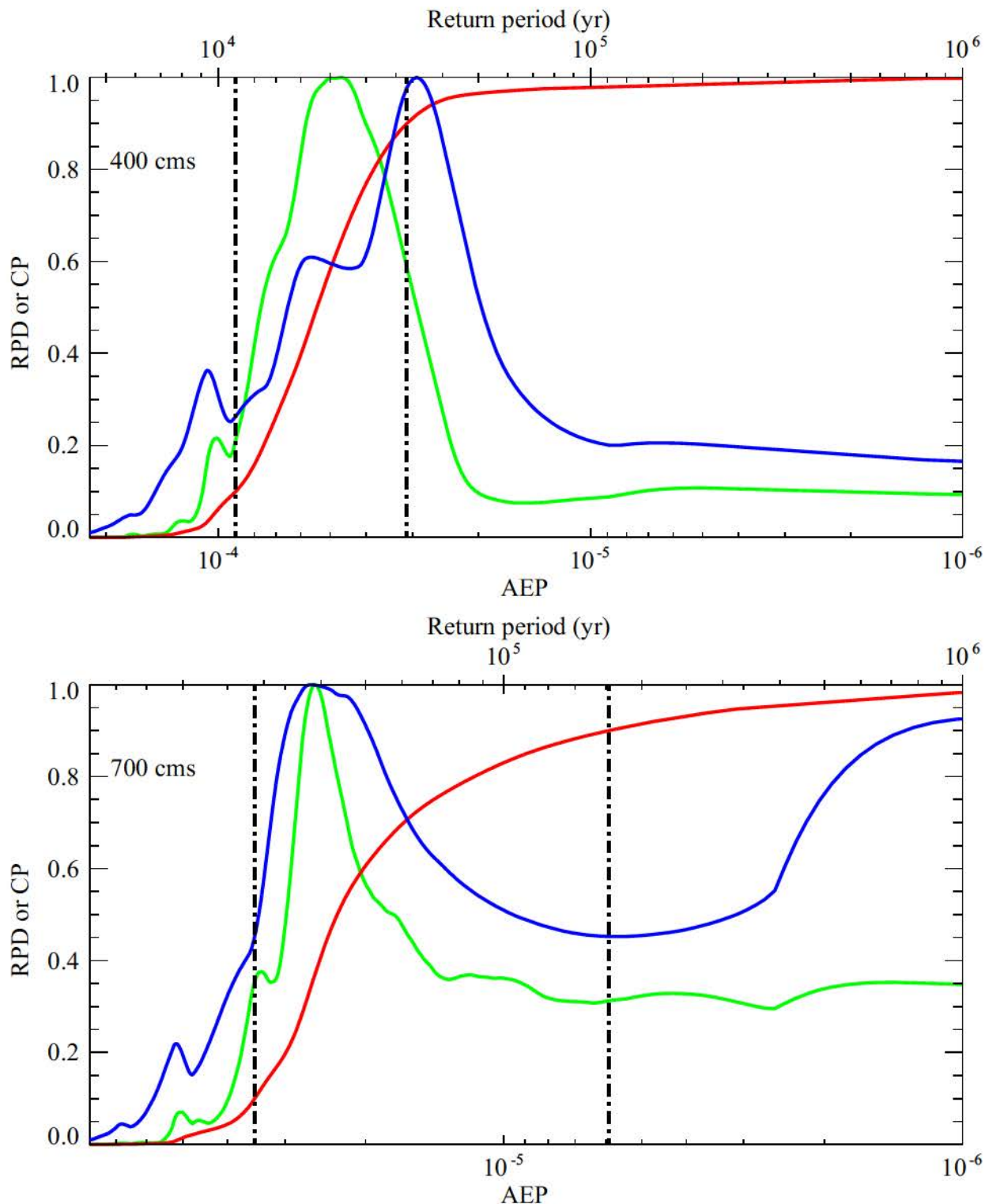


**Figure 4-11 AEP distributions for 400 m<sup>3</sup>/s and 700 m<sup>3</sup>/s on the Big Lost River at the INEEL Diversion Dam.** Red curves are cumulative probability, blue curves are sampling density, and green curves are probability density (from cumulative probability and transformed to AEP). Vertical lines represent 10% and 90% credible limits on AEP, but are not really defined here because nonzero density extends to AEP=0.

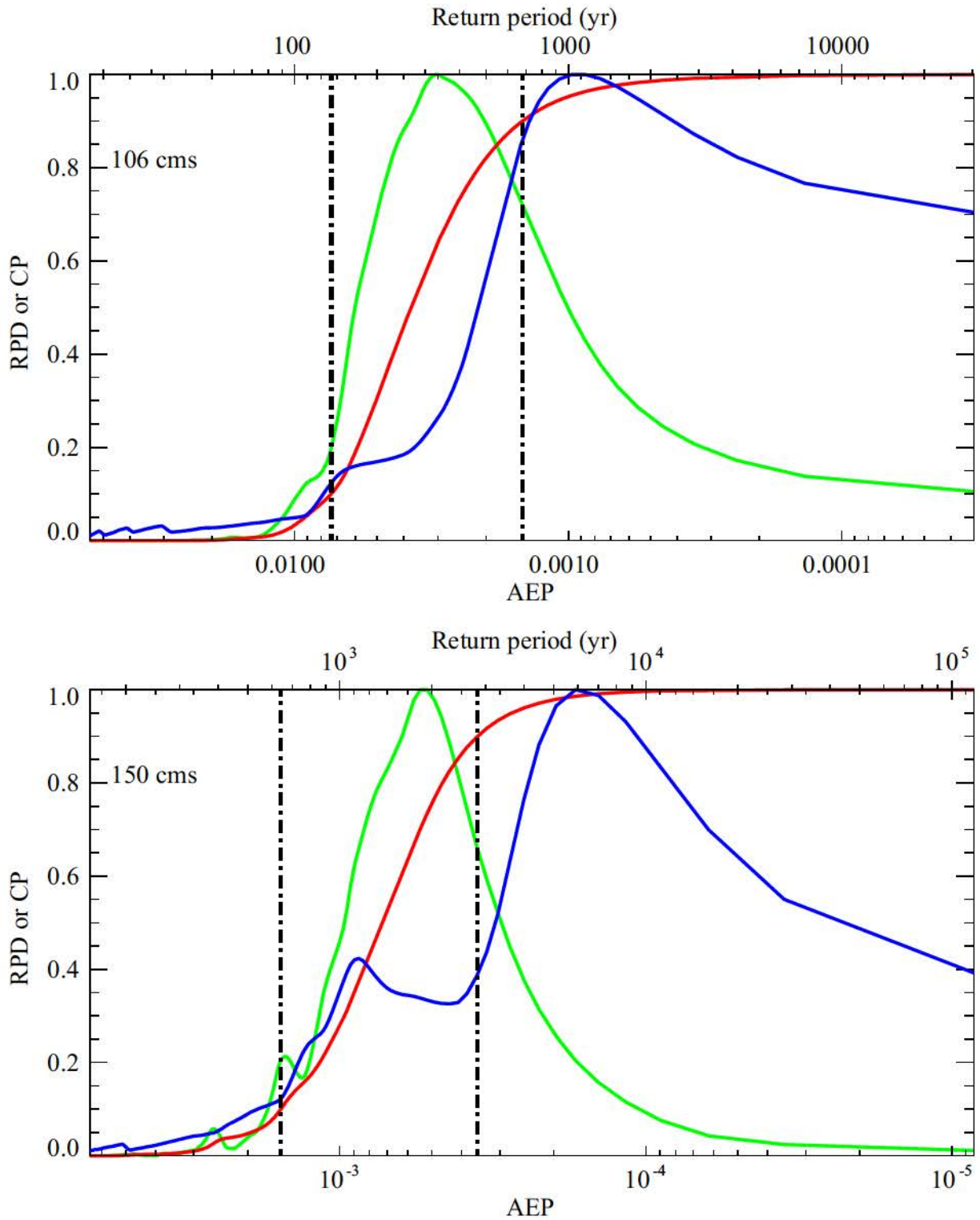


**Figure 4-12 AEP distributions for 106 m<sup>3</sup>/s and 150 m<sup>3</sup>/s on the Big Lost River at the INEEL Diversion Dam.** Red curves are cumulative probability, blue curves are sampling density, and green curves are probability density (from cumulative probability and transformed to AEP). Vertical lines represent 10% and 90% credible limits on AEP.

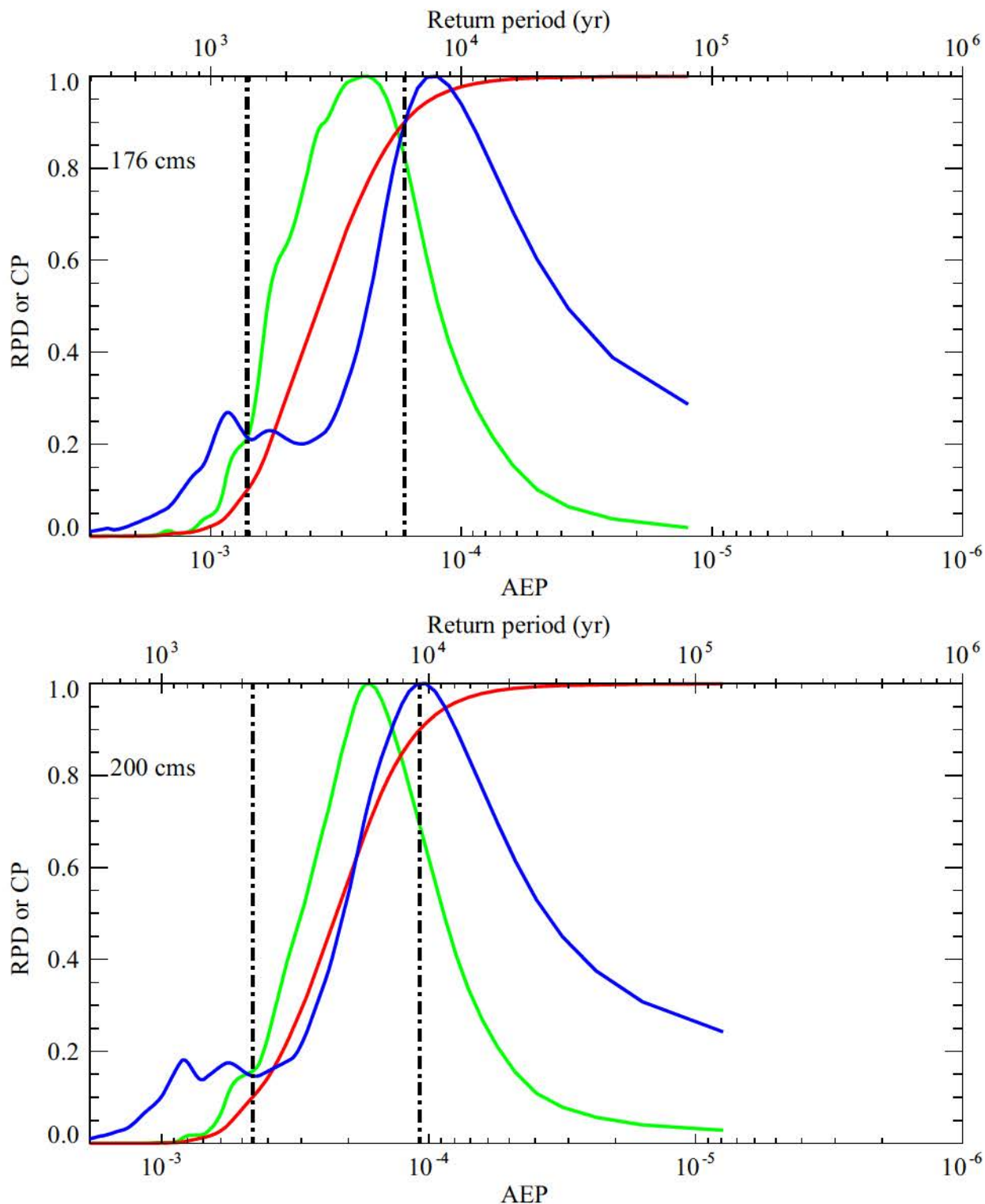


**Figure 4-13 AEP distributions for 176 m<sup>3</sup>/s and 200 m<sup>3</sup>/s on the Big Lost River at the INEEL Diversion Dam.** Red curves are cumulative probability, blue curves are sampling density, and green curves are probability density (from cumulative probability and transformed to AEP). Vertical lines represent 10% and 90% credible limits on AEP

**Tables for Section 4.0**

**Table 4-1 Least frequent peak discharge generation nodes.**

| $C_f$    | AEP (1/yr) | Return period (yr) |
|----------|------------|--------------------|
| 0.885662 | 0.114338   | 8.7                |
| 0.896279 | 0.103721   | 9.6                |
| 0.906895 | 0.093105   | 10.7               |
| 0.917511 | 0.082489   | 12.1               |
| 0.928128 | 0.071872   | 13.9               |
| 0.938744 | 0.061256   | 16.3               |
| 0.949360 | 0.050640   | 19.7               |
| 0.959976 | 0.040024   | 25.0               |
| 0.970593 | 0.029407   | 34.0               |
| 0.983657 | 0.016343   | 61.2               |
| 0.992182 | 0.007818   | 128.               |
| 0.995000 | 0.005000   | 200                |
| 0.997500 | 0.002500   | 400                |
| 0.998571 | 0.001429   | 700                |
| 0.999000 | 0.001000   | 1000               |
| 0.999231 | 0.000769   | 1300               |
| 0.999500 | 0.000500   | 2000               |
| 0.999750 | 0.000250   | 4000               |
| 0.999833 | 0.000167   | 6000               |
| 0.999875 | 0.000125   | 8000               |
| 0.999900 | 0.000100   | 10000              |
| 0.999933 | 0.000067   | 15000              |
| 0.999950 | 0.000050   | 20000              |
| 0.999967 | 0.000033   | 30000              |
| 0.999975 | 0.000025   | 40000              |

**Table 4-2 Nonparametric Flood Frequency for the Big Lost River at the Diversion Dam.**

| AEP<br>(1/yr)  | Return<br>period (yr) | 5%<br>(m <sup>3</sup> /s) | mean<br>(m <sup>3</sup> /s) | 95%<br>(m <sup>3</sup> /s) |
|--|-----------------------|---------------------------|-----------------------------|----------------------------|
| $5 \times 10^{-2}$   | 20                    | 63                        | 75                          | 83                         |
| $2.86 \times 10^{-2}$  | 35                    | 73                        | 81                          | 89                         |
| $2 \times 10^{-2}$   | 50                    | 75                        | 83                          | 91                         |
| $1.33 \times 10^{-2}$  | 75                    | 77                        | 86                          | 95                         |
| $10^{-2}$  | 100                   | 78                        | 87                          | 97                         |
| $6.67 \times 10^{-3}$  | 150                   | 80                        | 91                          | 104                        |
| $5 \times 10^{-3}$   | 200                   | 82                        | 96                          | 114                        |
| $2.86 \times 10^{-3}$  | 350                   | 86                        | 103                         | 127                        |
| $2 \times 10^{-3}$   | 500                   | 89                        | 110                         | 137                        |
| $1.33 \times 10^{-3}$  | 750                   | 95                        | 121                         | 151                        |
| $10^{-3}$  | 1000                  | 101                       | 131                         | 163                        |
| $5 \times 10^{-4}$   | 2000                  | 127                       | 159                         | 194                        |
| $2.86 \times 10^{-4}$  | 3500                  | 138                       | 172                         | 212                        |
| $2 \times 10^{-4}$   | 5000                  | 148                       | 188                         | 236                        |
| $1.33 \times 10^{-4}$  | 7500                  | 165                       | 224                         | 306                        |
| $10^{-4}$  | 10,000                | 185                       | 279                         | 412                        |
| $6.67 \times 10^{-5}$  | 15,000                | 209                       | 339*                        | 510*                       |
| $5 \times 10^{-5}$   | 20,000                | 245                       | 416*                        | 628*                       |
| * Values with diminished or little statistical significance. |                       |                           |                             |                            |

## 5.0 PROBABILISTIC FLOOD STAGE AT INTEC AND TRA

Two-dimensional hydraulic modeling using a broad range of discharges conducted for the reach of the Big Lost River downstream of the INEEL Diversion Dam to approximately the INEEL railroad grade downstream of INTEC and TRA provide one element needed for probabilistic flood stage estimates at these facilities. A conceptual framework for evaluating the model results and flood frequency information was developed in the early stages of this study to guide the evaluations. Uncertainties in probabilistic flood stage estimates are discussed in the context of that framework. Based on this framework, results and uncertainties for stage - probability curves for fifteen specific sites within INTEC and TRA are discussed.

### 5.1 Topographic Input to Two-Dimensional Models

The 5-ft-spaced reprocessed topographic data from the 1993 aerial photography at INEEL (**Appendix A**) were used to construct the computational meshes for TrimR2D and RiCOM flow modeling of INL inundation. Construction of the TrimR2D grid was relatively straightforward and simply involved subsampling a subset of the rotated topographic data to produce a 10-ft-spacing input file. Details of this process are provided in **Appendix C, Part A, Section 2**. TrimR2D flow results were used to define regions that warranted increased spatial sampling afforded by the finite-element capabilities of RiCOM. The construction of the RiCOM computational mesh was quite involved and is documented in **Appendix C, Part A, Section 2**.

In both grids the minimum elevation in the grid was removed from all points in the grid to maximize numerical precision in quantities involving elevations. Coordinate transformation equations were constructed for both flow grids to convert the local grid coordinates to their original INEEL state-plane coordinates and elevations.

### 5.2 Two Dimensional Hydraulic Modeling

Discharges were selected for modeling over the full range of flow probabilities to provide representative data from which to construct the stage - probability curves. Specific discharge values were chosen for relevance to historical flood events, system capacities, and flood estimates from previous studies (**Table 5-1**).

The TrimR2D grid consisted of approximately 3.3 million active cells. The RiCOM grid consisted of approximately 7.2 million active elements and nearly 14 million active sides and used a time step 1/5 of the TrimR2D time step. RiCOM calculations were much more computationally demanding than TrimR2D, with RiCOM calculations running at 1/10-1/20 real time, while TrimR2D ran at 1/2 to 1/4 real time. Consequently, TrimR2D was used to perform most of the sensitivity analyses concerning infiltration and culvert scenarios and RiCOM was used to concentrate calculations on the most important subset of flows identified from the TrimR2D flow calculations.

**5.2.1 Infiltration Implementation and Scenarios.** Infiltration was implemented in TrimR2D and RiCOM as discussed in **Appendix C, Part A, Section 3**. As discussed in **Appendix E**, infiltration estimates from Fiedler (2002) were modified to produce channel loss rates consistent with historical maximum channel discharge losses between the Diversion Dam and Lincoln Avenue of ~15%. The two scenarios in **Table 5-1** represent logical infiltration end-members of no infiltration and full infiltration consistent with the maximum observed historical channel losses between the Diversion Dam and Lincoln Avenue.

**5.2.2 Culvert Implementation and Scenarios.** As indicated in **Table 5-1**, TrimR2D was used to calculate flows for four scenarios for a full range of discharges. The four scenarios were constructed to determine the relative influence of infiltrations and culverts on estimated inundation. The scenarios represented in **Table 5-1** all assume full Big Lost River conveyance through Lincoln Avenue, the railroad embankment downstream of INTEC, and Highway 20/26. As discussed in detail in **Appendix C, Part A, Section 3**, culvert flow information from Berenbrock and Doyle (2003) was used for all other culverts. Since the RiCOM calculations indicated that topographic grid resolution had a significant impact on estimated inundation in the vicinity of INTEC, RiCOM was also used to estimate the impact of complete blockage of flow by Lincoln Avenue on estimated inundation for the case of full infiltration and full operation of the remaining culverts.

**5.2.3 Flow Initialization.** The TrimR2D inundation grid was initially wetted with springs distributed along the Big Lost River channel that were activated for several minutes of flow to partially fill the channels. To produce steady-state flows for specific discharges, springs

were activated immediately downstream of the Diversion Dam in the active channel with a total flux equal to the specific discharge. For the TrimR2D flows, 32 springs were used to minimize excess stages in the vicinity of the springs. Because RiCOM used 5-ft elements in the active channel, 886 springs were used to minimize excess stages in the vicinity of the springs. It is important to note, that despite these efforts to minimize excess stages in the vicinity of the input springs, stages near the springs may be up to 1 m higher than would occur if water flowed through the channel at typical velocities of 1-2 m/s. Consequently, inundation of areas immediately south of the channel downstream of the Diversion Dam are overestimated to some degree, particularly for discharges of 300 cms or larger. TrimR2D flows for all discharges started from the same initial low-flow channel wetting conditions so that all discharges in **Table 5-1** could be calculated in parallel. The TrimR2D stages upon completion of the flow simulations (about 40 hours of flow) were used as initial conditions to initialize the RiCOM flow calculations. The outlet flow boundary was located more than 1 km from any regions of interest. Consequently, a simple fixed water surface elevation boundary condition was imposed for simplicity, since the boundary condition had no impact on the interior points of interest in the grids.

**5.2.4 Flow Parameters.** Time steps were established at 20 s for the TrimR2D 20-ft grid to ensure Courant numbers of larger than 4 for main channel flow velocities for all discharges. A time step of 4 s was used for the RiCOM grid because all significant flow channels used 5-ft elements. This ensured Courant numbers larger than 4 in the main flow channels in the RiCOM flow calculations. Criteria for selection of time step and the impact of time step on computed flows are discussed in detail in **Appendix C, Part A - Section 1** and **Part B - Section 1**. Semi-implicit weights were set to 0.7 for all calculations.

**5.2.5 Flow Completion.** A total of 15 hydrograph monitoring positions were established throughout inundation grids in both channel and out-of-bank positions. These hydrographs were monitored to determine when the flows had reached steady state. Typically, flow times of about 20-40 hours were required to achieve steady-state conditions throughout the TrimR2D grid, when starting from a modest channel inundation condition. Steady-state flow conditions were obtained in the RiCOM flow calculations in 6-7 hours of flow time, when starting with the TrimR2D inundations at the same discharge. Steady-state conditions were defined as attaining an

essentially static water surface elevation at all the hydrograph monitoring positions (natural high-frequency water surface elevation oscillations, typically of several centimeters, were ignored).

**5.2.6 Flow Output. Appendix E - Electronic Supplement** presents maps depicting the results of two-dimensional hydraulic modeling conducted to estimate probabilistic flood stage at INTEC and TRA for the discharges listed in **Table 5-1**. These maps show results for both the entire reach downstream of the INEEL Diversion Dam as well as enlarged views in the immediate vicinity of the facilities. For TrimR2D, the output flow quantities included water surface elevations and vector flow velocities interpolated to the water surface elevation positions at cell-centered positions in the staggered grid. Using the known topography, derived quantities such as depth, shear stress, and power were obtained. For RiCOM, the output flow quantities included water surface elevations and vector flow velocities interpolated to the element vertices using the finite-element basis functions. The inverse transformation operators were then applied to produce flow quantities in the INEEL state-plane coordinate system. For most modeled discharges, results are presented for modeled flow depth, unit stream power, and bed shear stress based on the TrimR2D results. RiCOM results are presented mostly as plots showing the difference in water-surface elevation from TrimR2D results for the same input discharge. A full set of RiCOM results (depth, unit stream power, bed shear stress) are presented only for four quantile results of the 100- and 500- yr discharges from the flood frequency analyses. Additional depth difference plots from TrimR2D models depict end member differences for infiltration and culvert scenarios.

### **5.3 Conceptual Framework for Development of Probabilistic Inundation Maps and Flood Stage Estimates for Facility Sites at INL**

Each of the inundation maps for a specific discharge listed in **Table 5-1** could be associated with mean and credible limits on AEP associated with that discharge from **Section 4.0** and **Table 5-2**. However, such AEP's would not represent complete probabilistic inundation maps (PIM) for INL. There are additional probabilities (or weights) that must be assigned to aleatory (random-by-nature) parameters, such as infiltration and culvert conveyance. A conceptual framework for evaluating these uncertainties that was developed in the early stages of this study to guide the investigations is illustrated in **Figure 5-2**. Epistemic uncertainties include factors such as flow model variability and appropriate scenario terrain models used in the simulations. Elicitation and

assignments of weights to all aleatory and epistemic factors are required to produce comprehensive PIM's. Each of the major elements will be briefly described below.

### 5.3.1 Aleatory Uncertainties.

**5.3.1.1 Flood Frequency Analyses.** The flood frequency analysis (FFA) can be viewed as the primary input to the PIM process. This is the element by which the annual probability of floods (and hence inundation) are incorporated into the process. Several sources of uncertainty are brought into the PIM process through the FFA, including discharge measurement uncertainties and statistical uncertainties in estimated AEP. The flood frequency results from **Section 4.0** are used to establish probabilistic estimates of mean AEP, and 5% and 95% credible limits on AEP associated with the specific discharges in **Table 5-1**. For instance, a 5% credible limit on AEP roughly represents a 95% probability that the AEP is actually larger than the 5% credible limit AEP (low confidence the AEP will not be exceeded). Conversely, a 95% credible limit on AEP roughly represents a 5% probability that the AEP is actually larger than the 95% credible limit AEP (high confidence the AEP will not be exceeded). As these concepts may not be intuitive, it helps to remember that the conservative limits are represented by the upper hazard curves, which correspond to the 95% credible limit for AEP.

If multiple and complete estimates of flood frequency exist for the site, each of the alternative estimates could be weighted and carried through the PIM process. Because of the wide variation of previous flood frequency estimates for the INL site (**Section 1.0**), it was the original intent of this study to include alternative estimates and propagate this uncertainty through to the estimate of flood stage at the facilities. For example, flood frequency results based on earlier paleoflood studies of the Big Lost River (Ostenaar and others, 1999) would be weighted relative to present study results from **Section 4.0** based on expert opinion. However, because the present study found that the topography used as inputs to earlier paleoflood studies was inadequate (**Appendix A**) making hydraulic model results unreliable, it is now clear that the earlier results must be discounted and effectively given zero weight. As there are no other existing flood frequency analyses for the Big Lost River that can be extended with uncertainties significantly beyond an AEP of  $10^{-2}$ , only the revised analyses described in **Section 4.0** is used. Potential impacts of the differences associated with point estimates for floods of a specific AEP, such as the 100-yr flow

estimate of Hortness and Rousseau (2002) are separately evaluated against the final stage-probability curves later in this section.

**5.3.1.2 Hydrograph Shape.** The current modeling effort uses a specific hydrograph shape based on an assumption of unregulated long-duration “natural” flow. Here long-duration means sufficient duration to inundate the entire INL inundation grid to the point of steady-state flow. The time required to achieve steady-state flow from initially near-dry conditions (flow confined to the Big Lost River channel) can be as long as about 20 hours. Steady-state flow can be achieved across the entire INL inundation grid in as little as 5-10 hours for modest (~10%) changes in discharge. For the purposes of the PIM, the probabilistic stage estimates correspond to peak flow durations of 20 hours. The effects of regulation and potential dam failure on hydrograph shape would require separate investigations, that would focus on modeling transient flow behavior.

**5.3.1.3 Infiltration.** The potential variability in inundation due to infiltration is currently evaluated by including two distinct end-member values for this parameter. Interpretation of available data suggests infiltration losses between 0 (no infiltration) and 15% for the study reach of the Big Lost River (**Appendix E**). These two end member values provide information to assess the sensitivity of results to this parameter. The uncertainty in this parameter is composed of the intrinsic spatial variability in infiltration as well as a lack of knowledge regarding methods for estimating the parameter (especially for out-of-bank flows and long durations).

**5.3.1.4 Culverts.** The probabilistic stage calculations for INL include a simplified representation of the effect of culverts on flow, and hence inundation at the site. Three scenarios are considered. In two scenarios full conveyance of the active Big Lost River channel is allowed through Lincoln Avenue and either, full conveyance, or zero conveyance, occurs through the other culverts. The third scenario involves zero conveyance through the Lincoln Avenue culverts on the active channel of the Big Lost River and full conveyance through the remaining culverts.

### 5.3.2 Epistemic Uncertainties.

**5.3.2.1 Topography and Flow Model Uncertainty.** Uncertainties in the modeling of topography will exist in both the FFA results and in the PIM. Currently, these uncertainties are explicitly treated by calculating flow results using two grid resolutions to provide a first-order sensitivity analysis. Potential epistemic uncertainties associated with the two flow models are discussed in **Appendix C, Part B, Section 1**. These tests and output comparisons (difference plots in **Appendix E - Electronic Supplement**) show that negligible differences in water-surface elevation at most sites can be attributed to the choice of flow model. Much larger epistemic uncertainty is associated with the ability to accurately resolve subtle topographic features in the model inputs.

Efforts have been made to ensure that the topographic models will not have systematic biases (**Appendix A**). The observed sensitivity of the flow results to grid resolution suggest that the flow models are likely sensitive to random and transient variations in topography, particularly in regions near the Big Lost River channel and secondary channels associated with old diversions, roadways, ditches, and artificial barriers. These small-scale features play significant roles in determining the path of shallow flow across the broad Pleistocene surfaces near INTEC and TRA.

**5.3.3 Scope of Results.** Based on the study results, it was deemed unnecessary to attempt to assign weights to the various aleatory and epistemic uncertainty components to produce a comprehensive calculation of PIM. Hence, for this study, the conceptual framework portrayed in **Figure 5-2** has essentially one primary input from which calculated uncertainty is carried forward, that being the revised flood frequency analyses. For the present analyses, the other aleatory components of uncertainty are either beyond the scope of the present study (e.g., hydrograph variability), or can be shown to be not significant based on the modeling results (e.g., effects of infiltration and most culverts). Difference plots of the end member scenarios of infiltration and secondary culvert blockage show that the change in water surface between these scenarios is less than 0.25 ft except for isolated locations along the margin of the inundated area where a small increase in stage overtops a local threshold and leads to inundation of adjacent lower areas (**Appendix E - Electronic Supplement**). Examination of these results shows that in most cases the resulting stage differences are most typically on the order of ~ 0.1 ft.

Stage - AEP curves were constructed for fifteen TRA/INTEC sites of particular interest shown on **Figure 5-1** and listed in **Table 5-3**. Example curves from two INTEC and two TRA sites are shown here as **Figure 5-3** through **Figure 5-6** and a complete set of curves is displayed in **Appendix F**. Curves show mean, 5%, and 95% fractiles based on the associated discharge probabilities derived from the flood frequency analyses in **Section 4.0** and listed in **Table 5-2** and the stage (water-surface elevations) from the TrimR2D and RiCOM hydraulic models. Differences in equivalent fractile curves due to infiltration and culvert scenarios are typically on the order of ~0.1 ft. Differences due to discharge AEP are much larger. For AEP of 0.01 (100-yr) the typical range between the 5% and 95% curves is ~0.3 ft; for AEP of 0.0001 (10,000-yr) the range is typically 0.5- to 1.0 ft. These ranges thus depict the sensitivity of stage to uncertainty in input discharge AEP.

Epistemic uncertainty associated with the input topography for the hydraulic models is not quantified in a statistical sense, but is shown by the differences in stage hazard plots for TrimR2D compared to RiCOM. These effects are often largest for flows less than about 200 cms where the differences the ability of the input grids to resolution subtle features of the input topography leads to areas inundated to higher or lower levels between the flow models (See TrimR2D minus RiCOM difference plots in **Appendix E - Electronic Supplement**). A full appreciation of the impact of these factors on inundation characteristics is best provided by the large-scale inundation maps. On the stage - AEP curves for the fifteen TRA/INTEC sites suggest these effects are mostly less than ~ 0.5 ft (**Appendix F**), but it is the maps (**Appendix E - Electronic Supplement**) that provide the best illustrations of the strong sensitivity of portions of the inundation to topographic resolution and relatively subtle topographic features such as roads and old diversion structures.

## 5.4 Evaluation of Results

Flow patterns for the modeled flows near and through the facility sites are complex and strongly influenced by small-scale topographic features such as secondary channels, ditches, roads, berms, barriers, buildings and the overall topographic slope across each facility site. Water-surface elevations within the site areas are not always directly linked to the water-surface elevation in the main Big Lost River channel because flow reaches many areas of the site through channel networks that connect to the main Big Lost River as much as several kilometers upstream of the

facilities. In other cases, some areas within each facility are effectively isolated from most flows by local topographic high areas of unknown permanence or integrity. Thus, within each facility, the water-surface elevation shown on the stage-probability plots for a given probability may differ across the facility by as much as 10 ft. **Table 5-4** and **Table 5-5** show the variations in water-surface elevation based on TrimR2D simulations at the fifteen monitoring sites within TRA and INTEC for AEP of 0.01 (100-yr), 0.02 (500-yr), 0.005 (2000-yr), and 0.0001 (10,000).

**5.4.1 Flood Stage - Probability at TRA.** The situation at TRA illustrates that topographic features located far from TRA have the most profound impacts on potential inundation at TRA. For discharges of 225 cms or larger, flow backwaters behind the constriction upstream of BLR8 (upstream of Hwy 20/26), flows proceed into a channel that extends 1 km north of the Big Lost River, and are entrained on the north side of an old Pioneer diversion canal (that starts 3-4 km upstream of TRA), which delivers the flow directly to the west edge of the TRA (see inundation maps in **Appendix E - Electronic Supplement**). Similarly, inundation hazards for the southern side of the TRA are dominated by flows that escape the primary Big Lost River channel about 3.2 km upstream of Monroe Avenue for discharges of > 100 cms as illustrated in **Figure 5-3** and the inundation maps (**Appendix E - Electronic Supplement**). Other sites in the TRA, like TRA-632 (map ref #7), are influenced by large scale flow features and are almost completely insensitive to topographic resolution, infiltration, or culvert scenarios (**Figure 5-4**). Only topographic resolution (**Figure 5-4a**) has a non-negligible impact on the TRA-632 stage probabilities, but the effect is still small (compare **Figure 5-4a** to **Figure 5-3b** or **Figure 5-5a**).

**5.4.2 Flood Stage - Probability at INTEC.** Topographic grid resolution also has a profound impact on estimated inundation at several sites at INTEC (**Appendix E - Electronic Supplement; Figure 5-5**) However, full versus blocked conveyance of the Big Lost River at Lincoln Avenue has the strongest impact on estimated inundation at INTEC map ref site #13 (**Figure 5-5**). Similar results are obtained at the INTEC tank farm (map ref #10, **Figure 5-6**) except that RiCOM inundation actually exceeds TrimR2D inundation for discharges larger than 100 cms (**Figure 5-6a**). The contrasts between **Figure 5-5a** and **Figure 5-6a** demonstrate some of the complex dependencies of inundation on topographic grid resolution at INTEC and serve to

emphasize the importance of using the inundation maps (**Appendix E - Electronic Supplement**) to understand the primary factors influencing inundation at INL facilities.

## 5.5 Inundation Discussion

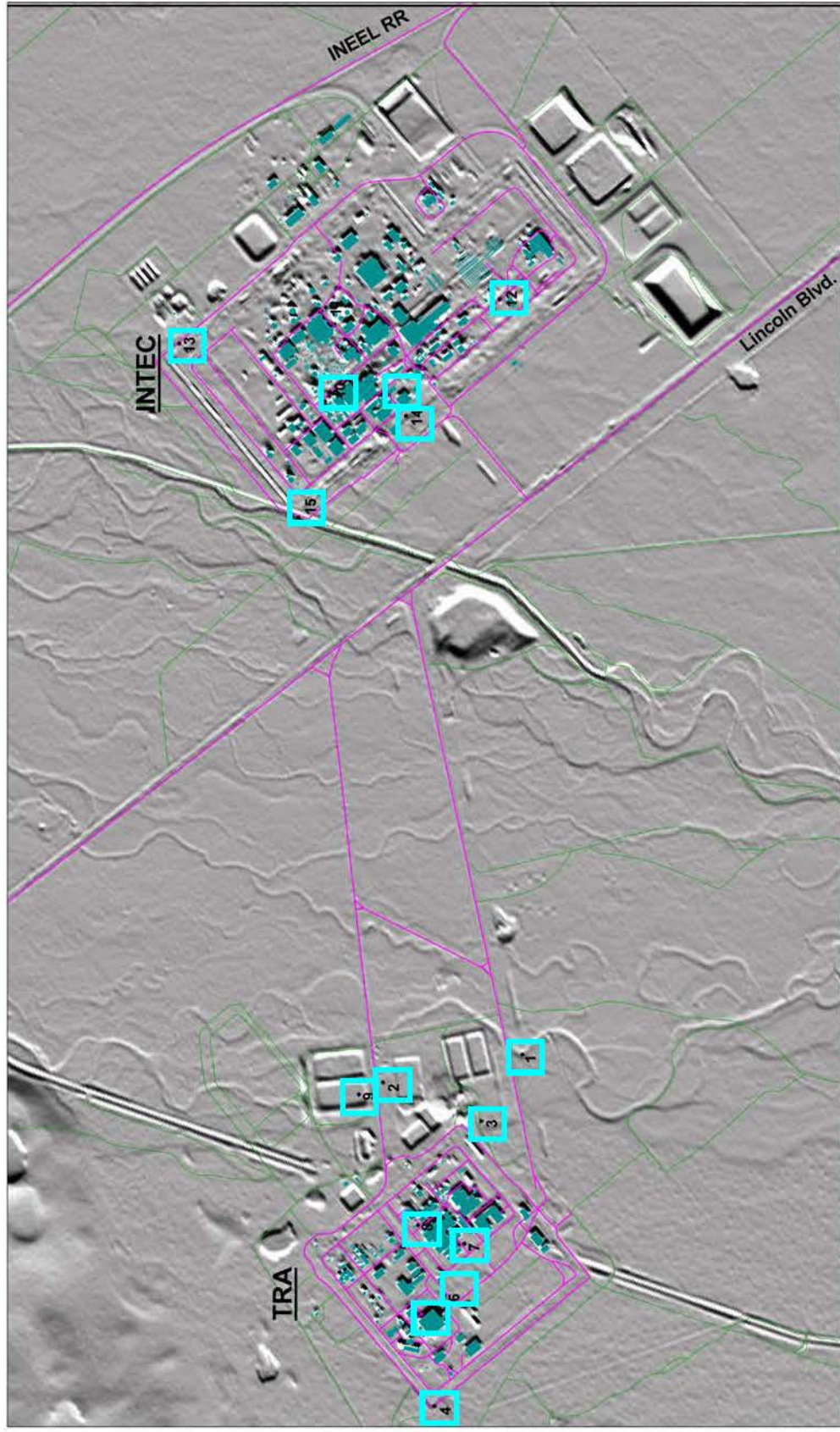
Stage hazard curves are provided in **Appendix F** for fifteen specific sites near TRA or INTEC as listed in **Table 5-3** and shown on **Figure 5-1**. For each site there are four plots of flow simulation results: 1) TrimR2D, 2) RiCOM, 3) TrimR2D - RiCOM comparisons, and 4) RiCOM Lincoln Ave blockage scenarios. Comparisons within and between these four sets of plots isolate or compare specific factors that could influence estimated stages. The TrimR2D simulations are the primary suite of results for final estimate of stage hazard curves and isolate the effects of variations in infiltration and secondary culvert blockage. Generally, the secondary culverts have virtually no impact on inundation at most sites, with only minor impacts on inundation at sites outside TRA along Monroe Avenue. Infiltration has only a modest impact on inundation and generally does not change the hazard curves much. The RiCOM simulations and TrimR2D - RiCOM simulations illustrate the impacts of topographic resolution and persistent topographic features such as roads, old diversions, etc. These factors have the strongest impacts on inundation over the entire site. The RiCOM simulations with blockage of the Big Lost River channel at Lincoln Avenue has the strongest impact on inundation for portions of INTEC, particularly for the simulations of discharges less than about 250 cms.

The inundation maps in **Appendix E - Electronic Supplement** provide an essential tool to understand the stage hazard curves in **Appendix F**. It is clear that small-scale (possibly transient) changes to topography can significantly impact inundation at TRA and INTEC. This is a consequence of the relatively flat terrain in the vicinity of the Big Lost River and these INL facilities. However, the maps also provide a tool to determine small-scale changes to topography that could substantially reduce inundation hazards at TRA and INTEC. For instance, flow along the northern side of the old diversion channel west of TRA could be blocked by rather small-scale topographic modifications about 3.2 km west of TRA near the western end of the old diversion channel. The inundation impacts of topographic modification scenarios could be easily investigated by running new flows with modifications to the detailed topographic RiCOM mesh. Clearly, the performance of the Big Lost River culverts at Lincoln Avenue have a profound

influence on stage hazards for several sites at INTEC, especially for the lower end of the discharges simulated. Similarly, although an explicit culvert blocking scenario was not constructed for the railroad embankment bridge downstream of INTEC, blockage of conveyance through the railroad embankment may also significantly influence stage hazards for portions of INTEC.

The stage hazard curves contained in **Appendix F** have the same limitations for extrapolation to small AEP ( $AEP < 0.0001$ ) as do the flood frequency results presented in **Section 4.0**. Because the flood frequency results are largely unconstrained for small AEP, no meaningful estimate of 95% limits is contained in the revised flood frequency analyses to promulgate into the stage probability estimate. Given the nearly unlimited upper bounds of extrapolation that might be possible for small AEP from the present flood frequency analyses, development of stage hazard curves for smaller AEP would also require additional hydraulic modeling for discharges much larger than 700 cms, which is the largest discharge considered in the present study.

**Figures for Section 5.0**



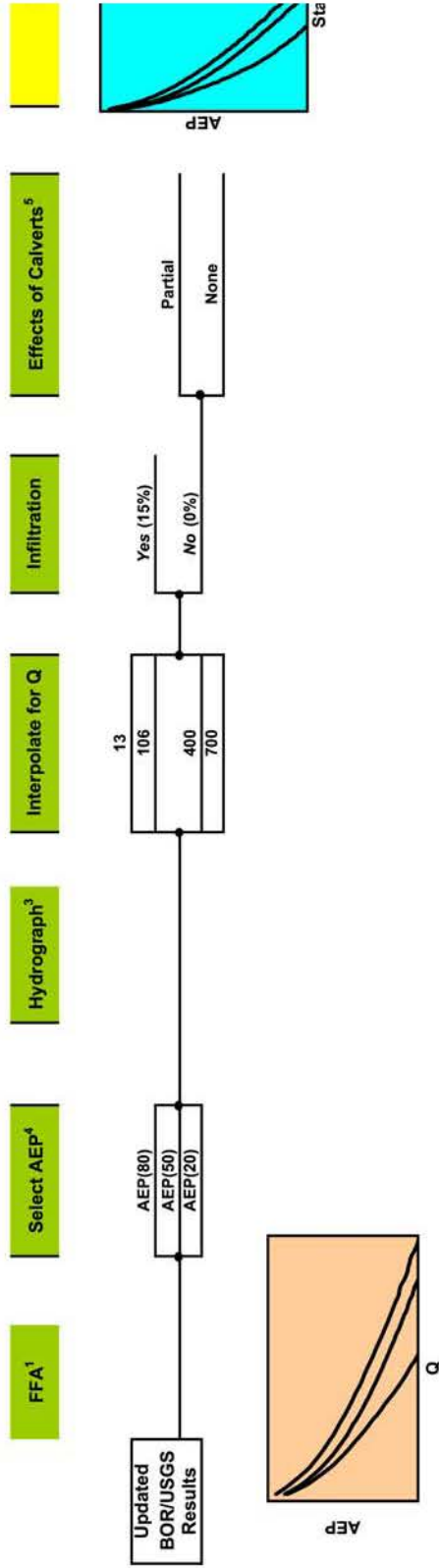
Base map is shaded relief image of 10 ft topographic grid from 1993 photography. Planimetric features are from INEEL Spatial Analyses Laboratory.



3 • Stage-probability estimate site

**Figure 5-1 Map of monitoring site locations (numbered black squares within blue boxes) for inundation at TRA and INTEC.** Sites 1 through 9 are located within and around TRA; sites 10 through 15 are located within and around INTEC. Numbers by each square are "Map Ref #" listed under "site" in **Table 5-3** and in the headings of each stage-AEP plot.

CONCEPTUAL LOGIC TREE FOR ESTIMATION OF PROBABILISTIC FLOOD STAGE



- Notes:
- <sup>1</sup>FFA - flood frequency analysis
  - <sup>2</sup>Could include regulated flow frequency and/or upstream dam failure probability estimates
  - <sup>3</sup>Hydrographic Shapes are based on assumption of natural, unregulated flow
  - <sup>4</sup>Flow simulations have been run for Q values = 13, 25, 63, 106, 150, 200, 250, 300, 400, 700 hrs
  - <sup>5</sup>For "partial" effect, main stem of river stays open; for "none," all culverts are assumed open

Figure 5-2 Conceptual logic tree for probabilistic INL inundation modeling.

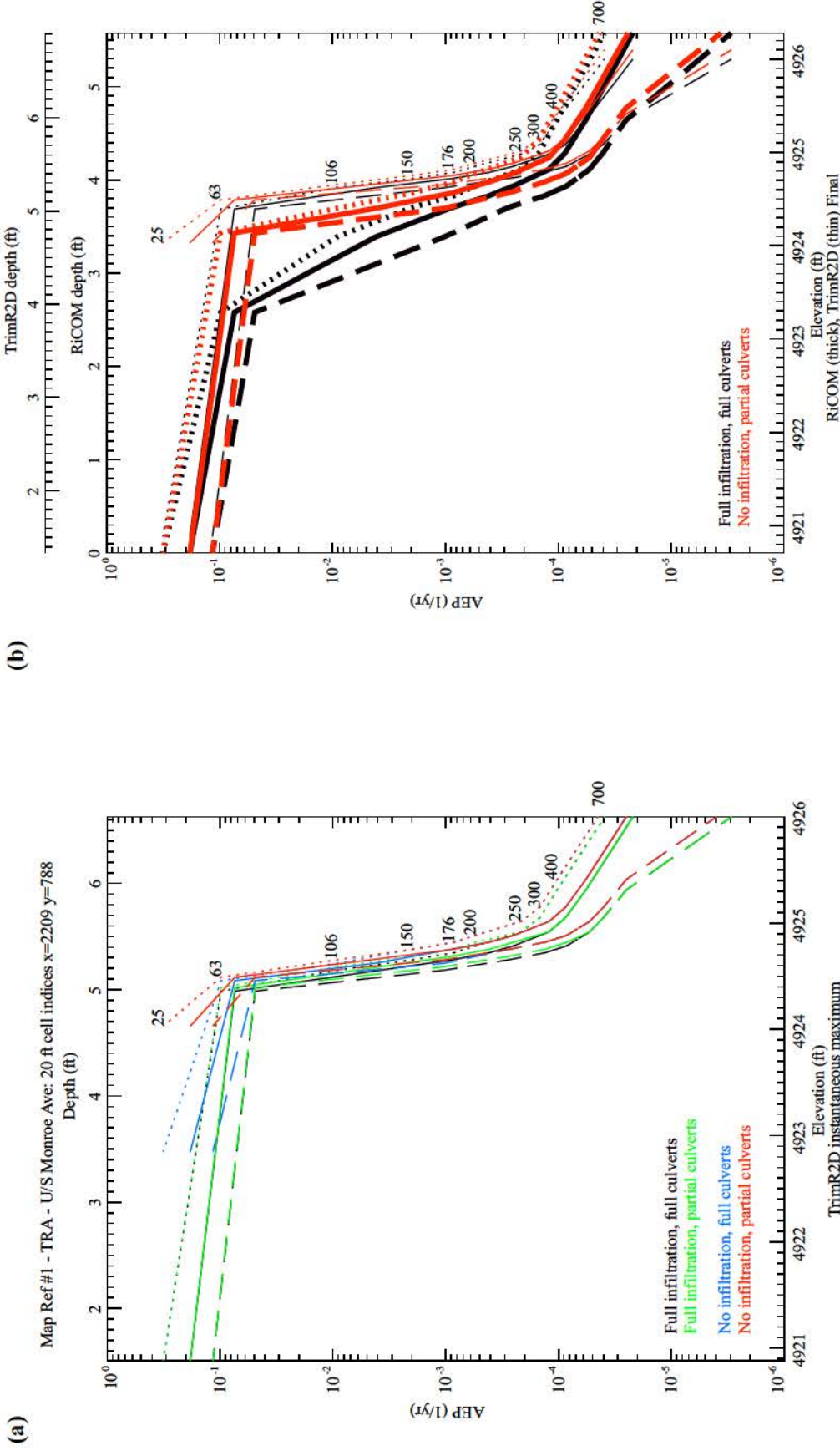
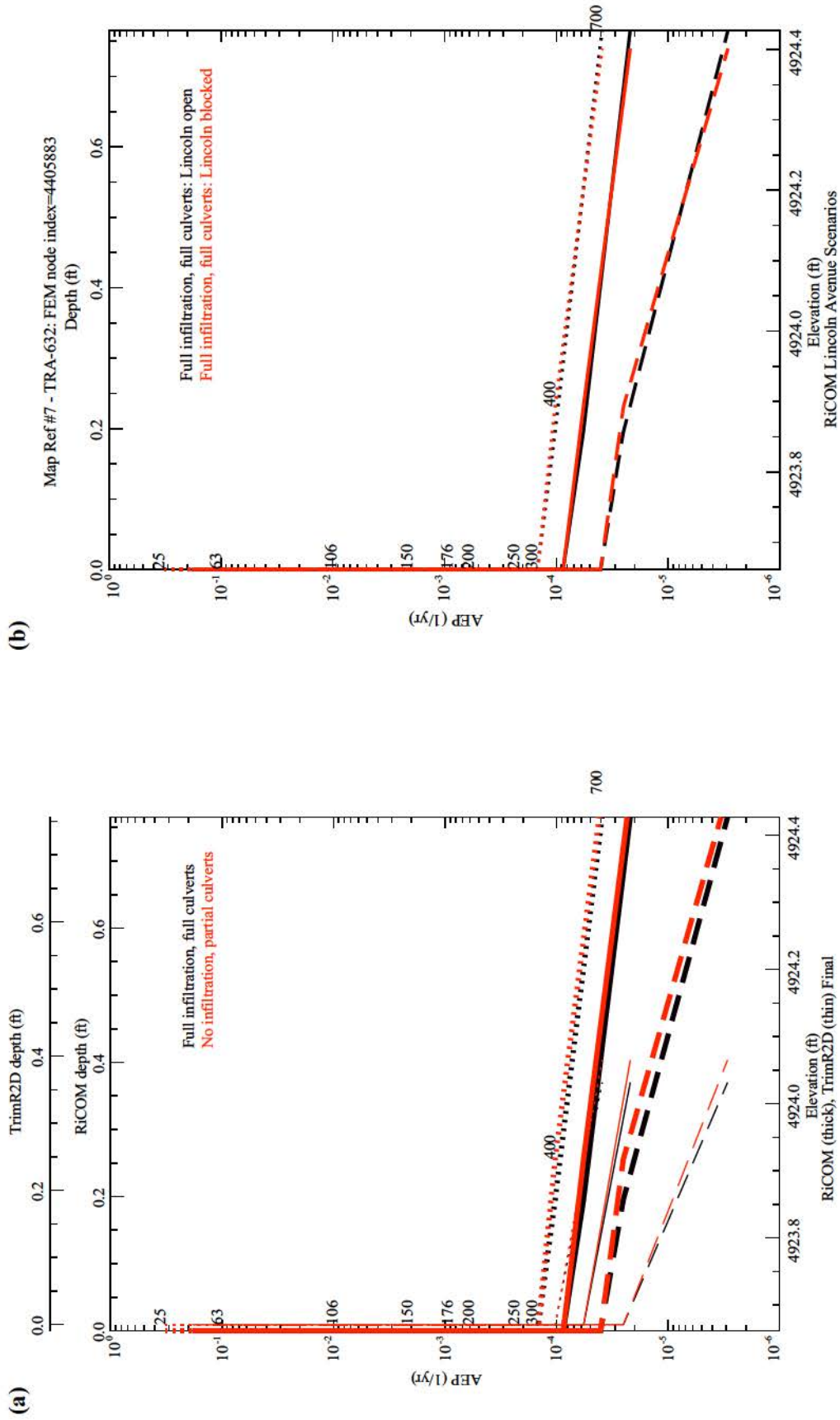
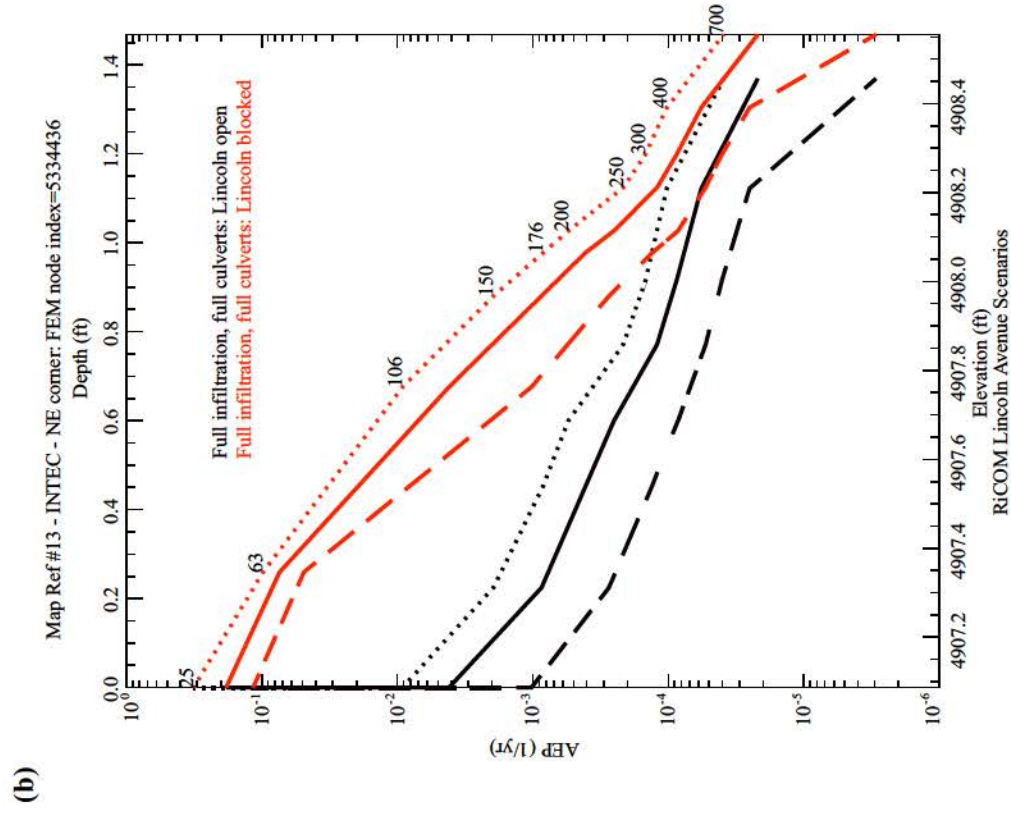
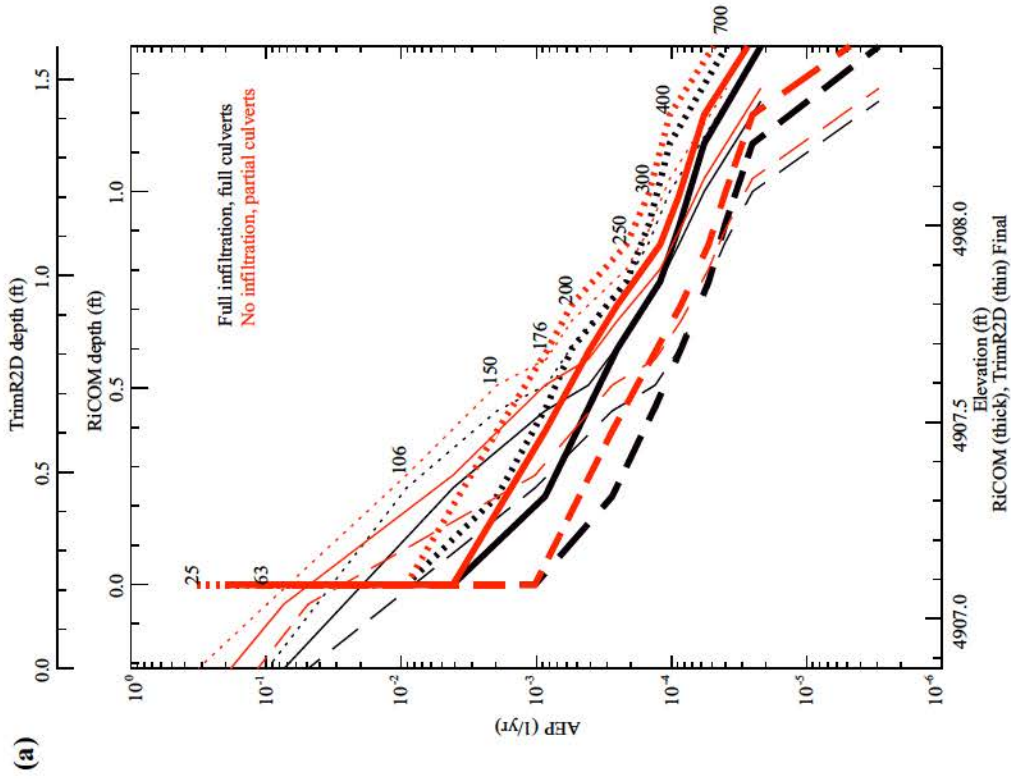


**Figure 5-3 Stage hazard curves for site TRA map ref #1.** TrimR2D results are shown in (a) and RiCOM results in (b). In the TrimR2D results (a) there are four color-coded infiltration-culvert scenarios (see legend) for fractiles of 5% (dashed curves), mean (solid curves), and 95% (dotted curves). When black or blue curves are not visible the inclusion of culverts outside the Big Lost River main channel had no influence at the site. In (b) comparison of TrimR2D (thin curves) and RiCOM (thick curves) results demonstrate that topographic resolution has the strongest impact on the site inundation. Numbers indicate discharge (cms) for specific points along the rightmost 95% curves. See **Figure 5-1** for site location.



Map Ref #7 - TRA-632: FEM node index=4405883

**Figure 5-4 Stage hazard curves for TRA-632 map ref #7.** (a) comparison of TrimR2D (thin curves) and RiCOM (thick curves) results demonstrate that topographic resolution has a stronger impact on site inundation than infiltration or culverts when the main channel is open. (b) blocking the Big Lost River at Lincoln Avenue (b) has virtually no impact on site inundation. Lines styles indicate fractiles of 5% (dashed curves), mean (solid curves), and 95% (dotted curves). Numbers indicate discharges (cms) for specific points along the rightmost 5% curves. See **Figure 5-1** for site location.



Map Ref #13 - INTEC - NE corner: FEM node index=5334436

**Figure 5-5 Stage hazard curves for INTEC map ref #13.** (a) comparison of TrimR2D (thin curves) and Ricom (thick curves) results demonstrate that topographic resolution has a stronger impact on site inundation than infiltration or culverts when the main channel is open. (b) blocking the Big Lost River at Lincoln Avenue has the strongest impact on site inundation. Lines styles indicate fractiles of 5% (dashed curves), mean (solid curves), and 95% (dotted curves). Numbers indicate discharges (cms) for specific points along the rightmost 95% curves. See **Figure 5-1** for site location.

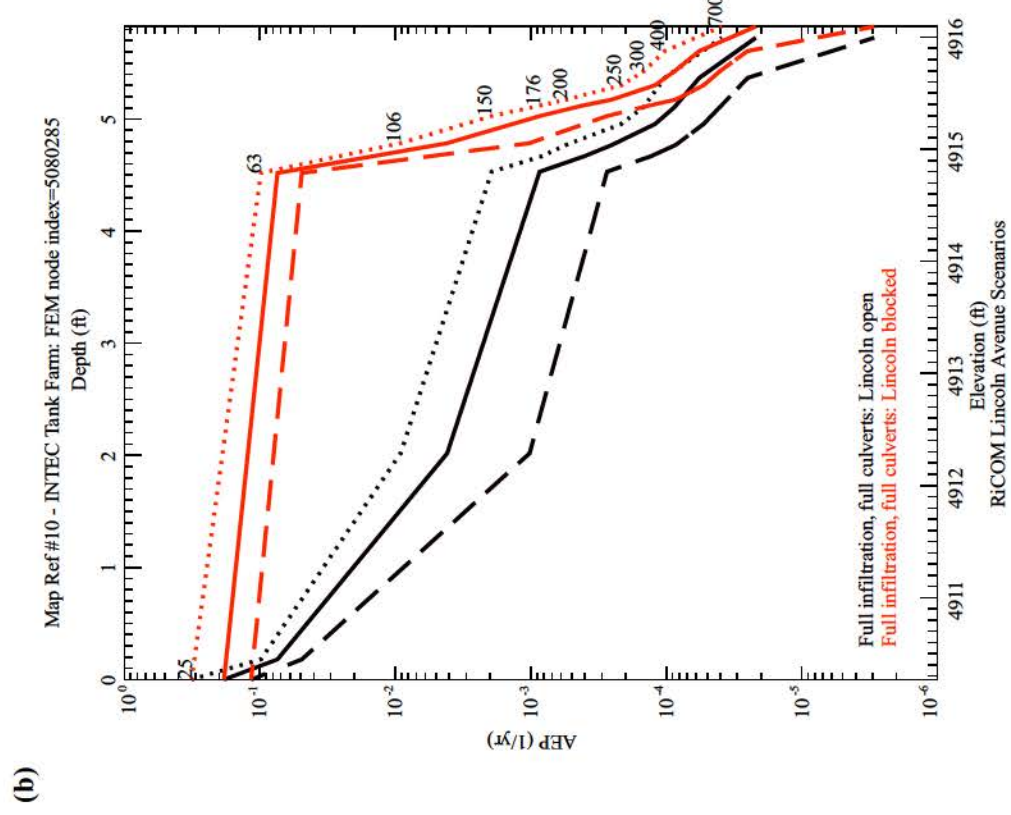
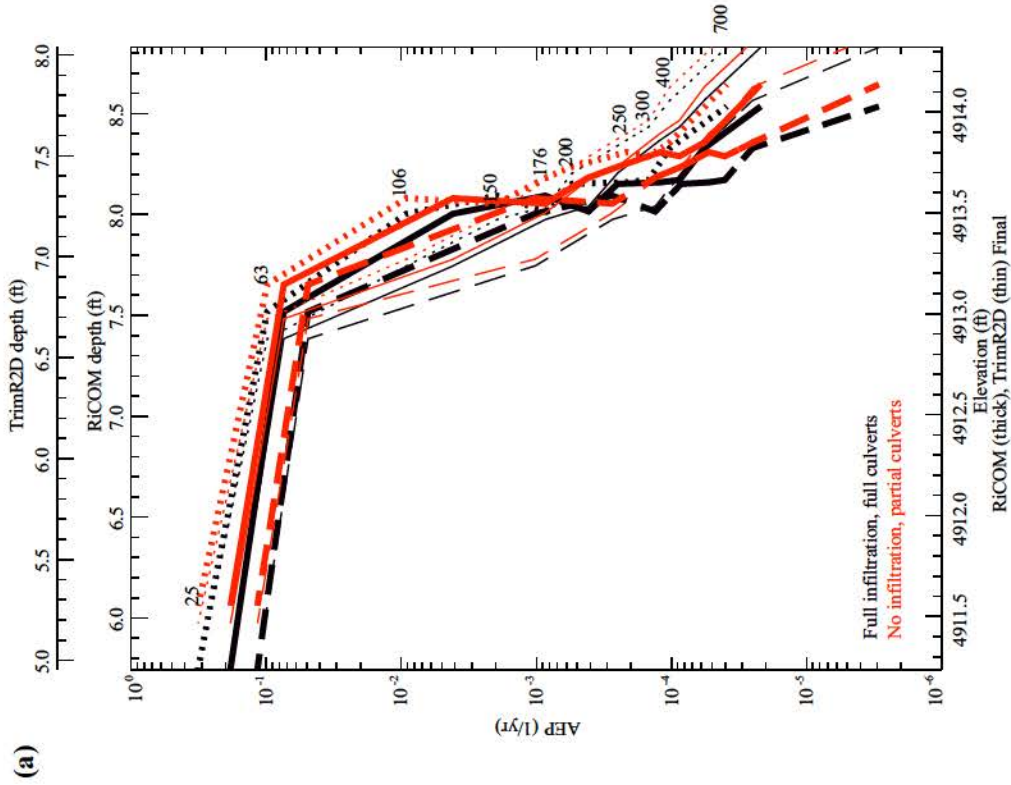


Figure 5-6 Stage hazard curves for the INTEC tank farm map ref #10.

(a) comparison of TrimR2D (thin curves) and Ricom (thick curves) results demonstrate that topographic resolution has a stronger impact on site inundation than infiltration or culverts when the main channel is open. (b) blocking the Big Lost River at Lincoln Avenue has the strongest impact on site inundation. Lines styles indicate fractiles of 5% (dashed curves), mean (solid curves), and 95% (dotted curves). Numbers indicate discharges (cms) for specific points along the rightmost 95% curves. See Figure 5-1 for site location.

**Tables for Section 5.0**

**Table 5-1 Discharge and modeling scenarios used to construct the stage - probability estimates**

| Modeled Discharge <sup>1</sup><br>m <sup>3</sup> /s (ft <sup>3</sup> /s) | Infiltration <sup>2</sup> |                  |                  |               | Potential Significance of Modeled Discharge   |
|--|---------------------------|------------------|------------------|---------------|---|
|  | None                      |                  | Full             |               |   |
|  | Full Culverts             | Partial Culverts | Partial Culverts | Full Culverts |   |
| 13 (~460)  | T                         | T                | T                | T             | Approximate maximum Big Lost River gaged flow downstream of INEEL Diversion (since 1984)  |
| 25 (~885)  | T                         | T,R              | T                | T,R           | Approximate INEEL Diversion Dam release capacity  |
| 63 (~2225)   | T                         | T,R              | T                | T,R           | Estimated maximum Big Lost River historic flood (1965) upstream of INEEL Diversion Dam  |
| 87   |                           | R                |                  | R             | Revised Big Lost River 100-yr flood (this study)  |
| 97   |                           | R                |                  | R             | 95% bound on revised Big Lost River 100-yr flood (this study)   |
| 106 (~3740)  | T                         | T,R              | T                | T,R           | Revised USGS Big Lost River 100-yr flood (Hortness and Rousseau, 2002)  |
| 110  |                           | R                |                  | R             | Revised Big Lost River 500-yr flood (this study)  |
| 130  |                           | R                |                  | R             | Data for stage-probability curves   |
| 150 (~5295)  | T                         | T,R              | T                | T,R           | Preferred discharge for Big Lost River 10,000-yr paleohydrologic bound (Ostenaar and others, 1999). Preferred discharge for late Holocene Big Lost River paleofloods (this study) |
| 176 (~6215)  | T                         | T,R              | T                | T,R           | USGS 100-yr flood downstream of INEEL Diversion Dam (Kjelstrom and Berenbrock, 1998)  |
| 200 (~7060)  | T                         | T,R              | T                | T,R           | Data for stage-probability curves   |
| 250 (~8830)  | T                         | T,R              | T                | T,R           | Preferred discharge for Big Lost River 10,000-yr paleohydrologic bound (this study)   |
| 300 (~10,595)  | T                         | T,R              | T                | T,R           | Data for stage-probability curves   |
| 400 (~14,125)  | T                         | T,R              | T                | T,R           | Data for stage-probability curves   |
| 700 (~24,720)  | T                         | T,R              | T                | T,R           | Adopted INEEL interim 100-yr flood; Estimated dam break flow at INTEC for Mackay Dam 100-yr flood failure (Koslow and Van Haaften, 1986)  |

**Notes:**

<sup>1</sup> Steady-state discharge input at upstream end of reach near INEEL Diversion Dam

<sup>2</sup> Entries in table indicate flow model used for each scenario: T - TRIMR2D with 20-ft rectangular grid as input topography; R - RICOM with 5-, 10-, and 20-ft variable grid as input topography. Limits of 5-ft mesh were defined by extent of inundation from TRIMR2D model of 100 m<sup>3</sup>/s with no infiltration and partial culverts; limits of 10-ft mesh by extent of TRIMR2D 200 m<sup>3</sup>/s inundation for same scenario.

**Table 5-2 Discharge-AEP Results from the FFA.**

| Discharge  | 5%                                | Mean                             | 95%                              |
|--|-----------------------------------|----------------------------------|----------------------------------|
| (cms)  | AEP (1/yr,T=yr)                   | AEP (1/yr,T=yr)                  | AEP (1/yr,T=yr)                  |
| 25   | $1.16 \times 10^{-01}$ (9)        | $1.84 \times 10^{-01}$ (5)       | $3.19 \times 10^{-01}$ (3)       |
| 63   | $4.901 \times 10^{-02}$ (20)      | $7.41 \times 10^{-02}$ (14)      | $9.82 \times 10^{-02}$ (10)      |
| 106  | $1.02 \times 10^{-03}$ (977)      | $4.15 \times 10^{-03}$ (241)     | $9.14 \times 10^{-03}$ (109)     |
| 150  | $2.74 \times 10^{-04}$ (3651)     | $8.61 \times 10^{-04}$ (1162)    | $1.95 \times 10^{-03}$ (513)     |
| 176  | $1.32 \times 10^{-04}$ (7588)     | $4.10 \times 10^{-04}$ (2436)    | $8.42 \times 10^{-04}$ (1188)    |
| 200  | $8.46 \times 10^{-05}$ (11,823)   | $2.51 \times 10^{-04}$ (3991)    | $5.44 \times 10^{-04}$ (1838)    |
| 250  | $5.30 \times 10^{-05}$ (18,872)   | $1.21 \times 10^{-04}$ (8269)    | $2.15 \times 10^{-04}$ (4660)    |
| 300  | $4.02 \times 10^{-05}$ (24,855)*  | $8.70 \times 10^{-05}$ (11,499)  | $1.47 \times 10^{-04}$ (6784)    |
| 400  | $2.51 \times 10^{-05}$ (39,851)*  | $5.71 \times 10^{-05}$ (17,513)  | $1.03 \times 10^{-04}$ (9737)    |
| 700  | $2.92 \times 10^{-06}$ (342,392)* | $2.18 \times 10^{-05}$ (45,839)* | $3.90 \times 10^{-05}$ (25,653)* |
| * Values with little or diminished statistical significance (See <b>Section 4.0</b> ). |                                   |                                  |                                  |

Table 5-3 Stage - Probability Sites

| Site <sup>1</sup>  |                          | x-coordinate | y-coordinate | Notes                              |
|--|--------------------------|--------------|--------------|------------------------------------|
| Map Ref #  | Description              | 20-ft grid   | 20-ft grid   |                                    |
| TRA Sites  |                          |              |              |                                    |
| 1  | TRA - Monroe Ave         | 2209         | 788          | upstream side in small channel     |
| 2  | TRA-715 (evap. pond)     | 2277         | 819          | sm. channel upstream of old Monroe |
| 3  | TRA southeast corner     | 2222         | 827          | outside fence                      |
| 4  | TRA northwest corner     | 2212         | 979          | outside fence                      |
| 5  | TRA-670 (ATR)            | 2225         | 926          | southeast corner                   |
| 6  | TRA-670 (ATR)            | 2220         | 921          | south side on Cod Street           |
| 7  | TRA-632                  | 2216         | 892          |                                    |
| 8  | TRA-621                  | 2242         | 888          |                                    |
| 9  | TRA-715 (evap. pond)     | 2288         | 828          | inside north pond                  |
| INTEC Sites  |                          |              |              |                                    |
| 10   | INTEC Tank Farm          | 2387         | 471          | NW corner                          |
| 11   | NWCF (Bldg 659)          | 2399         | 428          | SE corner                          |
| 12   | CPP-749                  | 2311         | 403          | West side                          |
| 13   | INTEC - NE corner        | 2470         | 464          | outside fence                      |
| 14   | INTEC -nr west gate      | 2345         | 474          |                                    |
| 15   | BLR - NW corner of INTEC | 2388         | 539          | in main channel                    |
| Notes:   |                          |              |              |                                    |
| <sup>1</sup> See Appendix E for plots that show Site No. locations at INTEC and TRA. |                          |              |              |                                    |

Table 5-4 Probabilistic Stage Estimates for INTEC and TRA Sites (100 and 500 floods).

| Map Ref #   | Site Description         | AEP = 10 <sup>-2</sup><br>Return period = 100 yr |                 |                 | AEP = 2 x 10 <sup>-3</sup><br>Return period = 500 yr |                 |                 |
|-------------|--------------------------|--|-----------------|-----------------|--|-----------------|-----------------|
|             |                          | 5%   | mean            | 95%             | 5%   | mean            | 95%             |
| TRA Sites   |                          |  |                 |                 |  |                 |                 |
| 1           | TRA - Monroe Ave         | 4924.49-4924.56                                  | 4924.55-4924.60 | 4924.61-4924.65 | 4924.58-4924.63                                      | 4924.67-4924.70 | 4924.72-4924.75 |
| 2           | TRA-715 (evap. pond)     | 4918.36-4918.56                                  | 4918.50-4918.64 | 4918.63-4918.71 | 4918.57-4918.67                                      | 4918.73-4918.81 | 4918.81-4918.91 |
| 3           | TRA southeast corner     | dry  | dry             | dry             | dry  | dry             | dry             |
| 4           | TRA northwest corner     | dry  | dry             | dry             | dry  | dry             | dry             |
| 5           | TRA-670 (ATR)            | dry  | dry             | dry             | dry  | dry             | dry             |
| 6           | TRA-670 (ATR)            | dry  | dry             | dry             | dry  | dry             | dry             |
| 7           | TRA-632                  | dry  | dry             | dry             | dry  | dry             | dry             |
| 8           | TRA-621                  | dry  | dry             | dry             | dry  | dry             | dry             |
| 9           | TRA-715 (evap. pond)     | dry  | dry             | dry             | dry  | dry             | dry             |
| INTEC Sites |                          |  |                 |                 |  |                 |                 |
| 10          | INTEC Tank Farm          | 4912.57-4913.12                                  | 4912.92-4913.29 | 4913.26-4913.45 | 4913.09-4913.37                                      | 4913.50-4913.65 | 4913.72-4913.85 |
| 11          | NWCF (Bldg 659)          | dry  | dry             | dry             | dry  | dry             | dry             |
| 12          | CPP-749                  | 4916.30-4916.40                                  | 4916.42-4916.51 | 4916.54-4916.60 | 4916.48-4916.55                                      | 4916.63-4916.69 | 4916.71-4916.78 |
| 13          | INTEC - NE corner        | 4907.04-4907.17                                  | 4907.18-4907.27 | 4907.31-4907.35 | 4907.25-4907.31                                      | 4907.42-4907.47 | 4907.53-4907.59 |
| 14          | INTEC -nr west gate      | 4916.30-4916.40                                  | 4916.42-4916.51 | 4916.54-4916.60 | 4916.48-4916.55                                      | 4916.63-4916.69 | 4916.71-4916.78 |
| 15          | BLR - NW corner of INTEC | 4913.03-4913.10                                  | 4913.13-4913.18 | 4913.22-4913.26 | 4913.18-4913.22                                      | 4913.34-4913.38 | 4913.46-4913.50 |

\* Values of 0.00-0.00 indicate that site is not inundated by modeled flows for stated AEP.

**Table 5-5 Probabilistic Stage Estimates for INTEC and TRA Sites (2000 and 10000 year floods).**

| Map Ref#    | Site Description         | AEP = 5 x 10 <sup>-4</sup><br>Return period = 2000 yr |                 |                 | AEP = 1 x 10 <sup>-4</sup><br>Return period = 10000 yr |                 |                 |
|-------------|--------------------------|---|-----------------|-----------------|--|-----------------|-----------------|
|             |                          | 5%  | mean            | 95%             | 5%   | mean            | 95%             |
| TRA Sites   |                          |   |                 |                 |  |                 |                 |
| 1           | TRA - Monroe Ave         | 4924.68-4924.71                                       | 4924.77-4924.80 | 4924.86-4924.90 | 4924.83-4924.86  | 4925.04-4925.09 | 4925.36-4925.43 |
| 2           | TRA-715 (evap. pond)     | 4918.74-4918.82                                       | 4918.91-4918.99 | 4919.06-4919.13 | 4919.01-4919.07  | 4919.36-4919.45 | 4919.89-4919.99 |
| 3           | TRA southeast corner     | dry   | dry-4922.21     | 4922.36-4922.45 | 4922.20-4922.37  | 4922.81-4922.96 | 4923.76-4924.02 |
| 4           | TRA northwest corner     | dry   | dry             | dry             | dry  | 4923.38-4923.52 | 4924.14-4924.20 |
| 5           | TRA-670 (ATR)            | dry   | dry             | dry             | dry  | dry             | dry             |
| 6           | TRA-670 (ATR)            | dry   | dry             | dry             | dry  | dry             | 4923.29-4923.32 |
| 7           | TRA-632                  | dry   | dry             | dry             | dry  | dry             | dry             |
| 8           | TRA-621                  | dry   | dry             | dry             | dry  | dry             | dry             |
| 9           | TRA-715 (evap. pond)     | dry   | dry             | dry             | dry  | dry             | dry             |
| INTEC Sites |                          |   |                 |                 |  |                 |                 |
| 10          | INTEC Tank Farm          | 4913.54-4913.68                                       | 4913.87-4913.98 | 4914.08-4914.18 | 4914.01-4914.11  | 4914.49-4914.57 | 4914.86-4914.89 |
| 11          | NWCF (Bldg 659)          | dry   | dry-4911.35     | 4911.77-4911.81 | 4911.22-4911.77  | 4911.93-4911.96 | 4912.03-4912.06 |
| 12          | CPP-749                  | 4916.64-4916.71                                       | 4916.79-4916.85 | 4916.93-4916.96 | 4916.88-4916.92  | 4917.15-4917.24 | 4917.45-4917.48 |
| 13          | INTEC - NE corner        | 4907.44-4907.49                                       | 4907.58-4907.64 | 4907.71-4907.77 | 4907.66-4907.72  | 4907.91-4907.95 | 4908.09-4908.13 |
| 14          | INTEC -nr west gate      | 4916.64-4916.71                                       | 4916.79-4916.85 | 4916.93-4916.96 | 4916.88-4916.92  | 4917.15-4917.22 | 4917.41-4917.45 |
| 15          | BLR - NW corner of INTEC | 4913.36-4913.40                                       | 4913.52-4913.62 | 4913.71-4913.75 | 4913.64-4913.71  | 4913.90-4913.93 | 4914.07-4914.13 |

\* Values of 0.00-0.00 indicate that site is not inundated by modeled flows for stated AEP.

## 6.0 REFERENCES

- Andrews, E.D., 1984, Bed-material entrainment and hydraulic geometry of gravel-bed rivers in Colorado: Geological Society of America Bulletin, v. 95, p. 371-378.
- Baker, V.R., and Costa, J.E., 1987, Flood power, in Mayer, L., and Nash, D., eds., Catastrophic Flooding: Boston, MA, Allen & Unwin, p. 1-21.
- Baker, V.R., Kochel, R.C., and Patton, P.C., eds., 1988, Flood geomorphology: New York, John Wiley and Sons, 503 p.
- Berenbrock, C., and Doyle, J.D., 2004, Stage-discharge relations for selected culverts and bridges in the Big Lost River flood plain at the Idaho National Engineering and Environmental Laboratory, Idaho: U.S. Geological Survey Water Resources Investigations Report 04-4066, Idaho Falls, ID, 62 p.
- Berenbrock, C., Rousseau, J.P., Orr, B.R., Twining, B.V., and Whnke, A., in prep., Flood flow and sediment characteristics of bedrock constrictions in the Big Lost River at the Idaho National Engineering and Environmental Laboratory, Idaho [DRAFT]: U.S. Geological Survey Water Resources Investigations Report 03-xxx, Idaho Falls, ID.
- Birkeland, P.W., 1999, Soils and geomorphology: New York, Oxford University Press, 430 p.
- Carson, M. A., and Griffiths, G.A., 1987, Bedload transport in gravel channels: Journal of Hydrology New Zealand, v. 26, no. 1, p. 1-151.
- Cerling, T.E., Poreda, R.J., and Rathburn, S.L., 1994, Cosmogenic  $^3\text{He}$  and  $^{21}\text{Ne}$  age of the Big Lost River flood, Snake River Plain, Idaho: Geology, v. 22, p. 227-230.
- Connor, M.A., 1998, Final report on the Jackson Lake archeological project, Grand Teton National Park, Wyoming: Report prepared for Bureau of Reclamation, Pacific Northwest Office, Boise, ID, with contributions by K.L. Pierce, S. Lundstrom, and J.M. Good, Technical Report No. 46, Department of the Interior, National Park Service, Midwest Archeological Center, Lincoln, Nebraska, 278 p.
- Cook, J.L., 1987, Quantifying peak discharges for historical floods: Journal of Hydrology, v. 96, p.29-40.
- Costa, J.E., 1978, Holocene stratigraphy in flood frequency analysis: Water Resources Research, v. 14, p. 626-632.
- Fiedler, F.R., 2002, Infiltration rates to support high-resolution hydraulic modeling at Idaho National Engineering and Environmental Laboratory, Department of Civil Engineering, University of Idaho, Moscow, ID, 13 p.
- Forman, S.L., Smith, R.P., Hackett, W.R., Tullis, J.A., and McDaniel, P.A., 1993, Timing of late Quaternary glaciations in the western United States based on the age of loess on the eastern Snake River Plain, Idaho: Quaternary Research, v. 40, p. 30-37.
- Geslin, J.K., Link, P.K., and Fanning, C.M., 2002, High-precision provenance determination using detrital-zircon ages and petrography of Quaternary sands on the eastern Snake River Plain, Idaho: Geology, v. 27, no. 4, p. 295-298.
- Good, J.M., and Pierce, K.L., 1996, Interpreting the landscapes of Grand Teton and Yellowstone National Parks, recent and ongoing geology: Grand Teton Natural History Association, Grand Teton National Park, Moose, Wyoming, 58 p.
- Harding, William M, 2002, Northwind Environmental, Inc. letter report to Dr. Kenneth Reid, State Historic Preservation Office, Boise, ID, dated September 6, 2002, 8 p.

- Hortness, J.E., and Rousseau, J.P., 2003, Estimating the magnitude of the 100-year peak flow in the Big Lost river at the Idaho National Engineering and Environmental Laboratory, Idaho: U.S. Geological Survey Water Resources Investigations Report 02-4299, Idaho Falls, ID, 36 p.
- House, P.K., Pearthree, P.A., and Klawon, J.E., 2002, Historical flood and paleoflood chronology of the lower Verde River, Arizona, *in*: House, P.K., Webb, R.H., Baker, V.R., and Levish, D.R., eds., Ancient Floods, Modern Hazards: Principles and Applications of Paleoflood Hydrology: Water and Science Application 5, American Geophysical Union, Washington, D.C., p. 267-293.
- Jarrett, R.D., and England, J.F., Jr., 2002, Reliability of paleostage indicators for paleoflood studies, *in* House, P.K., Webb, R.H., Baker, V.R., and Levish, D.R., eds, Ancient Floods, Modern Hazards: Principles and Applications of Paleoflood Hydrology: Water Science and Application Volume 5, American Geophysical Union, Washington, D.C., p. 91-109
- Johnson, D.L., and Johnson, D.N., 2003, Mima and other animal mounds as point-centered biomantles: Geol. Soc. Amer., Abstracts with Programs v.35;n. 6, p. 258.
- Kessler, M.A., and Werner, B.T., 2003, Self-organization of sorted patterned ground: Science, v. 299, p. 380-383.
- Kjelstrom, L.C., 1991, Idaho, floods and droughts, in Paulson, R.W., Chase, E.B., Roberts, R.S., and Moody, D.W., National Water Summary 1988-89 – Hydrologic events and floods and droughts: U.S. Geological Survey Water-Supply Paper 2375, p. 255-262.
- Kjelstrom, L.C., and Berenbock, C., 1996, Estimated 100-year peak flows and flow volumes in the Big Lost River and Birch Creek at the Idaho National Engineering and Environmental Laboratory, Idaho: U.S. Geological Survey Water-Resources Investigations Report 96-4163, 23 p.
- Koslow, K.N., and Van Haaften, D.H., 1986, Flood routing analysis for a failure of Mackay Dam: EG&G Idaho, Inc. report prepared for the U.S. Department of Energy, contract no. DE-AC07-76IDO1570, 33 p.
- Knudsen, K.L., Sowers, J.M., Ostenaar, D.A., and Levish, D.R., 2002, Evaluation of glacial outburst flood hypothesis for the Big Lost River, Idaho, *in*: House, P.K., Webb, R.H., Baker, V.R., and Levish, D.R., eds., Ancient Floods, Modern Hazards: Principles and Applications of Paleoflood Hydrology: Water and Science Application 5, American Geophysical Union, Washington, D.C., p. 217-235.
- Kuntz, M.A., Skipp, B., Lamphere, M.A., Scott, W.E., Pierce, K.L., Dalrymple, G.B., Champion, D.E., Embree, G.F., Page, W.R., Morgan, L.A., Smith, R.P., Hackett, W.R., and Rodgers, D.W., 1994, Geologic map of the Idaho National Engineering Laboratory and adjoining area, eastern Idaho, U.S. Geological Survey Miscellaneous Investigation Map I-2330, scale 1:100,000.
- Levish, D.R., 2002, Paleohydrologic bounds - non-exceedence information for flood hazard assessment, *in*: House, P.K., Webb, R.H., Baker, V.R., and Levish, D.R., eds., Ancient Floods, Modern Hazards: Principles and Applications of Paleoflood Hydrology: Water and Science Application 5, American Geophysical Union, Washington, D.C., p. 175-190.
- Levish, D.R., Ostenaar, D.A., and O'Connell, D.R.H., 1994, A non-inundation approach to paleoflood hydrology for the event-based assessment of extreme flood hazards, in 1994 Annual Conference Proceedings, Association of State Dam Safety Officials: Lexington, KY, Association of State Dam Safety Officials, p. 69-82.

- Levish, D.R., Ostenaar, D.A., and O'Connell, D.R.H., 1996, Paleohydrologic bounds and the frequency of extreme floods: in Gruntfest, E. (ed.), *Twenty years later what we have learned since the Big Thompson flood*: Boulder, University of Colorado, Natural Hazards Research and Applications Information Center, Special Publication No. 33, p. 171-182.
- Levish, D.R., Ostenaar, D.A., and O'Connell, D.R.H., 1997, Paleoflood hydrology and dam safety: *Waterpower '97*, Proceedings of the International Conference on Hydropower, Atlanta, GA, p. 2205-2214.
- Licciardi, J.M., Clark, P.U., Brook, E.J., Pierce, K.L., Kurz, M.D., Elmore, D., and Sharma, P., 2001, Cosmogenic  $^3\text{He}$  and  $^{10}\text{Be}$  chronologies of the late Pinedale northern Yellowstone ice cap, *Montana: Geology*, v. 29, p. 1095-1098.
- Licciardi, J.M., Clark, P.U., Brook, E.J., Elmore, D., and Sharma, P., 2004, Variable responses of western U.S. glaciers during the last deglaciation: *Geology*, v. 32, p. 81-84.
- Magilligan, F.J., 1992, Thresholds and the spatial variability of flood power during extreme floods: *Geomorphology*, v. 5, p. 373-390.
- McFadden, L.D., McDonald, E.V., Wells, S.G., Anderson, K., Quade, J., and Forman, S.L., 1998, The vesicular layer and carbonate collars of desert soils and pavements: formation, age and relation to climate change: *Geomorphology*, v. 24, p. 101-145.
- Miall, A.D., 1996, *The Geology of Fluvial Deposits: Sedimentary Facies, Basin Analysis, and Petroleum Geology*: Springer-Verlag, Berlin, Heidelberg, 582 p.
- Miller, A.J. and Cluer, B.L., 1998, Modeling considerations for simulation of flow in bedrock channels: in Tinkler, K.J. and Wohl, E.E., eds., *Rivers over rock: Fluvial processes in bedrock channels*: Washington, DC, American Geophysical Union, Geophysical Monograph 107, p. 61-104.
- NRC (National Research Council), 1995, *Natural climate variability on decade-to-century time scales*: Washington, D.C., National Academy Press, Climate Research Committee, 630 p.
- NRC (National Research Council), 1999, *Improving American River flood frequency analyses*: Washington, D.C., National Academy Press, Committee on American River Flood Frequencies, 120 p.
- O'Connell, D.R.H., 1998, FLDFRQ3 Three-parameter maximum likelihood flood-frequency estimation with optional probability regions using parameter grid integration: User's Guide (Release 1.0), <ftp://ftp.seismo.usbr.gov/pub/outgoing/geomagic/scr/fldfqr3/>, June 2000.
- O'Connell, D.R.H., 2005, Nonparametric Bayesian flood frequency estimation: *Journal of Hydrology*, v. 313, p. 79-96.
- O'Connell, D.R.H., Levish, D.R., and Ostenaar, D.A., 1996, Bayesian flood frequency analysis with paleohydrologic bounds for late Holocene paleofloods, Santa Ynez River, California: in *Twenty years later what we have learned since the Big Thompson flood*: Boulder, University of Colorado, Natural Hazards Research and Applications Information Center, Special Publication No. 33, p. 183-196.
- O'Connell, D.R.H., Levish, D.R., and Ostenaar, D.A., 1998, Risk-based hydrology: Bayesian flood-frequency analyses using paleoflood information and data uncertainties: *Proceedings of the First Federal Interagency Hydrologic Modeling Conference*, April 19 - 23, 1998, Tropicana Hotel, Las Vegas, Nevada, vol. 1, p. 4-101 to 4-108.
- O'Connell, D.R.H., Ostenaar, D.A., Levish, D.R., and Klinger, R.E., 2002, Bayesian flood frequency analysis with paleohydrologic bound data, *Water Resour. Res.* 38 (5), DOI 10.1029/2000WR000028.

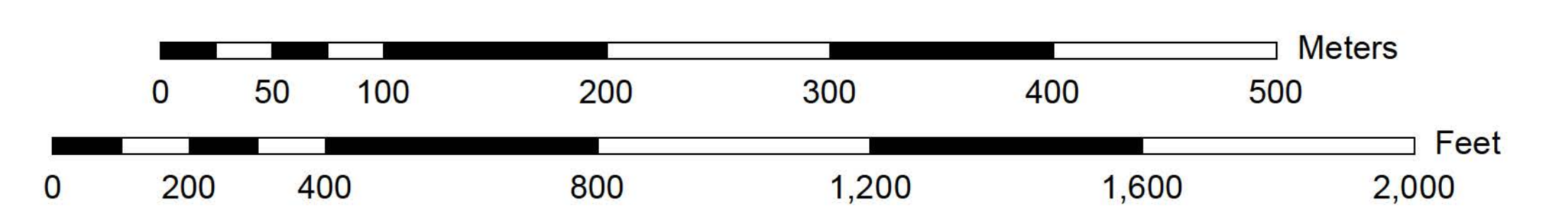
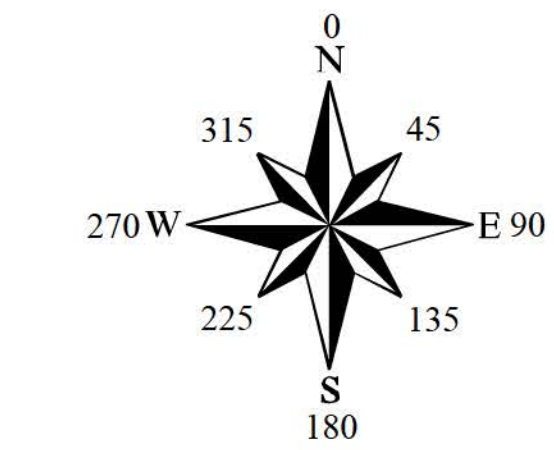
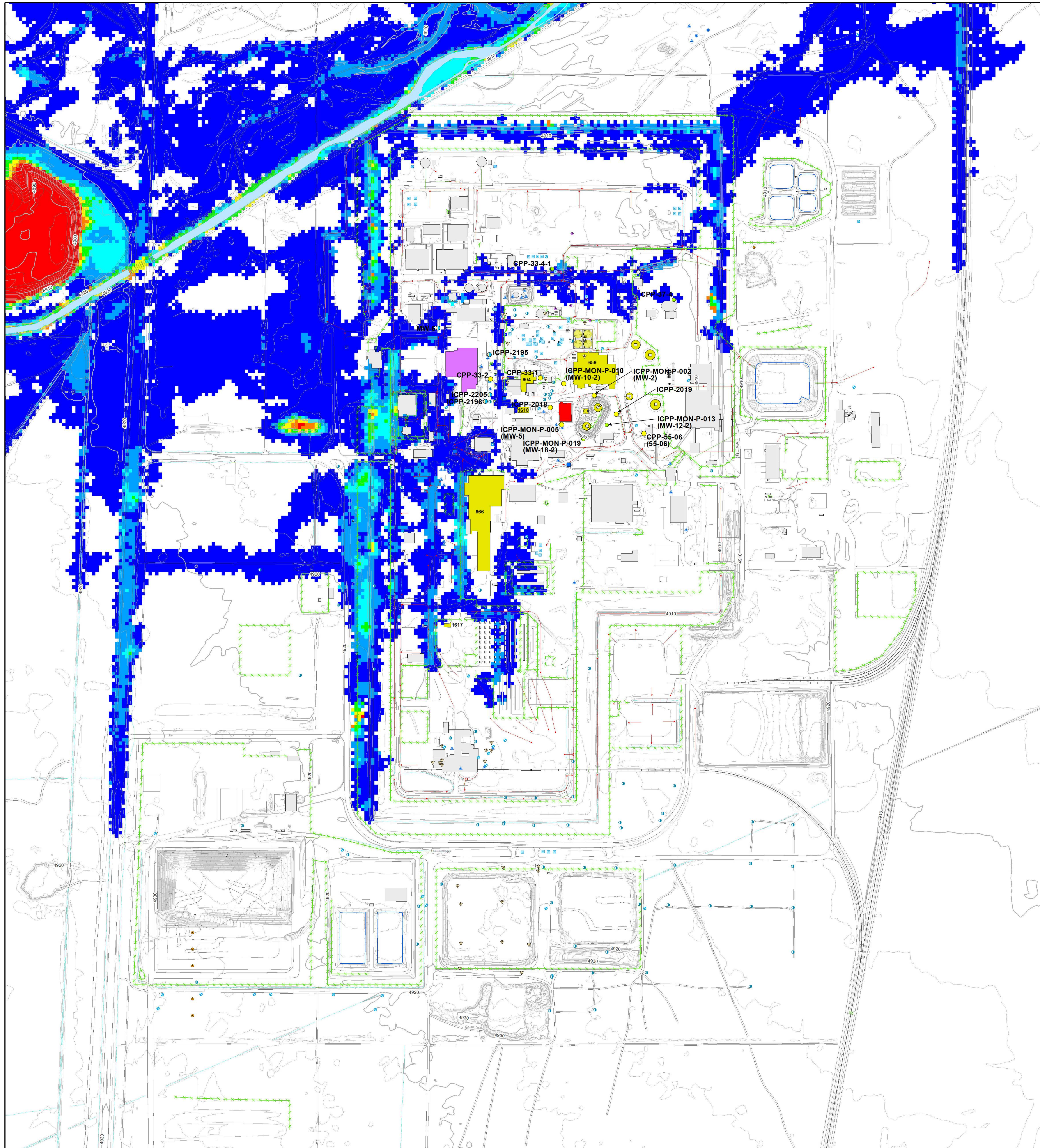
- Ostenaar, D.A., and Levish, D.R., 1996, Event-based assessment of extreme flood hazards for dam safety: in Proceedings, Association of State Dam Safety Officials Western Regional Conference, Association of State Dam Safety Officials, Lexington, KY, p. 41-54.
- Ostenaar, D.A., and Levish, D.R., 1997, Reconnaissance Paleoflood Study for Ochoco Dam, Crooked River Project, Oregon: Denver, CO, Bureau of Reclamation, Seismotectonic Report 96-2, 20 p., 1 folded plate, 2 appendices.
- Ostenaar D.A., Levish, D.R., and O'Connell, D.R.H., 1996, Paleoflood study for Bradbury Dam, Cachuma Project, California: Denver, CO, Bureau of Reclamation, Seismotectonic Report 96-3, 86 p., 1 folded plate, 4 appendices.
- Ostenaar D.A., Levish, D.R., O'Connell, D.R.H., and Cohen E.A., 1997, Paleoflood study for Causey and Pineview Dams, Weber Basin and Ogden River Projects, Utah: Denver, CO, Bureau of Reclamation, Seismotectonic Report 96-6, 69 p., 3 appendices.
- Ostenaar D.A., Levish, D.R., Klinger, R.E., and O'Connell, D.R.H., 1999, Phase 2 Paleohydrologic and Geomorphic Studies for the Assessment of Flood Risk for the Idaho National Engineering and Environmental Laboratory, Idaho: Denver, CO, Bureau of Reclamation, Geophysics, Paleohydrology and Seismotectonics Group, Report 99-7, 112 p., 1 folded plate, 4 appendices.
- Ostenaar, D.A., O'Connell, D.R.H., Walters, R.A., Creed, R.J., 2002, Holocene paleoflood hydrology of the Big Lost River, western Idaho National Engineering and Environmental Laboratory, Idaho *in*: Link, P.K., and Mink, L.L., eds., *Geology, Hydrology, and Environmental Remediation: Idaho National Engineering and Environmental Laboratory, Eastern Snake River Plain, Idaho*: Boulder, CO, Geological Society of America Special Paper 353, p. 91-110.
- Parker, G., 1978, Self-formed straight rivers with equilibrium banks and mobile bed. Part 2. The gravel river: *Journal of Fluid Mechanics*, v. 89, part 1, p. 127-146.
- Peterson, L. and Harding, W., 2002, Mitigation of site 10BT2189 (BLR-8) at the Idaho National Environmental and Engineering Laboratory, Butte County, Idaho: DRAFT, September, 2002, North Wind Environmental, Inc., NW Project 2072.202, Idaho Falls, ID, 51 p.
- Pierce, K.L., 1979, History and dynamics of glaciation in the northern Yellowstone National Park area: U.S. Geological Survey Professional Paper 729-F, 90 p.
- Pierce, K.L., and Good, J.D., 1992, Field guide to the Quaternary geology of Jackson Hole, Wyoming: US Geol. Surv. Open-File Report 92-504, 54 p.
- Pierce, K.L., and Morgan, L.A., 1992, The track of the Yellowstone hot spot: Volcanism, faulting, and uplift, in Link, Paul Karl, Kuntz, M.A., and Platt, Lucian B., eds., *Regional Geology of Eastern Idaho and Western Wyoming*: Geological Society of America Memoir 179, p. 1-53.
- Rathburn, S.L., 1991, Quaternary channel changes and paleoflooding along the Big Lost River, Idaho National Engineering Laboratory: TriHydro Corporation report prepared for EG&G Idaho, Inc., subcontract no. C90-132903, 33 p.
- Richmond, G.M., 1986, Stratigraphy and chronology of glaciations in Yellowstone National Park, *in* Sibrava, V., et al., eds., *Quaternary glaciations in the Northern Hemisphere: Quaternary Science Reviews*, v. 5, p. 83-98.
- Scott, W.E., 1982, Surficial geologic map of the eastern Snake River Plain and adjacent areas, 111° to 115° W., Idaho and Wyoming: U.S. Geological Survey Miscellaneous Investigations Series Map I-1372, scale 1:250,000.

- SSHAC, 1995, Recommendations for probabilistic seismic hazard analysis: Guidance on uncertainty and use of experts: NUREG/CR-6372, 170 p.
- Simpson, D.T., Kolbe, T.E., Ostenaar, D.A., Levish, D.R., and Klinger, R.E., 1999, Lower Big Lost River chronosequence - implications for glacial outburst flooding [abs.]: Geological Society of America, Abstracts with Programs, v. 31, no. 4, p. A-56.
- Stearns, H.T., Crandall, L., and Steward, W.G., 1938, Geology and ground-water resources of the Snake River Plain in southeastern Idaho: U.S. Geological Survey Water-Supply Paper 774, 268 p.
- Stedinger, J.R., and Cohn, T.A., 1986, Flood frequency analysis with historical and paleoflood information: Water Resources Research, v. 22, p. 785-793.
- Sturchio, N.C., Pierce, K.L., Murrell, M.T., and Sorey, M.L., 1994, Uranium-series ages of travertines and timing of the last glaciation in the northern Yellowstone area, Wyoming-Montana: Quaternary Research, v. 41, p. 265-277.
- Thackery, G.D., Lundeen, K.A., and Borgert, J.A., 2004, Latest Pleistocene alpine glacier advances in the Sawtooth Mountains, Idaho, USA: Reflections of midlatitude moisture transport at the close of the last glaciation: Geology, v. 32, no. 3, p. 225-228.
- Tullis, J.A., 1995, Characteristics and origin of earth-mounds on the eastern Snake River Plain, Idaho: Idaho Fall, Lockheed Martin Idaho Technologies, Idaho National Engineering Laboratory, INEL-95/0505, September 1995, 90 p.
- Whitlock, C., 1993, Postglacial vegetation and climate of Grand Teton and southern Yellowstone National Parks: Ecological Monographs, v. 63, p. 173-198.

**APPENDIX III**

**INTEC 100-YEAR FLOOD PLAIN MAP**  
(RICOM Flow Model) - INTEC facilities updated June 2013

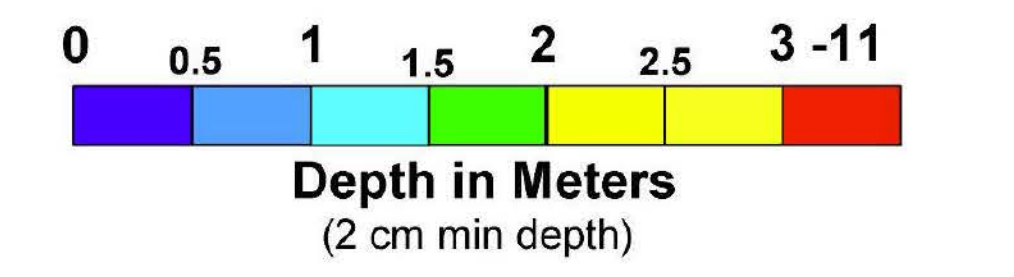
# Idaho Nuclear Technology and Engineering Center (INTEC)



## Legend

- WCF Footprint
- RCRA Treatment, Storage, and Disposal Units
- CPP-601/627/640 Footprint
- Buildings and Other Structures
- Roads
- Railroad Tracks
- Fences
- Berms
- Culverts
- Big Lost River
- Ditches
- Ponds
- 10-ft Index Contours
- 2-ft Contours
- 2-ft Depression Contours
- Surface Water Flow Paths
- Lift Station
- WCF Monitoring and Water Level Measurement Wells
- Water Level Measurement Wells
- CPP-601/627/640 Monitoring and Water Level Measurement Wells
- Borehole
- Corehole
- ▲ Injection
- Monitoring
- Observation
- Potable Water
- Production
- Scientific Instrumentation
- ▲ Shallow Injection
- ▼ Unknown

## 100 Year Flood Plain



## NOTES:

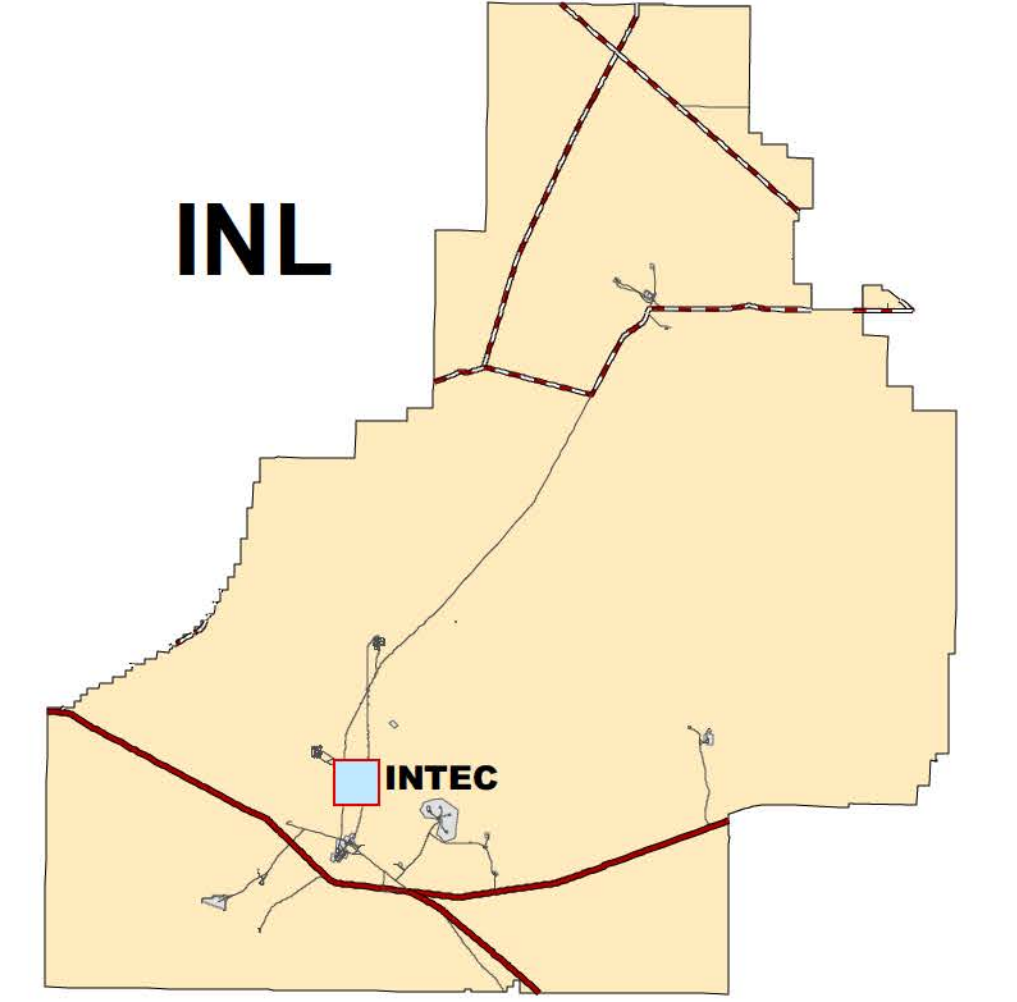
Landuse: INTEC facility boundaries are surrounded by restricted-access federal lands.

Legal Description: INTEC facility boundaries are located in Township 3 North, Range 29 East, Sections 24 and 25; and Range 30 East, Sections 19 and 30.

Base Map: INL Aerial Flyover: Aerial Mapping, October 2002, 2-ft. intervals.

Big Lost River Flood Hazard Study, Idaho National Laboratory, Idaho Report 2005-2, Dean A. Ostenaar and Daniel R. H. O'Connell, United States Bureau of Reclamation, Denver, Colorado (BOR, 2005).

In generating this map for a 100 year flow of 3,072 cubic feet per second it was conservatively assumed that the INL Diversion Dam does not exist and assumes no infiltration. The Federal Energy Regulatory Commission has recently determined that the INL Diversion Dam is adequate for handling flows up to 1 foot of freeboard (Operation Inspection Report For Department of Energy, Federal Energy Regulatory Commission, 2005) or approximately 7,300 cubic feet per second.





## **APPENDIX IV**

# **100-YEAR STORM WATER RUNOFF FLOODPLAIN AND 25-YEAR RUNOFF ANALYSIS FOR THE IDAHO NUCLEAR TECHNOLOGY AND ENGINEERING CENTER AT THE IDAHO NATIONAL ENGINEERING AND ENVIRONMENTAL LABORATORY**

**(INEEL/EXT-03-01174, REVISION 3, JANUARY 2004)**

INEEL/EXT-03-01174

Revision <sup>3</sup> *AWB*  
January 2004

# 100-Year Storm Water Runoff Floodplain and 25-Year Runoff Analyses for the Idaho Nuclear Technology and Engineering Center at the Idaho National Engineering and Environmental Laboratory



Idaho National Engineering and Environmental Laboratory

INEEL/EXT-03-01174

Revision 1<sup>3</sup>  
AMB

**100-Year Storm Water Runoff Floodplain and 25-Year  
Runoff Analyses for the Idaho Nuclear Technology  
and Engineering Center at the Idaho National  
Engineering and Environmental Laboratory**

Prepared By:

Clear Creek Hydrology, Inc.  
and  
Neil C. Hutten, INEEL

Published January 2004

**Idaho National Engineering and Environmental Laboratory  
Idaho Falls, Idaho 83415**

Prepared for the  
U.S. Department of Energy  
Assistant Secretary for Environmental Affairs  
Under DOE Idaho Operations Office

## PROFESSIONAL CERTIFICATION

**100-Year Storm Water Runoff Floodplain and 25-Year Runoff Analyses for the Idaho Nuclear Technology and Engineering Center at the Idaho National Engineering and Environmental Laboratory**

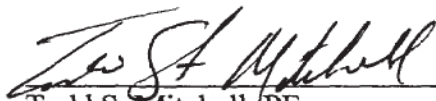
**Document No. INEEL/EXT-0301174**

**Bechtel BWXT Contract Number 19200**

**January, 2004**

The hydrologic analysis of the Idaho Nuclear Technology and Engineering Center was conducted in accordance with the scope, requirements, and limitations set forth by the Idaho National Engineering and Environmental Laboratory and Bechtel BWXT, LLC. The project was conducted, and this report prepared, under the professional supervision of the undersigned.

The data, analysis, and conclusions are presented, within the limits prescribed by the client, after being prepared in accordance with generally accepted professional civil, hydrologic and hydraulic engineering practices. This report was prepared for conditions existing at the site in May 2003, and any modifications to the study area since that time are not represented in the results and conclusions presented within.

  
\_\_\_\_\_  
Todd S. Mitchell, PE  
Civil Engineer  
Idaho PE Certificate No. 10628



exp 6/30/05

## ABSTRACT

This hydrologic study of the Idaho Nuclear Technology and Engineering Center (INTEC) at the Idaho National Engineering and Environmental Laboratory (INEEL) was conducted to identify the 100-year storm water runoff floodplain boundary for the drainage system and surface water channels in the vicinity of the site and to evaluate the capacity of the drainage system during the 25-year storm. The INTEC is subject to permitting under the Resource Conservation and Recovery Act (RCRA), which requires analysis of the 25-year runoff and 100-year floodplain associated with natural and man-made drainages. Storm water drainage diversions, channels, hydraulic control structures and retention areas have been constructed throughout and around the facility to minimize flooding potential and are the subject of these hydrologic and hydraulic analyses and report.

The hydrologic study was conducted to evaluate the largest 25-year and 100-year storm water flood flows through and in the vicinity of this facility. Summer, winter rain on snow, and winter rain on snow with frozen ground conditions were evaluated as a part of this study to identify the maximum flows anticipated for storms with the specified return intervals. Flood flows were generated using hydrologic models of the facility and incorporated into hydraulic models of storm water drainage systems and the Big Lost River. Peak water surface profiles were used to map the 100-year storm water runoff floodplain boundaries to represent conditions at the INTEC as of May 2003, and to evaluate the capacity of the storm water drainage system during the 25-year runoff event.

# CONTENTS

|   |  |     |
|---|--|-----|
| ABSTRACT .....  |  | iii |
| ACRONYMS .....  |  | vii |
| 1. INTRODUCTION .....   |  | 1   |
| 1.1 General .....   |  | 1   |
| 1.2 Objective .....   |  | 2   |
| 1.3 Previous Investigations .....                               |  | 4   |
| 1.4 Acknowledgements .....                                      |  | 5   |
| 1.5 Limitations .....   |  | 5   |
| 2. REGIONAL HYDROLOGY .....                                     |  | 6   |
| 2.1 Climatology and Historic Flooding Data Sources .....        |  | 6   |
| 2.2 Historical Flood Events .....                               |  | 7   |
| 2.3 Summer and Winter Design Storm Conditions .....             |  | 8   |
| 2.3.1 Design Storm Precipitation .....                          |  | 8   |
| 2.3.2 Snowmelt .....  |  | 11  |
| 2.3.3 Frozen Ground and Concrete Impermeable Frost .....        |  | 11  |
| 2.4 Summer and Winter Design Storm Parameters .....             |  | 13  |
| 3. FIELD INVESTIGATION AND DATA COLLECTION .....                |  | 15  |
| 3.1 Watershed and Subarea Boundary Verification .....           |  | 15  |
| 3.2 Hydraulic Structure Inventory .....                         |  | 15  |
| 3.3 Field Surveying and Measurements .....                      |  | 16  |
| 4. HYDROLOGIC MODELING .....                                    |  | 17  |
| 4.1 Hydrologic Characteristics and Modeling Parameters .....    |  | 17  |
| 4.1.1 Watershed and Sub Area Delineation .....                  |  | 17  |
| 4.1.2 Soil Type and Vegetation .....                            |  | 19  |
| 4.1.3 Impervious Surfaces .....                                 |  | 21  |
| 4.1.4 Natural and Man-Made Surface and Diversion Channels ..... |  | 22  |
| 4.1.5 Storm Water Retention Areas .....                         |  | 22  |
| 4.1.6 Big Lost River .....                                      |  | 22  |

|       |  |    |
|-------|--|----|
| 4.2   | Hydrologic Modeling and Analysis.....                                  | 23 |
| 4.2.1 | SCS Curve Numbers and Precipitation Losses .....                       | 23 |
| 4.2.2 | Time of Concentration .....  | 25 |
| 4.2.3 | HEC-1 Model Input and Output.....                                      | 29 |
| 4.2.4 | Hydrologic Modeling Approach.....                                      | 29 |
| 4.3   | Hydrologic Modeling Results .....                                      | 30 |
| 4.4   | Comparison of Results to Historic Rain/Snow/Frozen Ground Floods ..... | 38 |
| 5.    | HYDRAULIC ANALYSIS .....   | 39 |
| 5.1   | Big Lost River .....   | 39 |
| 5.1.1 | Channel Geometry .....   | 39 |
| 5.1.2 | Bridges and Culverts.....  | 39 |
| 5.1.3 | Roughness Coefficients .....   | 40 |
| 5.1.4 | Hydraulic Modeling Process and Equations .....                         | 40 |
| 5.1.5 | HEC-RAS Model Simulations, Big Lost River.....                         | 40 |
| 5.2   | INTEC Surface and Subsurface Drainage System Modeling.....             | 41 |
| 5.2.1 | SWMM Program Input Parameters .....                                    | 42 |
| 5.2.2 | Storm Water Runoff Hydrographs.....                                    | 42 |
| 5.2.3 | SWMM Analysis .....  | 42 |
| 5.2.4 | SWMM Modeling Results. ....  | 44 |
| 5.3   | 25-year and 100-year Floodplain Mapping.....                           | 45 |
| 6.    | CONCLUSIONS .....  | 46 |
| 7.    | REFERENCES.....  | 47 |

## TABLES

|   |    |
|---|----|
| 2-1. Precipitation depths (inches) for summer design storms. ....                                     | 9  |
| 2-2. Precipitation depths (inches) for winter design storms. ....                                     | 10 |
| 2-3. Precipitation depths (inches) for winter rain on frozen ground design storms. ....               | 10 |
| 4-1. SCS Curve Numbers for sage-grass complexes. ....   | 21 |
| 4-2. SCS Curve numbers used in hydrologic modeling. ....  | 23 |
| 4-3. Sub area flow parameters used in determining time of concentration ( $t_c$ ) and lag times ..... | 27 |
| 4-4. Time of concentration ( $t_c$ ) for sub areas. ....  | 28 |
| 4-5. Peak flow for individual sub areas. ....   | 32 |
| 4-6. Peak flows for key hydrograph combinations used in hydraulic analyses. ....                      | 33 |

## FIGURES

|   |    |
|---|----|
| Figure 1-1. INEEL and INTEC Location. ....  | 2  |
| Figure 1-2. INTEC Plan View. ....   | 3  |
| Figure 4-1. 25-year summer storm hydrographs for Lincoln Boulevard, Big Lost River. ....  | 34 |
| Figure 4-2. 25-year summer storm hydrographs for INTEC sub areas. ....                    | 34 |
| Figure 4-3. 100-year summer storm hydrographs for Lincoln Boulevard, Big Lost River. .... | 35 |
| Figure 4-4. 100-year summer storm hydrographs for INTEC sub areas. ....                   | 35 |
| Figure 4-5. 25-year winter storm hydrographs for Lincoln Boulevard, Big Lost River. ....  | 36 |
| Figure 4-6. 25-year winter storm hydrographs for INTEC sub areas. ....                    | 36 |
| Figure 4-7. 100-year winter storm hydrographs for Lincoln Boulevard, Big Lost River. .... | 37 |
| Figure 4-8. 100-year winter storm hydrographs for INTEC sub areas. ....                   | 37 |

## DRAWINGS

Sheet 1. INTEC Facility and Surrounding Area, Watershed and Sub Area Boundaries

Sheet 2. INTEC Facility Detail, 100-Year Floodplain

## ACRONYMS

|         |   |
|---------|---|
| AMC     | Antecedent moisture condition                           |
| amsl    | Above mean sea level                                    |
| CCH     | Clear Creek Hydrology, Inc.                             |
| CFA     | Central Facilities Area                                 |
| CFR     | Code of Federal Regulations                             |
| CFS     | Cubic feet per second                                   |
| CN      | Curve Number  |
| DDF     | Depth duration frequency                                |
| DOE     | Department of Energy                                    |
| EPA     | Environmental Protection Agency                         |
| F       | Fahrenheit  |
| FAA     | Federal Aviation Administration                         |
| FEMA    | Federal Emergency Management Agency                     |
| FT      | Feet  |
| GPS     | Global Positioning System                               |
| HEC     | Hydrologic Engineering Center                           |
| HEC-RAS | Hydrologic Engineering Center's River Analysis System   |
| ID      | Idaho   |
| IN      | Inches  |
| INEEL   | Idaho National Engineering and Environmental Laboratory |
| INTEC   | Idaho Nuclear Technology and Engineering Center         |
| LB      | Lincoln Boulevard                                       |
| MI      | Mile  |
| MIN     | Minutes   |
| NAD     | North American Datum                                    |
| NGVD    | National Geodetic Vertical Datum                        |
| NOAA    | National Oceanographic and Atmospheric Administration   |
| NRCS    | Natural Resource Conservation Service                   |
| NWS     | National Weather Service                                |
| RCRA    | Resource Conservation and Recovery Act                  |
| RWMC    | Radioactive Waste Management Complex                    |
| S       | Second(s), Slope  |
| SCS     | Soil Conservation Service                               |
| SWMM    | Storm Water Management Model                            |
| T       | Time  |
| $t_c$   | Time of Concentration                                   |
| US      | United States   |
| USCOE   | United States Army Corps of Engineers                   |
| USGS    | United States Geological Survey                         |

# 100-Year Storm Water Runoff Floodplain and 25-Year Runoff Analyses for the Idaho Nuclear Technology and Engineering Center at the INEEL

## 1. INTRODUCTION

### 1.1 General

The Idaho Nuclear Technology and Engineering Center (INTEC) is located approximately 50 miles west of Idaho Falls in the south-central portion of the Idaho National Engineering and Environmental Laboratory (INEEL) (Figure 1-1). The facility encompasses a total of 420 acres within a perimeter fence and adjoining areas (Figure 1-2).

The INTEC is located at the northeastern end of a large, relatively flat, fan-shaped area dominated by volcanic features including basalt flows. It is located immediately south of the Big Lost River in an arid portion of Idaho where storms are generally infrequent, producing little storm water runoff and flooding potential. Storm water runoff around INTEC generally infiltrates the soils or evaporates before reaching the Big Lost River. The Big Lost River itself generally flows very little near the INTEC due to the lack of precipitation, upgradient water withdrawal for irrigation and the presence of control structures upgradient of the site.

Historically, the INTEC has seen only minor localized flooding and ponding in depression areas inside and around the facility. No significant flooding due to storm water runoff was identified during discussions with INTEC and INEEL personnel, including periods when floods occurred in other locations near INTEC. A storm water drainage network constructed with open surface water channels, culverts, storm water catch basins and subsurface piping serves to manage storm water runoff through the facility, directing it to the northeast edge of the facility where it is discharged into a retention area. Excess water in the retention area overflows towards the Big Lost River during significant runoff events.

Modifications and improvements to the drainage system serving the INTEC facility have been constructed since the mapping and field investigation for this study were completed. Improvements include a new retention basin with additional storage volume for discharge from the facility and other minor drainage modifications and upgrades. The analyses conducted for this study were prepared for conditions existing at the site as of May 2003 and do not include alterations to the drainage system and facilities since that time.

The Big Lost River, immediately north of the INTEC, is controlled by a long barrier dike in the vicinity of the facility to limit flooding potential and flows northeast to its termination in the playas. Big Lost River flows have not entered the INTEC since operations began in the 1950's. This floodplain analysis for the INTEC facility is limited to storm water runoff from the contributing area around the facility. The potential for riverine flooding from the Big Lost River is being studied by others and is beyond the scope of this project and report.

## 1.2 Objective

The primary objective of this project is to determine the magnitude and extent of the largest 100-year return interval storm and develop a storm water runoff floodplain map for the hypothetical storm as required by state and federal regulations to determine whether INTEC facilities are within the floodplain boundaries and subject to potential flooding. The secondary objective is to ensure that the INTEC storm water drainage system will convey, at a minimum, the 25-year, 24-hour peak storm water runoff flow.

This hydrologic and hydraulic analysis of the INTEC facility was conducted according to the requirements of the Resource Conservation and Recovery Act found in 40 Code of Federal Regulations (CFR) Section 270.14(b)(11)(iii). Additionally, the modeling and mapping prepared for this study were conducted according to the procedures and methods required by the Federal Emergency Management Agency (FEMA).

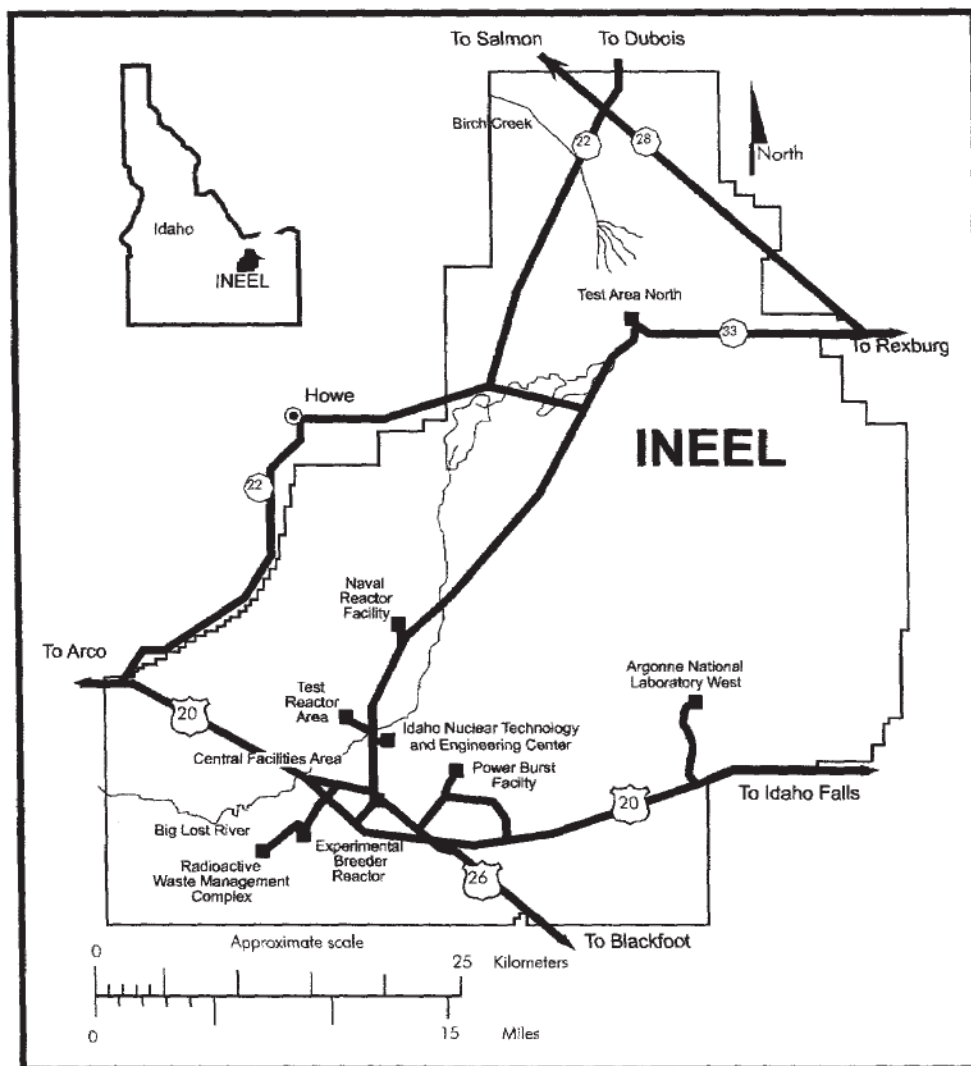


Figure 1-1. INEEL and INTEC location.



Figure 1-2. INTEC Plan View

### 1.3 Previous Investigations

Previous studies of the area around the INTEC and INEEL have been conducted to evaluate potential flooding events, storm water drainage systems and the Big Lost River. Specific aspects of these studies that are relevant to the current study are discussed in the following paragraphs and in subsequent sections of this report.

Tullis and Koslow (1983) characterized Big Lost River floods with recurrence intervals greater than 25 years by a statistical analysis of short-term historical records and through the study of slack water deposits. The United States Geological Survey (USGS) (Berenbrock and Kjelstrom, 1998) evaluated flood potential on the Big Lost River by utilizing a one-dimensional model to calculate water surface elevations and estimate inundated areas during the 100-year peak flow. Ostenaar, et al., (1999) performed a paleoflood study of the Big Lost River.

Koslow and Van Haaften (1986) utilized the National Weather Service (NWS) DAMBRK model to simulate four different hypothetical Mackay Dam failure scenarios. The magnitude of the combined probability of the 100-year recurrence interval flood with Mackay Dam failure was not specified in this report, but by definition is less than the probability of the 100-year event alone. Likewise, the probability of the hydrologic events discussed in this current report with the simultaneous occurrence of a hypothetical Mackay Dam failure is much less than 0.01. Analyses of the flood magnitude and potential associated with the Mackay Dam and the Big Lost River were considered beyond the scope of this project.

Taylor, et al., (1994) conducted a detailed study of flooding events at the INEEL that occurred in 1962, 1964, 1969 and 1972, resulting from combinations of precipitation, snowmelt and frozen ground. Results of the study concluded that the most significant flooding potential at the INEEL occurs during winter months with rain on snow in the presence of frozen ground. Mitchell, et al., (2002) conducted a detailed hydrologic analysis of the Radioactive Waste Management Complex (RWMC), including a comparison of summer and winter storm events, similar in nature to this current study. Results of the RWMC analysis verified Taylor's findings with the largest 100-year return interval event occurring during the winter rain on snow with frozen ground event and serves as a guideline for the current study of INTEC.

Burgess, J.D. (1991) conducted hydrologic and hydraulic analyses of the storm water drainage system within the INTEC facility perimeter to evaluate adequacy during the 25-year return period event. Results of the investigation included a comparison of the hydraulic capacity of surface channels, storm water piping, culverts and other features with storm water runoff during the 25-year, 24-hour event. It also included recommendations for improvements to the drainage system in order to minimize flooding potential. Results of the Burgess study were used as background information for the 25-year, 24-hour storm event analysis conducted as a part of the current study, however, the Burgess study was conducted prior to additional construction and improvements completed at the INTEC.

The current study was performed to include recent precipitation and temperature data and to address changes in topography and facility drainage structures made after previous investigations were completed. Topographic data used in the current study were collected in an aerial photogrammetry flight by Aerial Services, Inc. of Cedar Falls, Iowa on July 30, 2002.

## **1.4 Acknowledgements**

Appreciation is extended to Mr. Ken Beard of the INEEL and the INTEC facility for his assistance with site surveying and data. Mr. Beard provided extensive surveying of storm water control structures including surface water channels, storm drainage inlets and culverts. He conducted surveying in restricted access areas and provided surveying control point data utilized during the field investigation for this study.

## **1.5 Limitations**

This hydrologic and hydraulic study was conducted for the INTEC facility with base mapping and topography created in 2002, and additional field investigation data collected in May of 2003. Results of this study are presented for conditions at the site as of May, 2003.

Several areas in and around the INTEC facility, the surrounding watershed, and near other facilities were under construction at the time of the field investigation or were modified or improved after the field investigation. Changes in topography, drainage patterns, and facilities completed after May of 2003 are not represented in the analyses and results of this report.

## 2. REGIONAL HYDROLOGY

Regional hydrology of the southern portion of the INEEL was investigated in the current study for the area around the INTEC facility during the course of this investigation and in a recent study performed for the RWMC (Mitchell, et al., 2002). An investigation and review of available regional hydrology documentation was conducted in order to determine the appropriate design storm conditions and watershed parameters for use in hydrologic and hydraulic modeling of the site. Several sources of information were utilized to determine existing conditions during previous flooding events throughout southeastern Idaho and the surrounding area, which provides a measure of flood and regional hydrologic conditions for the INTEC. This section of the report discusses the sources of information reviewed as a part of the evaluation of regional hydrologic conditions and used to develop design storm parameters and precipitation statistics for the hydrologic modeling.

### 2.1 Climatology and Historic Flooding Data Sources

Several sources of information relating to climatology and historic flooding were utilized in determining regional hydrologic conditions for the INTEC and the INEEL. Regional hydrologic information is available for southeastern and central Idaho, however, there is limited information relating specifically to stream flows and storm water runoff for the INTEC and INEEL. Data used in this hydrologic study were obtained from the National Weather Service for the area within and surrounding the INEEL. In the absence of site-specific information, data were selected for areas with similar hydrologic regimes outside of the INEEL including southern Idaho, northern Utah, northern Nevada and southwestern Montana. Data sources utilized in this hydrologic investigation include the following:

- United States Geological Survey, Methods for Estimating Magnitude and Frequency of Floods in the Southwestern United States, Open File Report 93-419, 1994.
- National Weather Service, INEEL Winter Flood Events, Idaho Falls 46W Data (1952 - 2000).
- National Weather Service, Idaho Falls FAA, Idaho Falls Airport Gage data (1948 - 1952).
- National Weather Service, Idaho Falls 2ESE Gage Data (1952 - 1960).
- National Weather Service, Idaho Falls 16SE Gage Data (1960 - 1997).
- National Weather Service, Dubois Gage Data (1948 - 1997).
- National Weather Service, Twin Falls Gage Data (1978 - 1997).
- Soil Conservation Service, National Engineering Handbook, 1972.
- United States Army Corps of Engineers, Snow Hydrology Manual, 1998.

In addition to the data sources identified above, several reports and technical memoranda regarding the INTEC facility and other hydrologically similar areas were reviewed to evaluate previous flooding events and hydrologic studies including:

- Eugene L. Peck and E. Arlo Richardson, 1962, *An Analysis of the Causative Factors of the February 1962 Floods in Utah and Eastern Nevada*, National Weather Service, Salt Lake City, Utah.
- United States Army Corps of Engineers, 1975, *Humbolt River and Tributaries, Nevada*, Design Memorandum No. 1, Sacramento District.
- Dr. John H. Humphrey, 1994, *Meteorological Analysis, Flood Control Master Plan*, Washoe County, Nevada.
- CH2MHill, Inc., 1989, *Silver Bow Creek Flood Modeling Study*, Silver Bow County, Montana.
- Burgess, J.D., 1991, *25-year, 24-Hour Storm Analysis for the Idaho Chemical Processing Plant*.
- J. Sagendorf, 1991, *Meteorological Information for RWMC Flood Potential Studies*, National Oceanic Atmospheric Administration, Environmental Research Laboratories, Air Resources Laboratory Field Research Division, Idaho Falls, Idaho.
- J. Sagendorf, 1996, *Precipitation Frequency and Intensity at the Idaho National Engineering Laboratory*, National Oceanic and Atmospheric Administration, Technical Memorandum ERL ARL-215, Air Resources Laboratory, Silver Spring, Maryland.
- Mitchell, T., Mitchell, J. S., Humphrey, J., Kennedy, D., Funderburg, T., 2002, *100-Year Floodplain and 25-Year Runoff Analyses for the Radioactive Waste Management Complex at the Idaho National Engineering and Environmental Laboratory*, Document No. INEEL/EXT-02-00093.

## **2.2 Historical Flood Events**

There have been several significant flood events with documented information in southern Idaho, northern Utah and northern Nevada, dating from the early 1900's through the present. Four events in particular have enough recorded information to estimate conditions experienced during winter rain and snowmelt storms with return periods ranging from 25 to 100 years. The most significant events occurred in February 1962, January 1969, February 1980 and February 1982. Of these events, the 1962 rain-on-snow conditions were estimated to represent a storm with a return period of 50 to 100 years (DOE-ID, 1998). Climatologic and general flooding information was obtained for all of these events and used to evaluate anticipated conditions during a 100-year return period storm. The data provides an approximate measure of the peak flow anticipated for the INTEC facility.

All of the observed events required an unusual set of climatological conditions including a wet fall season, very cold temperatures through December, January, and February, little or no

snow cover, no thawing of the ground, and some accumulation of snow just prior to the flood. This set of conditions results in a shallow snow cover underlain by concrete impermeable frost. The development of concrete impermeable frost and its influence on storm water runoff are discussed further in section 2.3.3 of this report.

Based on historic flooding information (USCOE, 1975, CH2MHill, 1989) and according to limited United States Geological Survey (USGS) stream gage data in the area surrounding INEEL, peak flows of 30 to 60 cubic feet per second per square mile (cfs/mi<sup>2</sup>) can be expected during a 100-year rain on snow with frozen ground event in watersheds similar in size and nature to that of the INTEC. This regional flood flow information was used as an approximation of the 100-year flood model developed for the INTEC.

In addition to peak flow estimations provided by the USGS documentation, limited information relating to runoff volume was obtained from previous hydrologic studies. Sagendorf (1991) indicates that the 1962 flood event produced a runoff volume of approximately 30 acre-feet in a 3.435 mi<sup>2</sup> watershed (located at the Radioactive Waste Management Complex). This volume estimate of storm water was used as an indirect correlation to the runoff expected at the INTEC due to the locations of these facilities and their similar hydrologic conditions.

## **2.3 Summer and Winter Design Storm Conditions**

Three separate conditions were considered to evaluate the largest 25-year and 100-year storm water runoff events for the INTEC facility. Design storm data were developed separately for summer cloudburst storms, winter storms, and for winter rain on snow with frozen ground events. Separating the different conditions provides more accurate determination of precipitation depths for various return period storms and better representation of hydrologic conditions during the summer and winter seasons. Design storm parameters for summer and winter conditions are discussed in the following sections.

### **2.3.1 Design Storm Precipitation**

Precipitation depths for summer and winter storms were determined primarily from gage data collected from the City of Idaho Falls and the INEEL. Specific gage sites include the following:

- National Weather Service, INEEL Winter Flood Events, Idaho Falls 46W Data
- National Weather Service, Idaho Falls FAA, Idaho Falls Airport Gage Data

Gage data from these sources are available for approximately 50 years, providing sufficient data to conduct a statistical analysis for precipitation depths. Depth-duration-frequency (DDF) curves were developed for this study from the gage data obtained from the NWS using standard procedures of ranking maximum observed precipitation depths and plotting data on a lognormal probability distribution. Best-fit curves were developed for evaluating precipitation depth-duration-frequency statistics for the INTEC facility. The power curve equation is shown below.

$$D = a * t^b$$

- Where: D = design storm precipitation depth (in)  
 a = statistical parameter based on ranked gage data  
 b = statistical parameter based on ranked gage data  
 t = time (min)

Precipitation depths were determined for storms with durations ranging from 5 minutes to 24 hours and return periods from 2 to 100 years. The precipitation depths developed for design storms used in this hydrologic analysis were prepared independently from studies performed by others, including those prepared by J. Sagendorf (1991 and 1996), Keck (1998) and Dames and Moore (1993). Most significantly, the DDF statistics developed for this hydrologic analysis compare closely with those prepared by J. Sagendorf in 1996. Slight differences can be identified in precipitation depths for each design storm and return frequency due to specific data periods used in developing the statistics, differences in interpretation of best-fit curves and lines, and best engineering judgment.

Summer DDF curves were developed from gage data recorded between the months of May through September. Summer precipitation statistics are shown in Table 2-1.

**Table 2-1.** Precipitation depths (inches) for summer design storms.

| Summer Cloudburst Depth Duration Frequency<br>D=a*t <sup>b</sup> |       |       |       |        |       |       |       |       |       |       |
|--|-------|-------|-------|--------|-------|-------|-------|-------|-------|-------|
| Recurrence   | a     | b     | 5-min | 15-min | 1-hr  | 2-hr  | 3-hr  | 6-hr  | 12-hr | 24-hr |
| 2-year   | 0.095 | 0.305 | 0.155 | 0.217  | 0.331 | 0.409 | 0.463 | 0.572 | 0.707 | 0.873 |
| 5-year   | 0.154 | 0.282 | 0.242 | 0.331  | 0.489 | 0.594 | 0.666 | 0.810 | 0.985 | 1.197 |
| 10-year  | 0.199 | 0.269 | 0.307 | 0.412  | 0.599 | 0.721 | 0.804 | 0.969 | 1.168 | 1.408 |
| 25-year  | 0.262 | 0.257 | 0.396 | 0.525  | 0.750 | 0.897 | 0.995 | 1.189 | 1.421 | 1.698 |
| 50-year  | 0.302 | 0.253 | 0.454 | 0.599  | 0.851 | 1.014 | 1.124 | 1.339 | 1.596 | 1.901 |
| 100-year   | 0.359 | 0.243 | 0.531 | 0.693  | 0.971 | 1.149 | 1.268 | 1.501 | 1.776 | 2.102 |

Winter DDF curves were developed using precipitation gage data recorded during the months from November through March, when wet soil conditions will occur. Winter precipitation depths are shown in Table 2-2.

**Table 2-2.** Precipitation depths (inches) for winter design storms.

| <b>Winter Rainfall Depth Duration Frequency</b><br>$D=a*t^b$ |       |       |       |        |       |       |       |       |       |       |
|--|-------|-------|-------|--------|-------|-------|-------|-------|-------|-------|
| Recurrence   | a     | b     | 5-min | 15-min | 1-hr  | 2-hr  | 3-hr  | 6-hr  | 12-hr | 24-hr |
| 2-year   | 0.015 | 0.506 | 0.034 | 0.059  | 0.119 | 0.169 | 0.208 | 0.295 | 0.419 | 0.595 |
| 5-year   | 0.026 | 0.469 | 0.055 | 0.093  | 0.177 | 0.246 | 0.297 | 0.411 | 0.569 | 0.787 |
| 10-year  | 0.035 | 0.447 | 0.072 | 0.117  | 0.218 | 0.297 | 0.357 | 0.486 | 0.663 | 0.903 |
| 25-year  | 0.047 | 0.427 | 0.093 | 0.149  | 0.270 | 0.363 | 0.432 | 0.580 | 0.780 | 1.049 |
| 50-year  | 0.058 | 0.413 | 0.113 | 0.177  | 0.315 | 0.419 | 0.495 | 0.659 | 0.878 | 1.169 |
| 100-year   | 0.071 | 0.397 | 0.135 | 0.208  | 0.361 | 0.475 | 0.558 | 0.735 | 0.967 | 1.274 |

Winter rain on frozen ground DDF curves were developed using precipitation gage data recorded during the months of January and February, when impermeable conditions will occur. Rain on frozen ground precipitation depths are shown in Table 2-3.

**Table 2-3.** Precipitation depths (inches) for winter rain on frozen ground design storms.

| <b>Winter Rain on Frozen Ground Depth Duration Frequency</b><br>$D=a*t^b$ |       |       |       |        |       |       |       |       |       |       |
|---|-------|-------|-------|--------|-------|-------|-------|-------|-------|-------|
| Recurrence  | a     | b     | 5-min | 15-min | 1-hr  | 2-hr  | 3-hr  | 6-hr  | 12-hr | 24-hr |
| 2-year  | 0.011 | 0.506 | 0.024 | 0.042  | 0.084 | 0.119 | 0.147 | 0.208 | 0.296 | 0.420 |
| 5-year  | 0.018 | 0.469 | 0.039 | 0.065  | 0.125 | 0.172 | 0.209 | 0.289 | 0.400 | 0.553 |
| 10-year   | 0.025 | 0.447 | 0.051 | 0.083  | 0.154 | 0.210 | 0.252 | 0.343 | 0.467 | 0.637 |
| 25-year   | 0.033 | 0.427 | 0.066 | 0.106  | 0.191 | 0.257 | 0.305 | 0.411 | 0.552 | 0.742 |
| 50-year   | 0.041 | 0.413 | 0.079 | 0.124  | 0.221 | 0.294 | 0.347 | 0.462 | 0.615 | 0.819 |
| 100-year  | 0.050 | 0.397 | 0.094 | 0.145  | 0.252 | 0.332 | 0.390 | 0.513 | 0.675 | 0.889 |

The data and procedures used in developing DDF curves for the various seasonal events are standard meteorological methods used by the NWS and National Oceanographic and Atmospheric Administration (NOAA). Differences in the DDF statistics prepared for this study may be identified in precipitation depths associated with the various storm durations and return periods when compared to other DDF curves prepared for INEEL. The differences are the result of the specific seasonal periods used to develop the curves and judgment in best-fit curves for statistical representation of precipitation data.

In preparing the three different sets of DDF curves for this study, data were separated according to seasonal variations when summer, winter and winter frozen ground conditions exist. This separation of the data often results in lower precipitation depths and intensities used for modeling during the winter season as compared to summer and to the year as a whole. Winter storms typically have lower rainfall depth and intensity than other times of the year. Separation of these data from the entire period of record provides a more accurate determination of DDF statistics when evaluating specific seasonal storm events.

### **2.3.2 Snowmelt**

Snowmelt was incorporated into hydrologic models for the INTEC flood study in order to evaluate winter storm events. Data for snow depth and water content were developed from the winter precipitation statistics, and previous rain on snow events observed throughout the region surrounding INEEL. Contributing factors for snowmelt were established from temperature and wind speed gage data according to the following:

- Maximum daily temperature is 46° F and average daily temperature is 42° F
- Wind speed of 20 miles per hour
- Constant snowmelt during the 24-hour storm period
- Little delay for snowmelt contribution to runoff

Using equations presented in the USCOE Snow Hydrology Manual (USCOE, 1998), with a mean temperature of 42° F and wind speed of 20 mph, snowmelt was calculated as 0.06 in/hr. This constant snowmelt was added to the design storm precipitation for use in hydrologic modeling of the winter rain on snow and frozen ground events. The 0.06 in/hr is added to the precipitation depth duration frequency statistics identified earlier, based on the time period (i.e., 12-hour event adds 0.72 inches to the precipitation depth). Snowmelt adds 1.44 inches of water to the rainfall event throughout the duration of the 25-year and 100-year, 24-hour winter events.

### **2.3.3 Frozen Ground and Concrete Impermeable Frost**

Frozen ground and concrete impermeable frost increase runoff volume and associated peak flow during winter storms by limiting the infiltration capacity of the soil, and in the case of concrete impermeable frost, effectively increasing the amount of impervious surface within a watershed. Several climatological factors contribute to developing frozen ground and concrete impermeable frost including, but not limited to, the following:

- Wet fall and early winter season, sufficient to allow accumulation of water in the surface soil layers
- Continuous cold weather
- Little or no snow accumulation to insulate the ground

For the purposes of this study, it is necessary to distinguish between frozen ground and concrete impermeable frost in order to estimate the impervious surface area in the watershed. Frozen ground occurs annually during the winter season as cold temperatures freeze moisture

in surface and vadose zone soils. However, this condition does not preclude infiltration as cracks develop, porosity in the soil-ice structure still exists, and root structures provide additional pathways for water to enter the soil profile. To become a completely impervious frost layer, sufficient moisture must be present to saturate the soil and sustained freezing temperatures must develop frost and ice to eliminate all infiltration capability in the soil profile. This condition is described as concrete impermeable frost.

Previous investigations have been conducted to evaluate the presence and severity of concrete impermeable frost during winter rain on snow and frozen ground events (CH2MHill 1989). During this study, known gage data were used to calibrate hydrologic models of the watershed contributing to Silver Bow Creek during winter storm events in southwest Montana. It was determined through this study that although concrete impermeable frost existed in the watershed, it did not cover the entire surface area, was found to exist only in very narrow elevation ranges throughout the watershed, and that water infiltration occurs in areas where frozen ground (not impermeable frost) exists.

Results of the Silver Bow Creek investigation were used to develop and assign probability to the recurrence of concrete impermeable frost. The probability of concrete impermeable frost is based on rainfall, temperatures, snow and other climatological factors that allow concrete impermeable frost to develop. Statistical analyses of climatological data from the INEEL were used to evaluate the probability of concrete impermeable frost development as a part of this study. The recurrence interval of conditions required to develop impermeable frost is approximately every 5 to 10 years at the INEEL and INTEC based on available gage data from the site and surrounding area.

Additionally, an estimate of the percentage of the ground surface representing concrete impermeable frost was developed from site-specific conditions at INEEL and results of the Silver Bow Creek investigation. Vegetation, exposed surface soils, soil porosity and other factors contribute to the development of concrete impermeable frost. For the watershed surrounding the INTEC, vegetative cover was estimated to be 50% and exposed soils have fairly good water transmission properties (B group). Concrete impermeable frost was estimated to represent 33% of the watershed area during this study, based on the following assumptions:

1. Exposed surface soils represent 50% of the natural watershed area. 67% of exposed surface soils are subject to developing concrete impermeable frost. Total concrete impermeable frost in the natural watershed is then 33%.
2. Concrete impermeable frost will not develop in the remaining 50% of the watershed area due to the presence of vegetative cover and root structure.

Review of previous studies conducted at the INEEL further indicate that although concrete impermeable frost will exist in portions of the watershed, it is overly conservative to assume that the presence of frozen ground eliminates all infiltration. A report prepared in 1994 (Taylor et. al, 1994) states "...the assumption of frozen ground presumes zero infiltration of the surface...zero infiltration appears overly conservative...assumption of zero infiltration was used in order to obtain demonstrably conservative results." This previous study further supports the assumption that impermeable concrete frost does not exist over the entire watershed area.

Natural watershed areas can have concrete impermeable frost which occupies less than 100% of the natural watershed during winter.

There are no universally accepted methods for establishing recurrence interval or aerial extent of concrete impermeable frost during winter seasons. Generally accepted methods include estimations of impervious surfaces using hydrologic models of watersheds with available stream gage data. In the absence of site-specific data, it is necessary to estimate concrete impermeable frost and resulting impervious surface area from climatological data, known watershed properties, experience with similar sites, and comparison to other studies. Representing 33% of the natural watershed area as concrete impermeable frost provides a reasonable estimate of expected impervious ground conditions during winter storm events for the INEEL based on the hydrologic conditions of the watershed, available surface area for impermeable frost to develop, and experience with similar studies.

## **2.4 Summer and Winter Design Storm Parameters**

Summer and winter design storm parameters were developed for hydrologic modeling of the watershed contributing to the INTEC and surrounding areas. The storm parameters were developed from the statistical analyses of data collected primarily from the INEEL and Idaho Falls gages, with additional supporting information as described in previous sections. The following design storm parameters were used in hydrologic modeling of the various return period and seasonal conditions.

- 25-year and 100-year Summer Thunderstorms (Cloudburst)
  - 25-year and 100-year, 24-hour storm events
  - 1.70 and 2.10 inches of precipitation, respectively, from statistical analyses and data presented in Table 2-1.
  - Embedded peak 5-, 15- and 30-minute, 1-, 2-, 3-, 6-, 12- and 24-hour rainfall intensities.
- 25-year, 24-hour Winter Precipitation (Rain on Snow) with frozen ground
  - 5-year, 24-hour storm event
  - 5-year frozen ground conditions (33% impermeable frost in natural watershed areas)
  - 0.553 inches of direct precipitation
  - 0.06 inches/hour constant snowmelt (1.44 inches total depth for 24 hours)
  - Embedded peak 5-, 15-, and 30-minute, 1-, 2-, 3-, 6-, 12- and 24-hour rainfall intensities.
- 100-year, 24-hour Winter Precipitation (Rain on Snow) with Frozen Ground
  - 20-year, 24-hour storm event
  - 5-year frozen ground conditions
  - 0.72 inches of direct precipitation

- 0.06 inches/hour constant snowmelt (1.44 inches total depth for 24 hours)
- Embedded peak 5-, 15- and 30-minute, 1-, 2-, 3-, 6-, 12- and 24-hour rainfall intensities.

The design storm parameters for the various storms used in this hydrologic study are statistically equivalent to, or greater than, the return frequencies for the 25-year and 100-year events. The return interval for a particular storm event has a probability equal to the inverse of the return interval as shown in the following equation:

$$P = \frac{1}{\text{return period}}$$

Therefore, the probabilities of the 25-year and 100-year events are 0.04 and 0.01, respectively. Additionally, the probability of different events can be multiplied to determine combined probabilities representing statistically equivalent, larger return period events. Using the combined probability approach, a 20-year rainfall was used in conjunction with the 5-year frozen ground (impermeable frost) condition to generate a storm event that is statistically equivalent to the 100-year event according to the following:

$$P_{100} = P_{20} * P_5 = \frac{1}{20} * \frac{1}{5} = \frac{1}{100} = 0.01$$

The combined probability of the 20-year rainfall and 5-year frozen ground represents a 100-year return period probability. For the purposes of this study, the volume of snowmelt was added to the winter design storm events to provide additional runoff. Adding the snowmelt to the design storms increases the return period of the storms, as the presence of snow during the event has additional statistical probability, which should be multiplied in the combined probabilities. However, the probability of snowmelt runoff during the design storms was not included in the return period calculations. This was done to account for possible variations in truly frozen ground, design storm precipitation depths and other hydrologic parameters used to represent the watershed and sub areas. Neglecting the probability of snowmelt in the combined probabilities of the design storm events provides a conservative approach to estimating the peak flood flow anticipated for the INTEC facility and surrounding watershed area.

The probabilities for rainfall and frozen ground occurrence are sufficiently independent to allow their combination in a joint probability distribution. The design storm precipitation is developed from gage data from several different sites around the INTEC and INEEL for periods of record exceeding 50 years in many cases. Further, the probability of the presence of impermeable concrete frost accounts for several environmental factors including precipitation, temperature, snow, wind, and freezing temperature durations and was also developed from gage data for the INEEL and surrounding area. The probabilities for precipitation and the presence of concrete impermeable frost are prepared independently, allowing the use of the combined probability approach.

### **3. FIELD INVESTIGATION AND DATA COLLECTION**

A field investigation of the watershed area in and surrounding the INTEC facility was conducted to verify watershed and sub area boundaries, identify and inventory hydraulic control structures, measure channel cross-sections and gather other hydrologic and hydraulic information for the site. The field investigation was conducted during late April and early May 2003. Details of the specific tasks and data collected during the investigation are included in the following sections.

#### **3.1 Watershed and Sub Area Boundary Verification**

A preliminary watershed boundary and sub area map was developed prior to conducting the field investigation. Major and minor drainage boundaries were identified on topographic mapping developed for the site in 2002 and included both natural and manmade features. Natural features included ridges, depressions, drainage swales and others. Manmade features included roads, railroads, berms, channels, pits and others. This preliminary watershed and sub area map was further refined as a result of the field investigation.

Boundaries identified along roads and railroads were reviewed in the field to identify the presence of culverts, hydraulic structures, or other hydrologic features that may serve to alter drainage area boundaries. Where identified, culverts were added to the topographic mapping and sub area boundaries adjusted accordingly. Additionally, drainage ditches and berms were inspected for integrity and function and utilized to identify watershed and sub area boundaries as appropriate. Watershed and sub area boundaries prepared for this study from topographic mapping and investigation are shown on Sheet 1 included with this report.

#### **3.2 Hydraulic Structure Inventory**

Previous hydraulic structure investigations and surveys were utilized to generate an inventory for the INTEC facility and surrounding area, including Central Facilities Area, the Guard Training Facilities, and along US Highway 20. A summary of culverts located throughout the watershed area (Kingsford, 2002) was used as a starting point for the inventory and field investigation.

As part of this study, a detailed investigation of the hydraulic structures within the INTEC perimeter was conducted to further the existing database. Hydraulic structures measured in the field included catch basins, pipes, culverts, lift stations and surface drainage channels. Storm water flow paths and connectivity were also confirmed during the investigation for use in subsequent hydraulic modeling.

### **3.3 Field Surveying and Measurements**

Several areas in and around the INTEC facility were surveyed to collect data for use in modeling storm water drainage channels, flow in the Big Lost River and to confirm topographic drainage divides identified during the preliminary watershed and sub area delineation. Surveying was conducted by Mr. Ken Beard of INEEL and CCH, Inc. All surveying was conducted using horizontal and vertical control points established by Mr. Beard, using NGVD29 vertical and NAD27 horizontal Idaho State Plane datums.

Drainage channel geometry was measured using tapes and surveying rods in remote, localized areas to determine properties for use in hydraulic modeling and channel capacity estimates where surface flooding has no potential to impact buildings or areas of concern. Field measured sections were collected for constructed irrigation and diversion channels around the site.

## 4. HYDROLOGIC MODELING

The HEC-1 computer program was utilized for this hydrologic analysis as it provides flexibility in modeling methods and allows detailed input of watershed parameters, stage-storage-routing information, design storm precipitation, snowmelt and other hydrologic modeling parameters impacting storm water runoff. Specifically, the hydrologic modeling for this study was conducted using ProHEC1 Plus, an enhanced version of the Hydrologic Engineering Center's HEC-1 program (Dodson and Associates, ProHEC1 Plus, 1995). This program generates rainfall/runoff hydrographs for watersheds and sub basins based on several hydrologic parameters including, but not limited to, the following:

- Watershed and sub basin area
- Soil type and vegetative cover
- Impervious surfaces
- Surface features such as exposed bedrock and fractures
- Stream channel flow patterns
- Natural and constructed reservoirs or storm water retention areas
- Storm water runoff controls
- Unique hydrologic features

Details of the hydrologic modeling parameters and processes are included in the following sections.

### 4.1 Hydrologic Characteristics and Modeling Parameters

Hydrologic characteristics of the watershed are discussed in the following sections and, where applicable, modeling parameters based on conditions observed in the field are discussed.

#### 4.1.1 Watershed and Sub Area Delineation

Topographic mapping and field inspection of hydrologic and hydraulic features were used to delineate the contributing watershed and sub basins of the INTEC and surrounding area. Topographic mapping provided by INEEL (Aerial Services, Inc., 2002) and portions of a USGS quadrangle map were used to identify the outer boundary of the watershed. Sub areas were delineated within the outer watershed boundary based on several factors including the following:

- Major and minor surface water runoff drainage patterns and flow lengths
- Location of culverts, storm water runoff controls, local reservoir areas (storage)
- Key features and junctions in the diversion channels
- General hydrologic regime and field conditions

Aerial Services, Inc. prepared topographic mapping for the INTEC watershed and surrounding area in July 2002. A map of the entire watershed area evaluated during the course of this study is shown on Sheet 1 included with this report.

The watershed area west and south of the immediate vicinity of the INTEC facility was evaluated as a part of this study based on regional topography. During the field investigation, several drainage area divides, both natural and man-made were identified which influence the drainage area characteristics. More detailed discussion of the drainage areas delineated for subsequent hydrologic modeling is included in the following three sections.

The watershed and sub area delineations were completed using 2-foot topographic mapping, field surveying data and a thorough review of the digital elevation models developed during the aerial mapping of the site. The watershed sub areas were carefully delineated to ensure that subsequent hydrologic modeling results would be representative of flow conditions at the site.

#### **4.1.1.1 Areas Contributing Directly to the INTEC**

The INTEC has a perimeter road surrounding the facility area, outside of the secure fenced area. This road serves as a major drainage divide around the facility, with only one culvert on the southwest corner of the facility area that allows cross-drainage into the facility. Additionally, the INTEC facility is protected from unauthorized entry by a perimeter ditch constructed to prevent vehicle access to the site. This perimeter ditch functions as a drainage channel for the facility and areas within the perimeter of the INTEC. Due to its proximity to the facility, the perimeter ditch was surveyed and incorporated into hydrologic and hydraulic models to verify its function as a drainage ditch for the facility. The areas contributing directly to the INTEC are identified as INTEC-2 (INTEC perimeter) and INTEC-5 (via culvert flow) on the watershed and sub area map (Sheet 1). The watershed area contributing storm water runoff to the INTEC storm water drainage system is 0.40 square miles.

#### **4.1.1.2 Areas in the Vicinity of the INTEC Perimeter**

Several areas around the INTEC facility were included in the watershed mapping and delineation for the site in order to identify any storm water run-on and flooding potential. Additionally, areas in the immediate vicinity of the facility were included in order to evaluate the flow away from the INTEC drainage areas. The areas identified in the vicinity of the facility include sub areas INTEC 1, 3, 4, 6 and 7. The watershed area in the immediate vicinity of the facility included in these sub areas is 1.20 square miles.

#### **4.1.1.3 Area West of Lincoln Boulevard, Central Facilities and Non-Contributing Areas**

The INTEC is located at the northeastern edge of a large, fan-shaped regional watershed. The location of hydraulic structures, the lack of culverts or other drainage controls, constructed roads, pits and subtle natural topography breaks serve to limit the watershed contributing directly to the INTEC facility.

Areas west of Lincoln Boulevard were included in the hydrologic modeling for this study in order to evaluate any flooding potential due to flow over Lincoln Boulevard and in the

Big Lost River near the INTEC facility. There are no culverts under Lincoln Boulevard between Central Facilities and the Big Lost River and therefore it serves as a major divide between the INTEC and the watershed extending to the west of the road. Several cross-sections were surveyed along Lincoln Boulevard to confirm the capacity of the drainage ditch and road to convey storm water runoff from west of the road north to the Big Lost River. The watershed area contributing to the west side of Lincoln Boulevard is 10.30 square miles.

The Central Facilities Area was included in this investigation to evaluate potential contributing storm water flow towards the INTEC. There are several constructed pits located to the north of the Central Facilities Area which collect storm water runoff from the CFA sub areas. These pits, in conjunction with a subtle natural drainage divide along the northern end of sub area CFA-1 effectively divert and contain all storm water drainage from the CFA sub areas, eliminating storm water run-on and flooding potential to the INTEC. These areas were included in the hydrologic investigation conducted for INTEC in order to confirm the absence of any contributing flow from CFA. The sub areas included in the CFA are identified as CFA-1, 2, and 3 on Sheet 1 of this report. The watershed area contributing to the constructed pits north of CFA is 1.18 square miles.

Non-contributing areas identified on Sheet 1 include those areas east of the railroad grade, southeast of CFA, and north of the Big Lost River. These areas do not contribute any flow to the INTEC due to either their location hydrologically downgradient of the site, or the presence of drainage barriers, including the railroad grade and the Big Lost River. These areas were not included in the hydrologic investigation and models prepared for this study.

A total watershed area of 13.15 mi<sup>2</sup> was included in the hydrologic analysis of the site to evaluate any potential effects of storm water runoff and flooding potential outside of the INTEC facility. The watershed area contributing storm water run-on and runoff directly to the INTEC storm water drainage system is limited to 0.40 mi<sup>2</sup> due to the presence of several storm water diversions and controls.

#### **4.1.2 Soil Type and Vegetation**

Native soils in the area of the INTEC are primarily sandy silt loam, with sand fractions ranging in size from very fine to coarse. Soil depths range from very shallow to very deep and are intermixed with basalt flows. Regional data indicates that soils are primarily loess, and are characterized as Hydrologic Soil Group B. This soil group allows moderate infiltration and consists of silts, sands and to a lesser extent, clays.

The vegetation in the watershed surrounding the INTEC is a sage-grass community consisting of sagebrush and primarily wheat grasses. Cover was estimated at approximately 50% during the field investigation conducted at the site. Vegetation within the INTEC facility perimeter, while limited in area, consists of residential lawn grasses (fescue and blue grasses) where present.

The Soil Conservation Service (SCS) National Engineering Handbook provides representative curve numbers (CN) for sage-grass complexes in the Western United States (SCS, 1972). The curve number is used in hydrologic modeling to represent the soil and vegetation conditions within a watershed and accounts for precipitation losses and excesses. According to

the SCS reference, curve numbers may range from 28 to 96 for sage-grass complexes, depending on soil group and vegetative cover. The SCS method categorizes soils into one of four groups, known as Hydrologic Soil Groups A, B, C, or D, based upon their classification (silt, clay, sand, loam, etc.). Low curve numbers indicate Group A and B soils with high percentage of vegetative cover and high numbers indicate Group C and D soils with little or no vegetative cover.

Antecedent moisture conditions (AMC) are used to represent soil and moisture conditions in a watershed prior to the rainfall-runoff event being modeled. AMC II is the standard condition for hydrologic modeling according to the SCS methodology and is the basis for curve numbers presented in the National Engineering Handbook and other references. AMC II curve numbers are adjusted for varying conditions in a watershed, depending on anticipated soil moisture conditions prior to a modeled event. AMC I represents dry conditions typical of summer thunderstorms, with no precipitation prior to the model storm. AMC III represents wet soil conditions during winter and spring seasons, when it is likely that some moisture has been retained in the soils from previous storms and/or snowmelt. Curve numbers taken from the SCS handbook are shown in Table 4-1.

The curve numbers were selected from tables shown in the SCS National Engineering Handbook, Section 4, Hydrology, 1972, page 9.11. Curve numbers were selected to represent natural conditions identified in the field, with further support from SCS documentation and experience with similar sites. Curve numbers were also selected accordingly to represent antecedent moisture conditions anticipated in each storm. AMC III curve numbers were used to represent saturated soils during winter storms. Normal soils during summer events were represented by AMC II, although dry (AMC I) conditions are more likely in the summer.

Curve numbers for sage-grass complexes, Hydrologic Soil Group B and normal AMC (II) range from 28 to 74 for 100% to 0% cover, respectively. These values are shown in Table 4-1.

Based on the vegetative covers with a Hydrologic Soil Group B, a curve number of 52 was selected to represent natural watershed conditions. This CN was used for summer thunderstorm events, although it is more likely that AMC I conditions will be present during summer (dry, which would result in a lower CN). The CN of 52 was adjusted to AMC III conditions (saturated soil condition) for the winter storm events. A CN of 71 was selected to represent the unfrozen portion of soils in the natural watershed during the winter rain on snow and frozen ground events.

Curve numbers were adjusted for areas inside the INTEC facility perimeter based on an assumption that soils in this area are more compacted than natural conditions (allowing lower infiltration rates) due to construction activities, heavy traffic and constructed cover soil areas. A curve number of 80 was selected for modeling the watershed sub areas in the INTEC facility.

**Table 4-1.** SCS Curve Numbers<sup>1</sup> for sage-grass complexes.

| <b>Antecedent Moisture Condition II (Standard)</b>          |                                |                                |                                |
|---|--------------------------------|--------------------------------|--------------------------------|
| <b>Vegetative Cover (%)</b>                                 | <b>Hydrologic Soil Group B</b> | <b>Hydrologic Soil Group C</b> | <b>Hydrologic Soil Group D</b> |
| 0   | 74                             | 87                             | 96                             |
| 20  | 65                             | 78                             | 88                             |
| 40  | 56                             | 68                             | 79                             |
| 60  | 47                             | 59                             | 70                             |
| 80  | 37                             | 49                             | 61                             |
| 100   | 28                             | 40                             | 52                             |
| <b>Antecedent Moisture Condition I (Summer Condition)</b>   |                                |                                |                                |
| 0   | 55                             | 73                             | 89                             |
| 20  | 45                             | 60                             | 75                             |
| 40  | 36                             | 48                             | 62                             |
| 60  | 28                             | 39                             | 51                             |
| 80  | 20                             | 30                             | 41                             |
| 100   | 14                             | 22                             | 32                             |
| <b>Antecedent Moisture Condition III (Winter Condition)</b> |                                |                                |                                |
| 0   | 88                             | 95                             | 99                             |
| 20  | 82                             | 90                             | 95                             |
| 40  | 75                             | 84                             | 91                             |
| 60  | 67                             | 77                             | 85                             |
| 80  | 57                             | 69                             | 78                             |
| 100   | 48                             | 60                             | 71                             |
| <b>Impermeable Frost</b>                                    | 99                             | 99                             | 99                             |

<sup>1</sup>Section 4, Hydrology, SCS National Engineering Handbook, 1972.

### 4.1.3 Impervious Surfaces

There are limited areas of impervious surfaces within the natural watershed around the INTEC. Existing natural impervious surfaces include exposed bedrock outcrops, which, where present, were estimated to cover 5 percent of the surface in sub basins. Man-made impervious surfaces include roads, buildings, parking areas and other impervious surfaces. The impervious surface area created by man-made features was estimated from topographic

mapping and aerial photography of the site. A curve number of 99 was used for all impervious surface portions of the watershed, including areas within INTEC, during all storm events.

A curve number of 99 was also used to represent concrete impermeable ground for winter rain on snow with frozen ground events.

#### **4.1.4 Natural and Man-Made Surface and Diversion Channels**

Topography of the watershed at, and immediately around, the INTEC is generally low-lying and flat, with few defined natural drainage channels. In general, incised channels do not form within the natural watershed areas around INTEC due to the low-lying topography, low slope and lack of significant storm water runoff during times when soils are easily eroded (i.e., summer). Where necessary for modeling purposes, natural drainage channels were modeled as very wide-bottom trapezoid-shape channels with low side slopes.

Several man-made diversion and irrigation channels have been constructed in the watershed around INTEC and have been used for storm water runoff and historic irrigation. These channels are generally intact and function to control storm water runoff in the watershed area contributing to the west side of Lincoln Boulevard. The diversion channels were measured in the field in order to provide input data for subsequent hydraulic modeling.

#### **4.1.5 Storm Water Retention Areas**

Several storm water retention areas exist within the watershed area contributing to the INTEC, the West Side of Lincoln Boulevard, and CFA-1. The storm water retention areas used for stage-storage-routing in this hydrologic study are subject to flooding during the 25-year and 100-year storm events. Stage-storage-discharge relationships were developed for all storage areas utilized in hydrologic modeling for this study. Stage and storage volume relationships were generated from topographic mapping of the study area and discharge evaluated utilizing open channel flow equations for surface channels and culverts, as appropriate. Water surface elevations identified in the hydrologic models were used to identify inundated areas throughout the watershed. The inundated areas are considered a part of the storm water runoff floodplain delineated on the maps prepared for this study.

#### **4.1.6 Big Lost River**

The Big Lost River flows around the northwestern part of the INTEC facility and is bermed along the INTEC side to prevent floodwater from impacting the facility. The Big Lost River has several flow control measures along its length including a water spreading/control area upgradient of the site. Water generated in the watershed above the spreading areas can be effectively controlled by the spreading areas and the flood control gates associated with them.

A detailed analysis of flow in the Big Lost River generated from upgradient watersheds was not included in this study. Other on-going studies are in progress to evaluate flow in the Big Lost River and are not included in the scope of this project. However, in order to evaluate any potential flooding that may result from storm water runoff in the Big Lost River, a portion of the watershed area surrounding the INTEC was assumed to be contributing runoff to the river at the time of the modeled events. Approximately 17 square miles of watershed area were

estimated from topographic mapping as contributing area during the modeled storm events. This area includes the watershed extending upgradient from the INTEC facility to the large spreading areas located on the Big Lost River near the RWMC facility (southwest of INTEC).

Based on results of current and previous studies, a base flow (30 cfs/mi<sup>2</sup>) for the estimated contributing area was added to hydraulic models of the Big Lost River and used to identify flooding potential (in addition to runoff from the watershed delineated on Sheet-1 for INTEC). The base flow was combined in the Big Lost River with flows contributing to the west side of Lincoln Boulevard in order to identify any flooding potential resulting from insufficient channel or bridge/culvert capacity near the INTEC. Further discussion of the hydraulic modeling of the Big Lost River is included in Section 5.1 of this report.

## **4.2 Hydrologic Modeling and Analysis**

The rainfall-runoff modeling was conducted using ProHEC-1 Plus (Dodson and Associates, 1995), with input parameters based on the design storm statistics and hydrologic conditions of the watershed. The SCS method for storm water loss and excess was used in the hydrologic models to generate storm water runoff hydrographs for selected locations in the watershed area. Specific parameters incorporated into the models created as a part of this study are discussed in the following sections.

### **4.2.1 SCS Curve Numbers and Precipitation Losses**

SCS curve numbers were selected to represent the watershed condition based on soil type, vegetative cover, impervious surfaces and the presence of impermeable frost. For summer conditions, curve numbers were selected from tables presented in the SCS Engineering Handbook as previously described in this report.

Additionally, to represent impermeable conditions during the winter storm events, the sub areas were separated into two portions, designated as A and B in the model. Two-thirds (67%) of the basin was considered as unfrozen ground with AMC III soil conditions. One-third (33%) of the basin was represented as concrete impermeable frost with a curve number of 99 for impervious surface. Hydrographs for the two separate portions of each sub area during winter events were combined to determine peak flow from the whole sub area, prior to combining flows with other sub areas. SCS curve numbers selected for modeling are shown in Table 4-2.

**Table 4-2. SCS Curve Numbers used in hydrologic modeling**

| <b>Sub Area Description</b>                 | <b>SCS Curve Number Summer Events</b> | <b>SCS Curve Number Winter Events</b> |
|---|---------------------------------------|---------------------------------------|
| Natural conditions                          | 52                                    | 71                                    |
| INTEC-2, facility area                      | 80 <sup>(1)</sup>                     | 94 <sup>(1)</sup>                     |
| Central Facilities Area                     | 62 <sup>(1)</sup>                     | 80 <sup>(1)</sup>                     |
| Impervious surfaces including frozen ground | 99                                    | 99                                    |

(1) - SCS curve number increased assuming soils have been compacted over time by traffic and construction activities.

The SCS Unit Discharge method was used for modeling rainfall-runoff at the site. The Unit Discharge method requires calculation of a time of concentration and lag time for each watershed sub area, accounts for precipitation losses and excess within the curve number, allows channel routing for hydrographs, includes stage, storage and discharge information and other hydrologic parameters to generate storm water runoff models.

The SCS method accounts for precipitation losses from infiltration and evaporation and precipitation excess contributing to runoff within the curve number. Other methods including Kinematic wave, Muskingum, Muskingum-Cunge account for the losses using initial and constant loss parameters and were tested with variations of the HEC-1 models generated for this study. After evaluation of different methods for determining peak runoff, the SCS method was determined to be the most reasonable for the watershed, rainfall, snowmelt and frozen ground conditions. The Kinematic Wave, Muskingum, and Muskingum-Cunge methods utilize overland flow parameters, shallow concentrated flow conditions and channel flow parameters to determine time of concentration and peak flow within a sub area of the watershed. Input of the sub area parameters into the HEC-1 program generated widely varied results within the different sub areas due to long overland flow lengths anticipated at this site, variations in frozen ground and natural soil conditions, and a variety of other factors affecting the model results.

Precipitation losses are accounted for in the hydrologic models using two different parameters, initial losses and continuous losses. Initial losses are included in the hydrologic models as a depth of precipitation that is abstracted initially before infiltration and runoff begin. The initial loss accounts for depression storage areas on the surface that collect a small amount of precipitation and are generally included in all hydrologic models. The SCS National Engineering Handbook recommends initial losses of approximately 0.5 to 1.5 inches for the types of soils and conditions present in the INTEC and surrounding watersheds. Initial losses were set to 0.6 inches for summer events and 0.1 inches for winter storm events, assuming that the soil will not absorb precipitation during the winter and that depression storage is partially filled before the design storm occurs.

#### 4.2.2 Time of Concentration

The time of concentration is used to assist in the definition of runoff characteristics within the individual sub areas. The time of concentration for a watershed is defined as the travel time of water from the hydraulically most distant point of the watershed to the point of interest (generally the most downstream point). The time of concentration for each sub area was estimated by measuring three components of storm water runoff flow paths including overland flow, shallow concentrated flow, and channel flow, and determining appropriate roughness coefficients and other parameters that influence water flow. Topographic maps and site surveying were used to determine flow distances and slopes, and roughness coefficients were estimated using the aerial photography and observed field conditions. Properties of the individual sub areas used in determining the time of concentrations are shown in Table 4-3. A summary of the travel time associated with the three flow conditions (overland, shallow concentrated, channel flow) and time of concentration for each basin is presented in Table 4-4. The equations used in evaluating total time of concentration are standard equations for the three different flow components and are shown below.

$$t_{overland} = \frac{0.007(nL)^{0.8}}{\sqrt{P_2 S^{0.4}}}$$

$$t_{shallow} = \frac{L}{V}, \text{ where } V = 16.1345\sqrt{S}$$

$$t_{channel} = \frac{L}{V}, \text{ where } V = \frac{CR^{0.667} S^{0.5}}{n}$$

Where:  $n$  = Manning's roughness coefficient, unitless

$L$  = length of flow, ft

$P_2$  = 2-year, 24-hour precipitation depth, in

$S$  = slope, ft/ft

$R$  = hydraulic radius, ft

$V$  = velocity, ft/s

$C$  = 1.49 (constant)

These equations can be found in the ProHEC-1 Program Documentation (Dodson and Associates, 1995) and several other hydrologic modeling references. An example of the time of concentration calculations prepared for the watershed sub areas is shown for INTEC-1 in the following equations (parameters taken from Table 4-3).

INTEC-1: Overland Flow:  $L = 300$  ft,  $n = 0.175$ ,  $P_2 = 0.873$  inches (summer),  $S = 0.002$  ft/ft

$$t_{overland} = \frac{0.007 * (0.175 * 300)^{0.8}}{\sqrt{0.873 * 0.002^{0.4}}} = 2.14 \text{ min}$$

INTEC-1: Shallow Concentrated Flow: L = 1375, S = 0.0036

$$t_{shallow} = \frac{1375}{16.1345\sqrt{0.0036}} = 1420.35 \text{ sec} = 23.67 \text{ min}$$

INTEC-1: Channel Flow: L = 5450 ft, R = 0.349, S = 0.0018, n = 0.05

$$t_{channel} = \frac{5450}{\frac{1.49 * 0.349^{0.667} * 0.0018^{0.5}}{0.05}} = 8,696.18 \text{ sec} = 144.94 \text{ min}$$

The total time of concentration is the sum of the three component times for each basin (for some basins, with more defined channels contributing to the main channel, two channel flow sections may be used). The total time of concentration for INTEC-1 is shown below.

$$t_c = t_{overland} + t_{shallow} + t_{channel} = 2.14 \text{ min} + 23.67 \text{ min} + 144.94 \text{ min} = 170.75 \text{ min}$$

**Table 4-3.** Sub area flow parameters used in determining time of concentration ( $t_c$ ) and lag times.

|          |         | Kinematic Wave/Muskingum Basin Parameters |         |             |          |                                     |         |             |          |                     |        |         |        |              |        |         |        |      |
|----------|---------|---|---------|-------------|----------|-------------------------------------|---------|-------------|----------|---------------------|--------|---------|--------|--------------|--------|---------|--------|------|
|          |         | Collector Channel 1 - Contributor 1       |         |             |          | Collector Channel 1 - Contributor 2 |         |             |          | Collector Channel 1 |        |         |        | Main Channel |        |         |        |      |
| Sub Area | Area    | Length                                    | Slope   | Roughness   | % of     | Length                              | Slope   | Roughness   | % of     | Sub Area            | Length | Slope   | Shape  | Roughness    | Length | Slope   | Shape  |      |
| Number   | (sq mi) | (ft)                                      | (ft/ft) | (manning's) | Sub Area | (ft)                                | (ft/ft) | (manning's) | Sub Area | Number              | (ft)   | (ft/ft) | Shape  | (manning's)  | (ft)   | (ft/ft) | Shape  |      |
| CFA-1    | 0.5653  | 300                                       | 0.001   | 0.175       | 100      |                                     |         |             |          | 0                   | CFA-1  | 1375    | 0.0036 | TRAP         | 0.15   | 7625    | 0.0022 | TRAP |
| CFA-2    | 0.5772  | 300                                       | 0.001   | 0.175       | 70       | 200                                 | 0.005   | 0.175       | 30       | CFA-2               | 800    | 0.0075  | TRAP   | 0.175        | 8875   | 0.0041  | TRAP   |      |
| CFA-3    | 0.0324  | 150                                       | 0.005   | 0.175       | 100      |                                     |         |             |          | 0                   | CFA-3  | 750     | 0.0110 | TRAP         | 0.175  | 1375    | 0.0087 | TRAP |
| INTEC-1  | 0.3015  | 300                                       | 0.002   | 0.175       | 40       | 200                                 | 0.001   | 0.175       | 60       | INTEC-1             | 1375   | 0.0036  | TRAP   | 0.1          | 5450   | 0.0018  | TRAP   |      |
| INTEC-2  | 0.3495  | 100                                       | 0.002   | 0.1         | 50       | 100                                 | 0.002   | 0.1         | 50       | INTEC-2             | 500    | 0.0040  | TRAP   | 0.04         | 3000   | 0.0020  | TRAP   |      |
| INTEC-3  | 0.0671  | 300                                       | 0.002   | 0.175       | 60       | 100                                 | 0.005   | 0.08        | 40       | INTEC-3             | 1000   | 0.0030  | TRAP   | 0.05         | 1550   | 0.0030  | TRAP   |      |
| INTEC-4  | 0.0651  | 200                                       | 0.002   | 0.08        | 50       | 75                                  | 0.001   | 0.08        | 50       | INTEC-4             | 600    | 0.00167 | TRAP   | 0.065        | 800    | 0.00196 | TRAP   |      |
| INTEC-5  | 0.0434  | 200                                       | 0.0043  | 0.08        | 65       | 130                                 | 0.005   | 0.08        | 35       | INTEC-5             | 800    | 0.00260 | TRAP   | 0.042        | 590    | 0.00240 | TRAP   |      |
| INTEC-6  | 0.0889  | Not included in analysis - sink area      |         |             |          |                                     |         |             |          |                     |        |         |        |              |        |         |        |      |
| INTEC-7  | 0.7663  | 200                                       | 0.001   | 0.175       | 50       | 75                                  | 0.001   | 0.175       | 50       | INTEC-7             | 400    | 0.0010  | TRAP   | 0.175        | 7250   | 0.0022  | TRAP   |      |
| LB-1     | 0.2092  | 50  | 0.001   | 0.175       | 50       | 100                                 | 0.001   | 0.175       | 50       | LB-1                | 400    | 0.0015  | TRAP   | 0.175        | 7200   | 0.0029  | TRAP   |      |
| LB-2     | 0.5135  | 125                                       | 0.002   | 0.175       | 50       | 80                                  | 0.001   | 0.175       | 50       | LB-2                | 500    | 0.0015  | TRAP   | 0.175        | 10375  | 0.0029  | TRAP   |      |
| LB-3     | 0.2953  | 95  | 0.001   | 0.175       | 50       | 150                                 | 0.001   | 0.175       | 50       | LB-3                | 560    | 0.0035  | TRAP   | 0.175        | 9300   | 0.0030  | TRAP   |      |
| LB-4     | 0.1721  | 50  | 0.001   | 0.175       | 50       | 150                                 | 0.001   | 0.175       | 50       | LB-4                | 310    | 0.0015  | TRAP   | 0.175        | 5375   | 0.0029  | TRAP   |      |
| LB-5     | 0.1494  | 50  | 0.001   | 0.175       | 50       | 150                                 | 0.001   | 0.175       | 50       | LB-5                | 200    | 0.0035  | TRAP   | 0.175        | 3875   | 0.0033  | TRAP   |      |
| LB-6     | 0.4099  | 50  | 0.001   | 0.175       | 50       | 150                                 | 0.001   | 0.175       | 50       | LB-6                | 250    | 0.0016  | TRAP   | 0.175        | 9250   | 0.0031  | TRAP   |      |
| LB-7     | 0.4351  | 50  | 0.001   | 0.175       | 50       | 125                                 | 0.001   | 0.175       | 50       | LB-7                | 250    | 0.0025  | TRAP   | 0.175        | 6000   | 0.0030  | TRAP   |      |
| LB-8     | 0.7509  | 75  | 0.001   | 0.175       | 50       | 200                                 | 0.001   | 0.175       | 50       | LB-8                | 4000   | 0.0025  | TRAP   | 0.175        | 3250   | 0.0025  | TRAP   |      |
| LB-9     | 0.4458  | 200                                       | 0.045   | 0.175       | 60       | 250                                 | 0.025   | 0.175       | 40       | LB-9                | 800    | 0.0085  | TRAP   | 0.15         | 8000   | 0.0050  | TRAP   |      |
| LB-10    | 0.1559  | 300                                       | 0.001   | 0.175       | 50       | 200                                 | 0.001   | 0.175       | 50       | LB-10               | 400    | 0.0030  | TRAP   | 0.05         | 3350   | 0.0020  | TRAP   |      |
| LB-11    | 0.2317  | 75  | 0.001   | 0.175       | 50       | 185                                 | 0.001   | 0.175       | 50       | LB-11               | 750    | 0.0026  | TRAP   | 0.15         | 7000   | 0.0023  | TRAP   |      |
| LB-12    | 0.3234  | 75  | 0.001   | 0.175       | 50       | 185                                 | 0.001   | 0.175       | 50       | LB-12               | 430    | 0.0030  | TRAP   | 0.15         | 6500   | 0.0028  | TRAP   |      |
| LB-13    | 0.4537  | 75  | 0.001   | 0.175       | 50       | 175                                 | 0.001   | 0.175       | 50       | LB-13               | 300    | 0.0030  | TRAP   | 0.15         | 8850   | 0.0027  | TRAP   |      |
| LB-14    | 0.4064  | 100                                       | 0.001   | 0.175       | 50       | 200                                 | 0.001   | 0.175       | 50       | LB-14               | 250    | 0.0020  | TRAP   | 0.15         | 8500   | 0.0030  | TRAP   |      |
| LB-15    | 0.1885  | 150                                       | 0.001   | 0.175       | 50       | 300                                 | 0.001   | 0.175       | 50       | LB-15               | 250    | 0.0020  | TRAP   | 0.15         | 7500   | 0.0024  | TRAP   |      |
| LB-16    | 0.4806  | 75  | 0.001   | 0.175       | 50       | 150                                 | 0.001   | 0.175       | 50       | LB-16               | 400    | 0.0025  | TRAP   | 0.15         | 10000  | 0.0034  | TRAP   |      |
| LB-17    | 0.4356  | 75  | 0.001   | 0.175       | 50       | 150                                 | 0.001   | 0.175       | 50       | LB-17               | 400    | 0.0025  | TRAP   | 0.15         | 9500   | 0.0032  | TRAP   |      |
| LB-18    | 0.7317  | 150                                       | 0.001   | 0.175       | 70       | 200                                 | 0.005   | 0.175       | 30       | LB-18               | 500    | 0.0040  | TRAP   | 0.15         | 9000   | 0.0028  | TRAP   |      |
| LB-19    | 0.8361  | 75  | 0.001   | 0.175       | 50       | 150                                 | 0.001   | 0.175       | 50       | LB-19               | 1200   | 0.0065  | TRAP   | 0.15         | 12250  | 0.0057  | TRAP   |      |
| LB-20    | 2.0322  | 250                                       | 0.04    | 0.175       | 80       | 300                                 | 0.006   | 0.175       | 20       | LB-20               | 1800   | 0.0189  | TRAP   | 0.15         | 13250  | 0.0053  | TRAP   |      |
| LB-21    | 0.0193  | 200                                       | 0.01    | 0.175       | 100      |                                     |         |             | 0        | LB-21               | 375    | 0.0267  | TRAP   | 0.15         | 1225   | 0.0114  | TRAP   |      |
| LB-22    | 0.0988  | 300                                       | 0.013   | 0.175       | 80       | 200                                 | 0.02    | 0.175       | 20       | LB-22               | 600    | 0.0167  | TRAP   | 0.15         | 2250   | 0.0080  | TRAP   |      |
| LB-23    | 0.0197  | 100                                       | 0.01    | 0.175       | 100      |                                     |         |             | 0        | LB-23               | 375    | 0.0133  | TRAP   | 0.15         | 750    | 0.0146  | TRAP   |      |
| LB-24    | 0.3457  | 125                                       | 0.001   | 0.175       | 70       | 150                                 | 0.0267  | 0.175       | 30       | LB-24               | 1375   | 0.0065  | TRAP   | 0.15         | 5125   | 0.0047  | TRAP   |      |
| LB-25    | 0.0288  | 100                                       | 0.001   | 0.08        | 85       | 200                                 | 0.001   | 0.175       | 15       | LB-25               | 450    | 0.0044  | TRAP   | 0.15         | 3060   | 0.0013  | TRAP   |      |
| LB-26    | 0.1282  | 100                                       | 0.001   | 0.08        | 85       | 200                                 | 0.001   | 0.175       | 15       | LB-26               | 450    | 0.0089  | TRAP   | 0.15         | 11000  | 0.00127 | TRAP   |      |

**Table 4-4.** Time of concentration ( $t_c$ ) for sub areas.

| Sub Area<br>Number                              | Overland                             | Shallow<br>Concentrated | Channel       | $t_c$ (min) | lag<br>time<br>(hours) |
|---|--------------------------------------|-------------------------|---------------|-------------|------------------------|
|   | Flow<br>(min)                        | Flow<br>(min)           | Flow<br>(min) |             |                        |
| <b>INTEC sub areas</b>                          |                                      |                         |               |             |                        |
| INTEC-1   | 2.14                                 | 23.67                   | 144.94        | 170.75      | 1.71                   |
| INTEC-2   | 0.79                                 | 8.17                    | 52.98         | 61.93       | 0.62                   |
| INTEC-3   | 2.14                                 | 18.86                   | 38.32         | 59.32       | 0.59                   |
| INTEC-4   | 0.83                                 | 15.17                   | 24.47         | 40.46       | 0.40                   |
| INTEC-5   | 0.61                                 | 16.21                   | 13.59         | 30.40       | 0.30                   |
| INTEC-6   | Not included in analysis - sink area |                         |               |             |                        |
| INTEC-7   | 2.04                                 | 13.07                   | 261.61        | 276.71      | 2.77                   |
| <b>Lincoln Boulevard contributing sub areas</b> |                                      |                         |               |             |                        |
| LB-1  | 1.17                                 | 10.67                   | 226.28        | 238.13      | 2.38                   |
| LB-2  | 1.06                                 | 13.34                   | 326.07        | 340.47      | 3.40                   |
| LB-3  | 1.62                                 | 9.78                    | 287.37        | 298.77      | 2.99                   |
| LB-4  | 1.62                                 | 8.27                    | 168.93        | 178.82      | 1.79                   |
| LB-5  | 1.62                                 | 3.49                    | 114.17        | 119.28      | 1.19                   |
| LB-6  | 1.62                                 | 6.46                    | 281.18        | 289.26      | 2.89                   |
| LB-7  | 1.40                                 | 5.16                    | 185.40        | 191.97      | 1.92                   |
| LB-8  | 2.04                                 | 82.64                   | 110.01        | 194.69      | 1.95                   |
| LB-9  | 0.67                                 | 8.96                    | 191.48        | 201.12      | 2.01                   |
| LB-10   | 2.82                                 | 7.54                    | 168.27        | 178.64      | 1.79                   |
| LB-11   | 1.92                                 | 15.19                   | 247.03        | 264.15      | 2.64                   |
| LB-12   | 1.92                                 | 8.11                    | 207.90        | 217.93      | 2.18                   |
| LB-13   | 1.83                                 | 5.66                    | 288.26        | 295.75      | 2.96                   |
| LB-14   | 2.04                                 | 5.77                    | 262.65        | 270.47      | 2.70                   |
| LB-15   | 2.82                                 | 5.77                    | 259.11        | 267.70      | 2.68                   |
| LB-16   | 1.62                                 | 8.26                    | 290.26        | 300.14      | 3.00                   |
| LB-17   | 1.62                                 | 8.26                    | 284.23        | 294.12      | 2.94                   |
| LB-18   | 1.62                                 | 8.17                    | 287.86        | 297.65      | 2.98                   |
| LB-19   | 1.62                                 | 15.38                   | 228.84        | 245.84      | 2.46                   |
| LB-20   | 1.38                                 | 13.52                   | 256.70        | 271.60      | 2.72                   |
| LB-21   | 0.81                                 | 2.37                    | 16.18         | 19.36       | 0.19                   |
| LB-22   | 1.01                                 | 4.80                    | 35.48         | 41.29       | 0.41                   |
| LB-23   | 0.47                                 | 3.36                    | 8.75          | 12.58       | 0.13                   |
| LB-24   | 1.40                                 | 17.62                   | 105.44        | 124.45      | 1.24                   |
| LB-25   | 2.04                                 | 7.01                    | 95.76         | 104.81      | 1.05                   |
| LB-26   | 2.04                                 | 4.93                    | 348.27        | 355.24      | 3.55                   |
| <b>Central Facilities contributing areas</b>    |                                      |                         |               |             |                        |
| CFA-1   | 2.82                                 | 23.67                   | 183.43        | 209.92      | 2.10                   |
| CFA-2   | 2.82                                 | 9.54                    | 156.39        | 168.75      | 1.69                   |
| CFA-3   | 0.85                                 | 7.39                    | 16.63         | 24.87       | 0.25                   |

### 4.2.3 HEC-1 Model Input and Output

Hydrologic modeling was completed using the HEC-1 computer program with watershed and sub area properties incorporated into the models based on parameters discussed in the previous sections. The models were used to generate peak flows at key locations contributing to the INTEC facility drainage systems, Lincoln Boulevard, the Big Lost River, and the constructed pits in the Central Facilities Area to evaluate the 25-year and 100-year storm water runoff flood profiles.

HEC-1 input is completed using “cards” to represent different sub area parameters, rainfall statistics, reservoir and channel routing parameters, sub area connectivity and hydrograph combinations, and a number of model control and output parameters. The card identifier is the first two characters on the lines contained in the input file, which the HEC-1 program uses to perform the hydrologic modeling process. Limited information is included in text in the HEC-1 input files, identifying sub basins, routing reaches, hydrograph combinations and other significant steps within the models and can, to some degree, be used to follow the general modeling process. Complete descriptions of the “cards” used in the HEC-1 input files can be reviewed in HEC-1 User’s Manuals available from the USCOE website or other HEC-1 resources on the Internet.

The peak flow associated with each sub area within the contributing watershed was evaluated in the HEC-1 program for the modeled events including:

- 25-year, 24-hour summer thunderstorm
- 25-year, 24-hour winter rain on snow with frozen ground
- 100-year, 24-hour summer thunderstorm
- 100-year, 24-hour winter rain on snow with frozen ground

Combined hydrographs defining flow conditions throughout the watershed area were also evaluated in the HEC-1 models. A discussion of the modeling results for the INTEC and the surrounding watershed is included in the following.

### 4.2.4 Hydrologic Modeling Approach

The entire watershed contributing to the INTEC, Lincoln Boulevard and the Central Facilities Area was modeled to evaluate storm water runoff and determine any flooding potential. For modeling purposes, the HEC-1 models were created to evaluate runoff in the following manner:

1. Determine the 100-year runoff flow from all areas contributing to Lincoln Boulevard, using sequential analysis of the uppermost sub areas and combining flows according to flow path as the runoff approaches the intersection of the Big Lost River and Lincoln Boulevard. Account for stage-storage relationships in depressions storage areas, channel routing in interceptor and irrigation channels and determine the peak runoff entering the Big Lost River just above Lincoln Boulevard. Route flows through the Big Lost River channel and combine with the INTEC runoff below the railroad bridge.

2. Determine the 100-year runoff flow from all areas contributing to the constructed pits in the Central Facilities Area, using sequential analysis of the uppermost sub areas and combining flows according to flow path as the runoff approaches the pits. Allow the constructed pits to serve as the stage-storage area and determine if any flow exits the CFA sub areas and overflows towards the INTEC sub areas. If so, combine CFA flows with INTEC flows accordingly.
3. Determine the 100-year runoff flow from all areas contributing to the INTEC and surrounding area that drains to two culverts located under the railroad grade northeast of the facility area. Account for stage-storage areas and determine peak flow discharging from the facility towards the culverts.
4. Due to the limited area contributing directly to the storm water drainage systems at the INTEC, create a separate HEC-1 model of sub area INTEC-2 using further subdivided areas based on drainage flow paths to evaluate the 25-year runoff and drainage system capacity and the 100-year storm water runoff floodplain for the interior facility area at the INTEC.

A discussion of the results of this modeling approach is included in the following section.

### **4.3 Hydrologic Modeling Results**

The HEC-1 analyses of the different return period storm events indicate that the 25-year and 100-year rain on snow and frozen ground events generate the largest peak flows throughout the watershed sub areas as a whole. These storm events were used to identify the storm water runoff floodplain associated with the Big Lost River, stage-storage areas throughout the watershed, and to evaluate channel capacities outside of the INTEC-2 sub area (main facility).

Inside of the INTEC facility perimeter, the HEC-1 analysis indicates that the 25-year and 100-year summer storm events will generate the highest peak flow from the INTEC-2 (main facility area) sub area. These results are indicative of the amount of impervious surface in the INTEC facility and grounds. Summer events have a higher precipitation intensity, which generally drives peak flow in impervious areas. In order to evaluate the largest flood potential and more accurately identify the 100-year storm water runoff floodplain within the facility area, the summer runoff event was used in the INTEC-2 sub area (resulting from the separate INTEC-2 facility analysis).

A summary of the peak flow within each sub area is provided in Table 4-5 for the summer and winter events for the whole watershed area. A summary of peak flows for several key combinations of sub area hydrographs contributing to the Big Lost River and areas of potential concern is shown in Table 4-6. Representative hydrographs for peak flows are shown in Figure 4-1 (25-year, 24-hour summer storm hydrographs) through Figure 4-8 (100-year, 24-hour winter storm hydrographs). Discussion of specific results of the hydrologic modeling for each individual storm event is provided in the following.

1. The 25-year, 24-hour *winter* rain on snow with frozen ground event generates the highest peak flow in the watershed as a whole for the INTEC and surrounding area, for storms with this return period. The 25-year, 24-hour winter rain-on snow with frozen ground event was used to identify the 25-year storm water runoff floodplain for the Big Lost River and surrounding areas. This event generates 214 cubic feet per second (cfs) at the Lincoln Boulevard Bridge and 270 cfs at the junction downstream of the railroad bridge.
2. The 100-year, 24-hour *winter* rain on snow with frozen ground event generates the highest peak flow in the watershed as a whole for the INTEC and surrounding area, for storms with this return period. The 100-year, 24-hour winter rain-on snow with frozen ground event was used to identify the 100-year storm water runoff floodplain for the Big Lost River and surrounding areas. This event generates 314 cubic feet per second (cfs) at the Lincoln Boulevard Bridge and 393 cfs at the junction downstream of the railroad bridge.
3. The 25-year and 100-year *summer* events generate the highest peak flow for the INTEC-2 (main facility) sub area due to the amount of impervious surface in this basin. The amount of impervious surface within the INTEC-2 boundary was estimated to be 60 %, and when combined with the short time of concentration for this basin, generates approximately 75 cfs during the 25-year summer event, and 106 cfs during the 100-year summer event. The 25-year summer event was used to evaluate the capacity of all storm sewer systems and culverts located within the INTEC perimeter. The 100-year summer event was used to identify the 100-year floodplain in INTEC-2.

Table 4-5. Peak flow (cfs) for individual sub areas.

| <i>Intec Area</i>                               |                |                |                 |                 |
|---|----------------|----------------|-----------------|-----------------|
| Sub Area  | 25-year Summer | 25-year Winter | 100-year Summer | 100-year Winter |
| Intec 1   | 5              | 12             | 9               | 18              |
| Intec 2   | 75             | 28             | 106             | 46              |
| Intec 3   | 4              | 4              | 7               | 7               |
| Intec 4   | 2              | 3              | 9               | 5               |
| Intec 5   | 5              | 6              | 8               | 11              |
| Intec 6   | Sink           | Sink           | Sink            | Sink            |
| Intec 7   | 9              | 27             | 17              | 39              |
| <i>Lincoln Boulevard contributing sub areas</i> |                |                |                 |                 |
| Sub Area  | 25-year Summer | 25-year Winter | 100-year Summer | 100-year Winter |
| LB-1  | 3              | 8              | 5               | 11              |
| LB-2  | 5              | 17             | 10              | 24              |
| LB-3  | 3              | 10             | 6               | 15              |
| LB-4  | 3              | 7              | 5               | 10              |
| LB-5  | 3              | 6              | 6               | 10              |
| LB-6  | 5              | 14             | 9               | 21              |
| LB-7  | 6              | 17             | 12              | 25              |
| LB-8  | 11             | 29             | 21              | 44              |
| LB-9  | 6              | 17             | 12              | 26              |
| LB-10   | 2              | 6              | 5               | 9               |
| LB-11   | 3              | 8              | 5               | 12              |
| LB-12   | 4              | 12             | 8               | 18              |
| LB-13   | 5              | 16             | 9               | 23              |
| LB-14   | 5              | 14             | 9               | 21              |
| LB-15   | 2              | 7              | 4               | 10              |
| LB-16   | 5              | 16             | 10              | 24              |
| LB-17   | 5              | 15             | 9               | 22              |
| LB-18   | 8              | 25             | 15              | 37              |
| LB-19   | 10             | 30             | 20              | 45              |
| LB-20   | 24             | 71             | 45              | 105             |
| LB-21   | 2              | 2              | 3               | 4               |
| LB-22   | 4              | 7              | 9               | 12              |
| LB-23   | 2              | 2              | 4               | 5               |
| LB-24   | 7              | 15             | 14              | 24              |
| LB-25   | 2              | 1              | 2               | 2               |
| LB-26   | 3              | 5              | 4               | 6               |
| <i>Central Facilities contributing areas</i>    |                |                |                 |                 |
| Sub Area  | 25-year Summer | 25-year Winter | 100-year Summer | 100-year Winter |
| CFA-1   | 21             | 24             | 33              | 37              |
| CFA-2   | 42             | 33             | 60              | 51              |
| CFA-3   | 2              | 3              | 4               | 5               |

Hydrographs from individual sub areas were combined in the HEC-1 models according to storm water runoff flow paths as water from one sub area flows into the upper reach of the next downstream sub area or as several sub areas combine at their most downstream point. Combining the sub areas provides a representative model analysis of the entire watershed, allowing evaluation of peak storm water runoff flows at any location within the watershed.

Several locations where hydrographs were combined in the HEC-1 model were selected for hydraulic (HEC-RAS) modeling of the surface water channels to evaluate peak flows where significant flow changes occur. Significant flow changes were identified at channel junctions where combined sub area flows enter the Big Lost River or other key areas. Combined hydrographs and significant changes in peak flow incorporated into subsequent hydraulic models of the surface water drainage system are shown in Table 4-6. The flows identified in Table 4-6 were combined with the estimated base flow (30 cfs/mi<sup>2</sup>, see Section 4.1.6) in the Big Lost River and routed through the channel in hydraulic models created for this study to evaluate any backwater effects and identify any flooding potential from storm water runoff.

**Table 4-6.** Peak flows for key hydrograph combinations used in hydraulic analyses.

| Subarea Hydrograph Combination (CMB) | HEC-1 Combination Label | 25-year summer peak flow (cfs) | 25-year winter peak flow (cfs) | 100-year summer peak flow (cfs) | 100-year winter peak flow (cfs) |
|--------------------------------------|-------------------------|--------------------------------|--------------------------------|---------------------------------|---------------------------------|
| LB9, LB 8                            | CMB 1                   | 17                             | 45                             | 33                              | 69                              |
| LB 4-LB 9                            | CMB 4                   | 30                             | 82                             | 58                              | 124                             |
| LB 1-LB 9                            | CMB 7                   | 40                             | 116                            | 77                              | 173                             |
| LB 19-LB 24                          | CMB 11                  | 12                             | 110                            | 36                              | 158                             |
| LB 18-LB 24                          | CMB 12                  | 8                              | 118                            | 15                              | 144                             |
| LB 16-LB 24                          | CMB 13                  | 10                             | 32                             | 19                              | 46                              |
| LB 11-LB 24, LB 26                   | CMB 19                  | 30                             | 91                             | 56                              | 133                             |
| All Lincoln Boulevard sub areas      | CMB 20                  | 63                             | 214                            | 135                             | 314                             |
| All Central Facilities sub areas     | CMB 22                  | 63                             | 59                             | 95                              | 90                              |
| Intec 1 through Intec 5              | CMB 25                  | 76                             | 46                             | 116                             | 74                              |
| (CMB 25) Intec 1-5, Intec 7          | CMB 26                  | 18                             | 50                             | 37                              | 70                              |
| Entire watershed area                | CMB 27                  | 80                             | 270                            | 172                             | 393                             |

The hydrologic modeling approach used in this study identified storm water runoff peak flows in the watershed where flooding potential may exist. Flow contributing to the west side of Lincoln Boulevard was included in this study to determine if the road serves as a drainage divide or if overflow may enter the INTEC area. Flow in the CFA sub areas was evaluated to determine any potential overflow from the constructed pits. Peak flows identified in Tables 4-5 and 4-6 were utilized in hydraulic analyses of surface water channels and a comprehensive analysis of the INTEC facility storm water drainage system in order to identify the 100-year floodplain and evaluate capacity of the system during the 25-year, 24-hour runoff.

Figures 4-1 through 4-8 show the storm water runoff hydrographs generated from the HEC-1 program at several key locations for the INTEC and the surrounding watershed during the modeled storm events. Hydrographs for key locations include flows generated west of Lincoln Boulevard, within the INTEC facility perimeter, and in the Big Lost River where all flows combine from the watershed analyzed in this study.

The hydrographs for summer storms show a significant spike in the flow near hour 12 due to the rainfall distribution associated with summer storms. Rainfall intensity increases during a model summer storm near hour 12 causing the peak runoff to occur shortly thereafter. The hydrographs for winter storms show a smaller spike near hour 12, with a more drawn-out flow condition. Rainfall intensity during a winter storm is more consistent throughout the duration of the storm, with a smaller peak intensity near hour 12. Winter storm rainfall distributions create a longer runoff hydrograph, with the peak occurring near hour 12 and sustained flows for the remainder of the storm.

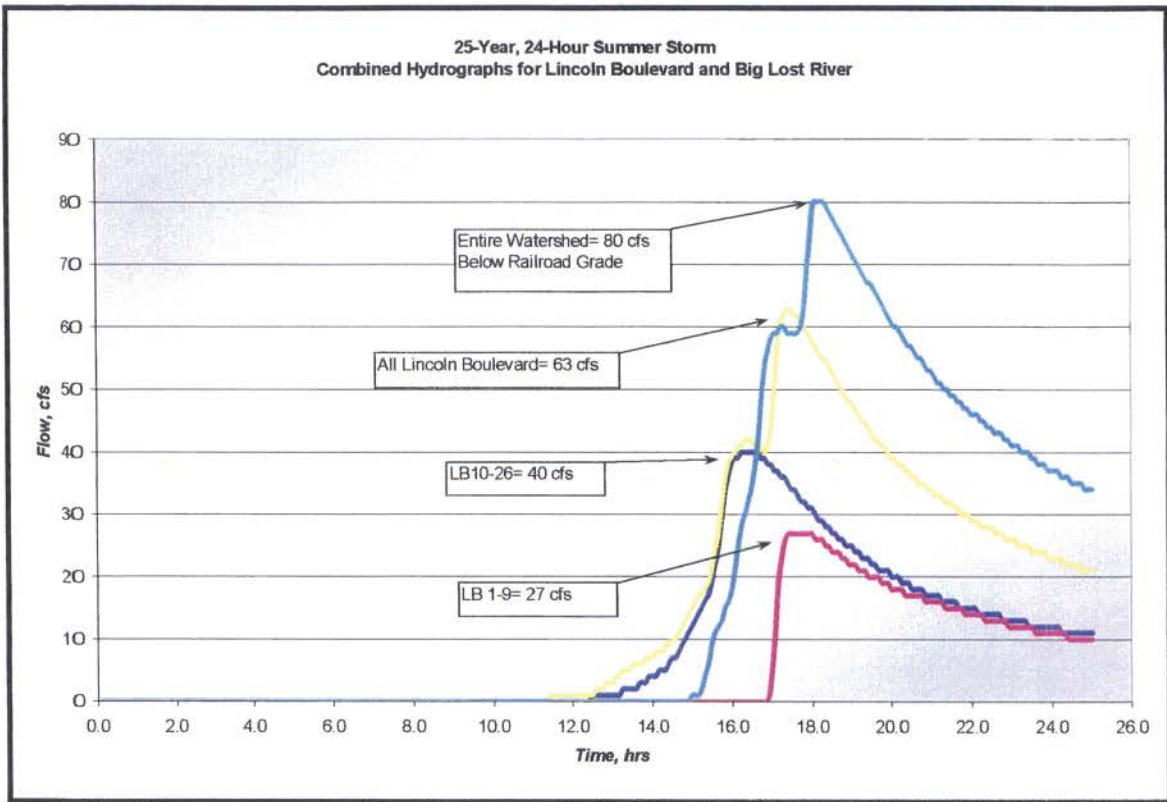


Figure 4-1. 25-year summer storm hydrographs for Lincoln Boulevard, Big Lost River.

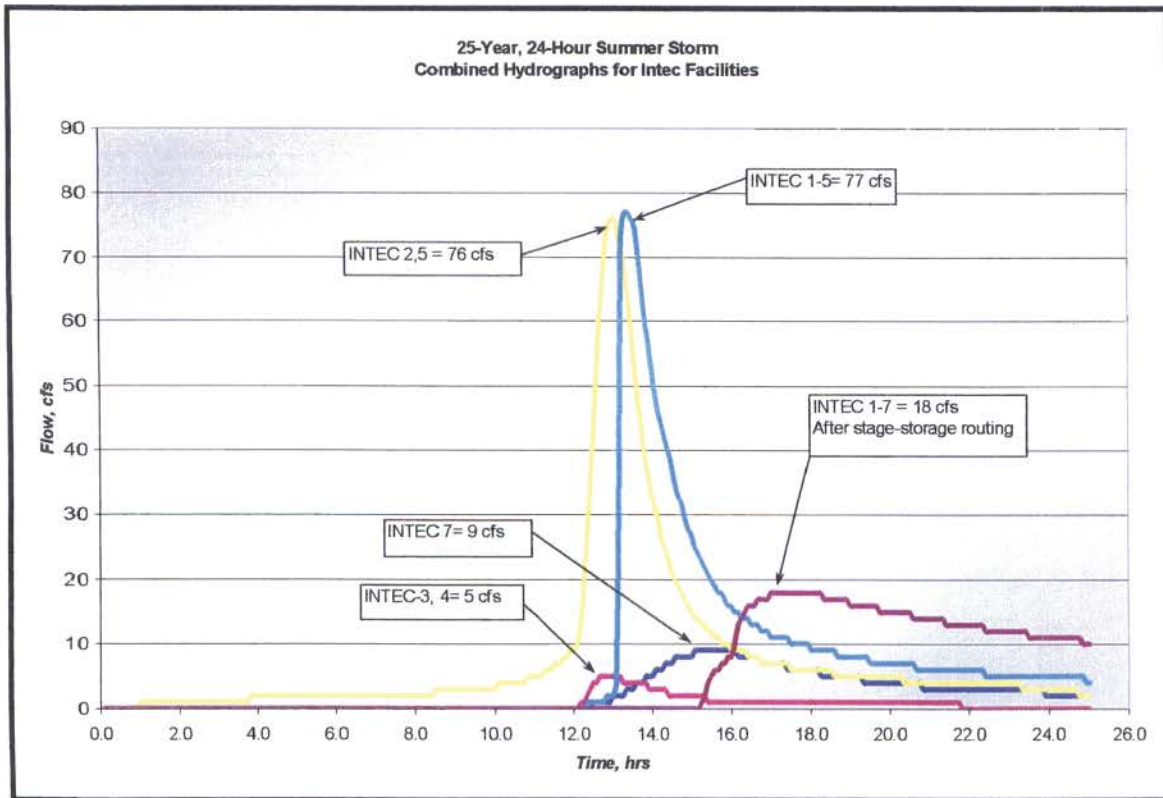


Figure 4-2. 25-year summer storm hydrographs for INTEC sub areas.

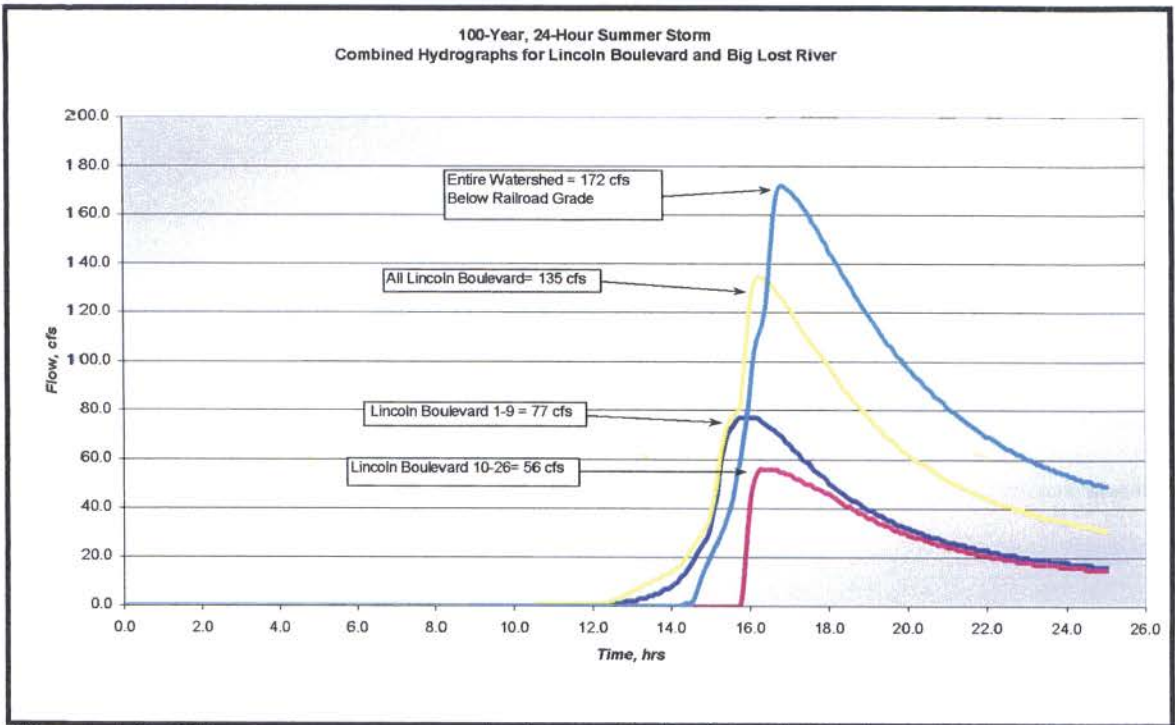


Figure 4-3. 100-year summer storm hydrographs for Lincoln Boulevard, Big Lost River.

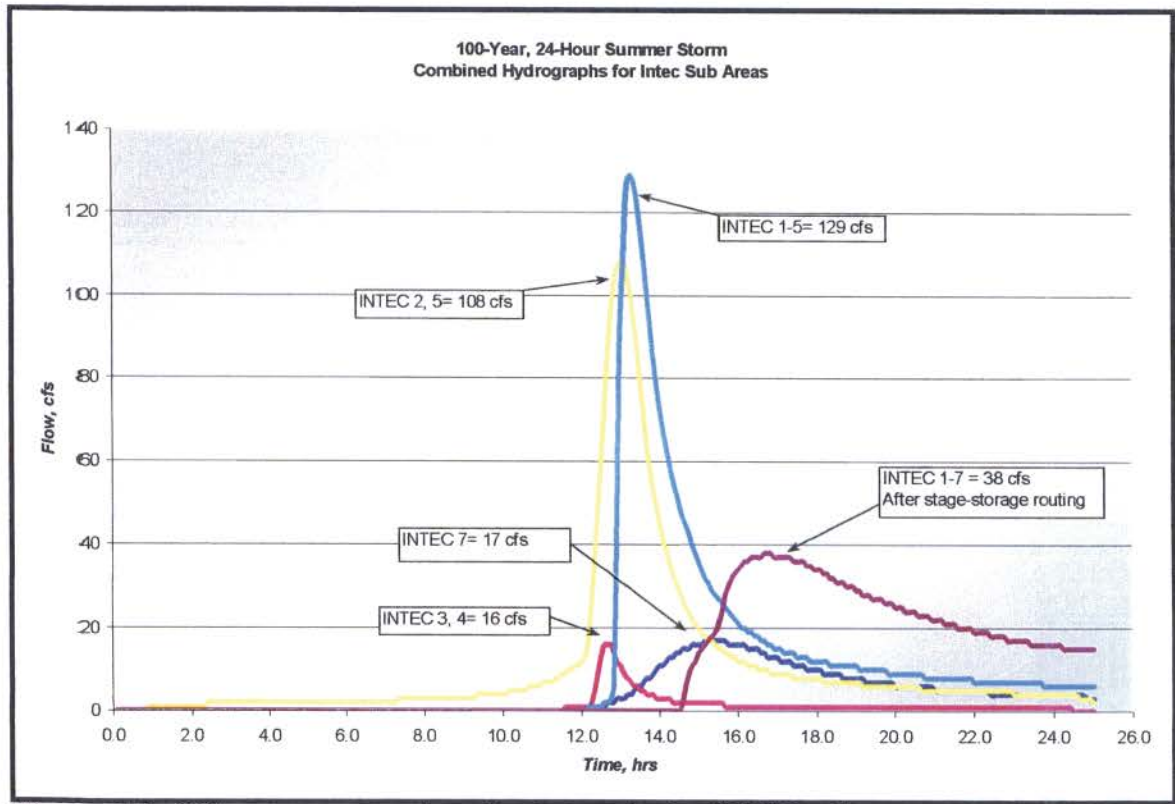
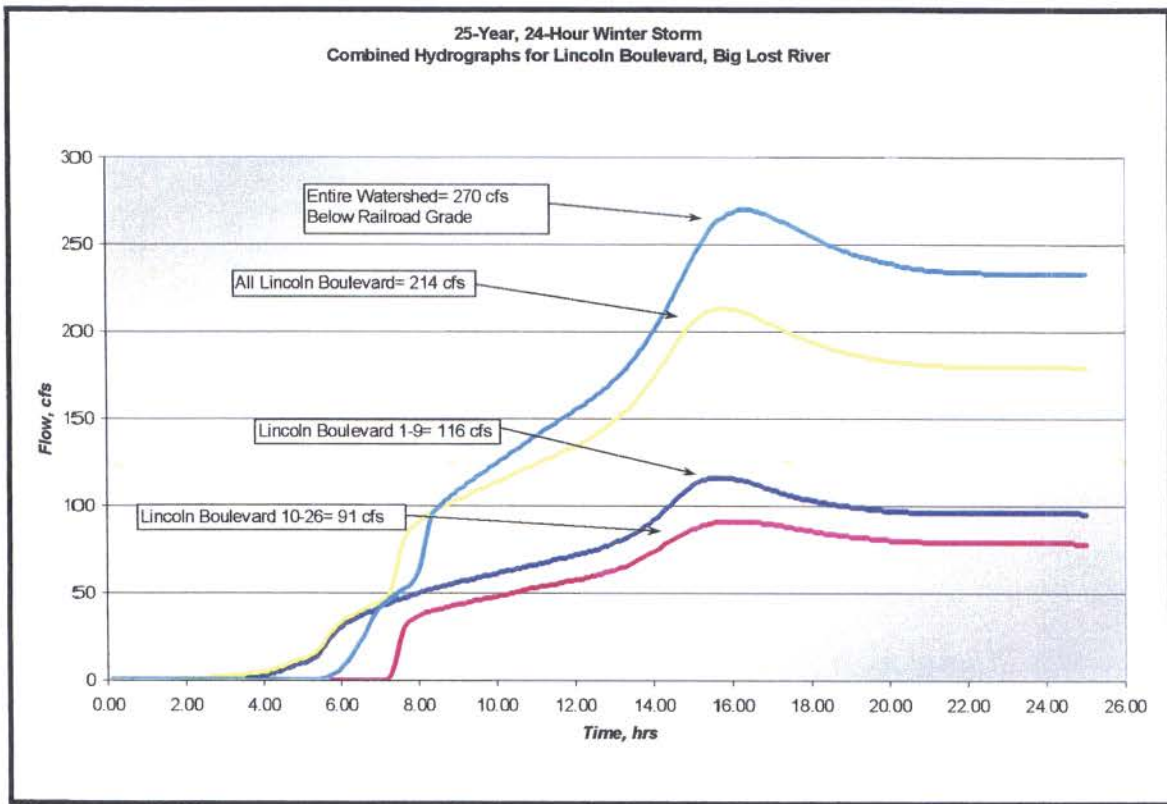
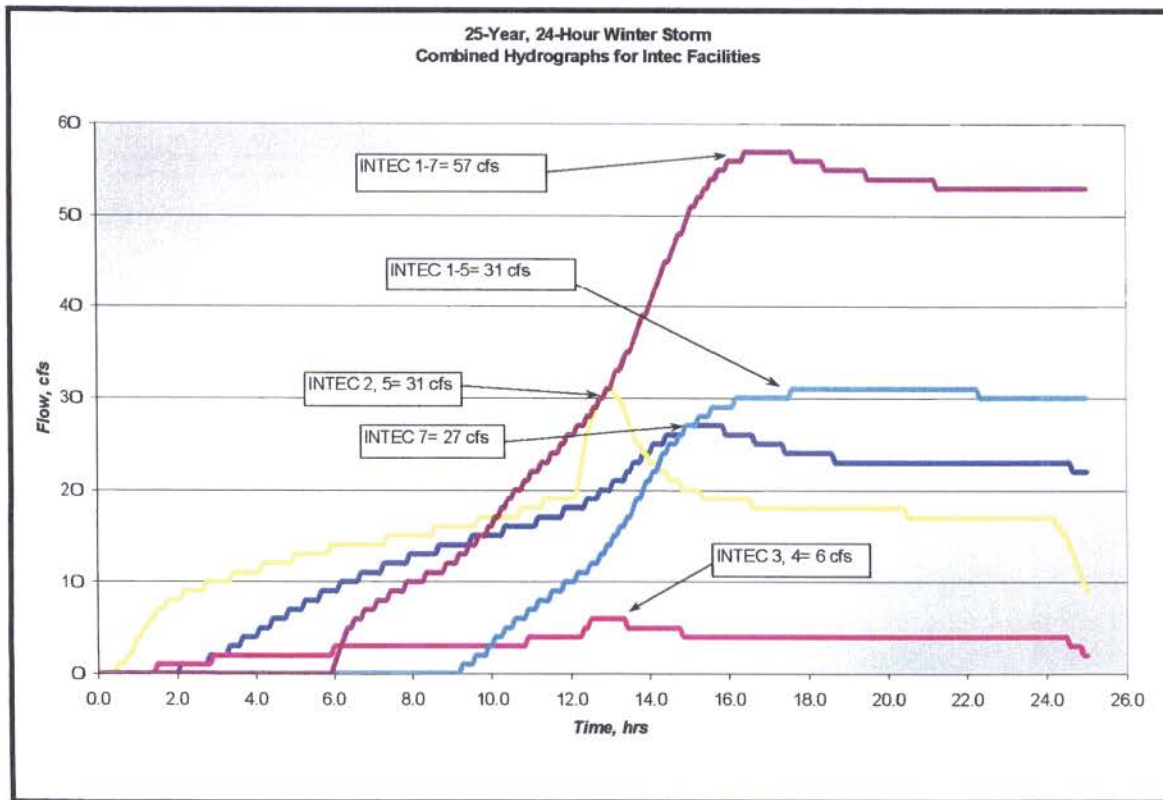


Figure 4-4. 100-year summer storm hydrographs for INTEC sub areas.



**Figure 4-5.** 25-year winter storm hydrographs for Lincoln Boulevard, Big Lost River.



**Figure 4-6.** 25-year winter storm hydrographs for INTEC sub areas.

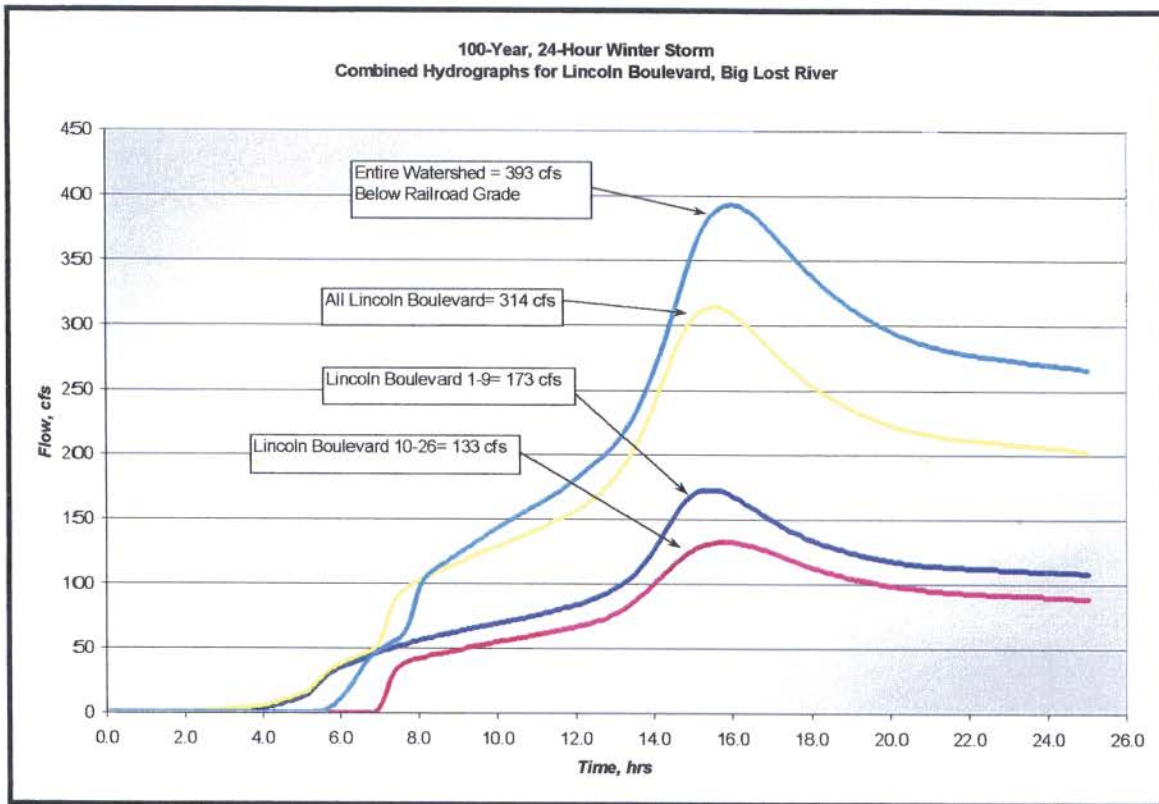


Figure 4-7. 100-year winter storm hydrographs for Lincoln Boulevard, Big Lost River.

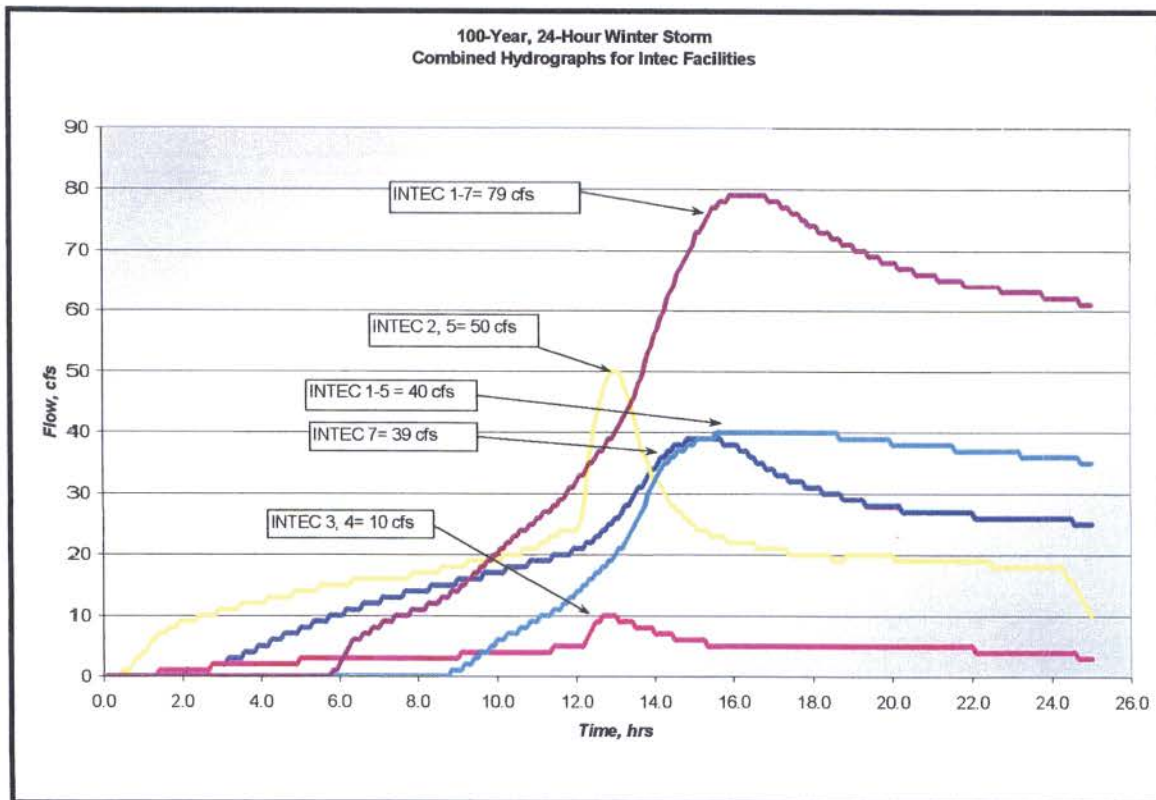


Figure 4-8. 100-year winter storm hydrographs for INTEC sub areas.

#### **4.4 Comparison of Results to Historic Rain/Snow/Frozen Ground Floods**

The 100-year peak flow associated with the watershed area contributing to Lincoln Boulevard is estimated to be 314 cfs, according to the HEC-1 analysis for this study. The contributing area to the Lincoln Boulevard is 10.3 square miles, resulting in an average peak flow of 30.5 cfs/mi<sup>2</sup>. The peak flow associated with the entire watershed modeled in this study including the INTEC facility, is 393 cfs, with a total contributing area of 11.98 square miles, resulting in an average peak flow of 32.8 cfs/mi<sup>2</sup> (does not include CFA sub areas due to the constructed pits and no outflow). The average peak flows are consistent with flows identified in the historic rain on snow and frozen ground events (~ 30-60 cfs/mi<sup>2</sup>) documented throughout the region surrounding the INTEC and INEEL. The consistency of the modeling results with documented flood events provides a measure of the reasonableness of watershed parameters, snowmelt and frozen ground parameters, and the overall model setup for the INTEC watershed and surrounding area.

A detailed model calibration was not performed for this hydrologic analysis due to limited availability of documented flood flow conditions throughout the Snake River Plain. There are no sufficient stream gage records throughout the region surrounding the INEEL which are representative of the hydrologic and hydraulic conditions at the INTEC. Typically, with known watershed area, hydrologic parameters, stream channel parameters and climatological, precipitation and stream flow gage data, a model calibration can be conducted, comparing model results to measured data in order to verify modeling results. As an alternative, regional hydrology was used to compare results of this study to historic data, including documented estimations of peak flow expected in upper watershed areas for rain on snow and frozen ground events. Regional hydrologic information compares closely with results of this study indicating that the models are representative of conditions that may occur at the site during the 25-year and 100-year events.

## 5. HYDRAULIC ANALYSIS

The water surface profiles for the 25-year and 100-year peak flood flows were developed using hydraulic models of the storm water drainage network within the INTEC facility area and the Big Lost River between Lincoln Boulevard and the railroad grade. The 100-year, 24-hour winter rain on snow event was used to identify the storm water runoff floodplain associated with the Big Lost River and key storm water retention areas throughout the watershed area. The 100-year summer event was used to identify the 100-year storm water runoff floodplain limit within the sub areas contributing runoff to the INTEC drainage system. The 25-year summer storm was used to evaluate the capacity of the storm water drainage network in the INTEC facility.

The methodology, assumptions and results of the hydraulic modeling of the surface water channels and storm water drainage systems are discussed in the following sections. Water surface profiles for the Big Lost River and other surface water features outside of the INTEC facility are discussed in Section 5.1. Water surface profiles and the storm water drainage system capacity in the INTEC boundary were developed using hydraulic models of the inlets, pipes, culverts, and surface drainage channels. The methodology, assumptions and results of the hydraulic modeling of the storm drainage systems in the INTEC are discussed in section 5.2.

### 5.1 Big Lost River

Storm water runoff flow in the Big Lost River was analyzed using the Hydrologic Engineering Center's River Analysis System (USCOE, 2001). Field data collected during the course of this investigation were incorporated into a model of the channel and storm water runoff hydrographs from HEC-1 simulations were input to determine the water surface profile during the different storm events. Additional base flow runoff was included in the HEC-RAS model based on the measured portion of the watershed assumed to be contributing to the Big Lost River upgradient of the study area. Model parameters and assumptions used in generating the water surface profiles are described in the following paragraphs.

#### 5.1.1 Channel Geometry

A portion of the Big Lost River adjacent to the INTEC was surveyed in the field during the course of this investigation using a total station in conjunction with GPS control points. Eleven cross-sections were surveyed in the channel for the purposes of conducting the hydraulic analysis, beginning just upstream of Lincoln Boulevard at the gated culvert entering the channel and continuing downstream past the railroad grade, encompassing the entire area that may influence the INTEC.

#### 5.1.2 Bridges and Culverts

Two hydraulic structures were included in the study reach of the Big Lost River. Three parallel culverts installed at Lincoln Boulevard and a bridge located at the railroad grade crossing were measured, surveyed and incorporated into the hydraulic models of the Big Lost River. Measurements taken at each structure include opening widths, heights and/or diameters as applicable, channel geometry at the faces of the structure, number of culverts, entrance and exit geometry and other parameters that may influence hydraulic capacity.

### 5.1.3 Roughness Coefficients

Roughness coefficients (Manning's  $n$  values) were estimated from field observations of conditions in the channel and overbank areas. The roughness coefficients vary little within the channel and overbank areas, with consistent conditions throughout the study reach. Manning's  $n$  values were set at 0.042 and 0.075 for the channel and overbank areas, respectively. These values were taken from the range of values identified in various engineering resource handbooks including the HEC-RAS User's Manual, with specific roughness values selected based on professional engineering judgment and experience with similar channel conditions.

### 5.1.4 Hydraulic Modeling Process and Equations

The HEC-RAS computer program is used to model water surface profiles in a channel and incorporates channel and overbank geometry, channel length and slope (profile), and roughness coefficients. Channel and flow properties modeled in HEC-RAS are used to evaluate a wide variety of flow conditions including flow depth, velocity, critical depths, and backwater effects from hydraulic structures. The program provides flow property solutions based on three equations; the energy equation, Manning's equation, and where necessary the momentum equation. The primary equation used to relate channel geometry, profile and roughness is Manning's equation:

$$Q = \frac{1.49}{n} A \left( \frac{A}{WP} \right)^{0.667} S^{0.5}$$

Where:  $Q$  = discharge, cfs

$n$  = Manning's roughness coefficient

$A$  = flow area, ft<sup>2</sup>

$WP$  = wetted perimeter, ft

$S$  = channel slope, ft/ft

This equation relates the discharge and channel geometry to evaluate the flow area and wetted perimeter, which, in turn, determines the flow depth and water surface elevation at each cross-section within the model. Using an iterative process of solving the energy equation, Manning's equation and where necessary, the momentum equation, HEC-RAS provides a detailed analysis of the flow conditions in the modeled stream channel.

### 5.1.5 HEC-RAS Model Simulations, Big Lost River

Peak flows from the 25-year and 100-year hydrographs were taken from the HEC-1 hydrologic simulations and input into the HEC-RAS model of the Big Lost River to identify water surface profiles during the simulated storm events. A total of 3 hydrographs; base flow from upgradient contributing watershed area, flows from the Lincoln Boulevard contributing sub areas, and all contributing flow from the study area, were combined and incorporated into the HEC-RAS model to accurately model channel junctions where flow enters the river.

The HEC-RAS model simulations indicate that the Big Lost River has sufficient capacity to convey all storm water runoff during the design storm events in the vicinity of the INTEC. The barrier dike constructed between Lincoln Boulevard and the railroad grade prevents flood flows in the Big Lost River from impacting the INTEC facility during the 25-year and 100-year events.

One location along the barrier dike was identified where floodwater may flow out of the banks of the river during the 100-year runoff event and is located upstream of Lincoln Boulevard. The dike has a low elevation in this location relative to the remainder of the dike and may be subject to flooding in the overbank area. This location is upgradient of Lincoln Boulevard and, with Lincoln Boulevard serving as an additional flow barrier, does not contribute flooding to the INTEC.

The storm water runoff floodplain for the 100-year event modeled in this study is shown on Sheet 2. The floodplain drawing includes the floodplain associated with storm water flow in the Big Lost River, stage-storage areas inundated during the modeled events, as well as floodplain areas within the INTEC perimeter resulting from the storm water drainage systems. Water surface elevations taken from hydraulic modeling of these areas are included in the floodplain mapping.

It should be noted that the floodplain map was generated using two different storm water runoff events. The Big Lost River storm water runoff floodplain was identified using the 100-year winter rain on snow with frozen ground event and the floodplain within the INTEC facility area was identified using the 100-year summer thunderstorm in order to identify the greatest floodplain extent for the respective areas. Detailed discussion of the flood modeling conducted within the INTEC facility is included in the following section.

## **5.2 INTEC Surface and Subsurface Drainage System Modeling**

The surface drainage channels and subsurface drainage piping system in the INTEC facility area were modeled using the Environmental Protection Agency's Storm Water Management Model (US EPA, SWMM 4.4gu, 1999). This model provides a detailed analysis of storm drainage surface channel and piping networks including pipe and inlet flow conditions, water surface elevations, flow velocities, and design capacities of drainage system components. The program generates detailed flow hydrographs resulting from storm water runoff input into the model, and simultaneously solves for flow conditions in all channels and pipes using the energy equation, Manning's equation and the momentum equation to evaluate the storm drain system as a whole.

The SWM modeling for the INTEC storm drainage system networks was conducted for the 25-year and 100-year summer storm events in order to identify any flooding that may occur and to delineate the 100-year floodplain for the storm water drainage system. Discussion of the SWMM program and modeling parameters used in this analysis are presented in the following sections.

### 5.2.1 SWMM Program Input Parameters

The SWMM program combines storm water drainage system parameters including open channel, piping and inlet characteristics and configurations and storm water runoff hydrographs to generate a flow model of the drainage network during a design storm event. All connected components of the storm drainage system can be modeled together in order to identify backwater influences and channels and pipes with insufficient capacity.

Input parameters for the SWMM program include the following:

- Pipe diameter, shape, length, upstream/downstream invert elevations and roughness
- Surface channel shapes, lengths and roughness
- Inlet type, surface and invert elevations
- Pipe and inlet connectivity data
- Storm water runoff hydrographs for the duration of the runoff event
- Outfall type and water surface elevation at the outfall during the runoff event (to identify backwater effects on the drainage system where outlet elevations are located near the bottom of surface channels).

The storm water drainage network inlets and culvert locations were surveyed during the field investigation at the INTEC. All necessary data to complete the storm water management model were collected for surface channels, catch basins, lift stations, and culverts in the INTEC area. Field data were incorporated into the SWMM input files and used to determine channel and pipe capacities and peak flow during the modeled runoff events.

### 5.2.2 Storm Water Runoff Hydrographs

Detailed storm water runoff hydrographs for the INTEC facility were developed from a HEC-1 model prepared specifically for the INTEC-2 sub area identified within the regional watershed area (main facility). The INTEC-2 sub area was further subdivided according to flow paths in the storm water drainage system and used to more accurately evaluate flows in the surface channels, culverts and pipes.

The runoff hydrographs for the INTEC-2 sub area were proportioned to various channels, culverts and inlets throughout the drainage system according to their respective contributing area and surface runoff flow paths. In each major segment of the drainage network, runoff was input into end of line inlets in order to evaluate all pipes and channels in the segment.

### 5.2.3 SWMM Analysis

The SWMM program analysis provides detailed information regarding peak flows, channel and pipe capacities, flow depths, and, where applicable, pipe surcharge depths in and above the catch basins (inlets). During the modeling process, the SWMM program computes the flow and velocity in each channel and pipe throughout the duration of the storm based on

size, roughness, slope, length and connectivity. The program also computes water surface elevations in the channels and catch basins, including surcharge in inlets and catch basins resulting from insufficient capacity. Water surface profiles and surface elevations computed by the program are used to identify areas where surface flooding may occur. The following is a detailed description of the information input to and output from the SWMM program and used in evaluating any surface flooding resulting from insufficient capacity.

#### Input information:

- Pipe segment describing upstream and downstream catch basin locations for each pipe or culvert modeled in the program.
- Pipe diameter and roughness (based on material), and pipe length. For modeling purposes, pipes include both subsurface piping and culverts.
- Inlet information including ground elevation and basin invert elevation.
- Surface water channel shape, depths, side slopes, channel slope based on pipe and culvert inlet elevations (as identified in connectivity data) and roughness.
- General connectivity information including upstream and downstream nodes for each surface channel, culvert and storm drain pipe. Outfall data to identify conditions at the downstream limit of the storm water drainage network.
- Storm water runoff hydrographs distributed to the appropriate inlet or node (nodes used to describe upstream and downstream ends of all channels, pipes and culverts).

#### Output information:

- Channel and pipe capacity (design capacity) and peak flow.
- Ratio of design capacity to peak flow. This ratio may identify channels and pipes where insufficient capacity can cause surface flooding. A ratio less than 1 shows sufficient capacity in the drainage segment for the storm water runoff input into the model. A ratio greater than 1 identifies drainage segments where surcharge is present and additional flow capacity is generated under pressure flow conditions.
- Junction surcharge elevation above ground elevation indicates inlets where surcharge water in the basin has reached the surface and can cause flooding. Values of zero for this output parameter indicate that, although surcharge water may be present in the basin, the water surface elevation does not rise above the ground elevation and cause flooding.

The ratio of design capacity to peak flow is one of the key output parameters utilized from the SWMM program to evaluate the drainage system and flooding potential. When the ratio is less than one, the peak flow is less than the pipe or channel capacity and indicates that the water surface profile and energy grade are contained within the pipe or channel with no backwater effects that can cause flooding. A ratio greater than one indicates that the peak flow

in the pipe or channel is greater than capacity under gravity flow conditions. However, a ratio greater than 1 does not necessarily indicate that the drainage system has insufficient capacity and that flooding will occur because additional flow capacity is generated under pressure flow conditions.

When the peak flow exceeds the design flow of a pipe or channel, water rises above the top of the pipe (surcharge) causing a pressure flow condition allowing greater flow than design capacity. However, in subsurface drainage systems, and in open channels with culverts, the surcharge may not reach the ground surface or top of the open channel and cause surface flooding. Where surcharge is present in the system and the ratio of peak flow to capacity exceeds 1, it is necessary to evaluate the depth of surcharge, site topography and other factors to determine if surface flooding occurs and to what extent.

#### **5.2.4 SWMM Modeling Results**

The INTEC storm water drainage system has adequate capacity to convey nearly all storm water runoff during the 25-year event. Insufficient pipe and channel capacity and physical condition deficiencies (improper construction) were identified in the drainage network near buildings T-1 and T-5. This area of the drainage network was constructed at an elevation above the apparent floor elevation of the buildings and during periods of significant runoff may overflow and cause localized flooding. Minor surface flooding at localized areas throughout the remainder of the storm water drainage network is limited to the immediate vicinity of the storm water surface channels and inlets and does not pose a flooding hazard to the surrounding areas.

During the 100-year storm, more extensive flooding will occur in the area around buildings T-1 and T-5, and shallow surface flooding will occur near buildings CPP-651 and CPP-796. This area of the storm water drainage network has insufficient capacity to convey all of the 100-year runoff and will cause localized shallow flooding in the vicinity of these buildings. According to topographic mapping of the site, the limit of the 100-year storm water runoff floodplain will encompass buildings T-1 and T-5. Buildings CPP-651 and CPP-796 are not within the 100-year floodplain boundary.

Surface flooding elevations are identified in the SWM models prepared for the 25-year and 100-year runoff events. The surface flooding elevations were subsequently used to identify floodplain limits for the storm water drainage networks. The storm water runoff floodplain for the 100-year event is shown on Sheet 2.

The SWMM modeling conducted for this study included surface water channels, culverts, catch basins, subsurface piping, lift stations and storm water retention areas. Modeling for storm water drainage network at the INTEC facility assumes that all culverts, pipes, channels and lift stations are maintained in a fully functioning condition. The results for the 25-year and 100-year events indicate that, in general, the storm water drainage network has sufficient capacity to convey runoff away from the facility towards the Big Lost River. With the exceptions described in the previous paragraphs, no surface flooding outside the limits of open surface water drainage channels within the INTEC facility area was identified.

### 5.3 25-year and 100-year Floodplain Mapping

The 25-year and 100-year storm water runoff floodplains were identified on topographic mapping of the INTEC facility using results of the SWMM and HEC-RAS model analyses. The water surface elevations resulting from the 25-year and 100-year flows were plotted on a base map of the storm water drainage network and the Big Lost River. In locations where the channel capacity was exceeded, surface flooding elevations were identified and delineated on topographic maps to determine the extent of the floodplain. Storm water retention area flood elevations were also identified for the 25-year and 100-year events in order to identify all inundated floodplain areas associated with storm water runoff. The 100-year floodplain boundary for the INTEC storm water drainage network, surface channels and storm water retention areas included in the modeling for this study is shown on Sheet 2.

Additionally, a storm water runoff floodplain for the Big Lost River was delineated to the extent of the water surface elevations identified in the HEC-RAS models created for this study. A short segment of the Big Lost River was modeled as a part of this study to evaluate the function of the barrier dike constructed along the southern bank of the river in the immediate vicinity of the INTEC, and to identify the floodplain limit associated with the 25-year and 100-year storm water runoff events. Using estimates of the base flow in the Big Lost River combined with runoff from the watershed contributing to Lincoln Boulevard, flood flows and water surface elevations in the Big Lost River were compared to the barrier dike profile to identify flooding potential. According to the results of the model analyses, storm water runoff from the watershed west of Lincoln Boulevard will be contained within the limits of the channel and low lying areas to the north of the river. The perimeter dike prevents storm water runoff from entering the area in the immediate vicinity of the INTEC. A detailed study of the 25-year and 100-year riverine floods in the Big Lost River is beyond the scope of this project and is being conducted by others.

## 6. CONCLUSIONS

Conclusions of this hydrologic and hydraulic study of the 25-year runoff and 100-year storm water runoff floodplain at the INTEC facility are presented in the following.

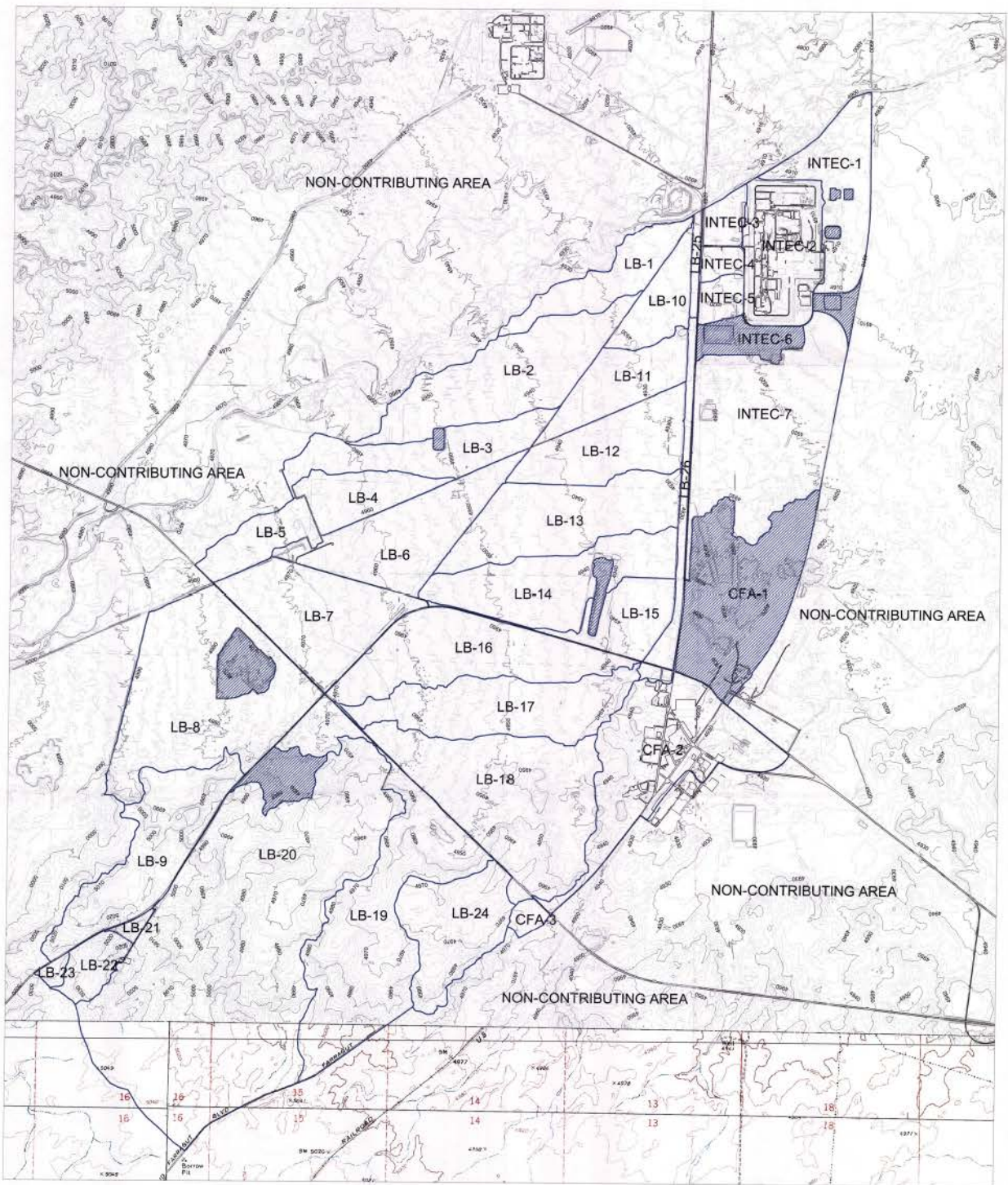
1. One area in the storm water drainage network serving the INTEC facility was identified as hydraulically deficient during the 25-year summer storm event. This surface channel is constructed at an elevation above the surrounding ground and will overflow during the 25-year event, causing localized flooding around Buildings T-1 and T-5.
2. Buildings T-1 and T-5 are located within the floodplain associated with an open surface channel and culverts in their vicinity. This surface channel is constructed at an elevation above the surrounding ground and will overflow during the 100-year event, causing localized flooding in the area. Buildings CPP-651 and CPP-796 are located outside of the limits of the 100-year floodplain according to surface water elevations and topographic mapping in the area.
3. The 25-year and 100-year flood flows throughout the remainder of the INTEC facility area are generally contained within the limits of surface water channels and local storm water retention areas. No other buildings beyond those discussed in items 1 and 2 were identified within the limits of the storm water runoff floodplain boundaries delineated during the course of this study.
4. The limits of the 100-year floodplain associated with flows entering the Big Lost River to the west (upgradient) side of Lincoln Boulevard, including estimated base flow, are contained on the southern side of the channel by the perimeter dike, with the exception of one small area. Immediately west of Lincoln Boulevard, a low elevation in the perimeter dike may allow flood flow to leave the channel. This flow does not have the potential to enter the INTEC facility area as Lincoln Boulevard serves as a drainage divide, with no culverts to allow cross flow.
5. The northern side of the Big Lost River was not thoroughly investigated to identify the full extent of the floodplain to the north of the perimeter dike. Other studies are being conducted to determine the magnitude and extent of the 25-year and 100-year floods associated with the Big Lost River.
6. Storm water retention areas identified throughout the watershed area will collect storm water runoff during the 25-year and 100-year events. These areas will fill to the elevations identified on the floodplain maps and where sufficient storm water accumulation occurs, will overflow into surface water drainage channels. No flooding identified in these areas has the potential to impact the INTEC facility.

## 7. REFERENCES

- Berenbrock, C., and Kjelstrom, L.C., 1998, *Preliminary Water-Surface Elevations and Boundary of the 100-year Peak Flow in the Big Lost River at the Idaho National Engineering and Environmental Laboratory, Idaho*, United States Geological Survey, Water-Resources Investigations Report 98-4065.
- Burgess, J.D., July 1991, *25-Year, 24-Hours Storm Analysis for the Idaho Chemical Processing Plant*, EG&G Geosciences.
- CH2MHill, Inc., 1989, *Silver Bow Creek Flood Modeling Study*, Butte, Montana.
- Dames and Moore, 1993, *Flood Evaluation Study, Radioactive Waste Management Complex*, Idaho National Engineering Laboratory, Idaho Falls, Idaho.
- DOE-ID, 1998, *Interim Risk Assessment and Contaminant Screening for the Waste Area Group 7 Remedial Investigation (Section 3.1.4, P. 3-6)*, US Department of Energy Idaho Operations Office, DEO/IDD-10569.
- Dodson and Associates, Inc., June 1995, *ProHEC1 Plus Program Documentation*, Houston, Texas.
- Humphrey, J. H., 1994, *Meteorological Analysis, Flood Control Master Plan*, Washoe County, Nevada.
- Kingsford, C.O., 2002, *Culvert Survey Summary*, Document No. INEEL/EXT-01-01179.
- Keck, K. N., 1998, *25-Year, 24-hour Storm Evaluation for the Transuranic Storage Area*, Idaho National Engineering and Environmental Laboratory, INEEL/EXT-98-00472.
- Koslow, K. N., Van Haaften, D. H., 1986, *Flood Routing Analysis for a Failure of a Mackay Dam*, EGG-EP-7-7184, EG&G Idaho, Inc.
- Mitchell, T. S., Mitchell, J. S., Humphrey, J. H., Kennedy, D., Funderburg, T., 2002, *100-year Floodplain and 25-Year Runoff Analyses for the Radioactive Waste Management Complex at the Idaho National Engineering and Environmental Laboratory*, Document No. INEEL/EXT-02-00093.
- National Weather Service, Dubois Gage Data (1948 – 1997).
- National Weather Service, Idaho Falls 16SE Gage Data (1960 – 1997).
- National Weather Service, Idaho Falls 2ESE Gage Data (1952 – 1960).
- National Weather Service, Idaho Falls FAA, Idaho Falls Airport Gage data (1948 – 1952).
- National Weather Service, INEEL Winter Flood Events, Idaho Falls 46W Data (1952 – 2000).
- National Weather Service, Twin Falls Gage Data (1978 – 1997).
- Ostenaar, D. A., Levish, D. R., Klingler, R. E., and O'Connell, D. R., 1999, *Phase II, Paleohydrologic and Geomorphic Studies for the Assessment of Flood Risk for the Idaho National Engineering and Environmental Laboratory, Idaho*, Report 99-7, Geophysics, Paleohydrology, and Seismotectonics Group, Technical Service Center, Bureau of Reclamation, Denver, Colorado.

- Peck, E. L., Richardson, E. A., 1962, *An Analysis of the Causative Factors of the February 1962 Floods in Utah and Eastern Nevada*, National Weather Service, Salt Lake City, Utah.
- Sagendorf, J., 1991, *Meteorological Information for RWMC Flood Potential Studies*, National Oceanic Atmospheric Administration, Environmental Research Laboratories, Air Resources Laboratory Field Research Division, Idaho Falls, Idaho.
- Sagendorf, J., 1996, *Precipitation Frequency and Intensity at the Idaho National Engineering Laboratory*, National Oceanic and Atmospheric Administration, Technical Memorandum ERL ARL-215, Air Resources Laboratory, Silver Spring, Maryland.
- Soil Conservation Service, 1972, *National Engineering Handbook*.
- Taylor, D. D., Hoskinson, R.L., Kingsford, C. O., Ball, L. W., 1994, *Preliminary Siting Activities for New Waste Handling Facilities at the Idaho National Engineering Laboratory*.
- Tullis, J. A., Koslow, K. N., 1983, *Characterization of Big Lost River Floods with Recurrence Intervals Greater than 25 Years*, EG&G Idaho, Inc. Internal Technical Report, RE-PB-83-044.
- United States Army Corps of Engineers, 1975, *Humbolt River and Tributaries, Nevada, Design Memorandum No. 1*, Sacramento District.
- United States Army Corps of Engineers, 1998, *Snow Hydrology Manual*, EM 1110-2-1406.
- United States Army Corps of Engineers, Hydrologic Engineering Center, 2001, *HEC-RAS River Analysis System, Version 3.0.1 User's Manual*.
- United States Environmental Protection Agency, 1999, *Storm Water Management Model, User's Manuals*, Office of Research and Development, Athens, Georgia.
- United States Geological Survey, 1994, *Methods for Estimating Magnitude and Frequency of Floods in the Southwestern United States*, Open File Report 93-419.

# **DRAWINGS**



**LEGEND:**

- MAJOR CONTOUR
- MINOR CONTOUR
- WATERSHED BOUNDARY
- SUB AREA BOUNDARY
- SUB AREA LABEL
- SINK AREA (STORAGE)
- PAVED ROADS
- RAILROAD
- USGS QUAD SECTION NUMBER

**NOTES:**

1. PLANIMETRIC AND TOPOGRAPHIC DATA DERIVED FROM AERIAL PHOTOGRAMMETRIC IMAGERY COLLECTED BY AERIAL SERVICES, INC., CEDAR FALLS, IOWA, DURING JULY 2002.
2. WATERSHED AND SUB AREA DELINEATIONS ARE BASED ON SEVERAL FACTORS INCLUDING, BUT NOT LIMITED TO, TOPOGRAPHY, STORM WATER FLOW PATHS, HYDRAULIC STRUCTURE LOCATIONS, SIGNIFICANT DRAINAGE AREA DIVIDES AND GENERAL HYDROLOGIC CONDITIONS.
3. THE SOUTHERN LIMITS OF THE WATERSHED AREA WERE IDENTIFIED USING PORTIONS OF A USGS QUADRANGLE (CIRCULAR BUTTE 3, USGS), IMPORTED AND SCALED TO APPROXIMATELY MEET THE TOPOGRAPHY WITHIN THE FLYOVER LIMITS.
4. AREAS WEST OF LINCOLN BOULEVARD (LB-##) WERE INCLUDED IN HYDROLOGIC MODELING TO EVALUATE ANY FLOODING POTENTIAL FROM FLOW OVER LINCOLN BOULEVARD OR IN THE BIG LOST RIVER NEAR THE INTEC FACILITY PERIMETER.
5. ALL CENTRAL FACILITIES SUB AREAS (CFA-##) FLOW INTO CFA-1 WHICH SERVES A STORM WATER RUNOFF SINK DUE TO THE PRESENCE OF SEVERAL LARGE OPEN PITS.

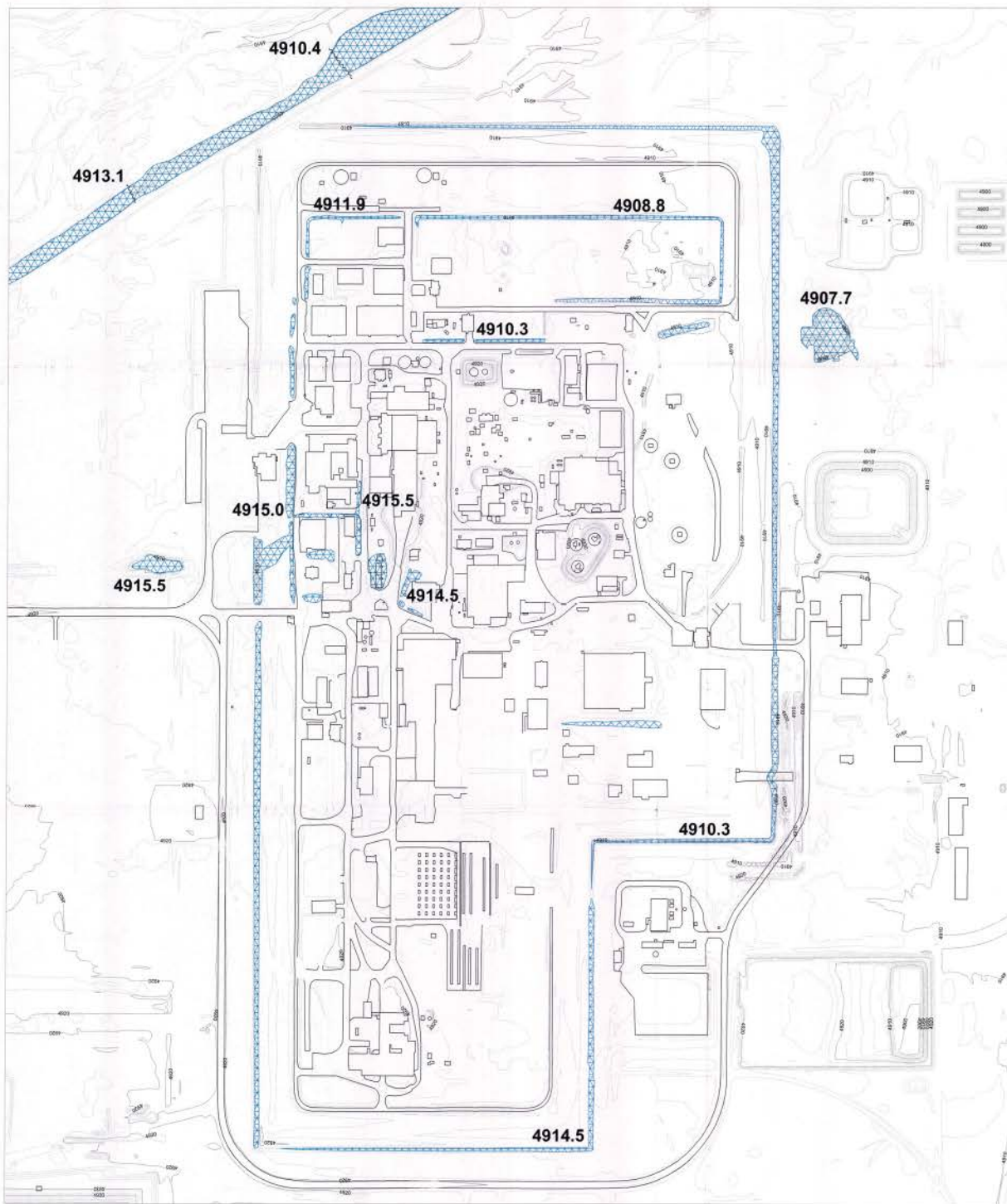


HORIZONTAL DATUM: NAD 27, IDAHO EAST ZONE, STATE PLANE COORDINATES

VERTICAL DATUM: NGVD 29

CONTOUR INTERVAL: 2 FEET

|   |  |  |                       |
|---|--|--|-----------------------|
| <b>INTEC FLOODPLAIN ANALYSES</b><br>  |  | <small>Idaho National Engineering and Environmental Laboratory<br/>         MICHEL, BRYANT &amp; ASSOCIATES, LLC</small> |                       |
| <small>Requestor: Neil Hutten<br/>         Drawn: Todd S. Mitchell, PE<br/>         Checked: K. Flynn/J.S. Mitchell</small> |  | <b>INTEC FACILITY AND SURROUNDING AREA, WATERSHED AND SUB AREA BOUNDARIES</b>  |                       |
| <small>Subcontract No. 00018206<br/>         Date: September, 2003</small>  | <small>Size Scale: 1-IN = 1,500 FT</small> | <small>Drawing No. SHEET 1</small>   | <small>Rev. 0</small> |



**LEGEND:**

- MAJOR CONTOUR
- MINOR CONTOUR
- 100-YEAR FLOODPLAIN LIMIT
- 4915.5 BASE FLOOD ELEVATION
- BUILDING
- PAVED ROADS

**NOTES:**

1. FLOODPLAIN AREAS INSIDE OF THE INTEC FACILITY WERE IDENTIFIED USING THE 100-YEAR SUMMER THUNDERSTORM (PEAK RUNOFF FOR FACILITY AREA).
2. BASE FLOOD ELEVATIONS SHOWN IN THE INTEC FACILITY AREA WERE TAKEN FROM DETAILED STORM WATER MANAGEMENT MODELS OF THE DRAINAGE SYSTEM.
3. FLOODPLAIN LIMITS OF THE BIG LOST RIVER ARE SHOWN FOR STORM WATER RUNOFF FROM THE WATERSHED AREAS WEST OF LINCOLN BOULEVARD AND ADDITIONAL WATERSHED AREA (~ 17 SQ. MI.) ASSUMED TO BE CONTRIBUTING TO THE RIVER AT THE TIME OF THE MODELED STORM EVENTS.



HORIZONTAL DATUM: NAD 27, IDAHO EAST ZONE, STATE PLANE COORDINATES

VERTICAL DATUM: NGVD 29

CONTOUR INTERVAL: 2 FEET

|                           |                        |   |  |   |   |
|---------------------------|------------------------|---|--|---|---|
| INTEC FLOODPLAIN ANALYSIS |                        |   |  | www.national-engineering-and-consulting.com<br>REGISTERED ENGINEERS, ARCHITECTS & PLANNERS, LLC |   |
| Requester:                | Nell Ruffen            |   |  |   |   |
| Drawn:                    | Todd S. Mitchell, PE   |   |  |   |   |
| Checked:                  | K. Flynn/J.S. Mitchell |   |  |   |   |
|                           |                        | <b>INTEC FACILITY DETAIL,<br/>100-YEAR FLOODPLAIN</b> |  |   |   |
| Subcontract No. 00019290  | <b>C</b>               | Size/Scale:   | 1-IN = 200 FT                                      | Drawing No.   | 0 |
| Date:                     | July 31, 2003          | File:   | x:\stem\map10\INTEC\final drawings\CGG Sheet 2.dwg |   |   |
|                           |                        |   |  | SHEET 2   | 0 |